m 53

Mohamed Gad-el-Hak Andrew Pollard
Jean-Paul Bonnet (Eds.)

Flow Control

Fundamentals and Practices

Springer

Lecture Notes in Physics

New Series m: Monographs

Editorial Board

H. Araki, Kyoto, Japan
R. Beig, Vienna, Austria
J. Ehlers, Potsdam, Germany
U. Frisch, Nice, France
K. Hepp, Zürich, Switzerland
R. L. Jaffe, Cambridge, MA, USA
R. Kippenhahn, Göttingen, Germany
H. A. Weidenmüller, Heidelberg, Germany
J. Wess, München, Germany
J. Zittartz, Köln, Germany

Managing Editor

W. Beiglböck
Assisted by Mrs. Sabine Lehr
c/o Springer-Verlag, Physics Editorial Department II
Tiergartenstrasse 17, D-69121 Heidelberg, Germany

Springer
Berlin
Heidelberg
New York
Barcelona
Budapest
Hong Kong
London
Milan
Paris
Santa Clara
Singapore
Tokyo

The Editorial Policy for Monographs

The series Lecture Notes in Physics reports new developments in physical research and teaching - quickly, informally, and at a high level. The type of material considered for publication in the New Series m includes monographs presenting original research or new angles in a classical field. The timeliness of a manuscript is more important than its form, which may be preliminary or tentative. Manuscripts should be reasonably self-contained. They will often present not only results of the author(s) but also related work by other people and will provide sufficient motivation, examples, and applications.
The manuscripts or a detailed description thereof should be submitted either to one of the series editors or to the managing editor. The proposal is then carefully refereed. A final decision concerning publication can often only be made on the basis of the complete manuscript, but otherwise the editors will try to make a preliminary decision as definite as they can on the basis of the available information.
Manuscripts should be no less than 100 and preferably no more than 400 pages in length. Final manuscripts should preferably be in English, or possibly in French or German. They should include a table of contents and an informative introduction accessible also to readers not particularly familiar with the topic treated. Authors are free to use the material in other publications. However, if extensive use is made elsewhere, the publisher should be informed. Authors receive jointly 50 complimentary copies of their book. They are entitled to purchase further copies of their book at a reduced rate. As a rule no reprints of individual contributions can be supplied. No royalty is paid on Lecture Notes in Physics volumes. Commitment to publish is made by letter of interest rather than by signing a formal contract. Springer-Verlag secures the copyright for each volume.

The Production Process

The books are hardbound, and quality paper appropriate to the needs of the author(s) is used. Publication time is about ten weeks. More than twenty years of experience guarantee authors the best possible service. To reach the goal of rapid publication at a low price the technique of photographic reproduction from a camera-ready manuscript was chosen. This process shifts the main responsibility for the technical quality considerably from the publisher to the author. We therefore urge all authors to observe very carefully our guidelines for the preparation of camera-ready manuscripts, which we will supply on request. This applies especially to the quality of figures and halftones submitted for publication. Figures should be submitted as originals or glossy prints, as very often Xerox copies are not suitable for reproduction. For the same reason, any writing within figures should not be smaller than 2.5 mm. It might be useful to look at some of the volumes already published or, especially if some atypical text is planned, to write to the Physics Editorial Department of Springer-Verlag direct. This avoids mistakes and time-consuming correspondence during the production period.
As a special service, we offer free of charge LaTeX and TeX macro packages to format the text according to Springer-Verlag's quality requirements. We strongly recommend authors to make use of this offer, as the result will be a book of considerably improved technical quality.
Manuscripts not meeting the technical standard of the series will have to be returned for improvement.
For further information please contact Springer-Verlag, Physics Editorial Department II, Tiergartenstrasse 17, D-69121 Heidelberg, Germany.

Mohamed Gad-el-Hak Andrew Pollard
Jean-Paul Bonnet (Eds.)

Flow Control

Fundamentals and Practices

Springer

Editors

Mohamed Gad-el-Hak
Department of Aero. & Mech. Engineering
University of Notre Dame
Notre Dame, IN 46556, USA
e-mail: mohamed.gad.el.hak.1@nd.edu

Andrew Pollard
Department of Mechanical Engineering
Queen's University
Kingston, Ontario K7L 3N6, Canada
e-mail: pollard@me.queensu.ca

Jean-Paul Bonnet
Centre d'Etudes Aérod. & Thermiq.
Université de Poitiers
F-86036 Poitiers Cedex, France
e-mail: bonnet@univ-poitiers.fr

CIP data applied for.

Die Deutsche Bibliothek - CIP-Einheitsaufnahme

Flow control : fundamentals and practices / Mohamed Gad-el-Hak ... (ed.). - Berlin ; Heidelberg ; New York ; Barcelona ; Budapest ; Hong Kong ; London ; Milan ; Paris ; Santa Clara ; Singapore ; Tokyo : Springer, 1998
(Lecture notes in physics : N.s. M, Monographs ; 53)
ISBN 3-540-63936-5

ISSN 0940-7677 (Lecture Notes in Physics. New Series m: Monographs)
ISBN 3-540-63936-5 Springer-Verlag Berlin Heidelberg New York

This work is subject to copyright. All rights are reserved, whether the whole or part of the material is concerned, specifically the rights of translation, reprinting, re-use of illustrations, recitation, broadcasting, reproduction on microfilms or in any other way, and storage in data banks. Duplication of this publication or parts thereof is permitted only under the provisions of the German Copyright Law of September 9, 1965, in its current version, and permission for use must always be obtained from Springer-Verlag. Violations are liable for prosecution under the German Copyright Law.

© Springer-Verlag Berlin Heidelberg 1998
Printed in Germany

The use of general descriptive names, registered names, trademarks, etc. in this publication does not imply, even in the absence of a specific statement, that such names are exempt from the relevant protective laws and regulations and therefore free for general use.

Typesetting: Camera-ready by authors/editors
Cover design: *design & production* GmbH, Heidelberg
SPIN: 10552601 55/3144-543210 - Printed on acid-free paper

Preface

No knowledge can be certain if it is not based upon mathematics.
(Leonardo da Vinci, 1452–1519)

Thinking is one of the greatest joys of humankind.
(Galileo Galilei, 1564–1642)

Now I think hydrodynamics is to be the root of all physical science, and is at present second to none in the beauty of its mathematics.
(William Thomson (Lord Kelvin), 1824–1907)

The present book contains the lecture notes of eight of the nine instructors at the short course Flow Control: Fundamentals and Practices, which was held in Cargèse, Corsica, France, during the week 24–28 June 1996, and repeated at the University of Notre Dame, Indiana, 9–13 September 1996. Following the course week in Corsica, a 5-day workshop on the same topic was held. Selected papers from the workshop are scheduled to appear early 1998 special volume of the *International Journal of Experimental Heat Transfer, Thermodynamics, and Fluid Mechanics.* All three events were organized by Jean-Paul Bonnet of Université de Poitiers, France, Andrew Pollard of Queen's University at Kingston, Canada, and Mohamed Gad-el-Hak of the University of Notre Dame, U.S.A.

The ability to actively or passively manipulate a flow field to effect a desired change is of immense technological importance, and this undoubtedly accounts for the fact that the subject is hotly pursued at present by more scientists and engineers than any other topic in fluid mechanics. The art of flow control is as old as prehistoric man, whose sheer perseverance resulted in the invention of streamlined spears, sickle-shaped boomerangs and fin-stabilized arrows. The German engineer Ludwig Prandtl pioneered the science of flow control at the beginning of the twentieth century.

The potential benefits of realizing efficient flow control systems range from saving billions of dollars in fuel cost for land, air and sea vehicles to achieving economically/environmentally more competitive industrial processes involving fluid flows. The purpose of both the short course and the workshop was

to provide an up-to-date view of the fundamentals of some basic flows and control practices, which can be employed to produce needed effects. Understanding of some basic mechanisms in free and wall-bounded turbulence has increased substantially in the last few years. This understanding suggests that taming of turbulence – the quintessential challenge in the field of flow control – is possible so as to eliminate some of its deleterious effects while enhancing others.

The Mediterranean island ambiance was fabulous by all accounts, and the two events in Corsica attracted an international audience/participants about 75 strong. The short course at Notre Dame was attended by 20 students, researchers and practicing engineers from academia, industry and the military. The events acted as forums for presentation of current ideas and methods for effecting such control to achieve transition delay, separation prevention, drag reduction, lift augmentation, turbulence suppression, noise abatement, and heat and mass transfer (including combustion) enhancement, in both free-shear and wall-bounded flows.

The present book, much like the short course, is intended for engineers, physicists and graduate students at universities and research laboratories, in government and industry, who have an interest in the physics and control of laminar, transitional and turbulent flows. The different contributions here are written in a clear, pedagogic style and are designed to attract newcomers to the field. A knowledge of basic fluid dynamics is assumed, and the book should help the reader in navigating through the colossal literature available on flow control fundamentals and practices.

The book is organized into nine chapters as follows. Mohamed Gad-el-Hak provides in Chapters 1 and 2 a broad introduction to flow control and its classical as well as modern developments. Gad-el-Hak maintains that the recent developments in chaos control, microfabrication and neural networks will make feasible, for future practical devices, efficient reactive control of turbulent flows where a distributed control input is optimally adjusted based on feedforward or feedback spatio-temporal measurements. In Chapter 3, Ron F. Blackwelder details the eddy structures in the near-wall region of bounded turbulent shear flows as well as their relationship to the momentum transfer, mixing and drag. Blackwelder suggests that transitional flows can be used as a model for near-wall turbulent flows and describes different control scenarios utilizing suction and mechanical actuators. In the following chapter, Joël Delville, Laurent Cordier and Jean-Paul Bonnet illustrate the use of proper orthogonal decomposition for large-scale structure identification and control of turbulent shear flows. Pierre Perrier surveys the multiscale theoretical, experimental and practical aspects of active flow control in Chapter 5. In Chapter 6, Heinrich E. Fiedler discusses in great detail the principles, methods and possibilities of control of turbulent free-shear flows. Passive and active control of near-wall events in turbulent boundary layers, with particular emphasis on roughness effects and phase randomization techniques, are

covered in Chapter 7 by Andrew Pollard. In Chapter 8, Edward Haile, Olivier Delabroy, Daniel Durox, François Lacas and Sébastien Candel describe applications of active control to optimize combustion system operations, with particular emphasis on strategies for reducing NO_x and other pollutant emission levels. Troy Shinbrot covers in the last chapter the control of low- and high-dimensional chaotic dynamical systems, and the potential for extending such control strategies to turbulent flows.

Chih-Ming Ho of UCLA presented four lectures at the short course, dealing with the emerging field of microelectromechanical systems (MEMS) and their use for flow control. Unfortunately, a written version of Professor Ho's contribution was not available in time for this book. Interested readers may look forward to a forthcoming article by Ho and Tai in the 1998 issue of the *Annual Review of Fluid Mechanics.*

Hans Wolfgang Liepmann, my academic grandfather, wrote in a recent retrospective of the early days of research on boundary-layer transition (Applied Mechanics Reviews, vol. 50, no. 2, pp. R1–R4, 1997): *The importance of asking the right question is as obvious in principle as it is nebulous in research. Always present is the temptation to look for the key under the street light and not in the dark corner where it was lost. Indeed, in my opinion, much of the extensive turbulence research today follows this line and fails to address the real problems.* How true those words of wisdom are to the field of flow control and especially to the difficult task of taming turbulence. The editors of the present volume aspire for the right questions to be asked and for the answers to be sought even in the darkest corners.

The course/workshop organizers would like to acknowledge the financial support received from Aérospatiale, Centre d'Etudes Spatiales, CNRS and Ministère de la Défense, all of France, Queen's University at Kingston and the CFD Society of Canada, University of Notre Dame, U.S.A., and the European Community on Flow Turbulence and Combustion (ERCOFTAC).

Notre Dame, Indiana, USA
October 1997

Mohamed Gad-el-Hak

Contributors

Professor Ron F. Blackwelder
Dept. of Aerospace Engineering
University of Southern California
Los Angeles, CA 90089
U.S.A.
ron@spock.usc.edu

Dr. Jean-Paul Bonnet
Centre d'Etudes Aérod. & Thermiq.
Université de Poitiers
F-86036 Poitiers Cedex
France
bonnet@univ-poitiers.fr

Professeur Sébastien Candel
Laboratoire E.M2.C.
École Centrale Paris et C.N.R.S.
Grande Voie des Vignes
F-92295 Châtenay-Malabry Cedex
France
candel@em2c.ecp.fr

Dr. Laurent Cordier
Centre d'Etudes Aérod. & Thermiq.
Université de Poitiers
F-86036 Poitiers Cedex
France
cordier@univ-poitiers.fr

Dr. Olivier Delabroy
Laboratoire E.M2.C.
École Centrale Paris et C.N.R.S.
Grande Voie des Vignes
F-92295 Châtenay-Malabry Cedex
France
delabroy@em2c.ecp.fr

Dr. Joël Delville
Centre d'Etudes Aérod. & Thermiq.
Université de Poitiers
F-86036 Poitiers Cedex
France
delville@univ-poitiers.fr

Dr. Daniel Durox
Laboratoire E.M2.C.
École Centrale Paris et C.N.R.S.
Grande Voie des Vignes
F-92295 Châtenay-Malabry Cedex
France
durox@em2c.ecp.fr

Professor Heinrich E. Fiedler
Hermann-Föttinger-Institut
für Strömungsmechanik
Technische Universtität Berlin
D-10623 Berlin
Germany
hfiedler@pi.tu-berlin.de

Professor Mohamed Gad-el-Hak
Dept. of Aero. & Mech. Engineering
University of Notre Dame
Notre Dame, IN 46556
U.S.A.
Mohamed.Gad-el-Hak.1@nd.edu

Dr. Edward Haile
Laboratoire E.M2.C.
École Centrale Paris et C.N.R.S.
Grande Voie des Vignes
F-92295 Châtenay-Malabry Cedex
France
edward@em2c.ecp.fr

Dr. François Lacas
Laboratoire E.M2.C.
École Centrale Paris et C.N.R.S.
Grande Voie des Vignes
F-92295 Châtenay-Malabry Cedex
France
francois@em2c.ecp.fr

Dr. Pierre C. Perrier
Dept. Aérodynamique Théorique
Dassault Aviation
F-92210 Saint Cloud Cedex
France
perrier@dassault-aviation.fr

Professor Andrew Pollard
Dept. of Mechanical Engineering
Queen's University
Kingston, Ontario K7L 3N6
Canada
pollard@me.queensu.ca

Dr. Troy Shinbrot
Dept. of Chemical Engineering
Northwestern University
Evanston, IL 60208
U.S.A.
shinbrot@nwu.edu

Contents

1. **Introduction to Flow Control**
   Mohamed Gad-el-Hak 1

2. **Frontiers of Flow Control**
   Mohamed Gad-el-Hak 109

3. **Some Notes on Drag Reduction in the Near-Wall Region**
   Ron F. Blackwelder 155

4. **Large-Scale-Structure Identification and Control in Turbulent Shear Flows**
   Joël Delville, Laurent Cordier and Jean-Paul Bonnet 199

5. **Multiscale Active Flow Control**
   Pierre C. Perrier 275

6. **Control of Free Turbulent Shear Flows**
   Heinrich E. Fiedler 335

7. **Near-Wall Turbulence Control**
   Andrew Pollard 431

8. **Combustion Enhancement by Active Control**
   Edward Haile, Olivier Delabroy, Daniel Durox, François Lacas and Sébastien Candel 467

9. **Chaos, Coherence and Control**
   Troy Shinbrot 501

1 Introduction to Flow Control

Mohamed Gad-el-Hak

University of Notre Dame, Notre Dame, Indiana 46556, U.S.A.

Abstract. The subject of flow control is broadly introduced in this first chapter, leaving much of the details to the subsequent chapters of the book. The ability to actively or passively manipulate a flow field to effect a desired change is of immense technological importance, and this undoubtedly accounts for the fact that the subject is more hotly pursued by scientists and engineers than any other topic in fluid mechanics. In this chapter classical tools of flow control are emphasized, leaving the more modern strategies to the following chapter. Methods of control to achieve transition delay, separation postponement, lift enhancement, drag reduction, turbulence augmentation, or noise suppression are considered. The treatment is tutorial at times, making the material accessible to the advanced graduate student in the field of fluid mechanics. Emphasis is placed on external boundary-layer flows although applicability of some of the methods reviewed for internal flows will be mentioned. An attempt is made to present a unified view of the means by which different methods of control achieve a variety of end results. Performance penalties associated with a particular method such as cost, complexity, or trade-off will be elaborated.

1 What Is Flow Control

Before we get started it might be a good idea to explain what is meant by flow control. The topic as discussed in this book is not related to flowrate control via manual or automatic valves. Rather it is the attempt to favorably alter the character or disposition of a flow field that is of concern to us here. Many definitions for the topic exist, and some differentiate between flow control and flow management (e.g., Fiedler's article in this volume). My favorite definition was offered by Flatt in 1961 as applied to wall-bounded flows, but could easily be extended to free-shear flows. *Boundary layer control includes any mechanism or process through which the boundary layer of a fluid flow is caused to behave differently than it normally would were the flow developing naturally along a smooth straight surface.* Prandtl (1904) pioneered the modern use of flow control in his epoch-making presentation to the third International Congress of Mathematicians held at Heidelberg, Germany. In just 8 pages (as required for acceptance by the Congress) of a paper entitled "Über Flüssigkeitsbewegung bei sehr kleiner Reibung," Prandtl introduced the boundary layer theory, explained the mechanics of steady separation, opened the way for understanding the motion of real fluids, and described several experiments in which the boundary layer was controlled.

M. Gad-el-Hak et al.: LNPm 53, pp. 1 - 107, 1998
© Springer-Verlag Berlin Heidelberg 1998

Prandtl (1904) used active control of the boundary layer to show the great influence such a control exerted on the flow pattern. He used suction to delay boundary-layer separation from the surface of a cylinder. Notwithstanding Prandtl's success, aircraft designers in the three decades following his convincing demonstration were accepting lift and drag of airfoils as predestined characteristics with which no man could or should tamper (Lachmann, 1961). This predicament changed mostly due to the German research in boundary layer control pursued vigorously shortly before and during the Second World War. In the two decades following the war, extensive research on laminar flow control, where the boundary layer formed along the external surfaces of an aircraft is kept in the low-drag laminar state, was conducted in Europe and the United States, culminating in the successful flight test program of the X-21 where suction was used to delay transition on a swept wing up to a chord Reynolds number of 4.7×10^7. The oil crisis of the early 1970s brought renewed interest in novel methods of flow control to reduce skin-friction drag even in turbulent boundary layers. In the 1990s, the need for supermaneuverable fighter planes, faster and quieter underwater vehicles, and hypersonic transport (e.g., the U.S. National Aerospace Plane) provides new challenges for researchers in the field of flow control.

The major goal of this chapter is to broadly introduce the subject and to present a unified view of the different control methods to achieve a variety of end results. At times, the treatment of the subject matter is pedagogical and is designed to attract newcomers to the field. Emphasis is placed on external boundary-layer flows. The same vorticity considerations brilliantly employed by Lighthill (1963) to place the boundary layer correctly in the flow as a whole is used to explain many of the flow control techniques reviewed in here.

2 Five Eras of Flow Control

Flow control involves passive or active devices to effect a beneficial change in wall-bounded or free-shear flows. Whether the task is to delay/advance transition, to suppress/enhance turbulence or to prevent/provoke separation, useful end results include drag reduction, lift enhancement, mixing augmentation and flow-induced noise suppression. Broadly, there are perhaps five distinct eras in the development of the art and science of this challenging albeit very useful field of research and technology: The empirical era (prior to 1900); the scientific era (1900–1940); the World War II era (1940–1970); the energy crisis era (1970–1990); and the 1990s and beyond. The art of flow control probably has its roots in prehistoric times when streamlined spears, sickle-shaped boomerangs, and fin-stabilized arrows evolved empirically by archaic Homo sapiens. Modern man also artfully applied flow control methods to achieve certain technological goals. Relatively soon after the dawn of civilization and the establishment of an agriculture way of life 8,000 years

ago, complex systems of irrigation were built along inhabited river valleys to control the water flow, thus freeing man from the vagaries of the weather. For centuries, farmers knew the value of windbreaks to keep top soil in place and to protect fragile crops.

The science of flow control originated with Prandtl (1904), who introduced the boundary layer theory, explained the physics of the separation phenomena and described several experiments in which a boundary layer was controlled. Thus the birth of the scientific method to control a flow field. Slowly but surely, the choice of flow control devices is no longer a trial and error feat, but physical reasoning and even first principles are more often than not used for rational design of such artifacts.

Stimulated by the Second World War and the subsequent cold war, that trend accelerated significantly during the third era (1940–1970). Military needs of the superpowers dictated the development of fast, highly maneuverable, efficient aircraft, missiles, ships, submarines and torpedoes, and flow control played a major role in achieving these goals. Natural laminar flow, laminar flow control and polymer drag-reduction are notable achievements during this era. Partial summaries of flow control research during this period are contained within the books edited by Lachmann (1961) and Wells (1969).

The energy crises exemplified by the 1973 Arab oil embargo brought about a noticeable shift of interest from the military sector to the civilian one. During the period 1970–1990, government agencies and private corporations around the world but particularly in the industrialized countries invested valuable resources searching for methods to conserve energy, and hence drag reduction for civilian air, sea and land vehicles, for pipelines and for other industrial devices was emphasized. The availability of fast, inexpensive computers made it possible to simulate numerically complex flow situations that have not been approachable analytically. Some control strategies, for example transition-delaying compliant coatings (Gad-el-Hak, 1996a), were rationally optimized using computational fluid dynamics. Large-eddy breakup devices (LEBUs) and riblets are examples of control methods developed during this period to reduce skin-friction drag in turbulent boundary layers. Good sources of information on these and other devices introduced during the fourth era are the books edited by Hough (1980), Bushnell and Hefner (1990), and Barnwell and Hussaini (1992). Numerous meetings devoted to flow control, particularly drag reduction, were held during this period. Plentiful fuel supplies during the 1990s and the typical short memory of the long gas lines during 1973 have, unfortunately, somewhat dulled the urgency and enthusiasm for energy conservation research as well as practice.

For the 1990s and beyond, more complex reactive control devices, geared specifically towards manipulating the omnipresent coherent structures in transitional and turbulent shear flows (Cantwell, 1981; Robinson, 1991), are pursued by several researchers. Theoretical advances in chaos control and developments of microelectromechanical systems (MEMS) and neural net-

works should help such efforts. Papers specifically addressing reactive control strategies include those by Wilkinson (1990), Moin and Bewley (1994), and Gad-el-Hak (1994; 1996b). Reactive flow control is emphasized in the following chapter of this book. All five eras of flow control are seen from the perspective of the *history of the universe* depicted in Figure 1.

3 Governing Equations

There is no doubt that rational design, i.e. based on first principles, of flow control devices is always preferable than a trial and error approach. That of course is not always possible due to the extreme complexity of the equations involved, but one tries either analytically or, more commonly to date, numerically. The proper first principles for flow control are those for fluid mechanics itself. The principles of conservation of mass, momentum and energy govern all fluid motions. In general, a set of partial, nonlinear differential equations expresses these principles, and together with appropriate boundary and initial conditions constitute a well-posed problem. It is of course beyond the scope of this chapter to derive these equations and the reader is referred to any advanced textbook in Fluid Dynamics (Batchelor, 1967; Hinze, 1975; Landau and Lifshitz, 1987; Kays and Crawford, 1993; Panton, 1996). The equations are first recalled in as general a form as possible. This approach will become particularly useful when discussing high-speed flows, surface heating/cooling (viscosity varies spatially), drag-reducing polymers (non-Newtonian fluid), and other nonconventional situations. For a continuum fluid, the continuity equation, Newton's second law, and thermal energy equation read in Cartesian tensor notation

$$\frac{\partial \rho}{\partial t} + \frac{\partial}{\partial x_k}(\rho u_k) = 0 \tag{1}$$

$$\rho\left(\frac{\partial u_i}{\partial t} + u_k \frac{\partial u_i}{\partial x_k}\right) = \frac{\partial \Sigma_{ki}}{\partial x_k} + \rho g_i \tag{2}$$

$$\rho\left(\frac{\partial e}{\partial t} + u_k \frac{\partial e}{\partial x_k}\right) = -\frac{\partial q_k}{\partial x_k} + \Sigma_{ki}\frac{\partial u_i}{\partial x_k} \tag{3}$$

In the above equations, ρ is the density, u_i is an instantaneous velocity component (u, v, w), Σ_{ki} is the second-order stress tensor, g_i is the body force per unit mass, e is the internal energy per unit mass, and q_i is the heat flux vector. The independent variables are time t and the three spatial coordinates x_1, x_2 and x_3 or (x, y, z).

Absent any body couples, the stress tensor is symmetric having only six independent components, which leaves 14 unknowns in the five Equations (1)–(3). To close these equations, relation between the stress tensor and deformation rate, relation between the heat flux vector and the temperature

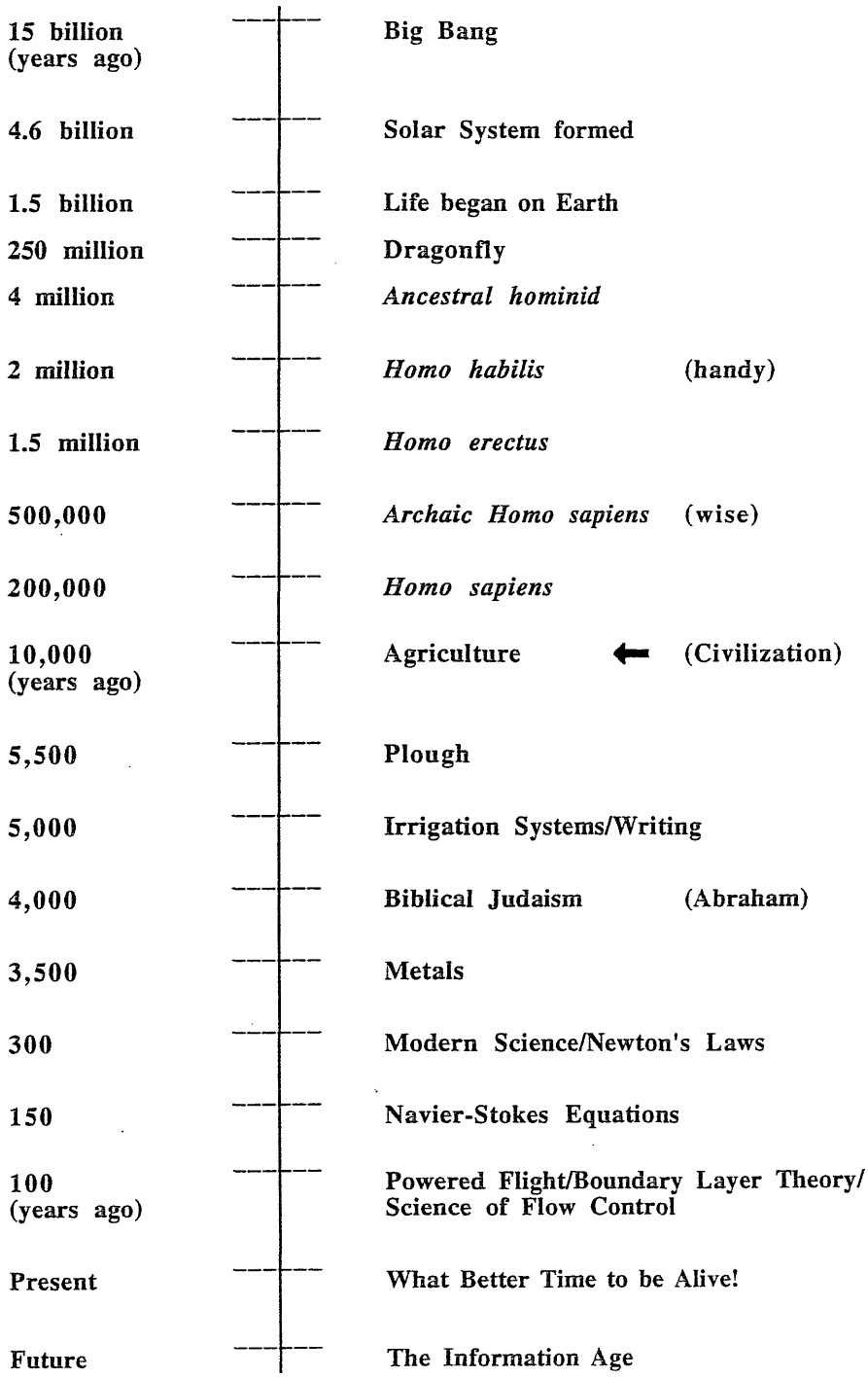

Fig. 1. History of the universe

field, and appropriate equations of state, relating the different thermodynamic properties, are needed. For a Newtonian, isotropic, Fourier,[1] ideal gas, for example, these relations read

$$\Sigma_{ki} = -p\,\delta_{ki} + \mu\left(\frac{\partial u_i}{\partial x_k} + \frac{\partial u_k}{\partial x_i}\right) + \lambda\left(\frac{\partial u_j}{\partial x_j}\right)\delta_{ki} \tag{4}$$

$$q_i = -\kappa\frac{\partial T}{\partial x_i} \tag{5}$$

$$\mathrm{d}e = c_v\,\mathrm{d}T \qquad \text{and} \qquad p = \rho\mathcal{R}T \tag{6}$$

where p is the thermodynamic pressure, μ and λ are the first and second coefficients of viscosity, respectively, δ_{ki} is the unit second-order tensor (Kronecker delta), κ is the thermal conductivity, T is the temperature field, c_v is the specific heat at constant volume, and $\mathcal{R}$ is the gas constant. The Stokes' hypothesis relates the first and second coefficients of viscosity, $\lambda + \frac{2}{3}\mu = 0$, although the validity of this assumption has occasionally been questioned (Gad-el-Hak, 1995). With the above constitutive relations, Equations (1)–(3) now read

$$\frac{\partial \rho}{\partial t} + \frac{\partial}{\partial x_k}(\rho u_k) = 0 \tag{7}$$

$$\rho\left(\frac{\partial u_i}{\partial t} + u_k\frac{\partial u_i}{\partial x_k}\right) = -\frac{\partial p}{\partial x_i} + \frac{\partial}{\partial x_k}\left[\mu\left(\frac{\partial u_i}{\partial x_k} + \frac{\partial u_k}{\partial x_i}\right) + \delta_{ki}\lambda\frac{\partial u_j}{\partial x_j}\right] + \rho g_i \tag{8}$$

$$\rho c_v\left(\frac{\partial T}{\partial t} + u_k\frac{\partial T}{\partial x_k}\right) = \frac{\partial}{\partial x_k}\left(\kappa\frac{\partial T}{\partial x_k}\right) - p\frac{\partial u_k}{\partial x_k} + \phi \tag{9}$$

where ϕ is the always positive dissipation function expressing the irreversible conversion of mechanical energy to internal energy as a result of the deformation of a fluid element. The viscous dissipation is given by

$$\phi = \frac{1}{2}\mu\left(\frac{\partial u_i}{\partial x_k} + \frac{\partial u_k}{\partial x_i}\right)^2 + \lambda\left(\frac{\partial u_j}{\partial x_j}\right)^2 \tag{10}$$

There are now six unknowns, ρ, u_i, p and T, and the five coupled Equations (7)–(9) plus the equation of state relating pressure, density and temperature. These six equations together with sufficient number of initial and boundary conditions constitute a well-posed, albeit formidable, problem.

[1] Newtonian implies a linear relation between the stress tensor and the symmetric part of the deformation tensor (rate of strain tensor). The isotropy assumption reduces the 81 constants of proportionality in that linear relation to two constants. Fourier fluid is that for which the heat flux vector is linearly related to the temperature gradient, and again isotropy implies that the constant in this relation is a single scalar.

Considerable simplification is achieved if the fluid is assumed incompressible, usually a reasonable assumption provided that the characteristic flow speed is less than 0.3 of the speed of sound. The (constant) density is assumed given and the governing equations for such fluid are

$$\frac{\partial u_k}{\partial x_k} = 0 \tag{11}$$

$$\rho\left(\frac{\partial u_i}{\partial t} + u_k \frac{\partial u_i}{\partial x_k}\right) = -\frac{\partial p}{\partial x_i} + \frac{\partial}{\partial x_k}\left[\mu\left(\frac{\partial u_i}{\partial x_k} + \frac{\partial u_k}{\partial x_i}\right)\right] + \rho g_i \tag{12}$$

$$\rho c_v\left(\frac{\partial T}{\partial t} + u_k \frac{\partial T}{\partial x_k}\right) = \frac{\partial}{\partial x_k}\left(\kappa \frac{\partial T}{\partial x_k}\right) + \phi^* \tag{13}$$

These are five equations for the five dependent variables u_i, p and T. Note that the system of equations (11)–(13) is coupled if either the viscosity or density depends on temperature, otherwise the energy equation is uncoupled from the continuity and momentum equations and can therefore be solved *after* the velocity and pressure fields are determined.

In nondimensional form, the incompressible flow equations read

$$\frac{\partial u_k}{\partial x_k} = 0 \tag{14}$$

$$\left(\frac{\partial u_i}{\partial t} + u_k \frac{\partial u_i}{\partial x_k}\right) = -\frac{\partial p}{\partial x_i} + \frac{\partial}{\partial x_k}\left[\frac{F_\nu(T)}{Re}\left(\frac{\partial u_i}{\partial x_k} + \frac{\partial u_k}{\partial x_i}\right)\right] + \frac{Gr}{Re^2} T\,\delta_{i3} \tag{15}$$

$$\left(\frac{\partial T}{\partial t} + u_k \frac{\partial T}{\partial x_k}\right) = \frac{\partial}{\partial x_k}\left(\frac{1}{Pe}\frac{\partial T}{\partial x_k}\right) + \frac{Ec}{Re} F_\nu(T)\,\phi^* \tag{16}$$

where $F_\nu(T)$ is a dimensionless function that characterizes the viscosity variation with temperature, and Re, Gr, Pe and Ec are, respectively, the Reynolds, Grashof, Péclet and Eckert numbers. These dimensionless parameters determine the relative importance of the different terms in the equations.

All the field equations recited thus far are valid at all points in space and time, and can be used for either laminar or turbulent flows. Three forms of the equations of motion are particularly useful to flow control; the x, y and z momentum equations written at the wall, the integral form of the differential equations, and, for turbulent flows, the ensemble average of the instantaneous equations. Those forms will be given in the next three subsections.

3.1 Equations of Motion at the Wall

In wall-bounded flows, the streamwise (x) and spanwise (z) momentum equations written at the wall give very useful expressions of the wall fluxes of, respectively, the spanwise and streamwise vorticity. For an incompressible fluid

over a non-moving wall, the streamwise, normal and spanwise momentum equations, written at $y = 0$, read

$$\rho v_{\rm w} \left.\frac{\partial u}{\partial y}\right|_{y=0} + \left.\frac{\partial p}{\partial x}\right|_{y=0} - \left.\frac{\partial \mu}{\partial y}\right|_{y=0} \left.\frac{\partial u}{\partial y}\right|_{y=0} = \mu \left.\frac{\partial^2 u}{\partial y^2}\right|_{y=0} \tag{17}$$

$$0 \quad + \quad \left.\frac{\partial p}{\partial y}\right|_{y=0} \quad - \quad 0 \quad = \mu \left.\frac{\partial^2 v}{\partial y^2}\right|_{y=0} \tag{18}$$

$$\rho v_{\rm w} \left.\frac{\partial w}{\partial y}\right|_{y=0} + \left.\frac{\partial p}{\partial z}\right|_{y=0} - \left.\frac{\partial \mu}{\partial y}\right|_{y=0} \left.\frac{\partial w}{\partial y}\right|_{y=0} = \mu \left.\frac{\partial^2 w}{\partial y^2}\right|_{y=0} \tag{19}$$

These equations are instantaneous and are valid for both laminar and turbulent flows. Here, $v_{\rm w}$ is the (positive) injection or (negative) suction velocity through the wall. Upward or downward motion of the wall act analogously to injection or suction. The right hand side of each of the three equations represents the curvature of the corresponding velocity profile, which in the case of the streamwise/spanwise equation is the same as the flux of spanwise/streamwise vorticity from the wall. Negative curvature implies that the velocity profile is fuller and that the wall is a source (positive flux) of vorticity. Whether the wall is a source or a sink of spanwise/streamwise vorticity, depends on whether fluid is sucked or injected from the wall, whether the streamwise/spanwise pressure gradient is favorable or adverse, and whether the wall viscosity is lower or higher than that above the surface. For a canonical turbulent flow, the instantaneous velocity profiles in all three directions change shape continuously as a result of the random changes in the pressure field.

3.2 The Kármán Integral Equation

The next useful equation results from integrating in the normal direction (from the wall to the edge of the shear layer) and combining the continuity and streamwise momentum equations. The result is known as the Kármán integral equation. For a two-dimensional (or axisymmetric) wall-bounded flow of a compressible fluid, this equation reads

$$\frac{C_f}{2} = \frac{1}{U_\infty^2} \frac{\partial}{\partial t} (U_\infty \delta^*) + \frac{\partial \delta_\theta}{\partial x} - \frac{\rho_{\rm w} v_{\rm w}}{\rho_\infty U_\infty} + \delta_\theta \left[\left(2 + \frac{\delta^*}{\delta_\theta} \right) \frac{1}{U_\infty} \frac{\partial U_\infty}{\partial x} + \frac{1}{\rho_\infty} \frac{\partial \rho_\infty}{\partial x} + \frac{1}{R} \frac{\partial R}{\partial x} \right] \tag{20}$$

Similar integral relations can be derived from the kinetic energy and thermal energy differential equations. In the momentum integral equation, the skin-friction coefficient, the displacement thickness and the momentum thickness are given by, respectively,

$$C_f \equiv \frac{\tau_{\rm w}}{\frac{1}{2} \rho_\infty U_\infty^2} \tag{21}$$

$$\delta^* \equiv \int_0^\infty \left(1 - \frac{\rho\, u}{\rho_\infty U_\infty}\right) \mathrm{d}y \tag{22}$$

$$\delta_\theta \equiv \int_0^\infty \frac{\rho\, u}{\rho_\infty U_\infty} \left(1 - \frac{u}{U_\infty}\right) \mathrm{d}y \tag{23}$$

Also, R is the transverse radius of curvature of the body of revolution (the corresponding term in Equation (20) drops for a two-dimensional flow), ρ_∞ and U_∞ are the density and velocity outside the boundary layer, respectively, ρ_w and v_w are the density and normal velocity of fluid injected (or sucked) through the surface, and τ_w is the shear stress at the wall.

Since the skin-friction coefficient in the momentum integral equation is defined in terms of the shear stress and not in terms of the velocity gradient at the wall, theKármán equation is, in fact, valid for both laminar and turbulent flows as well as for both Newtonian and non-Newtonian fluids; the only assumptions being made are that the flow is two-dimensional (or axisymmetric) in the mean. In case of a turbulent flow, the mean streamwise velocity, $\overline{U}(t, x, y)$ is used in the definition of δ^* and δ_θ. For a Newtonian fluid

$$\tau_\mathrm{w} = \mu \left.\frac{\partial u}{\partial y}\right|_{y=0} \tag{24}$$

3.3 Turbulent Flows

All the equations thus far are valid for nonturbulent as well as turbulent flows. However, in the latter case the dependent variables are in general random functions of space and time. No straightforward method exists for obtaining stochastic solutions of these nonlinear partial differential equations, and this is the primary reason why turbulence remains as the last great unsolved problem of classical physics. The recent attempts to use dynamical systems theory to study turbulent flows has not yet reached fruition especially at Reynolds numbers far above transition (Aubry et al., 1988), although advances in this theory have helped some with reducing and displaying the massive bulk of data resulting from numerical and experimental simulations (Sen, 1989). The brute-force numerical integration of the equations using the supercomputer is prohibitively expensive at practical Reynolds numbers. For the present at least, a statistical approach, where a temporal, spatial or ensemble average is defined and the equations of motion are written for the various moments of the fluctuations about this mean, is the only route available to get meaningful engineering results. Unfortunately, the nonlinearity of the Navier-Stokes equations guarantees that the process of averaging to obtain moments results in an open system of equations, where the number of unknowns is always greater than the number of equations, and more or less heuristic modeling is used to close the equations. This is known as the closure problem, and again makes obtaining first-principle solutions to the (averaged) equations of motion impossible.

To illustrate the closure problem, we consider the momentum equation for an incompressible fluid, Equation (12). As was first done by Osborne Reynolds over a century ago, all the field variables are decomposed into a mean and a fluctuation. Let $u_i = \overline{U}_i + u_i'$ and $p = \overline{P} + p'$, where $\overline{U}_i$ and $\overline{P}$ are ensemble averages for the velocity and pressure, respectively, and u_i' and p' are the velocity and pressure fluctuations about the respective averages. Note that temporal or spatial averages could be used in place of ensemble average if the flow field is stationary or homogeneous, respectively. In the former case, the time derivative of any statistical quantity vanishes. In the latter, averaged functions are independent of position. Substituting the decomposed pressure and velocity into (12), the equation governing the mean velocity for a Newtonian, incompressible, constant-viscosity, turbulent flow becomes

$$\rho\left(\frac{\partial \overline{U}_i}{\partial t} + \overline{U}_k \frac{\partial \overline{U}_i}{\partial x_k}\right) = -\frac{\partial \overline{P}}{\partial x_i} + \frac{\partial}{\partial x_k}\left(\mu \frac{\partial \overline{U}_i}{\partial x_k} - \rho \overline{u_i u_k}\right) + \rho \overline{g}_i \qquad (25)$$

This equation is written in a form that facilitates the physical interpretation of the turbulent stress tensor (Reynolds stresses), $-\rho \overline{u_i u_k}$, as additional stresses on a fluid element to be considered along with the conventional viscous stresses and pressure. An equation for the components of this tensor may be derived but it will contain third-order moments such as $\overline{u_i u_j u_k}$, and so on. The equations are closed by expressing the second- or third-order quantities in terms of the first- or second-moments, respectively. For a review of these first- and second-order closure schemes see Lumley (1983; 1987).

4 Unifying Principles

A particular control strategy is chosen based on the kind of flow and the control goal to be achieved. Flow control goals are strongly interrelated, and there are several different ways for classifying control strategies to achieve a desired effect. Presence or lack of walls, Reynolds and Mach numbers, and the character of the flow instabilities are all important considerations for the type of flow to be controlled. These issues are discussed in turn in the following five subsections.

4.1 Control Goals and Their Interrelation

Section 4.3 will contrast free-shear and wall-bounded flows. For the purposes of the present section, we focus on the latter particularly the technologically very important boundary layers. An external wall-bounded flow, such as that developing on the exterior surface of an aircraft or a submarine, can be manipulated to achieve transition delay, separation postponement, lift increase, skin-friction and pressure[2] drag reduction, turbulence augmentation,

[2] Pressure drag includes contributions from flow separation, displacement effects, induced drag, wave drag, and, for time-dependent flows, virtual mass.

heat transfer enhancement, or noise suppression. These objectives are not necessarily mutually exclusive. Figure 2 is a schematic representation of the interrelation between one control goal and another. To focus the discussion further, think of the flow developing on a lifting surface such as an aircraft wing. If the boundary layer becomes turbulent, its resistance to separation is enhanced and more lift could be obtained at increased incidence. On the other hand, the skin-friction drag for a laminar boundary layer can be as much as an order of magnitude less than that for a turbulent one. If transition is delayed, lower skin friction as well as lower flow-induced noise are achieved. However, the laminar boundary layer can only support very small adverse pressure gradient without separation and subsequent loss of lift and increase in form drag occur. Once the laminar boundary layer separates, a free-shear layer forms and for moderate Reynolds numbers transition to turbulence takes place. Increased entrainment of high-speed fluid due to the turbulent mixing may result in reattachment of the separated region and formation of a laminar separation bubble. At higher incidence, the bubble breaks down either separating completely or forming a longer bubble. In either case, the form drag increases and the lift-curve's slope decreases. The ultimate goal of all this is to improve the airfoil's performance by increasing the lift-to-drag ratio. However, induced drag is caused by the lift generated on a lifting surface with a finite span. Moreover, more lift is generated at higher incidence but form drag also increases at these angles.

All of the above points to potential conflicts as one tries to achieve a particular control goal only to adversely affect another goal. An ideal method of control that is simple, inexpensive to build and operate, and does not have any trade-off does not exist, and the skilled engineer has to make continuous compromises to achieve a particular design goal.

4.2 Classification Schemes

There are different classification schemes for flow control methods. One is to consider whether the technique is applied at the wall or away from it. Surface parameters that can influence the flow include roughness, shape, curvature, rigid-wall motion, compliance, temperature, and porosity. Heating and cooling of the surface can influence the flow via the resulting viscosity and density gradients. Mass transfer can take place through a porous wall or a wall with slots. Suction and injection of primary fluid can have significant effects on the flow field, influencing particularly the shape of the velocity profile near the wall and thus the boundary layer susceptibility to transition and separation. Different additives, such as polymers, surfactants, micro-bubbles, droplets, particles, dust or fibers, can also be injected through the surface in water or air wall-bounded flows. Control devices located away from the surface can also be beneficial. Large-eddy breakup devices (also called outer-layer devices, or OLDs), acoustic waves bombarding a shear layer from outside, additives

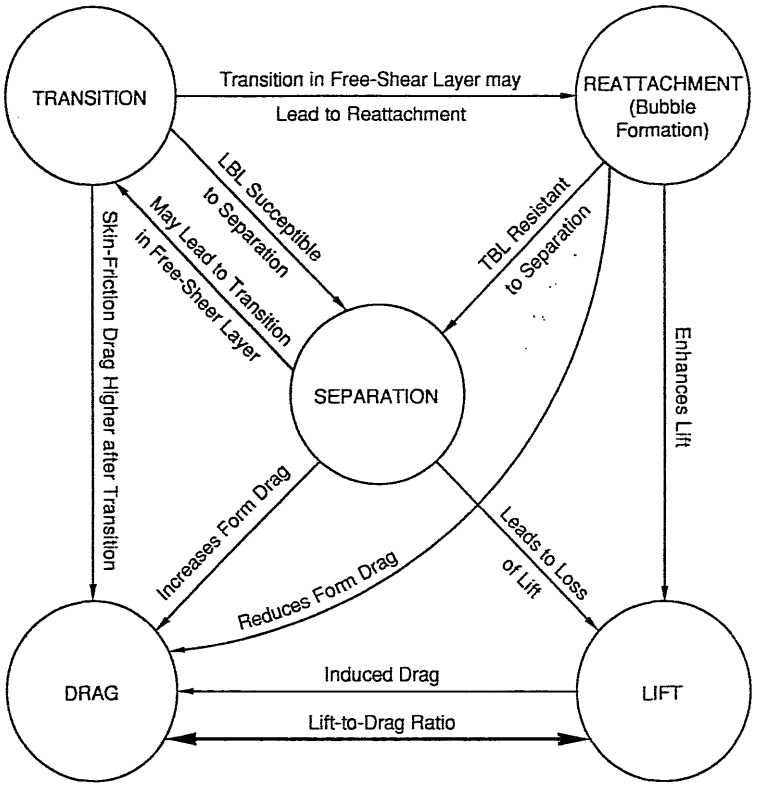

Fig. 2. Interrelation between flow control goals

introduced in the middle of a shear layer, manipulation of freestream turbulence levels and spectra, gust, and magneto- and electro-hydrodynamic body forces are examples of flow control strategies applied away from the wall.

A second scheme for classifying flow control methods considers energy expenditure and the control loop involved. As shown in the schematic in Figure 3, a control device can be passive, requiring no auxiliary power, or active, requiring energy expenditure. As for the action of passive devices, some prefer to use the term flow management rather than flow control (Fiedler and Fernholz, 1990), reserving the latter terminology for dynamic processes. Active control is further divided into predetermined or reactive. Predetermined control includes the application of steady or unsteady energy input without regard to the particular state of the flow. The control loop in this case is open as shown in Figure 4a, and no sensors are required. Reactive[3] control is a special class of active control where the control input is continuously

[3] Also termed by some interactive flow control. Reactive could be confused with chemically reacting flows, but is more proper linguistically to describe this particular control strategy.

adjusted based on measurements of some kind. The control loop in this case can either be an open, feedforward one (Figure 4b) or a closed, feedback loop (Figure 4c). Classical control theory deals, for the most part, with reactive control.

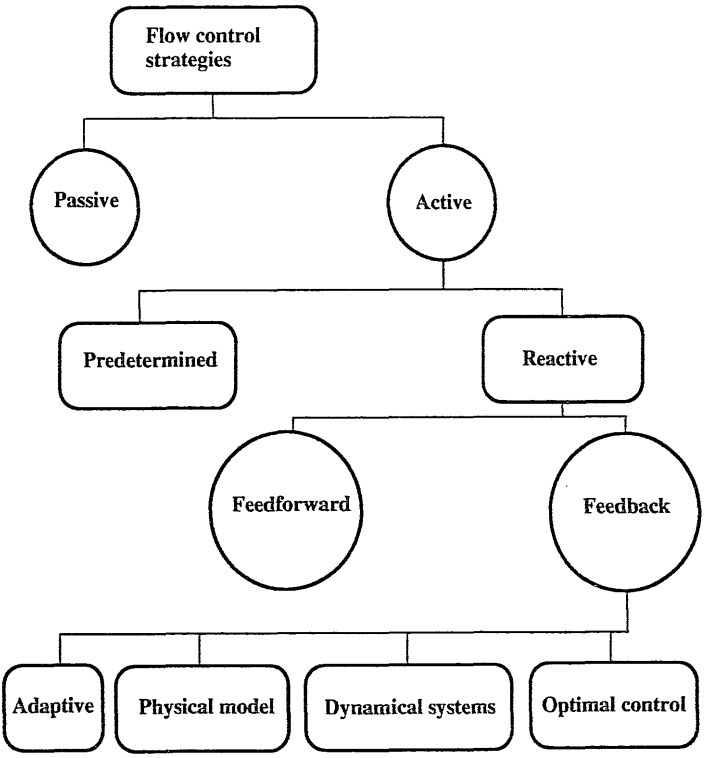

Fig. 3. Classification of flow control strategies

The distinction between feedforward and feedback is particularly important when dealing with the control of flow structures which convect over stationary sensors and actuators. In feedforward control, the measured variable and the controlled variable differ. For example, the pressure or velocity can be sensed at an upstream location, and the resulting signal is used together with an appropriate control law to trigger an actuator which in turn influences the velocity at a downstream position. Feedback control, on the other hand, necessitates that the controlled variable be measured, fed back and compared with a reference input. Reactive feedback control is further classified into four categories: Adaptive, physical model-based, dynamical systems-based, and optimal control (Moin and Bewley, 1994). We will return to these categories in the next chapter.

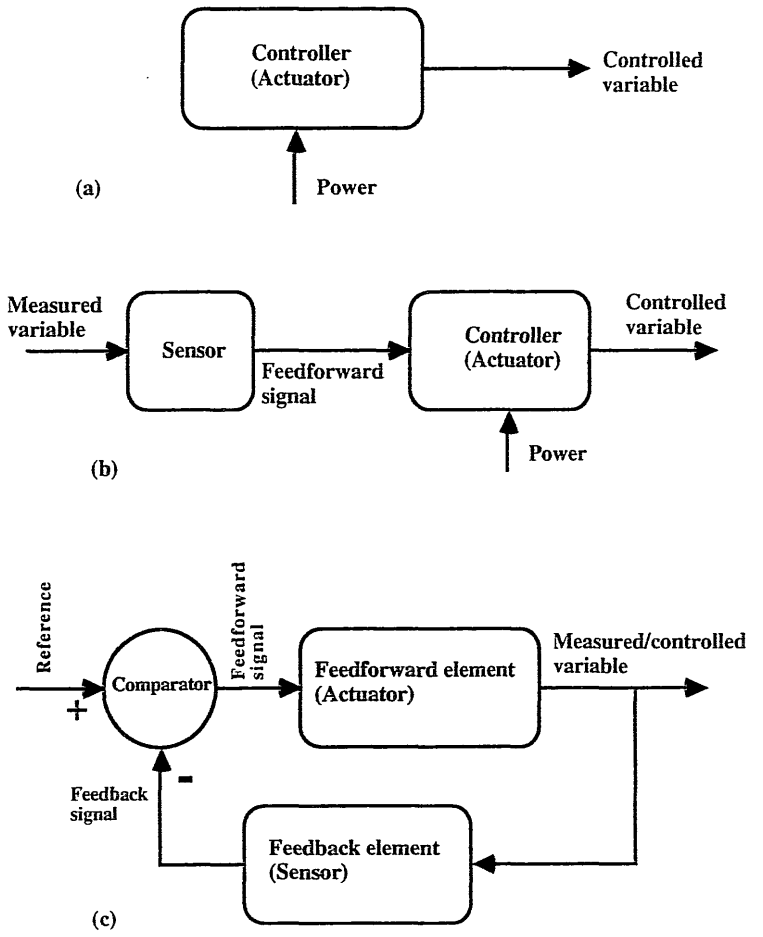

Fig. 4. Different control loops for active flow control

A yet another classification scheme is to consider whether the control technique directly modifies the shape of the instantaneous/mean velocity profile or selectively influence the small dissipative eddies. An inspection of the Navier-Stokes equations written at the surface (17)–(19), indicates that the spanwise and streamwise[4] vorticity fluxes at the wall can be changed, either instantaneously or in the mean, via wall motion/compliance, curvature, suction/injection, streamwise or spanwise pressure-gradient (respectively), or normal viscosity-gradient. These vorticity fluxes determine the fullness of the corresponding velocity profiles. For example, suction (or downward wall motion), favorable pressure-gradient or lower wall-viscosity results in vortic-

[4] Streamwise vorticity exists only if the velocity field is three-dimensional, instantaneously or in the mean.

ity flux away from the wall, making the surface a source of spanwise and streamwise vorticity. The corresponding fuller velocity profiles have negative curvature at the wall and are more resistant to transition and to separation but are associated with higher skin-friction drag. Conversely, an inflectional velocity profile can be produced by injection, adverse pressure-gradient or higher wall-viscosity. Such profile is more susceptible to transition and to separation and is associated with lower, even negative, skin friction. Note that many techniques are available to effect a wall viscosity-gradient; for example surface heating/cooling, film boiling, cavitation, sublimation, chemical reaction, wall injection of lower/higher viscosity fluid, and the presence of shear thinning/thickening additive.

Flow control devices can alternatively target certain scales of motion rather than globally changing the velocity profile. Polymers, riblets and LEBUs, for example, appear to selectively damp only the small dissipative eddies in turbulent wall-bounded flows. These eddies are responsible for the (instantaneous) inflectional profile and the secondary instability in the buffer zone, and their suppression leads to increased scales, a delay in the reduction of the velocity-profile slope, and consequent thickening of the wall region. In the buffer zone, the scales of the dissipative and energy containing eddies are roughly the same and, hence, the energy containing eddies will also be suppressed resulting in reduced Reynolds stress production, momentum transport and skin friction.

4.3 Free-Shear and Wall-Bounded Flows

Free-shear flows, such as jets, wakes or mixing layers, are characterized by inflectional mean-velocity profiles and are therefore susceptible to inviscid instabilities. Viscosity is only a damping influence in this case, and the prime instability mechanism is vortical induction. Control goals for such flows include transition delay/advancement, mixing enhancement and noise suppression. External and internal wall-bounded flows, such as boundary layers and channel flows, can too have inflectional velocity profiles, but, in the absence of adverse pressure-gradient and similar effects, are characterized by non-inflectional profiles and viscous instabilities are then to be considered. This kind of viscosity-dominated wall-bounded flows are intrinsically stable and therefore are generally more difficult to control. Free-shear flows and separated boundary layers, on the other hand, are intrinsically unstable and lend themselves more readily to manipulation.

Free-shear flows originate from some kind of surface upstream be it a nozzle, a moving body or a splitter plate, and flow control devices can therefore be placed on the corresponding walls albeit far from the fully-developed regions. Examples of such control include changing of the geometry of a jet exit from circular to elliptic (Gutmark and Ho, 1986), using periodic suction/injection in the lee side of a blunt body to affect its wake (Williams and Amato, 1989), and vibrating the splitter plate of a mixing layer (Fiedler

et al., 1988). These and other techniques are extensively reviewed by Fiedler and Fernholz (1990), who offer a comprehensive list of appropriate references, and more recently by Gutmark et al. (1995) and Viswanath (1995).

4.4 Regimes of Reynolds and Mach Numbers

Reynolds number determines whether the flow is laminar or turbulent. For low-to-moderate Reynolds numbers, the flow is laminar. Because of the nature of their instabilities, free-shear flows undergo transition at extremely low Reynolds numbers as compared to wall-bounded flows. Many techniques are available to delay laminar-to-turbulence transition for both kinds of flows, but none would do that to indefinitely high Reynolds numbers. Therefore, for Reynolds numbers beyond a reasonable limit, one should not attempt to prevent transition but rather deal with the ensuing turbulence. Of course early transition to turbulence can be advantageous in some circumstances, for example to achieve separation delay, enhanced mixing or augmented heat transfer. The task of advancing transition is generally simpler than trying to delay it.

Three Reynolds number regimes can be identified for the purpose of reducing skin friction in wall-bounded flows. First, if the flow is laminar, typically at Reynolds numbers based on distance from leading edge $< 10^6$, then methods of reducing the laminar shear stress are sought. These are usually velocity-profile modifiers, for example adverse-pressure gradient, injection, cooling (in water) and heating (in air), that reduce the fullness of the profile at the increased risk of premature transition and separation. Secondly, in the range of Reynolds numbers from 1×10^6 to 4×10^7, active and passive methods to delay transition as far back as possible are sought. These techniques can result in substantial savings and are broadly classified into two categories: stability modifiers and wave cancellation. The skin-friction coefficient in the laminar flat-plate can be as much as an order of magnitude less than that in the turbulent case. Note, however, that all the stability modifiers, such as favorable pressure-gradient, suction or heating (in liquids), result in an increase in the skin friction over the unmodified Blasius layer. The object is, of course, to keep this penalty below the potential saving; i.e., the net drag will be above that of the flat-plate laminar boundary-layer but presumably well below the viscous drag in the flat-plate turbulent flow. Thirdly, for $Re > 4 \times 10^7$, transition to turbulence cannot be delayed with any known practical method without incurring a penalty that exceeds the saving. The task is then to reduce the skin-friction coefficient in a turbulent boundary layer. Relaminarization (Narasimha and Sreenivasan, 1979) is an option, although achieving a net saving here is problematic at present.

Mach number determines whether the flow is incompressible ($Ma < 0.3$) or compressible ($Ma > 0.3$). The latter regime is further divided into subsonic ($Ma < 1$), transonic ($0.8 < Ma < 1.2$), supersonic ($Ma > 1$), and

hypersonic ($Ma > 5$). Each of those flow regimes lends itself to different optimum methods of control to achieve a given goal. Take laminar-to-turbulence transition control as an illustration (Bushnell, 1994). During transition, the field of initial disturbances is internalized via a process termed receptivity and the disturbances are subsequently amplified by various linear and nonlinear mechanisms. Assuming that by-pass mechanisms, such as roughness or high levels of freestream turbulence, are identified and circumvented, delaying transition then is reduced to controlling the variety of possible linear modes: Tollmien-Schlichting modes, Mack modes, crossflow instabilities and Görtler instabilities. Tollmien-Schlichting instabilities dominate the transition process for two-dimensional boundary layers having $Ma < 4$, and are damped by increasing the Mach number, by wall cooling (in gases), and by the presence of favorable pressure-gradient. Contrast this to the Mack modes which dominate for two-dimensional hypersonic flows. Mack instabilities are also damped by increasing the Mach number and by the presence of favorable pressure-gradient, but are destabilized by wall cooling. Crossflow and Görtler instabilities are caused by, respectively, the development of inflectional crossflow velocity profile and the presence of concave streamline curvature. Both of these instabilities are potentially harmful across the speed range, but are largely unaffected by Mach number and wall cooling. The crossflow modes are enhanced by favorable pressure-gradient, while the Görtler instabilities are insensitive. Suction suppresses, to different degrees, all the linear modes discussed in here.

4.5 Convective and Absolute Instabilities

In addition to grouping the different kinds of hydrodynamic instabilities as inviscid or viscous, one could also classify them as convective or absolute based on the linear response of the system to an initial localized impulse (Huerre and Monkewitz, 1990). A flow is convectively unstable if, at any fixed location, this response eventually decays in time. In other words, if all growing disturbances convect downstream from their source. Suppression of convective instabilities is particularly effective when applied near the point where the perturbations originate. If any of the growing disturbances has zero group velocity, the flow is absolutely unstable. This means that the local system response to an initial impulse grows in time. In this case, some of the growing disturbances can travel back upstream and continually disrupt the flow even after the initial disturbance is neutralized. Therefore, absolute instabilities are generally more dangerous and more difficult to control; nothing short of complete suppression will work. In some flows, for example two-dimensional blunt-body wakes, certain regions are absolutely unstable while others are convectively unstable.

5 Transition Delay

Delaying laminar-to-turbulence transition of a boundary layer has many obvious advantages. Depending on the Reynolds number, the skin-friction drag in the laminar state can be as much as an order of magnitude less than that in the turbulent condition (Figure 5). For an aircraft or an underwater body, the reduced drag means longer range, reduced fuel cost/volume, or increased speed. Flow-induced noise results from the pressure fluctuations in the turbulent boundary layer and, hence, is virtually nonexistent in the laminar case. Reducing the boundary layer noise is crucial to the proper operation of an underwater sonar. On the other hand, turbulence is an efficient mixer and rates of mass, momentum and heat transfer are much lower in the laminar state, so early transition may be sought in some applications as for example when enhanced heat transfer rates are desired or when rapid mixing is needed.

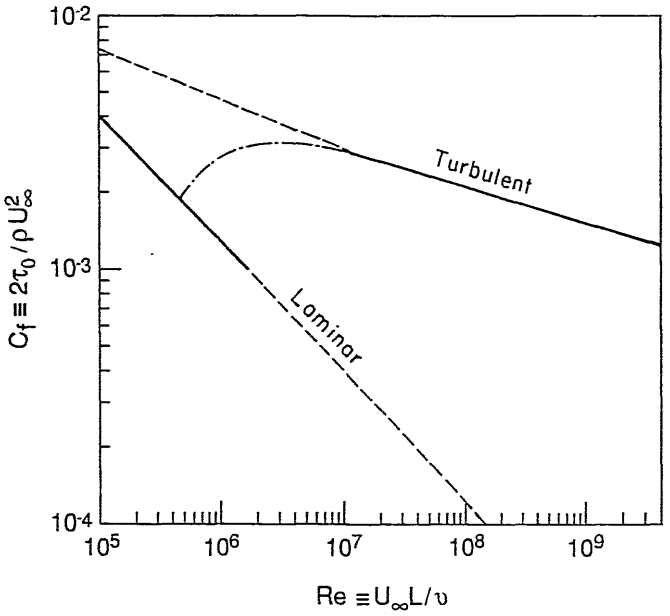

Fig. 5. Skin-friction coefficient for a smooth flat plate at zero incidence to uniform, incompressible flow

The routes to transition are many; some are more understood than others. On a semi-infinite, smooth flat plate placed in a clean, uniform, incompressible flow with as little external disturbances as possible, the laminar flow (somewhat downstream of the leading edge) is in the form of a Blasius profile and exists at low enough Reynolds number, typically $Re_x <$

6×10^4. This laminar shear layer is, however, unstable to small perturbations that invariably exist in any flow. Squire's (1933) theorem shows that two-dimensional traveling waves (Tollmien-Schlichting waves) are the most dangerous for incompressible-flow instability and become unstable when the Reynolds number exceeds a critical value. However, as soon as the T-S waves are amplified, gain a certain amplitude and nonlinear effects take place, three-dimensional disturbances can no longer be excluded (Itoh, 1987). Following the linear step, the originally two-dimensional waves inherently acquire a nearly periodic spanwise modulation and three-dimensional structures evolve as a result of a secondary instability. Hairpin vortices develop, perhaps due to a tertiary instability, and finally breakdown to turbulence occurs (Klebanoff et al., 1962). Not surprisingly, these nonlinear processes are far less understood than the linear step. The linear amplification step is, however, the slowest of the successive multiple steps in the transition process and, hence, factors that affect the linear amplification determine the magnitude of the transition Reynolds number.

Reshotko (1976; 1985; 1987) asserts that transition is a consequence of the nonlinear response of the laminar shear layer (a very complicated oscillator) to random forcing disturbances that result from freestream turbulence, radiated sound, surface roughness, surface vibrations, or combination of these environmental factors. If the initial disturbances are small, transition Reynolds number depends upon the nature and spectrum of these disturbances, their signature and excitation of the normal modes in the boundary layer (receptivity; see, for example, Morkovin, 1969; Goldstein and Hultgren, 1989), and the linear amplification of the growing normal modes. Once wave interaction and nonlinear processes set in, transition is quickly completed. If the initial disturbance levels are large enough, the relatively slow linear amplification step mentioned above is bypassed (Morkovin, 1984; 1988) and transition can occur at much lower Reynolds numbers. In fact, a sufficiently violent disturbance, $u_{\text{rms}}/U_\infty \sim 10\%$, can cause transition of a laminar boundary layer to advance to the position upstream of which perturbations of all wave numbers decay (Klebanoff et al., 1955).

Other routes to transition include the Taylor-Görtler vortices forming on a concave surface as a set of counter-rotating, streamwise standing eddies (Stuart, 1963; DiPrima and Swinney, 1985), the cross-flow instabilities occurring on a swept wing or a rotating disk (Reed and Saric, 1987; 1989), and any other situation where an instability will occur as a result of disturbing the equilibrium of body forces, inertia and surface forces (Drazin and Reid, 1981). Once again, these instabilities will generally occur at Reynolds numbers lower than the critical Reynolds number for the growth of Tollmien-Schlichting waves.

To delay transition to as far downstream position as possible, the following steps may be taken. First, since factors that affect the linear amplification of Tollmien-Schlichting waves determine the magnitude of the transition Reynolds number, these waves may be either inhibited or canceled. In the

former method of control, the growth of the linear disturbance is minimized using any or a combination of the so-called stability modifiers which alter the shape of the velocity profile. According to Equation (17), the stability modifiers include increased length of favorable pressure gradient, wall transpiration/wall motion, and surface heating/cooling. Wave cancellation of the growing perturbation is accomplished through exploiting but not altering the stability characteristics of the flow. Secondly, the forcing disturbances in the environment in which the laminar shear layer develops may be reduced. This is accomplished by using smooth surfaces, reducing the freestream turbulence and the radiated sound, minimizing body vibration, and ensuring a particulate-free incoming flow or, in case of a contaminated environment such as the ocean, using a particle-defense mechanism. Practically achieved surface smoothness and levels of radiated noise place an upper limit for unit Reynolds number required for a successful laminar flow control system. For aircraft, this typically translates into a requirement for high altitude operation (above 10 Km). Thirdly, one may provide a flow where other kind of instabilities, e.g., Taylor-Görtler vortices or cross-flow instabilities, will not occur or at least will not grow at a rapid rate. This is done by avoiding as much as possible concave surfaces or concave streamlines, minimizing the sweep on lifting surfaces, etc.

5.1 Stability Modifiers

Stability modifiers are those methods of laminar flow control which alter the shape of the velocity profile to minimize the linear growth of unstable waves. For a two-dimensional laminar boundary layer, vorticity is only in the spanwise direction and, within the boundary layer approximation, is given by $\omega_3 = -\partial u_1/\partial x_2$. The right-hand side of (17), therefore, represents the flux of vorticity at the surface, as demonstrated by Lighthill (1963). Any of the terms on the left-hand side of (17) can affect the sign of the second derivative of the velocity profile (or the direction of the vorticity flux) at the wall and, hence, the flow stability. Stability modifiers do just that and include wall suction (or downward wall motion), favorable pressure gradient, surface cooling in gases or surface heating in liquids. Any one or a combination of these methods will cause the curvature of the velocity profile at the wall to become more negative and, hence, increase the lower critical Reynolds number and reduce the spatial or the temporal amplification rates of unstable waves.

Boundary layers which are stabilized by extending the region of favorable pressure gradient are known as natural laminar flow (NLF), while the other methods to modify the stability of the shear flow are termed laminar flow control (LFC). It is clear from (17) that the effects of these methods are additive. The term hybrid laminar flow control normally refers to the combination of NLF and one of the LFC techniques.

Suction. An effective method for postponing transition is the application of wall suction. Small amounts of fluid withdrawn from the near-wall region of the boundary layer change the curvature of the velocity profile at the wall and can dramatically alter the stability characteristics of the boundary layer. Additionally, suction inhibits the growth of the boundary layer, so that the critical Reynolds number based on thickness may never be reached. Although laminar flow can be maintained to extremely high Reynolds number provided that enough fluid is sucked away, the goal is to accomplish transition delay with the minimum suction flow rate. Not only this will reduce the power necessary to drive the suction pump but also the momentum loss due to suction, and hence the skin friction, is minimized. This latter point can easily be seen from the momentum integral equation. Rewriting (20) for a steady, incompressible flow ($\rho = \rho_\infty = \text{constant}$) over a flat plate ($\mathrm{d}U_\infty/\mathrm{d}x = 0; \mathrm{d}R/\mathrm{d}x = 0$) with uniform suction through the wall (v_w negative), the equation reads

$$\frac{C_f}{2} = \frac{\mathrm{d}\delta_\theta}{\mathrm{d}x} + \frac{|v_\mathrm{w}|}{U_\infty} \tag{26}$$

The second term on the right-hand side is the suction coefficient, C_q, and although withdrawing the fluid through the wall leads to a decrease in the rate of growth of the momentum thickness, C_f increases directly with C_q. Fluid withdrawn through the wall has to come from outside the boundary layer where the streamwise momentum per unit mass is at the relatively high level of U_∞. The second term is proportional to the rate of momentum loss due to withdrawing a mass per unit time and area of $\rho|v_\mathrm{w}|$. Note that this term does not exist for pipe flows because of the mass flow constraint. Hence, this momentum penalty is not paid for channel flows with wall transpiration, an important distinction between internal and external flows.

Although Prandtl (1904) used suction to prevent flow separation from the surface of a cylinder near the beginning of this century, the first experimental demonstration that boundary-layer transition can be delayed by withdrawing near-wall fluid did not take place until about four decades later. Holstein (1940), Ackeret et al. (1941), Ras and Ackeret (1941), and Pfenninger (1946) used carefully shaped, single and multiple suction slits to demonstrate the decrease in drag associated with delaying transition. Braslow et al. (1951) used continuous suction through a porous wall to maintain laminar flow on an airfoil to chord Reynolds number of 2.0×10^7. Raspet (1952) conducted unique, noise-free experiments that confirmed the large decrease in drag when suction is applied through the wings of a sailplane. In the early 1960s, test flights of two X-21 aircrafts (modified U.S. Air Force B-66's) indicated the feasibility of maintaining a laminar flow on a swept wing to chord Reynolds number as high as 4.7×10^7 (Whites et al., 1966). The wing surfaces contained many thin and closely spaced spanwise suction slots, and the total airplane drag was reduced by 20% as compared to the no suction case.

Although discrete suction slots were used first, because of the unavailability of suitable porous surfaces in the early 1940s, the theoretical treatment

of the problem is considerably simplified by assuming continuous suction through a porous wall where the characteristic pore size is much smaller than a boundary layer thickness. In fact, the case of a uniform suction from a flat plate at zero incidence is an exact solution of the Navier-Stokes equation (12). Assuming weak enough suction that the potential flow outside the boundary layer is unaffected by the loss of mass at the wall (sink effects), the asymptotic velocity profile in the viscous region is exponential and has a negative curvature at the wall

$$u(y) = U_\infty \left[1 - \exp\left(-\frac{|v_w|\, y}{\nu}\right)\right] \tag{27}$$

The displacement thickness has the constant value $\delta^* = \nu/|v_w|$, where ν is the kinematic viscosity and $|v_w|$ is the absolute value of the normal velocity at the wall. In this case, (20) reads

$$C_f = 2\, C_q \tag{28}$$

Bussmann and Münz (1942) computed the critical Reynolds number for the above asymptotic velocity profile to be $Re_{\delta^*} \equiv U_\infty \delta^*/\nu = 70,000$. From the value of δ^* given above, the flow is stable to all small disturbances if $C_q \equiv |v_w|/U_\infty > 1.4 \times 10^{-5}$. The amplification rate of unstable disturbances for the asymptotic profile is an order of magnitude less than that for the Blasius boundary layer (Pretsch, 1942). This treatment ignores the development distance from the leading edge needed to reach the asymptotic state. When this is included into the computation, a higher C_q $\left(1.18 \times 10^{-4}\right)$ is required to ensure stability (Iglisch, 1944; Ulrich, 1944). Wuest (1961) presented a summary of transpiration boundary layer computations up to the early 1960s.

The more complicated analysis for the stability of a boundary layer with suction through discrete spanwise strips was only carried out satisfactorily relatively recently. Reed and Nayfeh (1986) conducted a numerical-perturbation analysis of a linearized, triple-deck, closed-form basic state of a flat plate boundary layer with suction through a finite number of spanwise porous strips. Their results were compared to interacting boundary layer calculations (Ragab and Nayfeh, 1980) as well as to the carefully conducted experiments of Reynolds and Saric (1986). Suction applied through discrete strips can be as effective as suction applied continuously over a much longer streamwise length. Reed and Nayfeh suggested a scheme for optimizing the strip configuration. Their results showed that suction should be concentrated nearer the leading edge (branch I of the neutral stability curve) when disturbances are still small in amplitude.

Suction may be applied through porous surfaces, perforated plates, or carefully machined slots. It is of course structurally impossible to make the whole surface of an aircraft's wing or the like out of porous material and

often strips of sintered bronze or steel are used. A relatively inexpensive woven stainless steel, Dynapore, is now available and provides some structural support (Reynolds and Saric, 1986). Superior surface smoothness and rigidity are obtained by drilling microholes in titanium using the recently developed electron-beam technology. The lower requirement for a pressure drop in the case of a perforated plate translates directly into pumping-power saving. However, outflow problems may result from regions of the wing having strong pressure gradients (Saric and Reed, 1986). Outflow in the aft region of a suction strip can cause large destabilizing effects and local three-dimensionality.

While structurally a surface with multiple slits is more rigid than a porous surface, slots are more expensive to fabricate accurately. Moreover, the higher mass flow rates associated with them may result in high Reynolds number instabilities such as separation and backflow, which adversely affect the stability of the basic flow. The rule of thumb is that the Reynolds number based on slot width (or hole diameter in the case of a perforated plate) and the local suction velocity should be kept below 10 to avoid adverse effects on the boundary layer stability, although Saric and Reed (1986) claim a hole Reynolds number an order of magnitude higher than that without destabilization of the basic flow.

Delaying transition using suction is a mature technology, where most of the remaining problems are in the maintainability and reliability of suction surfaces and the optimization of suction rate and distribution. To protect the delicate suction surfaces on the wing of an aircraft from insect impacts and ice formation at low altitudes, special leading edge systems are used (Wagner and Fischer, 1984; Wagner et al., 1984; 1988). Suction is less suited for underwater vehicles because of the abundance of suspended ocean particulate that can clog the suction surface as well as destabilize the boundary layer.

Shaping. The second method of control to delay laminar-to-turbulence transition is perhaps the simplest and involves the use of suitably shaped bodies to manipulate the pressure distribution. In (17), the pressure gradient term can affect the sign of the curvature of the velocity profile at the wall and, hence, change the stability characteristics of the boundary layer. According to the calculations of Schlichting and Ulrich (1940), the critical Reynolds number based on displacement thickness and freestream velocity changes from about 100 to 10,000 as a suitably nondimensionalized pressure gradient (the shape factor, Λ) varies from $\Lambda = -6$ (adverse) to $\Lambda = +6$ (favorable). Moreover, for the case of a favorable pressure gradient, no unstable waves exist at infinite Reynolds number. In contrast, the upper branch of the neutral stability curve in the case of an adverse pressure distribution tends to a non-zero asymptote so that a finite region of wavelengths at which disturbances are always amplified remains even as $Re \rightarrow \infty$.

Streamlining a body to prevent separation and reduce form drag is quite an old art, but the stabilization of a boundary layer by pushing the longitu-

dinal location of the pressure minimum to as far back as possible dates back to the 1930s and led to the successful development of the NACA 6-Series NLF airfoils. Newer, low-Reynolds-number lifting surfaces used in sailplanes, low-speed drones and executive business jets have their maximum thickness point far aft of the leading edge. The recent success of the Voyager's nine-day, unrefueled flight around the world was due in part to a wing design employing natural laminar flow to approximately 50% chord. Application of NLF technology to underwater vehicles is feasible but somewhat more limited (Granville, 1979).

The favorable pressure gradient extends to the longitudinal location of the pressure minimum. Beyond this point, the adverse pressure gradient becomes steeper and steeper as the peak suction is moved further aft. For an airfoil, the desired shift in the point of minimum pressure can only be attained in a certain narrow range of angles of incidence. Depending on the shape, angle of attack, Reynolds number, surface roughness and other factors, the boundary layer either becomes turbulent shortly after the point of minimum pressure or separates first and then undergoes transition. One of the design goals of NLF is to maintain attached flow in the adverse pressure gradient region and some method of separation control (Section 6) may have to be used there.

Factors that limit the utility of NLF include crossflow instabilities and leading edge contamination on swept wings, insect and other particulate debris, high unit Reynolds numbers at lower cruise altitudes, and performance degradation at higher angles of attack due to the necessarily small leading edge radius of NLF airfoils. Reductions of surface waviness and smoothness of modern production wings, special leading edge systems to prevent insect impacts and ice formation, higher cruise altitudes of newer airplanes, and higher Mach numbers all favor the application of NLF (Runyan and Steers, 1980). To paraphrase a recent statement by Holmes (1988), an NLF airfoil is no longer as finicky as Morris the Cat. It is true that a boundary layer that is kept laminar to extremely high Reynolds numbers is very sensitive to environmental factors such as roughness, freestream turbulence, radiated sound, etc. However, the flow is durable and reliable within certain conservative design corridors which must be maintained by the skillful designer and eventual operator of the vehicle. Current research concentrates on understanding the achievability and maintainability of natural laminar flow, expanding the practical applications of NLF technology, and extending the design methodology to supersonic aviation (Bushnell and Malik, 1988; Bushnell, 1989).

Wall Heating/Cooling. The last of the stability modifiers is the addition or removal of heat from a surface, which causes the viscosity to vary with distance from the wall. In general, viscosity increases with temperature for gases, while the opposite is true for liquids. Thus, if heat is removed from the surface of a body moving in air, the third term on the left-hand side of (17) is negative. In that case, the velocity gradient near the wall increases and

the velocity profile becomes fuller and more stable. The term containing the viscosity derivative will also be negative if the surface of a body moving in water is heated. With heating in water or cooling in air, the critical Reynolds number is increased, the range of amplified frequencies is diminished and the amplification rate of unstable waves is reduced. Substantial delay of transition is feasible with a surface that is only a few degrees hotter (in water) or colder (in air) than the freestream.

The first indirect evidence of this phenomenon was the observation that the drag of a flat plate placed in a wind tunnel increases by a large amount when the plate is heated (Linke, 1942). Both Frick and McCullough (1942) and Liepmann and Fila (1947) showed that the transition location of a flat-plate boundary layer in air at low subsonic speeds is moved forward as a result of surface heating. The stability calculations of Lees (1947) confirmed these experiments and, moreover, showed that cooling has the expected opposite effects. The critical Reynolds number based on distance from the leading edge increases from 10^5 to 10^7 when the wall of a flat plate placed in an air stream is cooled to 70% of the absolute ambient temperature. Even a modest cooling of the wall to $0.95T_\infty$ results in doubling of the critical Reynolds number (Kachanov et al., 1974). With cooling, the range of amplified frequencies is diminished and the growth rate of T-S waves is reduced resulting in a substantial increase in transition Reynolds number. These same trends were dramatically confirmed in subsonic and supersonic flights[5] by Dougherty and Fisher (1980) who studied the transition on an airborne cone over the Mach number range of 0.55–2.0. They reported a transition Reynolds number that varied approximately as T_w^{-7}, where T_w is the wall temperature. For aircraft, this method of transition delay is feasible only for a vehicle which uses a cryo-fuel such as liquid hydrogen or liquid methane. In that case, a sizable heat sink is readily available. The idea being that the fuel is used to cool the major aerodynamic surfaces of the aircraft as it flows from the fuel tanks to the engines. Reshotko (1979) examined the prospects for the method and concluded that, particularly for a hydrogen-fueled aircraft, substantial drag reductions are feasible. His engineering calculations indicated that the weight of the fuel saved is well in excess of the weight of the required cooling system.

The above effects are more pronounced in water flows due to the larger Prandtl number (good thermal coupling) and the stronger dependence of viscosity on temperature.[6] In a typical low-speed situation , a surface heating of 1°C in water has approximately the same effect on the curvature of the

[5] In hypersonic flows, a different mode of stability, Mack's Second Mode, dominates the transition process and cooling, in fact, promotes earlier transition to turbulence.

[6] For water at room temperature, $Pr \approx 7$ and absolute viscosity is decreased by approximately 2% for each 1°C rise in temperature. For room temperature air, $Pr \approx 0.7$ and absolute viscosity is decreased by approximately 0.2% for each 1°C drop in temperature.

velocity profile at the wall as a surface cooling of 20°C in air or a suction coefficient (in air or water) of 0.0003 (Liepmann et al., 1982). Wazzan et al. (1968;1970) used a modified fourth-order Orr-Sommerfeld equation combined with the e^9 method of Smith and Gamberoni (1956) and confirmed that wall heating can produce large increases in the transition Reynolds number of water boundary layers. They predicted a transition Reynolds number, based on freestream velocity and distance from the leading edge of a flat-plate, as high as 2×10^8 for wall temperatures that are only 40°C above the ambient water temperature.

Lowell and Reshotko (1974) refined Wazzan et al.'s (1968; 1970) calculations by introducing a coupled sixth-order system of vorticity and energy disturbance equations. The predicted critical Reynolds numbers for wall overheats of up to 2.8°C were confirmed by the experiments of Strazisar et al. (1977) who measured the growth rates of small disturbances generated by a vibrating ribbon in a heated flat-plate in water. These experiments did not yield data on transition or on stability at higher overheats. The transition predictions of Wazzan et al. (1968; 1970) at higher overheats were partially confirmed by the very carefully conducted experiments of Barker and Gile (1981) who used the entrance region of an electrically heated pipe. The displacement thickness was much smaller than the pipe radius and, thus, the boundary-layer development was approximately the same as that of a zero-pressure gradient flat-plate. Barker and Gile reported a transition Reynolds number of 4.7×10^7 for a wall overheat of 8°C. No further increase in $(Re|_{\text{transition}})$ was observed as the wall was heated further, in contradiction to the computations of Wazzan et al. (1968; 1970). Barker and Gile (1981) investigated possible causes of this discrepancy including buoyancy effects, wall roughness, effects of geometry, flow asymmetries, and suspended particulate matter. Their analysis and numerous related work (e.g., Kosecoff et al., 1976; Chen et al., 1979; Hendricks and Ladd, 1983; Lauchle and Gurney, 1984) indicate that increased concentration and size of suspended particulate diminish the stabilizing effect of surface heating until at some point surface heating no longer stabilizes the boundary layer but is in fact a destabilizing influence.

On a heated body of revolution in a high-speed water tunnel, Lauchle and Gurney (1984) observed an increase in transition Reynolds number from 4.5×10^6 to 3.6×10^7 for an average overheat of 25°C. Clearly, surface heating in water can be an extremely effective method of transition delay and, hence, drag reduction for small, high-speed underwater vehicles where the rejected heat from their propulsion system is used to increase the surface temperature along the body length. The detrimental effects of freestream particulate alluded to earlier are, however, a major obstacle at present for a practical implementation of this method of control. Suspended particulate having a wide-band concentration spectra are abundant in the oceans and "particle-defense" mechanisms must be sought before using any of the transition delay methods in a contaminated environment.

In addition to surface heating, several other techniques are available to lower the near-wall viscosity ($\partial\mu/\partial y > 0$) in a liquid boundary layer and, thus, favorably affect the stability of the flow. These include film boiling, cavitation, sublimation, chemical reaction, or wall injection of a gas or lower-viscosity liquid. Finally, a shear-thinning additive could be introduced into the boundary layer. Since the shear increases as the wall is approached, the effective viscosity of the non-Newtonian fluid decreases there and $(\partial\mu/\partial y)$ becomes positive.

5.2 Wave Cancellation

An alternative approach to increase the transition Reynolds number of a laminar boundary layer is wave cancellation. If the frequency, orientation and phase angle of the dominant element of the spectrum of growing linear disturbances in the boundary layer is detected, a control system and appropriately located disturbance generators may then be used to effect a desired cancellation or suppression of the detected disturbances. In this case, the stability characteristics of the boundary layer are exploited but not altered (Reshotko, 1985). Wave cancellation is feasible only when the disturbances are still relatively small, their growth is governed by a linear equation, and the principle of superposition is still valid.

The first reported use of wave cancellation is that due to Schilz (1965/66). He used a vibrating ribbon to excite a T-S wave on a test plate which had a flexible surface. A unique wall-motion device flush mounted into the plate moved the flexible wall in a transverse, wavelike manner with a variety of frequencies and phase speeds. A significant amount of cancellation resulted when the flexible wall motion had the opposite phase but the same frequency and phase speed as the T-S wave. Both Milling (1981) and Thomas (1983) used two vibrating wires, one downstream of the other, to generate and later cancel a single frequency T-S wave. Thomas (1983) observed that interaction between the primary disturbance and background excitations prevented complete cancellation of the primary wave. To further study the consequences of wave interactions, Thomas applied the same method of control to eliminate two interacting waves of different frequency. Although the primary waves were behaving linearly, a nonlinear interaction gave rise to a low-amplitude difference frequency that could only be partially reduced and ultimately led to transition. Thomas (1983) concluded that it is not possible to return the flow completely to its undisturbed base state because of wave interactions and that it is perhaps more appropriate to describe this control method as wave superposition rather than wave cancellation.

The same principle of wave superposition could be applied using wall heating/cooling (Liepmann et al., 1982; Liepmann and Nosenchuck, 1982; Ladd and Hendricks, 1988), plate vibration (Gedney, 1983), compliant wall (McMurray et al., 1983), or periodic suction/blowing (Biringen, 1984). Liepmann and Nosenchuck (1982) used flush-mounted hot-film probes to sense

natural T-S waves in a flat-plate boundary layer in a water tunnel. A feed-forward control loop was then used to synthesize and introduce disturbances of equal amplitude but of opposite phase via flush-mounted wall heaters. Ladd and Hendricks (1988) performed their experiment in a water tunnel on a 9:1 fineness-ratio ellipsoid. Strip heaters were again used to create and actively attenuate T-S waves. They applied digital filtering techniques to synthesize the attenuation signal. The filter was able to actively adapt the attenuation signal to changes in amplitude and frequency of the artificially introduced instability wave with no loss in attenuation downstream.

The transition delay achieved by active wave cancellation is modest, typically a factor of two or less increase in the transition Reynolds number based on distance from the leading edge. Reshotko (1985) maintains that to achieve significant delay in transition using this technique would require an extensive array of disturbance detectors and generators as well as prohibitively complicated control system that could cancel both the primary and residual disturbance spectra. Significant delay in transition is more readily achieved via the stability modifiers summarized in Section 5.1.

5.3 Compliant Coatings

Wall motion can be generated by either actively driving the surface or by using a flexible coating whose modulus of rigidity is low enough so that surface waves are generated under the influence of the stress field in the fluid. In the former case, the wall motion is precisely controlled and can be made to affect the shape of the velocity profile in a desired manner. This method of control is, however, quite impractical, at present at least, and is used mainly to provide controlled experiments to determine what type of wave motion is required to achieve a given result. The more practical passive flexible walls can be broadly classified into two categories: truly compliant coatings which have extremely small damping and modulus of elasticity and can therefore respond with little phase lag to the boundary layer flow; and the more readily available resonant walls in which vibration modes in the solid, acting as an active vibration damper, are excited by the flow-disturbance forcing function (Bushnell et al., 1977). The flow stabilization in this case may be a result of altering the phase relation in the viscous region rather than changing the curvature of the velocity profile at the wall.

Theoretical studies of boundary-layer stability in the presence of a flexible wall started in the early 1960s, stimulated in part by the pioneering experimental work of Kramer (1960). In both the classical work (e.g., Benjamin, 1960; Landahl, 1962; Kaplan, 1964) and the more recent research (e.g., Carpenter and Garrad, 1985; Willis, 1986; Yeo and Dowling, 1987), steady-state stability theory has been used with an assumed velocity profile which is not allowed to change as the wall moves. It is clear, however, that the wall displacement will induce a traveling pressure signal which in turn will modulate the mean velocity profile. Either a quasi-steady stability analysis

of the modulated flow or a true time-dependent calculations would be preferable to conventional linear-stability theory, but neither has been attempted yet due to the obvious complexities of the problem. Notwithstanding the shortcoming of present stability calculations, Willis (1986) obtained a very impressive agreement with the careful experiments conducted by Michael Gaster. Eigenvalue calculations were performed to predict the amplification factors for a range of modal frequencies. The flexible coating was a silicon-rubber/silicon-oil mix covered by a thin latex rubber skin stretched across the surface. The experiments were conducted in a water towing tank using a flat plate, and controlled, harmonic, two-dimensional disturbances were introduced upstream of the compliant surface. A reduction of the wave growth by an order of magnitude is feasible when this rather simple coating is used, almost eliminating transition due to Tollmien-Schlichting type of instability. The flexible wall itself is, however, susceptible to other kinds of instability and care must be taken to ensure that these surface waves will not grow to an amplitude that will promote transition through a roughness-like effect (see the recent review articles by Riley et al., 1988, and Gad-el-Hak, 1996a).

Although the original Kramer's (1960) experiments were discredited up until a few years ago, new theoretical and experimental evidence confirm Kramer's results (Carpenter and Garrad, 1985). Passive flexible coatings with density the order of the fluid density appear to be capable of considerable transition postponement. The density requirement makes this method of control suitable for water applications only. Transitional Reynolds numbers (based on distance from the leading edge) that are 5–10 times those for a rigid surface seem to be readily achievable with a simple method that does not require energy expenditure, slots, ducts, or internal equipment of any kind.

6 Separation Control

6.1 Steady Separation

Separation of a steady, two-dimensional boundary layer was explained first by Prandtl (1904) in his milestone presentation cited earlier "On the Motion of a Fluid with Very Small Viscosity (translated)," in which he introduced the Boundary-Layer Theory. Fluid particles near the surface are retarded by the friction of the wall and by any adverse pressure gradient present in the freestream. If the near-wall fluid has insufficient momentum for it to continue its motion, it will be brought to rest at the separation point (line). Further downstream, the adverse pressure forces will cause reverse flow. Since the velocity at the wall is always zero, the gradient $[\partial u/\partial y]_{y=0}$ must be positive upstream of separation, zero at the point of separation, and negative in the reverse flow region. For an axially symmetric flow, the line of separation becomes a circle, and the point of vanishing shear still coincides with the point of separation.

In Prandtl's view, the separation point is entirely determined by external conditions. Boundary-layer separation is accompanied by a thickening of the rotational flow region and ejection of vorticity. Downstream of the separation point the shear layer either passes over the region of recirculating fluid and reattaches to the body surface or forms a wake and never reattaches to the body. The characteristic dimension of the recirculating region is quite large in the latter case and is of the order of the body height.

Analytically, the solution of the steady, two-dimensional, laminar boundary-layer equations with a prescribed external-pressure (or external-velocity) distribution breaks down at the point of separation, and this is commonly known as the Goldstein's singularity. The singularity of the boundary-layer equations at separation is obviously not a physical property of the flow and can be overcome by prescribing either the displacement thickness or the wall shear distribution instead of the external pressure. This kind of analysis is termed inverse calculation.

6.2 Unsteady Separation

For two-dimensional flow over moving walls, two-dimensional unsteady flows, and three-dimensional steady and unsteady flows, the point (line) of vanishing wall shear does not necessarily coincide with separation, and this greatly complicates the problem. This was first observed by Rott (1956) while analyzing the unsteady flow in the vicinity of a stagnation point. He observed that, while the wall shear vanished with an accompanying reverse flow, there was no singularity or breakdown of the boundary-layer assumptions. In seeking a generalized model for separation, Sears (1956) postulated that the unsteady separation point is characterized by the simultaneous vanishing of the shear and the velocity at a point within the boundary later as seen by an observer moving with the velocity of the separation point .

Moore (1958), while investigating a steady flow over a moving wall, arrived at the same model for unsteady separation. Based on an intuitive relationship between steady flow over a moving wall and unsteady flow over a fixed wall, Moore was able to sketch the expected velocity profiles for both cases as seen in Figures 6 and 7. He considered the possibility that a Goldstein-type singularity occurs at the location where the velocity profile has simultaneously zero velocity and shear at a point above the moving wall. Equivalently, for unsteady separation on a fixed wall, the separation point is the location at which both the shear and velocity vanish in a singular fashion in a frame of reference moving with the separation point. The main drawback of this Moore-Rott-Sears (MRS) model in the fixed wall case is that the speed of the separation point is not known *a priori*, making it difficult to locate this point and forcing researchers to rely on more qualitative measures for unsteady separation. Sears and Telionis (1972; 1975) were the first to prove that the boundary-layer separation singularity accompanies detachment of unsteady flows. They suggested that the existence of such singularity could serve as a

criterion for unsteady separation when integrating numerically the boundary-layer equations.

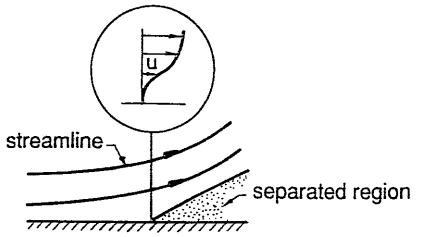

a. Fixed wall.

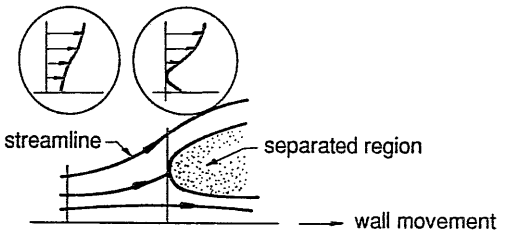

b. Wall moving downstream.

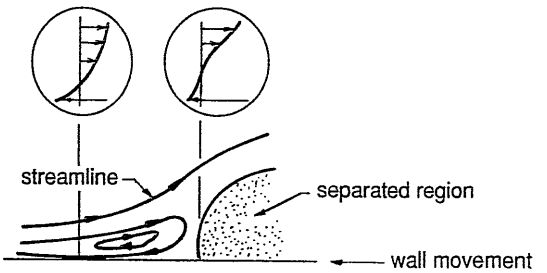

c. Wall moving upstream.

Fig. 6. Streamlines and velocity profiles when a boundary layer over a fixed or moving wall separates

Because of the above difficulty, early attempts to verify this important Moore-Rott-Sears model of unsteady separation considered the more tractable problem of steady separation over moving walls. Both Vidal (1959) and Ludwig (1964) investigated experimentally a shrouded rotating cylinder in steady flow. As expected, separation was delayed (moved downstream) when the wall moved in the freestream direction and was advanced when the wall moved opposite the main flow. The measured velocity profiles corresponded to those hypothesized by Moore (1958). Telionis and Werle (1973) presented an an-

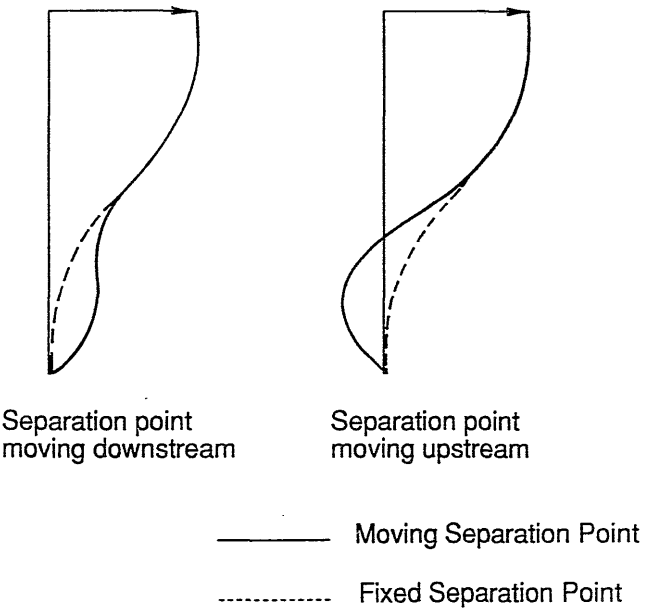

Fig. 7. Moor's (1958) postulated velocity profiles for unsteady separation on a fixed wall

alytical verification of the separation model for the case of a downstream moving wall.

Until the work of Williams and Johnson (1974a; 1974b), the relationship between unsteady boundary-layer separation over fixed walls and steady separation over moving walls has been an intuitive one. By considering the rather general class of unsteady, two-dimensional boundary-layer problems which could be treated by the method of semi-similar solutions, Williams and Johnson (1974a) were able to transform an unsteady problem in three independent variables into an equivalent problem in two independent variables. This transformation made it then possible to use conventional numerical techniques for solving steady, nonsimilar boundary-layer problems, and allowed the authors to investigate some time-dependent flows where separation occurs in a coordinate system for which unsteady separation is most easily identified and analyzed. As a practical example, Williams and Johnson (1974a) verified the MRS model for unsteady separation for a particular time-dependent retarded flow the steady flow equivalent of which is the classical linearly retarded flow studied by Howarth (1938).

In a subsequent paper, Williams and Johnson (1974b) established a rigorous analytical link between unsteady separation over a fixed wall and steady separation over a moving wall for the special case in which the external velocity distribution in the fixed coordinate system is a function only of a linear

combination of the streamwise coordinate and time and where the wall moves downstream with the (constant) speed of the unsteady separation point. Once more, Williams and Johnson were able to transform a given unsteady flow into a steady flow over a wall moving with the speed of the separation point and then to relate this back to the unsteady flow.

6.3 Velocity Profile Modifiers

As mentioned, Prandtl (1904) was the first to explain the mechanics of separation. He provided a precise criterion for its onset for the case of a steady, two-dimensional boundary layer developing over a fixed wall. If such a flow is retarded, the near-wall fluid may have insufficient momentum to continue its motion and will be brought to rest at the point of separation. Fluid particles behind this point move in a direction opposite to the external stream and the original boundary-layer fluid passes over a region of recirculating flow. Since the velocity at the wall is always zero, the gradient $[\partial u/\partial y]_{y=0}$ will be positive upstream of separation, zero at the point of separation, and negative in the reverse flow region. The velocity profile at separation must then have a positive curvature at the wall. However, $[\partial^2 u/\partial y^2]$ is negative at a large distance from the wall, which means the velocity profile at separation must have a point of inflection somewhere above the wall. Since $[\partial^2 u/\partial y^2]_0 > 0$ is a necessary condition for a steady, two-dimensional boundary layer to separate, the opposite, i.e. a negative curvature of the velocity profile at the wall, must be a sufficient condition for the boundary-layer flow to remain attached.

The above arguments naturally lead to several possible methods of control to delay (or advance) steady, two-dimensional separation that rely on modifying the shape of the velocity profile near the wall. Namely, the object is to keep $[\partial^2 u/\partial y^2]_0$ as negative as possible, or in other words to make the velocity profile as full as possible. In this case, the magnitude of the spanwise vorticity decreases monotonically away from the wall and the surface vorticity flux is in the positive y direction. Not surprisingly, then, methods of control to postpone separation that rely on changing the velocity profile are similar to those used to delay laminar-to-turbulence transition. For example, beyond the point of minimum pressure on a streamlined body the pressure gradient is adverse and the boundary layer will separate if the pressure rise is sufficiently steep; however, enough suction may be applied there to overcome the retarding effects of the adverse pressure gradient and to prevent separation.

Shaping. For any two-dimensional, subsonic flow over a closed-surface body, adverse pressure gradient always occurs somewhere in the aft region. Streamlining can greatly reduce the steepness of the pressure rise, leading to the prevention or postponement of separation. Numerous biological species are endowed with body shapes that avoid separation and allow for minimum fluid

resistance to their motion in air or water. Archaic Homo sapiens discovered, through scores of trials and errors, the value of streamlining spears, sickle-shaped boomerangs, and fin-stabilized arrows (Williams, 1987). In supersonic flows, pressure always rises across a shock wave and a boundary layer may separate as a result of the wave interaction with the viscous flow (Young, 1953; Lange, 1954).

Laminar boundary layers can only support very small adverse pressure gradients without separation. In fact, if the ambient incompressible fluid decelerates in the streamwise direction faster than $U_\infty \sim x^{-0.09}$, the flow separates (Schlichting, 1979). On the other hand, a turbulent boundary layer, being an excellent momentum *conductor*, is capable of overcoming much larger adverse pressure gradients without separation. In this case, separation is avoided for external flow deceleration up to $U_\infty \sim x^{-0.23}$ (Schlichting, 1979). The efficient momentum transport that characterizes turbulent flows provides the mechanism for mixing the slower fluid near the wall with the faster fluid particles further out. The forward movement of the boundary-layer fluid against pressure and viscous forces is facilitated and separation is, thus, postponed. According to the experimental results of Schubauer and Spangenberg (1960), a larger total pressure increase without separation is possible in the turbulent case by having larger adverse pressure gradient in the beginning and continuing at a progressively reduced rate of increase.

To expand the attached flow operational envelope to off-design conditions using the concept of pressure gradient mitigation generally requires some form of variable geometry such as vanes, slats, or flaps. These can be combined with other separation control techniques such as active or passive blowing, rotating cylinder at the flap knee, or use of an injection-stabilized trapped vortex. For low-speed flows, bodies can now be designed for incipiently separated flow over large surface areas using the so-called Stratford closure (Smith, 1977; Smith et al., 1981). While minimizing skin friction drag, this approach exacerbates the attached-flow, viscous-induced form drag, and the minimum drag body is actually a less extreme design. Also, such bodies tend to generate large separated flow regions off-design, and therefore some form of standby flow separation control would probably be required to ensure reasonable off-design performance.

Zero Skin Friction. The skin friction downstream of the separation line is negative. However, the increase in pressure drag that results from flow detachment is far greater than the saving in skin-friction drag. The papers by Stratford (1959a; 1959b) provide useful discussion on the prediction of turbulent-boundary-layer separation and the concept of flow with continuously zero skin-friction throughout its region of pressure rise. By specifying that the turbulent boundary layer be just at the condition of separation, without actually separating, at all positions in the pressure rise region, Stratford (1959b) experimentally verified that such flows achieve a specified pressure

rise in the shortest possible distance and with the least possible dissipation of energy. A lifting surface which could utilize the Stratford's distribution immediately after transition from laminar to turbulent flow would be expected to have very low skin friction as well as pressure drag. Liebeck (1978) successfully followed this strategy using a highly polished wing to achieve the best lift-to-drag ratio (over 200) of any airfoil tested in the low-Reynolds-number range of 5×10^5–2×10^6. He argued that the entire pressure-recovery region of an airfoil's upper surface would be operating at its maximum capacity if the adverse pressure distribution was uniformly critically close to separation. By assuming an incipient-separation turbulent profile, Liebeck calculated the pressure field required then used an inverse calculation procedure to derive the airfoil shape from the given critical-velocity distribution.

When attempting to reduce skin-friction drag by driving the boundary layer towards separation, a major concern is the flow behavior at off-design conditions. A slight increase in angle of attack for example can lead to separation and consequent large drag increase as well as loss of lift. High performance airfoils with lift-to-drag ratio of over 100 utilize carefully controlled adverse pressure gradient to retard the near-wall fluid, but their performance deteriorates rapidly outside a narrow envelope (Carmichael, 1974).

Separation Bubbles. Laminar-to-turbulence transition on the upper surface of a lifting surface typically occurs at the first onset of adverse pressure gradient if the Reynolds number exceeds 10^6. The separation-resistant turbulent boundary layer that evolves in the pressure recovery region results in higher maximum lift and a relatively larger angle of stall. At lower Reynolds numbers and depending on the severity of the initial adverse gradient (hence on the airfoil shape), laminar separation may take place prior to transition. For sufficiently low Re, the separated flow will not reattach to the surface. However, in the intermediate Reynolds number range of typically 10^4–10^6, transition to turbulence takes place in the free-shear layer due to its increased susceptibility. Subsequent turbulent entertainment of high-speed fluid causes the flow to return to the surface, thus forming what is known as a laminar separation bubble. Regardless of whether or not the flow subsequently reattaches, the laminar separation leads to higher form drag and lower maximum lift. Delicate contouring of the airfoil near the minimum pressure point to lessen the severity of the adverse pressure gradient may be used to accomplish separation-free transition (Pfenninger and Vemuru, 1990).

Transpiration. The second method to avert separation by changing the curvature of the velocity profile at the wall involves withdrawing the near-wall fluid through slots or porous surfaces. Prandtl (1904) applied suction through a spanwise slit on one side of a circular cylinder. His flow visualization photographs convincingly showed that the boundary layer adhered to the suction side of the cylinder over a considerably larger portion of its surface. By re-

moving the decelerated fluid particles in the near-wall region, the velocity gradient at the wall is increased, the curvature of the velocity profile near the surface becomes more negative, and separation is avoided. In the following, an approximate method to compute the amount of suction needed to prevent laminar separation is briefly recalled (Prandtl, 1935).

For a laminar boundary layer, the ratio of pressure forces to viscous forces is proportional to the shape factor, Λ,

$$\Lambda = \frac{\delta^2}{\nu}\frac{\mathrm{d}U_\infty}{\mathrm{d}x} = -\frac{\mathrm{d}p_\infty}{\mathrm{d}x}\frac{\delta^2}{\mu U_\infty} \tag{29}$$

where δ is the boundary layer thickness, U_∞ is the velocity outside the boundary layer, ν is the kinematic viscosity, μ is the dynamic viscosity, and $(\mathrm{d}p_\infty/\mathrm{d}x)$ is the pressure gradient in the streamwise direction. At separation, $[\partial u/\partial y]_0 = 0$ and Equation (17) reads

$$\frac{\mathrm{d}p_\infty}{\mathrm{d}x} = \mu\left[\frac{\partial^2 u}{\partial y^2}\right]_0 \tag{30}$$

The shape factor at the point of separation of a laminar boundary layer is $\Lambda = -12$, and from Equations (29) and (30) the expressions for the curvature of the velocity profile at the wall and the boundary-layer thickness become, respectively

$$\left[\frac{\partial^2 u}{\partial y^2}\right]_0 = \frac{12\,U_\infty}{\delta^2} \tag{31}$$

$$\delta = \sqrt{\frac{-12\,\nu}{(\mathrm{d}U_\infty/\mathrm{d}x)}} \tag{32}$$

The velocity distribution, $(\mathrm{d}U_\infty/\mathrm{d}x)$, is determined from the potential flow solution. As an example, suppose we wish to compute the suction coefficient, $C_q \equiv (|v_\mathrm{w}|/U_\infty)$, which is just sufficient to prevent laminar separation from the surface of a cylinder. By assuming that the velocity profiles in the vicinity of separation are identical with that at the point of separation and computing $\mathrm{d}U_\infty/\mathrm{d}x$ at the downstream stagnation point, Prandtl (1935) used the momentum integral equation, (20), and the above results to make a simple estimate of the required suction

$$C_q = 4.36\,Re^{-0.5} \tag{33}$$

where Re is the Reynolds number based on the cylinder diameter and the freestream velocity.

Several researchers have used similar approximate methods to calculate the laminar boundary layer on a body of arbitrary shape with arbitrary suction distribution (see, e.g., Schlichting and Pechau, 1959; Chang, 1970). A particularly simple calculation is due to Truckenbrodt (1956). He reduces the

problem to solving a first-order ordinary differential equation. As an example, for a symmetrical Zhukovskii airfoil with uniform suction, Truckenbrodt predicts a suction coefficient just sufficient to prevent separation of

$$C_q = 1.12\,Re^{-0.5} \tag{34}$$

where Re is the Reynolds number based on the airfoil chord and the freestream velocity.

For turbulent boundary-layers, semi-empirical methods of calculation are inevitably used due to the well-known closure problem. Suction coefficients in the range of $C_q = 0.002$–0.004 are sufficient to prevent separation on a typical airfoil (Schlichting, 1959; Schlichting and Pechau, 1959). Optimally, the suction should be concentrated on the low-pressure side of the airfoil just a short distance behind the nose where, at large angles of attack, the largest local adverse pressure gradient occurs.

Passive Suction. For the high-speed, shock-boundary-layer interaction case, a passive porous surface can be used to mitigate the local pressure gradients and obviate separation as well as reduce wave drag/shock losses (Bahi et al., 1983; Savu and Trifu, 1984; Nagamatsu et al., 1985; 1987; Raghunathan, 1985; Stanewsky and Krogmann, 1985; Barnwell et al., 1985; Koval'nogov et al., 1987) in both transonic and supersonic flows (Bauer and Hernandez, 1988). The basic device is an empty subsurface plenum covered by a porous surface and located underneath the shock-boundary-layer interaction region. Such a passive porous surface allows mass to self-bleed from downstream of the shock to upstream, resulting in a more gradual viscous-inviscid interaction, a series of weaker shock waves and reduced pressure gradients. Flow separation is then delayed and wave drag is minimized. Suction implemented via passive bleed is employed as an integral part of the technologically important case of high-speed inlet design (Delery, 1985; Viswanath, 1988).

Suction Optimization. Flow separation control by suction is the other conventional technique which, along with blowing, is within the capacity of contemporary CFD for design and optimization via tailored and perhaps distributed flow profiles and is well reviewed in readily available literature. Suction can be instituted via active or passive systems, with the boundary-layer diverter constituting the *reductio ad absurdum*. The parameter space for separation control by suction (or injection) includes: distribution of mass transfer location vis-a-vis adverse pressure gradient regions; spatial distribution (discrete, continuous); exit orientation; tailoring of orifice velocity profiles; active or passive source/sink; and distribution of suction/injection both chordwise and spanwise.

In summary, studies of suction control at high speeds indicate that suction holes should probably be inclined in the upstream direction (Purohit,

1987); that upstream control is less effective than direct control of the separated flow region; and that optimum distributed suction requires several independent plenum chambers to avoid local backflow and consequent loss of suction control. An additional possibility for high-speed flows is to utilize the embedded near-wall spanwise vortex structure associated with swept shocks to remove the inner portion of the incident boundary layer (S. M. Bogdonoff; private communication). This may require provision of an additional control shock upstream of the interaction.

The increased interest in, and favorable flight experience with, hybrid laminar flow control (where suction is employed in the leading-edge region ahead of wing box) has revived interest in suction control for the subsonic case. Preliminary studies indicate that the LFC suction system for cruise application is not incompatible with leading-edge region suction separation control or high-lift requirements for both CTOL and SST (supersonic transport) applications. Flight experiments of leading-edge suction systems for high lift (e.g., Hunter and Johnson, 1954) and LFC (Hefner and Sabo, 1987) do not indicate any stoppers. A combined approach has considerable promise, using the same suction surface and system for both LFC at cruise and leading-edge-region high lift for takeoff and landing. For LFC, there is the added benefit of eliminating the joints, etc., associated with conventional leading-edge, variable-geometry devices.

Wall Heat Transfer. The third term in Equation (17) points to yet another method to delay boundary-layer separation. By transferring heat from the wall to the fluid in liquids or from the fluid to the wall in gases, this term adds a negative contribution to the curvature of the velocity profile at the wall and, hence, causes the separation point to move farther aft. If the surface of a body in a compressible gas is cooled, the near-wall fluid will have larger density and smaller viscosity than that in the case with no heat transfer. The smaller viscosity results in a fuller velocity profile and higher speeds near the wall. Combined with the larger density, this yields a higher momentum for the near-wall fluid particles and, hence, the boundary layer becomes more resistant to separation. Although this method of control has been successfully applied to delay transition in both water and air flows, its use to prevent separation has been demonstrated only for high-speed gaseous flows. These effects are confirmed via the analytical results of Libby (1954), Illingworth (1954), and Morduchow and Grape (1955). Experimental verification is provided by the work of Gadd et al. (1958), Bernard and Siestrunck (1959), and Lankford (1960; 1961). Excellent summaries of the problem of heat transfer effects on the separation of a compressible boundary layer are available in Gadd (1960) and Chang (1970; 1976).

Active separation control by wall cooling in air is straightforward. The technique might be particularly appropriate for high-altitude, long-endurance vehicles (HALE) having thick, low-Reynolds-number wings and cryogenic fuel

to provide the requisite heat sink (e.g., Baullinger and Page, 1989). Unfortunately the method is mainly restricted to cryogenically-fueled aircraft. This makes it particularly appropriate for hypersonic applications such as shock-boundary-layer interactions on hydrogen-fueled vehicles. Cooling in air works according to both experiment and theory for low (Macha et al., 1972; Lin and Ash, 1986) as well as high (Spaid, 1972; Ogorodnikov et al., 1972) speeds.

In liquids, surface heating lowers the near-wall viscosity but the density remains essentially unchanged. Using simple asymptotic analysis of the coupled energy and momentum equations, Aroesty and Berger (1975) compared the effectiveness of wall heating to suction as a means of delaying separation for a prescribed adverse pressure gradient in a water boundary layer. They concluded that surface heating can be used in water to delay separation somewhat. However, it seems that this analytical result has not been confirmed experimentally.

In addition to surface heating/cooling, several other methods are available to establish a viscosity gradient in a wall-bounded flow and thus to affect the location of separation. These include as indicated earlier film boiling, cavitation, sublimation, chemical reaction, wall injection of a secondary fluid having lower/higher viscosity, and the introduction into the boundary layer of shear-thinning/shear-thickening additive.

6.4 Moving Walls

The moving-wall effects can be exploited to postpone separation. For a surface moving downstream, the relative motion between the wall and the freestream is minimized and thus the growth of the boundary layer is inhibited. Furthermore, the surface motion injects additional momentum into the near-wall flow. Prandtl (1925) demonstrated the effects of rotating a cylinder placed in a uniform stream at right angles to its axis. Separation is completely eliminated on the side of the cylinder where the wall and the freestream move in the same direction. On the other side of the cylinder separation is developed only incompletely. In fact, for high enough values of circulation, the entire flow field can be approximated by the potential flow theory. The asymmetry causes a force on the cylinder at right angle to the mean flow direction. This important phenomenon, known as the Magnus effect (Magnus, 1852; Swanson, 1961), is exploited in several sport balls (Mehta, 1985a) and even in an experimental device used for propelling ships, known as the Flettner's (1924) rotor.

From a practical point of view, wall motion for body shapes other than circular cylinders or spheres is prohibitively complicated, although it is feasible to replace a small portion of the surface of, say, an airfoil by a rotating cylinder thus energizing the boundary-layer and avoiding separation (Alvarez-Calderon, 1964). Rotating cylinders have been successfully employed to delay separation at the leading and trailing edges of airfoils and control surfaces (Johnson et al., 1975; Mokhtarian and Modi, 1988; Mokhtarian et al., 1988a;

1988b; Modi et al., 1989) at flap junctures (Alvarez-Calderon, 1964; Lee, 1974; Tennant et al., 1975; Modi et al., 1980), and in diffusers (Tennant, 1973). Critical parameters include rotational speed and cylinder-to-fixed surface gap.

Flight tests were conducted on an YOV-10A STOL-type aircraft having flaps with rotating cylinders at their leading edges (Cichy et al., 1972; Weiberg et al., 1973; Cook et al., 1974). With the flaps in lowered position, the cylinders were rotated at high speed and lift coefficients as high as 4.3 were recorded at a modest flying speed of 30 m/sec along approaches up to $-8°$. Modi and his colleagues (Modi et al., 1981; Mokhtarian and Modi, 1988) carried out a comprehensive wind tunnel test program involving a family of airfoils each having one or more rotating cylinders located at the leading edge, the trailing edge or the upper surface, as sketched in Figure 8. Under optimum conditions, the lift coefficient increased by as much as 200% and the stall angle was delayed to 48°.

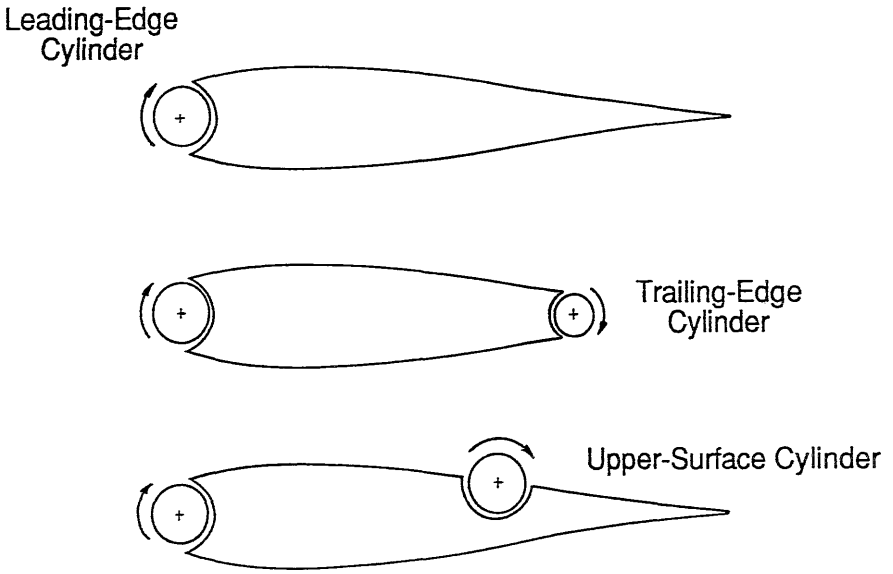

Fig. 8. Various rotating cylinder configurations used to increase lift and delay stall of an airfoil

Recently, Modi et al. (1990) extended the concept of moving surface boundary-layer control to reduce the drag of land vehicles. On a scale-model of a typical tractor-trailer truck configuration having a splined rotating cylinder at the top leading edge of the trailer (Figure 9), drag was lowered by as much as 27%, when the cylinder surface velocity was 3.7 times the freestream

speed. Modi et al. maintain that this separation control concept is essentially semi-passive in character requiring negligible amount of power for its implementation.

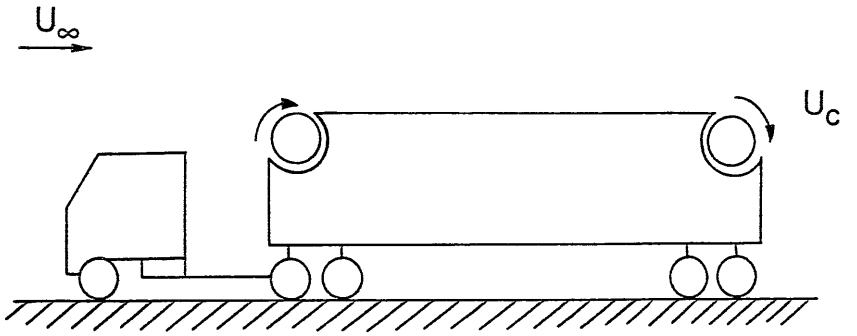

Fig. 9. Tractor-trailer truck with rotating cylinders

Creating a wall-slip layer biases the mean flow such that a larger pressure gradient can be tolerated before separation occurs. There are essentially two techniques for establishing a slip layer on the wall to mitigate separation. The first of these is to actually translate the wall itself, e.g., moving belts or embedded rotating cylinders as discussed above. The other approach is the establishment of stabilized cavity vortex flows. Either small-scale (Migay, 1960a; 1960b; 1961; 1962a; 1962b; 1962c; Stull and Velkoff, 1975; Howard and Goodman, 1985) or large-scale (Ringleb,1961; Adkins, 1975; Adkins et al., 1980; Burd, 1981; Chow et al., 1985; Krall and Haight, 1972; Haight et al., 1974) vortex stabilization is necessary, otherwise the trapped vortex will generally periodically shed downstream causing disrupted operation and higher drag and losses. Stabilization techniques include injection (Krall and Haight, 1972; Haight et al., 1974); suction (Adkins, 1975; 1977; Adkins et al., 1980; Burd, 1981; Chow et al., 1985); and/or viscous forces via low-cavity-Reynolds number (e.g., Howard and Goodman, 1985). The vortex flap is the latest version of such a device. These slip-layer separation control techniques work for moderately separated flows, but in extreme cases reverse flow can still occur away from the surface (Zhuk and Ryzhov, 1980).

6.5 Time-Dependent Separation

For time-dependent flows, the separation point is no longer stationary but rather moves along the surface of the body. In analogy to the moving wall case, unsteady separation is (temporally) postponed when the separation

point moves upstream as is the case on the suction side of an airfoil undergoing a pitching motion from small to large angles of attack. Conversely, when an airfoil is pitched from large to small attack angle, the separation point on the suction side moves downstream and separation is advanced, much the same as the case of a wall moving upstream.

An airfoil oscillating sinusoidally through high angles of attack can produce very high lift coefficients and maintain flow attachment well beyond static stall attack angles (McCroskey, 1977; 1982). During the upstroke, the separation point moves upstream and reverse flow exists in an attached and mathematically well-behaved boundary layer. The global aerodynamic properties of a pitching airfoil are strongly influenced by the local unsteady separation. Sudden changes of lift, drag, and pitching moment occur near the onset of separation and the spillage of a leading edge vortex. These effects are particularly significant at high frequencies and large amplitudes. Moment stall is observed when the reverse-flow region extends over most of the airfoil and a large-scale vortex is formed near the leading edge. A discontinuous increase in circulation is associated with the spilled vortex. During this phase of the cycle, lift continues to increase. Lift stall follows moment stall and occurs when the separation vortex reaches the latter half of the airfoil and a double-peaked pressure distribution results on the suction side. In other words, the suction on the upper surface of the airfoil continues to increase at the initial stages of separation, and a sudden decrease in suction does not occur until the leading edge is in the wake of separation.

Similar phenomena are observed on three-dimensional lifting surfaces undergoing pitching motion (Gad-el-Hak, 1986a; 1988a; 1988b; Gad-el-Hak and Ho, 1986a). For highly swept wings, both steady as well as unsteady flows are vortex dominated. The latter flow is characterized by the existence of unsteady large- and small-scale vortices that go through a growth-decay cycle with hysteresis during each period (Gad-el-Hak and Ho, 1985; 1986b; Kandil and Chuang, 1988; Atta and Rockwell, 1990; Huyer et al., 1990).

According to Ericsson (1967; 1988), the forces on an airfoil oscillating in pitch will deviate from the static forces realized at the instantaneous angle of attack due to the superposition of two effects. First, the frequency-induced normal velocity distribution over the airfoil. This so-called q effect can be visualized as a frequency-induced camber. Secondly, the effect of attack angle rate of change, the so-called $\dot{\alpha}$ effect. This can be visualized as a frequency-induced change of the mean velocity vector or plunging. During the upstroke, a pitching airfoil will appear as having a positive camber and as plunging. According to the unsteady Bernoulli's equation, the local pressure gradient is less adverse in the dynamic case. Thus, the boundary layer at a particular α during the upstroke has a more favorable upstream time history as compared to the static case. The opposite effects take place during the downstroke. Insects, most of whom mate and eat while airborne, exploit unsteady separation effects to achieve remarkable aerodynamic characteristics. The dragonfly,

in existence for approximately 250 million years, presumably survived innumerable life and death aerodynamic struggles (Luttges et al., 1984; Luttges, 1989). The enviably large lift coefficients generated by the chalcid wasp during hovering suggest the existence of an efficient unsteady lift generation mechanism (Weis-Fogh, 1973; Lighthill, 1973; Maxworthy, 1979; 1981).

6.6 Three-Dimensional Separation

Three-dimensional boundary layers are more common in practical flow situations than two-dimensional ones. Bodies of revolution at some angle of attack, flow near wing tips, turbine blades, pump impellers, and low-aspect-ratio wings are examples of flow fields in which three-dimensional effects dominate. As mentioned earlier, the point of boundary-layer separation from a three-dimensional body does not necessarily coincide with the point of vanishing wall shear. Instead, the shear stress at the wall is equal to zero only at a limited number of points along the separation line. The number and type of these critical or singular points must satisfy certain topological laws (Lighthill, 1963; Tobak and Peake, 1982). The projection of the limiting streamlines as the distance from the wall goes to zero coincides with the skin-friction lines on the surface of the body. Oil-streak techniques and the like are usually used to obtain separation and attachment patterns for steady, three-dimensional flows (Maltby, 1962). A necessary condition for the occurrence of flow separation is the convergence of skin-friction lines onto a particular line. Because of the three-dimensionality of the flow, the near-wall fluid may move in a direction in which the pressure gradient is more favorable and not against the adverse pressure in the direction of the main flow as is the case for two-dimensional flows. Consequently, three-dimensional boundary-layers are in general more capable of overcoming an adverse pressure gradient without separation. Three-dimensional relief of the streamwise adverse pressure gradient may be exploited to delay separation. Properly designed corrugated trailing edges can provide sufficient easement to postpone the separation at higher angles of attack. In nature, three-dimensional serrated geometry is to be found in the trailing edges of the fins and wings of many aquatic animals and birds (Norman and Fraser, 1937; Lighthill, 1975). For man-made lifting surfaces, the same concept was tested in the low-Reynolds-number regime by Vijgen et al. (1989). They reported a modest 5% increase in the maximum lift-to-drag ratio when triangular serration were added to the trailing edge of a natural-laminar-flow airfoil.

6.7 Turbulators

A turbulent boundary layer is more resistant to separation than a laminar one and mostly for that reason transition advancement may be desired in some situations. In low-Reynolds-number terminology, the transition promoting devices are called turbulators. For a zero-pressure-gradient boundary

layer, transition typically occurs at a Reynolds number based on distance from leading edge of the order of 10^6. The critical Re below which perturbations of all wave numbers decay is about 6×10^4. To advance the transition Reynolds number, one may attempt to lower the critical Re, increase the growth rate of Tollmien-Schlichting waves, or introduce large disturbances that can cause bypass transition. The first two routes involve altering the shape of the velocity profile using wall motion, injection, adverse pressure gradient, or surface heating in gases or cooling in liquids. The third route, exposing the boundary layer to large disturbances, is much simpler to implement though more difficult to analyze (Smith and Kaups, 1968; Cebeci and Chang, 1978; Nayfeh et al., 1986; Cebeci and Egan, 1989).

Morkovin (1984) broadly classifies the large disturbances that can cause bypass transition into steady or unsteady ones originating into the freestream or at the body surface. The most common example is single, multiple or distributed roughness elements placed on the wall. The mechanical roughness elements, in the form of serrations, strips, bumps or ridges, are typically placed near the airfoil's leading edge. If the roughness characteristic-length is large enough, the disturbance introduced is nonlinear and bypass transition takes place. For a discrete three-dimensional roughness element of height-to-width ratio of one, Tani (1969) reports a transition Reynolds number of $Re_{\delta^*} \approx 300$ for a roughness Reynolds number of $Re_\kappa \approx 10^3$. In here, Re_{δ^*} is based on the velocity outside the boundary layer and the displacement thickness ($Re_{\delta^*} \equiv U_\infty \, \delta^*/\nu$), and Re_κ is based on the height of the roughness element and the velocity in the undisturbed boundary layer at the height of the element ($Re_\kappa \equiv u(\kappa) \, \kappa/\nu$). Note that the transition Reynolds number, Re_{δ^*}, indicated above is below the critical $Re_{\delta^*} = 420$ predicted from the linear stability theory. For a roughness Reynolds number of about 600, transition occurs at $Re_{\delta^*} \approx 10^3$. For a smooth surface, transition typically takes place at $Re_{\delta^*} \approx 2.6 \times 10^3$. An important consideration when designing a turbulator is to produce turbulence and suppress laminar separation without causing the boundary layer to become unnecessarily thick. A thick turbulent wall-bounded flow suffers more drag and is more susceptible to separation than a thin one. Consistent with this observation, available data (Figure 10) indicates that a rough airfoil has higher lift-to-drag ratio than a smooth one for $Re_c < 10^5$, but that this trait is reversed at higher Reynolds numbers.

For low-Reynolds-number airfoils, performance may be improved by reducing the size of the laminar separation bubble through the use of transition ramps (Eppler and Somers, 1985), boundary layer trips (Davidson, 1985; Van Ingen and Boermans, 1986), or even pneumatic turbulators (Pfenninger and Vemuru, 1990). Donovan and Selig (1989) provide extensive data using both methods for 40 airfoils in the Reynolds number range of 6×10^4–3×10^5. A long region of roughly constant adverse pressure gradient on the upper surface of a lifting surface (termed a bubble ramp) achieves a lower drag than the more conventional laminar-type velocity distribution in which initially the pressure

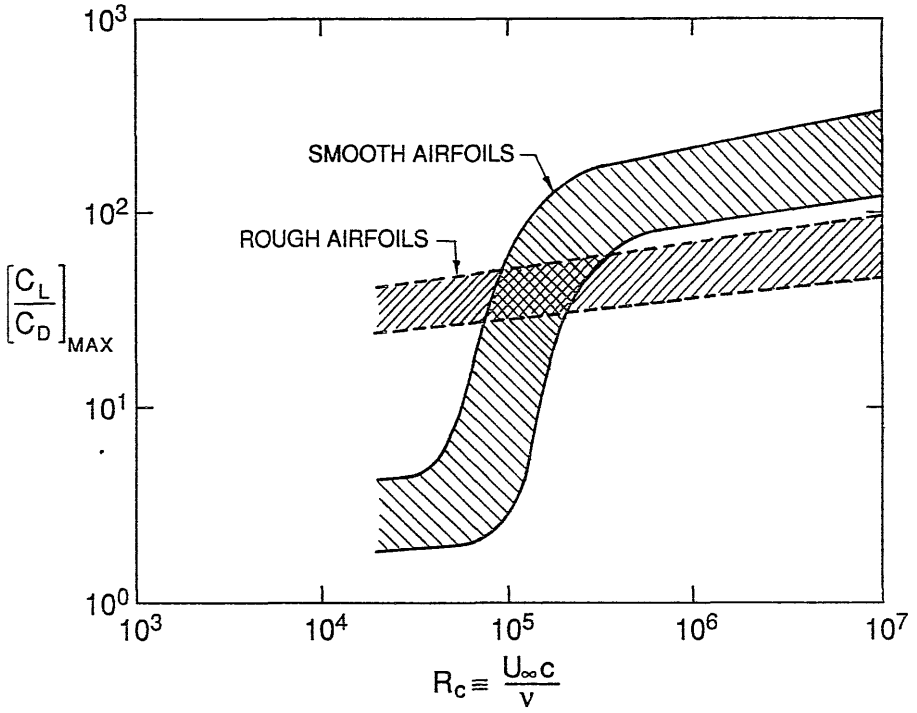

Fig. 10. Airfoil performance as a function of chord Reynolds number

remains approximately constant and then quickly recovers. Trips were also used to shorten the separation bubble. A simple two-dimensional trip performed as well or better than zig-zag tape, hemisphere bumps, and normal blowing. Donovan and Selig concluded that an airfoil which performs poorly at low Reynolds numbers can be improved through the use of turbulators. Trips were less effective, however, at improving airfoils which normally had low drag.

Other large disturbances that could lead to early transition include high turbulence levels in the freestream, external acoustic excitations, particulate contamination, and surface vibration. These are often termed environmental tripping. Transition could also be effected by detecting naturally occurring T-S waves and artificially introducing in-phase waves. Transition could be considerably advanced, on demand, using this wave superposition principle. Early transition could also be achieved by exploiting other routes to turbulence such as Taylor-Görtler or cross-flow vortices (Taylor, 1923; Görtler, 1955; Gregory et al., 1955; Reed and Saric, 1987; 1989). For example, a very mild negative curvature of $(0.003/\delta^*)$ results in the generation of strong

streamwise vortices. In this case, transition Reynolds number is lowered from $Re_{\delta^*} \approx 2600$ for the flat-plate case to $Re_{\delta^*} \approx 700$ for the curved surface (Tani, 1969). For high Mach number flows, the general decay in spatial amplification rate of T-S waves makes conventional tripping more difficult as the Mach number increases (Reshotko, 1976). For these flows, trips that generate oblique vorticity waves of appropriate wavelength may be most effective to advance the transition location.

The last issue to be considered in this section is augmentation of the turbulence for a shear flow that has already undergone transition. Notwithstanding that the turbulence levels and the Reynolds stresses are highest immediately following transition (Harvey et al., 1969), the newly developed turbulent flow is in general less capable of resisting separation than a corresponding flow at higher speeds (Lissaman, 1983). Turbulence augmentation in the low-Reynolds-number case is then a useful control goal to energize the flow and to enhance its ability to resist separation at higher angles of attack. Roughness will enhance the turbulence, but its associated drag must be carefully considered. Other devices to enhance the turbulent mixing include vane-type vortex generators, which draw energy from the external flow, or wheeler-type or Kuethe-type generators, which are fully submerged within the boundary layer and presumably have less associated drag penalty (Rao and Kariya, 1988). These and other devices will be detailed in the next section.

6.8 Momentum Addition to Near-Wall Flow

Near-wall momentum addition is the usual approach of choice for control of residual flow separation remaining after mitigation of the causative pressure field or for off-design conditions. Common to all these control methods is the supply of additional energy to the near-wall fluid particles which are being retarded in the boundary layer. The additional longitudinal momentum is provided either from an external source or through local redirection into the wall region. Passive techniques do not require auxiliary power, but do have an associated drag penalty, and include intentional tripping of transition from laminar to turbulent flow upstream of what would be a laminar separation point (Mangalam et al., 1986; Harvey, 1986), boundary-layer fences to prevent separation at the tips of swept-back wings, placing an array of vortex generators on the body to raise the turbulence level and enhance the momentum and energy in the neighborhood of the wall (Mehta, 1985b; Rao and Kariya, 1988), rippled trailing edge (Werle et al., 1987), streamwise corrugations (Mabey, 1988), stepped afterbodies to form a system of captive vortices in the base of a blunt body (Kentfield, 1985a; 1985b; Kidd et al., 1990), or using a screen to divert the flow and increase the velocity gradient at the wall.

Active methods to postpone separation require energy expenditure. Obviously, the energy gained by the effective control of separation must exceed

that required by the device. In addition to suction or heat transfer reviewed in Section 6.3, fluid may be injected parallel to the wall to augment the shear-layer momentum or normal to the wall to enhance the mixing rate (Horstmann and Quast, 1981). Either a blower is used or the pressure difference that exists on the aerodynamic body itself is utilized to discharge the fluid into the retarded region of the boundary layer. The latter method is found in nature in the thumb pinion of a pheasant, the split-tail of a falcon, or the layered wing feathers of some birds.

In man-made devices, passive blowing through leading-edge slots and trailing-edge flaps is commonly used on aircraft wings, as sketched in Figure 11. Although in this case direct energy expenditure is not required, the blowing intensity is limited by the pressure differentials obtainable on the body itself. Nevertheless, the effect of passive blowing on lift and drag could be dramatic. Compared to the clean (no flap) case, when a single trailing-edge flap is used the maximum lift is increased by about 175% while the section drag at $C_{L\max}$ is increased by more than 180%. The corresponding numbers when a double-slotted flap is used are, respectively, 230% and 500%. The induced drag, which must be considered in addition to the section drag, is proportional to C_L^2, and the total drag, therefore, rises sharply at low aircraft speeds.

Many of the control methods discussed in this section could be used for external as well as internal flows. For example, Viets (1980) used an asymmetrical rotating cam embedded in the wall to produce large eddies in a turbulent boundary layer with zero- and adverse-pressure gradients. By using this device in a wide-angle diffuser, Viets et al. (1981) were able to postpone the natural separation and dramatically improve the diffuser's performance.

Passive Vortex Generation. Passive momentum addition is most commonly carried out via one of two general approaches, either macro overturning of the mean flow using embedded streamwise vortices generated by fixed lifting surfaces, or Reynolds stress amplification which leads to increased cross-stream momentum transfer. Conventional passive vortex generators (VGs) date from the 1940s (Taylor, 1948a) and are simple, effective and generally the first tried as a fix to an existing flow separation problem. Passive VGs have been applied, for example, to compressor blades (Staniforth, 1958), diffusers (Henry et al., 1956; Feir, 1965; Brown et al., 1968), airfoils (Pearcey, 1961; Nickerson, 1986; Bragg and Gregorek, 1987), and the afterbody of aircraft fuselages (Calarese et al., 1985; Wortmann, 1987). What these embedded vortices do is cause overturning of the near-wall flow via macro motions. Fluid particles with high streamwise momentum are swept along helical paths toward the surface to mix with and, to a certain extent, to replace the retarded near-wall flow. The vortex influence upon the turbulence can actually be debilitating due to streamline curvature-induced stabilization.

Essentially small-aspect-ratio airfoils mounted normal to the surface, vor-

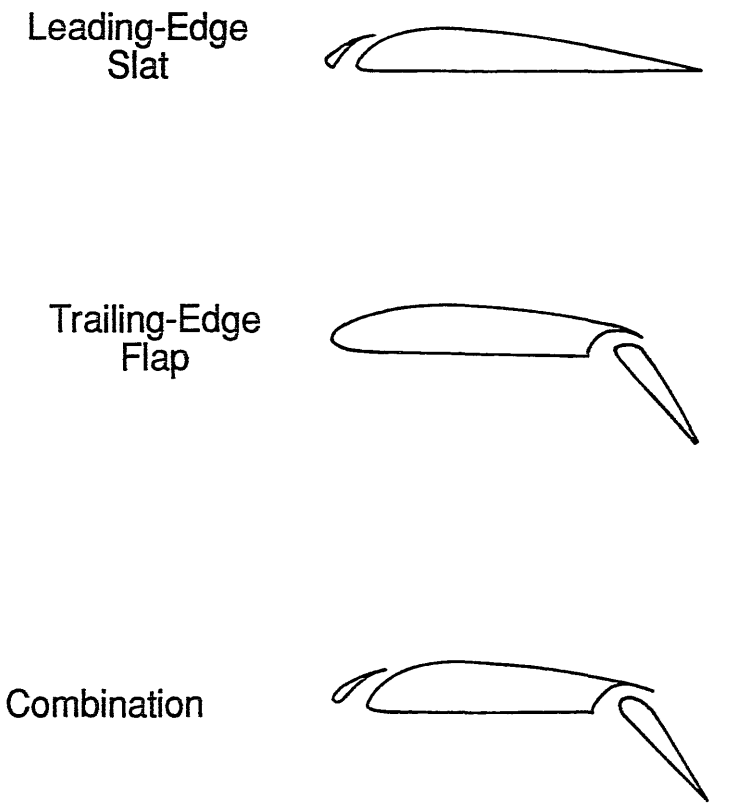

Fig. 11. Passive blowing through leading-edge slats and trailing-edge flaps

tex generators' individual parametrization include planform shape, section profile and camber, yaw angle, aspect ratio, and height with respect to the boundary-layer thickness. The spatial relationship of the devices is also critical, e.g., co-rotating versus contra-rotating bi-plane and wing, use of downstream reinforcers, and spacing. Counter-rotating vortices force large regions of vorticity to rise above the surface and hence are often not as efficient as co-rotating devices. However, co-rotating vortices with too close a spacing undergo mutual vorticity cancellation, therefore spacing is critical in this case.

Nominal guidelines for conventional VGs are given in the papers by Taylor (1948b); Henry et al. (1956); and Pearcey (1961): aspect ratio of 0.5–1; rectangular or triangular planform with either simple flat plate or low-Reynolds-number airfoil cross-section; yaw angle less than 15°; and individual height on the order of the boundary-layer thickness. For co-rotating devices, the spanwise spacing should be greater than 3 times the device height to avoid interactive cancellation or annihilation of the vortical structures. The recommended nominal spanwise spacing for contra-rotating vortex production

devices is on the order of 4–5 device heights. These conventional vortex generating devices produce sizable parasitic drag. When employed to handle off-design problems, the VGs cause a reduction in cruise performance, unless the devices are retracted when not needed. The papers by Schubauer and Spangenberg (1960); Gadetskii et al. (1972); Liandrat et al. (1986); Cutler and Bradshaw (1986; 1989); Inger and Siebersma (1988); Mehta (1988); and Briedenthal and Russell (1988) provide generic studies of vortex generator physics and operation. Application to supersonic flows is summarized by Gartling (1970).

Several approaches are now available to optimize the performance of passive vortex generators. The first of these is the use of downstream reinforcers; which are vortex generators of the same sense located in the path of the upstream-generated vortex to maintain the strength of the overturning motion (Kuethe, 1973; Wheeler, 1984; Lin and Howard, 1989; Rao and Kariya, 1988). A second optimization approach is surprisingly recent and consists of simply reducing the device height from the order δ to $\mathcal{O}[\delta/5]$ or less (Rao and Kariya, 1988; Lin and Howard, 1989; Lin et al., 1990a). This size reduction significantly diminishes the parasitic drag and is enabled by the extreme fullness of the mean velocity profile in a turbulent boundary layer. In other words, with sizable longitudinal momentum levels readily available quite close to the surface, it is not necessary to have $\mathcal{O}[\delta]$ devices. Such sub-δ devices must be placed closer to the nominal separation location and therefore may be less suitable than larger devices for situations where the separation region is not relatively localized.

Alternative approaches for separation control by streamwise vortices are the V-shaped cutouts of the NACA's flush inlet, leading-edge serrations (Harris and Bartlett, 1972; Soderman, 1972; Barker, 1986) and use of large-scale (flow field vs. boundary-layer scale) vortical motions to control separation on highly swept wings. Such motions can be generated by either auxiliary lifting devices, e.g. canards, or by simple abrupt planform variations such as wing leading-edge extensions (LEXs). Such large-scale vortical motions alter both the near-wall momentum and the basic pressure field, generating increased lift. Problems with such an approach include vortex bursting, usually caused primarily by adverse pressure gradients. Control of bursting is actually control *of* vortices and is a subsidiary problem of separation control *by* vortices (Vakili, 1990).

Passive Turbulence Amplification. The fundamental flow separation control approach associated with turbulence amplification is augmentation of the cross-stream momentum via Reynolds stresses in as much as the overall pressure rise for incipient separation is directly proportional to the square root of the skin-friction coefficient of the undisturbed boundary layer (Hayakawa and Squire, 1982). The zeroth order consideration for most separation control is to ensure a turbulent rather than laminar boundary-layer state. For Reynolds

numbers less than $\mathcal{O}\left[10^7\right]$, this may necessitate use of various boundary-layer tripping devices such as roughness and waviness, passive or active mass transfer, acoustic fields, body vibration, or even elevated freestream disturbance levels.

Once a turbulent boundary-layer flow is established, large-scale, dynamic, transverse vortical entities can be generated to augment the innate turbulent Reynolds stress field beyond the usual amplification concomitant with the adverse pressure gradients usually associated with separation. Applicable devices include transverse cylinders or flow control rails mounted just above, or in the outer part of, the boundary layer (Sajben et al., 1976). Airfoils with chord of the $\mathcal{O}\left[\delta\right]$ mounted parallel to the body in the outer part of the boundary layer and set at angle of attack also generate large transverse dynamic vortical motions (Corke et al., 1980), as can embedded cavity (Helmholtz) resonator surfaces. Dynamic three-dimensional horse-shoe or hairpin eddies can be generated in the tip flow of three-dimensional stubs mounted normal to the surface. Except for the flow control rail, which works quite well, these passive devices have received only limited attention and development for flow separation control.

Howard and Goodman (1985; 1987) recently investigated the effectiveness of two passive techniques to reduce flow separation, transverse rectangular grooves and longitudinal V-grooves placed in the aft shoulder region of a bluff body. Both types of grooves were beneficial in reducing the form drag on a body at zero and moderate angles of yaw. Basically, the grooves work by redirecting the outer-flow momentum to the near-wall region through the three-dimensionalization of a two-dimensional flow. This is an example of locally mitigating the adverse pressure gradient through partial boattailing. Lin et al. (1990b) extended the longitudinal groove approach to the low-speed, two-dimensional rearward-facing ramp. Their closely packed grooves resulted in a reduction of the reattachment distance by up to 66%. Selby and Miandoab (1990) reported that the base pressure of a blunt trailing-edge airfoil with surface grooves increased with increasing groove depth and angle. They speculated that minimally attached flow in the grooves is the mechanism by which fluid of higher momentum is redirected to the base flow region to effect an increase in the pressure.

Additional turbulence amplification ploys include destabilizing longitudinal surface curvature in order to increase wall shear, concave for boundary layers and convex for wall jets (coanda effect). For high speeds, use of upstream shock-wave-interaction, which can amplify turbulence significantly (Anyiwo and Bushnell, 1982; Zang et al., 1984), also delays separation (Schofield, 1985; Gol'd Fel'd and Zatoloka, 1979). The use and/or generation of freestream turbulence/disturbance fields with intermediate scale motions also amplifies turbulence in the boundary layer and delays separation (Hoffmann, 1981; Sasaki and Kiya, 1985; Hoffmann et al., 1988; Isomoto and Honami, 1989).

Active Wall-Region Momentum Enhancement. Active momentum addition techniques include streamwise vortex generation via discrete blowing or injection, turbulence/Reynolds stress amplification through use of dynamically activated or driven devices, and direct tangential injection of high-velocity fluid. The two passive techniques discussed above, vortex generation and turbulence amplification, can also be employed via active systems. Of particular interest is the use of discrete jet injection for streamwise vortex generation. This concept arose in the 1950s (Wallis and Stuart, 1958; Pearcey, 1961; Kukainis, 1969; Wimpenny, 1970) and is the subject of current research (Zhang and Sheng, 1987; Reynolds et al., 1988; Johnston and Nishi, 1989; 1990; Compton and Johnston, 1991). What is particularly appealing is the ability to deploy or retract the vortex generators as required, which eliminates parasitic drag in the retracted nonblowing condition. The associated fluid supply lines operate at high pressure and are thus relatively small. They might even be utilizable as structural reinforcement elements. The status of research in this area is such that, while it is clear that discrete jets will generate vortices and delay separation, the approach has not yet been optimized. Research is required to determine optimal injection orientation, spacing, individual hole geometry and size, velocity, pressure, and finally location vis-a-vis the adverse pressure gradient regions. Papell (1984) addresses vortex generation within the injection jet itself. Another use of injection for vortex generation is spanwise injection along the leading edges of swept wings for upper surface separation control (e.g., Bradley and Wray, 1974). Employing spanwise arrays of small, skewed, pitched jets from holes in the surface, Johnston and Nishi (1990) have shown that the jets can produce longitudinal vortices strong enough to substantially reduce and nearly eliminate a large stalled region of a turbulent separated flow.

A relatively recent development in flow separation control is active turbulence amplification in the bounding shear layer for flows already separated. The fundamental concept is excitation and, through phasing, enhanced interaction of large transverse eddy structures near and downstream of the separation point, thereby amplifying the mixing in the shear layer bounding the separated flow region. This increases entrainment and generally reduces the extent of separation. For initially laminar flows, the zeroth order influence of dynamic forcing is to both trip transition and enhance the eddy dynamics of the low-Reynolds-number shear-layer (e.g., Collins, 1979; 1981; Mullin et al., 1980; Sigurdson and Roshko, 1985; DeMeis, 1986; Durbin and McKinzie, 1987; Huang et al., 1987; Neuburger and Wygnanski, 1988; Zaman and McKinzie, 1989; Bar-Sever, 1989).

Various dynamic devices have been tried for the initially turbulent flow case including acoustic drivers (Bhattacharjee et al., 1985), oscillating embedded plates, spoilers and flaps (Reisenthel et al., 1985; Roos and Kegelman, 1986; Miau et al., 1988; Chen and Shi Ying, 1989; Katz et al., 1989a; 1989b), both chordwise and spanwise dynamic blowing (Oyler and Palmer, 1972; Ely

and Berrier, 1975; Vakili et al., 1988; Vakili, 1990), rotating cams (Viets et al., 1979; 1981a; 1981b; 1981c; 1984), and even dynamic motions of the entire body. One of the few large-scale dynamic experiments thus far is also one of the earliest (Oyler and Palmer, 1972). The same incremental increase in lift was achieved with only 50% of the blowing mass flow required for the steady-state case. What is obvious from the initially turbulent, dynamic-input separation control research thus far is that, once again, the method works. What is not so obvious is how well it would work in engineering applications and the nature and operating range of the optimal dynamic devices.

Wall Jets. Direct tangential injection, wall jet, was and still is the preferred and straightforward flow separation control technique which has been applied to military fighters and STOL transports. High-pressure air can be used enabling relatively small interior lines as opposed to suction control which, while generally more energy efficient than blowing at both low and high speeds, usually requires larger interior ducting (Gratzer, 1971). In some applications, a lighter gas is introduced to reduce the rate at which heat is exchanged between the wall and the external stream and, thus, to provide thermal protection at high supersonic velocities.

High-pressure bleed air was readily available from the early jet engines but less so for modern high-bypass-ratio turbofans. CFD can now be used to design the system and optimize the injection velocity profile for a given mass flow for optimal separation delay (see Saripalli and Simpson, 1980). Performance can be further enhanced by convex longitudinal curvature (coanda effect). Tangential blowing is also used to stabilize a trapped vortex, particularly in the knee region of wing flaps. The literature for the steady blowing case is both extensive and readily available, with most information dating from the 1950s. Separation control by blowing at high speeds is covered in the reviews by Delery (1985) and Viswanath (1988). Of possible interest for separation control via direct tangential injection is the application of turbulence control techniques to reduce the mixing between the injected and incident flows and thereby preserve the high near-wall momentum for a larger extent downstream (McInville et al., 1985).

Tangential jet blowing over the upper surface of a rounded trailing-edge airfoil sets an effective Kutta condition by fixing the location of separation. This circulation control concept was initially described by Cheeseman and Seed (1967), and a substantial data base has been gathered since then for the purpose of performance evaluation (Kind, 1967; Wood and Nielsen, 1985; Novak et al., 1987). More recently, McLachlan (1989) conducted an experimental study of the flow past a two-dimensional circulation control airfoil under steady leading/trailing-edge blowing. In the range of chord Reynolds numbers of 1.2×10^5–3.9×10^5, McLachlan observed a dramatic increase in the lift coefficient when trailing-edge blowing was used to control the location of the rear separation points. He reported a gain in the lift coefficient of

the order of 80 times the injected momentum coefficient. When leading-edge blowing was employed simultaneously, a slight decrease in lift was observed.

Although not directly related to separation control, jets in the form of thin sheets exiting in the spanwise direction from the tips of a straight wing can be used to enhance the lift through an effective enlargement of the wing span (Wu et al., 1983; 1984; Tavella et al., 1988; Lee et al., 1989; Vakili, 1990). This application was first reported in 1956 by Ayers and Wild, and suggests the possibility of using such an arrangement in place of conventional ailerons or flaps to alter the aerodynamic forces acting on an aircraft (Tavella et al., 1986b). Either a single long slot (Lee et al., 1986; Tavella et al., 1986a) or several short ones (Wu et al., 1983; 1984) are used along the entire chord at the wing tips. The enlargement of the aspect ratio associated with the lateral displacement of the tip vortices via blowing leads also to a reduction of the induced drag as well as to a beneficial effect on stall.

Additional Active Control Methods. Other active methods for controlling boundary layer separation and reattachment include the use of acoustic excitations (Collins and Zelenevitz, 1975; Ahuja et al., 1983; Ahuja and Burrin, 1984, Zaman et al., 1987; Huang et al., 1987), periodic forcing of the velocity field via an oscillating flap or wire (Koga et al. 1984; Sigurdson and Roshko, 1985; Reisenthel et al., 1985; Roos et al., 1986; Katz et al., 1989a; 1989b; Bar-Sever, 1989), and oscillatory surface heating (Maestrello et al., 1988).

As early as 1947, Schubauer and Skramstad observed that sound at particular frequencies and intensities could enhance the momentum exchange within a boundary layer and could, therefore, advance the transition location. Collins and Zelenevitz (1975) and Collins (1979; 1981) introduced the external acoustic excitation technique to enhance the lift of an airfoil. In this case, sound is radiated onto the wall from a source outside the boundary layer. Using the same technique at chord Reynolds number up to 1×10^6, Ahuja et al. (1983) and Ahuja and Burrin (1984) successfully demonstrated that sound at a preferential frequency and sufficient amplitude can postpone turbulent separation on an airfoil in both pre- and post-stall regimes. The optimum frequency was found to be $4U_\infty/c$ (i.e. Strouhal number $= 4$), where U_∞ is the freestream velocity and c is the airfoil chord. Goldstein (1984) speculates that the delay in separation in Ahuja et al.'s (1983) experiment resulted from enhanced entrainment promoted by instability waves that were triggered on the separated shear layer by the acoustic excitation.

Zaman et al. (1987) conducted further study of the beneficial interaction between external acoustic excitation and the separated flow around an airfoil at high angle of attack. They found that the most effective separation control is achieved at frequencies at which the acoustic standing waves in their wind tunnel induce transverse velocity fluctuations in the vicinity of the lifting surface. The loudspeakers used by Zaman et al. (1987) as well as by Ahuja

et al. (1983) essentially excited the resonant modes in their respective wind tunnels and one of these modes forced the shear layers separating from their respective airfoils. Extremely high level of excitation was required, however, to maintain these wind tunnel resonance modes, making the external acoustic excitation technique impractical for actual applications. Zaman et al. (1987) speculated that a more effective separation control can be obtained by direct introduction of velocity disturbances.

Huang et al. (1987) introduced the internal acoustic excitation technique, in which sound is emanated from a hole or a slot on the surface of a lifting surface. The loudspeaker in this case is essentially used as a piston to produce localized vorticity perturbations at the leading edge of the airfoil. Recently, Hsiao et al. (1990) reported improved aerodynamic performance of a two-dimensional airfoil using sound emitted from three narrow wall slots located near the leading edge. The sound pressure levels used in their experiment was substantially lower than that used externally by other researchers. Additionally, a correct Strouhal number scaling was achieved. Hsiao et al. (1990) concluded that the enhancement of momentum transport resulting from the sound excitation produce a suction peak at the leading edge, an increase of lift and a narrower wake, as long as the excitation frequency is locked-in to the most unstable frequency of the separated shear layer.

To directly disturb the velocity field, Koga et al. (1984) used a computer-controlled spoiler-like flap in a flat-plate turbulent boundary layer with and without modeled upstream separation. They were able to manipulate the separated flow region and its reattachment length characteristics by varying the frequency, amplitude and waveform of the oscillating flap. Reynolds and Carr (1985) offer a plausible explanation, from the viewpoint of a vorticity framework, for the experimental observations of Koga et al. It seems that the large-scale vortical structures produced by forcing play a major role in enhancing mixing and entrainment, thus leading to reattachment. The active flap controls the size of the separated region by providing an additional mechanism for removing vorticity from this zone, namely, large-scale vortex convection. Recent experiments by Nelson et al. (1987; 1990) seem to confirm that the dominant mechanism of vorticity transport behind an oscillating spoiler is convective.

Periodic forcing of the velocity field has been shown to reduce reattachment length in both laminar and turbulent flows on a number of other basic geometrical configurations (Sigurdson and Roshko, 1985; Roos et al., 1986; Katz et al., 1989a; 1989b; Bar-Sever, 1989) At a chord Reynolds number in the range of 1×10^5–3×10^5, Bar-Sever (1989) used an oscillating wire to introduce transverse velocity fluctuations into a separated shear layer on an airfoil at high incidence.

6.9 Separation Provocation

Although most of the control methods reviewed thus far are designed to prevent separation, under certain circumstances the designer may wish to provoke separation. Controlled separation is associated with the formation of jets, throttling action in household faucets, and noisy as well as musical acoustic effects generated by flow. During takeoff and landing of a supersonic aircraft, a freestream flap may be used to provoke leading-edge separation followed by reattachment at the leading edge of the flap, thus forming a thicker pseudo-body with the desired aerodynamic shape (Hurley, 1961). The airfoil has then a relatively high lift coefficient, although its lift-to-drag ratio is quite low.

The detached bow shock forming upstream of a blunt body in supersonic flight may be changed into a weaker, attached oblique shock by placing a spike in front of the body. The pressure rise and the presence of a solid surface on which a boundary layer forms causes the flow to separate downstream of the spike tip. A properly designed spike may result in lower drag, higher lift, and corresponding change in pitching moment (Wood, 1961).

Periodic separation may also be provoked by changes in the wall geometry. Francis et al. (1979) initiated separation on an airfoil by periodically inserting and removing a spoiler at the wall. Viets et al. (1984) studied separation inducement and control by use of a cam-shaped rotor mounted on an airfoil. The cam, either driven or free-wheeling, periodically extended out into the flow causing the boundary layer to separate. Large-scale coherent spanwise structures were periodically generated and were responsible for the flow detachment as explained by Reynolds and Carr (1985).

On a sharp-leading-edge delta wing, the separation position is fixed and a strong shear layer is formed along the entire edge (Lee and Ho, 1989; 1990). The shear layer is wrapped up in a spiral fashion, which results in a large-bound vortex on each side of the wing. The two vortices appear on the suction surface of the wing in the form of an expanding helix when viewed from the apex. The low pressure associated with the vortices produces additional lift on the wing, often called nonlinear or vortex lift, which is particularly important at large angles of attack. The experiments of Gad-el-Hak and Blackwelder (1985) have indicated that small discrete vortices are shed parallel to the leading edge at a repeatable frequency, determined by the angle of attack and Reynolds number. Repeated vortex pairings result in the formation of progressively larger vortices. This process can be modulated by weak, periodic suction/injection through a leading edge slot. In particular, when the perturbation frequency is a subharmonic of the natural shedding frequency, the evolution of the bounded shear layer is dramatically altered (Gad-el-Hak and Blackwelder, 1987a; Blackwelder et al., 1987).

Wood and Roberts (1986; 1988) examined the feasibility of vortex control by tangential mass injection at the leading edge of a 60° delta wing. Their initial experimental results indicate that modest continuous blowing was ca-

pable of extending the regime of stable, controlled vortical flow over the upper surface of the wing by approximately 30° angle of attack. Increases in maximum normal force of 30% were achieved and significant rolling moments were produced at attack angles of 35–60°. On a delta wing with rounded leading edges, the blowing seems to control the location of the crossflow separation points and hence the trajectories of the ensuing vortices. Wood and Roberts (1988) propose that this blowing scheme may be a practical solution for changing the normal force without changing attitude, for the production of both steady and transient control moments at extremely high angles of attack, and for increasing the lift-to-drag ratio of very slender bodies at modest attack angles. In a recent experiment, Wood et al. (1990) have shown that the effects of asymmetric leading-edge blowing are uncoupled at prestall angles of attack. In this case, the overall forces and moments for symmetric blowing can be simply deduced by superposition of asymmetric blowing situations. On the other hand, the response of the vortical flowfield is strongly coupled for asymmetric blowing at poststall conditions. Wood et al.'s results imply that tangential leading-edge blowing may result in substantial rolling moments at conditions where other control devices cease to be effective.

Controllable leading-edge flaps provide an active method of influencing the large vortices on a delta wing (Rao, 1979; Marchman et al., 1980). These devices appear to be capable of improving L/D ratio of a given wing, primarily through drag reduction. Unlike the control by blowing discussed above, the use of flabs results in only a modest improvement in the angle-of-attack envelope.

7 Drag Reduction

7.1 Introductory Remarks

Whenever there is relative motion between a solid body and the fluid in which it is immersed, the body experiences a net force due to the action of the fluid. The component of this force parallel to the direction of motion is termed the drag, and the body will move at a constant speed when the thrust generated by its propulsion system is equal to the drag force. The total drag consists of skin friction, equal to the streamwise component of the integral of all shearing stresses over the body's surface, and pressure drag, equal to the streamwise component of the integral of all normal forces. Flow Separation is the major source of pressure drag with additional contributions due to displacement effects of the boundary layer, wave resistance in a supersonic flow or at an air/water interface, and drag induced by lift on a finite body. The object of this section is to review available methods to reduce the total drag. For a vehicle, the reduced drag means longer range, reduced fuel cost/volume, higher payload, or increased speed. For pipes and channels, where close to 100% of the drag is due to skin friction, drag reduction can result in improved throughput, reduced pumping power, or reduced duct size and cost.

Nature provides numerous instances where drag reduction is essential for the survival of many species of air and marine animals. In here, we cite instead two examples of the importance of minimizing the drag of man-made vehicles. At present, the annual fuel bill for all commercial airlines in the United States is about \$10 billion (Hefner, 1988). At subsonic cruising speeds, approximately half of the total drag of conventional takeoff and landing aircraft is due to skin friction. Hence, a reduction in skin-friction drag of 20% translates into an annual fuel saving of \$1 billion. Not only is this a substantial sum, but also many believe that a return of the 1973's energy crisis is inevitable (Phillips, 1979; Kannberg, 1988). While the world may have another 100-year supply of natural petroleum, it is estimated that the United States supply will be virtually exhausted early in the next century (Nagel et al., 1975). Fuel conservation is certainly an important tool to ward off future shortages. The second example is from the military sector. The amount of propulsive power available for an underwater vehicle is limited by the volume allocated to its power plant and the efficiency of the various propulsive components. For these vehicles, about 90% of the total drag is due to skin friction. Accordingly, a reduction in skin-friction drag of 20% translates into an increase in speed of 6.8%. Although modest, this extra speed may be vital for the survival of a submarine being chased by another underwater vehicle.

Attempts to reduce drag go back to antiquity as mentioned in Section 2. Streamlining and other control methods summarized in Section 6 can eliminate most of the pressure drag due to flow separation. Some form drag remains, however, even when the flow remains attached to the trailing edge. Due to the displacement effects of the boundary layer, the pressure distribution around the body differs from the symmetric distribution predicted by potential flow theory. This remnant drag can be reduced by keeping the boundary layer as thin as possible. For a blunt body, passive and active methods to reduce wake momentum defect are available (Viswanath, 1995). Boundary layer tripping for advancing transition and trailing-edge splitter plate for disrupting the vortex formation process are among the passive techniques to modify the flow field around a bluff body. Continuous or pulsating base bleed is used to modify the flow in the separated region. The latter with zero net mass addition has been shown to be very effective when pulsating at twice the Kármán shedding frequency (Williams and Amato, 1989).

Wave resistance and induced drag can also be reduced by geometric design. By sweeping the wings of a subsonic aircraft, drag divergence is delayed to higher Mach numbers, thus allowing the aircraft to fly at higher speeds without experiencing a sudden increase in drag. Additionally, the so-called area rule or coke-bottle effect typically leads to a factor of 2 reduction in wave drag at Mach number of 1 (Whitcomb, 1956). For surface ships, where typically half the drag is due to wave resistance, bow and stern bulbs can reduce the energy dissipated into waves at the air/water interface. An even simpler solution to reduce wave drag is to operate the ship well below the

hull design speed, as is the case for supertankers. The induced drag of an aircraft's wing, about 25% of the airplane's total drag at subsonic cruising speeds, is inversely proportional to its aspect ratio and, hence, a lifting surface is typically designed with as large an aspect ratio as permissible by structural considerations and desired degree of maneuverability. End plates or other vortex diffusers can also be used to further reduce the induced drag.

Most of the current research efforts are directed towards reducing the skin-friction drag, and this topic will occupy the remainder of this section. According to Bushnell (1983), the leverage in this area of research is quite considerable and justifies the study of unusual or high-risk approaches on an exploratory basis.

Let us start by estimating typical Reynolds number for the vehicles whose drag is to be minimized. A commercial aircraft traveling at a speed of 300 m/s would have a unit Reynolds number of $2\times10^7/m$ at sea level and $1\times10^7/m$ at an altitude of 10 km. Due to the much smaller kinematic viscosity of water, an underwater vehicle moving at a modest speed of 10 m/s ($\approx$ 20 knots) would have the same unit Reynolds number of $1 \times 10^7/m$.

Three flow regimes can be identified for the purpose of reducing skin friction. First, if the flow is laminar, typically at Reynolds numbers based on distance from leading edge $< 10^6$, then methods of reducing the laminar shear stress are sought. Any or a combination of the following techniques can be used to lower the laminar skin friction: wall motion; injection of fluid normal to the wall; adverse pressure gradient; wall heating in air; or wall cooling in water. Note that any of these methods will promote flow instability and separation. These tendencies have to be carefully considered when deciding how far to go with the attempt to lower C_f. Two other techniques can be used to lower laminar skin-friction. Narasimha and Ojha (1967) considered the higher order effects of moderate longitudinal surface curvature. Their similarity solutions show a definite decrease in skin friction when the surface has convex curvature in all cases including zero pressure gradient. Narasimha and Ojha attributed the decrease in C_f to the fact that the velocity in the potential flow region tends to decrease away from the surface. The second technique is used in rarefied gas flows. Appropriate surface preparation could be used to introduce a slip velocity at the wall and, thus, lower the tangential momentum accommodation coefficient (Steinheil et al., 1977; Gampert et al., 1980).

Secondly, in the range of Reynolds numbers from 1×10^6 to 4×10^7, active and passive methods to delay transition as far back as possible are sought. These techniques were reviewed in Section 5, and can result in substantial savings. As shown in Figure 5, the skin-friction coefficient in the laminar flat plate can be as much as an order of magnitude less than that in the turbulent case. Note, however, that all the stability modifiers discussed in Section 5.1 result in an increase in the skin friction over the unmodified Blasius layer. The object is, of course, to keep the penalty below the saving, i.e., the net

drag will be above that of the flat-plate laminar boundary-layer but well below the viscous drag in the flat-plate turbulent flow.

Thirdly, for $Re > 4 \times 10^7$, transition to turbulence cannot be delayed with any known practical method without incurring a penalty that exceeds the saving. The task is then to reduce the skin-friction coefficient in a turbulent boundary layer. This topic will be covered in the following section. Relaminarization will be covered in Section 7.3, although achieving a net saving here is problematic at present.

For a vehicle with a unit Reynolds number of $1 \times 10^7/m$, the first regime exists in the first few centimeters and, hence, is of no great consequence. Transition delay is feasible on the wing and other appendages of an aircraft but not on its much longer fuselage. On the fuselage, where half of the skin-friction drag takes place, some alteration of the turbulence structure is sought. Short underwater bodies, such as torpedoes, are ideal targets for applying transition control methods. On the much longer submarine, these techniques are feasible on the first few meters of its surface. Beyond that, turbulence drag reduction or relaminarization is sought.

7.2 Turbulent Flows

At very large Reynolds numbers, transition can no longer be postponed and the boundary layer becomes turbulent and, thus, an excellent momentum conductor. Such a flow is less prone to separation but is characterized by large skin friction. Several techniques are available to reduce the turbulent skin-friction coefficient, but only very few are in actual use, the basic reason being that the majority of these methods are relatively new and, thus, are still in the research and development stage. The various drag reduction methods will be grouped into three categories: techniques that reduce the near-wall momentum; methods involving the introduction of foreign substances; and techniques involving the geometry. Three excellent reviews of the various turbulent skin-friction reduction methods are available, Bushnell (1983), Bandyopadhyay (1986), and Wilkinson et al. (1988). Bushnell and McGinley (1989) provide a more general article addressing turbulence control in wall flows to achieve a variety of desired goals. They summarize the known sensitivities of wall-bounded flows to various inputs having a first-order influence upon the flow structures.

Reduction of Near-Wall Momentum. Methods of skin-friction drag reduction in turbulent boundary layers that rely on reducing the near-wall momentum are reviewed in this section. One brute force way of achieving drag reduction is to lower the mean-velocity gradient at the wall or make the curvature of the velocity profile there as positive as possible, as was done in the laminar case. The influence of wall transpiration, shaping or heat transfer on the mean velocity profile is complicated by the additional effects of these

modulations on the Reynolds stress term. However, these influences are qualitatively in the same direction as in the simpler laminar case. Thus, lower skin friction is achieved by driving the turbulent boundary layer towards separation. This is accomplished by injecting fluid normal to the wall, shaping to produce adverse pressure gradient, surface heating in air, or surface cooling in water. These methods of control in general result in an increase in turbulence intensity (Wooldridge and Muzzy, 1966).

Although in the reverse flow region downstream of the separation line the skin friction is negative, the increase in pressure drag is far more than the saving in skin-friction drag. The goal of these methods of control is to avoid actual separation, i.e., lower C_f but not any lower than zero (the criterion for steady, two-dimensional separation).

Two additional methods to reduce the near-wall momentum are tangential injection and ion wind. In the former, a low-momentum fluid is tangentially injected from a wall slot. For some distance downstream, the wall senses the lower injection velocity and not the actual freestream. Bushnell (1983) terms this situation a wall wake as opposed to a wall jet (used in high lift devices to keep the flow attached). Ion wind, generated by an electrode in the wall and discharging either to space or to a ground on the wall further downstream, causes an increase in the normal velocity component near the wall. Since there is no net mass transfer through the surface, the near-wall longitudinal momentum is again reduced and the boundary layer is driven towards separation (Malik et al., 1983). The source and amount of power to produce a measurable drag reduction are among the outstanding issues to be considered with this technique. Among the possibilities is the use of the natural buildup of static electricity on an aircraft which at present is dissipated at discharge points to avoid large-scale arcing.

In the case of tangential or normal injection, the source of fluid to be injected is important. Large ram drag penalty is associated with using freestream fluid, and reaching a break-even point is highly problematic. A lower loss source is fluid withdrawn from somewhere else to control transition or separation, for example from the wings and empennage of an aircraft. This point will be discussed further in a later subsubsection.

Howard et al. (1975) conducted finite-difference calculations to show the effect of single- and multi-slot injection on skin-friction drag of a fuselage shape typical of long-haul subsonic transport. The beneficial effect of injection is most pronounced immediately downstream of the slot exit and diminishes with distance from the slot. Performance deterioration is clearly a result of the mixing between the low-momentum slot flow and the high-momentum boundary-layer flow. Note, however, that the asymptotic level of skin friction with multi-slots is lower than that in the unperturbed flow. Without taking into account the system penalties for collecting, ducting, and injecting the secondary flow, Howard et al. (1975) computed a reduction in total skin-friction drag of the order of 50%. They maintain that further optimization

may provide even greater skin-friction reductions to help compensate for system losses.

Introduction of Foreign Substance. Turbulent skin-friction drag can be reduced by the addition of several foreign substances. Examples include long-chain molecules, surface-active agents and microbubbles in liquid flows, and small solid particles or fibers in either gases or liquids. In general, the addition of these substances leads to a suppression of the Reynolds stress production in the buffer zone that links the linear and the logarithmic portions of the mean velocity profile. Thus, the turbulent mixing is inhibited and a consequent reduction in the viscous shear stress at the wall is achieved.

Drag reduction by solutions of macromolecules (molecular weight $> 10^5$) is perhaps the more mature technology with close to 5000 research papers in existence (Virk, 1975; White and Hemmings, 1976; Hoyt, 1979; Hendricks et al., 1989; Nadolink and Haigh, 1995). Toms (1948) observed that the addition of few parts per million of polymethyl methacrylate to a turbulent pipe flow of monochlorobenzene reduced the pressure drop substantially below that of the solvent alone at the same flow rate. Successful long-chain molecules for water flow include carboxymethyl cellulose, guar gum, copolymer of polyacrylamide and polyacrylic acid, and polyethylene oxide. Skin-friction drag reduction of up to 80% is possible in both external and internal flows with 100 ppm or less of the largest molecules.

The viscosity of these dilute solutions of polymers is typically 10% higher than that of the solvents, although most polymer solutions are detectably shear thinning at higher concentrations (Berman, 1978). The polymer molecules at rest are in the form of spherical random coils in which each monomer is joined to the preceding one at a random angle. The onset of drag reduction is associated with the expansion of these coils outside the viscous sublayer. Hinch (1977) asserts that this unfolding explains the dramatic effects of few parts per million (by weight) on the drag. The effective hydrodynamic volume fraction shows large concentration once the polymer molecules are stretched. Therefore, it is the volume fraction of spheres just enclosing the separate polymers rather than the weight which is the appropriate measure of the added substance.

When the macromolecules are coiled, the viscosity of the dilute solution changes by a few percent, while if they are fully stretched the apparent viscosity increases by several orders of magnitude. Onset of drag reduction occurs when $D_M\, u_\tau/\nu = 0.015$, where D_M is the effective molecular diameter. This diameter is about two orders of magnitude less than the shortest dynamically significant length in a typical turbulent flow (Virk et al., 1967; Lumley, 1969). Numerous experiments have indicated that the drag reduction is associated with a thickening of the buffer layer and a corresponding shift of the logarithmic part to accommodate the larger buffer zone (Reischman and Tiederman, 1975). The effect of the additive may then be represented as a virtual slip at the wall (Virk et al., 1967).

The percentage drag reduction increases as the polymer concentration is increased and the buffer layer is thickened. This process tends to an asymptote when the buffer layer reaches the center of the pipe or the edge of the boundary layer. As the Reynolds number is increased at a given concentration, a second limit in drag reduction is reached when the macromolecules become fully stretched. Moreover, degradation or breaking of the molecules by the flow occurs at sufficiently high strain rates, with a consequent loss of the ability to reduce the drag (Berman and George, 1974). Because of this latter point, care has to be exercised when mixing the macromolecules into the solvent as well as when delivering the solution into the flow.

By injecting the polymer in different regions of the boundary layer, Wells and Spangler (1967), Wu and Tulin (1972) and McComb and Rabie (1979) have shown that the additive must be in the wall region for drag reduction to occur. Furthermore, the channel flow experiments of Tiederman et al. (1985) have clearly demonstrated that drag reduction is measured downstream of the location where the additives injected into the viscous sublayer begin to mix in significant quantities with the buffer region, i.e., $10 < u_\tau y/\nu < 100$. At streamwise locations where drag reduction does occur, the dimensionless spanwise streak spacing increases and the average bursting rate decreases, although the decrease in bursting frequency is larger than the corresponding increase in low-speed streak spacing. Tiederman et al. (1985) conclude that the polymers have a direct effect on the flow processes in the buffer region and that the linear sublayer appears to have a rather passive role in the interaction of the inner and outer portions of a turbulent wall layer.

Many mechanisms have been proposed to explain the experimental observations. Notable among these is the work of Lumley (1973; 1977), Landahl (1973; 1977), and the more recent quantitative theory by Ryskin (1987). According to Lumley's model, the macromolecules are expanded outside the viscous sublayer due to the fluctuating strain rate. The resulting increase in effective viscosity damps only the small dissipative eddies. The suppression of small eddies in the buffer layer leads to increased scales, a delay in the reduction of the velocity profile slope, and consequent thickening of the wall region. In the viscous sublayer, the scales remain unchanged since the effective viscosity of the dilute solution in steady shear is only slightly affected. In the buffer zone, the scales of the dissipative and energy containing eddies are roughly the same and, hence, the energy containing eddies will also be suppressed resulting in reduced momentum transport and reduced drag.

Lumley's more conservative general hypothesis is not incompatible with Landahl's specific, rather speculative mechanism (Lumley and Kubo 1984). The polymer suppresses the small eddies responsible for the inflectional profile and the secondary instability in the buffer zone. Kim et al. (1971) have shown that the greatest turbulent kinetic energy production for a Newtonian boundary layer occurs near the beginning of the buffer zone at $y \approx 12\nu/u_\tau$.

A sharp maximum in the turbulent intensity, $\sqrt{\overline{u^2}}$, occurs at the same location. For a dilute solution of drag-reducing polymer, the peak of $\sqrt{\overline{u^2}}$ moves away from the wall and becomes much broader as compared to the solvent alone. Production of Reynolds stress in this important buffer zone is, thus, diminished.

The use of drag-reducing polymers in pipe lines is cost effective in some applications. When it was discovered that the winter cooling of crude oil in the Alaskan Pipeline had been underestimated, polymer additives offered an inexpensive alternative to increasing the number or power of the pumping stations. Long-chain molecules are presently used in waste-disposal plants, fire-fighting equipment and high-speed water-jet cutting. For surface ships or underwater vehicles practical considerations include cost of polymer, how, with what, and when to mix it, as well as how to eject it into the boundary layer, i.e. using pumps or pressurized tanks, through slots or porous surfaces, etc. A very important additional consideration is the portion of the payload that has to be displaced to make room for the additive. Oil companies appear to have concluded that the use of polymer for supertankers is just at the break-even point economically. For submarines and torpedoes, where space is a prime consideration, it seems that the volume occupied by the additive is a more important obstacle to its routine use.

Other substances that can be added to a clear fluid to reduce the skin-friction drag include surfactants (Savins, 1967; Patterson et al., 1969; Zakin et al., 1971; Aslanov et al., 1980), microbubbles (McCormick and Bhattacharya, 1973; Bogdevich and Malyuga, 1976; Bogdevich et al., 1977, Madavan et al., 1984; 1985; Merkle and Deutch, 1985; 1989), large length-to-diameter particles, e.g. fibers, (Hoyt, 1972; Lee et al., 1974; McComb and Chan, 1979; 1981), and spherical particles (Soo and Trezek, 1966; Pfeffer and Rosetti, 1971; Radi, 1974; Radin et al., 1975; Povkh et al., 1979). Lumley (1977; 1978) argues that the same mechanism discussed in conjunction with the polymer case governs the interaction of most of these substances with the turbulent boundary layer. The additives affect only the dissipative scales of the turbulence and thus increasing the scales of dissipation in the buffer layer. The energy containing eddies are also suppressed and, consequently, the momentum transport is reduced.

A surface-active substance, such as soap, is that which when dissolved in water or in an aqueous solution reduces its surface tension. The majority of surfactants appear to reduce the turbulent skin-friction drag only in the presence of electrolytes. These additives are stable against mechanical destruction, a certain advantage over polymer molecules which break down when the strain rate is sufficiently high. Although drag-reducing polymer flows undergo transition at a lower Reynolds number than Newtonian flows (Lumley and Kubo, 1984), some recent experiments indicate that surfactants are very effective in delaying laminar-to-turbulence transition (A. J. Smits, private communication; Sabadell, 1988).

The idea of placing a thin layer of gas between the wall and its water boundary layer dates back to the last century. Substantial drag reductions are potentially possible due to the lower density of the gas. Unfortunately, the various instabilities associated with gas/liquid interface result in drag increase. Extremely small gas bubbles (microbubbles) injected through a porous wall or produced by electrolysis do not suffer from the stability problems of a gas film and result in skin-friction reduction as high as 80%. Maximum reduction is obtained when the gas volume fraction approaches the bubble packing limit. Skin friction is reduced because of the substantially lower density and also because of the usual increase in bulk viscosity due to particles (Batchelor and Green, 1972), which damps the small scale motions in the buffer layer. Legner (1984) presents a simple phenomenological model to predict microbubble drag-reduction in turbulent boundary layers. Application of the microbubbles technique for surface ships is quite feasible. Compressed atmospheric air is injected through a micro-porous skin over portions of the hull. This has the additional advantage of reducing fouling drag and fouling maintenance costs, since water is kept away from the hull surface. The situation is different for underwater vehicles. There, a source of air is not readily available and using electrolysis for bubble production will not yield net energy saving. Moreover, the presence of bubbles may adversely affect the flow-induced noise, an important consideration for naval vehicles.

Spherical or large length-to-diameter particles can be used in both air and water flows. For spherical particles, drag reduction of up to 50% is feasible for certain parameter values, although drag increase is also possible. Heavy but small particles may reduce the drag by inducing a stable density stratification near the wall thus driving the turbulence towards relaminarization. Lighter particles that are large enough to interact with the smallest turbulence scales reduce the drag through the same mechanism as in the polymer case, i.e. suppressing the dissipative eddies and increasing the scale of dissipation.

McComb and Chan (1981) report up to 80% drag reduction using the naturally occurring macro-fiber chrysotile asbestos dispersed at a nominal concentration of 300 ppm by weight in a 0.5% aqueous solution of Aerosol OT. The individual fibrils of chrysotile asbestos have a mean diameter of $40\,nm$ and a mean length-to-diameter ratio in an undegraded suspension in the range of 10^3–10^4. Like polymers, macro-fibers readily break down (McComb and Chan, 1979) and have to be carefully dispersed into the solvent and delivered to the boundary layer. In principle, fibers can also be used in gases, although their drag-reduction potential has yet to be demonstrated.

Methods Involving Geometry. Under this classification are some of the most recently researched techniques to reduce the turbulent skin-friction drag. These include large eddy breakup devices, riblets, compliant surfaces, wavy walls, and other surface modifications. The book edited by Bushnell and Hefner (1990) offers comprehensive reviews of these and other drag re-

duction strategies. With few exceptions, there is little theoretical basis for how these geometrical modifications affect the skin friction and most of the present knowledge comes from experiments. Needless to say, the lack of analytical framework makes optimization for a given flow condition as well as extension to other flow regimes very tedious tasks.

The large eddy breakup devices (LEBUs) are designed to sever, alter or break up the large vortices that form the convoluted outer edge of a turbulent boundary layer. A typical arrangement consists of one or more splitter plates placed in tandem in the outer part of a turbulent boundary layer. It is of course very easy to reduce substantially the skin friction in a flat-plate boundary layer by placing an obstacle above the surface. What is difficult is to ensure that the device's own skin-friction and pressure drags do not exceed the saving. The original screen fence device of Yajnik and Acharya (1978) and the various sized honeycombs used by Hefner et al. (1980) did not yield a net drag reduction. In low-Reynolds-number experiments, very thin elements placed parallel to a flat plate have a device's total drag that is nearly equal to laminar skin friction. A net drag reduction of the order of 20% is feasible with two elements placed in tandem with a spacing of $\mathcal{O}\,[10\,\delta]$ (Corke et al. 1980; 1981). These ribbons have typically a thickness and a chord of the order of 0.01δ and δ, respectively, and are placed at a distance from the wall of 0.8δ. Several experiments report a more modest drag reduction (Hefner et al., 1983) or even a drag increase, but it is believed that a slight angle of attack of the thin element can result in a laminar separation bubble and a consequent increase in the device pressure drag. Flat ribbons at small, positive angles of attack produce larger skin-friction reductions. This is consistent with the analytical result that a device producing positive lift away from the wall is more effective (Gebert, 1988). In any case, a net drag reduction should be achievable, at least for devices having chord Reynolds numbers $< 10^6$, if extra care is taken to polish and install the LEBU.

Net drag reduction has been documented even in the presence of favorable or adverse pressure gradient in the main flow (Bertelrud et al., 1982; Plesniak and Nagib, 1985). Additionally, Anders and Watson (1985) have demonstrated that an LEBU having an airfoil shape is nearly as effective in reducing the net drag as a flat ribbon. A wing is several orders of magnitude stiffer than a thin ribbon, a certain advantage for extending the technique to field conditions. At flight Reynolds and Mach numbers, the possibility of paying for transitional or turbulent skin-friction as well as wave drag on the device itself is real (Anders et al., 1984; 1988) and achieving net drag reduction in this circumstance is problematic at present (Anders, 1990). For an airplane, an LEBU is likely to take the form of a ring around the fuselage.

Two analytical attempts to explain the mechanisms involved with the large eddy breakup devices are noted in here. Basically, the LEBU acts as an airfoil on a gusty atmosphere and a vortex unwinding mechanism is activated. Dowling's (1985) inviscid model indicates that the vorticity shed

from the LEBU's trailing edge as a result of an incident line vortex convected past the device tends to cancel the effect of the incoming vortex and to reduce the velocity fluctuations near the wall. Atassi and Gebert (1987) and Gebert (1988) model the incoming turbulent rotational flow as two- or three-dimensional harmonic disturbances. They use the rapid distortion approximation and unsteady aerodynamic theory to compute the fluctuating velocity downstream of thin-plate and airfoil-shaped devices. The fluctuating normal velocity component is most effectively suppressed for a range of frequencies that scales with the freestream velocity and the device chord. This important result determines the optimum size of an LEBU by selecting this frequency range to correspond to that of the large-scale eddies in a given turbulent boundary layer.

The second geometrical modification is the riblets. Small longitudinal striations in the surface, interacting favorably with the near-wall structures in a turbulent boundary layer, can produce a modest drag reduction in spite of the increase in surface area. The early work employed rectangular fins with height and spacing of $\mathcal{O}\,[100\,\nu/u_\tau]$. The turbulent bursting rate was reduced by about 20% and a modest 4% net drag reduction was observed (Liu et al., 1966). In a later refinement of this technique, Walsh and his colleagues at NASA-Langley examined the drag characteristics of longitudinally ribbed surfaces having a wide variety of fin shapes that included rectangular grooves, V-grooves, razor blade grooves, semi-circular grooves, and alternating transverse curvature (Walsh and Weinstein, 1978; Walsh, 1980; 1982; 1983; 1990; Walsh and Lindemann, 1984). A net drag reduction of 8% is obtained with V-groove geometry with sharp peak and either sharp or rounded valley. Optimum height and spacing of the symmetric grooves are about $15\,\nu/u_\tau$. Although these dimensions would be extremely small for the typical Reynolds numbers encountered on an airplane or a submarine (peak-to-valley height $\sim 35\,\mu m$), such riblets need not be machined on the surface. Thin, low specific gravity plastic films with the correct geometry on one side and an adhesive on the other side are presently available commercially and existing vehicles could be readily retrofitted. In fact, these tapes were successfully tested at $M = 0.7$ on a T-33 airplane and on a Lear jet. The performance of the riblets in flight was similar to that observed in the laboratory (Anders et al., 1988). In water, riblets were employed on the rowing shell during the 1984 Summer Olympic by the United States rowing team. Similar riblets were also used on the submerged hull of the winner of the 1987 America's Cup yacht race, the Stars and Stripes, with apparent success.

Riblets are effective in the presence of moderate adverse and favorable pressure gradients. The loss of drag-reducing effectiveness as flow conditions vary off-design is gradual. Moreover, the percentage drag reduction slowly decreases to zero as the yaw angle between the flow and the grooves goes up to 30°. Surprisingly, drag does not increase at yaw angles $> 30°$. Remaining practical problems include cost, weight penalty, particulate clogging, ultravi-

olet radiation, and film porosity and resistance to hydraulic fluids and fuel.

Curiously, fast sharks have a surface covering of dermal denticles with flow-aligned keels having the optimal riblet spacing as determined by Walsh (Bechert et al., 1985). As the shark grows, new keels are added onto the sides of the denticles without changing the keel-to-keel spacing. A clue to how riblets result in a net drag reduction despite the increase in wetted area is provided by the experiment of Hooshmand et al. (1983) who showed that, for an optimum V-grooved surface, C_f is reduced by 40% in the valleys and increased by 10% at the peaks. It appears that the riblets severely retard the flow in the valleys, which places a slip boundary condition upon the turbulence production process. Lumley and Kubo (1984) argue that the streamwise vortices in the near-wall region are forced to negotiate the sharp peaks of the riblets, causing increased losses. To stay in equilibrium, the eddies must increase their energy gain, and one way to do that is to grow larger (energy gain $\sim$ (size)^2; loss $\sim$ (size)). As was the case with polymers, the larger scales result in the secondary instability and the sharp change in profile slope occurring farther from the wall. The mean velocity is, thus, higher for the same friction velocity and the coefficient of skin friction is reduced.

The third geometrical modification to reduce the skin friction is fixed or moving wavy walls. Kendall (1970) observed that the integrated skin-friction in a turbulent boundary layer over rigid, sinusoidal waves can be as much as 25% below that over an equivalent flat surface. Kendall's waves were relatively shallow having a height-to-wavelength ratio of $h/\lambda = 0.028$, with $\lambda = \mathcal{O}[\delta]$. Sigal (1971) reported a reduction in integrated skin-friction of about 12% when using a 10% larger amplitude waves ($h/\lambda = 0.031$) than that used by Kendall. The transverse waves provide alternating regions of longitudinal concave and convex curvatures along with alternating adverse and favorable pressure gradients. The coincidence of convex curvature and favorable pressure gradient promote relaminarization as the wave crests are approached, and the near-wall momentum is reduced in regions having adverse pressure gradient. Accordingly, the integrated skin-friction drag is reduced. Unfortunately, viscous forces cause a downstream phase shift between the pressure distribution and the wave relative to the 180° out-of-phase relationship predicted from potential flow theory for a sinusoidal wave. This phase shift causes an additional pressure drag not present in the flat-surface case. The net result is that the total drag for the wavy surface increases despite the decrease in skin friction. Cary et al. (1980) argue that there may be two approaches to overcome this problem. First, since pressure drag varies as $(h/\lambda)^2$, further reduction of h/λ may yield a net drag reduction. Secondly, certain non-sinusoidal waves may have more favorable pressure and curvature effects on the viscous drag and a less skewed pressure distribution relative to the waves and, therefore, less pressure drag. Cary et al.'s numerical results indicate the soundness of the first approach. Net drag reduction of about 13% is attained for the optimum h/λ of 0.005. This result seems to be insensitive

to the ratio of wave height to the viscous scale at least for $hu_\tau/\nu < 33$. Experiments to test the second approach were only partially successful (Lin et al., 1983). Skewed waves with gradual, straight downstream-facing slope and steeper, sinusoidal upstream-facing surface have lower pressure drag than a symmetric sine-wave. However, the asymmetric surface is not as effective in reducing the viscous drag, with the result that the net drag reduction is only 1–2%, hardly worth the effort (Wilkinson et al., 1988).

Moving wavy walls are divided into two categories: driven, non-interactive walls and compliant surfaces. In the former technique, a flat or wavy wall is translated in the streamwise direction. The rectilinear wall motion essentially acts as a slip boundary condition and reduces the skin friction. Obviously the boundary layer could be completely eliminated when $U_{\text{wall}} = U_\infty$. A moving wavy wall can produce a thrust at high enough translational speed but causes an additional pressure drag at lower speed. In any case, this method of control is in general impractical and is used mainly to provide controlled experiments to determine what type of wave motion is required to achieve a given result, much the same as the laminar flow control case.

Wall motion can also be generated by using a flexible coating with sufficiently low modulus of rigidity. The idea is very appealing if a particular kind of fluid/solid interaction yields a net drag reduction. Covering a vehicle with a compliant coating is relatively simple, does not require modification of existing design, does not require slots, ducts or internal equipment of any kind, and no energy expenditure is needed. The search for such a surface has been very elusive, however, despite reports of substantial drag reduction by some researchers. Irreproducibility seems to be an outstanding characteristic of the body of compliant coating experimental evidence (Bushnell et al., 1977; McMichael et al., 1980; Gad-el-Hak, 1986b; 1986c; 1987). The window of opportunity for a favorable coating response is rather narrow. For flow speeds below the transverse wave speed in the solid, no significant interaction between the fluid and the compliant surface takes place. Above the transverse wave speed, ample opportunity for interaction exists; however, hydroelastic instabilities appear and the resulting large-amplitude surface waves increase the drag because of the roughness-like effects (Gad-el-Hak et al., 1984; Gad-el-Hak, 1986c; 1996a). A second constraint concerns the density ratio of the fluid and the solid. The extremely low density of air makes finding a reasonable coating material highly unlikely, although in liquids the situation is different. Flexible surfaces that interact favorably with Tollmien-Schlichting waves in water boundary layers are readily available (Gad-el-Hak, 1996a). For turbulent boundary layers, the task is to find a coating that responds to the flow, particularly to its preburst wall pressure signature, with a surface motion that can alter, modify or interrupt the sequence of events leading to a burst. The analytical work of Purshouse (1977) indicates that an anisotropic coating would be more likely to achieve a net drag reduction in a turbulent boundary layer.

Other geometric modifications on the surface with a drag-reducing potential include fixed waves aligned with the flow (essentially large-scale riblets), micro air-bearings, compound or three-dimensional riblets, sieves, furry (wheatfield-type) surfaces, and sword-fish configuration. These techniques have been reviewed by Bushnell (1983) and more recently by Wilkinson et al. (1988). The last of these methods is the most straightforward. As a boundary layer thickens, the Reynolds number increases and the coefficient of skin friction decreases, with the result that the local skin friction is higher in the forward part of a vehicle and quite low in the aft end. Consider, for example, a 50-meter-long aircraft with a unit Reynolds number of $10^7/m$, and ignore pressure gradient and other effects. Near the nose, the skin-friction coefficient is about 0.003 (Figure 5). Near the tail, $Re \approx 5 \times 10^8$ and $C_f \approx 0.0018$, i.e. 40% lower . By substantially reducing the wetted area of the forebody, the sword-fish configuration, drag reduction may be attainable. This technique is particularly useful when combined with a convex aftbody.

7.3 Relaminarization

Several articles define and explain the reversion of a turbulent flow to the laminar state, variously also known as retransition, inverse or reverse transition, or relaminarization (Preston, 1958; Patel and Head, 1968; Bradshaw, 1969). Narasimha and Sreenivasan (1979) provide a comprehensive review and analysis of the phenomenon. Instances of relaminarization may be found in a stably stratified atmosphere, spatially or temporally accelerated shear flows, coiled pipes, swirling flames, tip vortices behind finite lifting surfaces, far wakes of finite drag-producing bodies, air flow as it progresses from the trachea to the segmental bronchi in human lungs, and shear flows subjected to magnetic fields. Various authors use one or more of the following syndromes to diagnose the reversion of a turbulent flow: reduction in heat transfer or skin-friction coefficient, cessation of bursting events near the wall or entrainment of potential flow at the outer region of a boundary layer, reduction in high-frequency velocity fluctuations, breakdown of the log-law in the wall layer, spreading of intermittency to wall region, and overlapping of energy-containing and dissipating eddy scales. In the quasi-laminar state, the velocity fluctuations are not necessarily zero but rather their contribution to the dynamics of the mean flow becomes inconsequential. In other words, the turbulent fluctuations inherited from the previous history of the flow are no longer influencing the transport of mass, momentum or energy. Narasimha and Sreenivasan (1979) adopt a pragmatic definition of reversion. They maintain that a flow has relaminarized if its subsequent development can be understood without recourse to any model for turbulent shear flow.

The most obvious mechanism for the occurrence of relaminarization is dissipation. When the Reynolds number goes down in a turbulent flow, for example by enlarging a duct or by branching a channel flow, the viscous dissipation may exceed the production of turbulent energy and the flow may

revert to a quasi-laminar state. This type of reversion tends to be rather slow. Turbulent energy can also be destroyed or absorbed by the work done against external forces such as buoyancy (e.g., in stably stratified fluids), centrifugal (e.g., in convex boundary layers), or Coriolis (e.g., in rotating channel flows). The governing parameter in these absorptive-type reversion is the Richardson number (Ri) and relaminarization proceeds rapidly once the critical value of Ri is exceeded. In both dissipative- and absorptive-type of reversion, the turbulence energy is decreased but more significantly the velocity components that generate the crucial Reynolds stresses are "decorrelated." This explains the strong effects on turbulence of, say, a very mild positive curvature (So and Mellor, 1973; Smits and Wood, 1985). In this case, the amplitude as well as the phase of the different components of the fluctuating motion are affected by the additional strain rate imposed upon the flow, particularly away from the wall.

The third mechanism to effect relaminarization is observed in highly accelerated flows. Narasimha and Sreenivasan (1973) argue that, in the outer layer of such flows, the pressure forces dominate over nearly frozen Reynolds stress field. The $\overline{uv}$ term remains at about the same level as the zero-pressure-gradient case over much of the boundary layer. Near the wall, however, dissipation dominates and the flow is stabilized by the acceleration. The turbulence-re-energizing bursts diminish in frequency and may stop altogether and a thin new laminar boundary layer grows from the wall within the old boundary layer. According to Morkovin (1988), the turbulence in the outer layer is "starved" and the inner laminar layer is "buffeted" by the decaying, wake-like turbulence of the outer region. The skin friction and the heat transfer rate in the relaminarized inner layer is less than those expected in a corresponding turbulent flow.

Narasimha and Sreenivasan (1979) assert that a number of different reverting flows can be considered in light of the three archetypes summarized above. It is not uncommon, however, to effect relaminarization through a combination of mechanisms rather than a single one. In internal flows, relaminarization can be accomplished by gentle wall injection (to avoid separation) or by wall heating (for gases). In both these cases, the flow accelerates thus activating the third mechanism above. Moreover, when a gas is heated its kinematic viscosity is increased resulting in a lower Reynolds number that may fall below the critical value, thus activating the first mechanism.

In external flows, equation (17) indicates that wall suction, surface heating in liquids or surface cooling in gases, may have the same effect on the near-wall region of a turbulent boundary layer as favorable pressure gradient. It appears that only the first of these stimuli has been experimentally demonstrated. Dutton (1960) observed that a suction coefficient $C_q \approx 0.01$ is sufficient to relaminarize a boundary layer at $Re = \mathcal{O}\left[10^6\right]$. The initially turbulent flow approaches the laminar asymptotic state (Section 5.1) appropriate to the particular value of C_q used. Although the mean velocity gradient near the

wall is increased, the Reynolds shear stress is reduced at a faster rate leading to a reduction in the turbulent energy production.

The question of immediate concern to this section is whether or not suction, or in fact any of the other reversion stimuli, is a viable drag reduction method for turbulent boundary layers. The suction rate necessary for relaminarization is too high to be applied profitably over an entire surface, although it may be feasible to apply massive suction through a spanwise slot (perhaps enough to ingest the entire mass flow in the boundary layer) followed by gentle suction (or any of the other stability modifiers discussed in Section 5.1) to prevent transition of the newly formed laminar sublayer. This issue will be discussed again in the next subsubsection.

Convex (or positive) curvature affects the boundary layer locally in much the same way as a large eddy breakup device. With a relatively large radius of curvature, of the order of $10\,\delta$, positive Reynolds stress is produced in the outer flow and the wall shear is reduced. Downstream of the end of the curvature region, the flow relaxes very slowly to its unperturbed state. Wilkinson et al. (1988) suggest that a convex surface may be better suited for drag reduction than an LEBU device, particularly in supersonic flows where wave drag penalty on the LEBU blade is rather large. Obviously a vehicle surface cannot be all convex and short regions of concave curvature on the way to the convex portions are unavoidable. Bushnell (1983) speculates that the limited extent of the concave regions may not allow formation of any lasting alterations to the turbulent structures. Net reductions of drag of the order of 20% appear to be obtainable using surface curvature. Little research is available on the feasibility of using other relaminarization techniques to achieve drag reduction.

7.4 Synergism

Ideally, one searches for combinations of drag reduction methods where the total favorable effect is greater than the sum. For example, Lee et al. (1974) have shown that the use of polymers and fibers together can produce much larger reduction in skin friction than either additive alone. A slightly different strategy, but perhaps no less beneficial, is to employ a second control method that reduces the drag penalty of a given technique while adding some saving of its own. An example of that is the use of fluid that is being withdrawn from a certain portion of a vehicle for injection into another location, thus avoiding the ram drag penalty associated with blowing freestream fluid. For an aircraft, tangential slot injection or normal distributed injection may be used to reduce the skin friction on portions of the fuselage as discussed earlier. Possible sources of low-loss air include LFC suction from the wings and empennage, relaminarization slots on the fuselage, and active or passive bleed air for separation control.

Several possible combinations of drag reduction techniques were briefly mentioned elsewhere in this article. The sword-fish configuration (small wet-

ted area) may be used in the forward part of a vehicle where the local skin friction is high followed by the rest of the body where the boundary layer is thicker and the skin-friction coefficient is low. A nose spike followed by a short region of concave curvature then a longer convex portion may be used in supersonic flows. Massive suction through a spanwise slot may be used to ingest the entire mass flow in a turbulent boundary layer followed by any of the stability modifiers discussed in Section 5.1 to maintain the growing laminar boundary layer downstream.

The suction rate necessary for establishing an asymptotic turbulent boundary layer independent of streamwise coordinate ($\mathrm{d}\delta_\theta/\mathrm{d}x = 0$) is much lower than the rate required for relaminarization, but still not low enough to yield net drag reduction. For $Re = \mathcal{O}\left[10^6\right]$, Favre et al. (1966), Rotta (1970) and Verollet et al. (1972), among others, report an asymptotic suction coefficient of $C_q \approx 0.003$. From equation (20) rewritten for a steady, incompressible, zero-pressure-gradient boundary layer on a flat plate, the corresponding skin-friction coefficient is $C_f = 2\,C_q = 0.006$, indicating higher skin friction than if no suction was applied. The problem is that fluid withdrawn through the wall has to come from outside the boundary layer where the streamwise momentum per unit mass is at the relatively high level of U_∞, as was discussed in Section 5.1 in connection with using suction for transition delay. To achieve a net drag reduction with suction, the process must be further optimized. The results of Eléna (1975; 1984) and more recently of Antonia et al. (1988) indicate that suction causes an appreciable stabilization of the low-speed streaks in the near-wall region. The maximum turbulence level at $y^+ \approx 13$ drops from 15 to 12% as C_q varies from 0 to 0.003. More dramatically, the tangential Reynolds stress near the wall drops by a factor of 2 for the same variation of C_q. The dissipation length scale near the wall increases by 40% and the integral length scale by 25% with the suction.

Gad-el-Hak and Blackwelder (1987b; 1989) suggest that one possible means of optimizing the suction rate is to be able to identify where a low-speed streak is presently located and apply a small amount of suction under it. Assuming that the production of turbulent energy is due to the instability of an inflectional $U(y)$ velocity profile, one needs to remove only enough fluid so that the inflectional nature of the profile is alleviated. An alternative technique that could conceivably reduce the Reynolds stress is to inject fluid selectively under the high-speed regions. The immediate effect would be to decrease the viscous shear at the wall resulting in less drag. In addition, the velocity profiles in the spanwise direction, $U(z)$, would have a smaller shear, $\partial U/\partial z$, because the injection would create a more uniform flow. Since Swearingen and Blackwelder (1984) have found that inflectional $U(z)$ profiles occur as often as inflection points are observed in $U(y)$ profiles, injection under the high-speed regions would decrease this shear and hence the resulting instability. Since the inflectional profiles are all inviscidly unstable with growth rates proportional to the shear, the resulting instabilities would be weak-

ened by the suction/injection process. Gad-el-Hak and Blackwelder propose to combine suction with non-planar surface modifications. Minute longitudinal roughness elements if properly spaced in the spanwise direction greatly reduce the spatial randomness of the low-speed streaks (Johansen and Smith, 1986). By withdrawing the streaks forming near the peaks of the roughness elements, less suction should be required to achieve an asymptotic boundary layer. Recent experiments by Wilkinson and Lazos (1987) and Wilkinson (1988) combine suction/blowing with thin-element riblets. Although no net drag reduction is yet attained in these experiments, their results indicate some advantage of combining suction with riblets as proposed by the patent of Blackwelder and Gad-el-Hak (1990).

A large eddy breakup device influencing the outer structures of a turbulent boundary layer may be combined with drag reduction methods that mainly influence the near-wall region. Walsh and Lindemann (1984) show that the performance of riblets in the presence of an LEBU is approximately additive, not quite a synergetic effect. Wilkinson et al. (1988) propose using an LEBU device to reduce the free mixing between tangentially injected fluid and the boundary layer flow, thus extending the low skin-friction region. Bushnell (1983) suggests that the suction mass flow rate required to achieve relaminarization of a turbulent boundary layer may be reduced by the use of a large eddy breakup device ahead of the suction region.

The LEBU model of Gebert (1988) indicates that the fluctuating normal velocity component is most effectively suppressed for a particular incoming harmonic disturbance. The modest drag reduction currently achieved using an LEBU device in a natural boundary layer may, therefore, be greatly enhanced by cyclically generating the large outer structures using the method developed by Gad-el-Hak and Blackwelder (1987c). In this case, the large eddies arrive at a given location at a precisely controlled period that matches the optimum frequency for the LEBU device. Alternatively, Goodman's (1985) technique to generate closely spaced turbulent spots in the spanwise and streamwise directions may be used for tripping a laminar boundary layer. An LEBU device placed downstream will encounter more uniformly paced large eddies and its performance may be enhanced. Of course, in both schemes the penalty associated with artificially generating the large eddy structures must be considered.

Most of the combined drag reduction techniques discussed or proposed in this section are speculative, the reason being the scarcity of research in the area of synergism. Unguided by any theoretical framework and faced with the complexity of each of the methods used individually, one is tempted to stay away from the much more difficult situation when two or more techniques are combined. However, the potential for achieving a total effect larger than the sum should stimulate more research for combinations of method. In fact, in some situations one may not have much of a choice. Certain techniques, e.g. suction, may not yield net drag reduction and must, therefore, be combined

with something else to achieve the desired goal. Other methods, e.g. riblets, yield such modest drag reductions (less than 10%) that it may not be worth the effort implementing the individual technique.

8 Turbulence Augmentation

For some applications, the efficient mixing or transport mechanisms of turbulence may be required. For example, a turbulent boundary layer is in general more resistant to separation than a laminar one; turbulence is used to homogenize fluid mixtures and to accelerate chemical reactions; and turbulent heat exchangers are much more efficient than laminar ones. As an additional example, earlier transition may be required for some low-speed wind or water tunnel testing to simulate high Reynolds number conditions.

Consider the three flow regimes discussed in Sect. 7.1. For a zero-pressure-gradient boundary layer, transition is completed typically at a Reynolds number based on distance from leading edge of the order of 10^6. The critical Re below which perturbations of all wave numbers decay is about 6×10^4. To advance the transition Reynolds number, one may attempt to lower the critical Re, increase the growth rate of Tollmien-Schlichting waves, or introduce large disturbances that can cause bypass transition. The next issue is how to augment the turbulence for a shear flow that has already undergone transition, i.e. for $Re = 10^6$ and beyond. The obvious answer is to reverse the stimuli discussed earlier in connection with relaminarization. Injection instead of suction in external flows, decelerating flows instead of accelerating ones, negative curvature (concave) instead of positive curvature (convex), and so on. These stimuli will lead to an increase in turbulence production and enhanced mass, momentum and heat transfers. Roughness will also enhance the turbulence, but its associated drag must be carefully considered. Other devices to enhance the turbulent mixing include vane-type vortex generators, or wheeler-type or Kuethe-type generators as discussed earlier.

The turbulence levels in the near-wall region could be modestly augmented by freestream excitation. In a unique experiment, Bandyopadhyay (1988) used a pitching airfoil located outside a turbulent boundary layer to resonate the viscosity-dominated unsteady flow in a row of minute transverse square cavities at the wall. In a narrow band of pitching frequencies, the near-wall turbulence levels increased by as much as 6% while the rest of the boundary layer seemed transparent to the external disturbances. This result is particularly significant since it demonstrates that near-wall events may be controlled from the freestream and, therefore, that a dynamic coupling between disparate scales may exist.

The size, performance and efficiency of many engineering systems are often limited by the ability to transfer heat to or from the system. Consider the supercomputer, where the speed of computing is limited by the distance through which the electrons must travel at nearly the speed of light.

Electronic chips and other components must, therefore, be miniaturized and packaged tightly. Tremendous amounts of heat must be removed from a very modest surface area. The central processing unit of a present generation supercomputer is not much larger than, say, a refrigerator. In order to limit the temperature of the CRAY-2 to a tolerable range, its entire CPU is immersed in a dielectric liquid coolant (trade name FC-75). This is obviously an expensive, but perhaps unavoidable, approach to achieve the desired goal.

Convective heat transfer enhancement methods are reviewed by Bergles and Morton (1965), Bergles (1978), Bergles and Webb (1985), and Nakayama (1986). The simplest scheme involves the introduction of distributed roughness on the heat transfer surfaces. This would destabilize the wall region and intensify the mixing process leading to an increase in the convective heat transfer coefficient. Patera (1986) and Patera and Mikić (1986) introduced the concept of resonant heat transfer enhancement based on excitation of shear-layer instabilities in internal separated flows. In a two-dimensionally periodically grooved channel, Tollmien-Schlichting-like waves forced by the Kelvin-Helmholtz shear layer instabilities at the grooves' edge become unstable and take the form of self-sustained oscillations for Reynolds numbers greater than a critical value. For lower Re, oscillatory perturbation results in subcritical resonant excitation. For both laminar and turbulent flows, the resulting large-scale motions lead to significant lateral mixing and correspondingly dramatic enhancement of convective heat transfer coefficient.

9 Noise Control

Noise, or undesired sound, is generated from machines, vehicles moving in a fluid, or even natural phenomena. It is estimated that a single modern jet plane generates at takeoff more noise than the combined shouting power of the entire world's population! Noise control, a relatively young field of research, is required to maintain an acceptable (even pleasant) environment, to avoid detection of certain vehicles, and for the proper operation of sonars on underwater vehicles. Heckl (1988) broadly classifies noise suppression methods as follows: (1) Common sense application. For example, load or speed reduction, increase of mass, enclosures, or mufflers. (2) Add-on measures. These include multiple walls and floors, tuned absorbers and vibration coatings, impedance mismatches in the propagation paths, and shift of resonances away from exciting frequencies. (3) Changes at the source. For example, interruption of feedback loops or other instabilities, reduction of roughness and free clearances, and reduction of time derivatives. (4) Active methods of control such as sound reflection and absorption in wave guides, or compensation of periodic excitation.

For the purpose of this chapter flow-induced noise and its control are of primary interest. In 1952, Lighthill developed a very powerful theory that identified the sources of aerodynamic sound. Use the compressible continuity

equation (1) into the momentum equation and neglect body forces, (2) reads

$$\frac{\partial \rho u_i}{\partial t} + \frac{\partial (\rho u_i u_k)}{\partial x_k} = \frac{\partial \Sigma_{ki}}{\partial x_k} \tag{35}$$

By subtracting $\partial/\partial x_i$ of (35) from $\partial/\partial t$ of (1), an equation for the density results

$$\frac{\partial^2 \rho}{\partial t^2} = \frac{\partial^2}{\partial x_i \, \partial x_k} \left(\rho u_i u_k - \Sigma_{ki} \right) \tag{36}$$

Let $\rho = \rho_o + \rho'$, where ρ' is the density perturbation due to sound, and subtract $c^2 \nabla^2 \rho'$ from both sides of (36), where c is the constant propagation speed of acoustic waves. The resulting Lighthill's equation reads

$$\frac{\partial^2 \rho'}{\partial t^2} - c^2 \nabla^2 \rho' = \frac{\partial^2 T_{ik}}{\partial x_i \, \partial x_k} \tag{37}$$

where $T_{ik} \equiv \rho u_i u_k - \Sigma_{ik} - c^2 \rho' \delta_{ik}$, the Lighthill's stress tensor. The source field for the acoustic waves is a quadrupole distribution whose strength per unit volume is T_{ik}. Turbulence generates sound equivalently to a quadrupole source distribution. Organized structures in a turbulent flow play an important role in the source process and, therefore, controlling these eddies may be the key to noise suppression (Ffowcs Williams, 1977). At the low Mach number typically encountered in underwater applications ($\mathcal{O}[0.01]$), unbounded turbulent flows have an extremely low acoustic efficiency according to Lighthill's (1952) theory. The large differences between the noise levels predicted by the quadrupole theory and those actually generated by a turbulent boundary layer are often explained via acoustic scattering processes (Crighton, 1984). Small rigid bodies, gas bubbles, or sharp edges (Blake and Gershfeld, 1989) can destroy the cancellation between opposing elements of the quadrupole and may lead to the more efficient radiation of a dipole or even a monopole. Thus, for noise suppression, these efficient sound generators should be avoided.

At present, sonars are placed at the nose of underwater vehicles where the boundary layer is laminar. Search rates of these listening devices is improved by placing additional hydrophones farther downstream. However, the turbulence-induced noise is sufficient to interfere with the proper operations of these devices, and must therefore be suppressed before the search rate could be improved. A second example comes from the aeronautics field. On commercial aircraft, the turbulent boundary layer outside the fuselage contributes significantly to cabin noise. Techniques to reduce flow-induced noise are therefore sought. Methods to delay transition (Section 5) or to relaminarize an already turbulent boundary layer (Section 7.3) should be useful to suppress the turbulence-induced noise in both examples above. It is feasible to delay transition on both vehicles, where the unit Re is about $10^7/m$, for the first few meters. Beyond that relaminarization or at least partial suppression of turbulence is the only option. As indicated in Section 7.3, achieving

relaminarization over the entire length of an aircraft or a submarine may require large energy expenditure and is, therefore, not very practical. However, it may not be necessary to relaminarize an entire vehicle. Instead, selected portions of the boundary layer, where, for example, a hydrophone is to be placed, are treated.

A compliant coating that causes transition delay or reduction in turbulence skin friction will also lead to attenuation of sound radiated by the boundary layer. This is because the wall pressure fluctuations are dependent on turbulence levels, which in turn are related to the wall shear stress. The reverse is not necessarily true; i.e. a coating may attenuate the flow noise without affecting the hydrodynamic drag. In fact the technology exists today for manufacturing energy-absorbent compliant liners for sound absorption, vibration reduction, and noise shielding, while the search for a drag-reducing coating has thus far eluded researchers for about 40 years (Riley et al. 1988; Gad-el-Hak, 1996a).

Flow noise is influenced by surface flexibility through two distinct mechanisms: either the surface acts as a sounding board excited by the turbulent pressure field, or the surface compliance induces a change in the turbulence structure and, hence, modifies the pressure fluctuations (Ffowcs Williams, 1965; Purshouse, 1976; Dowling, 1983; 1986). As mentioned earlier, flow noise is currently considered the limiting performance factor for sonar systems placed on surface ships, submarines, and towed arrays. Major advances in the reduction of "self-noise" have been achieved by exploiting the first mechanism above, and further reductions may be possible if the nature of the turbulent boundary layer and its wall pressure fluctuations can be altered. Von Winkle (1961) and Barger and Von Winkle (1961) report pressure fluctuations measurements on a streamlined body of revolution free-falling in a water tank. Flush-mounted hydrophones fabricated from lead-zirconate titanite are used to measure the instantaneous pressure. Their experiment indicates a dramatic reduction in the pressure coefficient when the body is covered with a Kramer-type compliant coating. This result may, however, be due to transition delay caused by the flexible surface and not due to changes in the turbulence structure.

Active noise suppression systems are based on generating sound by auxiliary source with such an amplitude and phase that in the region of interest the sound wave interference from the original and auxiliary source results in considerable reduction of the noise levels. What makes these systems possible is, of course, the linearity of the governing equations.[7] The older systems with fixed gain in the feedback loop could not achieve high noise reduction. However, with the recent availability of adaptive filter systems, much more impressive suppression of noise is feasible (Tichy et al., 1984). These systems are capable of adjusting the feedback loop for the magnitude and phase re-

[7] The pressure fluctuations associated with sound at the threshold of pain (140 dB) are only 0.1% of the atmospheric pressure.

lationship of the spectral components and can quickly compensate for the sound path changes. These active control devices seem to work best for low frequency sound, where passive silencers are relatively ineffective, and when the source is localized and accessible. Local control is obviously easier than global one. Moreover, effective control is achieved when the system response within the frequency band of interest is dominated by relatively few modes. Review papers on active control of noise are available by Warnaka (1980), Ericksson et al. (1988), Van Laere and Sas (1988), and Warner et al. (1988). Anti-sound techniques seem to have gone from the laboratory to application in a remarkably short time.

10 Concluding Remarks

This chapter has attempted the very ambitious task of presenting a unified view of the different control methods available or contemplated for, particularly, external boundary-layer flows to achieve a variety of goals. These goals are not necessarily mutually exclusive and include transition delay, separation postponement, lift enhancement, drag reduction, turbulence augmentation, and noise control. In both laminar and turbulent boundary layers, the effect of many of the control methods is explained in terms of the behavior of the vorticity flux at the wall. The fullness of the normal velocity profile is related to the direction of this vorticity flux, which in turn has a direct influence on the stability, separation, skin friction, and turbulence levels. The broad range of topics covered precludes in-depth review of a particular flow control technique and the reader is referred to selected original publications detailing these methods and referenced throughout this chapter.

Both the science and technology to maintain a laminar boundary layer to a Reynolds number of about 4×10^7 are well established, although some details remain to be worked out. The linear stability theory provides a solid analytical framework, at least for the important first stage of transition. Barring large disturbances in a conventional boundary-layer flow, the linear amplification of Tollmien Schlichting waves is the slowest of the successive multiple steps in the transition process. Stability modifiers inhibit this linear amplification and, therefore, determine the magnitude of the transition Reynolds number. Shaping to provide extended regions of favorable pressure gradient is the simplest method of control and is well suited for small underwater vehicles or for the wings of low- or moderate-speed aircraft. Flight tests have demonstrated the feasibility of using suction to maintain a laminar flow on a swept wing to $Re \approx 4.7 \times 10^7$. The required suction rate is very modest and 20% net drag reduction is possible. Remaining problems are technological in nature and include maintainability and reliability of suction surfaces and further optimization of the suction rate and its distribution. Suction is less suited for underwater vehicles because of the abundance of particulate matters that can clog the suction surface as well as destabilize the boundary layer. For wa-

ter applications, compliant coatings that increase the transitional Reynolds number by a factor of 5–10 are available in the laboratory but performance in the field is still unknown. This technique is very appealing because of its simplicity and absence of energy requirement. Moderate surface heating also increases the transition Re by an order of magnitude, but a source of reject heat must be available to achieve net drag reduction. Additionally, a particle-defense mechanism is needed before the technique could successfully be used in the ocean. For futuristic aircraft using cryo-fuel, surface cooling may be a feasible method to delay transition.

The above stability modifiers change the shape of the velocity profile making it more full. Therefore, two-dimensional, steady separation can be postponed using the same techniques. Other separation control methods include passive ones, such as intentional tripping, fences or vortex generators, and active devices, such as tangential injection, acoustic excitations or oscillating surface flaps. A drag penalty is associated with both passive and active devices.

For time-dependent flows, upstream movement of the separation point results in a delay in boundary layer detachment, analogous to a wall moving in the same direction as the freestream. Three-dimensional boundary layers are in general more capable of overcoming an adverse pressure gradient without separation. In this case, the near-wall fluid is capable of moving in a direction in which the pressure gradient is more favorable, thus avoiding the adverse pressure in the direction of the main flow.

Techniques to reduce the pressure drag are more well established than turbulent skin-friction reduction techniques. Streamlining and other methods to postpone separation can eliminate most of the pressure drag. The wave and induced drag contributions to the pressure drag can also be reduced by geometric design. The skin friction constitutes about 50%, 90% and 100% of the total drag on commercial aircraft, underwater vehicles and pipelines, respectively. Most of the current research effort concerns reduction of skin-friction drag for turbulent boundary layers.

Three flow regimes are identified. First, for $Re < 10^6$, the flow is laminar and skin friction may be lowered by reducing the near-wall momentum. Adverse pressure gradient, blowing and surface heating/cooling could lower the skin friction, but increase the risk of transition and separation. Secondly, for $10^6 < Re < 4 \times 10^7$, active and passive methods to delay transition could be used, thus avoiding the much higher turbulent drag. Thirdly, at the Reynolds number encountered after the first few meters of a fuselage or a submarine, methods to reduce the large skin friction associated with turbulent flows are sought. These methods are classified in the following categories: Reduction of near-wall momentum; introduction of foreign substance; geometrical modification.

The second category above leads to the most impressive results. Introduction of small concentration of polymers, surfactants, particles or fibers into a

turbulent boundary layer lead to a reduction in the skin friction coefficient of as much as 80%. Among the practical considerations requiring further study are the cost of the additive, methods of delivering it to the boundary layer, potential for recovering and recycling, degradation, and the portion of the payload that has to be displaced to make room for the additive.

Recently introduced techniques mostly fall under the third category above and seem to offer more modest net drag reduction. These methods are, however, still in the research stage and include riblets ($\sim$ 8%), large eddy breakup devices ($\sim$ 20%), and convex surfaces ($\sim$ 20%). Potential improvement in these and other methods will perhaps involve combining more than one technique aiming at achieving a favorable effect that is greater than the sum. Due to its obvious difficulties, this area of research has not been very popular in the past but deserves future attention.

Along these lines, the selective suction technique, reviewed in Section 7.4, combines suction to achieve an asymptotic turbulent boundary layer and longitudinal riblets to fix the location of low-speed streaks. Although far from indicating net drag reduction, the available results are encouraging and further optimization is needed. Potentially the selective suction method is capable of skin friction reduction that approaches 60%.

Techniques to augment the turbulence for non-reacting mixing, combustion, heat transfer, and other applications were reviewed in Section 8. In the last section, methods to suppress noise, particularly flow-induced sound, were summarized. The most recent of these techniques exploits the linearity of the acoustic field. Active noise control using anti-sound is a new research area that, remarkably, seems to have gone into applications in just a few years.

The present chapter was part of the author's contribution to the short course Flow Control: Fundamentals and Practices, held in Cargèse, Corsica, France, 24–28 June 1996, and repeated at the University of Notre Dame, Notre Dame, Indiana, U.S.A., 9–13 September 1996. Part of the material in this chapter is excerpted from two review articles by the same author (*Applied Mechanics Reviews*, vol. 42, no. 10, pp. 261–293, 1989, and *Journal of Fluids Engineering*, vol. 113, no. 1, pp. 5–30, 1991).

References

Ackeret J., Ras M., Pfenninger W. (1941): Verhinderung des Turbulentwerdens einer Grenzschicht durch Absaugung. *Naturwissenschaften* **29**, 622–623.

Adkins R.C. (1975): A Short Diffuser with Low Pressure Loss. *J. Fluids Eng.* **97**, 297–302.

Adkins R.C. (1977): Diffusers and Their Performance Improvement by Means of Boundary Layer Control. *AGARD Special Course on Concepts for Drag Reduction*, AGARD Report No. R-654, Paper No. 6, Rhode-Saint-Génèse, Belgium.

Adkins R.C., Mathaus D.S., Yost J.O. (1980): The Hybrid Diffuser. ASME Paper No. 80-GT-136, New York.

Ahuja K.K., Burrin R.H. (1984): Control of Flow Separation by Sound. AIAA Paper No. 84-2298, New York.

Ahuja K.K., Whipkey R.R., Jones G.S. (1983): Control of Turbulent Boundary Layer Flows by Sound. AIAA Paper No. 83-0726, New York.

Alvarez-Calderon A. (1964): Rotating Cylinder Flaps of V/STOL Aircraft. *Aircraft Eng.* **36**, 304–309.

Anders J.B., Jr. (1990): Outer-Layer Manipulators for Turbulent Drag Reduction. *Viscous Drag Reduction in Boundary Layers*, eds. D.M. Bushnell and J.N. Hefner, *Progress in Astronautics & Aeronautics*, vol. 123, (AIAA, Washington, D.C.), 263–284.

Anders J.B., Hefner J.N., Bushnell D.M. (1984): Performance of Large-Eddy Breakup Devices at Post-Transitional Reynolds Numbers. AIAA Paper No. 84-0345, New York.

Anders J.B., Walsh M.J., Bushnell D.M. (1988): The Fix for Tough Spots. *Aerospace America* **26**, January, 24–27.

Anders J.B., Watson R.D. (1985): Airfoil Large-Eddy Breakup Devices for Turbulent Drag Reduction. AIAA Paper No. 85-0520, New York.

Antonia R.A., Fulachier L., Krishnamoorthy L.V., Benabid T., Anselmet F. (1988): Influence of Wall Suction on the Organized Motion in a Turbulent Boundary Layer. *J. Fluid Mech.* **190**, 217–240.

Anyiwo J.C., Bushnell D.M. (1982): Turbulence Amplification in Shock Wave-Boundary Layer Interaction. *AIAA J.* **20**, 893–899.

Aroesty J., Berger S.A. (1975): Controlling the Separation of Laminar Boundary Layers in Water: Heating and Suction. RAND Corporation Report No. R-1789-ARPA, Santa Monica, CA. (Also available from U.S. NTIS; Document Number AD-AO20026.)

Aslanov P.V., Maksyutenko S.N., Povkh I.L., Simonenko A.P., Stupin A.B. (1980): Turbulent Flows of Solutions of Surface-Active Substances. *Izvestiya Akademii Nauk SSSR*, Mekhanika Zhidkosti i Gaza, no. 1, 36–43.

Atassi H.M., Gebert G.A. (1987): Modification of Turbulent Boundary Layer Structure by Large-Eddy Breakup Devices. *Proc. Int. Conf. on Turbulent Drag Reduction by Passive Means*, vol. 2, (Royal Aeronautical Society, London, United Kingdom), 432–456.

Atta R., Rockwell D. (1990): Leading-Edge Vortices Due to Low Reynolds Number Flow Past a Pitching Delta Wing. *AIAA J.* **28**, 995–1004.

Aubry N., Holmes P., Lumley J.L., Stone E. (1988): The Dynamics of Coherent Structures in the Wall Region of a Turbulent Boundary Layer. *J. Fluid Mech.* **192**, 115–173.

Ayers R.F., Wilde M.R. (1956): An Experimental Investigation of the Aerodynamic Characteristics of a Low Aspect Ratio Swept Wing with Blowing in a Spanwise Direction from the Tips. College of Aeronautics, Note No. 57, Cranfield, England.

Bahi L., Ross J.M., Nagamatsu H.T. (1983): Passive Shock Wave/Boundary Layer Control for Transonic Airfoil Drag Reduction. AIAA Paper No. 83-0137, New York.

Bandyopadhyay P.R. (1986): Review-Mean Flow in Turbulent Boundary Layers Disturbed to Alter Skin Friction. *J. Fluids Eng.* **108**, 127–140.

Bandyopadhyay P.R. (1988): Resonant Flow in Small Cavities Submerged in a Boundary Layer. *Proc. R. Soc. Lond. A* **420**, 219–245.

Bar-Sever A. (1989): Separation Control on an Airfoil by Periodic Forcing. *AIAA J.* **27**, 820–821.

Barger J.E., Von Winkle W.A. (1961): Evaluation of a Boundary Layer Stabilization Coating. *J. Acoustical Soc. of America* **33**, 836.

Barker R.A. (1986): The Aerodynamic Effects of a Serrated Strip Near the Leading Edge of an Airfoil. M.S. Thesis, Royal Air Force College, Report No. ETN-87-99480, Cranwell, England.

Barker S.J., Gile D. (1981): Experiments on Heat-Stabilized Laminar Boundary Layers in Water. *J. Fluid Mech.* **104**, 139–158.

Barnwell R., Bushnell D.M., Nagamatsu H.T., Bahi L., Ross J. (1985): Passive Drag Control of Airfoils at Transonic Speeds. U.S. Patent No. 4,522,360.

Barnwell R.W., Hussaini M.Y. (editors) (1992): *Natural Laminar Flow and Laminar Flow Control* (Springer-Verlag, Berlin).

Batchelor G.K. (1967): *An Introduction to Fluid Dynamics.* (Cambridge University Press, London).

Batchelor G.K., Green J.T. (1972): The Determination of the Bulk Stress in a Suspension of Spherical Particles to Order c^2. *J. Fluid Mech.* **56**, 401–427.

Bauer S.X.S., Hernandez G. (1988): Reduction of Cross-Flow Shock-Induced Separation with a Porous Cavity at Supersonic Speeds. AIAA Paper No. 88-2567, New York.

Baullinger N., Page V. (1989): High Altitude Long Endurance (HALE) RPV. AIAA Paper No. 89-2014, New York.

Bechert D.W., Hoppe G., Reif W.-E. (1985): On the Drag Reduction of the Shark Skin. AIAA Paper No. 85-0546, New York.

Benjamin T.B. (1960): Effects of a Flexible Boundary on Hydrodynamic Stability. *J. Fluid Mech.* **9**, 513–532.

Bergles A.E. (1978): Enhancement of Heat Transfer. *Proc. Sixth Int. Heat Transfer Conference*, vol. 6, (Hemisphere, Washington, D.C.), 89–108.

Bergles A.E., Morton L.H. (1965): Survey and Evaluation of Techniques to Augment Convective Heat Transfer. Dept. of Mech. Eng., Report No. EPL 5382-34, MIT, Cambridge, MA.

Bergles A.E., Webb R.L. (1985): A Guide to the Literature on Convective Heat Transfer Augmentation. *Twenty-Third National Heat Transfer Conference: Advances in Enhanced Heat Transfer*, Denver, CO.

Berman N.S. (1978): Drag Reduction by Polymers. *Ann. Rev. Fluid Mech.* **10**, 47–64.

Berman N.S., George W.K. (1974): Time Scale and Molecular Weight Distribution Contributions to Dilute Polymer Solution Fluid Mechanics. *Proc. Heat Transfer Fluid Mech. Inst.*, eds. L.R. Davis and R.E. Wilson, (Stanford Univ. Press, CA), 348–364.

Bernard J.J., Siestrunck R. (1959). Échanges de Chaleur dans les Écoulements Présentant des Décollements. *Proc. First Int. Congr. Aero. Sci.*, , eds. Th. von Karman et al., Madrid, Spain, *Adv. in Aero. Sci* 1 (Pergamon Press, London, England), 314–332.

Bertelrud A., Truong T.V., Avellan F. (1982): Drag Reduction in Turbulent Boundary Layers Using Ribbons. AIAA Paper No. 82-1370, New York.

Bhattacharjee S., Scheelke B., Troutt T.R. (1985): Modification of Vortex Interactions in a Reattaching Separated Flow. AIAA Paper No. 85-0555, New York.

Biringen S. (1984): Active Control of Transition by Periodic Suction-Blowing. *Phys. Fluids* **27**, 1345–1347.

Blackwelder R.F., Gad-el-Hak M. (1990): Method and Apparatus for Reducing Turbulent Skin Friction. United States Patent No. 4,932,612.

Blackwelder R.F., Gad-el-Hak M., Srnsky R.A. (1987): Method and Apparatus for Controlling Bound Vortices in the Vicinity of Lifting Surfaces. U.S. Patent No. 4,697,769.

Blake W.K., Gershfeld J.L. (1989): The Aeroacoustics of Trailing Edges. *Frontiers in Experimental Fluid Mechanics*, ed. M. Gad-el-Hak, *Lecture Notes in Engineering*, vol. 46, (Springer-Verlag, Berlin), 457–532.

Bogdevich V.G., Evseev A.R., Malyuga A.G., Migirenko G.S. (1977): Gas-Saturation Effect on Near-Wall Turbulence Characteristics. *Second Int. Conf. on Drag Reduction*, Paper No. D2, (BHRA Fluid Engineering, Cranfield, United Kingdom).

Bogdevich V.G., Malyuga A.G. (1976): The Distribution of Skin Friction in a Turbulent Boundary Layer of Water beyond the Location of Gas Injection. *Studies on the Boundary Layer Control* (in Russian), eds. S.S. Kutateladze and G.S. Migirenko, (Institute of Thermophysics, Novosibirsk, U.S.S.R.), 62.

Bradley R.G., Wray W.O. (1974): A Conceptual Study of Leading-Edge-Vortex Enhancement by Blowing. *J. Aircraft* **11**, 33–38.

Bradshaw P. (1969): A Note on Reverse Transition. *J. Fluid Mech.* **35**, 387–390.

Bragg M.B., Gregorek G.M. (1987): Experimental Study of Airfoil Performance with Vortex Generators. *J. Aircraft* **24**, 305–309.

Braslow A.L., Burrows D.L., Tetervin N., Visconti F. (1951): Experimental and Theoretical Studies of Area Suction for the Control of Laminar Boundary Layer. NACA Report No. 1025, Washington, D.C.

Briedenthal R.E., Jr., Russell D.A. (1988): Aerodynamics of Vortex Generators. NASA Contractor Report No. CR-182511, Washington, D.C.

Brown A.C., Nawrocki H.F., Paley P.N. (1968): Subsonic Diffusers Designed Integrally with Vortex Generators. *J. Aircraft* **5**, 221–229.

Burd J.E. (1981): Flow Control for a High Energy Laser Turret Using Trapped Vortices Stabilized by Suction. M.Sc. Thesis, Naval Postgraduate School, Monterey, CA. (Also available from U.S. NTIS; Document Number AD-A115263.)

Bushnell D.M. (1983): Turbulent Drag Reduction for External Flows. AIAA Paper No. 83-0227, New York.

Bushnell D.M. (1989): Applications and Suggested Directions of Transition Research. *Fourth Symp. on Numerical and Physical Aspects of Aerodynamic Flows*, Long Beach, CA, 16–19 January.

Bushnell D.M. (1994): Viscous Drag Reduction in Aeronautics. *Proceedings of the Nineteenth Congress of the International Council of the Aeronautical Sciences*, vol. 1, Paper No. ICAS-94-0.1, (AIAA, Washington, D.C.), XXXIII–LVI.

Bushnell D.M., Hefner J.N. (editors) (1990): *Viscous Drag Reduction in Boundary Layers, Progress in Astronautics & Aeronautics*, vol. 123, (AIAA, Washington, D.C.).

Bushnell D.M., Hefner J. N., Ash R.L. (1977): Effect of Compliant Wall Motion on Turbulent Boundary Layers. *Phys. Fluids* **20**, S31–S48.

Bushnell D.M., Malik M.R. (1988): Compressibility Influences on Boundary-Layer Transition. *Symp. on Physics of Compressible Turbulent Mixing*, Princeton, NJ, 25–27 October.

Bushnell D.M., McGinley C.B. (1989): Turbulence Control in Wall Flows. *Ann. Rev. Fluid Mech.* **21**, 1–20.

Bushnell D.M., Trimpi R.L. (1986): Optimum Supersonic Wind Tunnel. AIAA Paper No. 86-0773, New York.

Bussmann K., Münz H. (1942): Die Stabilität der laminaren Reibungsschicht mit Absaugung. *Jahrb. Dtsch. Luftfahrtforschung* **1**, 36–39.

Calarese W., Crisler W.P., Gustafson G.L. (1985): Afterbody Drag Reduction by Vortex Generators. AIAA Paper No. 85-0354, New York.

Cantwell B.J. (1981): Organized Motion in Turbulent Flow. it Ann. Rev. Fluid Mech. **13**, 457–515.

Carmichael B.H. (1974): Application of Sailplane and Low-Drag Underwater Vehicle Technology to the Long-Endurance Drone Problem. AIAA Paper No. 74-1036, New York.

Carpenter P.W., Garrad A.D. (1985): The Hydrodynamic Stability of Flow over Kramer-Type Compliant Surfaces. Part 1. Tollmien-Schlichting Instabilities. *J. Fluid Mech.* **155**, 465–510.

Cary A.M., Jr., Weinstein L.M., Bushnell D.M. (1980): Drag Reduction Characteristics of Small Amplitude Rigid Surface Waves. *Viscous Flow Drag Reduction*, ed. G.R. Hough, *Progress in Astronautics & Aeronautics*, vol. 72, (AIAA, New York), XXXIII–LVI.

Cebeci T., Chang K.C. (1978): Calculation of Incompressible Rough-Wall Boundary-Layer Flows. *AIAA J.* **16**, 730–735.

Cebeci T., Egan D.A. (1989): Prediction of Transition due to Isolated Roughness. *AIAA J.* **27**, 870–875.

Chang P.K. (1970): *Separation of Flow*, (Pergamon Press, Oxford, England).

Chang P.K. (1976): *Control of Flow Separation*, (Hemisphere, Washington, D.C.).

Cheeseman I.C., Seed A.R. (1967): The Application of Circulation Control by Blowing to Helicopter Rotors. *J. Royal Aeronautical Society* **71**, 451–467.

Chen C.P., Goland Y., Reshotko E. (1979): Generation Rate of Turbulent Patches in the Laminar Boundary Layer of a Submersible. *Viscous Flow Drag Reduction*, ed. G.R. Hough, *Progress in Astronautics & Aeronautics*, vol. 72, (AIAA, New York), 73–89.

Chen D., Shi Ying Z. (1989): Control of Separation in Diffusers Using Forced Unsteadiness. AIAA Paper No. 89-1015, New York.

Chow C.Y., Chen C.L., Huang M.K. (1985): Trapping of Free Vortex by Airfoils with Surface Suction. AIAA Paper No. 85-0446, New York.

Cichy D.R., Harris J.W., MacKay, J.K. (1972): Flight Tests of a Rotating Cylinder Flap on a North American Rockwell YOV-10A Aircraft. NASA Contractor Report No. CR-2135, Washington, D.C.

Collins F.G. (1979): Boundary Layer Control on Wings Using Sound and Leading Edge Serrations. AIAA Paper No. 79-1875, New York.

Collins F.G. (1981): Boundary Layer Control on Wings Using Sound and Leading-Edge Serrations. *AIAA J.* **19**, 129–130.

Collins F.G., Zelenevitz J. (1975): Influence of Sound upon Separated Flow over Wings. *AIAA J.* **13**, 408–410.

Compton D.A., Johnston J.P. (1991): Streamwise Vortex Development by Pitched and Skewed Jets in a Turbulent Boundary Layer. AIAA Paper No. 91-0038, New York.

Cook W.L., Mickey D.M., Quigley H.G. (1974): Aerodynamics of Jet Flap and Rotating Cylinder Flap STOL Concepts. AGARD Fluid Dynamics Panel on V/STOL Aerodynamics, Paper No. 10, Delft, Netherlands.

Corke T.C., Guezennec Y., Nagib H.M. (1980): Modification in Drag of Turbulent Boundary Layers Resulting from Manipulation of Large-Scale Structures. *Viscous Flow Drag Reduction*, ed. G.R. Hough, *Progress in Astronautics & Aeronautics*, vol. 72, (AIAA, New York), 128–143.

Corke T.C., Nagib H.M., Guezennec Y. (1981): A New View on Origin, Role and Manipulation of Large Scales in Turbulent Boundary Layers. NASA Contractor Report No. 165861, Washington, D.C.

Crighton D.G. (1984): Long-Range Acoustic Scattering by Surface Inhomogeneities Beneath a Turbulent Boundary Layer. *J. Vibration, Acoustics, Stress & Reliability in Design* **106**, 376–382.

Cutler A., Bradshaw P. (1986): The Interaction Between a Strong Longitudinal Vortex and a Turbulent Boundary Layer. AIAA Paper No. 86-1071, New York.

Cutler A., Bradshaw P. (1989): Vortex/Boundary-Layer Interactions. AIAA Paper No. 89-0083, New York.

Davidson C.J. (1985): The Experimental Investigation of the Effects of Roughness upon Aerofoil Characteristics at Low Reynolds Numbers. M.Sc. Thesis, Cranfield Institute of Technology, Cranfield, England.

Delery, J.M. (1985): Shock Wave/Turbulent Boundary Layer Interaction and Its Control. *Prog. Aerospace Sci.* **22**, 209–280.

DeMeis R. (1986): Sounding a Happy Note for Lift. *Aerospace America* **24**, August, 10–11.

DiPrima R.C., Swinney H.L. (1985): Instabilities and Transition in Flow Between Concentric Rotating Cylinders *Hydrodynamic Instabilities and the Transition to Turbulence*, eds. H.L. Swinney and J.P. Gollub, second edition, (Springer-Verlag, Berlin), 139–180.

Donovan J.F., Selig M.S. (1989): Low Reynolds Number Airfoil Design and Wind Tunnel Testing at Princeton University. *Low Reynolds Number Aerodynamics*, ed. T.J. Mueller, *Lecture Notes in Engineering*, vol. 54, (Springer-Verlag, Berlin), 39–57.

Dougherty N.S., Fisher D.F. (1980): Boundary Layer Transition on a 10-Degree Cone. AIAA Paper No. 80-0154, New York.

Dowling A.P. (1983): Flow-Acoustic Interaction Near a Flexible Wall. *J. Fluid Mech.* **128**, 181–198.

Dowling A.P. (1985): The Effect of Large-Eddy Breakup Devices on Oncoming Vorticity. *J. Fluid Mech.* **160**, 447–463.

Dowling A.P. (1986): Mean Flow Effects on the Low-Wavenumber Pressure Spectrum on a Flexible Surface. *J. Fluids Eng.* **108**, 104–108.

Drazin P., Reid W. (1981): *Hydrodynamic Stability* (Cambridge University Press, London).

Durbin P.A., McKinzie D.J. (1987): Corona Anemometry for Qualitative Measurement of Reversing Surface Flow with Application to Separation Control by Ex-

ternal Excitation. *Proc. Forum on Unsteady Flow Separation*, ed. K.N. Ghia, (ASME, New York), 15–18.

Dutton R.A. (1960): The Effects of Distributed Suction on the Development of Turbulent Boundary Layers. Aeronautical Research Council R&M No. 3155, London, England.

Eléna M. (1975): Etude des Champs Dynamiques et Thermiques d'un Ecoulement Turbulent en Conduit avec Aspiration à la Paroi. Thèse de Doctoratès Sciences, Université d'Aix-Marseille, Marseille, France.

Eléna M. (1984): Suction Effects on Turbulence Statistics in a Heated Pipe Flow. *Phys. Fluids* **27**, 861–866.

Ely W.L., Berrier F.C. (1975): Performance of Steady and Intermittent Blowing Jet Flaps and Spanwise Upper Surface Slots. Air Force Flight Dynamics Laboratory Report No. AFFDL-TR-75-128, Wright-Patterson Air Force Base, OH.

Eppler R., Somers D.M. (1985): Airfoil Design for Reynolds Numbers between 50,000 and 500,000. *Proc. Conf. on Low Reynolds Number Airfoil Aerodynamics*, ed. T.J. Mueller, (University of Notre Dame, Notre Dame, IN), 1–14.

Ericsson L.E. (1967): Comment on Unsteady Airfoil Stal. *J. Aircraft* 4, 478–480.

Ericsson L.E. (1988): Moving Wall Effects in Unsteady Flow. *J. Aircraft* **25**, 977–990.

Eriksson L.J., Allie M.C., Bremigan C.D., Gilbert J.A. (1988): Active Noise Control and Specificiations for Fan Noise Problems. *Proc. Noise Control Design: Methods and Practice*, ed. J.S. Bolton, (Noise Control Foundation, Poughkeepsie, NY), 273–278.

Favre A., Dumas R., Verollet E., Coantic M. (1966): Couche Limite Turbulente sur Paroi Poreuse avec Aspiration. *J. Mecanique* **5**, 3–28.

Feir J.B. (1965): The Effects of an Arrangement of Vortex Generators Installed to Eliminate Wind Tunnel Diffuser Separation. Institute for Aerospace Studies, University of Toronto, UTIAS Technical Note No. 87, Toronto, Canada.

Ffowcs Williams J.E. (1965): Sound Radiation from Turbulent Boundary Layers Formed on Compliant Surfaces. *J. Fluid Mech.* **22**, 347–358.

Ffowcs Williams J.E. (1977): Aeroacoustics. *Ann. Rev. Fluid Mech.* **9**, 447–468.

Fiedler H.E., Fernholz H.H. (1990): On Management and Control of Turbulent Shear Flows. *Prog. Aerospace Sci.* **27**, 305–387.

Fiedler H.E., Glezer A., Wygnanski I. (1988): Control of Plane Mixing Layer: Some Novel Experiments. *Current Trends in Turbulence Research*, eds. H. Branover, M. Mond and Y. Unger, *Progress in Astronautics & Aeronautics*, vol. 112, (AIAA, Washington, D.C.), 30–64.

Flatt J. (1961): The History of Boundary Layer Control Research in the United States of America. *Boundary Layer and Flow Control*, ed. G.V. Lachmann, vol. 1, (Pergamon Press, Oxford, England), 122–143.

Flettner A. (1924): Die Anwendung der Erkenntnisse der Aerodynamik zum Windantrieb von Schiffen. *Jb. Schiffbautech. Ges.* **25**, 222–251.

Francis M.S., Keesee J.E., Lang J.D., Sparks G.W., Sisson G.E. (1979): Aerodynamic Characteristics of an Unsteady Separated Flow. *AIAA J.* **17** 1332–1339.

Frick C.W., McCullough C.B. (1942): Tests of a Heated Low Drag Airfoil. NACA ARR, Washington, D.C., December.

Gad-el-Hak M. (1986a): The Use of the Dye-Layer Technique for Unsteady Flow Visualization. *J. Fluids Eng.* **108**, 34–38.

Gad-el-Hak M. (1986b): Boundary Layer Interactions With Compliant Coatings: An Overview. *Appl. Mech. Rev.* **39**, 511–523.

Gad-el-Hak M. (1986c): The Response of Elastic and Viscoelastic Surfaces to a Turbulent Boundary Layer. *J. Appl. Mech.* **53**, 206–212.

Gad-el-Hak M. (1987): Compliant Coatings Research: A Guide to the Experimentalist. *J. Fluids & Struct.* **1**, 55–70.

Gad-el-Hak M. (1988a): Review of Flow Visualization Techniques for Unsteady Flows. *Flow Visualization IV*, ed. C. Véret, (Hemisphere, Washington, D.C.), 1–12.

Gad-el-Hak M. (1988b): Visualization Techniques for Unsteady Flows: An Overview. *J. Fluids Eng.* **110**, 231–243.

Gad-el-Hak M. (1994): Interactive Control of Turbulent Boundary Layers: A Futuristic Overview. *AIAA J.* **32**, 1753–1765.

Gad-el-Hak M. (1995): Questions in Fluid Mechanics: Stokes' Hypothesis for a Newtonian, Isotropic Fluid. *J. Fluids Eng.* **117**, 3-5.

Gad-el-Hak M. (1996a): Compliant Coatings: A Decade of Progress. *Appl. Mech. Rev.* **49**, no. 10, part 2, S147–S157.

Gad-el-Hak M. (1996b): Modern Developments in Flow Contro. *Appl. Mech. Rev.* **49**, 365–379.

Gad-el-Hak M., Blackwelder R.F. (1985): The Discrete Vortices from a Delta Wing. *AIAA J.* **23**, 961–962.

Gad-el-Hak M., Blackwelder R.F. (1987a): Control of the Discrete Vortices from a Delta Wing. *AIAA J.* **25**, 1042–1049.

Gad-el-Hak M., Blackwelder R.F. (1987b): A Drag Reduction Method for Turbulent Boundary Layers. AIAA Paper No. 87-0358, Washington, D.C.

Gad-el-Hak M., Blackwelder R.F. (1987c): Simulation of Large-Eddy Structures in a Turbulent Boundary Layer. *AIAA J.* **25**, 1207–1215.

Gad-el-Hak M., Blackwelder R.F. (1989): Selective Suction for Controlling Bursting Events in a Boundary Layer *AIAA J.* **27**, 308–314.

Gad-el-Hak M., Blackwelder R.F., Riley J.J. (1984): On the Interaction of Compliant Coatings With Boundary Layer Flows. *J. Fluid Mech.* **140**, 257–280.

Gad-el-Hak M., Ho C.-M. (1985): The Pitching Delta Wing. *AIAA J.* **23**, 1660–1665.

Gad-el-Hak M., Ho C.-M. (1986a): Unsteady Vortical Flow Around Three-Dimensional Lifting Surfaces. *AIAA J.* **24**, 713–721.

Gad-el-Hak M., Ho C.-M. (1986b): Unsteady Flow Around An Ogive-Cylinder. *J. Aircraft* **23**, 520–528.

Gadd G.E. (1960): Boundary Layer Separation in the Presence of Heat Transfer. NATO Advisory Group for Aerospace Research and Development, AGARD Report No. R-280, Rhode-Saint-Génèse, Belgium.

Gadd G.E., Cope W.F., Attridge J.L. (1958): Heat-Transfer and Skin-Friction Measurements at a Mach Number of 2.44 for a Turbulent Boundary Layer on a Flat Surface and in Regions of Separated Flow. Aeronautical Research Council R&M No. 3148, London, England.

Gadetskii V.M., Serebriiskii I.A.M., Fomin V.M. (1972): Investigation of the Influence of Vortex Generators on Turbulent Boundary Layer Separation. *Uchenye Zapiski TSAGI* **3**, 22–28.

Gampert B., Homann K., Rieke H.B. (1980): The Drag Reduction in Laminar and Turbulent Boundary Layers by Prepared Surfaces with Reduced Momentum Transfer. *Israel J. Technology* **18**, 287–292.

Gartling D.K. (1970): Tests of Vortex Generators to Prevent Separation of Supersonic Flow in a Compression Corner. Applied Research Laboratory, University of Texas, Report No. ARL-TR-70-44, Austin, TX. (Also available from U.S. NTIS; Document Number AD-734154.)

Gebert G.A. (1988): Turbulent Boundary Layer Modification by Streamlined Devices. Ph.D. Thesis, University of Notre Dame, Notre Dame, IN.

Gedney C.J. (1983): The Cancellation of a Sound-Excited Tollmien-Schlichting Wave with Plate Vibration. *Phys. Fluids* **26**, 1158–1160.

Gol'd Fel'd M.A., Zatoloka V.V. (1979): On the Improvement of Separating Properties of a Turbulent Boundary Layer as a Result of the Effect of a Shock Wave. *Izvestiya Sibirskogo Otdeleniya*, Akademii Nank **3**, 40–47.

Goldstein M.E. (1984): Generation of Instability Waves in Flows Separating from Smooth Surfaces. *J. Fluid Mech.* **145**, 71–94.

Goldstein M.E., Hultgren L.S. (1989): Boundary-Layer Receptivity to Long-Wave Free-Stream Disturbances. *Ann. Rev. Fluid Mech.* **21**, 137–166.

Goodman W.L. (1985): Emmons Spot Forcing for Turbulent Drag Reduction. *AIAA J.* **23**, 155–157.

Granville P.S. (1979): Drag of Underwater Bodies. *Hydroballistics Design Handbook*, vol. 1, (Naval Sea Systems Command, SEAHAC TR 79-1, Washington, D.C.), 309–341.

Gratzer L.B. (1971): Analysis of Transport Applications for High Lift Schemes. *AGARD Course on Assessment of Lift Augmentation Devices*, eds. P.E. Colin and J. Williams, AGARD-LS-43-71, Paper No. 7, Rhode-Saint-Génèse, Belgium.

Gregory N., Stuart J.T., Walker W.S. (1955): On the Stability of Three-Dimensional Boundary Layers with Applications to the Flow due to a Rotating Disk. *Phil. Trans. R. Soc. London A* **248**, 155–199.

Gutmark E., Ho C.-M. (1986): Visualization of a Forced Elliptical Jet. *AIAA J.* **24**, 684–685.

Gutmark E.J., Schadow K.C., Yu K.H. (1995): Mixing Enhancement in Supersonic Free Shear Flows. *Annu. Rev. Fluid Mech.* **27**, 375–417.

Görtler H. (1955): Dreidimensionales zur Stabilittstheorie laminarer Grenzschichten. *ZAMM* **35**, 362–363.

Haight C.H., Reed T.D., Morland B.T. (1974): Design Studies of Transonic and STOL Airfoils with Active Diffusion Control. Advanced Technology Center Report No. ATC-B-94300/4CR-24, Dallas, TX. (Also available from U.S. NTIS; Document Number AD-A011928/9.)

Harris C.D., Bartlett D.W. (1972): Wind-Tunnel Investigation of Effects of Underwing Leading Edge Vortex Generators on a Supercritical-Wing Research Airplane Configuration. NASA Technical Memorandum No. TMX-2471, Washington, D.C.

Harvey W.D. (1986): Low-Reynolds Number Aerodynamics Research at NASA Langley Research Center. *Proc. Int. Conf. on Aerodynamics at Low Reynolds Numbers*, vol II, Royal Aeronautical Society, London, England, 19.1–19.49.

Harvey W.D., Bushnell D.M., Beckwith I.E. (1969): On the Fluctuating Properties of Turbulent Boundary Layers for Mach Numbers up to 9.0. NASA Technical Document No. TND-5496, Washington, D.C.

Hayakawa L., Squire L.C. (1982): The Effect of the Upstream Boundary Layer State on the Shock Interaction at a Compression Corner. *J. Fluid Mech.* **122**, 369–394.

Heckl M. (1988): The Use of Mathematical Methods in Noise Control Design. *Proc. Noise Control Design; Methods and Practice*, ed. J.S. Bolton, (Noise Control Foundation, Poughkeepsie, NY), 27–38.

Hefner J.N. (1988): Dragging Down Fuel Costs. *Aerospace America* **26**, January, 14–16.

Hefner J.N., Anders J.B., Bushnell D.M. (1983): Alteration of Outer Flow Structures for Turbulent Drag Reduction. AIAA Paper No. 83-0293, New York.

Hefner J.N., Sabo F.E. (editors) (1987): *Research in Natural Laminar Flow and Laminar Flow Control*, part 1, NASA Conference Proceedings No. CP-2487, Washington, D.C.

Hefner J.N., Weinstein L.M., Bushnell D.M. (1980): Large-Eddy Breakup Scheme for Turbulent Viscous Drag Reduction. *Viscous Flow Drag Reduction*, ed. G.R. Hough, *Progress in Astronautics & Aeronautics*, vol. 72, (AIAA, New York), 110–127.

Hendricks E.W., Ladd D.M. (1983): Effect of Surface Roughness on the Delayed Transition on 9:1 Heated Ellipsoid. *AIAA J.* **21**, 1406–1409.

Hendricks E.W., Lawler J.V., Horne M.P., Handler R.A., Swearingen J.D. (1989): Experiments in Drag-Reducing Polymer Flows. *Advances in Fluid Mechanics Measurements*, ed. M. Gad-el-Hak, *Lecture Notes in Engineering*, vol. 45, (Springer-Verlag, Berlin), 535–568.

Henry J.R., Wood C.C., Wilbur S.W. (1956): Summary of Subsonic Diffuser Data. NACA Report No. RML-56F05, Washington, D.C.

Hinch E.J. (1977): Mechanical Models of Dilute Polymer Solutions in Strong Flows. *Phys. Fluids* **20**, S22–S30.

Hinze J. O. (1975): *Turbulence*, second edition, (McGraw-Hill, New York).

Hoffmann J.A. (1981): Effects of Free Stream Turbulence on Diffuser Performance. *J. Fluids Eng.* **103**, 385–390.

Hoffmann J.A., Kassir S.M., Larwood S.M. (1988): The Influence of Free Stream Turbulence on Turbulent Boundary Layers with Mild Adverse Pressure Gradients. NASA Contractor Report No. CR-184677, Washington, D.C.

Holmes B. J. (1988): NLF Technology is Ready to Go. *Aerospace America* **26**, January, 16–20.

Holstein H. (1940): Messungen zur Laminarhaltung der Grenzschicht an einem Flügel. *Lilienthal-Bericht* **S10**, 17–27.

Hooshmand A., Youngs R., Wallace J.M., Balint J.-L. (1983): An Experimental Study of Changes in the Structure of a Turbulent Boundary Layer Due to Surface Geometry Changes. AIAA Paper No. 83-0230, New York.

Horstmann K.-H., Quast A. (1981): Widerstandsverminderung durch Blasturbulatoren. DFVLR Report No. FB-81-33, Braunschweig, Federal Republic of Germany.

Hough G.R. (editor) (1980): *Viscous Flow Drag Reduction. Progress in Astronautics &Aeronautics*, vol. 72, (AIAA, New York).

Howard F.G., Hefner J.N., Srokowski A.J. (1975): Multiple Slot Skin Friction Reduction. *J. Aircraft* **12**, 753–754.

Howard F.G., Goodman W.L. (1985): Axisymmetric Bluff-Body Drag Reduction Through Geometrical Modification. *J. Aircraft* **22**, 516–522.

Howard F.G., Goodman W.L. (1987): Drag Reduction on a Bluff Body at Yaw Angles to 30 Degrees. *J. Spacecraft & Rockets* **24**, 179–181.

Howarth L. (1938): On the Solution of the Laminar Boundary Layer Equations. *Proc. R. Soc. Lond. Ser. A* **164**, 547–579.

Hoyt J.W. (1972): Turbulent Flow of Drag-Reducing Suspensions. Naval Undersea Center Report No. TP 299, San Diego, CA.

Hoyt J.W. (1979): Polymer Drag Reduction - A Literature Review. *Second Int. Conf. on Drag Reduction*, Paper No. A1, (BHRA Fluid Engineering, Cranfield, United Kingdom).

Hsiao F.-B., Liu C.-F., Shyu J.-Y. (1990): Control of Wall-Separated Flow by Internal Acoustic Excitation. *AIAA J.* **28**, 1440–1446.

Huang L.S., Maestrello L., Bryant T.D. (1987): Separation Control over an Airfoil at High Angles of Attack by Sound Emanating from the Surface. AIAA Paper No. 87-1261, New York.

Huerre P., Monkewitz P.A. (1990): Local and Global Instabilities in Spatially Developing Flows. *Annu. Rev. Fluid Mech.* **22**, 473–537.

Hunter P.A., Johnson H.I. (1954): A Flight Investigation of the Practical Problems Associated with Porous Leading-Edge Suction. NACA Technical Note No. TN-3062, Washington, D.C.

Hurley D.G. (1961): The Use of Boundary Layer Control to Establish Free Streamline Flows. *Boundary Layer and Flow Control*, ed. G.V. Lachmann, vol. 1, (Pergamon Press, New York), 295-341.

Huyer S.A., Robinson M.C., Luttges M.W. (1990): Unsteady Aerodynamic Loading Produced by a Sinusoidally Oscillating Delta Wing. AIAA Paper No. 90-1536, New York.

Iglisch R. (1944): Exakte Berechnung der laminaren Reibungsschicht an der längsangeströmten ebenen Platte mit homogener Absaugung. *Schr. Dtsh. Akad, Luftfahrtforschung* **8B**, 1–51.

Illingworth C.R. (1954): The Effect of Heat Transfer on the Separation of a Compressible Laminar Boundary Layer. *Quart. J. Mech. Appl. Math.* **7**, 8–34.

Inger G.R., Siebersma T. (1988): Computational Simulation of Vortex Generator Effects on Transonic Shock/Boundary Layer Interaction. AIAA Paper No. 88-2590, New York.

Isomoto K., Honami S. (1989): The Effect of Inlet Turbulence Intensity on the Reattachment Process over a Backward-Facing Step. *J. Fluids Eng.* **111**, 87–92.

Itoh N. (1987): Another Route to the Three-Dimensional Development of Tollmien-SchlichtingWaves with Finite Amplitude. *J. Fluid Mech.* **181**, 1–16.

Johansen J.B., Smith C.R. (1986): The Effects of Cylindrical Surface Modifications on Turbulent Boundary Layers. *AIAA J.* **24**, 1081–1087.

Johnson W.S., Tennant J.S., Stamps R.E. (1975): Leading-Edge Rotating Cylinder for Boundary Layer Control on Lifting Surfaces. *J. Hydronautics* **9**, 76–78.

Johnston J., Nishi M. (1989): Vortex Generator Jets—A Means for Passive and Active Control of Boundary Layer Separation. AIAA Paper No. 89-0564, New York.

Johnston J., Nishi M. (1990): Vortex Generator Jets—Means for Flow Separation Control. *AIAA J.* **28**, 989–994.

Kachanov Y.S., Koslov V.V., Levchenko V. Ya. (1974): Experimental Study of the Influence of Cooling on the Stability of Laminar Boundary Layers. *Izvestia*

Sibirskogo Otdielenia Ak. Nauk SSSR, Seria Technicheskikh Nauk, Novosibirsk, no. 8-2, 75–79.

Kandil O.A., Chuang H.A. (1988): Unsteady Vortex-Dominated Flows around Maneuvering Wings over a Wide Range of Mach Numbers. AIAA Paperr No. 88-0317, New York.

Kannberg L.D. (1988): The Urgency Will Return. *Mechanical Engineering* **110**, 33.

Kaplan R. E. (1964): The Stability of Laminar Incompressible Boundary Layers in the Presence of Compliant Boundaries. Sc.D. Thesis, Massachusetts Institute of Technology, Cambridge, MA.

Katz Y., Nishri B., Wygnanski I. (1989a): The Delay of Turbulent Boundary Layer Separation by Oscillatory Active Control. AIAA Paper No. 89-0975, New York.

Katz Y., Nishri B., Wygnanski I. (1989b): The Delay of Turbulent Boundary Layer Separation by Oscillatory Active Control. *Phys. of Fluids* **1**, 179–181.

Kays W.M., Crawford M.E. (1993): *Convective Heat and Mass Transfer*, third edition, (McGraw-Hill, New Yor).

Kendall J.M. (1970): The Turbulent Boundary Layer over a Wall with Progressive Surface Waves. *J. Fluid Mech.* **41**, 259-281.

Kentfield J.A.C. (1985a): Drag Reduction of Controlled Separated Flows. AIAA Paper No. 85-1800, New York.

Kentfield J.A.C. (1985b): Short, Multi-Step, Afterbody Fairings. *J. Aircraft* **21**, 51–352.

Kidd J.A., Wikoff D., Cottrell C.J. (1990): Drag Reduction by Controlling Flow Separation Using Stepped Afterbodies. *J. Aircraft* **27**, 564–566.

Kim H.T., Kline S.J., Reynolds W.C. (1971): The Production of Turbulence Near a Smooth Wall in a Turbulent Boundary Layer. *J. Fluid Mech.* **50**, 133-160.

Kind R.J. (1967): A Proposed Method of Circulation Control. Ph.D. Dissertation, Cambridge University, Cambridge, England.

Klebanoff P.S., Schubauer G.B., Tidstrom K.D. (1955): Measurements of the Effect of Two-Dimensional and Three-Dimensional Roughness Elements on Boundary-Layer Transition. *J. Aero. Sci.* **22**, 803–804.

Klebanoff P.S., Tidstrom K.D., Sargent L.M. (1962): The Three-Dimensional Nature of Boundary Layer Instability. *J. Fluid Mech.* **12**, 1–34.

Koga D.J., Reisenthel P., Nagib H.M. (1984): Control of Separated Flowfields Using Forced Unsteadiness. Illinois Institute of Technology, Fluids & Heat Transfer Report No. R84-1, Chicago, IL.

Kosecoff M.A., Ko D.R.S., Merkle C.L. (1976): An Analytical Study of the Effect of Surface Roughness on the Stability of a Heated Water Boundary Layer. Dynamics Technology, Inc., Final Report No. PDT 76-131, Torrance, CA.

Koval'nogov S.A., Fomin V.M., Shapovalov G.K. (1987): Experimental Study of the Possibility of Passive Control of Shock-Boundary Layer Interactions. *Uchemye kZapiski TSAGI* **18**, 112–116.

Krall K.M., Haight C.H. (1972): Wind Tunnel Tests of a Trapped Vortex-High Lift Airfoil. Advanced Technology Center Report No. ATC-B-94300/3TR-10, Dallas, TX. (Also available from U.S. NTIS; Document Number AD-762 077.)

Kramer M.O. (1960): Boundary Layer Stabilization by Distributing Damping. *J. Am. Soc. Naval Engrs.* **72**, 25–33.

Kuethe A.M. (1973): Boundary Layer Control of Flow Separation and Heat Exchange. U.S. Patent No. 3,741,285.

Kukainis J. (1969): Effects of Three-Dimensional Boundary Layer Control Devices on a Quasi-Two-Dimensional Swept Wing at High Subsonic Speeds. Arnold Engineering Development Center Technical Report No. AEDC-TR-69-251, Arnold Air Forc Base, TN.

Lachmann G.V. (1961): *Boundary Layer and Flow Control*, volumes 1 and 2, (Pergamon Press, New York).

Ladd D.M., Hendricks E.W. (1988): Active Control of 2-D Instability Waves on an Axisymmetric Body. *Exp. Fluids* **6**, 69–70.

Landahl M.T. (1962): On the Stability of a Laminar Incompressible Boundary Layer over a Flexible Surface. *J. Fluid Mech.* **13**, 609–632.

Landahl M.T. (1973): Drag Reduction by Polymer Addition. *Proc. 13th IUTAM Congress*, eds. E. Becker and G.K. Mikhailov, (Springer-Verlag, Berlin), 177–199.

Landahl M.T. (1977): Dynamics of Boundary Layer Turbulence and the Mechanism of Drag Reduction. *Phys. Fluids* **20**, S55–S63.

Landau L.D., Lifshitz E.M. (1987): *Fluid Mechanics*, second edition, translated from the Russian, (Pergamon Press, Oxford).

Lange R.H. (1954): Present Status of Information Relative to the Prediction of Shock-Induced Boundary Layer Separation. NACA Technical Note No. TN-3065, Washington, D.C.

Lankford J.L. (1960): Investigation of the Flow over an Axisymmetric Compression Surface at High Mach Numbers. U.S. Naval Ordnance Laboratory Report No. 6866, Corona, CA.

Lankford J.L. (1961): The Effect of Heat Transfer on the Separation of Laminar Flow over Axisymmetric Compression Surfaces: Preliminary Results at Mach No. 6.78. U.S. Naval Ordnance Laboratory Report No. 7402, Corona, CA.

Lauchle G.C., Gurney G.B. (1984): Laminar Boundary-Layer Transition on a Heated Underwater Body. *J. Fluid Mech.* **144**, 79–101.

Laufer J. (1975): New Trends in Experimental Turbulence Research. *Ann. Rev. Fluid Mech.* **7**, 307–326.

Lee C.S., Tavella D.A., Wood N.J., Roberts L. (1986): Flow Structure of Lateral Wing-Tip Blowing. AIAA Paper No. 86-1810, New York.

Lee C.S., Tavella D.A., Wood N.J., Roberts L. (1989): Flow Structure and Scaling Laws in Lateral Wing-Tip Blowing. *AIAA J.* **2**, 1002–1007.

Lee D.G. (1974): Subsonic Force Characteristics of a Low Aspect Ratio Wing Incorporating a Spinning Cylinder. DTNSRDC Report No. ASED-329, Bethesda, MD. (Also available from U.S. NTIS; Document Number AD-AOO11135.)

Lee M., Ho C.-M. (1989): Vortex Dynamics of Delta Wings. *Frontiers in Experimental Fluid Mechanics*, ed. M. Gad-el-Hak, *Lecture Notes in Engineering*, vol. 46, (Springer-Verlag, Berlin), 365–428.

Lee M., Ho C.-M. (1990): Lift Force of Delta Wings. *Appl. Mech. Rev.* **43**, 209–221.

Lee W.K., Vaseleski R.C., Metzner A.B. (1974): Turbulent Drag Reduction in Polymeric Solutions Containing Suspended Fibers. *AIChE J.* **20**, 128-133.

Lees L. (1947): The Stability of the Laminar Boundary Layer in a Compressible Fluid. NACA Report No. 876, Washington, D.C.

Legner H.H. (1984): A Simple Model for Gas Bubble Drag Reduction. *Phys Fluids* **27**, 2788–2790.

Liandrat J., Aupoix B., Cousteix T. (1986): Calculation of Longitudinal Vortices embedded in a Turbulent Boundary Layer. *Fifth Symposium on Turbulent Shear*

Flows, eds. F. Durst, B.E. Launder, F.W. Schmidt and J.H. Whitelaw, (Springer-Verlag, Berlin), 7.17–7.22.

Libby P.A. (1954): Method for Calculation of Compressible Laminar Boundary Layer with Axial Pressure Gradient and Heat Transfer. NACA Technical Note No. TN-3157, Washington, D.C.

Liebeck R.H. (1978): Design of Subsonic Airfoils for High Lift. *J. Aircraft* **15**, 547–561.

Liepmann H.W., Brown G.L., Nosenchuck D.M. (1982): Control of Laminar Instability Waves Using a New Technique. *J. Fluid Mech.* **118**, 187–200.

Liepmann H.W., Fila G.H. (1947): Investigations of Effects of Surface Temperature and Single Roughness Elements on Boundary Layer Transition. NACA Report No. 890, Washington, D.C.

Liepmann H.W., Nosenchuck D.M. (1982): Active Control of Laminar-Turbulent Transition. *J. Fluid Mech.* **118**, 201–204.

Lighthill M.J. (1952): On Sound Generated Aerodynamically. I. General Theory. *Proc. Roy.Soc. London A* **211**, 564–587.

Lighthill M. J. (1963): Introduction—Boundary Layer Theory. *Laminar Boundary Layers*, ed. L. Rosenhead, (Clarendon Press, Oxford), 46–113.

Lighthill M.J. (1973): On the Weis-Fogh Mechanism of Lift Generation. *J. Fluid Mech.* **60**, 1–17.

Lighthill, M.J. (1975): Aerodynamic Aspects of Animal Flight. *Swimming and Flying in Nature*, eds. T.Y. Wu, C.J. Brokaw and C. Brennen, vol. 2, (Plenum, New York), 423–491.

Lin J.C., Ash R.L. (1986): Wall Temperature Control of Low-Speed Body Drag. *J. Aircraft* **23**, 93–94.

Lin J.C., Howard F.G. (1989): Turbulent Flow Separation Control Through Passive Techniques. AIAA Paper No. 89-0976, New York.

Lin J.C., Howard F.G., Bushnell D.M., Selby G.V. (1990a): Investigation of Several Passive and Active Methods for Turbulent Flow Separation Control. AIAA Paper No. 90-1598, New York.

Lin J.C., Howard F.G., Selby G.V. (1990b): Control of Turbulent Separated Flow over a Rearward-Facing Ramp Using Longitudinal Grooves. *J. Aircraft* **27**, 283–285.

Lin J.C., Weinstein L.M., Watson R.D., Balasubramanian R. (1983): Turbulent Drag Characteristic of Small Amplitude Rigid Surface Waves. AIAA Paper No. 83-0228, New York.

Linke W. (1942): Über den Strömungswiderstand einer beheizten ebenen Platte. *Luftfahrtforschung* **19**, 157–160.

Lissaman P.B.S. (1983): Low-Reynolds-Number Airfoils. *Ann. Rev. Fluid Mech.* **15**, 223–239.

Liu C.K., Kline S.J., Johnston J.P. (1966): Experimental Study of Turbulent Boundary Layer on Rough Walls. Department of Mechanical Engineering Report No. MD-15, Stanford University, Stanford, CA.

Lowell R.L., Reshotko E. (1974): Numerical Study of the Stability of a Heated Water Boundary Layer. Case Western University Report No. FTAS/TR-73-93, Cleveland, OH.

Ludwig G.R. (1964): An Experimental Investigation of Laminar Separation from a Moving Wall. AIAA Paper No. 64-6, New York.

Lumley J.L. (1969): Drag Reduction by Additives. *Ann. Rev. Fluid Mech.* **1**, 367–384.

Lumley J.L. (1973): Drag Reduction in Turbulent Flow by Polymer Additives. *J. Polym. Sci.: Macromol. Rev.* **7**, 263–290.

Lumley J.L. (1977): Drag Reduction in Two Phase and Polymer Flows. *Phys. Fluids* **20**, S64–S71.

Lumley J.L. (1978): Two-Phase and Non-Newtonian Flows. *Turbulence*, ed. P. Bradshaw, second edition, (Springer-Verlag, Berlin), 289–324.

Lumley J.L. (1983): Turbulence Modeling. *J. Applied Mechanics* **105**, 1097–1103.

Lumley J.L. (1987): Turbulence Modeling. *Proc. l0th U.S. National Cong. of Applied Mechanics*, ed. J.P. Lamb, (ASME, New York), 33–39.

Lumley J.L., Kubo I. (1984): Turbulent Drag Reduction by Polymer Additives: A Survey. Sibley School of Mechanical and Aerospace Engineering Report No. FDA-84-07, Cornell University, Ithaca, NY.

Luttges M.W. (1989): Accomplished Insect Fliers. *Frontiers in Experimental Fluid Mechanics*, ed. M. Gad-el-Hak, *Lecture Notes in Engineering*, vol. 46, (Springer-Verlag, Berlin), 429-456.

Luttges M.W., Somps C., Kliss M., Robinson M. (1984): Unsteady Separated Flows: Generation and Use by Insects. *Unsteady Separated Flows*, eds. M.S. Francis and M.W. Luttges, (University of Colorado, Boulder, CO), 127–136.

Mabey D.G. (1988): Design Features Which Influence Flow Separations on Aircraft. *Aero. J.* **92**, 409–415.

Macha J.M., Norton D.J., Young J.C. (1972): Surface Temperature Effect on Subsonic Stall. AIAA Paper No. 72-960, New York.

Madavan N.K., Deutsch S., Merkle C.L. (1984): Reduction of Turbulent Skin Friction by Microbubbles. *Phys. Fluids* **27**, 356–363.

Madavan N.K., Deutsch S., Merkle C.L. (1985): Measurements of Local Skin Friction in a Microbubble-Modified Turbulent Boundary Layer. *J. Fluid Mech.* **156**, 237–256.

Maestrello L., Badavi F.F., Noonan K.W. (1988): Control of the Boundary Layer Separation about an Airfoil by Active Surface Heating. AIAA Paper No. 88-3545-CP, New York.

Magnus G. (1852): On the Deflection of a Projectile. Abhandlung der Akademie der Wissenschaften, Berlin, Germany.

Malik M.R., Weinstein L.M., Hussaini M.Y. (1983): Ion Wind Drag Reduction. AIAA Paper No. 83-0231, New York.

Maltby R.L. (1962): Flow Visualization in Wind Tunnels Using Indicators. NATO Advisory Group for Aerospace Research and Development, AGARDograph No. 70, Rhode-Saint-Génèse, Belgium.

Mangalam S.M., Bar-Sever A., Zaman K.B.M.Q., Harvey W.D. (1986): Transition and Separation Control on a Low-Reynolds number Airfoil. *Proc. Int. Conf. on Aerodynamics at Low Reynolds Numbers*, vol. I, (Royal Aeronautical Society, London, England), 10.1–10.19.

Marchman J.F., Manor D., Plentovich E.B. (1980): Performance Improvement of Delta Wings at Subsonic Speeds Due to Vortex Flaps. AIAA Paper No. 80-1802, New York.

Maxworthy T. (1979): Experiments on the Weis-Fogh Mechanism of Lift Generation by Insects in Hovering Flight. Part 1. Dynamics of the 'Fling'. *J. Fluid Mech.* **93**, 47–63.

Maxworthy T. (1981): The Fluid Dynamics of Insect Flight. *Ann. Rev. Fluid Mech.* **13**, 329–350.

McComb W.D., Chan K.T.J. (1979): Drag Reduction in Fibre Suspensions: Transitional Behavior due to Fibre Degradation. *Nature* **280**, 45–46.

McComb W.D., Chan K.T.J. (1981): Drag Reduction in Fibre Suspension. *Nature* **292**, 520–522.

McComb W.D., Rabie L.H. (1979): Development of Local Turbulent Drag Reduction Due to Nonuniform Polymer Concentration. *Phys. Fluids* **22**, 183–185.

McCormick M.E., Bhattacharyya R. (1973): Drag Reduction of a Submersible Hull by Electrolysis. *Nav. Eng. J.* **85**, 11–16.

McCroskey W.J. (1977): Some Current Research in Unsteady Fluid Dynamics. *J. Fluids Eng.* **99**, 8–39.

McCroskey W.J. (1982): Unsteady Airfoils. *Ann. Rev. Fluid Mech.* **14**, 285–311.

McInville R.M., Hassan H.A., Goodman W.L. (1985): Mixing Layer Control for Tangential Slot Injection in Turbulent Flows. AIAA Paper No. 85-0541, New York.

McLachlan B.G. (1989): Study of a Circulation Control Airfoil with Leading/Trailing-Edge Blowing. *J. Aircraft* **26**, 817–821.

McMichael J.M., Klebanoff P.S., Meese N.E. (1980): Experimental Investigation of Drag on a Compliant Surface. *Viscous Flow Drag Reduction*, ed. G.R. Hough, *Progress in Astronautics & Aeronautics*, vol. 72, (AIAA, New York), 410–438.

McMurray J.T., Metcalfe R.W., Riley J.J. (1983): Direct Numerical Simulations of Active Stabilization of Boundary Layer Flows. *Proc. Eighth Biennial Symp. on Turbulence*, ed. J.L. Zakin and G.K. Patterson, Paper No. 36, (University of Missouri, Rolla, MO).

Mehta R.D. (1985a): Aerodynamics of Sports Balls. *Ann. Rev. Fluid Mech.* **17**, 151–189.

Mehta R.D. (1985b): Effect of a Longitudinal Vortex on a Separated Turbulent Boundary Layer. AIAA Paper No. 85-0530, New York.

Mehta R.D. (1988): Vortex/Separated Boundary-Layer Interactions at Transonic Mach Numbers. *AIAA J.* **26**, 15–26.

Merkle C.L., Deutsch, S. (1985): Drag Reduction by Microbubbles: Current Research Status. AIAA Paper No. 85-0537, New York.

Merkle C.L., Deutsch S. (1989): Microbubble Drag Reduction. *Frontiers inExperimental Fluid Mechanics*, ed. M. Gad-el-Hak, *Lecture Notes in Engineering*, vol. 46, (Springer-Verlag, Berlin), 291–336.

Miau J.J., Chen M.H., Chow J.H. (1988): Flow Structures of a Vertically Oscillating Plate Immersed in a Flat-Plate Turbulent Boundary Layer. *Proc. Eleventh Biennial Symp. on Turbulence*, Paper No. A28, (University of Missouri, Rolla, MO).

Migay V.K. (1960a): Diffuser with Transverse Fins (English translation from Russian). *Energomashinostroenie*, no. 4, 31.

Migay V.K. (1960b): On Improving the Effectiveness of Diffuser Flows with Separation (English translation from Russian). *Mekhanika i Mashinostroyeniye*, no. 4, 171–173.

Migay V.K. (1961): Increasing the Efficiency of Diffusers by Fitting Transverse Fins (English translation from Russian). *Teploenergetika*, no. 4, 41–43.

Migay V.K. (1962a): The Efficiency of a Cross-Ribbed Curvilinear Diffuser (English translation from Russian). *Energomashinostroenie*, no. 1, 45–46.

Migay V.K. (1962b): The Aerodynamic Effectiveness of a Discontinuous Surface (English translation from Russian). *Inzhenerno-Fizicheskiy Zhurnal* **5**, 20–24.

Migay V.K. (1962c): Investigating Finned Diffusers: Effects of Geometry on Effectiveness of Finned Body Diffusers (English translation from Russian). *Teploenergetika*, no. 10, 55–59.

Milling R.W. (1981): Tollmien-Schlichting Wave Cancellation. *Phys. Fluids* **24**, 979–981.

Modi V.J., Fernando M., Yokomizo T. (1990): Drag Reduction of Bluff Bodies Through Moving Surface Boundary Layer Control. AIAA Paper No. 90-0298, New York.

Modi V.J., Mokhtarian F., Fernando M., Yokomizo T. (1989): Moving Surface Boundary Layer Control as Applied to 2-D Airfoils. AIAA Paper No. 89-0296, New York.

Modi V.J., Sun J.L.C., Akutsu T., Lake P., McMillan K., Swinton P.G., Mullins D. (1980): Moving Surface Boundary Layer Control for Aircraft Operations at High Incidence. AIAA Paper No. 80-1621, New York.

Modi V.J., Sun J.L.C., Akutsu T., Lake P., McMillian K., Swinton P.G., Mullins D. (1981): Moving Surface Boundary Layer Control for Aircraft Operation at High Incidence. *J. Aircraft* **18**, 963–968.

Moin P., Bewley T. (1994): Feedback Control of Turbulence. *Appl. Mech. Rev.* **47**, S3–S13.

Mokhtarian F., Modi V.J. (1988): Fluid Dynamics of Airfoils with Moving Surface Boundary Layer Control. *J. Aircraft* **25**, 163–169.

Mokhtarian F., Modi V.J., Yokomizo T. (1988a): Effect of Moving Surfaces on the Airfoil Boundary Layer Control. AIAA Paper No. 88-4337-CP, New York.

Mokhtarian F., Modi V.J., Yokomizo T. (1988b): Rotating Air Scopp as Airfoil Boundary Layer Control. *J. Aircraft* **25**, 973–975.

Moore F.K. (1958): On the Separation of the Unsteady Laminar Boundary Layer. *Boundary-Layer Research*, ed. H. Görtler, (Springer-Verlag, Berlin), 296–310.

Morduchow M., Grape R.G. (1955): Separation, Stability, and Other Properties of Compressible Laminar Boundary Layer with Pressure Gradient and Heat Transfer. NACA Technical Note No. TN-3296, Washington, D.C.

Morkovin M.V. (1969): Critical Evaluation of Transition from Laminar to Turbulent Shear Layers with Emphasis on Hypersonically Traveling Bodies. Air Force Flight Dynamics Laboratory Report No. AFFDL-TR-68-149, Wright-Patterson AFB, OH.

Morkovin M.V. (1984): Bypass Transition to Turbulence and Research Desiderata. *Transition in Turbines Symposium*, NASA CP-2386, Washington, D.C.

Morkovin M.V. (1988): Recent Insights into Instability and Transition to Turbulence in Open-Flow Systems. AIAA Paper No. 88-3675, New York.

Mullin T., Greated C.A., Grant I. (1980): Pulsating Flow over a Step. *Phys. Fluids* **23**, 669–674.

Nadolink R.H., Haigh W.W. (1995): Bibliography on Skin Friction Reduction with Polymers and other Boundary-Layer Additives. *Appl. Mech. Rev.* **48**, 351–460.

Nagamatsu H.T., Dyer R., Ficarra R.V. (1985): Supercritical Airfoil Drag Reduction by Passive Shock Wave/Boundary Layer Control in the Mach Number Range .75 to .9. AIAA Paper No. 85-0207, New York.

Nagamatsu H.T., Trilling T.W., Bossard J.A. (1987): Passive Drag Reduction on a Complete NACA 0012 Airfoil at Transonic Mach Numbers. AIAA Paper No. 87-1263, New York.

Nagel A.L., Alford W.J., Jr., Dugan J.F. (1975): Future Long-Range Transports—Prospects for Improved Fuel Efficiency. NASA Technical Memorandum No. X-72659, Washington, D.C.

Nakayama W. (1986): Thermal Management of Electronic Equipment. *App. Mech. Rev.* **39**, 1847–1868.

Narasimha R., Ojha S.K. (1967): Effect of Longitudinal Surface Curvature on Boundary Layers. *J. Fluid Mech.* **29**, 187–199.

Narasimha R., Sreenivasan K.R. (1973): Relaminarization in Highly Accelerated Turbulent Boundary Layers. *J. Fluid Mech.* **61**, 417–447.

Narasimha R., Sreenivasan K.R. (1979): Relaminarization of Fluid Flows. *Advances in Applied Mechanics*, ed. C.-S. Yih, vol. 19, (Academic Press, New York), 221–309.

Nayfeh A.H., Ragab S.A., Al-Maaitah A. (1986): Effects of Roughness on the Stability of Boundary Layers. AIAA Paper No. 86-1044, New York.

Nelson C.F., Koga D.J., Eaton J.K. (1987): Control of the Unsteady Separated Flow behind an Oscillating Two-Dimensional Flap. AIAA Paper No. 89-1027, New York.

Nelson C.F., Koga D.J., Eaton J.K. (1990): Unsteady, Separated Flow behind an Oscillating, Two-Dimensional Spoiler. *AIAA J.* **2**, 845–852.

Neuburger D., Wygnanski I. (1988): The Use of a Vibrating Ribbon to Delay Separation on Two-Dimensional Airfoils: Some Preliminary Observations. *Proc. Workshop II on Unsteady Separated Flow*, ed. J.M. Walker, Frank J. Seiler Research Laboratory, U.S. Air Force Systems Command Report No. FJSRL-TR-88-0004, Colorado Springs, CO, 333–341.

Nickerson J.D. (1986): A Study of Vortex Generators at Low Reynolds Numbers. AIAA Paper No. 86-0155, New York.

Norman J.R., Fraser F.C. (1937): *Giant Fishes, Whales and Dolphins.* (Putnam, London, England).

Novak C.J., Cornelius K. C., Roads R.K. (1987): Experimental Investigations of the Circular Wall Jet on a Circulation Control Airfoil. AIAA Paper No. 87-0155, New York.

Ogorodnikov D.A., Grin V.T., Zakharov N.N. (1972): Boundary Layer Control of Hypersonic Air Inlets. NASA Report No. TTF-13927, Washington, D.C.

Oyler T.E., Palmer W.E. (1972): Exploratory Investigation of Pulse Blowing for Boundary Layer Control. Columbus Aircraft Division, North American Rockwell Corp. Report No. NR 72H-12, Columbus, OH. (Also available from U.S. NTIS; Document Number AD-742 085.)

Panton R.L. (1996): *Incompressible Flow*, second edition, (Wiley-Interscience, New York).

Papell S.S. (1984): Vortex Generating Flow Passage Design for Increased Film-Cooling Effectiveness and Surface Coverage. NASA Technical Memorandum No. TM-83617, Washington, D.C.

Patel V.C., Head M.R. (1968): Reversion of Turbulent to Laminar Flow. *J. Fluid Mech.* **34**, 371–392.

Patera A.T. (1986): Spectral Element Simulation of Flow in Grooved Channels: Cooling Chips with Tollmien-Schlichting Waves. *Supercomputers and Fluid Dynamics*, eds. K. Kuwahara, R. Mendez, and S.A. Orszag, (Springer-Verlag, Berlin), 41–51.

Patera A.T., Mikić B.B. (1986): Exploiting Hydrodynamic Instabilities—Resonant Heat Transfer Enhancement. *Int. J. Heat Mass Transfer* **29**, 1127–1138.

Patterson G.K., Zakin J.L., Rodriguez J.M. (1969): Drag Reduction. Polymer Solutions, Soap Solutions, and Solid Particle Suspensions in Pipe Flow. *Indus. & Eng. Chem.* **61**, 22–30.

Pearcey H.H. (1961): Shock Induced Separation and Its Prevention by Design and Boundary Layer Control. *Boundary Layer and Flow Control—Its Principle and Applications*, ed. G.V. Lachmann, vol. 2, (Pergamon Press, Oxford, England), 1166–1344.

Pfeffer R., Rosetti S.J. (1971): Experimental Determination of Pressure Drop and Flow Characteristics of Dilute Gas-Solid Suspensions. NASA Contractor Report No. 1894, Washington, D.C.

Pfenninger W. (1946): Untersuchungen über Reibungsverminderung an Tragflügeln, insbesondere mit Hilfe von Grenzschichtabsaugung. Institute of Aerodynamics Report No. 13, ETH, Zürich, Switzerland.

Pfenninger W., Vemuru C.S. (1990): Design of Low Reynolds Number Airfoils. *J. Aircraft* **27**, 204–210.

Phillips O.M. (1979): *The Last Chance Energy Book* (Johns Hopkins Univ. Press, Baltimore, MD).

Plesniak M.W., Nagib H.M. (1985): Net Drag Reduction in Turbulent Boundary Layers Resulting from Optimized Manipulation. AIAA Paper No. 85-0518, New York.

Povkh I.L., Bolonov N.I., Eidel'man A.Ye. (1979): The Average Velocity Profile and the Frictional Loss in Turbulent Flow of an Aqueous Suspension of Clay. *Fluid Mech.—Soviet Research* **8**. 118–124.

Prandtl L. (1904): Über Flüssigkeitsbewegung bei sehr kleiner Reibung. *Proc. Third Int. Math. Congr.*, (Heidelberg, Germany), 484–491.

Prandtl L. (1925): Magnuseffeckt und Windkraftschiff. *Naturwissenschaften* **13**, 93–108.

Prandtl L. (1935): The Mechanics of Viscous Fluids. *Aerodynamic Theory*, ed. W.F. Durand, vol. III, (Springer-Verlag, Berlin), 34–208.

Preston J.H. (1958): The Minimum Reynolds Number for a Turbulent Boundary Layer and the Selection of a Transition Device. *J. Fluid Mech.* **3**, 373–384.

Pretsch J. (1942): Umschlagbeginn und Absaugung. *Jahrb. Dtsch. Luftfahrtforschung* **1**, 54–71.

Purohit S.C. (1987): Effect of Vectored Suction on a Shock-Induced Separation. *AIAA J.* **25**, 759–760.

Purshouse M. (1976): On the Damping of Unsteady Flow by Compliant Boundaries. *J. Sound & Vibration* **49**, 423–436.

Purshouse M. (1977): Interaction of Flow with Compliant Surfaces. Ph.D. Thesis, Cambridge University, Cambridge, United Kingdom.

Radin I. (1974): Solid-Fluid Drag Reduction. Ph.D. Thesis, University of Missouri, Rolla, MO.

Radin I., Zakin J.L., Patterson G.K. (1975): Drag Reduction in Solid-Fluid Systems. *AIChE J.* **21**, 358–371.

Ragab S.A., Nayfeh A.H. (1980): A Comparison of the Second-Order Triple-Deck Theory and Interacting Boundary Layers for Incompressible Flows Past a Hump. AIAA Paper No. 80-0072, New York.

Raghunathan S. (1985): Passive Control of Shock-Boundary Layer Interaction. *Prog. Aerospace Sci.* **25**, 271–296.

Rao D.M. (1979): Leading-Edge Vortex Flap Experiments on a 74-Deg. Delta Wing. NASA Contractor Report No. CR-159161, Washington, D.C.

Rao D.M. Kariya T.T. (1988): Boundary-Layer Submerged Vortex Generators for Separation Control—An Exploratory Study. AIAA Paper No. 88-3546-CP, New York.

Ras M., Ackeret J. (1941): Über Verhinderung der Grenzschicht-Turbulenz durch Absaugung. *Helv. Phys. Acta* **14**, 323.

Raspet A. (1952): Boundary-Layer Studies on a Sailplane. *Aeronaut. Eng. Rev.* **11**, 52–60.

Reed H.L., Nayfeh A.H. (1986): Numerical-Perturbation Technique for Stability of Flat-Plate Boundary Layers with Suction. *AIAA J.* **24**, 208–214.

Reed H.L., Saric W.S. (1987): Stability and Transition of Three-Dimensional Flows. *Proc. 10th U.S. Nat. Cong. Applied Mech.*, ed. J.P. Lamb, (ASME, New York), 457–468.

Reed H.L., Saric W.S. (1989): Stability of Three-Dimensional Boundary Layers. *Ann. Rev. Fluid Mech.* **21**, 235–284.

Reischman M.M., Tiederman W.G. (1975): Laser-Doppler Anemometer Measurements in Drag-Reducing Channel Flows. *J. Fluid Mech.* **70**, 369–392.

Reisenthel P.H., Nagib H.M., Koga D. J. (1985): Control of Separated Flows Using Forced Unsteadiness. AIAA Paper No. 85-0556, New York.

Reshotko E. (1976): Boundary-Layer Stability and Transition. *Ann. Rev. Fluid Mech.* **8**, 311-349.

Reshotko E. (1979): Drag Reduction by Cooling in Hydrogen-Fueled Aircraft. *J. Aircraft* **16**, 584–590.

Reshotko E. (1985): Control of Boundary Layer Transition. AIAA Paper No. 85-0562, New York.

Reshotko E. (1987): Stability and Transition—How Much Do We Know?. *Proc. 10th U.S. National Cong. of App. Mech.*, ed. J.P. Lamb, (ASME, New York), 421–434.

Reynolds G.A., Saric W.S. (1986): Experiments on the Stability of the Flate-Plate Boundary Layer with Suction. *AIAA J.* **24**, 202–207.

Reynolds W.C., Carr, L.W. (1985): Review of Unsteady, Driven, Separated Flows. AIAA Paper No. 85-0527, New York.

Reynolds W.C., Eaton J.K., Johnston J.P., Hesselink L., Powell D.J., Roberts L., Kroo E. (1988): Flow Control for Unsteady and Separated Flows and Turbulent Mixing. AFOSR Technical Report No. TR-89-0232, Washington, D.C. (Also available from U.S. NTIS; Document Number AD-A205989.)

Riley J.J., Gad-el-Hak M. (1985): The Dynamics of Turbulent Spots. *Frontiers in Fluid Mechanics*, eds. S.H. Davis and J.L. Lumley, (Springer-Verlag, Berlin), 123–155.

Riley J.J., Gad-el-Hak M., Metcalfe R.W. (1988): Compliant Coatings. *Ann. Rev. Fluid Mech.* **20**, 393–420.

Ringleb E.O. (1961): Separation Control by Trapped Vortices. *Boundary Layer and Flow Control*, ed. G.V. Lachmann, vol. 1, (Pergamon Press, Oxford, England), 265–294.

Robinson S.K. (1991): Coherent Motions in the Turbulent Boundary Layer. *Annu. Rev. Fluid Mech.* **23**, 601–639.

Roos F.W., Kegelman J.T. (1986): Control of Coherent Structures in Reattaching Laminar and Turbulent Shear Layers. *AIAA J.* **24**, 1956–1963.

Rott N. (1956): Unsteady Viscous Flow in the Vicinity of a Stagnation Point. *Q. Appl. Math.* **13**, 444–451.

Rotta J.C. (1970): Control of Turbulent Boundary Layers by Uniform Injection and Suction of Fluid. *Seventh Congress of the International Council of the Aeronautical Sciences*, ICAS Paper No. 70-10, Rome, Italy.

Runyan L.J., Steers L. L. (1980): Boundary Layer Stability Analysis of a Natural Laminar Flow Glove on the F-111 TACT Airplane. *Viscous Flow Drag Reduction*, ed. G.R. Hough, *Progress in Astronautics & Aeronautics*, vol. 72, (AIAA, New York), 17–32

Ryskin G. (1987): Turbulent Drag Reduction by Polymers: A Quantitative Theory. *Phys. Rev. Letters* **59**, 2059–2062.

Sabadell L.A. (1988): Effects of a Drag Reducing Additive on Turbulent Boundary Layer Structure. M.Sc. Thesis, Princeton University, Princeton, NJ.

Sajben M., Chen C.P., Kroutil J.C. (1976): A New, Passive Boundary Layer Control Device. AIAA Paper No. 76-700, New York.

Saric W.S., Reed H.L. (1986): Effect of Suction and Weak Mass Injection on Boundary-Layer Transition. *AIAA J.* **24**, 383–389.

Saripalli K.R., Simpson R.L. (1980): Investigation of Blown Boundary Layers with an Improved Wall Jet System. NASA Contractor Report No. CR-3340, Washington, D.C.

Sasaki K., Kiya M. (1985): Effect of Free-Stream Turbulence on Turbulent Properties of a Separation-Reattachment Flow. *Bulletin of JSME* **28**, 610–616.

Savins J.G. (1967): A Stress-Controlled Drag-Reduction Phenomenon. *Rheologica Acta* **6**, 323–330.

Savu G., Trifu O. (1984): Porous Airfoils in Transonic Flow. *AIAA J.* **22**, 989–991.

Schilz W. (1965/66): Experimentelle Untersuchungen zur Akustischen Beeinflussung der Strömungsgrenzschicht in Luft. *Acustica* **16**, 208–223.

Schlichting H. (1959): Einige neuere Ergebnisse über Grenzschichtbeein flussung. *Proc. First Int. Congr. Aero. Sci.*, eds. Th. von Karman et al., *Adv. in Aero. Sci.*, vol. 2, (Pergamon Press, London, England), 563–586.

Schlichting H. (1979): *Boundary-Layer Theory*, seventh edition, (McGraw-Hill, New York).

Schlichting H., Pechau W. (1959): Auftriebserhöhung von Tragflügeln durch kontinuierlich verteilte Absaugung. *ZFW* **7**, 113–119.

Schlichting H., Ulrich A. (1940): Zur Berechnung des Umschlages laminar-turbulent. *Jahrb. Dtsch. Luftfahrtforschung* **1**, 8–35.

Schofield W.H. (1985): Turbulent Boundary Layer Development in an Adverse Pressure Gradient After an Interaction with a Normal Shock Wave. *J. Fluid Mech.* **154**, 43–62.

Schubauer G.B., Skramstad H.K. (1947): Laminar Boundary-Layer Oscillations and Stability of Laminar Flow. *J. Aero. Sci.* **14**, 69–78.

Schubauer G.B., Spangenberg W.G. (1960): Forced Mixing in Boundary Layers. *J. Fluid Mech.* **8**, 10–32.

Scott M.R., Watts H.A. (1977): Computational Solution of Linear Two-Point Boundary Value Problems via Orthonormalization. *J. Numerical Analysis* **14**, 40–70.

Sears W.R. (1956): Some Recent Developments in Airfoil Theory. *J. Aeronaut. Sci.* **23**, 490–499.

Sears W.R., Telionis D.P. (1972): Unsteady Boundary-Layer Separation. *Recent Research on Unsteady Boundary Layers*, ed. E.A. Eichelbrenner, vol. 1,(Presses de l'Universite Laval, Quebec, Canada), 404–442.

Sears W.R., Telionis D.P. (1975): Boundary-Layer Separation in Unsteady Flow. *J. Appl. Math.* **28**, 215-235.

Selby G.V., Miandoab, F.H. (1990): Effect of Surface Grooves on Base Pressure for a Blunt Trailing-Edge Airfoil. *AIAA J.* **28**, 1133–1135.

Sen M. (1989): The Influence of Developments in Dynamical Systems Theory on Experimental Fluid Mechanics. *Frontiers in Experimental Fluid Mechanics*, ed. M. Gad-el-Hak, *Lecture Notes in Engineering*, vol. 46, (Springer-Verlag, Berlin), 1–24.

Shiloh K., Shivaprasad B.G., Simpson R.L. (1981): The Structure of a Separating Turbulent Boundary Layer. Part 3: Transverse Velocity Measurements. *J. Fluid Mech.* **113**, 75–90.

Sigal A. (1971): An Experimental Investigation of the Turbulent Boundary Layer over a Wavy Wall. Ph.D. Thesis, California Institute of Technology, Pasadena, CA.

Sigurdson L.W., Roshko A. (1985): Controlled Unsteady Excitation of a Reattaching Flow. AIAA Paper No. 85-0552, New York.

Smith A.M.O. (1957): Transition, Pressure Gradient, and Stability Theory. *Actes IX Congrès International de Mécanique Appliquée*, vol. 4, (Université de Bruxelles, Belgique), 234–244.

Smith A.M.O. (1977): Stratford's Turbulent Separation Criterion for Axially-Symmetric Flows. *J. Applied Math. & Physics* **28**, 929–939.

Smith A.M.O., Gamberoni N. (1956): Transition, Pressure Gradient and Stability Theory. Douglas Aircraft Company Report No. ES-26388, El Segundo, CA.

Smith A.M.O., Kaups K. (1968): Aerodynamics of Surface Roughness and Imperfections. Society of Automotive Engineers Paper No. SAE-680198, New York.

Smith A.M.O., Stokes T.R., Jr., Lee R.S. (1981): Optimum Tail Shapes for Bodies of Revolution. *J. Hydronautics* **15**, 67–73.

Smits A.J., Wood, D.H. (1985): The Response of Turbulent Boundary Layers to Sudden Perturbations. *Ann. Rev. Fluid Mech.* **17**, 321–358.

So R.M.C., Mellor G.L. (1973): Experiment on Convex Curvature Effects in Turbulent Boundary Layers. *J. Fluid Mech.* **60**, 43–62.

Soderman P.T. (1972): Aerodynamic Effects of Leading Edge Separation on a Two-Dimensional Airfoil. NASA Technical Memorandum No. TMX-2643, Washington, D.C.

Soo S.L., Trezek G.J. (1966): Turbulent Pipe Flow of Magnesia Particles in Air. *I&EC Fundamentals* **5**, 388–392.

Spaid F.W. (1972): Cooled Supersonic Turbulent Boundary Layer Separated by a Forward Facing Step. *AIAA J.* **19**, 1117–1119.

Squire H.B. (1933): On the Stability for Three-Dimensional Disturbances of Viscous Fluid Flow Between Parallel Walls. *Proc. R. Soc. Lond. A* **142**, 621–628.

Stanewsky E., Krogmann P. (1985): Transonic Drag Rise and Drag Reduction by Active/Passive Boundary Layer Control. *Aircraft Drag Prediction and Reduction*, AGARD Report No. R-723, Rhode-Saint-Génèse, Belgium, 11.1–11.41.

Staniforth R. (1958): Some Tests on Cascades of Compressor Blades Fitted with Vortex Generators. National Gas Turbine Establishment Memorandum No. NGTE-M-314, Farnborough, England. (Also Aeronautical Research Council, CP-487, London, England.)

Steinheil E., Scherber W., Seidl M., Rieger H. (1977): Investigations on the Interaction of Gases and Well-Defined Solid Surfaces with Respect to Possibilities for Reduction of Aerodynamic Friction and Aerothermal Heating. *Rarefied Gas Dynamics*, ed. J.L. Potter, *AIAA Progress in Aeronautics & Astronautics*, vol. 51, (AIAA, New York), 589–602.

Stratford B.S. (1959a): The Prediction of Separation of the Turbulent Boundary Layer. *J. Fluid Mech.* **5**, 1–16.

Stratford B.S. (1959b): An Experimental Flow with Zero Skin Friction Throughout its Region of Pressure Rise. *J. Fluid Mech.* **5**, 17–35.

Strazisar A.J., Reshotko E., Prahl J.M. (1977): Experimental Study of the Stability of Heated Laminar Boundary Layers in Water. *J. Fluid Mech.* **83**, 225–247.

Stuart J.T. (1963): Hydrodynamic Stability. *Laminar Boundary Layer Theory*, ed. L. Rosenhead, (Clarendon Press, Oxford), 492-579.

Stull F.D., Velkoff H.R. (1975): Flow Regimes in Two-Dimensional Ribbed Diffusers. *J. Fluids Eng.* **97**, 87–96.

Swanson W.M. (1961): The Magnus Effect: A Summary of Investigations to Date. *J. Basic Eng.* **83**, 461–470.

Swearingen J.D., Blackwelder R.F. (1984): Instantaneous Streamwise Velocity Gradients in the Wall Region. *Bull. Am. Phys. Soc.* **29**, 1528.

Tani I. (1969): Boundary-Layer Transition. *Ann. Rev. Fluid Mech.* **1**, 169–196.

Tavella D.A., Lee C.S., Wood N.J. (1986a): Influence of Wing Tip Configuration on Lateral Blowing Efficiency. AIAA Paper No. 86-0475, New York.

Tavella D.A., Wood N.J., Lee C.S., Roberts L. (1986b): Two Blowing Concepts for Roll and Lateral Control of Aircraft. Department of Aeronautics and Astronautics Report No. TR-75, Stanford University, Stanford, CA.

Tavella D.A., Wood N.J., Lee C.S., Roberts L. (1988): Lift Modulation with Lateral Wing-Tip Blowing. *J. Aircraft* **25**, 311–316.

Taylor G.I. (1923): Stability of a Viscous Liquid Contained between Two Rotating Cylinders. *Phil. Trans. R. Soc. London A* **223**, 289–343.

Taylor H.D. (1948a): Application of Vortex Generator Mixing Principles to Diffusers. Research Department Concluding Report No. R-15064-5, United Aircraft Corporation, East Hartford, CN.

Taylor H.D. (1948b): Design Criteria for and Applications of the Vortex Generator Mixing Principle," Research Department Report No. M-15038-1, United Aircraft Corporation, East Hartford, CN.

Telionis D.P., Werle M.J. (1973): Boundary-Layer Separation from Downstream Moving Boundaries. *J. Appl. Mech.* **40**, 369–374.

Tennant J.S. (1973): A Subsonic Diffuser with Moving Walls for Boundary Layer Control. *AIAA J.* **11**, 240–242.

Tennant J.S., Johnson W.S., Keanton D.D., Krothapalli A. (1975): The Application of Moving Wall Boundary Layer Control to Submarine Control Surfaces. University of Tennesse, Report No. MAE-75-01210-1, Knoxville, TN. (Also available from U.S. NTIS; Document Number AD-AO23536.)

Thomas A.S.W. (1983): The Control of Boundary-Layer Transition Using a Wave Superposition Principle. *J. Fluid Mech.* **137**, 233–250.

Tichy J., Warnaka G.E., Poole L.A. (1984): A Study of Active Control of Noise in Ducts. *J. Vibration, Acoustics, Stress & Reliability in Design* **106**, 399–404.

Tiederman W.G., Luchik T.S., Bogard D.G. (1985): Wall-Layer Structure and Drag Reduction. *J. Fluid Mech.* **156**, 419–437.

Tobak M., Peake D.J. (1982): Topology of Three-Dimensional Separated Flows. *Ann. Rev. Fluid Mech.* **14**, 61–85.

Toms B.A. (1948): Some Observations on the Flow of Linear Polymer Solutions Through Straight Tubes at Large Reynolds Numbers. *Proc. 1st Int. Congr. Rheol.*, vol. 2, (North-Holland, Amsterdam), 135–141.

Truckenbrodt E. (1956): Ein einfaches Näherungsverfahren zum Berechnen der laminaren Reibungsschicht mit Absaugung. *Forschg. Ing.-Wes.* **22**, 147–157.

Ulrich A. (1944): Theoretische Untersuchungen über die Widerstandsersparnis durch Laminarhaltung mit Absaugung. *Schriften Dtsch. Akad. Luftfahrtforschung B* **8**, 53.

Vakili A.D. (1990): Review of Vortical Flow Utilization. AIAA Paper No. 90-1429, New York.

Vakili A.D., Wu J.M., Bhat M.K. (1988): High Angle of Attack Aerodynamics of Excitation of the Locked Leeside Vortex. Society of Automotive Engineers Paper No. SAE-88-1424, New York.

Van Ingen J.L., Boermans L.M.M. (1986): Aerodynamics at Low Reynolds Numbers: A Review of Theoretical and Experimental Research at Delft University of Technology. *Proc. Int. Conf. on Aerodynamics at Low Reynolds Numbers*, vol. I, (Royal Aeronautical Society, London, England), 1.1–1.40.

Van Laere L., Sas P. (1988): Principles and Applications of Active Noise Cancellation. *Proc. Noise Control Design: Methods and Practice*, ed. J.S. Bolton, (Noise Control Foundation, Poughkeepsie, NY), 279–284.

Verollet E., Fulachier L., Dumas R., Favre A. (1972): Turbulent Boundary Layer with Suction and Heating to the Wall. *Heat and Mass Transfer in Boundary Layers*, eds. N. Afgan, Z. Zaric and P. Anastasijevec, vol. 1, (Pergamon Presss, Oxford), 157–168.

Vidal R.J. (1959): Research on Rotating Stall in Axial-Flow Compressors: Part III—Experiments on Laminar Separation from a Moving Wall. Wright Air Development Center Technical Report No. 59-75, Wright-Patterson Air Force Base, OH.

Viets H. (1980): Coherent Structures in Time Dependent Shear Flows. *Turbulent Boundary Layers*, AGARD/NATO CPP-271, Paper No. 5, Nevilly Sur Seine, France.

Viets H., Ball M., Bougine D. (1981a): Performance of Forced Unsteady Diffusers. AIAA Paper No. 81-0154, New York.

Viets H., Palmer G.M., Bethke R.J. (1984): Potential Applications of Forced Unsteady Flows. *Unsteady Separated Flows*, eds. M.S. Francis and M.W. Luttges, (University of Colorado, Boulder, CO), 21–27.

Viets H., Piatt M., Ball M. (1979): Unsteady Wing Boundary Layer Energization. AIAA Paper No. 79-1631, New York.

Viets H., Piatt M., Ball M. (1981b): Forced Vortex Near a Wall. AIAA Paper No. 81-0256, New York.

Viets H., Piatt M., Ball M. (1981c): Boundary Layer Control by Unsteady Vortex Generation. *J. Wind Eng. & Industrial Aerodynamics* **7**, 135–144.

Vijgen P.M.H.W., van Dam C.P., Holmes B.J., Howard F.G. (1989): Wind-Tunnel Investigations of Wings with Serrated Sharp Trailing Edges. *Low Reynolds Number Aerodynamics*, ed. T.J. Mueller, *Lecture Notes in Engineering*, vol. 54, (Springer-Verlag, Berlin), 295–313.

Virk P.S. (1975): Drag Reduction Fundamentals. *AIChE J.* **21**, 625–656.

Virk P.S., Merrill E.W., Mickley H.S., Smith K.A., Mollo-Christensen E.L. (1967). The Toms Phenomenon: Turbulent Pipe Flow of Dilute Polymer Solutions. *J. Fluid Mech.* **30**, 305–328.

Viswanath P.R. (1988): Shockwave-Turbulent Boundary Layer Interaction and Its Control: A Survey of Recent Developments. *Sādhanā* **12**, 45–104.

Viswanath P.R. (1995): Flow Management Techniques for Base and Afterbody Drag Reduction. *Prog. Aero. Sci.* **32**, 79–129.

Von Winkle W.A. (1961): An Evaluation of a Boundary Layer Stabilization Coating. Naval Underwater Systems Center Technical Memorandum No. 922-111-61, New London, CT.

Wagner R.D., Bartlett D.W., Maddalond.V. (1988): Laminar Flow Control is Maturing. *Aerospace America* **26**, January, 20–24.

Wagner R.D., Fischer M.C. (1984): Fresh Attack on Laminar Flow. *Aerospace America* **22**, March, 72–76.

Wagner, R.D. Maddalon D.V., Fischer M.C. (1984): Technology Development for Laminar Boundary Control on Subsonic Transport Aircraft. AGARD CP-365, Paper No. 16, Rhode-Saint-Génèse, Belgium.

Wallis R.A., Stuart C.M. (1958): On the Control of Shock Induced Boundary Layer Separation with Discrete Jets. Aeronautical Research Council Current Paper No. 494, London, England.

Walsh M.J. (1980): Drag Characteristics of V-Groove and Transverse Curvature Riblets. *Viscous Flow Drag Reduction*, ed. G.R. Hough, *Progress in Astronautics & Aeronautics*, vol. 72, (AIAA, New York), 168–184.

Walsh M.J. (1982): Turbulent Boundary Layer Drag Reduction Using Riblets. AIAA Paper No. 82-0169, New York.

Walsh M.J. (1983): Riblets as a Viscous Drag Reduction Technique. *AIAA J.* **21**, 485–486.

Walsh M.J. (1990): Riblets. *Viscous Drag Reduction in Boundary Layers*, eds. D.M. Bushnell and J.N. Hefner, *Progress in Astronautics & Aeronautics*, vol. 123, (AIAA, Washington, D.C.), 203–261.

Walsh M.J., Lindemann A.M. (1984): Optimization and Application of Riblets for Turbulent Drag Reduction. AIAA Paper No. 84-0347, New York.

Walsh M.J., Weinstein M. (1978): Drag and Heat Transfer on surfaces with Small Longitudinal Fins. AIAA Paper No. 78-1161, New York.

Warnaka G.E. (1982): Active Attenuation of Noise: The State of the Art. *Noise Control Eng.* **18**, 100–110.

Warner J.V., Waters D.E., Bernhard R.J. (1988): Adaptive Active Noise Control in Three Dimensional Enclosures. *Proc. Noise Control Design: Methods and Practice*, ed. J.S. Bolton, (Noise Control Foundation, Poughkeepsie, NY), 285–290.

Wazzan A.R., Okamura T.T., Smith A.M.O. (1968): Stability of Water Flow over Heated and Cooled Flat Plates. *J. Heat Transfer* **90**, 109–114.

Wazzan A.R., Okamura T.T., Smith A.M.O. (1970): The Stability and Transition of Heated and Cooled Incompressible Boundary Layers. *Proc. 4th Int. Heat Transfer Conf.*, eds. U. Grigull and E. Hahne, vol. 2, FC 1.4, (Elsevier, New York).

Weiberg J.A., Giulianettij D., Gambucci B., Innis R.C. (1973): Takeoff and Landing Performance and Noise Characteristics of a Deflected STOL Airplane with Interconnected Propellers and Rotating Cylinder Flaps. NASA Technical Memorandum No. TM-X-62,320, Washington, D.C.

Weis-Fogh T. (1973): Quick Estimates of Flight Fitness in Hovering Animals, Including Novel Mechanisms for Lift Production. *J. Exp. Biol.* **59**, 169–230.

Wells C.S. (editor) (1969): *Viscous Drag Reduction* (Plenum Press, New York).

Wells C.S., Jr., Spangler J.G. (1967): Injection of a Drag-Reducing Fluid into Turbulent Pipe Flow of a Newtonian Fluid. *Phys. Fluids* **10**. 1890–1894.

Werle M.J., Paterson R.W., Presz W.M., Jr. (1987): Trailing-Edge Separation/Stall Alleviation. *AIAA J.* **25**, 624–626.

Wheeler G.O. (1984): Means for Maintaining Attached Flow of a Flow Medium. U.S. Patent No. 4,455,045.

Whitcomb R.T. (1956): A Study of the Zero-Lift Drag-Rise Characteristics of Wing-Body Combinations Near the Speed of Sound. NACA Report No. 1273, Washington, D.C.

White A., Hemmings J.A.G. (1976): *Drag Reduction by Additives: Review and Bibliography* (BHRA Fluid Engineering, Cranfield, United Kingdom).

Whites R.C., Sudderth R.W., Wheldon W.G. (1966): Laminar Flow Control on the X-21. *Astro. & Aero.* 4, 38–43.

Wilkinson S.P. (1988): Direct Drag Measurements on Thin-Element Riblets with Suction and Blowing. AIAA Paper No. 88-3670-CP, New York.

Wilkinson S.P. (1990): Interactive Wall Turbulence Control. *Viscous Drag Reduction in Boundary Layers*, eds. D.M. Bushnell and J.N. Hefner, *Progress in Astronautics & Aeronautics*, vol. 123, (AIAA, Washington, D.C.), 479–509.

Wilkinson S.P., Anders J.B., Lazos B.S., Bushnell D.M. (1988): Turbulent Drag Reduction Research at NASA Langley: Progress and Plans. *Int. J. Heat and Fluid Flow* **9**, 266–277.

Wilkinson S.P., Lazos B.S. (1987): Direct Drag and Hot-Wire Measurements on Thin-Element Riblet Arrays. *Turbulence Management and Relaminarization*, eds. H.W. Liepmann and R. Narasimha, (Springer-Verlag, Berlin), 121–131.

Williams D.R., Amato C.W. (1989): Unsteady Pulsing of Cylinder Wakes. *Frontiers in Experimental Fluid Mechanics*, ed. M. Gad-el-Hak, *Lecture Notes in Engineering*, vol. 46, (Springer-Verlag, Berlin), 337–364.

Williams J.C., III, Johnson W.D. (1974a): Semisimilar Solutions to Unsteady Boundary-Layer Flows Including Separation. *AIAA J.* **12**, 1388–1393.

Williams J.C., III, Johnson W.D. (1974b): Note on Unsteady Boundary-Layer Separation. *AIAA J.* **12**, 1427–1429.

Williams T. I. (1987): *The History of Invention* (Facts on File Publications, New York).

Willis G.J.K. (1986): Hydrodynamic Stability of Boundary Layers over Compliant Surfaces. Ph.D. Thesis, University of Exeter, United Kingdom.

Wimpenny J.C. (1970): Vortex Generators. U.S. Patent No. 3,525486.

Wood C.J. (1961): A Study of Hypersonic Separated Flow. Ph.D. Thesis, University of London, England.

Wood N.J., Nielsen J. N. (1985): Circulation Control Airfoils—Past, Present, Future. AIAA Paper No. 85-0204, New York.

Wood N.J., Roberts L. (1986): Experimental Results of the Control of a Vortical Flow by Tangential Blowing. Stanford University Report No. JIAA TR-71, Stanford, CA.

Wood N.J., Roberts L. (1988): Control of Vortical Lift on Delta Wings by Tangential Leading-Edge Blowing. *J. Aircraft* **25**, 236–243.

Wood N.J., Roberts L., Celik Z. (1990): Control of Asymmetric Vortical Flows over Delta Wings at High Angles of Attack. *J. Aircraft* **27**, 429–435.

Wooldridge C.E., Muzzy R.J. (1966): Boundary-Layer Turbulence Measurements with Mass Addition and Combustion. *AIAA J.* 4, 2009–2016.

Wortmann A. (1987): Alleviation of Fuselage from Drag Using Vortex Flows. Department of Energy Report No. DOE/CE/15277-T1, Washington, D.C.

Wu J., Tulin M.P. (1972): Drag Reduction by Ejecting Additive Solutions into a Pure-Water Boundary Layer. *ASME J. Basic Eng.* **94**, 749–756.

Wu J.M., Vakili A.D., Chen Z.L. (1983): Investigation on the Effects of Discrete Wingtip Jets. AIAA Paper No. 83-0546, New York.

Wu J.M., Vakili A.D., Gilliam F.T. (1984): Aerodynamic Interactions of Wingtip Flow with Discrete Wingtip Jets. AIAA Paper No. 84-2206, New York.

Wuest W. (1961): Survey of Calculation Methods of Laminar Boundary Layers With Suction in Incompressible Flow. *Boundary Layer and Flow Control—Its Principle and Applications*, ed. G.V. Lachmann, vol. 2, (Pergamon Press, New York), 771–800.

Yajnik K.S., Acharya M. (1978): Non-Equilibrium Effects in a Turbulent Boundary Layer due to the Destruction of Large Eddies. *Structure and Mechanisms of Turbulence*, ed. H. Fiedler, vol. 1, (Springer-Verlag, Berlin), 249–260.

Yeo K.S., Dowling A.P. (1987): The Stability of Inviscid Flows over Passive Compliant Walls. *J. Fluid Mech.* **183**, 265–292.

Young A.D. (1953): Boundary Layers. *Modern Developments in Fluid Dynamics: High Speed Flow*, ed. L. Howarth, vol. 1, (Clarendon Press, Oxford), 375–475.

Zakin J.L., Poreh M., Brosh A., Warshavsky M. (1971): Exploratory Study of Friction Reduction in Slurry Flows. *Chem. Eng. Prog. Symp. Seri.*, no. 67, vol. 111, (AIChE, New York), 85–89.

Zaman K.B.M.Q., Bar-Sever A., Mangalam S.M. (1987): Effect of Acoustic Excitation on the Flow over a Low-Re Airfoil. *J. Fluid Mech.* **182**, 127–148.

Zaman K.B.M.Q., McKinzie D.J. (1989): Control of 'Laminar Separation' over Airfoils by Acoustic Excitation. AIAA Paper No. 89-0565, New York. (Also NASA Technical Memorandum No. TM-101379, Washington, D.C.)

Zang T.A., Hussaini M.Y., Bushnell D.M. (1984): Numerical Computations of Turbulence Amplification in Shock Wave Interactions. *AIAA J.* **22**, 13–22.

Zhang F., Sheng C. (1987): A Prediction Method for Optimum Velocity Ratio of Air Jet Vortex Generator. *J. Aerospace Power* **2**, 55–60, 92, 93.

Zhuk V.I., Ryzhov O.S. (1980): Formation of Recirculation Zones in the Boundary Layer on a Moving Surface. *Fluid Dynamics* **15**, 637–644.

2 Frontiers of Flow Control

Mohamed Gad-el-Hak

University of Notre Dame, Notre Dame, Indiana 46556, U.S.A.

Abstract. In contrast to the first chapter, in the present chapter I shall emphasize the frontiers of the field of flow control, pondering mostly the control of turbulent flows. I shall review the important advances in the field that took place during the past few years and are anticipated to dominate progress in the near future, essentially covering the fifth era outlined in Sect. 2 of the previous chapter. By comparison with laminar flow control or separation prevention, the control of turbulent flow remains a very challenging problem. Flow instabilities magnify quickly near critical flow regimes, and therefore delaying transition or separation are relatively easier tasks. In contrast, classical control strategies are often ineffective for fully turbulent flows. Newer ideas for turbulent flow control to achieve, for example, skin-friction drag reduction focus on the direct onslaught on coherent structures. Spurred by the recent developments in chaos control, microfabrication and soft computing tools, reactive control of turbulent flows, where sensors detect oncoming coherent structures and actuators attempt to favorably modulate those quasi-periodic events, is now in the realm of the possible for future practical devices. In this article, I shall provide estimates for the number, size, frequency and energy consumption of the sensor/actuator arrays needed to control the turbulent boundary layer on a full-scale aircraft or submarine.

1 Introduction

1.1 The Taming of the Shrew

Considering the extreme complexity of the turbulence problem in general and the unattainability of first-principles analytical solutions in particular, it is not surprising that controlling a turbulent flow remains a challenging task, mired in empiricism and unfulfilled promises and aspirations. Brute force suppression, or *taming*, of turbulence via active, energy-consuming control strategies is always possible, but the penalty for doing so often exceeds any potential benefits. The artifice is to achieve a desired effect with minimum energy expenditure. This is of course easier said than done. Indeed, suppressing turbulence is as arduous as the taming of the shrew. The former task will be emphasized throughout this chapter, but for now we reflect on a short verse from the latter.

From William Shakespeare's The Taming of the Shrew:
Curtis (Petruchio's servant, in charge of his country house): Is she so hot a shrew as she's reported?
Grumio (Petruchio's personal lackey): She was, good Curtis, before this frost.

M. Gad-el-Hak et al.: LNPm 53, pp. 109 - 153, 1998
© Springer-Verlag Berlin Heidelberg 1998

But thou know'st winter tames man, woman, and beast; for it hath tamed my old master, and my new mistress, and myself, fellow Curtis.

1.2 Control of Turbulence

Numerous methods of flow control have already been successfully implemented in practical engineering devices. Such classical techniques have been reviewed in the first chapter of this book and by, among others, Barnwell and Hussaini (1992), Bushnell (1983; 1994), Wilkinson et al. (1988), Bushnell and McGinley (1989), Gad-el-Hak (1989), Bushnell and Hefner (1990), Fiedler and Fernholz (1990), Gad-el-Hak and Bushnell (1991), Viswanath (1995), and Joslin et al. (1996). Yet, very few of the classical strategies are effective in controlling free-shear or wall-bounded turbulent flows. Serious limitations exist for some familiar control techniques when applied to certain turbulent flow situations. For example, in attempting to reduce the skin-friction drag of a body having a turbulent boundary layer using global suction, the *penalty* associated with the control device often exceeds the *saving* derived from its use. What is needed is a way to reduce this penalty to achieve a more efficient control.

Flow control is most effective when applied near the transition or separation points; in other words, near the critical flow regimes where flow instabilities magnify quickly. Therefore, delaying/advancing laminar-to-turbulence transition and preventing/provoking separation are relatively easier tasks to accomplish. To reduce the skin-friction drag in a non-separating turbulent boundary layer, where the mean flow is quite stable, is a more challenging problem. Yet, even a modest reduction in the fluid resistance to the motion of, for example, the world-wide commercial air fleet is translated into fuel savings estimated to be in the billions of dollars. Newer ideas for turbulent flow control focus on the direct onslaught on coherent structures. Spurred by the recent developments in chaos control, microfabrication and soft computing tools, reactive control of turbulent flows is now in the realm of the possible for future practical devices.

The primary objective of the present chapter is to advance possible scenarios by which viable control strategies of turbulent flows could be realized. As will be argued in the following presentation, future systems for control of turbulent flows in general and turbulent boundary layers in particular could greatly benefit from the merging of the science of chaos control, the technology of microfabrication, and the newest computational tools collectively termed soft computing. Control of chaotic, nonlinear dynamical systems has been demonstrated theoretically as well as experimentally, even for multi-degree-of-freedom systems. Microfabrication is an emerging technology which has the potential for producing inexpensive, programmable sensor/actuator chips that have dimensions of the order of a few microns. Soft computing tools include neural networks, fuzzy logic and genetic algorithms and are now more advanced as well as more widely used as compared to just few

years ago. These tools could be very useful in constructing effective adaptive controllers.

Such futuristic systems are envisaged as consisting of a large number of intelligent, interactive, microfabricated wall sensors and actuators arranged in a checkerboard pattern and targeted towards specific organized structures that occur randomly within the boundary layer. Sensors detect oncoming coherent structures, and adaptive controllers process the sensors information and provide control signals to the actuators which in turn attempt to favorably modulate the quasi-periodic events. Finite number of wall sensors perceive only partial information about the entire flow field above. However, a low-dimensional dynamical model of the near-wall region used in a Kalman filter can make the most of the partial information from the sensors. Conceptually all of that is not too difficult, but in practice the complexity of such a control system is daunting and much research and development work still remain.

1.3 Outline

The present chapter reviews the important developments in the field of flow control that took place during the past few years and suggests avenues for future research. The emphasis will be on reactive flow control for future vehicles and other industrial devices. The present chapter is organized into eight sections. A particular example of a classical control system, suction, is described in the following section. This will serve as a prelude to introducing the selective suction concept. In Sect. 3, the different hierarchy of coherent structures that dominate a turbulent boundary layer and that constitute the primary target for direct onslaught are briefly recalled. Reactive flow control and the selective suction concept are described in Sect. 4. The number, size, frequency and energy consumption of the sensor/actuator units required to tame the turbulence on a full-scale air or water vehicle are estimated in that same section. Sections 5, 6 and 7 consider the emerging areas of chaos control, microfabrication and soft computing, respectively, particularly as they relate to reactive control strategies. Finally, brief concluding remarks are given in Sect. 8.

2 Suction

To set the ground for introducing the concept of targeted control in Sect. 4, I shall first discuss in this section global control as applied to wall-bounded flows. Part of the material in the present section was already included in the previous chapter but is repeated here for completeness. A viscous fluid which is initially irrotational will acquire vorticity when an obstacle is passed through the fluid. This vorticity controls the nature and structure of the boundary layer flow in the vicinity of the obstacle. For an incompressible,

wall-bounded flow, the flux of spanwise or streamwise vorticity at the wall, and hence whether the surface is a sink or a source of vorticity, is affected by the wall motion (e.g. in the case of a compliant coating), transpiration (suction or injection), streamwise or spanwise pressure gradient, wall curvature, and normal viscosity gradient near the wall (caused by, for example, heating/cooling of the wall or introduction of a shear-thinning/shear thickening additive into the boundary layer). As demonstrated in Sect. 3.1 of the previous chapter, these alterations separately or collectively control the shapes of the instantaneous as well as the mean velocity profiles which in turn determine the skin friction at the wall, the boundary layer ability to resist transition and separation, and the intensity of turbulence and its structure.

For illustration purposes, we focus on global wall suction as a generic control tool. The arguments presented here and in subsequent sections are equally valid for other global control techniques, such as geometry modification (body shaping), surface heating/cooling, etc. As has been shown in Chap. 1, transpiration provides a good example of a single control technique that is used to achieve a variety of goals. Suction leads to a fuller velocity profile (vorticity flux away from the wall) and can, therefore, be employed to delay laminar-to-turbulence transition, postpone separation, achieve an asymptotic turbulent boundary layer (i.e. constant momentum thickness), or relaminarize an already turbulent flow. Unfortunately, global suction can not be used to reduce the skin-friction drag in a turbulent boundary layer. The amount of suction required to inhibit boundary-layer growth is too large to effect a net drag reduction. This is a good illustration of a situation where the penalty associated with a control device might exceed the saving derived from its use.

Small amounts of fluid withdrawn from the near-wall region of a boundary layer change the curvature of the velocity profile at the wall and can dramatically alter the stability characteristics of the flow. Concurrently, suction inhibits the growth of the boundary layer, so that the critical Reynolds number[1] based on thickness may never be reached. Although laminar flow can be maintained to extremely high Reynolds numbers provided that enough fluid is sucked away, the goal is to accomplish transition delay with the minimum suction flow rate. This will reduce not only the power necessary to drive the suction pump, but also the momentum loss due to the additional freestream fluid entrained into the boundary layer as a result of withdrawing fluid from the wall. That momentum loss is, of course, manifested as an increase in the skin-friction drag.

The case of uniform suction from a flat plate at zero incidence is an exact solution of the Navier-Stokes equation. The asymptotic velocity profile in the viscous region is exponential and has a negative curvature at the wall. The displacement thickness has the constant value $\delta^* = \nu/|v_w|$, where ν is

[1] The lowest Reynolds number at which linear Tollmien-Schlichting waves would grow in a particular laminar flow.

the kinematic viscosity and $|v_w|$ is the absolute value of the normal velocity at the wall. In this case, the familiar von Kármán integral equation reads: $C_f = 2\,C_q$. Bussmann and Münz (1942) computed the critical Reynolds number for the asymptotic suction profile to be $Re_{\delta^*} \equiv U_\infty \delta^*/\nu = 70,000$. From the value of δ^* given above, the flow is stable to all small disturbances if $C_q \equiv |v_w|/U_\infty > 1.4 \times 10^{-5}$. The amplification rate of unstable disturbances for the asymptotic profile is an order of magnitude less than that for the Blasius boundary layer (Pretsch, 1942). This treatment ignores the development distance from the leading edge needed to reach the asymptotic state. When this is included into the computation, a higher C_q $\left(1.18 \times 10^{-4}\right)$ is required to ensure stability (Iglisch, 1944; Ulrich, 1944).

In a turbulent wall-bounded flow, the results of Eléna (1975; 1984) and more recently of Antonia et al. (1988) indicate that suction causes an appreciable stabilization of the low-speed streaks in the near-wall region. The maximum turbulence level at $y^+ \approx 13$ drops from 15 to 12% as C_q varies from 0 to 0.003. More dramatically, the tangential Reynolds stress near the wall drops by a factor of 2 for the same variation of C_q. The dissipation length scale near the wall increases by 40% and the integral length scale by 25% with the suction.

The suction rate necessary for establishing an asymptotic turbulent boundary layer independent of streamwise coordinate ($\mathrm{d}\delta_\theta/\mathrm{d}x = 0$) is much lower than the rate required for relaminarization ($C_q \approx 0.01$), but still not low enough to yield net drag reduction. For Reynolds number based on distance from leading edge $Re = \mathcal{O}\left[10^6\right]$, Favre et al. (1966), Rotta (1970) and Verollet et al. (1972), among others, report an asymptotic suction coefficient of $C_q \approx 0.003$. For a zero-pressure-gradient boundary layer on a flat plate, the corresponding skin-friction coefficient is $C_f = 2\,C_q = 0.006$, indicating higher skin friction than if no suction was applied. To achieve a net skin-friction reduction with suction, the process must be further optimized. One way to accomplish that is to target the suction towards particular organized structures within the boundary layer and not to use it globally as in classical control schemes. This point will be revisited in Sect. 4, but the coherent structures to be targeted are first described in Sect. 3.

3 Coherent Structures

The discussion in Sect. 2 indicates that achieving a particular control goal is always possible. The challenge is reaching that goal with a penalty that can be tolerated. Suction, for example, would lead to a net drag reduction, if only we could reduce the suction coefficient necessary for establishing an asymptotic turbulent boundary layer to below one-half of the unperturbed skin-friction coefficient. A more efficient way of using suction, or any other global control method, is to aim at a particular coherent structure within the turbulent boundary layer. Before discussing this *selective control* idea, we

briefly describe in this section the different hierarchy of organized structures in a wall-bounded flow.

The classical view that turbulence is essentially a stochastic phenomenon having a randomly fluctuating velocity field superimposed on a well-defined mean has been changed in the last few decades by the realization that the transport properties of all turbulent shear flows are dominated by quasi-periodic, large-scale vortex motions (Laufer, 1975; Cantwell, 1981; Fiedler, 1988; Robinson, 1991). Despite the extensive research work in this area, no generally accepted definition of what is meant by coherent motion has emerged. In physics, coherence stands for well-defined phase relationship. For the present purpose we adopt the rather restrictive definition given by Hussain (1986): *a coherent structure is a connected turbulent fluid mass with instantaneously phase-correlated vorticity over its spatial extent.* In other words, underlying the random, three-dimensional vorticity that characterizes turbulence, there is a component of large-scale vorticity which is instantaneously coherent over the spatial extent of an organized structure. The apparent randomness of the flow field is, for the most part, due to the random size and strength of the different types of organized structures comprising that field.

In a wall-bounded flow, a multiplicity of coherent structures have been identified mostly through flow visualization experiments, although some important early discoveries have been made using correlation measurements (e.g., Townsend, 1961; 1970; Bakewell and Lumley, 1967). Although the literature on this topic is vast, no research-community-wide consensus has been reached particularly on the issues of the origin of and interaction between the different structures, regeneration mechanisms, and Reynolds number effects. What follow are somewhat biased remarks addressing those issues, gathered mostly via low-Reynolds number experiments.[2] The interested reader is referred to the large number of review articles available (e.g., Kovasznay, 1970; Laufer, 1975; Willmarth, 1975a; 1975b; Saffman, 1978; Cantwell, 1981; Fiedler, 1986; 1988; Blackwelder, 1988; Robinson, 1991). The last reference in particular summarizes many of the different, sometimes contradictory, conceptual models offered thus far by different research groups. Those models are aimed ultimately at explaining how the turbulence maintains itself, and range from the speculative to the rigorous but none, unfortunately, is self-contained and complete. Furthermore, the structure research dwells largely on the kinematics of organized motion and little attention is given to the dynamics of the regeneration process.

In a boundary layer, the turbulence production process is dominated by three kinds of quasi-periodic eddies: the large outer structures, the intermediate Falco eddies, and the near-wall events. The large, three-dimensional structures scale with the boundary layer thickness, δ, and extend across the entire layer (Kovasznay et al., 1970; Blackwelder and Kovasznay, 1972). These

[2] See Gad-el-Hak and Bandyopadhyay (1994) for a discussion of Reynolds number effects.

eddies control the dynamics of the boundary layer in the outer region, such as entrainment, turbulence production, etc. They appear randomly in space and time, and seem to be, at least for moderate Reynolds numbers, the residue of the transitional Emmons spots (Zilberman et al., 1977; Gad-el-Hak et al., 1981). The Falco eddies are also highly coherent and three dimensional. Falco (1974; 1977) named them typical eddies because they appear in wakes, jets, Emmons spots, grid-generated turbulence, and boundary layers in zero, favorable and adverse pressure gradients. They have an intermediate scale of about $100\,\nu/u_\tau$ (100 wall units; u_τ is the friction velocity and ν/u_τ is the viscous length-scale). The Falco eddies appear to be an important link between the large structures and the near-wall events.

The third kind of eddies exists in the near-wall region ($0 < y < 100\,\nu/u_\tau$) where the Reynolds stress is produced[3] in a very intermittent fashion. Half of the total production of turbulence kinetic energy $\left(-\overline{uv}\,\partial\overline{U}/\partial y\right)$ takes place near the wall in the first 5% of the boundary layer at typical laboratory Reynolds numbers (smaller fraction at higher Reynolds numbers), and the dominant sequence of eddy motions there are collectively termed the bursting phenomenon. This dynamically significant process was reviewed by Willmarth (1975) and Blackwelder (1978) and more recently by Robinson (1991). Qualitatively, the process, according to at least one school of thought, begins with elongated, counter-rotating, streamwise vortices having diameters of approximately $40\,\nu/u_\tau$. The vortices exist in a strong shear and induce low- and high-speed regions between them as sketched in Fig. 1. The vortices and the accompanying eddy structures occur randomly in space and time. However, their appearance is regular enough that an average spanwise wavelength of approximately 80 to $100\,\nu/u_\tau$ has been identified by Kline et al. (1967) and others. Kline et al. also observed that the low-speed regions grow downstream and develop inflectional $U(y)$ profiles. At approximately the same time, the interface between the low- and high-speed fluid begins to oscillate, apparently signaling the onset of a secondary instability. The low-speed region lifts up away from the wall as the oscillation amplitude increases, and then the flow rapidly breaks down into a completely chaotic motion. Since this latter process occurs on a very short time scale, Kline et al. called it a *burst*. Corino and Brodkey (1969) showed that the low-speed regions are quite narrow, i.e., $z = 20\,\nu/u_\tau$, and may also have significant shear in the spanwise direction. Virtually all of the net production of turbulence kinetic energy in the near-wall region occurs during these bursts.

Considerably more has been learned about the bursting process during the last decade. For example, Falco (1980; 1983; 1991) has shown that when a typical eddy, which may be formed in part by ejected wall-layer fluid, moves

[3] In high-Reynolds-number flows, the Reynolds stress peaks, and therefore is produced, outside the near-wall region (see Gad-el-Hak and Bandyopadhyay, 1994). This contrasts the production of turbulence kinetic energy which always peaks near the wall, say $y^+ \approx 13$.

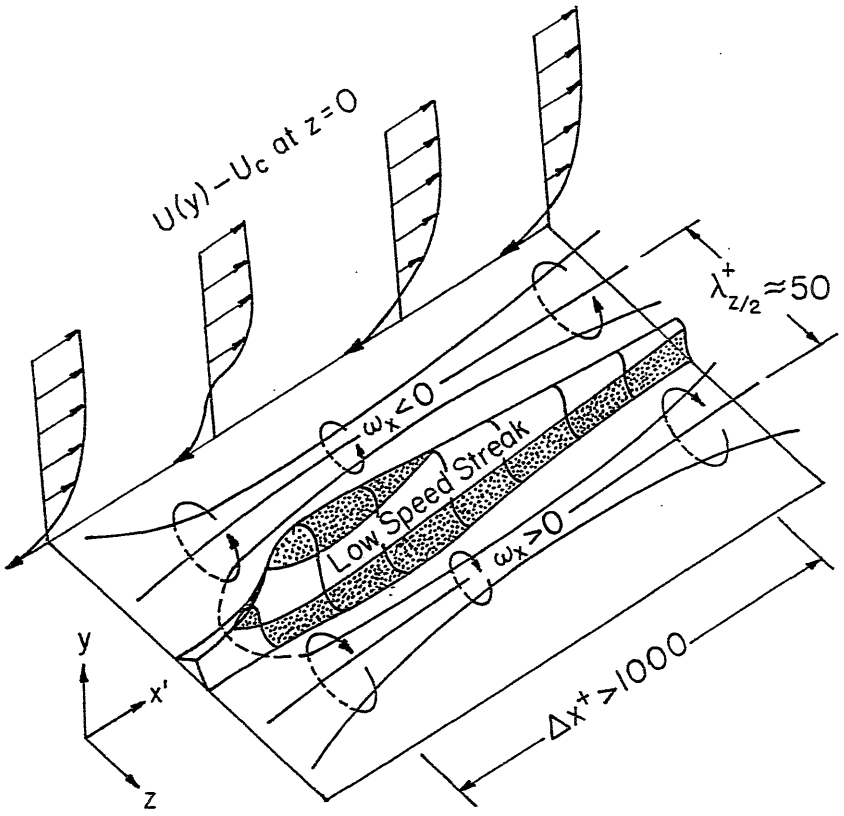

Fig. 1. Model of near-wall turbulent boundary-layer structure (adapted from Blackwelder, 1978)

over the wall it induces a high uv sweep (positive u and negative v). The wall region is continuously bombarded by *pockets* of high-speed fluid originating in the logarithmic and possibly the outer layers of the flow. These pockets tend to promote and/or enhance the inflectional velocity profiles by increasing the instantaneous shear leading to a more rapidly growing instability. Blackwelder and Haritonidis (1983) have shown convincingly that the frequency of occurrence of these events scales with the viscous parameters consistent with the usual boundary layer scaling arguments. An excellent review of the dynamics of turbulent boundary layers has recently been provided by Sreenivasan (1989). More information about coherent structures in high-Reynolds number boundary layers is given by Gad-el-Hak and Bandyopadhyay (1994).

4 Reactive Control

4.1 Introductory Remarks

Targeted control implies sensing and reacting to a particular quasi-periodic structure in the boundary layer. The wall seems to be the logical place for such reactive control, because of the relative ease of placing something in there, the sensitivity of the flow in general to surface perturbations, and the proximity and therefore accessibility to the dynamically all important near-wall coherent events. According to Wilkinson (1990), there are very few actual experiments that use embedded wall sensors to initiate a surface actuator response (Alshamani et al., 1982; Wilkinson and Balasubramanian, 1985; Nosenchuck and Lynch, 1985; Breuer et al., 1989). This six-year-old assessment is fast changing, however, with the introduction of microfabrication technology that has the potential for producing small, inexpensive, programmable sensor/actuator chips. Witness the more recent reactive control attempts by Kwong and Dowling (1993), Reynolds (1993), Jacobs et al. (1993), Jacobson and Reynolds (1993a; 1993b; 1994; 1995), Fan et al. (1993), James et al. (1994), and Keefe (1997). Fan et al. and Jacobson and Reynolds even consider the use of self-learning neural networks for increased computational speeds and efficiency. Recent reviews of reactive flow control include those by Gad-el-Hak (1994; 1996), Lumley (1996), McMichael (1996), Mehregany et al. (1996), and Ho and Tai (1996).

Numerous methods of flow control have already been successfully implemented in practical engineering devices. Yet, limitations exist for some familiar control techniques when applied to specific situations. For example, in attempting to reduce the drag or enhance the lift of a body having a turbulent boundary layer using global suction, the *penalty* associated with the control device often exceeds the *saving* derived from its use. What is needed is a way to reduce this penalty to achieve a more efficient control. Reactive control geared specifically towards manipulating the coherent structures in turbulent shear flows, though considerably more complicated than passive control or even predetermined active control, has the potential to do just that. As will be argued in this and the following three sections, future systems for control of turbulent flows in general and turbulent boundary layers in particular could greatly benefit from the merging of the science of chaos control, the technology of microfabrication, and the newest computational tools collectively termed soft computing. Such systems are envisaged as consisting of a large number of intelligent, communicative wall sensors and actuators arranged in a checkerboard pattern and targeted towards controlling certain quasi-periodic, dynamically significant coherent structures present in the near-wall region.

4.2 Targeted Control

As discussed in Chap. 1, successful techniques to reduce the skin friction in a turbulent flow, such as polymers, particles or riblets, appear to act indirectly through local interaction with discrete turbulent structures, particularly small-scale eddies, within the flow. Common characteristics of all these methods are increased losses in the near-wall region, thickening of the buffer layer, and lowered production of Reynolds shear stress (Bandyopadhyay, 1986). Methods that act directly on the mean flow, such as suction or lowering of near-wall viscosity, also lead to inhibition of Reynolds stress. However, skin friction is increased when any of these velocity-profile modifiers is applied globally.

Could these seemingly inefficient techniques, e.g. global suction, be used more sparingly and be optimized to reduce their associated penalty? It appears that the more successful drag-reduction methods, e.g. polymers, act selectively on particular scales of motion and are thought to be associated with stabilization of the secondary instabilities. It is also clear that energy is wasted when suction or heating/cooling is used to suppress the turbulence throughout the boundary layer when the main interest is to affect a near-wall phenomenon. One ponders, what would become of wall turbulence if specific coherent structures are to be targeted, by the operator through a reactive control scheme, for modification? The myriad of organized structures present in all shear flows are instantaneously identifiable, quasi-periodic motions (Cantwell, 1981; Robinson, 1991). Bursting events in wall-bounded flows, for example, are both intermittent and random in space as well as time. The random aspects of these events reduce the effectiveness of a predetermined active control strategy. If such structures are nonintrusively detected and altered, on the other hand, net performance gain might be achieved. It seems clear, however, that temporal phasing as well as spatial selectivity would be required to achieve proper control targeted towards random events.

A nonreactive version of the above idea is the *selective suction technique* which combines suction to achieve an asymptotic turbulent boundary layer and longitudinal riblets to fix the location of low-speed streaks. Although far from indicating net drag reduction, the available results are encouraging and further optimization is needed. When implemented via an array of reactive control loops, the selective suction method is potentially capable of skin-friction reduction that approaches 60%.

The genesis of the selective suction concept can be found in the papers by Gad-el-Hak and Blackwelder (1987; 1989) and the patent by Blackwelder and Gad-el-Hak (1990). These researchers suggest that one possible means of optimizing the suction rate is to be able to identify where a low-speed streak is presently located and apply a small amount of suction under it. Assuming that the production of turbulence kinetic energy is due to the instability of an inflectional $U(y)$ velocity profile, one needs to remove only enough fluid so that the inflectional nature of the profile is alleviated. An alternative tech-

nique that could conceivably reduce the Reynolds stress is to inject fluid selectively under the high-speed regions. The immediate effect of normal injection would be to decrease the viscous shear at the wall resulting in less drag. In addition, the velocity profiles in the spanwise direction, $U(z)$, would have a smaller shear, $\partial U/\partial z$, because the suction/injection would create a more uniform flow. Since Swearingen and Blackwelder (1984) have found that inflectional $U(z)$ profiles occur as often as inflection points are observed in $U(y)$ profiles, suction under the low-speed streaks and/or injection under the high-speed regions would decrease this shear and hence the resulting instability. The combination of selective suction and injection is sketched in Fig. 2. In Fig. 2a, the vortices are idealized by a periodic distribution in the spanwise direction. The instantaneous velocity profiles without transpiration at constant y and z locations are shown by the dashed lines in Figs. 2b and 2c, respectively. Clearly, the $U(y_o, z)$ profile is inflectional, having two inflection points per wavelength. At z_1 and z_3, an inflectional $U(y)$ profile is also evident. The same profiles with suction at z_1 and z_3 and injection at z_2 are shown by the solid lines. In all cases, the shear associated with the inflection points would have been reduced. Since the inflectional profiles are all inviscidly unstable with growth rates proportional to the shear, the resulting instabilities would be weakened by the suction/injection process.

The feasibility of the selective suction as a drag-reducing concept has been demonstrated by Gad-el-Hak and Blackwelder (1989) and is indicated in Fig. 3. Low-speed streaks were artificially generated in a laminar boundary layer using three spanwise suction holes as per the method proposed by Gad-el-Hak and Hussain (1986), and a hot-film probe was used to record the near-wall signature of the streaks. An open, feedforward control loop with a phase lag was used to activate a predetermined suction from a longitudinal slot located in between the spanwise holes and the downstream hot-film probe. An equivalent suction coefficient of $C_q = 0.0006$ was sufficient to eliminate the artificial events and prevent bursting. This rate is five times smaller than the asymptotic suction coefficient for a corresponding turbulent boundary layer. If this result is sustained in a naturally developing turbulent boundary layer, a skin-friction reduction of close to 60% would be attained. Gad-el-Hak and Blackwelder (1989) propose to combine suction with non-planar surface modifications. Minute longitudinal roughness elements if properly spaced in the spanwise direction greatly reduce the spatial randomness of the low-speed streaks (Johansen and Smith, 1986). By withdrawing the streaks forming near the peaks of the roughness elements, less suction should be required to achieve an asymptotic boundary layer. Experiments by Wilkinson and Lazos (1987) and Wilkinson (1988) combine suction/blowing with thin-element riblets. Although no net drag reduction is yet attained in these experiments, their results indicate some advantage of combining suction with riblets as proposed by Gad-el-Hak and Blackwelder (1987; 1989).

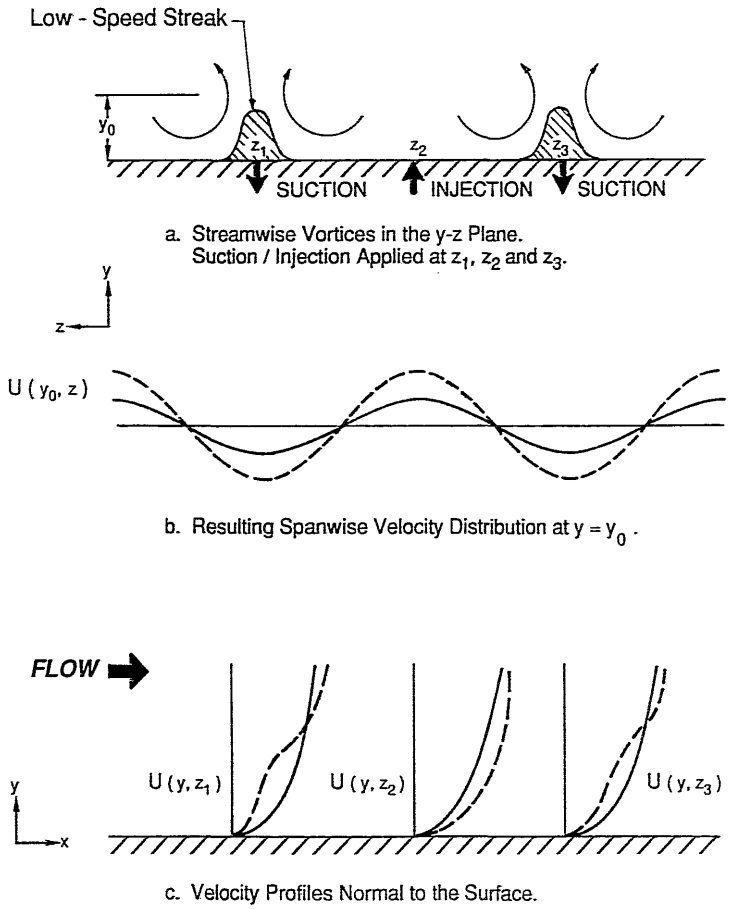

Fig. 2. Effects of suction/injection on velocity profiles. Broken lines: reference profiles. Solid lines: profiles with transpiration applied. (a) Streamwise vortices in the y-z plane, suction/injection applied at z_1, z_2 and z_3. (b) Resulting spanwise velocity distribution at $y = y_o$. (c) Velocity profiles normal to the surface.

The recent numerical experiments of Choi et al. (1994) also validate the concept of targeting suction/injection to specific near-wall events in a turbulent channel flow. Based on complete interior flow information and using the rather simple, heuristic control law proposed earlier by Gad-el-Hak and Blackwelder (1987), Choi et al.'s direct numerical simulations indicate a 20% net drag reduction accompanied by significant suppression of the near-wall structures and the Reynolds stress throughout the entire wall-bounded flow. When only wall information was used, a drag reduction of 6% was observed; a rather disappointing result considering that sensing and actuation took place at *every* grid point along the computational wall. In a practical implemen-

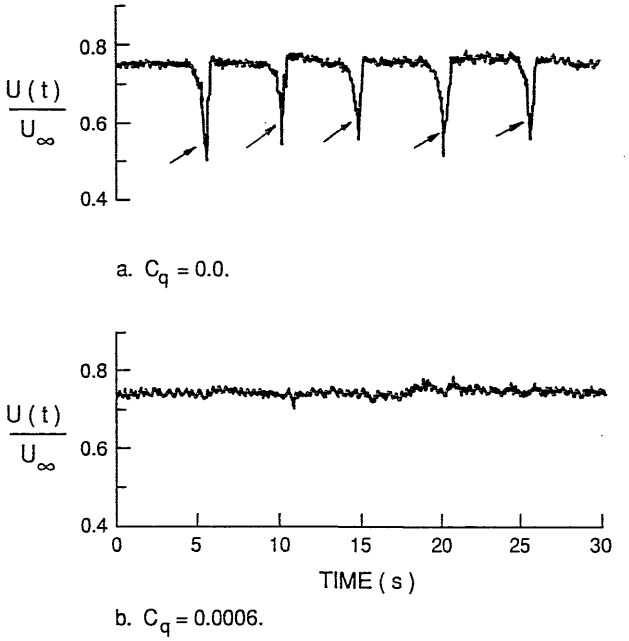

Fig. 3. Effects of suction from a streamwise slot on five artificially induced burstlike events in a laminar boundary layer (from Gad-el-Hak and Blackwelder, 1989). (a) $C_q = 0.0$. (b) $C_q = 0.0006$

tation of this technique, even fewer wall sensors would perhaps be available, measuring only a small subset of the accessible information and thus requiring even more sophisticated control algorithms to achieve the same degree of success. Low-dimensional models of the near-wall flow (Sect. 5) and soft computing tools (Sect. 7) can help in constructing more effective control algorithms.

Time sequences of the numerical flow field of Choi et al. (1994) indicate the presence of two distinct drag-reducing mechanisms when selective suction/injection is used. First, deterring the sweep motion, without modifying the primary streamwise vortices above the wall, and consequently moving the high-shear regions from the surface to the interior of the channel, thus directly reducing the skin friction. Secondly, changing the evolution of the wall vorticity layer by stabilizing and preventing lifting of the near-wall spanwise vorticity, thus suppressing a potential source of new streamwise vortices above the surface and interrupting a very important regeneration mechanism of turbulence.

Three new developments have relevance to the issue at hand. Firstly, the recently demonstrated ability to revert a chaotic system to a periodic one may provide optimal nonlinear control strategies for further reduction in the amount of suction (or the energy expenditure of any other active wall-

modulation technique) needed to attain a given degree of flow stabilization. This is important since, as seen from Equation (20) of Chap. 1, net drag reduction achieved in a turbulent boundary layer increases as the suction coefficient decreases. Secondly, to selectively remove the randomly occurring low-speed streaks, for example, would ultimately require reactive control. In that case, an event is targeted, sensed and subsequently modulated. Microfabrication technology provides opportunities for practical implementation of the required large array of inexpensive, programmable sensor/actuator chips. Thirdly, newly introduced soft computing tools include neural networks, fuzzy logic and genetic algorithms and are now more advanced as well as more widely used as compared to just few years ago. These tools could be very useful in constructing effective adaptive controllers. All three novel developments will be discussed in turn in Sects. 5–7.

4.3 Reactive Feedback Control

As was schematically depicted in Fig. 3 of Chap. 1, a control device can be passive, requiring no auxiliary power, or active, requiring energy expenditure. Active control is further divided into predetermined or reactive. Predetermined control includes the application of steady or unsteady energy input without regard to the particular state of the flow. The control loop in this case is open as was shown in Fig. 4a of Chap. 1, and no sensors are required. Reactive control is a special class of active control where the control input is continuously adjusted based on measurements of some kind. The control loop in this case can either be an open, feedforward one (Fig. 4b) or a closed, feedback loop (Fig. 4c).

The distinction between feedforward and feedback is particularly important when dealing with the control of flow structures which convect over stationary sensors and actuators. In feedforward control, the measured variable and the controlled variable differ. For example, the pressure or velocity can be sensed at an upstream location, and the resulting signal is used together with an appropriate control law to trigger an actuator which in turn influences the velocity at a downstream position. Feedback control, on the other hand, necessitates that the controlled variable be measured, fed back and compared with a reference input.

Moin and Bewley (1994) categorize reactive feedback control strategies by examining the extent to which they are based on the governing flow equations. Four categories are discerned: adaptive, physical model-based, dynamical systems-based, and optimal control (Fig. 3 of Chap. 1). Note that except for adaptive control, the other three categories of reactive feedback control can also be used in the feedforward mode or the combined feedforward-feedback mode. Also, in a convective environment such as that for a boundary layer, a controller would perhaps combine feedforward and feedback information and may include elements from each of the four classifications. Each of the four categories is briefly described below.

Adaptive schemes attempt to develop models and controllers via some learning algorithm without regard to the details of the flow physics. System identification is performed independently of the flow dynamics or the Navier-Stokes equations which govern this dynamics. An adaptive controller tries to optimize a specified performance index by providing a control signal to an actuator. In order to update its parameters, the controller thus requires feedback information relating to the effects of its control. The most recent innovation in adaptive flow control schemes involves the use of neural networks which relate the sensor outputs to the actuator inputs through functions with variable coefficients and nonlinear, sigmoid saturation functions. The coefficients are updated using the so-called back-propagation algorithm, and complex control laws can be represented with a sufficient number of terms. Hand tuning is required, however, to achieve good convergence properties. The nonlinear adaptive technique has been used with different degrees of success by Fan et al. (1993) and Jacobson and Reynolds (1993b; 1995) to control, respectively, the transition process and the bursting events in turbulent boundary layers. We will return to this subject in Sect. 7.

Heuristic physical arguments can instead be used to establish effective control laws. That approach obviously will work only in situations in which the dominant physics are well understood. An example of this strategy is the active cancellation scheme, used by Gad-el-Hak and Blackwelder (1989) in a physical experiment and by Choi et al. (1994) in a numerical experiment, to reduce the drag by mitigating the effect of near-wall vortices. As mentioned earlier, the idea is to oppose the near-wall motion of the fluid, caused by the streamwise vortices, with an opposing wall control, thus lifting the high-shear region away from the surface and interrupting the turbulence regeneration mechanism.

Nonlinear dynamical systems theory allows turbulence to be decomposed into a small number of representative modes whose dynamics are examined to determine the best control law. The task is to stabilize the attractors of a low-dimensional approximation of a turbulent chaotic system. The best known example is the OGY method which, when applied to simpler, small-number of degrees of freedom systems, achieves stabilization with minute expenditure of energy. This and other chaos control strategies, especially as applied to the more complex turbulent flows, will be revisited in Sect. 5.2.

Finally, optimal control theory applied directly to the Navier-Stokes equations can, in principle, be used to minimize a cost function in the space of the control. This strategy provides perhaps the most rigorous theoretical framework for flow control. As compared to other reactive control strategies, optimal control applied to the full Navier-Stokes equations is also the most computer-time intensive. In this method, feedback control laws are derived systematically for the most efficient distribution of control effort to achieve a desired goal. Abergel and Temam (1990) developed such optimal control theory for suppressing turbulence in a numerically simulated, two-dimensional

Navier-Stokes flow, but their method requires an impractical full flow-field information. Choi et al. (1993) developed a more practical, wall-information-only, sub-optimal control strategy which they applied to the one-dimensional stochastic Burgers equation. Later application of the sub-optimal control theory to a numerically simulated turbulent channel flow is reported by Moin and Bewley (1994).

4.4 Required Characteristics

The randomness of the bursting events necessitates temporal phasing as well as spatial selectivity to effect selective control. Practical applications of methods targeted at controlling a particular turbulent structure to achieve a prescribed goal would therefore require implementing a large number of surface sensors/actuators together with appropriate control algorithms. That strategy for controlling wall-bounded turbulent flows has been advocated by, among others and in chronological order, Gad-el-Hak and Blackwelder (1987; 1989), Lumley (1991; 1996), Choi et al. (1992), Reynolds (1993), Jacobson and Reynolds (1993b; 1995), Moin and Bewley (1994), Gad-el-Hak (1994; 1996), McMichael (1996), and Mehregany et al. (1996).

It is instructive to estimate some representative characteristics of the required array of sensors/actuators. Consider a typical commercial aircraft cruising at a speed of $U_\infty = 300$ m/s and at an altitude of 10 km. The density and kinematic viscosity of air and the unit Reynolds number in this case are, respectively, $\rho = 0.4\,\mathrm{kg/m^3}$, $\nu = 3 \times 10^{-5}\,\mathrm{m^2/s}$, and $Re = 10^7/\mathrm{m}$. Assume further that the portion of fuselage to be controlled has a turbulent boundary layer characteristics which are identical to those for a zero-pressure-gradient flat plate at a distance of 1 m from the leading edge. In this case, the skin-friction coefficient and the friction velocity are, respectively, $C_f = 0.003$ and $u_\tau = 11.62$ m/s.[4] At this location, one viscous wall unit is only $\nu/u_\tau = 2.6$ microns. In order for the surface array of sensors/actuators to be hydraulically smooth, it should not protrude beyond the viscous sublayer, or $5\,\nu/u_\tau = 13\,\mu$.

Wall-speed streaks are the most visible, reliable and detectable indicators of the preburst turbulence production process. The detection criterion is simply low velocity near the wall, and the actuator response should be to accelerate (or to remove) the low-speed region before it breaks down. Local wall motion, tangential injection, suction or heating triggered on sensed wall-pressure or wall-shear stress could be used to cause local acceleration of near-wall fluid.

The recent numerical experiments of Berkooz et al. (1993) indicate that effective control of bursting pair of rolls may be achieved by using the equiv-

[4] Note that the skin friction decreases as the distance from the leading increases. It is also strongly affected by such things as the externally imposed pressure gradient. Therefore, the estimates provided in here are for illustration purposes only.

alent of two wall-mounted shear sensors. If the goal is to stabilize or to eliminate *all* low-speed streaks in the boundary layer, a reasonable estimate for the spanwise and streamwise distances between individual elements of a checkerboard array is, respectively, 100 and 1000 wall units,[5] or $260\,\mu$ and $2600\,\mu$, for our particular example. A reasonable size for each element is probably one-tenth of the spanwise separation, or $26\,\mu$. A (1 m $\times$ 1 m) portion of the surface would have to be covered with about $n = 1.5$ million elements. This is a colossal number, but the density of sensors/actuators could be considerably reduced if we moderate our goal of targeting every single bursting event (and also if less conservative assumptions are used).

It is well known that not every low-speed streak leads to a burst. On the average, a particular sensor would detect an incipient bursting event every wall-unit interval of $P^+ = P u_\tau^2/\nu = 250$, or $P = 56\,\mu$s. The corresponding dimensionless and dimensional frequencies are $f^+ = 0.004$ and $f = 18$ kHz, respectively. At different distances from the leading edge and in the presence of nonzero-pressure gradient, the sensors/actuators array would have different characteristics, but the corresponding numbers would still be in the same ballpark as estimated in here.

As a second example, consider an underwater vehicle moving at a speed of $U_\infty = 10$ m/s. Despite the relatively low speed, the unit Reynolds number is still the same as estimated above for the air case, $Re = 10^7$/m, due to the much lower kinematic viscosity of water. At one meter from the leading edge of an imaginary flat plate towed in water at the same speed, the friction velocity is only $u_\tau = 0.39$ m/s, but the wall unit is still the same as in the aircraft example, $\nu/u_\tau = 2.6\,\mu$. The density of required sensors/actuators array is the same as computed for the aircraft example, $n = 1.5 \times 10^6$ elements/m^2. The anticipated average frequency of sensing a bursting event is, however, much lower at $f = 600$ Hz .

Similar calculations have been recently made by Gad-el-Hak (1993; 1994), Reynolds (1993) and Wadsworth et al. (1993). Their results agree closely with the estimates made here for typical field requirements. In either the airplane or the submarine case, the actuator's response need not be too large. As will be shown in Sect. 6, wall displacement on the order of 10 wall units ($26\,\mu$ in both examples), suction coefficient of about 0.0006, or surface cooling/heating on the order of 40°C/2°C (in the first/second example, respectively) should be sufficient to stabilize the turbulent flow.

[5] These are equal to, respectively, the average spanwise wavelength between two adjacent streaks and the average streamwise extent for a typical low-speed region. One can argue that those estimates are too conservative: once a region is *relaminarized*, it would perhaps stay as such for quite a while as the flow convects downstream. The next row of sensors/actuators may therefore be relegated to a downstream location well beyond 1000 wall units. Relatively simple physical or numerical experiments could settle this issue.

As computed in the two examples above, both the required size for a sensor/actuator element and the average frequency at which an element would be activated are within the presently known capabilities of microfabrication technology. The number of elements needed per unit area is, however, alarmingly large. The unit cost of manufacturing a programmable sensor/actuator element would have to come down dramatically, perhaps matching the unit cost of a conventional transistor, before the idea advocated in here would become practical.

An additional consideration to the size, amplitude and frequency response is the energy consumed by each sensor/actuator element. Total energy consumption by the entire control system obviously has to be low enough to achieve net savings. Consider the following calculations for the aircraft example. One meter from the leading edge, the skin-friction drag to be reduced is approximately $54\,\mathrm{N/m^2}$. Engine power needed to overcome this retarding force per unit area is $16\,\mathrm{kW/m^2}$, or $10^4\,\mu\mathrm{W}$/sensor. If a 60% drag-reduction is achieved,[6] this energy consumption is reduced to $4320\,\mu\mathrm{W}$/sensor. This number will increase by the amount of energy consumption of a sensor/actuator unit, but hopefully not back to the uncontrolled levels. The voltage across a sensor is typically in the range of $V = 0.1$–1 V, and its resistance in the range of $R = 0.1$–$1\,\mathrm{M}\Omega$. This means a power consumption by a typical sensor in the range of $\mathcal{P} = V^2/R = 0.1$–$10\,\mu\mathrm{W}$, well below the anticipated power savings due to reduced drag. For a single actuator in the form of a spring-loaded diaphragm with a spring constant of $k = 100\,\mathrm{N/m}$ and oscillating up and down at the bursting frequency of $f = 18$ kHz with an amplitude of $y = 26$ microns, the power consumption is $\mathcal{P} = (1/2)\,k\,y^2\,f = 600\,\mu\mathrm{W}$/actuator. If suction is used instead, $C_q = 0.0006$, and assuming a pressure difference of $\Delta p = 10^4\,\mathrm{N/m^2}$ across the suction holes/slots, the corresponding power consumption for a single actuator is $\mathcal{P} = C_q\,U_\infty\,\Delta p/n = 1200\,\mu\mathrm{W}$/actuator. It is clear then that when the power penalty for the sensor/actuator is added to the lower-level drag, a net saving is still achievable. The corresponding actuator power penalties for the submarine example are even smaller ($\mathcal{P} = 20\,\mu\mathrm{W}$/actuator for the wall motion actuator, and $\mathcal{P} = 40\,\mu\mathrm{W}$/actuator for the suction actuator), and larger savings are therefore possible.

5 Chaos Control

5.1 Nonlinear Dynamical Systems Theory

In the theory of dynamical systems, the so-called butterfly effect denotes sensitive dependence of nonlinear differential equations on initial conditions. The solution of such equations may be in the form of a strange attractor whose

[6] A not-too-farfetched goal according to the selective suction results discussed in Sect. 4.2.

intrinsic structure contains a well-defined mechanism to produce a chaotic behavior without requiring random forcing. A question arises naturally: just as small disturbances can radically grow within a deterministic system to yield rich, unpredictable behavior, can minute adjustments to a system parameter be used to reverse the process and control, i.e. regularize, the behavior of a chaotic system? Recently, that question was answered in the affirmative theoretically as well as experimentally, at least for system orbits which reside on low-dimensional strange attractors (see the review by Lindner and Ditto, 1995). Before describing such strategies for controlling chaotic systems, we first summarize the recent attempts to construct a low-dimensional dynamical systems representation of turbulent boundary layers. Such construction is a necessary first step to be able to use chaos control strategies for turbulent flows. Additionally, as argued by Lumley (1996), a low-dimensional dynamical model of the near-wall region used in a Kalman filter (Banks, 1986) can make the most of the partial information assembled from a finite number of wall sensors. Such filter minimizes in a least square sense the errors caused by incomplete information, and thus globally optimizes the performance of the control system.

Boundary layer turbulence is described by a set of nonlinear partial differential equations and is characterized by an infinite number of degrees of freedom. This makes it rather difficult to model the turbulence using a dynamical systems approximation. The notion that a complex, infinite-dimensional flow can be decomposed into several low-dimensional subunits is, however, a natural consequence of the realization that quasi-periodic coherent structures dominate the dynamics of seemingly random turbulent shear flows. This implies that low-dimensional, localized dynamics can exist in formally infinite-dimensional extended systems—such as open turbulent flows. Reducing the flow physics to finite-dimensional dynamical systems enables a study of its behavior through an examination of the fixed points and the topology of their stable and unstable manifolds. In Lumley's (1991) view, a bursting event corresponds to a dynamical system leaving one fixed point and jumping to another along a heteroclinic cycle. Delaying this jump by holding the system near the first fixed point should lead to lower momentum transport in the wall region and, therefore, to lower skin-friction drag.

In one significant attempt the proper orthogonal, or Karhunen-Loève, decomposition method has been used to extract a low-dimensional dynamical system from experimental data of the wall region (Aubry et al. 1988; Aubry, 1990). Aubry et al. (1988) expanded the instantaneous velocity field of a turbulent boundary layer using experimentally determined eigenfunctions which are in the form of streamwise rolls. They expanded the Navier-Stokes equations using these optimally chosen, divergence-free, orthogonal functions, applied a Galerkin projection, and then truncated the infinite-dimensional representation to obtain a ten-dimensional set of ordinary differential equations. These equations represent the dynamical behavior of the rolls, and are shown

to exhibit a chaotic regime as well as an intermittency due to a burst-like phenomenon. However, Aubry et al.'s ten-mode dynamical system displays a *regular* intermittency, in contrast both to that in actual turbulence as well as to the chaotic intermittency encountered by Pomeau and Manneville (1980) in which event durations are distributed stochastically. Nevertheless, the major conclusion of Aubry et al.'s study is that the bursts appear to be produced autonomously by the wall region even without turbulence, but are triggered by turbulent pressure signals from the outer layer. More recently, Berkooz et al. (1991) generalized the class of wall-layer models developed by Aubry et al. (1988) to permit uncoupled evolution of streamwise and cross-stream disturbances. Berkooz et al.'s results suggest that the intermittent events observed in Aubry et al.'s representation do not arise solely because of the effective closure assumption incorporated, but are rather rooted deeper in the dynamical phenomena of the wall region.

In addition to the reductionist viewpoint exemplified by the work of Aubry et al. (1988) and Berkooz et al. (1991), attempts have been made to determine directly the dimension of the attractors underlying specific turbulent flows. Again, the central issue here is whether or not turbulent solutions to the infinite-dimensional Navier-Stokes equations can be asymptotically described by a finite number of degrees of freedom. Grappin and Léorat (1991) computed the Lyapunov exponents and the attractor dimensions of two- and three-dimensional periodic turbulent flows without shear. They found that the number of degrees of freedom contained in the large scales establishes an upper bound for the dimension of the attractor. Deane and Sirovich (1991) and Sirovich and Deane (1991) numerically determined the number of dimensions needed to specify chaotic Rayleigh-Bénard convection over a moderate range of Rayleigh numbers, Ra. They suggested that the *intrinsic* attractor dimension is $\mathcal{O}\left[Ra^{2/3}\right]$.

The corresponding dimension in wall-bounded flows appears to be dauntingly high. Keefe et al. (1992) determined the dimension of the attractor underlying turbulent Poiseuille flows with spatially periodic boundary conditions. Using a coarse-grained numerical simulation, they computed a lower bound on the Lyapunov dimension of the attractor to be approximately 352 at a pressure-gradient Reynolds number of 3200. Keefe et al. (1992) argue that the attractor dimension in fully-resolved turbulence is unlikely to be much larger than 780. This suggests that periodic turbulent shear flows are deterministic chaos and that a strange attractor does underlie solutions to the Navier-Stokes equations. Temporal unpredictability in the turbulent Poiseuille flow is thus due to the exponential spreading property of such attractors. Although finite, the computed dimension invalidates the notion that the global turbulence can be attributed to the interaction of a *few* degrees of freedom. Moreover, in a physical channel or boundary layer, the flow is not periodic and is open. The attractor dimension in such case is not known but

is believed to be even higher than the estimate provided by Keefe et al. for the periodic *(quasi-closed)* flow.

In contrast to closed, absolutely unstable flows, such as Taylor-Couette systems, where the number of degrees of freedom can be small, local measurements in open, convectively unstable flows, such as boundary layers, do not express the global dynamics, and the attractor dimension in that case may inevitably be too large to be determined experimentally. According to the estimate provided by Keefe et al. (1992), the colossal data required (about 10^D, where D is the attractor dimension) for measuring the dimension simply exceeds current computer capabilities.

5.2 Chaos Control

There is another question of greater relevance here. Given a dynamical system in the chaotic regime, is it possible to stabilize its behavior through some kind of active control? While other alternatives have been devised (e.g., Fowler, 1989; Hübler and Lüscher, 1989; Huberman, 1990; Huberman and Lumer, 1990), the recent method proposed by workers at the University of Maryland (Ott et al., 1990a; 1990b; Shinbrot et al., 1990; 1992a; 1992b; 1992c; Romeiras et al., 1992) promises to be a significant breakthrough. Comprehensive reviews and bibliographies of the emerging field of chaos control can be found in the articles by Shinbrot et al. (1993), Shinbrot (1993; 1995), and Lindner and Ditto (1995).

Ott et al. (1990a) demonstrated, through numerical experiments with the Henon map, that it is possible to stabilize a chaotic motion about any prechosen, unstable orbit through the use of relatively small perturbations. The procedure consists of applying minute time-dependent perturbations to one of the system parameters to control the chaotic system around one of its many unstable periodic orbits. In this context, targeting refers to the process whereby an arbitrary initial condition on a chaotic attractor is steered toward a prescribed point (target) on this attractor. The goal is to reach the target as quickly as possible using a sequence of small perturbations (Kostelich et al., 1993a).

The success of the Ott-Grebogi-Yorke's (OGY) strategy for controlling chaos hinges on the fact that beneath the apparent unpredictability of a chaotic system lies an intricate but highly ordered structure. Left to its own recourse, such a system continually shifts from one periodic pattern to another, creating the appearance of randomness. An appropriately controlled system, on the other hand, is locked into one particular type of repeating motion. With such a reactive control the dynamical system becomes one with a stable behavior. The OGY-method can be simply illustrated by the schematic in Fig. 4. The state of the system is represented as the intersection of a stable manifold and an unstable one. The control is applied intermittently whenever the system departs from the stable manifold by a prescribed tolerance, otherwise the control is shut off. The control attempts to put the system

back onto the stable manifold so that the state converges toward the desired trajectory. Unmodeled dynamics cause noise in the system and a tendency for the state to wander off in the unstable direction. The intermittent control prevents that and the desired trajectory is achieved. This efficient control is not unlike trying to balance a ball in the center of a horse saddle (Moin and Bewley, 1994). There is one stable direction (front/back) and one unstable direction (left/right). The restless horse is the unmodeled dynamics, intermittently causing the ball to move in the wrong direction. The OGY-control needs only be applied, in the most direct manner possible, whenever the ball wanders off in the left/right direction.

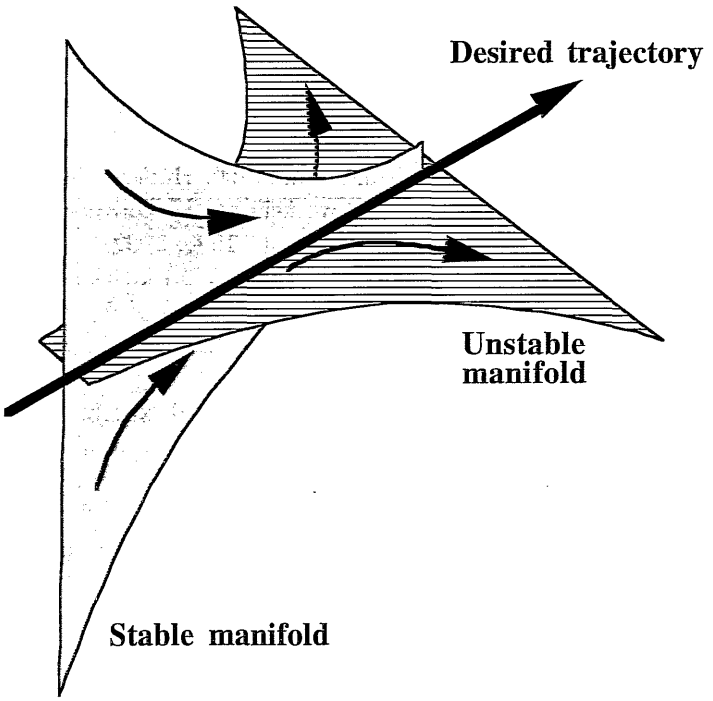

Fig. 4. The OGY method for controlling chaos

The OGY-method has been successfully applied in a relatively simple experiment by Ditto et al. (1990) and Ditto and Pecora (1993) at the Naval Surface Warfare Center, in which reverse chaos was obtained in a parametrically driven, gravitationally buckled, amorphous magnetoelastic ribbon. Garfinkel et al. (1992) applied the same control strategy to stabilize drug-induced cardiac arrhythmias in sections of a rabbit ventricle. Other extensions, improvements and applications of the OGY-strategy include higher-dimensional targeting (Auerbach et al., 1992; Kostelich et al., 1993b), con-

trolling chaotic scattering in Hamiltonian (i.e., nondissipative, area conservative) systems (Lai et al., 1993a; 1993b), synchronization of identical chaotic systems that govern communication, neural or biological processes (Lai and Grebogi, 1993), use of chaos to transmit information (Hayes et al., 1993), control of transient chaos (Lai et al., 1994), and taming spatio-temporal chaos using a sparse array of controllers (Chen et al., 1993; Qin et al., 1994; Auerbach, 1994).

In a more complex system, such as a turbulent boundary layer, there exist numerous interdependent modes and many stable as well as unstable manifolds (directions). Factors that make turbulence control a challenging task are the potentially quite large perturbations caused by the unmodeled dynamics of the flow, the non-stationary nature of the desired dynamics, and the complexity of the saddle shape describing the dynamics of the different modes. Nevertheless, the OGY-control strategy has several advantages that are of special interest in the control of turbulence: the mathematical model for the dynamical system need not be known; only **small** changes in the control parameter are required; and noise can be tolerated (with appropriate penalty).

Recently, Keefe (1993a; 1993b) made a useful comparison between two nonlinear control strategies as applied to fluid problems. Ott-Grebogi-Yorke's feedback method described above and the model-based control strategy originated by Hübler (see, for example, Hübler and Lüscher, 1989; Lüscher and Hübler, 1989), the H-method. Both novel control methods are essentially generalizations of the classical perturbation cancellation technique: apply a prescribed forcing to subtract the undesired dynamics and impose the desired one. The OGY-strategy exploits the sensitivity of chaotic systems to stabilize existing periodic orbits and steady states. Some feedback is needed to steer the trajectories toward the chosen fixed point, but the required control signal is minuscule. In contrast, Hübler's scheme does not explicitly make use of the system sensitivity. It produces general control response (periodic or aperiodic) and needs little or no feedback, but its control inputs are generally large. The OGY-strategy exploits the nonlinearity of a dynamical system; indeed the presence of a strange attractor and the extreme sensitivity of the dynamical system to initial conditions are essential to the success of the method. In contrast, the H-method works equally for both linear and nonlinear systems.

Keefe (1993a) first examined numerically the two schemes as applied to fully-developed and transitional solutions of the Ginzburg-Landau equation, an evolution equation that governs the initially weakly nonlinear stages of transition in several flows and that possesses both transitional and fully-chaotic solutions. The Ginzburg-Landau equation has solutions that display either absolute or convective instabilities, and is thus a reasonable model for both closed and open flows. Keefe's main conclusion is that control of nonlinear systems is best obtained by making maximum use possible of the underlying natural dynamics. If the goal dynamics is an unstable nonlinear

solution of the equation and the flow is nearby at the instant control is applied, both methods perform reliably and at low-energy cost in reaching and maintaining this goal. Predictably, the performance of both control strategies degrades due to noise and the spatially discrete nature of realistic forcing. Subsequently, Keefe (1993b) extended the numerical experiment in an attempt to reduce the drag in a channel flow with spatially periodic boundary conditions. The OGY-method reduces the skin friction to 60–80% of the uncontrolled value at a mass-flux Reynolds number of 4408. The H-method fails to achieve any drag reduction when starting from a fully-turbulent initial condition but shows potential for suppressing or retarding laminar-to-turbulence transition. Keefe (1993a) suggests that the H-strategy might be more appropriate for boundary layer control, while the OGY-method might best be used for channel flows.

It is also relevant to note here the work of Bau and his colleagues at the University of Pennsylvania (Singer et al., 1991; Wang et al., 1992), who devised a feedback control to stabilize (*relaminarize*) the naturally occurring chaotic oscillations of a toroidal thermal convection loop heated from below and cooled from above. Based on a simple mathematical model for the thermosyphon, Bau and his colleagues constructed a reactive control system that was used to alter significantly the flow characteristics inside the convection loop. Their linear control strategy, perhaps a special version of the OGY's chaos control method, consists simply of sensing the deviation of fluid temperatures from desired values at a number of locations inside the thermosyphon loop and then altering the wall heating either to suppress or to enhance such deviations. Wang et al. (1992) also suggested extending their theoretical and experimental method to more complex situations such as those involving Bénard convection (Tang and Bau, 1993a; 1993b). Hu and Bau (1994) used a similar feedback control strategy to demonstrate that the critical Reynolds number for the loss of stability of planar Poiseuille flow can be significantly increased or decreased.

Other attempts to use low-dimensional dynamical systems representation for flow control include the work of Berkooz et al. (1993), Corke et al. (1994), and Coller et al. (1994a; 1994b). Berkooz et al. (1993) applied techniques of modern control theory to estimate the phase-space location of dynamical models of the wall-layer coherent structures, and used these estimates to control the model dynamics. Since discrete wall-sensors provide incomplete knowledge of phase-space location, Berkooz et al. maintain that a nonlinear observer, which incorporates past information and the equations of motion into the estimation procedure, is required. Using an extended Kalman filter, they achieved effective control of a bursting pair of rolls with the equivalent of two wall-mounted shear sensors. Corke et al. (1994) used a low-dimensional dynamical system based on the proper orthogonal decomposition to guide control experiments for an axisymmetric jet. By sensing the downstream velocity and actuating an array of miniature speakers located at the lip of the

jet, their feedback control succeeded in converting the near-field instabilities from spatial-convective to temporal-global. Coller et al. (1994a; 1994b) developed a feedback control strategy for strongly nonlinear dynamical systems, such as turbulent flows, subject to small random perturbations that kick the system intermittently from one saddle point to another along heteroclinic cycles. In essence, their approach is to use local, weakly nonlinear feedback control to keep a solution near a saddle point as long as possible, but then to let the natural, global nonlinear dynamics run its course when *bursting* (in a low-dimensional model) does occur. Though conceptually related to the OGY-strategy, Coller et al.'s method does not actually stabilize the state but merely holds the system near the desired point longer than it would otherwise stay.

Shinbrot and Ottino (1993a; 1993b) offer yet another strategy presumably most suited for controlling coherent structures in area-preserving turbulent flows. Their geometric method exploits the premise that the dynamical mechanisms which produce the organized structures can be remarkably simple. By repeated stretching and folding of "horseshoes" which are present in chaotic systems, Shinbrot and Ottino have demonstrated numerically as well as experimentally the ability to create, destroy and manipulate coherent structures in chaotic fluid systems. The key idea to create such structures is to intentionally place folds of horseshoes near low-order periodic points. In a dissipative dynamical system, volumes contract in state space and the co-location of a fold with a periodic point leads to an isolated region that contracts asymptotically to a point. Provided that the folding is done properly, it counteracts stretching. Shinbrot and Ottino (1993a) applied the technique to three prototypical problems: a one-dimensional chaotic map; a two-dimensional one; and a chaotically advected fluid. Shinbrot (1995; 1997) provides recent reviews of the stretching/folding as well as other chaos control strategies.

6 Microfabrication

Manufacturing processes that can create extremely small machines have been developed in recent years (Angell et al., 1983; Gabriel et al., 1988; Gravesen et al., 1993; Gabriel, 1995). In this emerging microfabrication technology, under intensive development only since 1990, electronic and mechanical components are combined on a single silicon chip using photolithographic micromachining techniques. Motors, electrostatic actuators, pneumatic actuators, valves, gears and tweezers of typical size $\mathcal{O}[10\,\mu]$ have been fabricated. These have been used as sensors for pressure, temperature, velocity, mass flow, or sound, and as actuators for linear and angular motions. Current usage for microelectromechanical systems (MEMS) includes accelerometers for airbags and guidance systems, pressure sensors for engine air intake and blood analysis, rate gyroscopes for antilock brakes, microrelays and microswitches for semiconductor automatic test equipment, and microgrippers for surgical pro-

cedures (O'Connor, 1992; Hogan, 1996; Paula, 1996; Ouellette, 1996; Ashley, 1996; Robinson et al., 1996a; 1996b). There is considerable work under way to include other applications, one example being the micro-steam engine described by Lipkin (1993). A second example is the digital light processor which contains 500,000 individually addressable micromirrors which Texas Instruments, Inc., is currently developing for future high-definition televisions. The company maintains that when mass produced, such device would cost around $ 100, a mere 0.02 cent per actuator!

The new *Journal of Microelectromehanical Systems* and *Journal of Micromechanics and Microengineering* are dedicated to this technology, and the older Sensors and Actuators is increasingly allotting more of its pages to MEMS. Entire sessions in scientific meetings have been increasingly assigned to MEMS applications in fluid mechanics (see, for example, the presentations by McMichael, Tai, Mehregany, Mastrangelo, and Yun, all made at the *AIAA Third Shear Flow Control Conference,* Orlando, Florida, 6-9 July 1993, and the volumes edited by Bandyopadhyay et el., 1994, and Breuer et al., 1996). Recent reviews of the use, or potential use, of MEMS in flow control include those by Gad-el-Hak (1994; 1996), Lumley (1996), McMichael (1996), Mehregany et al. (1996), Ho and Tai (1996), and Keefe (1997).

MEMS would be ideal for the reactive flow control concept advocated in the present chapter. Methods of flow control targeted towards specific coherent structures involve nonintrusive detection and subsequent modulation of events that occur randomly in space and time. To achieve proper targeted control of these quasi-periodic vortical events, temporal phasing as well as spatial selectivity are required. Practical implementation of such an idea necessitates the use of a large number of intelligent, communicative wall sensors and actuators arranged in a checkerboard pattern. Section 4.4 provided estimates for the number, characteristics and energy consumption of such elements required to modulate the turbulent boundary layer which develops along a typical commercial aircraft or nuclear submarine. An upper-bound number to achieve total turbulence suppression is about one million sensors/actuators per square meter of the surface, although as argued earlier the actual number needed to achieve effective control could perhaps be 1–2 orders of magnitude below that.

The sensors would be expected to measure the amplitude, location, and phase or frequency of the signals impressed upon the wall by incipient bursting events. Instantaneous wall-pressure or wall-shear stress can be sensed, for example. The normal or in-plane motion of a minute membrane is proportional to the respective point force of primary interest. For measuring wall pressure, microphone-like devices respond to the motion of a vibrating surface membrane or an internal elastomer. Several types are available including variable-capacitance (condenser or electret), ultrasonic, optical (e.g., optical-fiber and diode-laser), and piezoelectric devices (see, for example, Löfdahl et al., 1993; 1994). A potentially useful technique for our purposes has been

recently tried at MIT (J. H. Haritonidis, private communications). An array of extremely small (0.2 mm in diameter) laser-powered microphones (termed picophones) was machined in silicon using integrated circuit fabrication techniques, and was used for field measurement of the instantaneous surface pressure in a turbulent boundary layer. The wall-shear stress, though smaller and therefore more difficult to measure than pressure, provides a more reliable signature of the near-wall events.

Actuators are expected to produce a desired change in the targeted coherent structures. The local acceleration action needed to stabilize an incipient bursting event can be in the form of adaptive wall, transpiration or wall heat transfer. Traveling surface waves can be used to modify a locally convecting pressure gradient such that the wall motion follows that of the coherent event causing the pressure change. Surface motion in the form of a Gaussian hill with height $y^+ = \mathcal{O}[10]$ should be sufficient to suppress typical incipient bursts (Lumley, 1991; Carlson and Lumley, 1996). Such time-dependent alteration in wall geometry can be generated by driving a flexible skin using an array of piezoelectric devices (dilate or contract depending on the polarity of current passing through them), electromagnetic actuators, magnetoelastic ribbons (made of nonlinear materials that change their stiffness in the presence of varying magnetic fields), or Terfenol-d rods (a novel metal composite, developed at Grumman Corporation, which changes its length when subjected to a magnetic field). Note should also be made of other exotic materials that can be used for actuation. For example, electrorheological fluids (Halsey and Martin, 1993) instantly solidify when exposed to an electric field, and may thus be useful for the present application. Recently constructed microactuators specifically designed for flow control include those by Wiltse and Glezer (1993), James et al. (1994), Jacobson and Reynolds (1995), Vargo and Muntz (1996), and Keefe (1997).

Suction/injection at many discrete points can be achieved by simply connecting a large number of minute streamwise slots, arranged in a checkerboard pattern, to a low-pressure/high-pressure reservoir located underneath the working surface. The transpiration through each individual slot is turned on and off using a corresponding number of independently controlled microvalves. Alternatively, positive-displacement or rotary micropumps (see, for example, Sen et al., 1996; Sharatchandra et al., 1997) can be used for blowing or sucking fluid through small holes/slits. Based on the results of Gad-el-Hak and Blackwelder (1989), equivalent suction coefficients of about 0.0006 should be sufficient to stabilize the near-wall region. Assuming that the skin-friction coefficient in the uncontrolled boundary layer is $C_f = 0.003$, and assuming further that the suction used is sufficient to establish an asymptotic boundary layer ($\mathrm{d}\delta_\theta/\mathrm{d}x = 0$, where δ_θ is the momentum thickness), the skin friction in the reactively controlled case is then $C_f = 0 + 2\,C_q = 0.0012$, or 40% of the original value. The net benefit will, of course, be reduced by

the energy expenditure of the suction pump (or micropumps) as well as the array of microsensors and microvalves.

Finally, if the bursting events are to be eliminated by lowering the near-wall viscosity, direct electric-resistance heating can be used in liquid flows and thermoelectric devices based on the Peltier effect can be used for cooling in the case of gaseous boundary layers. The absolute viscosity of water at 20°C decreases by approximately 2% for each 1°C rise in temperature, while for room-temperature air, μ decreases by approximately 0.2% for each 1°C drop in temperature. The streamwise momentum equation written at the wall can be used to show that a suction coefficient of 0.0006 has approximately the same effect on the wall-curvature of the instantaneous velocity profile as a surface heating of 2°C in water or a surface cooling of 40°C in air (Liepmann and Nosenchuck, 1982; Liepmann et al., 1982).

Sensors and actuators of the types discussed in this section can be combined on individual electronic chips using microfabrication technology. The chips can be interconnected in a communication network that is controlled by a massively parallel computer or a self-learning neural network (Sect. 7), perhaps each sensor/actuator unit communicating only with its immediate neighbors. In other words, it may not be necessary for one sensor/actuator to exchange signals with another far away unit. Factors to be considered in an eventual field application of chips produced using microfabrication processes include sensitivity of sensors, sufficiency and frequency response of actuators' action, fabrication of large arrays at affordable prices, survivability in the hostile field environment, and energy required to power the sensors/actuators. As argued by Gad-el-Hak (1994), sensor/actuator chips currently produced are small enough for typical field application, and they can be programmed to provide a sufficiently large/fast action in response to a certain sensor output (see also Jacobson and Reynolds, 1995). Present prototypes are, however, still quite expensive as well as delicate. But so was the transistor when first introduced! It is hoped that the unit price of future sensor/actuator elements would follow the same dramatic trends witnessed in case of the simple transistor and even the much more complex integrated circuit. The price anticipated by Texas Instruments for an array of half a million mirrors hints that the technology is well in its way to mass-produce phenomenally inexpensive microsensors and microactuators. Additionally, current automotive applications are a rigorous proving ground for MEMS: under-the-hood sensors can already withstand harsh conditions such as intense heat, shock, continual vibration, corrosive gases, and electromagnetic fields.

7 Soft Computing

The term soft computing was coined by Lotfi Zadeh of the University of California, Berkeley, to describe several ingenious modes of computations that exploit tolerance for imprecision and uncertainty in complex systems

to achieve tractability, robustness and low cost (Yager and Zadeh, 1992; Bouchon-Meunier et al., 1995a; 1995b). The principle of complexity provides the impetus for soft computing: as the complexity of a system increases, the ability to predict its response diminishes until a threshold is reached beyond which precision and relevance become almost mutually exclusive (Noor and Jorgensen, 1996). In other words, precision and certainty carry a cost. By employing modes of reasoning, probabilistic reasoning, that are approximate rather than exact, soft computing can help in searching for globally optimal design or achieving effectual control while taking into account system uncertainties and risks.

Soft computing refers to a domain of computational intelligence which loosely lies in between purely numerical (hard) computing and purely symbolic computations. Alternatively, one can think about symbolic computations as a form of artificial intelligence lying in between biological intelligence and computational intelligence (soft computing). The schematic in Fig. 5 illustrates the general idea. Artificial intelligence relies on symbolic information processing techniques and uses logic as representation and inference mechanisms. It attempts to approach the high level of human cognition. In contrast, soft computing is based on modeling low-level cognitive processes and strongly emphasizes modeling of uncertainty as well as learning. Computational intelligence mimics the ability of the human brain to employ modes of reasoning that are approximate. Soft computing provides a machinery for the numeric representation of the types of constructs developed in the symbolic artificial intelligence. The boundaries between these paradigms are of course *fuzzy*.

The principal constituents of soft computing are neurocomputing, fuzzy logic and genetic algorithms, as depicted in Fig. 5. These elements, together with probabilistic reasoning, can be combined in hybrid arrangements resulting in better systems in terms of parallelism, fault tolerance, adaptivity and uncertainty management. To my knowledge, only neurocomputing has been employed for fluid flow control, but the other tools of soft computing may be just as useful to construct powerful controllers and have in fact been used as such in other fields such as large-scale subway controllers and video cameras. A brief description of those three constituents follows.

Neurocomputing is inspired by the neurons of the human brain and how they work. Neural networks are information processing devices that can learn by adapting synaptic weights to changes in the surrounding environment, can handle imprecise, fuzzy, noisy and probabilistic information, and can generalize from known tasks (examples) to unknown ones. Actual engineering oriented hardware are termed artificial neural networks (ANN) while algorithms are called computational neural networks (CNN). The nonlinear, highly parallel networks can perform any of the following tasks: classification, pattern matching, optimization, control and noise removal. As modeling and optimization tools, neural networks are particularly useful when good analytic

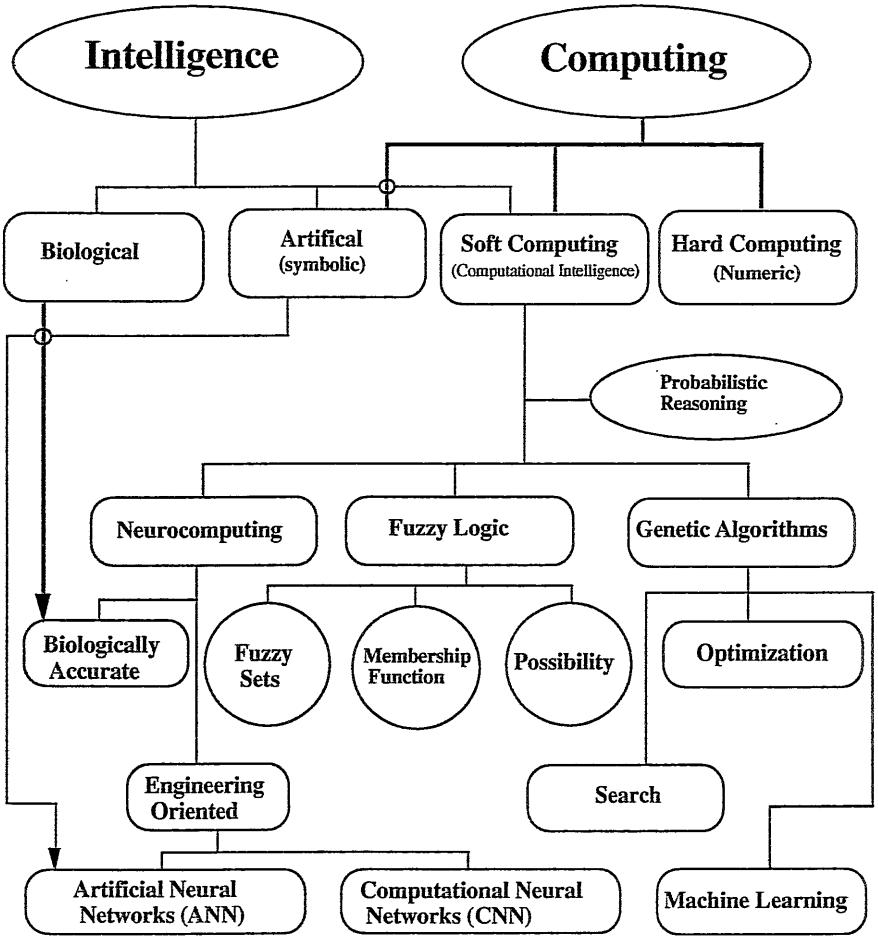

Fig. 5. Tools for soft computing

models are either unknown or extremely complex. Neural networks as used in fluid flow control will be covered in the following subsection.

Fuzzy logic was introduced by Lotfi Zadeh in 1965 as a mathematical tool to deal with uncertainty and imprecision. The book by Yager and Zadeh (1992) is an excellent primer to the field. For computing and reasoning, general concepts (such as size) are implemented into a computer algorithm by using mostly words (such as small, medium or large). Fuzzy logic, therefore, provides a unique methodology for computing with words. Its rationalism is based on three mathematical concepts: fuzzy sets, membership function and possibility. As dictated by a membership function, fuzzy sets allow a gradual transition from belonging to not belonging to a set. The concept of possibility provides a mechanism for interpreting factual statements involving fuzzy sets. Three processes are involved in solving a practical problem using fuzzy logic: fuzzification, analysis and defuzzification. Given a complex, unsolvable problem in real space, those three steps involve enlarging the space and searching for a solution in the new superset, then specializing this solution to the original real constraints.

Genetic algorithms are search algorithms based loosely on the mechanics of natural selection and natural genetics. They combine survival of the fittest among string structures with structured yet randomized information exchange, and are used for search, optimization and machine learning. For control, genetic algorithms aim at achieving minimum cost function and maximum performance measure while satisfying the problem constraints. The books by Goldberg (1989), Davis (1991) and Holland (1992) provide gentle introduction to the field.

In the Darwinian principle of natural selection, the fittest members of a species are favored to produce offspring. Even biologists cannot help but being awed by the complexity of life observed to evolve in the relatively short time suggested by the fossil records. A living being is an amalgam of characteristics determined by the (typically tens of thousands) genes in its chromosomes. Each gene may have several forms or alternatives called alleles which produce differences in the set of characteristics associated with that gene. The chromosomes are therefore the organic devices through which the structure of a creature is encoded, and this living being is created partly through the process of decoding those chromosomes. Genes transmits hereditary characters and form specific parts of a self-perpetuated deoxyribonucleic acid (DNA) in a cell nucleus. Natural selection is the link between the chromosomes and the performance of their decoded structures. Simply put, the process of natural selection causes those chromosomes that encode successful structures to reproduce more often than those that do not.

In an attempt to solve difficult problems, John H. Holland of the University of Michigan introduced the man-made version of the procedure of natural evolution in the early 1970s. The candidate solutions to a problem are ranked by the genetic algorithm according to how well they satisfy a certain criterion,

and the fittest members are the most favored to combine amongst themselves to form the next generation of the members of the *species*. Fitter members presumably produce even fitter offspring and therefore better solutions to the problem at hand. Solutions are represented by binary strings, each trial solution is coded as a vector called chromosome. The elements of a chromosome are described as genes, and its varying values at specific positions are called alleles. Good solutions are selected for reproduction based on a fitness function using genetic recombination operators such as crossover and mutation. The main advantage of genetic algorithms is their global parallelism in which the search efforts to many regions of the search area are simultaneously allocated.

Genetic algorithms have been used for the control of different dynamical systems, as for example the optimization of robot trajectories. But to my knowledge and at the time of writing this chapter (late 1996), the control of fluid flow is yet to benefit from this powerful soft computing tool. In particular, when a finite number of sensors are used to gather information about the state of the flow, a genetic algorithm perhaps combined with a neural network can adapt and learn to use current information to eliminate the uncertainty created by insufficient a priori information.

7.1 Neural Networks

Biologically inspired neural networks are finding increased applications in many fields of science and technology. Modeling of complex dynamical systems, adaptive noise canceling in telephones and modems, bomb sniffers, mortgage-risk evaluators, sonar classifiers, and word recognizers are but a few of existing usages of neural nets. The book by Nelson and Illingworth (1991) provides a lucid introduction to the field, and the review article by Antsaklis (1993) focuses on the use of neural nets for the control of complex dynamical systems. For flow control applications, neural networks offer the possibility of adaptive controllers that are simpler and potentially less sensitive to parameter variations as compared to conventional controllers. Moreover, if a colossal number of sensors and actuators is to be used, the massively parallel computational power of neural nets will surely be needed for real-time control.

The basic elements of a neural network are schematically shown in Fig. 6. Several inputs are connected to the nodes (neurons or processing elements) that form the input layer. There are one or more hidden layers, followed by an output layer. Note that the number of connections is higher than the total number of nodes. Both numbers are chosen based on the particular application and can be arbitrarily large for complex tasks. Simply put, the multi-task, albeit simple, job of each processing element is to evaluate each of the input signals to that particular element, calculate the weighted sum of the combined inputs, compare that total to some threshold level, and finally determine what the output should be. The various weights are the

adaptive coefficients which vary dynamically as the network *learns* to perform its assigned task; some inputs are more important than others. The threshold, or transfer, function is generally nonlinear; the most common one being the continuous sigmoid, or S-shaped, curve, which approaches a minimum and maximum value at the asymptotes. If the sum of the weighted inputs is larger than the threshold value, the neuron generates a signal; otherwise no signal is *fired*. Neural networks can operate in feedforward or feedback mode.[7] Complex systems, for which dynamical equations may not be known or may be too difficult to solve, can be modeled using neural nets.

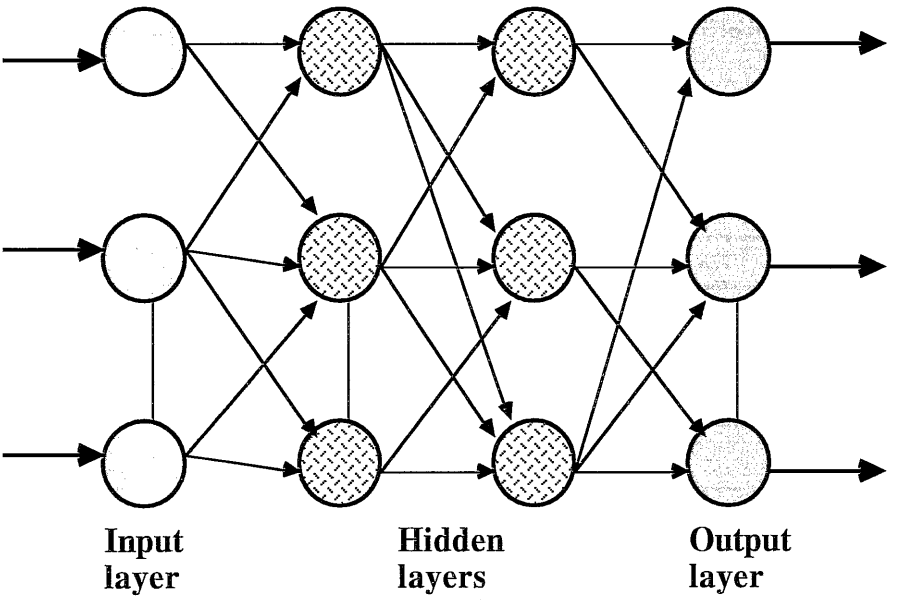

Fig. 6. Elements of a neural network

For flow control, neural networks provide convenient, fast, nonlinear adaptive algorithms to relate sensor outputs to actuator inputs via variable-coefficient functions and nonlinear, sigmoid saturation functions. With no prior knowledge of the pertinent dynamics, a self-learning neural network

[7] Note that this terminology refers to the direction of information through the network. When a neural net is used as a controller, the overall control loop is, however, a feedback, closed loop: the self-learning network dynamically updates its various parameters by comparing its output to a desired output, thus requiring feedback information relating to the effect of its control.

develops a model for that dynamics through observations of the applied control and sensed measurements. The network is by nature nonlinear and can therefore better handle nonlinear dynamical systems, a difficult task when classical, linear or weakly nonlinear, control strategies are attempted. The feedforward type of neural network acts as a nonlinear filter forming an output from a set of input data. The output can then be compared to some desired output, and the difference (error) is typically used in a back-propagation algorithm which updates the network parameters.

The number of researchers using neural networks to control fluid flows is growing rapidly. In here, we provide only a small sample. Using a pre-trained neural network, Fan et al. (1993) conducted a conceptual reactive flow control experiment to delay laminar-to-turbulence transition. Numerical simulations of their flow control system demonstrate almost complete cancellation of single and multiple artificial wave disturbances. Their controller also successfully attenuated a natural disturbance signal with developing wave packets from an actual wind-tunnel experiment.

Jacobson and Reynolds (1993b; 1995) used neural networks to minimize the boundary velocity gradient of three model flows: the one-dimensional stochastic Burgers equation; a two-dimensional computational model of the near-wall region of a turbulent boundary layer; and a real-time turbulent flow with a spanwise array of wall actuators together with upstream and downstream wall-sensors. For all three problems, the neural network successfully learned about the flow and developed into proficient controllers. However, for the laboratory experiments, Jacobson and Reynolds (1995) report that the neural network training time was much longer and the performance was no better than a simpler ad hoc controller that they developed. Jacobson and Reynolds emphasize that alternative neural net configurations and convergence algorithms may, however, greatly improve the network performance.

Using the angle of attack and angular velocity as inputs, Faller et al. (1994) trained a neural network to model the measured unsteady surface pressure over a pitching airfoil (see also Schreck et al., 1995). Following training and using the instantaneous angle of attack and pitch rate as the only inputs, their network was able to accurately predict the surface pressure topology as well as the time-dependent aerodynamic forces and moments. The model was then used to develop a neural network controller for wing-motion actuator signals which in turn provided direct control of the lift-to-drag ratio across a wide range of time-dependent motion histories.

Most recently, Kawthar-Ali and Acharya (1996) developed a neural network controller for use in suppressing the dynamic-stall vortex that periodically develops in the leading edge of a pitching airfoil. Based on the current state of the unsteady pressure field, their control system specified the optimum amount of leading-edge suction to achieve complete vortex suppression.

8 Concluding Remarks

The present chapter emphasized the frontiers of the filed of flow control, reviewing the important advances that took place during the past few years. An attempt has been made to place the field in a unifying framework and to properly categorize the different control strategies. Developments in chaos control, microfabrication and soft computing tools are making it more feasible to perform reactive control of turbulent flows. Field applications, however, have to await further progress in those three areas. Other less complex control schemes, passive as well as active, are more market ready and are also witnessing resurgence of interest.

As is clear from both this and the previous chapter, there is no lack of flow control methods to achieve a particular goal for free as well as wall-bounded flows across the entire range of Mach and Reynolds numbers. Ranging from simple to complex, from inexpensive to expensive, from passive to active to reactive, and from market ready to futuristic, the fluid engineer has a great variety of control devices to choose from. Flow control is most effective when applied near the transition or separation points; in other words, near the critical flow regimes where flow instabilities magnify quickly. Therefore, delaying/advancing laminar-to-turbulence transition and preventing/provoking separation can be readily accomplished. To reduce the skin-friction drag in a non-separating turbulent boundary layer, where the mean flow is quite stable, is a more challenging problem.

Market-ready techniques include passive and predetermined active control. Shaping, suction, heating/cooling and compliant coatings can be used to delay transition by an order of magnitude in Reynolds number, and, except for the latter technique (at least at this point of time), can also be used to prevent boundary layer separation. The use of polymers, microbubbles, riblets and LEBUs can lead to skin-friction reduction in turbulent boundary layers. Numerous other techniques are available to reduce form drag, induced drag and wave drag. Remaining issues for field application of market-ready techniques include cost, maintenance and reliability. Potential further improvements in classical flow control techniques will perhaps involve combining more than one technique aiming at achieving a favorable effect that is greater than the sum. Examples include combining suction or polymer injection with riblets for increased effectiveness and saving. Due to its obvious difficulties, synergism has not been extensively studied in the past but deserves future consideration.

Classical control techniques, though spectacularly successful in the past, have been extended to near their physical limits. Conventional strategies are often ineffective for turbulent flows. Substantial gains are potentially possible, however, when reactive flow control methods are used. Particularly for turbulent flows, reactive control requires large number of sensors and actuators and will not be practical until the technology for manufacturing inexpensive, robust microsensors and microactuators becomes available. Autonomous con-

trol algorithms and associated computers to handle the required colossal data in real time must also be developed. Further research is needed in dynamical systems theory particularly chaos control, microelectromechanical systems, and alternative neural network configurations, convergence algorithms and distributed flow control. The difficulties are daunting but the potential payoffs are enormous.

The outlook is, however, quite optimistic. Soft computing tools and nonlinear dynamical systems theory are developing at fast pace. MEMS technology is improving even faster. The ability of Texas Instruments to produce an array of 500,000 individually addressable mirrors for around 0.02 cent per actuator is a sign of the spectacular advances anticipated in the near future. Existing automotive applications of MEMS have already proven the ability of such devices to withstand the harsh environment under the hood. What is needed now is a focused, well-funded research and development program to make it all come together for field application of reactive flow control systems.

In parting, it might be worth recalling that a mere 10% reduction in the total drag of an aircraft translates into a saving of one billion dollars in annual fuel cost for the commercial fleet in the United States alone. Contrast this benefit to the annual worldwide cost of perhaps a few million dollars for all basic research in the broad field of flow control. Taming turbulence, though difficult, will pay for itself in gold.

A parting verse from William Shakespeare's The Taming of the Shrew:
Hortensio (a gentleman of Padua): Now go thy ways, thou hast tam'd a curst shrew.
Lucentio (a gentleman of Pisa): 'Tis a wonder, by your leave, she will be tam'd so.

The present chapter was part of the author's contribution to the short course Flow Control: Fundamentals and Practices, held in Cargèse, Corsica, France, 24-28 June 1996, and repeated at the University of Notre Dame, Notre Dame, Indiana, U.S.A., 9-13 September 1996. Part of the material in this chapter is excerpted from a recent review article written by the same author for the *Applied Mechanics Reviews*, vol. 49, no. 7, pp. 365-379, 1996.

References

Abergel F., Temam R. (1990): On Some Control Problems in Fluid Mechanics. *Theor. Comput. Fluid Dyn.* **1**, 303–325.

Alshamani K.M.M., Livesey J.L., Edwards F.J. (1982): Excitation of the Wall Region by Sound in Fully Developed Channel Flow. *AIAA J.* **20**, 334–339.

Angell J.B., Terry S.C., Barth P.W. (1983): Silicon Micromechanical Devices. *Scientific American* **248**, April, 44–55.

Antonia R.A., Fulachier L., Krishnamoorthy L.V., Benabid T., Anselmet F. (1988): Influence of Wall Suction on the Organized Motion in a Turbulent Boundary Layer. *J. Fluid Mech.* **190**, 217–240.

Antsaklis P.J. (1993): Control Theory Approach. *Mathematical Approaches to Neural Networks*, ed. J.G. Taylor, (Elsevier, Amsterdam), 1–23.

Ashley S. (1996): Getting a Microgrip in the Operating Room. *Mechanical Engineering* **118**, September, 91–93.

Aubry N. (1990): Use of Experimental Data for an Efficient Description of Turbulent Flows. *Appl. Mech. Rev.* **43**, S240–S245.

Aubry N., Holmes P., Lumley J.L., Stone E. (1988): The Dynamics of Coherent Structures in the Wall Region of a Turbulent Boundary Layer. *J. Fluid Mech.* **192**, 115–173.

Auerbach D. (1994): Controlling Extended Systems of Chaotic Elements. *Phys. Rev. Lett.* **72**, 1184–1187.

Auerbach D., Grebogi C., Ott E., Yorke J.A. (1992): Controlling Chaos in High Dimensional Systems. *Phys. Rev. Lett.* **69**, 3479–3482.

Bakewell H.P., Lumley J.L. (1967): Viscous Sublayer and Adjacent Wall Region in Turbulent Pipe Flow. *Phys. Fluids* **10**, 1880–1889.

Bandyopadhyay P.R. (1986): Review—Mean Flow in Turbulent Boundary Layers Disturbed to Alter Skin Friction. *J. Fluids Eng.* **108**, 127–140.

Bandyopadhyay P.R., Breuer K.S., Blechinger C.J. (editors) (1994): *Application of Microfabrication to Fluid Mechanics*, FED vol. 197, (American Society of Mechanical Engineers, New York).

Banks S.P. (1986): *Control Systems Engineering* (Prentice-Hall International, Englewood Cliffs, New Jersey).

Barnwell R.W., Hussaini M.Y. (editors) (1992): *Natural Laminar Flow and Laminar Flow Control* (Springer, Berlin).

Berkooz G., Fisher M., Psiaki M. (1993): Estimation and Control of Models of the Turbulent Wall Layer. *Bul. Am. Phys. Soc.* **38**, 2197.

Berkooz G., Holmes P., Lumley J.L. (1991): Intermittent Dynamics in Simple Models of the Turbulent Wall Layer. *J. Fluid Mech.* **230**, 75–95.

Blackwelder R.F. (1978): The Bursting Process in Turbulent Boundary Layers. *Workshop on Coherent Structure of Turbulent Boundary Layers*, eds. C.R. Smith and D.E. Abbott, (Lehigh University, Bethlehem, Pennsylvania), 211–227.

Blackwelder R.F. (1988): Coherent Structures Associated with Turbulent Transport. *Transport Phenomena in Turbulent Flows*, eds. M. Hirata and N. Kasagi, (Hemisphere, New York), 69–88.

Blackwelder R.F., Gad-el-Hak M. (1990): Method and Apparatus for Reducing Turbulent Skin Friction. United States Patent No. 4,932,612.

Blackwelder R.F., Haritonidis J.H. (1983): Scaling of the Bursting Frequency in Turbulent Boundary Layers. *J. Fluid Mech.* **132**, 87–103.

Blackwelder R.F., Kovasznay L.S.G. (1972): Time-Scales and Correlations in a Turbulent Boundary Layer. *Phys. Fluids* **15**, 1545–1554.

Bouchon-Meunier B., Yager R.R., Zadeh L.A. (editors) (1995a): *Fuzzy Logic and Soft Computing* (World Scientific, Singapore).

Bouchon-Meunier B., Yager R.R., Zadeh L.A. (editors) (1995b): *Advances in Intelligent Computing—IPMU'94, Lecture Notes in Computer Science*, vol. 945, (Springer-Verlag, Berlin).

Breuer K.S., Bandyopadhyay P.R., Gad-el-Hak M. (editors) (1996): *Application of Microfabrication to Fluid Mechanics*, DSC-Volume 59, 468 pages, (American Society of Mechanical Engineers, New York).

Breuer K.S., Haritonidis J.H., Landahl M.T. (1989): The Control of Transient Disturbances in a Flat Plate Boundary Layer Through Active Wall Motion. *Phys. Fluids A* **1**, 574–582.

Bushnell D.M. (1983): Turbulent Drag Reduction for External Flows. AIAA Paper No. 83-0227, New York.

Bushnell D.M. (1994): Viscous Drag Reduction in Aeronautics. *Proceedings of the Nineteenth Congress of the International Council of the Aeronautical Sciences*, vol. 1, Paper No. ICAS-94-0.1, (American Institute of Aeronautics and Astronautics, Washington, D.C.), XXXIII–LVI.

Bushnell D.M., Hefner J.N. (editors) (1990): *Viscous Drag Reduction in Boundary Layers, Progress in Astronautics & Aeronautics*, vol. 123, (AIAA, Washington, D.C.).

Bushnell D.M., McGinley C.B. (1989): Turbulence Control in Wall Flows, *Annu. Rev. Fluid Mech.* **21**, 1–20.

Bussmann K., Münz H. (1942): Die Stabilität der laminaren Reibungsschicht mit Absaugung. *Jahrb. Dtsch. Luftfahrtforschung* **1**, 36–39.

Cantwell B.J. (1981): Organized Motion in Turbulent Flow. *Annu. Rev. Fluid Mech.* **13**, 457–515.

Carlson H.A., Lumley/J.J. (1996): Flow over an Obstacle Emerging from the Wall of a Channel. *AIAA J.* **34**, 924–931.

Chen C.-C., Wolf E.E., Chang H.-C. (1993): Low-Dimensional Spatiotemporal Thermal Dynamics on Nonuniform Catalytic Surfaces. *J. Phys. Chemistry* **97**, 1055–1064.

Choi H., Moin P., Kim J. (1992): Turbulent Drag Reduction: Studies of Feedback Control and Flow Over Riblets. Department of Mechanical Engineering Report No. TF-55, Stanford University, Stanford, California.

Choi H., Moin P., Kim J. (1994): Active Turbulence Control for Drag Reduction in Wall-Bounded Flows. *J. Fluid Mech.* **262**, 75–110.

Choi H., Temam R., Moin P., Kim J. (1993): Feedback Control for Unsteady Flow and its Application to the Stochastic Burgers Equation. *J. Fluid Mech.* **253**, 509–543.

Coller B.D., Holmes P., Lumley J.L. (1994a): Control of Bursting in Boundary Layer Models. *Appl. Mech. Rev.* **47**, S139–S143.

Coller B.D., Holmes P., Lumley J.L. (1994b): Control of Noisy Heteroclinic Cycles. *Physica D* **7**, 135–160.

Corino E.R., Brodkey R.S. (1969): A Visual Investigation of the Wall Region in Turbulent Flow. *J. Fluid Mech.* **37**, 1–30.

Corke T.C., Glauser M.N., Berkooz G. (1994): Utilizing Low-Dimensional Dynamical Systems Models to Guide Control Experiments. *Appl. Mech. Rev.* **47**, S132–S138.

Davis L. (editor) (1991) *Handbook of Genetic Algorithms* (Van Nostrand Reinhold, New York).

Deane A.E., Sirovich L. (1991): A Computational Study of Rayleigh-Bénard Convection. Part 1. Rayleigh-Number Scaling. *J. Fluid Mech.* **222**, 231–250.

Ditto W.L., Pecora L.M. (1993): Mastering Chaos. *Scientific American* **269**, August, 78–84.

Ditto W.L., Rauseo S.N., Spano M.L. (1990): Experimental Control of Chaos. *Phys. Rev. Lett.* **65**, 3211–3214.

Eléna M. (1975): Etude des Champs Dynamiques et Thermiques d'un Ecoulement Turbulent en Conduit avec Aspiration à la Paroi. Thèse de Doctoratès Sciences, Université d'Aix-Marseille, Marseille, France.

Eléna M. (1984): Suction Effects on Turbulence Statistics in a Heated Pipe Flow. *Phys. Fluids* **27**, 861–866.

Falco R.E. (1974): Some Comments on Turbulent Boundary Layer Structure Inferred from the Movements of a Passive Contaminant. AIAA Paper No. 74-99, New York.

Falco R.E. (1977): Coherent Motions in the Outer Region of Turbulent Boundary Layers. *Phys. Fluids* **20**, S124–S132.

Falco R.E. (1980): The Production of Turbulence Near a Wall. AIAA Paper No. 80-1356, New York.

Falco R.E. (1983): New Results, a Review and Synthesis of the Mechanism of Turbulence Production in Boundary Layers and its Modification. AIAA Paper No. 83-0377, New York.

Falco R.E. (1991): A Coherent Structure Model of the Turbulent Boundary Layer and its Ability to Predict Reynolds Number Dependence. *Phil. Trans. R. Soc. London A* **336**, 103–129.

Faller W.E., Schreck S.J., Luttges M.W. (1994): Real-Time Prediction and Control of Three-Dimensional Unsteady Separated Flow Fields Using Neural Networks. AIAA Paper No. 94-0532, Washington, D.C.

Fan X., Hofmann L., Herbert T. (1993): Active Flow Control with Neural Networks. AIAA Paper No. 93-3273, Washington, D.C.

Favre A., Dumas R., Verollet E., Coantic M. (1966): Couche Limite Turbulente sur Paroi Poreuse avec Aspiration. *J. Mecanique* **5**, 3–28.

Fiedler H.E. (1988): Coherent Structures in Turbulent Flows. *Prog. Aerospace Sci.* **25**, 231–269.

Fiedler H.E., Fernholz H.-H. (1990): On Management and Control of Turbulent Shear Flows. *Prog. Aerospace Sci.* **27**, 305–387.

Fowler T.B. (1989): Application of Stochastic Control Techniques to Chaotic Nonlinear Systems. *IEEE Trans. Autom. Control* **34**, 201–205.

Gabriel K.J. (1995): Engineering Microscopic Machines. *Scientific American* **273**, September, 150–153.

Gabriel K.J., Jarvis J., Trimmer W. (editors) (1988): Small Machines, Large Opportunities: A Report on the Emerging Field of Microdynamics. National Science Foundation, (AT&T Bell Laboratories, Murray Hill, New Jersey).

Gad-el-Hak M. (1989): Flow Control. *Appl. Mech. Rev.* **42**, 261–293.

Gad-el-Hak M. (1993): Innovative Control of Turbulent Flows. AIAA Paper No. 93-3268, Washington, D.C.

Gad-el-Hak M. (1994): Interactive Control of Turbulent Boundary Layers: A Futuristic Overview. *AIAA J.* **32**, 1753–1765.

Gad-el-Hak M. (1996): Modern Developments in Flow Control. *Appl. Mech. Rev.* **49**, 365–379.

Gad-el-Hak M., Bandyopadhyay P.R. (1994): Reynolds Number Effects in Wall-Bounded Flows. *Appl. Mech. Rev.* **47**, 307–365.

Gad-el-Hak M., Blackwelder R.F. (1989): Selective Suction for Controlling Bursting Events in a Boundary Layer. *AIAA J.* **27**, 308–314.

Gad-el-Hak M., Bushnell D.M. (1991): Separation Control: Review. *J. Fluids Eng.* **113**, 5–30.

Gad-el-Hak M., Hussain A.K.M.F. (1986): Coherent Structures in a Turbulent Boundary Layer. Part 1. Generation of "Artificial" Bursts. *Phys. Fluids* **29**, 2124–2139.

Gad-el-Hak M., Blackwelder R.F., Riley J.J. (1981): On the Growth of Turbulent Regions in Laminar Boundary Layers. *J. Fluid Mech.* **110**, 73–95.

Garfinkel A., Spano M.L., Ditto W.L., Weiss J.N. (1992): Controlling Cardiac Chaos. *Science* **257**, 1230–1235.

Goldberg D.E. (1989) *Genetic Algorithms in Search, Optimization, and Machine Learning* (Addison-Wesley, Reading, Massachusetts).

Grappin R., Léorat J. (1991): Lyapunov Exponents and the Dimension of Periodic Incompressible Navier-Stokes Flows: Numerical Measurements. *J. Fluid Mech.* **222**, 61–94.

Halsey T.C., Martin J.E. (1993): Electrorheological Fluids. *Scientific American* **269**, October, 58–64.

Ho C.-M., Tai Y.-C. (1996): Review: MEMS and Its Applications for Flow Control. *J. Fluids Eng.* **118**, 437–447.

Hogan H. (1996): Invasion of the micromachines. *New Scientist* **29**, June, 28–33.

Holland J.H. (1992) *Adaptation in Natural and Artificial Intelligence* (MIT Press, Cambridge, Massachusetts).

Hu H.H., Bau H.H. (1994): Feedback Control to Delay or Advance Linear Loss of Stability in Planar Poiseuille Flow. *Proc. Roy. Soc. Lond. A* **447**, 299–312.

Huberman B. (1990): The Control of Chaos. *Proc. Workshop on Applications of Chaos*, 4–7 December, San Francisco, California.

Huberman B.A., Lumer E. (1990): Dynamics of Adaptive Systems. *IEEE Trans. Circuits Syst.* **37**, 547–550.

Hübler A., Lüscher E. (1989): Resonant Stimulation and Control of Nonlinear Oscillators. *Naturwissenschaften* **76**, 67–69.

Hussain A.K.M.F. (1986): Coherent Structures and Turbulence. *J. Fluid Mech.* **173**, 303–356.

Iglisch R. (1944): Exakte Berechnung der laminaren Reibungsschicht an der längsangeströmten ebenen Platte mit homogener Absaugung. *Schr. Dtsh. Akad, Luftfahrtforschung* **8B**, 1–51.

Jacobs J., James R., Ratliff C., Glazer A. (1993): Turbulent Jets Induced by Surface Actuators. AIAA Paper No. 93-3243, Washington, D.C.

Jacobson S.A., Reynolds W.C. (1993a): Active Boundary Layer Control Using Flush-Mounted Surface Actuators. *Bul. Am. Phys. Soc.* **38**, 2197.

Jacobson S.A., Reynolds W.C. (1993b): Active Control of Boundary Layer Wall Shear Stress Using Self-Learning Neural Networks. AIAA Paper No. 93-3272, Washington, D.C.

Jacobson S.A., Reynolds W.C. (1994): Active Control of Transition and Drag in Boundary Layers. *Bul. Am. Phy. Soc.* **39**, 1894.

Jacobson S.A., Reynolds W.C. (1995): An Experimental Investigation Towards the Active Control of Turbulent Boundary Layers. Department of Mechanical Engineering Report No. TF-64, Stanford University, Stanford, California.

James R.D., Jacobs J.W., Glezer A. (1994): Experimental Investigation of a Turbulent Jet Produced by an Oscillating Surface Actuator. *Appl. Mech. Rev.* **47**, S127–S1131.

Joslin R.D., Erlebacher G., Hussaini M.Y. (1996): Active Control of Instabilities in Laminar Boundary Layers—Overview and Cncept Validation. *J. Fluids Eng.* **118**, 494–497.

Kawthar-Ali M.H., Acharya M. (1996): Artificial Neural Networks for Suppression of the Dynamic-Stall Vortex over Pitching Airfoils. AIAA Paper No. 96-0540, Washington, D.C.

Keefe L.R. (1993a): Two Nonlinear Control Schemes Contrasted in a Hydrodynamic Model. *Phys. Fluids A* **5**, 931–947.

Keefe L.R. (1993b): Drag Reduction in Channel Flow Using Nonlinear Control. AIAA Paper No. 93-3279, Washington, D.C.

Keefe L.R. (1997): A MEMS-Based Normal Vorticity Actuator for Near-Wall Modification of Turbulent Shear Flows. *Exp. Thermal & Fluid Science* **13**, to appear.

Keefe L.R., Moin P., Kim J. (1992): The Dimension of Attractors Underlying Periodic Turbulent Poiseuille Flow. *J. Fluid Mech.* **242**, 1–29.

Kline S.J., Reynolds W.C., Schraub F.A., Runstadler P.W. (1967): The Structure of Turbulent Boundary Layers. *J. Fluid Mech.* **30**, 741–773.

Kostelich E.J., Grebogi C., Ott E., Yorke J.A. (1993a): Targeting from Time Series. *Bul. Am. Phys. Soc.* **38**, 2194.

Kostelich E.J., Grebogi C., Ott E., Yorke J.A. (1993b): Higher-Dimensional Targeting. *Phys. Rev. E* **47**, 305–310.

Kovasznay L.S.G. (1970): The Turbulent Boundary Layer. *Annu. Rev. Fluid Mech.* **2**, 95–112.

Kovasznay L.S.G., Kibens V., Blackwelder R.F. (1970): Large-Scale Motion in the Intermittent Region of a Turbulent Boundary Layer. *J. Fluid Mech.* **41**, 283–325.

Kwong A., Dowling A. (1993): Active Boundary Layer Control in Diffusers. AIAA Paper No. 93-3255, Washington, D.C.

Lai Y.-C., Grebogi C. (1993): Synchronization of Chaotic Trajectories Using Control. *Phys. Rev. E* **47**, 2357–2360.

Lai Y.-C., Deng M., Grebogi C. (1993a): Controlling Hamiltonian Chaos. *Phys. Rev. E* **47**, 86–92.

Lai Y.-C., Grebogi C., Tél T. (1994): Controlling Transient Chaos in Dynamical Systems. *Towards the Harnessing of Chaos*, ed. M. Yamaguchi, (Elsevier, Amsterdam).

Lai Y.-C., Tél T., Grebogi C. (1993b): Stabilizing Chaotic-Scattering Trajectories Using Control. *Phys. Rev. E* **48**, 709–717.

Laufer J. (1975): New Trends in Experimental Turbulence Research. *Annu. Rev. Fluid Mech.* **7**, 307–326.

Liepmann H.W., Nosenchuck D.M. (1982): Active Control of Laminar-Turbulent Transition. *J. Fluid Mech.* **118**, 201–204.

Liepmann H.W., Brown G.L., Nosenchuck D.M. (1982): Control of Laminar Instability Waves Using a New Technique. *J. Fluid Mech.* **118**, 187–200.

Lindner J.F., Ditto W.L. (1995): Removal, Suppression and Control of Chaos by Nonlinear Design. *Appl. Mech. Rev.* **48**, 795–808.

Lipkin R. (1993): Micro Steam Engine Makes Forceful Debut. *Science News* **144**, 197.

Löfdahl L., Glavmo M., Johansson B., Stemme G. (1993): A Silicon Transducer for the Determination of Wall-Pressure Fluctuations in Turbulent Boundary Layers. *Appl. Scientific Res.* **51**, 203–207.

Löfdahl L., Kälvesten E., Stemme G. (1994): Small Silicon Based Pressure Transducers for Measurements in Turbulent Boundary Layers. *Exp. Fluids* **17**, 24–31.

Lumley J.L. (1991): Control of the Wall Region of a Turbulent Boundary Layer. *Turbulence: Structure and Control*, ed. J.M. McMichael, 1-3 April, Ohio State University, Columbus, Ohio, 61–62.

Lumley J.L. (1996): Control of Turbulence. AIAA paper No. 96-0001, Washington, D.C.

Lüscher E., Hübler A. (1989): Resonant Stimulation of Complex Systems. *Helv. Phys. Acta* **62**, 544–551.

Mastrangelo C. (1993): Integration, Partition, and Reliability of Microelectromechanical Systems. Invited oral presentation at the *AIAA Third Flow Control Conference*, Orlando, Florida, 6–9 July.

McMichael J.M. (1993): MEMS and Challenges of Flow Control. Invited oral presentation at the *AIAA Third Flow Control Conference*, Orlando, Florida, 6–9 July.

McMichael J.M. (1996): Progress and Prospects for Active Flow Control Using Microfabricated Electromechanical Systems (MEMS). AIAA Paper No. 96-0306, Washington, D.C.

Mehregany M. (1993): Overview of Microelectromechanical Systems. Invited oral presentation at the *AIAA Third Flow Control Conference*, Orlando, Florida, 6–9 July.

Mehregany M., DeAnna R.G., Reshotko E. (1996): Microelectromechanical Systems for Aerodynamics Applications. AIAA Paper No. 96-0421, Washington, D.C.

Moin P., Bewley T. (1994): Feedback Control of Turbulence. *Appl. Mech. Rev.* **47**, S3–S13.

Nelson M.M., Illingworth W.T. (1991): *A Practical Guide to Neural Nets* (Addison-Wesley, Reading, Massachusetts).

Noor A., Jorgensen C.C. (1996): A Hard Look at Soft Computing. *Aerospace America* **34**, September, 34–39.

Nosenchuck D.M., Lynch M.K. (1985): The Control of Low-Speed Streak Bursting in Turbulent Spots. AIAA Paper No. 85-0535, New York.

O'Connor L. (1992): MEMS: Micromechanical Systems. *Mechanical Engineering* **114**, February, 40–47.

Ott E., Grebogi C., Yorke J.A. (1990a): Controlling Chaos. *Phys. Rev. Lett.* **64**, 1196–1199.

Ott E., Grebogi C., Yorke J.A. (1990b): Controlling Chaotic Dynamical Systems. *Chaos: Soviet-American Perspectives on Nonlinear Science*, ed. D.K. Campbell, (American Institute of Physics, New York), 153–172.

Ouellette J. (1996): MEMS: Mega Promise for Micro Devices. *Mechanical Engineering* **118**, October, 64–68.

Paula G. (1996): MEMS Sensors Branch Out. *Aerospace America* **34**, September, 26–32.

Pomeau Y., Manneville P. (1980): Intermittent Transition to Turbulence in Dissipative Dynamical Systems. *Commun. Math. Phys.* **7**, 189–197.

Pretsch J. (1942): Umschlagbeginn und Absaugung. *Jahrb. Dtsch. Luftfahrtforschung* **1**, 54–71.

Qin F., Wolf E.E., Chang H.-C. (1994): Controlling Spatiotemporal Patterns on a Catalytic Wafer. *Phys. Rev. Lett.* **72**, 1459–1462.

Reynolds W.C. (1993): Sensors, Actuators, and Strategies for Turbulent Shear-Flow Contro. Invited oral presentation at the *AIAA Third Flow Control Conference*, Orlando, Florida, 6–9 July.

Robinson S.K. (1991): Coherent Motions in the Turbulent Boundary Layer. *Annu. Rev. Fluid Mech.* **23**, 601–639.

Robinson E.Y., Helvajian, Jansen S.W. (1996a): Small and Smaller: The World of MNT. *Aerospace America* **34**, September, 26–32.

Robinson E.Y., Helvajian, Jansen S.W. (1996b): Big Benefits from Tiny Technologies. *Aerospace America* **34**, October, 38–43.

Romeiras F.J., Grebogi C., Ott E., Dayawansa W.P. (1992): Controlling Chaotic Dynamical Systems. *Physica D* **58**, 165–192.

Rotta J.C. (1970): Control of Turbulent Boundary Layers by Uniform Injection and Suction of Fluid. *Seventh Congress of the International Council of the Aeronautical Sciences*, ICAS Paper No. 70-10, Rome, Italy.

Saffman P.G. (1978): Problems and Progress in the Theory of Turbulence. *Structure and Mechanisms of Turbulence*, ed. H. Fiedler, vol. 2, *Lecture Notes in Physics*, vol. 76, (Springer-Verlag, Berlin), 273–306.

Schreck S.J., Faller W.E., Luttges M.W. (1995): Neural Network Prediction of Three-Dimensional Unsteady Separated Flow Fields. *J. Aircraft* **32**, 178–185.

Sen M., Wajerski D., Gad-el-Hak M. (1996): A Novel Pump for MEMS Applications. *J. Fluids Eng.* **118**, 624–627.

Sharatchandra, M.C., Sen, M., and Gad-el-Hak, M. (1997): Navier-Stokes Simulations of a Novel Viscous Pump. *J. Fluids Eng.* **119**, no. 2.

Shinbrot T. (1993): Chaos: Unpredictable Yet Controllable? *Nonlinear Science Today* **3**, 1–8.

Shinbrot T. (1995): Progress in the Control of Chaos. *Adv. Physics* **44**, 73–111.

Shinbrot T. (1997): Prospects for Spatio-Temporal Chaos Control. In this volume.

Shinbrot T., Ottino J.M. (1993a): Geometric Method to Create Coherent Structures in Chaotic Flows. *Phys. Rev. Lett.* **71**, 843–846.

Shinbrot T., Ottino J.M. (1993b): Using Horseshoes to Create Coherent Structures in Chaotic Fluid Flows. *Bul. Am. Phys. Soc.* **38**, 2194.

Shinbrot T., Ditto W., Grebogi C., Ott E., Spano M., Yorke J.A. (1992a): Using the Sensitive Dependence of Chaos (the "Butterfly Effect") to Direct Trajectories in an Experimental Chaotic System. *Phys. Rev. Lett.* **68**, 2863–2866.

Shinbrot T., Grebogi C., Ott E., Yorke J.A. (1992b): Using Chaos to Target Stationary States of Flows. *Phys. Lett. A* **169**, 349–354.

Shinbrot T., Grebogi C., Ott E., Yorke J.A. (1993): Using Small Perturbations to Control Chaos. *Nature* **363**, 411–417.

Shinbrot T., Grebogi C., Ott E., Yorke J.A. (1990): Using Chaos to Direct Trajectories to Targets. *Phys. Rev. Lett.* **65**, 3215–3218.

Shinbrot T., Grebogi C., Ott E., Yorke J.A. (1992c): Using Chaos to Direct Orbits to Targets in Systems Describable by a One-Dimensional Map. *Phys. Rev. A* **45**, 4165–4168.

Singer J., Wang Y.-Z., Bau H.H. (1991): Controlling a Chaotic System. *Phys. Rev. Lett.* **66**, 1123–1125.

Sirovich L., Deane A.E. (1991): A Computational Study of Rayleigh-Bénard Convection. Part 2. Dimension Considerations. *J. Fluid Mech.* **222**, 251–265.

Sreenivasan K.R. (1989): The Turbulent Boundary Layer. *Frontiers in Experimental Fluid Mechanics*, ed. M. Gad-el-Hak, *Lecture Notes in Engineering*, vol. 46, (Springer-Verlag, Berlin), 159–210, .

Swearingen J.D., Blackwelder R.F. (1984): Instantaneous Streamwise Velocity Gradients in the Wall Region. *Bull. Am. Phys. Soc.* **29**, 1528.

Tai Y.-C. (1993): Silicon Micromachining and Micromechanics. Invited oral presentation at the *AIAA Third Flow Control Conference*, Orlando, Florida, 6–9 July.

Tang J., Bau H.H. (1993a): Stabilization of the No-Motion State in Rayleigh-Bénard Convection through the Use of Feedback Control. *Phys. Rev. Lett.* **70**, 1795–1798.

Tang J., Bau H.H. (1993b): Feedback Control Stabilization of the No-Motion State of a Fluid Confined in a Horizontal Porous Layer Heated from Below. *J. Fluid Mech.* **257**, 485–505.

Townsend A.A. (1961): Equilibrium Layers and Wall Turbulence. *J. Fluid Mech.* **11**, 97–120.

Townsend A.A. (1970): Entrainment and the Structure of Turbulent Flow. *J. Fluid Mech.* **41**, 13–46.

Ulrich A. (1944): Theoretische Untersuchungen über die Widerstandsersparnis durch Laminarhaltung mit Absaugung. *Schriften Dtsch. Akad. Luftfahrtforschung B* **8**, 53.

Vargo S.E., Muntz E.P. (1996): A Simple Micromechanical Compressor and Vacuum Pump for Flow Control and Other Distributed Applications. AIAA Paper No. 96-0310, Washington, D.C.

Verollet E., Fulachier L., Dumas R., Favre A. (1972): Turbulent Boundary Layer with Suction and Heating to the Wall. *Heat and Mass Transfer in Boundary Layers*, eds. N. Afgan, Z. Zaric and P. Anastasijevec, vol. 1, (Pergamon Presss, Oxford), 157–168.

Viswanath P.R. (1995): Flow Management Techniques for Base and Afterbody Drag Reduction. *Prog. Aero. Sci.* **32**, 79–129.

Wadsworth D.C., Muntz E.P., Blackwelder R.F., Shiflett/ G.R. (1993): Transient Energy Release Pressure Driven Microactuators for Control of Wall-Bounded Turbulent Flows. AIAA Paper No. 93-3271, Washington, D.C.

Wang Y., Singer J., Bau H.H. (1992): Controlling Chaos in a Thermal Convection Loop. *J. Fluid Mech.* **237**, 479–498.

Wilkinson S.P., Balasubramanian R. (1985): Turbulent Burst Control Through Phase-Locked Surface Depressions. AIAA Paper No. 85-0536, Washington, D.C.

Willmarth W.W. (1975). Structure of Turbulence in Boundary Layers. *Adv. Appl. Mech.* **15**, 159–254.

Wiltse J.M., Glezer A. (1993): Manipulation of Free Shear Flows Using Piezoelectric Actuators. *J. Fluid Mech.* **249**, 261–285.

Wilkinson S.P. (1990): Interactive Wall Turbulence Control. *Viscous Drag Reduction in Boundary Layers*, eds. D.M. Bushnell and J.N. Hefner, *Progress in Astronautics and Aeronautics*, vol. 123, (AIAA, Washington, D.C.), 479–509.

Wilkinson S.P., Lazos B.S. (1987): Direct Drag and Hot-Wire Measurements on Thin-Element Riblet Arrays. *Turbulence Management and Relaminarization*, eds. H.W. Liepmann and R. Narasimha, (Springer-Verlag, Berlin), 121–131.

Wilkinson S.P., Anders J.B., Lazos B.S., Bushnell D.M. (1988). Turbulent Drag Reduction Research at NASA Langley: Progress and Plans. *Int. J. Heat and Fluid Flow* **9**, 266–277.

Willmarth W.W. (1975a): Structure of Turbulence in Boundary Layers. *Adv. Appl. Mech.* **15**, 159–254.

Willmarth W.W. (1975b): Pressure Fluctuations Beneath Turbulent Boundary Layers. *Annu. Rev. Fluid Mech.* **7**, 13–37.

Yager R.R., Zadeh L.A. (editors) (1992): *An Intorduction to Fuzzy Logic Applications in Intelligent Systems* (Kluwer Academic, Boston).

Yun W. (1993): System Considerations for Integration of Microsensors and Electronics. Invited oral presentation at the *AIAA Third Flow Control Conference*, Orlando, Florida, 6–9 July.

Zilberman M., Wygnanski I., Kaplan R.E. (1977): Transitional Boundary Layer Spot in a Fully Turbulent Environment. *Phys. Fluids* **20**, S258–S271.

3 Some Notes on Drag Reduction in the Near-Wall Region

Ron F. Blackwelder

University of Southern California, Los Angeles, California 90089, U.S.A.

Abstract. The last thirty years has seen an explosion of information concerning the structure of the near-wall region of bounded shear flows. Kline et al. (1967) were one of the first to examine its eddy structure and provide a detailed description using primarily visualization methods. They showed the existence of the ubiquitous low-speed streaks and coined the word "burst" to describe the violent lift-up and mixing. The intervening thirty years have provided many details about this region and its importance to the dynamics of bounded shear flows. It is well known that the eddies in this region control the production of turbulence and the drag due to the boundary. The general structure of the eddies and processes in this region is covered in the next section followed by a discussion of the similarities between this region and transitional flows. The use of suction and actuators for manipulating and controlling the eddies follow.

1 The Structure of the Bursting Process

Since the original work by Kline et al. (1967), many authors have added terminology to the observations in the wall region that has been summarized by Robinson (1991). It has become clear that the entire eddy structure within the wall region is an ongoing process that is quite dynamic and is statistically repeatable. Hereafter, this process will be called the bursting process or bursting phenomenon and denoted by BP. It consists of many individual eddies and events that are summarized in the flow chart presented in Fig. 1. This schematic is obviously a simplification of a complicated process, but provides a beginning point for the discussion. The major components of the BP are streamwise vortices, the low-speed streaks, the inflectional profiles and the resulting instabilities. There is no universal agreement within the community as to the details of the elements within Fig. 1. Many of the differing points of view result from the random environment of the bursting phenomenon. It occurs near the wall in the presence of turbulence having an rms value of 10–12% of the freestream or centerline velocity. This allows fluctuating swings of more than 50% of the local mean flow which makes the BP difficult to study. For example, it is extremely difficult to follow any eddy in the wall region long enough to observe its complete life cycle. Indeed, this turbulent environment may be more correctly viewed as the result of the BP. When the BP is artificially removed, the turbulent intensity decreases significantly.

Another reason for the lack of agreement of the elements in Fig. 1 is because the different eddy structures are observed via many different methods.

M. Gad-el-Hak et al.: LNPm 53, pp. 155 - 198, 1998
© Springer-Verlag Berlin Heidelberg 1998

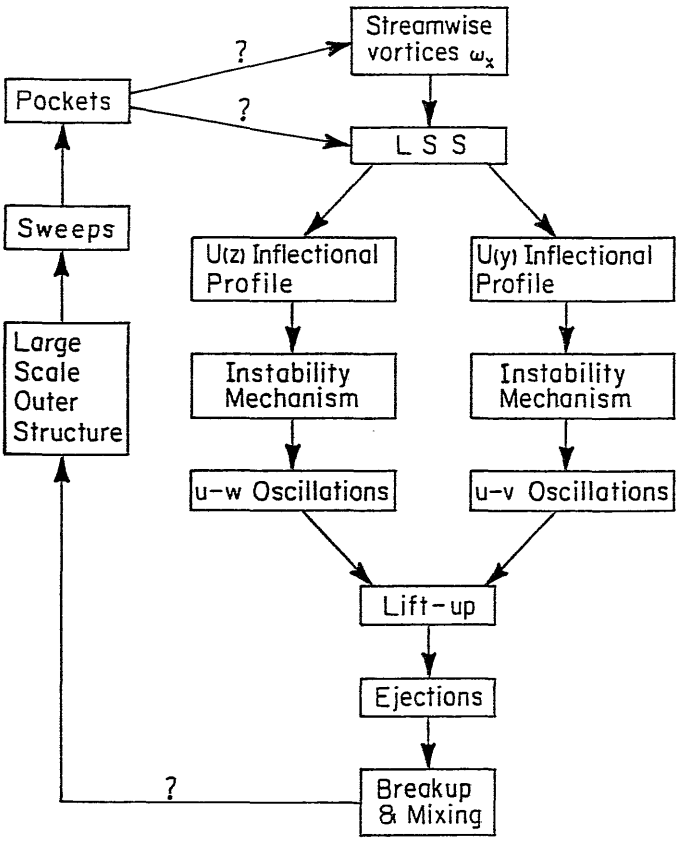

Fig. 1. The proposed sequence of the bursting process. The arrows indicate the sequential events and the '?' indicate relationships with less supporting evidence.

Most of the knowledge about the BP has been obtained from visualization methods, hot-wire/film anemometry and direct numerical simulations. Lately some impressive results have been obtained from particle image velocimetry. However within each type of measurement system, there are almost as many variations as there are investigators. The result is that often different aspects of the eddies are observed in "similar" investigations. For example different initial conditions or threshold levels can yield different views and impressions of the eddies under study. In addition, the BP has a Reynolds number dependence that is not well known. To obtain a near-wall region having sufficient spatial resolution with any of the methods mentioned above, a low Reynolds number is required. Consequently most of the results in the literature have been obtained at a "low" Reynolds number, thus excluding a large range of Reynolds number testing. In addition, the Reynolds number can be viewed as a ratio between the spatial scales of the large eddies of the flow field and

the scales describing the near-wall structure. Hence if there is a dynamical relationship between these two sets of eddies as suggested later, then the structure of the near-wall region is bound to change as the Reynolds number changes.

1.1 Length and Velocity Scales

The coordinate system used throughout will follow the traditional Cartesian boundary layer system with the orthogonal directions of x,y and z having velocity components of u, v and w. The mean flow will be aligned with the x direction and y is perpendicular to the wall. The mean flow field is denoted by U, V, and W so that a two dimensional canonical boundary layer will have $W = 0$ and $U \gg V$. The three velocity components can also be denoted by $u_i = U_i + u_i'$ with $i = 1, 2$ or 3. The three vorticity components are denoted by w_x, w_y and w_z or by w_i.

The length scale of the near-wall region is called the viscous scale and is obtained from the magnitude of the mean vorticity in the region and its viscous diffusion away from the wall. The mean vorticity in the region is characterized by the velocity gradient at the wall; i.e. $\partial U/\partial y\big|_w$. The inverse of the vorticity provides the time scale for the region; $t_\nu = \left[\partial U/\partial y\big|_w\right]^{-1}$. The viscous length scale, ℓ_ν, is determined by the distance the vorticity is diffused from the wall given by

$$\ell_\nu = \sqrt{\frac{\nu}{\frac{\partial U}{\partial y}\big|_w}} \tag{1}$$

where ν is the kinematic viscosity. The velocity scale consistent with the above time and length scales is ℓ_ν/t_ν which yields $u_\tau = \sqrt{\nu \frac{\partial U}{\partial y}\big|_w}$. This characteristic velocity is called the 'friction velocity.' These scales have been used universally in the near-wall region of bounded turbulent shear flows for half a century. Ludwig and Tilman (1949) showed that they were independent of the imposed pressure gradient. When the physical variables are scaled with the viscous scales, the usual $()^+$ notation will be used; e.g. $y^+ = y/\ell_\nu$.

The large eddies in the outer or core region of a bounded turbulent shear flow scale with δ which is either the boundary layer thickness, radius, or half channel height depending upon the type of shear flow. The ratio of the scale of the outer eddies to the scale of the near-wall eddies is δ/ℓ_ν denoted by δ^+. This is a form of the Reynolds number, $Re_\tau = \delta \cdot u_\tau/\nu$. It is easily shown that

$$Re_\tau = \sqrt{\frac{C_f}{2}} \cdot \frac{\delta U_\infty}{\nu} \tag{2}$$

where $\delta \cdot U_\infty/\nu = Re_\delta$ is the Reynolds number based upon the large scale eddies. Re_τ must usually exceed 10^2 to maintain a turbulent flow. In practical applications, values Re_τ of up to 10^5 and 10^6 occur. Since Re_τ is the ratio of

the outer length scale to the viscous scale and $Re_\tau \gg 1$, it follows that the size of the near-wall region is quite small compared to the larger scales in the flow. However the wall region must be sufficiently large to provide adequate spatial resolution in any wall investigation. These two opposing requirements have been met by using flow fields at small Reynolds numbers; i.e. in the range $10^2 < \delta^+ < 10^3$.

Fig. 2 illustrates the mean velocity profile and the turbulent production in a turbulent boundary layer. The plot is semi-logarithmic and has three primary regions. They are the near-wall region defined by $0 < y^+ < 30$, the log region bounded by $y^+ \simeq 30$ and $y/\delta \simeq 1/4$ and the outer region or wake region at $1/4 < y/\delta$. The log region is often called the overlap region between the two other regions. The region near the wall is subdivided between the viscous sublayer which is defined as the region where the mean velocity gradient, $\partial U/\partial y$, is approximately constant in the region $0 < y^+ \leq 5$. The buffer region is defined by $5 \leq y^+ \leq 30$. It is the location of the maximum values of many of the turbulence quantities, such as the turbulent production plotted in the figure . It and the turbulent velocity intensities, u' and w', have a maximum in the region approximated by $12 < y^+ < 15$ which makes this region the most dynamical location in bounded shear flows.

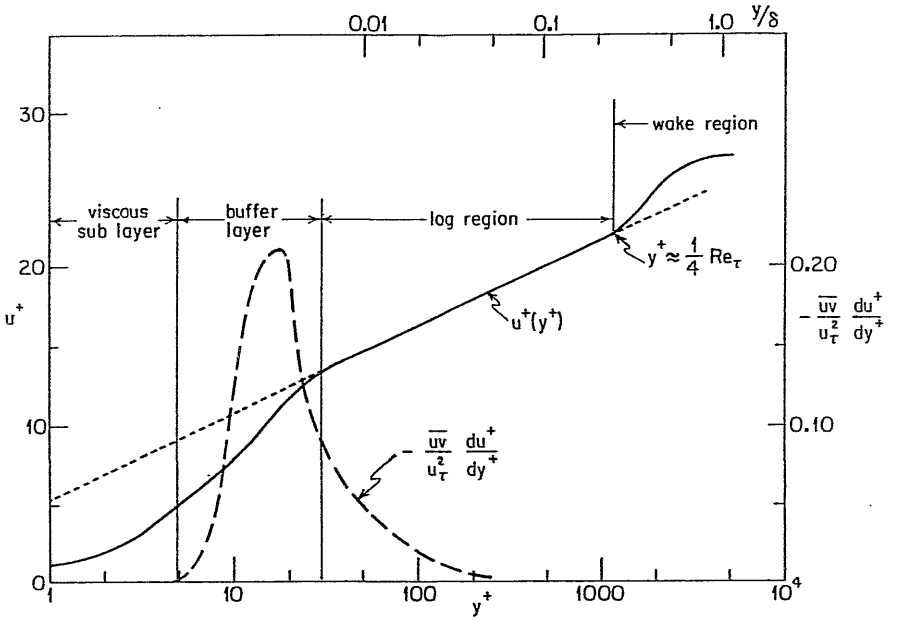

Fig. 2. The logarithmic mean velocity profile and turbulent production in a turbulent boundary layer showing the near-wall region, the log region and the wake (i.e. outer) region.

1.2 The Principal Eddies in the Bursting Process

The most common characteristic of the near-wall region is the presence of the low-speed regions called 'low-speed streaks.' They were first noticed by Hama (see Corrsin, 1957) and reported in detail by Kline et al. (1967) and many others since. They are most easily visualized by allowing small amounts of dye to seep into the wall region via a spanwise slot in the wall. The dye is quickly coagulated into streaks as seen in Kline et al. Alternatively, small hydrogen bubbles can be introduced into the region which also form elongated regions as seen in Fig. 3. The low-speed streaks have a width of about twenty ℓ_ν and a length of several hundred to a thousand ℓ_ν. Smith and Metzler (1983) have shown that they have a lifetime of typically $500\nu/u_\tau^2$ but lifetimes up to $2500\nu/u_\tau^2$ were observed. The average spacing between them is approximately $100\ell_\nu$ with a median spacing of $80\ell_\nu$ as seen in Fig. 4. This figure plots the probability distribution of the spanwise spacing, λ_z, between the streaks using data from Lee et al. (1974) and Oldaker and Tiederman (1977). The spacing between the streaks and other variables in the near-wall region are always random due to the turbulent environment. The distribution in the figure shows that values of λ_z^+ can be found between 20 and 200. Kline et al. (1967) have indicated that during the relatively dormant state of the streaks, they extend about $10\ell_\nu$ outward from the wall. But they often move away from the wall to $20 < y^+ < 50$ in a violent action that results in considerable mixing.

Another common eddy structure in the near-wall region is the streamwise vortices that occur typically on the sides of the low-speed streaks. These vortices are much more difficult to study for several reasons. First there is not a commonly accepted definition of a vortex, contrary to the precise mathematical definition of vorticity. Secondly, there is no small vorticity meter that is useful in experimental studies of the near-wall region, however the DNS studies have been very illuminating in describing the vorticity. Kim and Moin (1986) have shown that there are large amounts of fluctuating streamwise vorticity in the near-wall region and have traced out vortex lines. The coherent sections of the streamwise vorticity only extended a hundred ℓ_ν or so in the streamwise direction. They found very little evidence that the vorticity looped over the low-speed streaks in the shape of a horseshoe vortex as had been speculated in the literature. The streamwise vortices had diameters of 10–$30\ell_\nu$ and lengths of approximately $100\ell_\nu$. The remaining elements of the BP shown in Fig. 1 can best be described by referring to a model of the eddies in the near-wall region. Fig. 5 shows three low-speed streaks in an undisturbed state in the x'-z plane. The x'-coordinate is a convected x-coordinate with a convection speed equal to that of the low-speed streaks which is approximately 5–$10u_\tau$. The streamwise meandering and randomness shown in Fig. 3 appears to be important in the dynamics of the streaks only after they have lifted away from the wall region. Thus for simplification, the streaks are presented in Fig. 5 as being straight with an average spacing

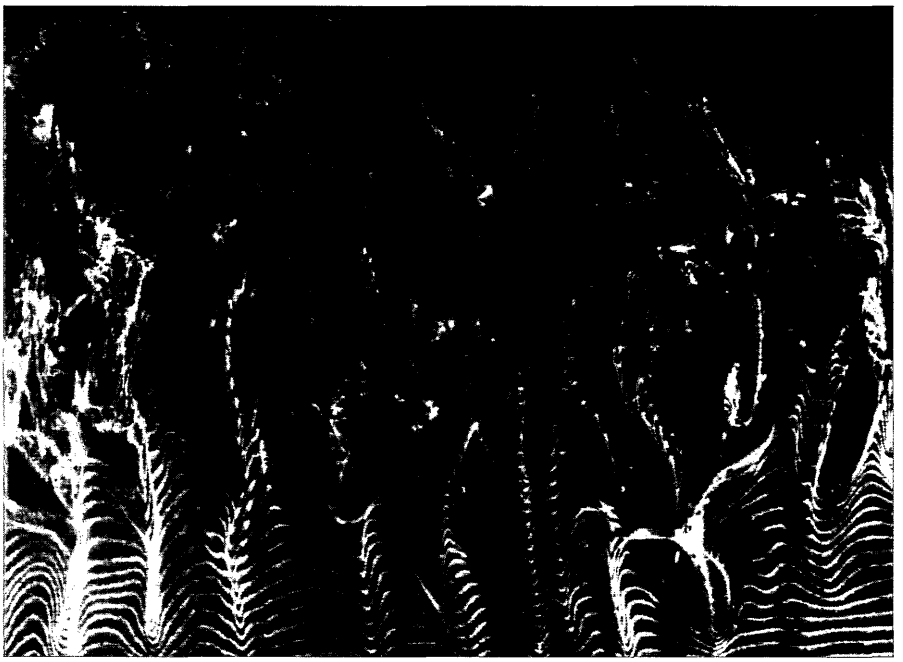

Fig. 3. A photograph of the low-speed streaks visualized by hydrogen bubbles. The bubbles were placed in the flow at the bottom of the photograph by electrically pulsing a small wire which produced a line of bubbles that were convected downstream, i.e. towards the top of the figure . The bubble wire was located at $y^+ = 5$.

between them. One can also image relatively short regions of streamwise vorticity lying besides the low-speed streaks as discussed above. The origin of the streaks is still unknown. Several authors have suggested different mechanisms for their origin but there is no universally accepted theory for the spacing of approximately $100\ell_\nu$.

The location of the streaks in the near-wall region implies that they will be surrounded by intense regions of strong shear. First, on their sides large values of $\partial u/\partial z$ are present because there is alternating high- and low-speed fluid in the spanwise direction as indicated in Fig. 6 and as seen in Fig. 3. Also in the normal direction, large values of shear are present associated with the $U(y)$ velocity profile. Swearingen and Blackwelder (1988) have shown that the magnitudes of $\partial u/\partial z$ and $\partial u/\partial y$ are approximately equal in the near-wall region. In addition, both have characteristic values of u_τ/ℓ_ν in this region. Hence the shear regions are indeed intense suggesting that they are important in the ensuing dynamics. The strength of the spanwise gradient also implies that the normal vorticity component, ω_y, will be large. Indeed Robinson (1991) found that ω_y was the only other flow quantity to have a streaky structure in the wall region.

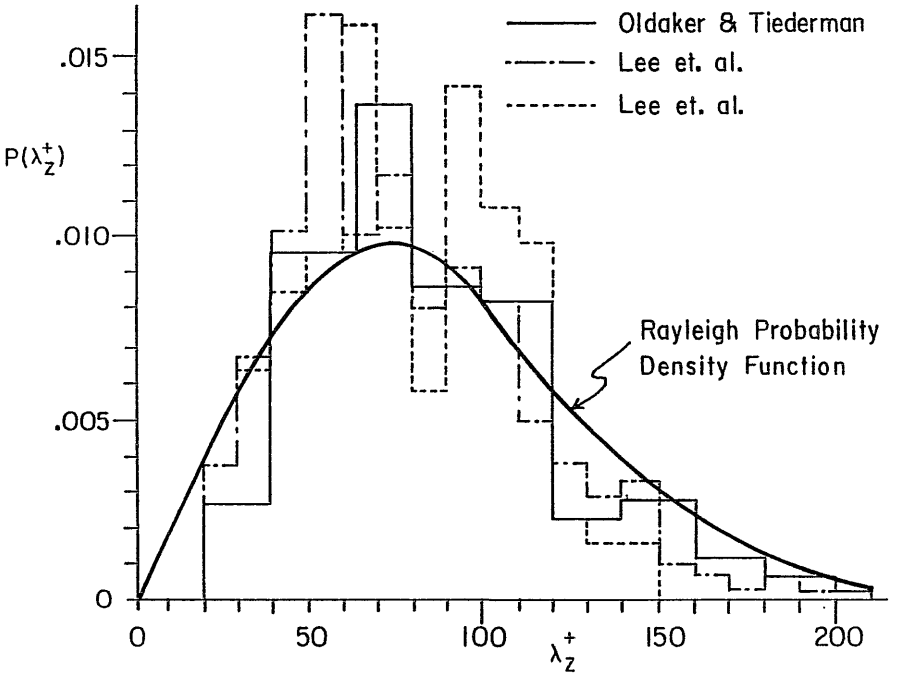

Fig. 4. The probability distribution of the spanwise spacing between the low-speed streaks.

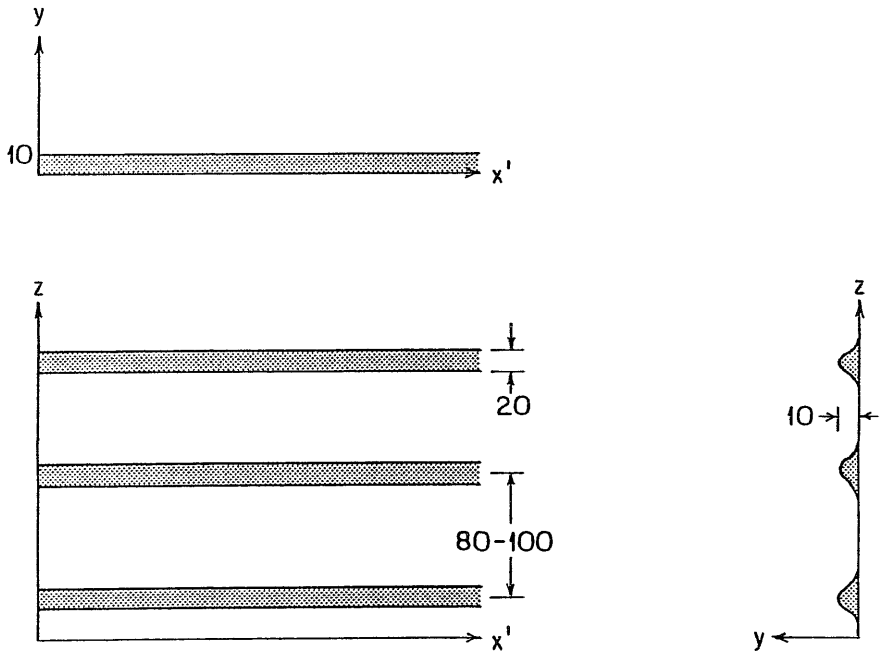

Fig. 5. An idealized model of the undisturbed low-speed streaks shown in three views in the convected coordinate, x'.

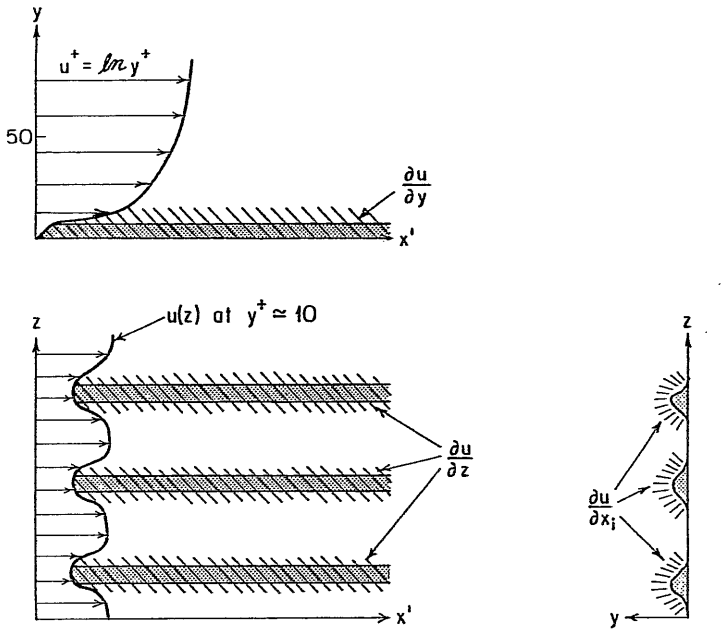

Fig. 6. The regions of the intense velocity shear surrounding the streaks in the normal and spanwise directions.

The next important element in the sequence shown in Fig. 1 are the inflectional profiles that develop in the normal and spanwise directions. In the spanwise direction, an inflectional velocity profile, $U''(z) = 0$, develops as soon as a low-speed region is formed because as one moves from high to low and back to high speed regions in the spanwise region, two inflection points are encountered. In the normal direction, an inflectional $U(y)$ profile forms only after the low-speed streak has had sufficient time to develop; i.e. in its earlier stages the low-speed deficit may not be sufficient to form an inflectional profile. The inflection points in any streamwise velocity profile are numerous as can be seen in Fig. 7 which shows profiles in the normal and spanwise directions. The number of inflection points decreases as the distance from the boundary increases as seen by comparing Fig. 7b and 7c. Since the low-speed streaks are three dimensional, the loci of all of the inflectional points must be a two dimensional surface. This inflectional surface will be random in space and time and need not be continuous.

The inflectional profiles are important because they are a harbinger of an inviscid instability; thus they are one of the more important aspects of the turbulent production in the near-wall region. Viscous instabilities grow on a time scale given by the viscous diffusion. These time scales are usually slow compared to the other time scales in the flow, such as those associated with an inflection point. Hence even in transitional bounded shear flows, where

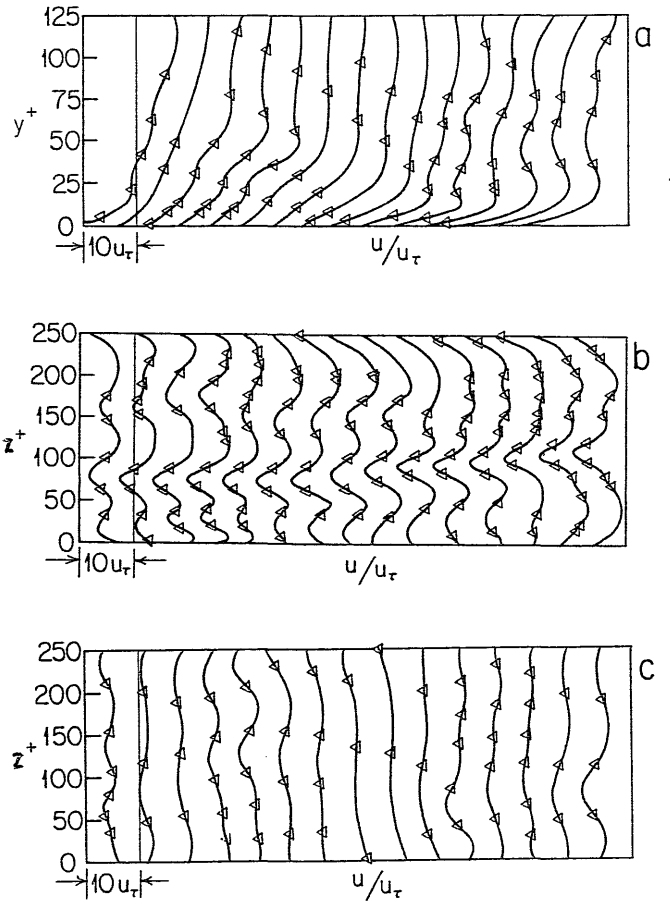

Fig. 7. Instantaneous velocity profiles in the normal (a) and spanwise (b and c) directions from a direct simulation of a channel flow. The spanwise data were obtained at $y^+ = 15$ in (b) and at 66 in (c). The inflection points are denoted by the $\triangleleft$ symbol.

the initial instability is a Tollmien-Schlichting type viscous instability, the final breakdown into turbulence is often due to an inviscid instability. As soon as an inflection point occurs in the flow field, a Kelvin-Helmholtz type instability rapidly develops.

Consider the inflectional profile, $U(\xi)$ shown in Fig. 8 where ξ can be any direction in the flow. For such a hyperbolic tangent profile, Michalke (1965) has shown that the maximum growth rate according to linear theory is $0.19U_o/\Delta$ where Δ is the half width of the shear layer. This growth rate can be shown to be an order of magnitude larger than the growth rates in viscous instabilities. Michalke points out that the most amplified wave has a wavelength of approximately 14Δ and will increase its amplitude by a factor

of thirty while it travels only one wave length downstream. Correspondingly, the energy of the disturbance will increase by almost 10^3 during the same travel time. Such rapid growth implies that the disturbance probably will not be able to travel more than a couple of wave lengths downstream before it has increased in amplitude sufficiently that the linear analysis no long holds. For this reason only one or two wavelengths are observed in well controlled transitional flow fields such as in a jet flow. In the random environment of a turbulent shear flow, the coherent portion of the growth will be even more difficult to observe.

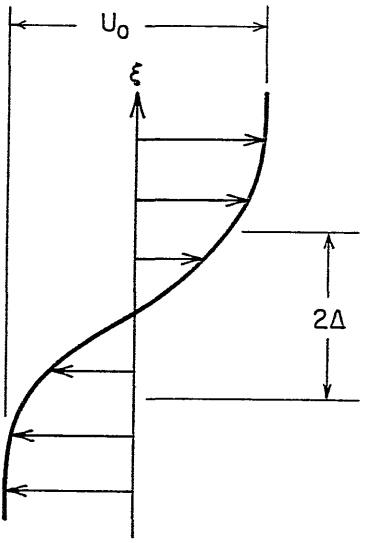

Fig. 8. Schematic of an inflectional profile associated with an inviscid instability.

The analysis of Michalke (1965) had several restrictions that should be mentioned. First his velocity profile was assumed to extend to infinity in the $\pm\xi$ directions. Huerre (1983) has added an inviscid wall into the analysis and shown that there are no significant changes to the analysis as long as the inflection point is greater that $10\ell_\nu$ removed from the wall. Secondly, Michalke considered only an inflection point in a two dimensional profile. However Nishioka et al. (1980) have shown that the results accurately predict the wavelength and breakdown of a three dimensional transitional flow in the presence of a wall. Lastly, the above analysis is for a steady flow. However the time scales of the disturbance are so small compared to the longer time scales of the low-speed streaks that this condition is well satisfied. This can be seen by examining the time scale of the velocity profile which is $[\partial U/\partial\xi]^{-1} \approx \Delta/U_o$. Swearingen and Blackwelder (1988) examined a boundary layer and found experimentally that Δ was approximately $10\ell_\nu$ and U_o was roughly $5u_\tau$ in the near-wall region. Compared with the time scale of the low-speed

streaks of approximately $500\nu/u_\tau^2$ as given by Smith and Metzler (1983), it is seen that the instability occurs very rapidly compared to the changes occurring in the streaks.

Inflectional profiles have been observed by many investigators in the near-wall region of bounded shear flows. Any visualization study that injects a passive contaminant along a line such as the bubbles in Fig. 3 or studies by Grass (1971) and others quickly sees distortions due to inflectional profiles. Blackwelder and Kaplan (1976), Willmarth and Lu (1972), and others have observed similar profiles using hot-wire anemometry. Results from the direct numerical simulations such as seen in Fig. 7 and elsewhere have also produced such profiles. Observations of growing wavelike disturbances associated with the inflectional profiles have been more rare. This is possibly due to the rapid growth of the disturbance, but it is probably also due to the fact that the disturbances are occurring in a highly turbulent environment. Some evidence of oscillations can be found in the literature. Kline et al. (1967) observed that the low-speed streaks oscillated after they lifted away from the wall. Smith (1978) observed wavelike formations as the result of a strong interaction between the low-speed fluid in the near-wall region and the higher speed fluid moving toward the wall. Blackwelder and Kaplan (1976) and Bacher and Smith (1986) obtained conditionally averaged data and found some evidence of waves having wavelengths of $\lambda_x^+ \approx 150$ in agreement with Michalke's (1965) predictions.

Although the oscillations are not readily observed, the process of the lift-up of the low-speed streak has been documented in the visualization studies. These studies suggest that the low-speed streak is disturbed by the background turbulence which triggers the inviscid instability discussed above. This instability grows rapidly with an oscillation from side to side in response to a growing inflectional instability of $U(z)$ or away from the wall with a $U(y)$ instability. Since the instability may be in any other plane aligned with the x axis, the instability need not occur in only the xz or the xy planes. However when visualized in the xz plane, a projection of the oscillation will be seen. Similarly, when viewed in the xy plane, its projection in that plane will be seen. Fig. 9 suggests how an oscillation may appear based upon this information. Although a single wave is more commonly seen, two are often seen and are shown in the cartoon. In the xy plane, the low-speed steak is seen to move away from the wall in a motion called lift-up. This is commonly seen in the visual studies and is usually defined when a portion of the streak raises up above $y^+ \approx 15$.

As the lift-up continues outward, it comes into contact with higher speed fluid which seems to accelerate its motion. This phase of the motion is termed an 'ejection' and involves a strong outward motion of low-speed fluid. Hence there is a strong Reynolds shear stress associated with this motion with the uv product often exceeding ten times its mean value. Corino and Brodkey (1969) found a second ejection often associated with an earlier one. They also

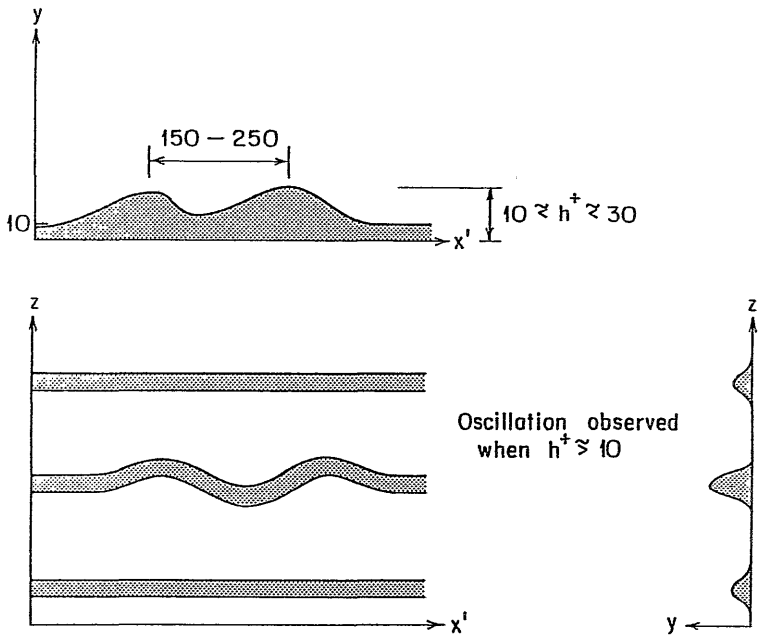

Fig. 9. Model of the disturbed low-speed streaks shown at the stage of lift-up. Sinuous motions are often observed when the lift-up moves to $y^+ > 10$.

suggested that the ejections were associated with a sweep of large scale high-speed fluid that appeared to be associated with the outer motion. Tiederman et al. (1985) defined the ejections as a marked fluid element originating from $y^+ < 15$ which moved outward at least $20\ell_\nu$ over a distance downstream of $350\ell_\nu$. In another study, Bogard and Tiederman (1986) studied multiple lift-ups and ejections and find that when they occur, the multiple ejections were separated by $\Delta t^+ = 25$. In this near-wall region, the convection velocity is roughly $6–10u_\tau$ yielding a wavelength of approximately $150–250\ell_\nu$.

As the ejection motion continues, the coherence appears to decrease. In the visualization studies, the tracing contaminant, usually dye or bubbles, becomes diffuse in this stage making it difficult to follow the motion. It has also been problematical to observe coherent motion using probes or direct numerical simulations. It appears that the ejected fluid produces its most violent mixing during this stage thus diluting the contaminant and making it impossible to follow. In any case, the coherency of the motion that is so evident in the earlier stages decreases dramatically which leads to a 'breakup' of the coherent motion.

1.3 Inner-Outer Relationship in the Shear Flow

Several authors have speculated about the nature of the process after the breakup. Kovasznay (1970) suggested that several of the mixed regions may coagulate and eventually form a large scale structure in the outer region. Alternatively, these mixed regions may grow and ultimately reach an distance from the wall that is proportional to their energy or to their normal velocity component. At that point their outward energy would have been spent and they would begin a decay process that continues until they are displaced by other ejections moving outward. Most of the ejections would probably end their outward motion in the log region and then decay as they are convected downstream. But the highly energetic motions would move further outward into the wake region and the most energetic ones would find their way to the interface of a turbulent boundary layer or would cross the centerline of a pipe or channel flow. There presently is no hard evidence confirming a relationship between the breakup of the BP and the large scale outer structure and hence the '?' on that portion of the flow diagram in Fig. 1.

On the other hand, there is more evidence to suggest that the outer region may influence the events that occur in the near-wall region. Corino and Brodkey (1969) were the first to point out the significance of regions of high-speed fluid that regularly disturb this region. They termed this high-speed fluid 'sweeps' and suggested that they were associated with the larger eddies in the logarithmic and outer regions. They found that after the ejection phase of the process, the larger scale high-speed fluid would sweep everything downstream and leave the region in a more quiescent state until the BP began again. Offen and Kline (1974) found that the lift-ups in the near-wall region seemed to be correlated with the passage of an eddy structure in the outer region having a negative normal velocity component. Chen and Blackwelder (1978) used a temperature contaminant introduced at the wall to study a turbulent boundary layer. They found that the upstream side of the large structures in the wake region had a sharp temperature discontinuity separating the warmer temperature inside the turbulent region from the cooler fluid in the non-turbulent fluid. Because the large outer eddies were strongly three-dimensional, the discontinuity did not always extend through the logarithmic region. But sometimes it did extend into the near-wall region suggesting a possible linkage between the these two diverse regions.

Falco (1977) has also shown that there is a smaller eddy structure that rides on the upstream side of the large outer eddies in turbulent boundary layers. These 'typical eddies' appear to have length scales of roughly 100–$200\ell_\nu$ and move toward the wall as the large structures evolve. Although Falco could not follow these typical eddies into the near-wall region, he speculated that they may interact with the region thus forming a link between the wake and the wall region. In a separate study, Falco (1979) found a similarly shaped disturbance in the near-wall region. He introduced smoke through a slot into the wall region and initially observed only the streaks. By increasing

the amount of smoke injected through the wall, he obscured the streaks and observed regions that were clear of smoke which he termed 'pockets.' The clear fluid could have only come from regions further removed from the wall, hence the pockets must be associated with some eddies in the log or wake region. They also had a spanwise and streamwise scale of 100–$200\ell_\nu$ suggesting that they may be related to the typical eddies, or possibly are the typical eddies as they reach the wall. Falco speculated that the pockets are related to the streamwise vortices and low-speed streaks in the wall region. However there is still a need to substantiate this evidence and hence the '?' in these two linkages in the flow chart of Fig. 1.

There are still many unknown aspects of the near-wall region. The effect of the Reynolds number is one of the most vexing. As mentioned earlier, most of the investigations in the wall region are by necessity done at low Reynolds number to improve the spatial resolution in experiments or to conform to the computer memory and calculation speed in the numerical simulations. Although there is universal usage of the viscous variables to describe the wall flow, Sreenivasan (1989) has pointed out that there are some parameters that remain a function of the outer variables. One such example is the distance from the wall to the peak in the Reynolds stress, y_m^+. For channel flows with half height δ, the Reynolds equation is

$$-\overline{uv} = -\nu\left(\frac{dU}{dy}\right) + u_\tau^2 \cdot \left(1 - \frac{y}{\delta}\right) \tag{3}$$

Assuming the mean profile is approximately logarithmic in the region of y_m^+, the location of the maximum of $-\overline{uv}$ is given by

$$y_m^+ = \sqrt{\frac{\delta^+}{\kappa}} \tag{4}$$

where κ is von Kármán's constant. Thus the location of the maximum of the Reynolds shear stress depends directly upon the outer length scale, δ. Sreenivasan supports this conclusion with experimental data from boundary layers, pipes and channels. Furthermore, the value of Reynolds stress at its maximum is

$$\frac{-\overline{uv}\,(y_m^+)}{u_\tau^2} = 1 - \frac{2}{\sqrt{\kappa\delta^+}} \tag{5}$$

which also depends upon the outer scale. Other turbulence quantities in the near-wall region also display an effect of the Reynolds number and more study is required of this aspect of the near-wall region.

2 Analogies with Transitional Flows

To understand the nature of the near-wall region of bounded shear flows, it is instructive to examine similar flow fields. This section compares the

similarities and differences between the transitional flow and the wall region of a fully developed bounded shear flow. Most of the comparisons will be with boundary layers since more work has been done on this flow; however the results generally hold for pipe and channel flows as well.

The gross characteristics of the transitional boundary layer and the near-wall region of a turbulent boundary are quite evident. They both are bounded by a solid surface, which together with the no slip condition, produces a strong shear flow, $\partial U/\partial y$. This gradient yields a strong spanwise vorticity field in both flows. The Navier-Stokes equations evaluated at the wall are identical for both the transitional and the turbulent flow having the same boundary conditions. For an isothermal wall with no suction, the equations show that when the instantaneous $\partial p/\partial x \neq 0$, the wall is a source of spanwise vorticity. Similarly, when $\partial p/\partial z \neq 0$, the wall is a source of streamwise vorticity. Thus when the transitional and the turbulent flows have three-dimensional disturbances, they both produce ω_x and ω_z vorticity at the wall. In both flows, the vorticity in the near-wall region is diffused away from the wall by viscosity. The length scale associated with diffusion in both flows is ℓ_ν and the velocity scale is u_τ. Although these scales were introduced earlier for the turbulent case, they can be utilized in the transitional case which provides the basis of the similarity. For a Blasius boundary layer, the boundary layer solution yields

$$\frac{u_\tau}{U_\infty} = 0.58 Re_x^{-1/4} \tag{6}$$

Thus the viscous scale, ℓ_ν, grows as $Re_x^{1/4}$ and $\delta^+ \approx 3Re_x^{1/4}$ in the Blasius layer. For a flat plate boundary layer in a zero pressure gradient, transition occurs at approximately $Re_x = 10^6$, which implies that $\delta^+ \approx 90$. Correspondingly, on a curved plate where the transition is dominated by a Görtler instability, transition occurs at a Görtler number of Gö ≈ 7 which has a corresponding δ^+ of 70.

There has been evidence of streamwise vortices for many years in several types of transitional boundary layers. These vortices usually have diameters of the order of the boundary layer thickness and are related to an instability. The best documented case is the Görtler boundary layer where counter-rotating vortices are a first order result of the initial instability. Klebanoff, et al. (1962) also documented the existence of counter-rotating streamwise vortices in a transitional Blasius boundary layer in zero pressure gradient. These vortices appeared as a secondary instability following the growth of the Tollmien-Schlichting instability. In addition, co- and counter-rotating streamwise vortices have been predicted and observed in swept wing instabilities.

In the past, the vortices observed in transitional flows have not been compared with the turbulent case because they did not appear to have the same length scales as sketched in Fig. 10. The usual argument was that in the transitional case, the vortices filled the boundary layer so the ratio of spanwise wavelength to boundary layer thickness, λ_z/δ, was approximately unity whereas the same ratio in the turbulent case was much smaller than

unity. However, if the viscous scales are used for the comparison, the *spanwise length scales are comparable.* That is, it has been well documented in the turbulent case that the average spacing between the low-speed streaks is $\lambda_z^+ \approx 100$. In transitional boundary layers, the counter-rotating vortices usually fill the boundary layer and have diameter of approximately δ^+. Since the spanwise length scale includes two vortices, λ_z^+ in transitional boundary layers should be approximately 100–200.

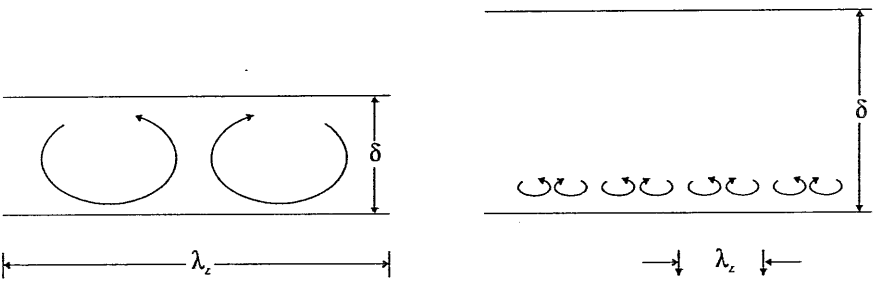

Fig. 10. Sketch of the counter-rotating streamwise vortices in the transitional (left) and the turbulent boundary layer (right).

Data for several cases of transitional boundary layers are shown in Table I. The transitional boundary layer spans a large range of Reynolds numbers and λ_z^+. The seven values at the end of the table are for flat plate transitional boundary layers which often generate streamwise vortices as a result of a secondary instability. Many of these investigations had spanwise irregularities placed on the flat plate to enforce a particular value of λ_z^+. This may explain why these λ_z^+ values seem large. The data from this table are plotted in Fig. 11. Except for the forced flat plate results, most of the data fall within the range of $20 < \lambda_z^+ < 200$ which is the same range of the low-speed streak data found in Fig. 4.

In experiments, the vorticity is much more difficult to measure than the velocity. Thus in transitional and turbulent boundary layers, the vorticity is often inferred from velocity measurements. On the flat plate, the streamwise vortices appear in phase with the Tollmien-Schlichting waves and are thus non-stationary. The T-S waves are roughly 7δ long which is several hundred ℓ_ν in this flow. Klebanoff et al. (1962) phase averaged the spanwise velocity at several times during the cycle of the T-S wave and found a structure consistent with streamwise vortices. They found that during the passage of each wave, the spanwise velocity would increase and decrease during each wave. Correspondingly, the ω_x vortex would grow, reach a maximum and

Table I

Reference	Re_x	Gö	δ^+	λ_z^+
Bippes (1972)	33,000	6.3	37	39
Bippes (1972)	54,000	6.8	39	46
Aihara (1979)	72,000	6.5	47	103
Aihara & Sonoda (1981)	80,000	5.9	40	70
Ito (1980)	100,000	7.4	51	81
Bippes (1972)	130,000	7.2	49	82
Tani & Sakagami (1962)	233,000	4.9	64	220
Wortmann (1969)	250,000	4.0	56	110
Swearingen & Blackwelder (1988)	330,000	7.5	69	200
Tani & Aihara (1969)	420,000	6.8	68	211
Tani (1962)	600,000	4.6	82	296
Anders & Blackwelder (1979)	210,000		62	287
Hama & Nutant (1963)	220,000		54	280
Wortmann (1979)	370,000		77	610
Saric et al. (1981)	490,000		70	335
Kovasznay et al. (1962)	660,000		83	660
Saric et al. (1981)	850,000		87	365
Klebanoff et al. (1962)	1,200,000		95	460

Table 1. The spanwise wavelength for Görtler and transitional boundary layers for various Reynolds numbers and Görtler numbers.

decay to approximately zero. Their data are plotted in Fig. 12a along with the reference T-S wave. The data are scaled with the viscous parameters. The primary T-S wave was obtained at $y^+ = 10$ and is plotted at the top of the figure with the reference time chosen at the midpoint of the acceleration. The data were obtained at the spanwise location where the maximum amplitude of w occurred. The individual $w(y^+)/u_\tau$ profiles are plotted at several values of the time delay. At $\tau^+ = -17$, they found the initial profile began and it increased in strength up to $\tau^+ \approx -5$. Thereafter it decayed as shown. The beginning of the following cycle can be see at $\tau^+ \approx +11$. By moving one half wavelength in the spanwise direction, similar profile were seen with the opposite sign. They noted that the $w(y)$ profile at $\tau^+ = -5$ is consistent with a streamwise vortex having its center at roughly $y^+ = 17$.

The similarity between the transitional and the turbulent case is seen by observing the comparable profiles in a turbulent channel flow obtained from the data of Blackwelder and Eckelmann (1979) shown in Fig. 12b. Since the

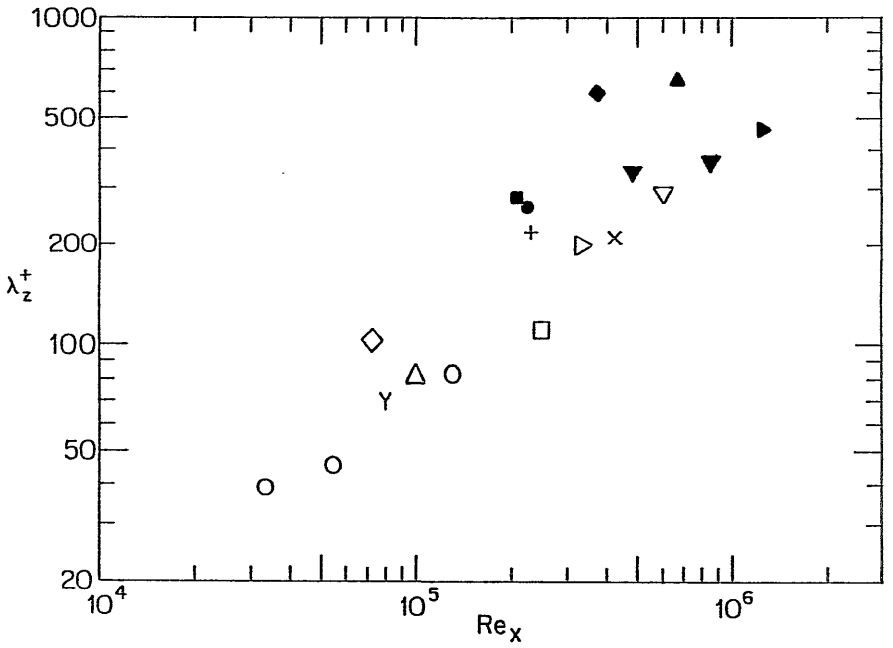

Fig. 11. The spanwise length scale in transitional boundary layers versus the Reynolds number. The data are from Table I.

flow was turbulent, the structure appeared randomly in space and time so the VITA technique was used to detect the bursting events. Upon detection at $y^+ = 15$, the spanwise velocity obtained from hot-film sensors was sampled at the indicated distances from the wall at $\Delta z^+ = 17$ to the side of the detection probe. These data were ensemble averaged over about 300 events to obtain $< w(y^+)/u_\tau >$. τ^+ is the time delay with respect to the point of the detection. At $\tau^+ = -20$, the beginning of the spanwise velocity structure is seen which builds up to a maximum amplitude at $\tau^+ = -5$ directly before the point of detection. Thereafter a gradual decay in the w velocity component occurs until there no structure is observed beyond $\tau^+ = 15$. These results are quite remarkable when it is considered that the associated streamwise vortices are of random size and shape. Similar results with the opposite sign were obtained at $\Delta z^+ = -17$ indicating that the flow is statistically symmetrical. That is, similar streamwise vortices of both signs must occur in the flow field but at random times. Guezennec et al. (1989) pointed out that in the turbulent flow the vortices do not occur in pairs of equal magnitude. Hence this aspect differs from the transitional flow in Fig. 12a. But otherwise, the sequence of the growth and decay of the spanwise velocity profiles associated with the streamwise vortices is similar in the bounded transitional and turbulent flows.

The spanwise velocity profiles from the flat plate transitional boundary layer(i.e. the profile at $\tau^+ = -5$ in Fig. 12a) and the turbulent channel flow (i.e. the $\tau^+ = -5$ profile in Fig. 12b) are compared with one from a transitional Görtler boundary layer in Fig. 13. The profile from the Görtler case was obtained from Bippes (1972). The Görtler flow is the only one of the three flows which is stationary allowing the profile to be obtained by regular time averaging techniques. Since the profiles in the transitional case are continuing to grow in the downstream direction, no standard normalizing velocity exists. Thus, to compare the three profiles in Fig. 13, they were normalized with their maximum values, w_{max}. The distance from the wall is normalized with the viscous scale, ℓ_ν, in all three cases. When compared in this manner, all three profiles are quite similar. In particular, this result supports the argument that the viscous scaling is the proper scale for these flows. A further result from the figure is that the vortices have a diameter of roughly $50\ell_\nu$.

Another similarity between the transitional boundary layers and the turbulent boundary layer is the presence of inflectional profiles of the mean velocity. In the transitional case, the profiles are stationary and easier to study than in the turbulent case. In addition, the lack of the background turbulence often makes it easier to follow the ensuing instability in the transitional boundary layer. Several authors have examined the inflectional profiles in transitional boundary layers and their profiles are shown in Fig. 14. Nishioka et al. (1979) have also measured similar inflectional profiles in a transitional Poiseuille flow (not shown). The profiles are all plotted with the viscous scales. In the transitional cases, the profiles are usually observed over a longer period of time possibly because there is less background disturbance to seed and thus trigger the ensuing instability. In addition, since the values of u_τ/U_∞ are smaller in transitional boundary layers, the profiles are seen to extend to larger values of u^+. One interesting aspect of the two transitional profiles is that the maximum shear exhibited is approximately the same and has a value slightly greater than u_τ/ℓ_ν. Kovasznay et al. (1962) were this first to note that this maximum could exceed the mean shear value at the wall. In the transitional boundary layer, the location of the maximum value of the shear moves away from the wall as the layer develops. The conditionally averaged value in the turbulent boundary layer has a much smaller value of shear; however that is due to the fact that the location of the maximum is a random variable as seen in Fig. 7. Thus the profiles become smeared in the averaging process. When individual profiles are examined, as the two shown in Fig. 14, it is seen that they also have a maximum shear of approximately u_τ/ℓ_ν. It is also interesting to note that the thickness of the shear layer is approximately the same in all three flow fields; i.e. $\Delta^+ \approx 10$–12.

As in the turbulent case discussed earlier, the inflectional profiles observed in transitional flows are usually followed by a growing oscillation and breakdown. Several authors have used the results from two-dimensional shear lay-

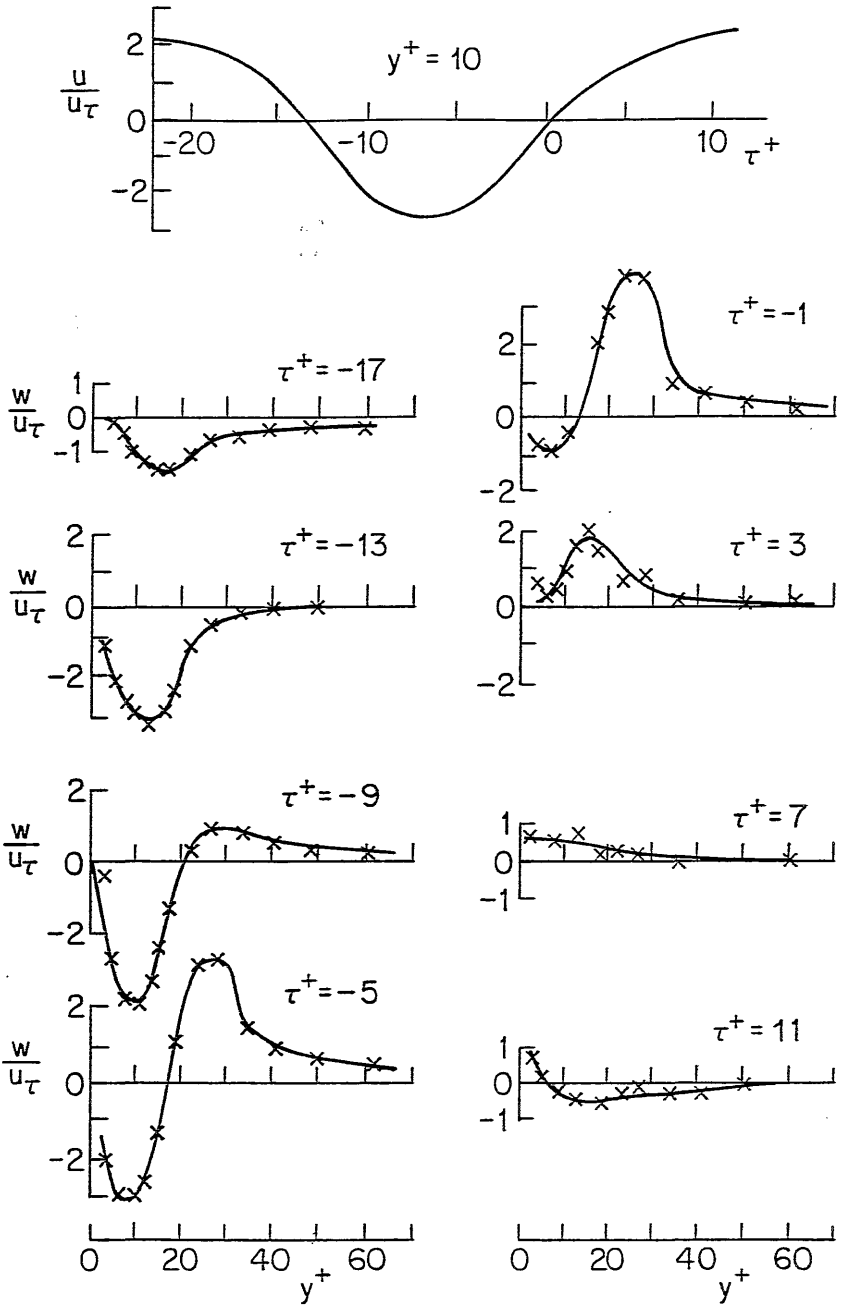

Fig. 12. (a) The spanwise velocity component conditionally averaged with respect to the Tollmien-Schlichting waves from Klebanoff et al. (1962). The T-S wave is shown at the top and the spanwise velocity profiles at several values of the time delay, τ^+, are plotted below.

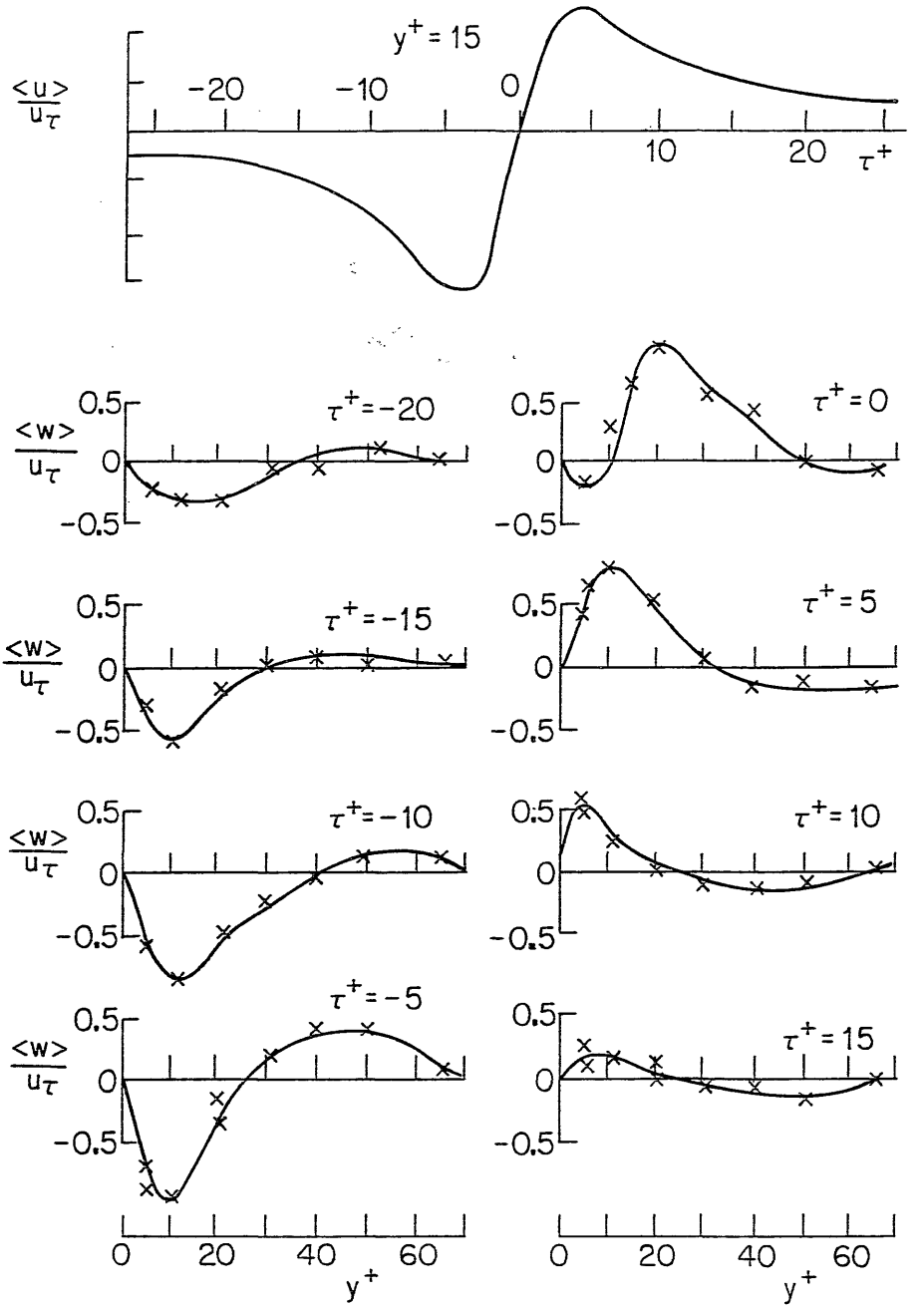

Fig. 12. (b) The spanwise velocity component conditionally averaged with respect to the VITA detection in a turbulent channel flow. The data are indicated by 'x' at the corresponding y^+ values. Data were taken at $\Delta z^+ = 17$ from the detection probe and at the indicated time delay, τ^+. The detection was at $y^+ = 15$ which produced the conditional average of the streamwise velocity shown at the top.

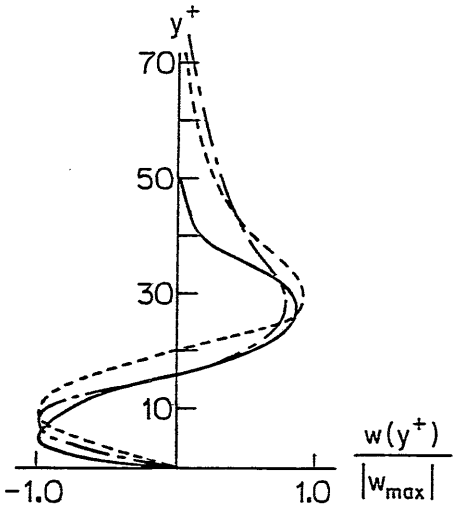

Fig. 13. Comparison of the spanwise velocity profiles associated with the streamwise vorticity in transitional and turbulent boundary layers. The data are from: a Görtler instability (Bipps, 1972), ——; a transitional boundary layer (Fig. 12a), – – – –; and a turbulent channel flow (Fig. 12b), – – – – – –

ers to explain the oscillations in the transitional boundary layer. Greenspan and Benny (1963) added an unsteady component to the mean velocity in a flat plate transitional boundary layer and found a secondary instability with wavelengths and frequencies similar to those measured by Klebanoff et al. (1962). Swearingen and Blackwelder (1987) have used similar arguments for the Görtler case. In both cases, the authors have shown that the wavelength was about 12–15 times the length scale of the inflectional profile. Fig. 15 shows that the wavelength observed during breakdown of the inflectional flow instability in the transitional and turbulent flow fields are similar when compared using viscous length scales. The data were obtained from 10 different authors listed in Table II. The streamwise wavelength of the instability, λ_x^+, is seen to be roughly between 100 and $200\ell_\nu$ for both the transitional and turbulent cases. This value agrees with the results of Michalke (1965) quoted earlier.

Of course, there are some differences between transitional and turbulent boundary layers. The most obvious is that the turbulent flow has two distinct regions; namely the near-wall region and the outer region or core region in pipe and channel flows. Associated with the outer region is an additional set of eddies often termed the large scale outer eddies. They promote mixing in the outer region and control the entrainment in turbulent boundary layers. The turbulent boundary layers grow as $x^{0.8}$ via turbulent diffusion in the outer region whereas transitional boundary layers grow by laminar diffusion as $x^{0.5}$. The additional set of eddies in the turbulent flow provides an additional

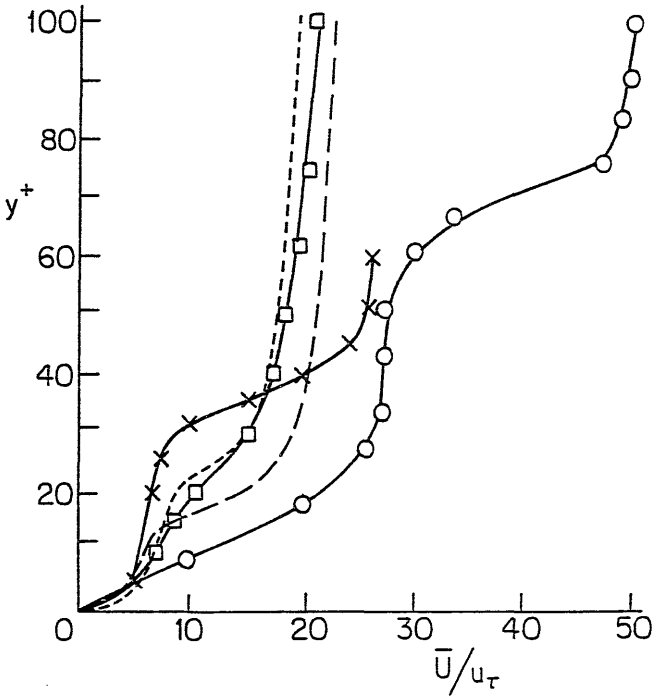

Fig. 14. Inflectional velocity profiles from transitional and turbulent boundary layers. The maximum shear in all three cases is approximately u_τ/ℓ_ν. The data are from: a concave wall (Aihara and Sonoda, 1981), ×; a transitional flat plate (Kovasznay, Komoda and Vasudeva, 1962), ○; a conditional average in a turbulent boundary layer (Blackwelder and Kaplan, 1976), □; and two instantaneous turbulent boundary layer profiles, ——— and - - - - -.

length scale; i.e. in addition to the viscous scales that dominate the inner region, there is a larger scale that describes the large eddy structures in the outer region. The existence of the large eddies in the outer region always promotes large disturbances to the near-wall region. For this reason, there are always large amplitude disturbances to seed the instabilities in the wall region of bounded turbulent flows that do not exist in the transitional cases. This may explain the reason that the waves developing on the inflectional profiles are much more readily seen in the transitional cases than in the turbulent case.

3 Aspects of Control of Bounded Turbulent Flows

The large amount of evidence assembled over the past three decades suggests there may be some methods of manipulating these bounded shear flows to enhance the performance of engineering flow fields. Such efforts generally are

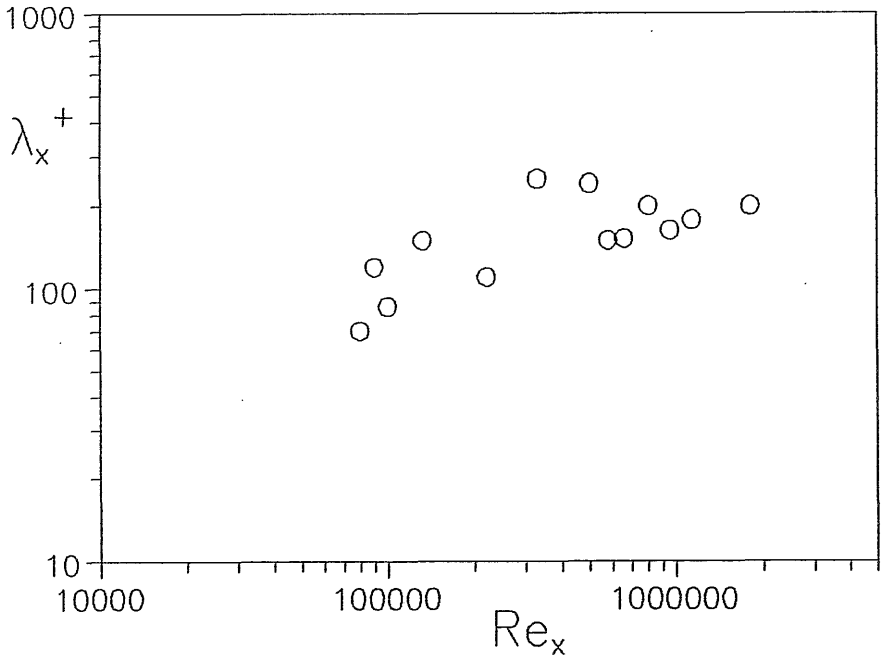

Fig. 15. The streamwise wavelength associated with the inflectional profiles and corresponding instabilities obtained in transitional and turbulent boundary layers.

considered to 'control' the shear flow in order to obtain a desired goal at a lower cost such as enhanced mixing, reduced drag, etc. Liepmann (1979) has stated that the most important aspect of the existence of deterministic eddies in turbulent flows is the possibility of turbulence control. For the particular case of drag reduction, efforts in the first half of this century were primarily aimed at streamlining to reduce drag due to separation and later smoothing the surface to reduce the roughness drag. With the development of low turbulence wind tunnels and the experimental confirmation of T-S waves by Schubauer and Skramstad (1947), new efforts were undertaken to further reduce drag by attempting to maintain a laminar boundary layer at increased Reynolds numbers. The discovery by Toms (1949) at mid century that a small amount of long chain polymer added to a liquid flow could reduce the base drag of a turbulent flow up to 80% set the stage for further advances in drag reduction. Although the details of how the polymers actually reduce the drag are still not understood, it is realized that they alter the eddy structures in the near-wall region which thereby reduces the drag. This concept has opened the doors for other ideas of drag reduction that have been pursued intermittently with vigor during the last twenty years. These efforts have included Large Eddy Break-Up Devices, riblets, polymers, etc.

Table II

Reference	Re_x	Type	δ^+	λ_x^+
Aihara and Sonoda (1981)	80,000	G	40	70
Bippes (1972)	90,000	G	48	120
Ito (1980)	100,000	G	51	86
Bippes (1972)	132,000	G	55	150
Hama and Nutant (1963)	220,000	B	54	110
Swearingen and Blackwelder (1987)	330,000	G	69	250
Kline et al. (1967)	500,000	T	210-480	240
Klebanoff et al. (1962)	580,000	B	83	150
Kovasznay et al. (1962)	660,000	B	83	152
Emmerling (1973)	800,000	T	820	200
Klebanoff et al. (1962)	950,000	B	90	163
Klebanoff et al. (1962)	1,130,000	B	98	178
Blackwelder and Kaplan (1976)	1,800,000	T	930	200

Table 2. Data at various Reynolds numbers for the breakdown wavelength, λ_x^+, for various δ^+. The boundary layer types are: G-Görtler, B-transitional Blasius and T-turbulent.

There are many other reasons why one would like to be able to control the turbulence in bounded shear flows. The augmentation of heat transfer has been pursued for years in heat exchangers, etc. Similar enhancement has been investigated for mass transfer. Other control applications include the reduction of noise from a flow, separation control, reduced pressure fluctuations, etc. Many techniques are available, but most of them also increase the power required through increased pressure loss, etc. These complicated problems not only require control of the turbulent eddies, but may also involve altered boundary conditions, initial conditions, etc. Since drag reduction has been the focus of much effort in the past and displays considerable promise in engineering applications, the following will focus on this aspect of control in bounded shear flows. Other aspects of control in bounded shear flows follow similar reasoning as presented below. Control of free-shear layers are discussed in the other chapters in this book.

The use of a model for the near-wall region would be of great help in the study of control of the eddies in this region. However the complexity of the dynamics of the region essentially preclude such models, although Lumley (1996) reports some progress using a truncated model. Not only is the turbulence four-dimensional(three spatial coordinates plus time) but it is random as well. Although some Reynolds averaged equations can well

predict the mean flow around a streamlined body, their turbulence models are usually not sufficiently detailed to describe the effects of perturbations on the eddy structure within the near-wall region. Consequently these models do not perform well when applied to the prediction of incipient separation, the addition of polymers, selective suction, etc.

It should be emphasized that control of the turbulent shear flows differs from attempting to maintain a laminar flow over as much of the flow field as possible. These two goals are quite different in nature and application of the same technique in laminar and turbulent flows may have grossly different effects on the flow. For example, suction under a laminar boundary layer can alter the base flow and change the stability characteristics of the boundary layer. This will delay the transition to turbulence and thus lower the overall drag on a body. However suction applied globally under a turbulent boundary layer will increase the drag unless massive suction is used to remove the entire boundary layer. This is demonstrated by examination of the von Kármán relation

$$\frac{c_f}{2} = \frac{d\theta}{dx} - \frac{v_{wall}}{U_\infty} \tag{7}$$

which is valid in both laminar and turbulent boundary layers with zero pressure gradient. For small values of suction, $d\theta/dx$ changes only slightly. Thus a uniform suction($v_{wall} < 0$ everywhere) will increase the skin friction, c_f. However in the laminar case, small amounts of suction (i.e. $-v_{wall}/U_\infty \approx 10^{-5}$) alters the streamwise velocity profile in such a manner that the location of the critical instability is moved far downstream and a reduction in the growth of the incipient Tollmien-Schlichting waves occurs. Consequently the flow transitions to turbulence at a much greater distance downstream. In this case, the larger values of c_f due to the turbulence are delayed and the integrated drag on the body is decreased. The primary effect of the suction in this case is to delay the onset of the T-S waves and decrease their growth.

However T-S waves have no dynamical significance in turbulent boundary layers and suction has a completely different effect; namely it increases the velocity gradient at the wall and thus increases the skin friction. Consequently techniques that delay transition will not necessarily be successful in fully developed turbulent flows. For this reason, drag reduction methods in turbulent shear flows often concentrate upon controlling the eddy structures within such flows.

The control of transition in bounded shear flows can and does lend a lot of information and ideas that are useful in turbulent shear flows. Since the base flow in transition is a laminar flow, it usually has a more concise and tractable mathematical description than its turbulent counter part. Many control scenarios are often attempted in a transitional setting first and then adapted to the more difficult turbulent case. One instance is the control of Tollmien-Schlichting waves in a transitional boundary layer. Liepmann et al. (1982) used surface-film heaters with a fast time response to introduce two-dimensional T-S waves into an unstable laminar boundary layer in a water

channel. As the waves grew downstream, a second set of heaters were used to increase and decrease the amplitude of the traveling waves by changing the phase of the second heater. This clearly showed that cancellation of T-S waves could be achieved under controlled conditions. Liepmann and Nosenchuck (1982) added a wall shear stress sensor to detect the passage of naturally occurring T-S waves. By using a feedback loop to drive the downstream heater, they were able to decrease the amplitude of the natural waves and increase the transition Reynolds number. These two-dimensional results in a controlled environment suggest that more complicated three-dimensional disturbances can possibly also be controlled as discussed by Fan et al. (1993) in a transitional boundary layer. Similar attempts have now progressed to fully developed turbulent flows as discussed below.

3.1 Global versus Selective Control

In the past, boundary layer control has been studied by applying some external condition globally; i.e. the condition is applied everywhere within the flow field without regard to how it effects the individual eddies in the flow. For example, to decrease the shedding behind a circular cylinder, suction can be selectively applied in the vicinity of the separation region on the cylinder. Applying suction globally around the entire cylinder may achieve the same result, but with a much greater expenditure of energy. The control of turbulent boundary layers may display similar results. Instead of applying a control mechanism globally, it could be applied only selectively; i.e. locally with respect to the eddy structure that one is attempting to control. For example, to alter the low-speed streaks, the external condition may need be applied only under or around the streaks. This implies that the controlling mechanism must have dimensions comparable to those of the streaks or other structures that they are attempting to control.

A second important criteria for control is the phase of the controlling parameter with respect to the eddy structure. Phase is used here in its traditional sense in the temporal domain. (The spatial phase variability is taken care of by the selectivity parameter discussed above.) Just as suction would not necessarily need be applied everywhere around the cylinder example above, it also need not be applied continuously in time either. Short bursts of suction having a duty factor of 0.2 or less may be sufficient to control the shedding of vortices. Of course the suction would need to be applied at the appropriate phase of the shedding process to have the desired effect. If the phasing is incorrect, the vortex shedding process could be enhanced instead of suppressed. This aspect is extremely important in the control of turbulent production within the turbulent boundary layer because it is well known that the production is a very intermittent and random process. The frequency of occurrence of the bursting phenomenon yields a good estimate of the intermittency and duty factor of the control mechanism.

As additional information about the dynamics of the eddy structures has become available, ideas for utilizing that information has been developed. The concept of 'selective control' was proposed by Gad-el-Hak and Blackwelder (1987; 1989) to apply a control mechanism such as suction/blowing, heating/cooling, etc. on only selected aspects of the eddies. They proposed to interact with a particular feature of the eddies, such as an instability, to reduce or eliminate the turbulent mixing that would occur if no control action were taken. This effort obviously requires a deeper understanding of the dynamics of the eddy structure than a global control system would require. It also requires that the eddies location in space and time be known a priori so that the control can be applied. As mentioned above, the spatial and temporal scales of the controlling mechanism must be similar to the scale of the eddies; i.e. in the near-wall region, it must be on a viscous scale. These requirements suggests that selective control will involve some 'intelligence' about the flow that is not needed in global control systems. Blackwelder (1989) proposed the concept of a "smart wall" with embedded sensors, actuators and feedback as a means of controlling the eddy structures in the near-wall region. To date, few investigations have used temporal phasing and spatial selectivity to control the eddies in a turbulent boundary layer primarily because of the limited knowledge of the eddy structure and because of the practical problems that need to be surmounted. It is interesting to speculate that nature has accomplished some means of controlling and possibly reducing the drag in limited cases. Bechert et al. (1985) have proposed that the scales of fast sharks may offer a "streak cancellation mechanism" that inhibits the momentum exchange and thus decrease the turbulent shear stress. Close examination of fish scales reveal that their motion may be instrumental in the prevention of local separation and control of the boundary layer eddies. Birds may use feathers in an analogous manner to alter the eddies in their unsteady motion in flight.

3.2 Selective Suction

The application of selective control described by Gad-el-Hak and Blackwelder (1987; 1989) involve the use of suction at specified spanwise locations as illustrated in Fig. 16. If the location of the low-speed streaks could be determined a priori, they reasoned that one means of reducing the intensity and the magnitude of the shear at the spanwise inflection point would be to apply a small amount of suction under the streaks. This action would reduce the quantity of low-speed fluid in the streaks, thereby reducing the velocity difference between the low-speed streak and the nearby high-speed region, $\Delta u(z)$. If the ejection of the streak from the wall region and the subsequent mixing were due to the inflectional instability described earlier, then these phases of the BP should also be reduced or delayed. To avoid accumulation of the low-speed fluid, they proposed that it be re-injected into the flow under the high-speed regions. This would possibly further reduce the velocity difference,

$\Delta u(z)$, and also reduce the velocity gradient at the wall. Thus the suction would reduce the mixing and the blowing would help reduce the local skin friction so that both actions would reduce the drag. In addition, since the suction/blowing is only applied selectively, the amount of pumping power should be greatly reduced from that which would be required for a global application. Preliminary testing by Gad-el-Hak and Blackwelder (1987) were conducted by artificially generating streaks and the results were promising.

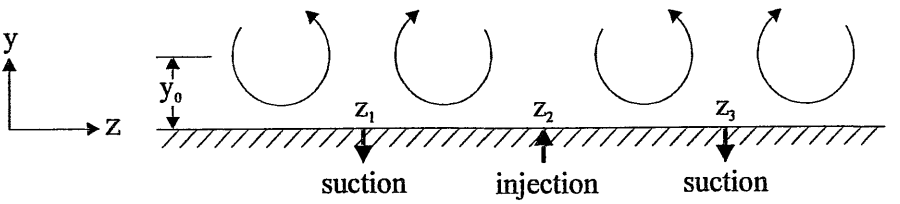

Fig. 16. Selective suction as proposed by Gad-el-Hak and Blackwelder (1987). The suction/blowing is actively programmed to be applied selectively in space and time to interact with specific eddy structures.

Myose and Blackwelder (1994) tested this concept in a model flow field consisting of a laminar boundary layer embedded with Görtler streamwise vortices. This flow modeled the flow in the near-wall region and was used as a test bed for control scenarios. They applied the suction selectively under the low-speed regions between the vortices as sketched in Fig. 16 and studied the resulting flow downstream. As the amount of suction increased from zero, the breakdown of the low-speed region moved downstream until an optimum amount of suction was applied. Increasing the amount of suction further, caused the breakdown to move back upstream. Smoke wire visualization showed that the breakdown of the low-speed regions could be delayed up to $20\delta^*$ downstream. Velocity profiles taken by hot-wire anemometers indicated that as the suction increased, the inflectional profile in the normal direction, $U(y)$, disappeared. In the spanwise direction, the suction has less effect on the inflectional profile and large amounts of suction added an additional inflection point into the $U(z)$ profile. The optimum amount of suction was more than one order of magnitude smaller than the asymptotic value of suction required to maintain a stable laminar boundary layer. They suggested that the ultimate breakdown further downstream was due to the inflectional spanwise profile. Thus although the suction was able to eliminate the normal inflectional profile and the associated instability, the spanwise profile remained and became unstable, albeit further downstream.

Selective suction has been demonstrated in direct numerical simulations by Choi et al. (1994). They used a two-dimensional channel simulation with $Re_\theta = 150$ and applied suction and blowing at the wall in a non-uniform

manner. Their wall condition was that the normal velocity at the wall was given by $v_{wall} = -v(y_d)$ where y_d was the location of a detection plane. This action would tend to counter the ejections and the higher speed sweeps. Since the amount of suction and blowing were equal, there was no net mass flow. They found a maximum of 25% drag reduction when $y_d^+ = 15$. At this value the thickness of the sublayer increased and the fluctuations of the velocity, pressure and vorticity decreased everywhere. They also observed that the spacing of the low-speed streaks increased suggesting that the scales increased along with the drag reduction. As y_d^+ increased above 20, they also observed that the drag began to increase rapidly.

A more interesting aspect of the investigation by Choi et al. (1994) was the use of a selective spanwise velocity perturbation at the wall in the same flow field. They reasoned that a spanwise disturbance at the wall would hinder the action of streamwise vortices in the wall region. Hence they numerically imposed the boundary condition $w_{wall} = -w(y_d)$ everywhere on the wall where y_d is the detection distance above the wall. With $y_d^+ = 10$, a drag reduction of 30% was obtained; i.e. the drag reduction was larger than when the normal velocity was used as a perturbation. This result is shown in Fig. 17 which illustrates the pressure gradient in the channel after the control disturbance at the wall was turned on. It is apparent that there is reduced drag for $y_d^+ < 25$ and the optimum is near $y_d^+ = 10$. The velocity, pressure and vorticity fluctuations decreased everywhere and the spacing of the low-speed streaks increased. When the authors applied a combination of the normal and a spanwise control, relaminarization occurred which may have been a result of the low Reynolds number of the simulation. Irrespective, the larger reduction for the spanwise velocity disturbance strongly suggests that the phase of the control disturbance is quite important and may be more important than the amplitude of the disturbance.

3.3 Spanwise Wall Disturbances

It has been noted for years that some turbulent boundary layers with a three dimensional mean flow appear to have a reduced level of Reynolds stress and turbulent production. This has been observed in pressure driven flows such as on swept wings by Bradshaw and Terrell (1969) and in shear driven flows such as on rotating cylinders aligned in the streamwise direction by Bissonnette and Mellor (1974). This has instigated several studies that have imposed controlled three dimensional disturbances into a nominally two dimensional mean flow with the idea of suppressing the turbulence and drag.

To add three dimensionality to the mean flow, Moin et al. (1990) performed a direct numerical simulation of this phenomenon by utilizing a suddenly imposed spanwise pressure gradient on a 2D fully developed turbulent channel flow with a Reynolds number of $\delta^+ = 180$. As in the other investigations, there was a decrease in the Reynolds shear stress and the turbulent

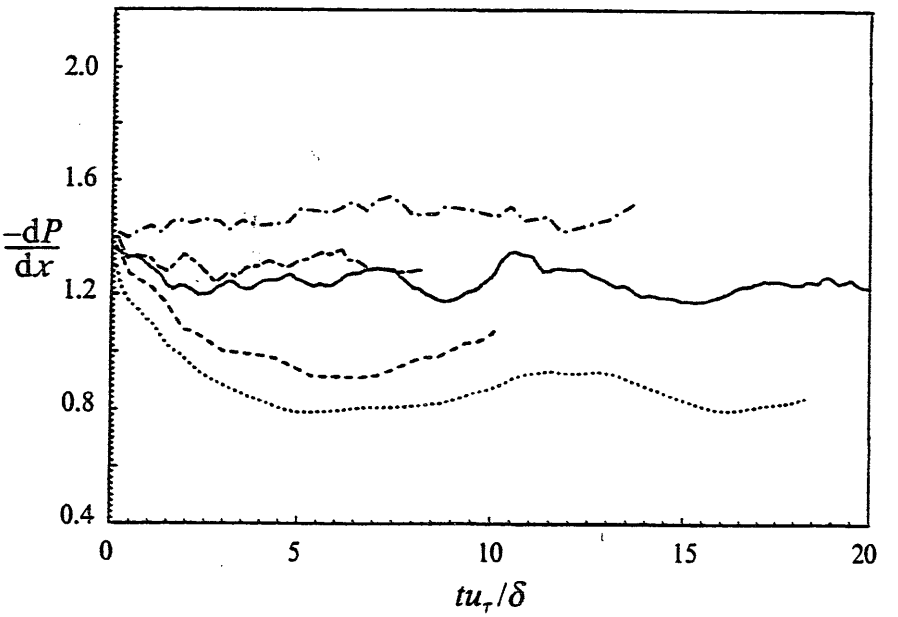

Fig. 17. Time history of the pressure gradient required to maintain constant mass flow while utilizing selective boundary conditions on the spanwise velocity (from Choi et al. (1994)) —, unmanipulated channel; – – – –, manipulated channel with sensors at $y_d^+ \approx 5$; · · · · ·, $y_d^+ \approx 10$; – – – – – – – $y_d^+ \approx 20$; – · – · – · $y_d^+ \approx 26$.

kinetic energy. Sendstad and Moin (1991) reported that the probability density functions showed that lower u' fluctuation levels occurred primarily due to a reduction of the intensely negative u' values. Moin et al. (1990) noted that in theirs and other similar investigations, there is an observed difference between the alignment of the Reynolds shear stress vector and the mean velocity gradient vector. Moin et al. also computed the terms in the Reynolds stress transport equations and determined that the turbulent production was decreased and the turbulent dissipation increased, however no drag measurements were reported.

Instead of the steady flow of Moin et al., Jung et al. (1992) imposed an oscillating spanwise cross flow in a numerically simulated channel flow. Their Reynolds number was $\delta^+ = 200$ and the imposed flow had an amplitude of $0.8U_{avg.}$. The period of oscillation, $f = \omega/2\pi$, was in the range of $0.002 < f^+ < 0.04$. They found they could reduce the drag up to 40% when the oscillation frequency was $f^+ = 0.01$. Low-frequency oscillations, $f^+ < 0.005$, tended to increase the drag. The large amplitude oscillations appeared to destroy the vorticity structure and the low-speed streaks. In addition, it decreased all three fluctuating velocity components. For the case

of $f^+ = 0.01$, they used the mean two dimensional channel flow and oscillated one of the walls with an amplitude of $0.8U_{avg}$. This disturbance produced a 40% drag reduction similar to the pressure driven flow.

In an experimental verification of this phenomenon, Laadhari et al. (1994) oscillated a section of a wall under a fully developed turbulent boundary layer with $Re_\theta = 950$. They oscillated the plate with an amplitude of $\Delta z^+ = 160$ and frequencies of $0.0033 \leq f^+ \leq 0.017$ which allowed velocity oscillations with amplitudes of $3.3 < w_{wall}/u_\tau < 16$. Although the drag could not be measured, they found that the mean streamwise velocity was reduced for $y^+ < 30$ along with a reduction of $\partial U/\partial y$ in the region $y^+ < 8$. The turbulent fluctuations were reduced throughout the near-wall region with the largest reduction occurring in u' and $\overline{uv}$.

More recently, Trujillo, et al. (1997) investigated a spanwise oscillating wall under a boundary layer in a water channel with $Re_\theta = 1500$. They tested three amplitudes of $\Delta z^+ = 120, 240$ and 360 over frequencies of $0.003 \leq f^+ \leq 0.018$. The drag was inferred from the measured turbulence shear stress profile and from measurements of the local wall mean shear. The amount of drag reduction increased as the frequency and the amplitude increased. The authors were able to measure a maximum drag reduction of 25% over their parameter range and speculated that larger values may be found. Their probability density function of the streamwise velocity showed that the decreased mean velocity near the wall was due to a decrease in the high-velocity fluctuations in the near-wall region. This observation differs with Sendstad and Moin (1991) possibly because Trujillo et al. worked with an oscillating wall instead of a pressure driven disturbance. The decreased probability of finding high-speed fluid near the wall suggests that the spanwise oscillations prohibited the influx of the higher speed fluid toward the wall and provided longer periods of time when the streamwise velocity remained at a lower velocity. They further found that the spanwise oscillations inhibited the strong ejections and sweeps so that the intermittently large values of $\overline{uv}$ did not occur as often. The lower amplitude sweeps and ejections were not significantly altered.

Note that none of the spanwise disturbances utilized selective control since the disturbances were implemented over the entire flow field. In addition, there was no concern for the amount of energy added with the disturbance which is important in engineering applications. However these and other studies have shown that the structures in the near-wall region can be significantly altered by three-dimensional changes in the mean flow and that lower drag states can be obtained. The imposition of a spanwise velocity, $w(y)$, evidently alters the equilibrium between the low-speed streaks and the nominally two-dimensional flow in a manner that is still unknown. These studies also point out that there are differences between the pressure driven and the shear driven methods of imposing the three dimensionality. Consequently, there may be differences in the manner that the pressure and shear driven flows alter the eddy structure in the near-wall region.

3.4 Actuators in the Wall Region

Several attempts have been made to use active actuators to control the turbulence in the near-wall region. Most of these techniques have employed a flush mounted actuator or other actuators near the wall to alter the flow parameters and/or the boundary conditions. Many different approaches to the problem have been attempted. Some investigations have developed a known eddy structure upstream and then attempted to manipulate it as it develops downstream. This simplification reduces the temporal and spatial randomness of the eddies and makes the control easier. On the other hand, direct numerical simulations compute a complete solution of the flow field and can simulate possible interactions with the flow at every point in the flow.

Most studies with actuators have attempted to interact and alter particular aspects of the eddy structure in the wall region. Consequently one of the more important questions that need to be addressed in any control scenario is "Which eddy structures or elements thereof does one want to control?" The earlier discussion on the eddies in the near-wall region has shown that several structures may be amenable to control. For example, one might focus on the low-speed streaks since they are the most ubiquitous structures in the wall region. But if the goal is to reduce the drag, the streaks may not be a good candidate because their low speed indicates that they will have a smaller gradient at the wall and hence less skin friction than the nearby higher speed regions. On the other hand, if the goal is to increase mixing, the breakup of the low-speed regions may be desirable. Similar arguments can be made about injecting vorticity or altering the vortex structures and/or interactions with other regions. Alternatively, one would like to be able to identify a rapidly developing instability mechanism and then increase or decrease its natural growth since a smaller expenditure of external energy would presumably be required. The inflectional instabilities discussed earlier are likely candidates for this method and changes in their growth rates will decease their breakdown and mixing.

Another decision that must be made is to determine the desired response of the actuator. This will depend upon whether the operator desires to control the turbulent eddies or to control the flow; i.e. a microscopic or macroscopic control. The type of actuator needs to be considered and whether it is to be passive or active. Cost will play a major role in any of these decisions. Passive actuators may have a non-zero initial cost but very little operating costs. On the other hand, active actuators may be expensive to install and operate but may be more effective. If active actuators are to be used, sensors must also be employed to detect the state of the fluid or eddies. This necessitates the addition of algorithms to process the data and determine the actuator response to the flow conditions. The algorithms may involve a feed back system, a feed forward algorithm, an artificial neural network, etc. Since the

use of actuators to control turbulent flows is still in its infancy, the work to date has generally chosen a subset of the problem and explored a limited domain of response. Some of these investigations are mentioned below.

One of the first to use an active actuator to control eddies in the near-wall region was Jacobson and Reynolds (1995). They utilized a small cavity below the wall with a flush mounted cantilevered actuator mounted over the cavity as shown on Fig. 18. The actuator was driven by an amplitude modulated signal supplied to a piezo-ceramic unimorph mounted on the under side of the actuator. This provided a means to control the amplitude of the actuator with a fast time response using low power. Since the cavity was closed, there was no net mass addition. The cantilevered actuator was designed to be asymmetric with respect to the cavity which produced a diffuse influx of fluid into the cavity and a more concentrated and directed efflux. This resulted in a pair of ω_x counter-rotating vortices over the narrow side gap of the cantilever. The test flow field was a laminar boundary layer with superimposed streamwise vortices generated upon demand by small suction holes upstream. The vortices were sensed by shear stress sensors located upstream of the actuator. Various algorithms using the mean and fluctuating shear stress controlled the action of the actuators. Using neural networks, they were able to obtain a reduction of 8% in the average wall shear stress downstream of the actuators and a 30% reduction in the fluctuating shear stress.

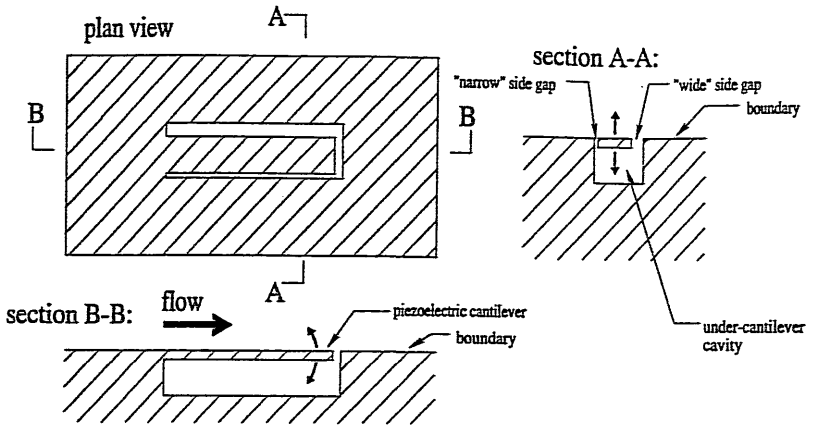

Fig. 18. Sketch of the flush mounted actuator used by Jacobson and Reynolds (1995). Note the asymmetry in the plan view that led to different flow patterns during influx and efflux.

Lorkowski et al. (1997) performed a similar experiment by using an elongated slit with dimensions $1.5\ell_\nu$ by $150\ell_\nu$ aligned in the streamwise direction. They forced it with a relatively high frequency ($f^+ = 0.1$) oscillations forcing the air out of a cavity below the slit in the form of a two dimensional jet. They speculated that this created a pair of counter-rotating streamwise vortices and measured the resulting changes in the flow structure. The peak in the $u'(y)$ distribution moved away from the wall indicating that ℓ_ν was slightly increased. However the authors did not effectively reduce the turbulence intensities and suggested that their geometry may not be optimum. Using more optimum conditions, Rathnasingham and Breuer (1997) found a 31% reduction in the streamwise velocity fluctuations and a 17% reduction in the pressure fluctuations.

Carlson and Lumley (1996) used a numerical laminar channel flow as a test bed to study the flow's response to a bump type actuator that was nominally stowed flush with the wall. The bump was a three-dimensional Gaussian hump that could be deployed upon demand to a height of approximately $10\ell_\nu$. They varied the symmetry of the bump in the plane parallel to the wall with the typical length scales in the plane being $15\ell_\nu$. When the bump was raised, up to three pairs of counter-rotating vortices appeared above the hump at different times. The Reynolds number and shape of the bump determined the pattern and strengths of the vortical structures. The speed of deployment (i.e. the acceleration of the hump's vertical motion) affected the intensification of the vortices and was a significant parameter in the flow patterns that formed.

In another direct numerical simulation, Mito and Kasagi (1997) allowed one wall of their two dimensional channel flow to oscillate with the wall displacement given by

$$y_w = a \cdot \sin\left(\frac{2\pi z}{s}\right) \cdot \sin(2\pi f t) \tag{8}$$

Thus the wall moved only in the normal direction and the disturbance was uniform in the streamwise direction. Two amplitudes of $a^+ = 2.5$ and 5.0 and two spanwise wavelengths of $s^+ = 45$ and 90 were computed for two frequencies of $f^+ = 0.01$ and 0.02. These disturbances did not produce any significant drag reduction. In fact, the larger amplitude perturbations slightly increased the skin coefficient.

Small flush mounted delta wings have been used as actuators by Blackwelder et al. (1998) to delay the breakdown of the low-speed regions between streamwise vortices in a boundary layer undergoing Görtler transition. This test flow developed large streamwise vortices in a steady state environment. The delta wing actuator was attached to a rectangular base and the base had a piezo-ceramic unimorph or bimorph on its surfaces. By applying a sinusoidal signal to the piezo-ceramic material, the delta wing would oscillate with amplitudes up to $12\ell_\nu$. The best results were obtained with the delta wing pointed downstream as shown in Fig. 19. Visualization of the actuator in a water channel showed that the oscillations of the delta wing produced

a streaming flow from under the wing that coagulated into two low-speed streaks downstream. The amount of displaced fluid depended upon the oscillation frequency which was typically $0.01 < f^+ < 0.15$. The actuator was positioned so that it produced the low-speed regions in the location of the naturally occurring high-speed region between the Görtler vortices. The net result was a more uniform velocity field downstream shown by the isovelocity contours in Fig. 20. The mean and fluctuating wall shear stresses were reduced. In addition, the spanwise shear, $\partial U/\partial z$, was weaker downstream which delayed the breakdown of the low-speed streaks by $20\delta^*$. At that point the breakdown appeared to be due more to the inflectional profile in the normal direction rather than the spanwise inflectional profile.

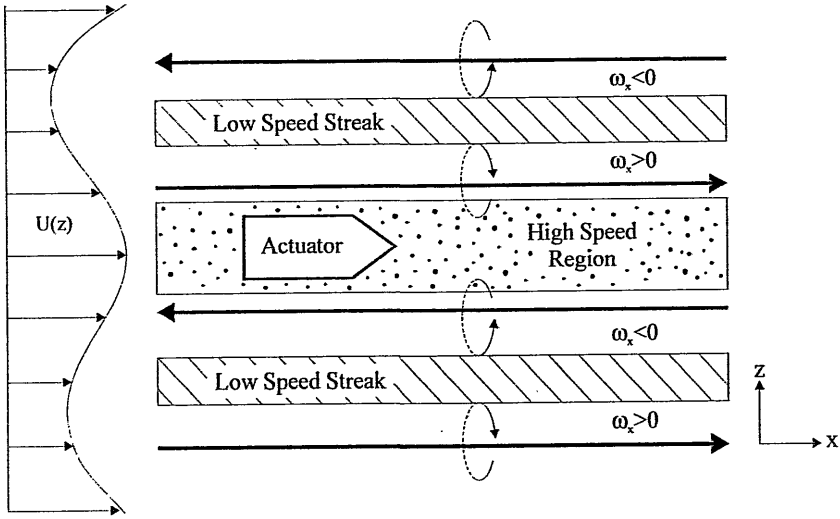

Fig. 19. Sketch of the delta wing actuator used by Blackwelder et al. (1987). Its orientation pumped low-speed fluid into the existing high-speed region.

As the Reynolds number increases in these flow fields, the viscous scales become smaller compared to the outer flow necessitating smaller actuators. This has helped spawn the field of microelectromechanical systems (MEMS) which has successfully produced small sensors and actuators. Tung et al. (1995) have measured the velocity field behind a scaled up version of such an actuator similar to the delta wing actuators discussed above. Ho and Tai (1996) have reviewed the recent developments in the use of MEMS technology for flow control and discuss future trends in utilizing these devices for drag reduction. Small sensors that can be flush mounted or embedded in the wall have been manufactured using MEMS technology. They have been successfully used to measure the shear stress on the wall at large Reynolds numbers by Hites et al. (1997).

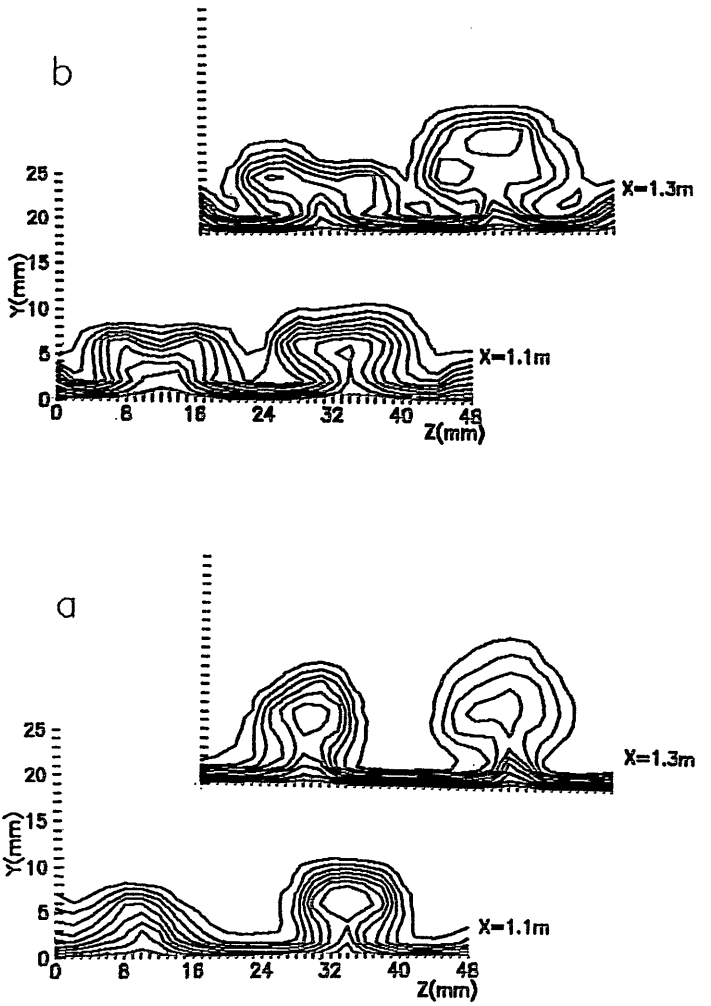

Fig. 20. Iso-velocity contours of the streamwise velocity downstream of the actuator. The base flow with no oscillation is shown in a (below) and the results with the actuator operating are found in (b) above. The actuator was located at 40cm from the leading edge of the curved plate and the data shown were taken at $x = 1.1$ and 1.3m downstream from the leading edge.

3.5 Control Algorithms

With the advent of MEMS technology, the possibility of combining computers and actuators for the control of turbulence is being considered. At present the marriage of sensors, actuators and computers to build a "smart wall" is still in its infancy, but the concept has progressed to the state that some applications may be on the horizon. The nonlinearity and multi-dimensionality of the problem will require considerable effort before solutions become practical.

Although it is relatively easy to consider how sensors can be employed to locate the eddies, it is more problematical to determine which actuators and hardware will be necessary to modify the eddies and the flow field. As difficult as these choices may be, an equally important problem is to determine and develop necessary software and algorithms for decision making and control. This may prove to be a more difficult hurdle than the hardware. These issues have been discussed in the literature and at symposiums, but no consensus has been reached upon the types of solutions required.

Artificial neural networks have proven useful in designing control software for the actuators. This technique is quite general and can be designed for linear or nonlinear systems with any number of inputs and outputs. The inputs are sensor signals obtained upstream. The signals are processed in a multi-layered feed-forward mode producing one or more output signals which are used to drive the actuators. Each node in the network has a weight that must be determined via an auxiliary technique. The weights may be specified by the operator using prior results and research. Alternatively, the system of weights can be 'learned' by a training algorithm so that they are assigned values to produce a desired result, such as a minimum drag as used by Lee et al. (1997). They used information obtained at the wall and were able to reduce the skin friction by 20% in a numerically simulated channel flow. With an additional system of sensors downstream of the actuators, the system of weights can be altered in real time to optimize the desired result. For example if the flow conditions changed in real time so that the drag was no longer minimized, the additional sensors could be used to train the weights for the new conditions. Kim (1997) and his co-workers have used neural networks in channel flows to control suction and blowing at the wall. They have suggested that the actuators are actually controlling the streamwise vortices in the near-wall region and that the neural networks must contain some nonlinearity.

Another method of deriving a control algorithm for the wall region assumes that the turbulence can be described using nonlinear dynamical systems theory. By using the proper orthogonal decomposition theory of Lumley (1967), the eigenfunctions corresponding to the most energetic eddies can be extracted from the correlations of the velocity components as shown by Aubrey et al. (1988) and others. A set of model equations is used to represent the dynamics of these eddies in the near-wall region. Aubrey et al. found that the system displays an intermittent character similar to the ejection events in the wall region and the average frequency of the events was linked by the pressure to the outer part of the turbulent boundary layer. Coller and Holmes (1997) have used similar equations and added a control signal to delay the ejection character. They were able to increase the average time between the ejections up 70% suggesting that less turbulent mixing would be achieved in such a system. Lumley (1996) discusses this method in more detail.

Another encompassing method for designing control software is to examine optimum control methods as discussed by Temam et al. (1997) and

others. They define a cost function which includes the cost of implementing the control variable, such as suction, plus the fluid flow quantity that is to be minimized, such as the average value of $\partial\overline{U}/\partial y\big|_w$ to reduce the drag. Abergel and Temam (1990) have shown that solutions can be found to this optimization problem which involves solving an adjoint equation for the velocity field and the control function. Bewley (1997) has implemented this method for a numerical channel flow with $Re_\tau = 100$, and found that the drag could be reduced to 42% of its original value, which is approximately the laminar value at this Reynolds number. Numerical constraints limited his results to computational times of only a couple thousand viscous time scales and the low Reynolds number. Both of these constraints should be relaxed as more efficient algorithms are developed. One means of extending the results is to attempt a sub-optimal control which places some limits on the extent of the variables in the problem, such as examining only the state of the flow on or near the wall.

4 Conclusions

A review of the near-wall eddy structure in bounded shear flows has shown that there are many important components in the bursting phenomenon including the streamwise vortices, low-speed streaks, inflectional velocity profiles, etc. The low-speed streaks are surrounded by two dimensional surfaces that are the loci of inflectional profiles. The streaks and inflectional surfaces have a long time scale compared to the instabilities that develop on the inflection profiles. Consequently the inflectional instability grows rapidly and break down into chaotic motion involving a lot of turbulent mixing. The extremely random nature of this phenomenon has made it difficult to study. However transitional bounded shear flows have a similar set of eddies and dynamics but with less randomness. A review of the transition process highlighted the similarities and differences between these two classes of flow fields. The inflectional velocity profiles appear to be a key element in the breakdown into turbulence in both the transitional flow and the bursting process. Lastly several investigators have attempted to control these eddies with promising results. Values of drag reduction exceeding 50% have been reported with several researchers finding 20-30% using suboptimal methods. However the full control of bounded turbulent flows must await the development of control algorithms that will sense the state of the turbulent flow, process this information and operate actuators to alter it in a beneficial sense.

Acknowledgments

This work was supported by the Office of Naval Research through Grants N00014-94-1-0590 and N00014-92-J-1062 monitored by Pat Purtell. ONR's continuing support through the years is greatly appreciated.

References

Abergel R., Temam R. (1990): On some control problems in fluid mechanics. *Theor. and Comp. Fluid Dynamics* **1**, 303.

Aihara Y. (1979): Görtler vortices in the nonlinear region. In *Theoretical and Experimental Mechanics*, eds. U. MåAller, K.G. Roesner & B. Schmidt, Springer, Berlin, 331.

Aihara Y., Sonada T. (1981): Effects of Pressure Gradient on the secondary instability of Görtler vortices. AIAA Paper No. 81-0197.

Anders J.B., Blackwelder R.F. (1979): Longitudinal vortices in a transitioning boundary layer. In *Laminar Turbulent Transition*, ed. R. Eppler and H. Fasel, Springer Verlag, Berlin, 110.

Aubrey N., Holmes P., Lumley J.L., Stone E. (1988): The dynamics of coherent structures in the wall region of a turbulent boundary layer. *J. Fluid Mech.* **192**, 115.

Bacher E.V., Smith C.R. (1986): Turbulent boundary layer by surface riblets. *AIAA J.* **24**, 1382.

Bechert D.W., Hoppe G., Reif W.-E. (1985): On the drag reduction of the shark skin. AIAA Paper No. 85-0546.

Bewley T. (1997): Optimal and robust control and estimation of transition and turbulence. Ph.D. Thesis, Mechanical Engineering, Stanford University.

Bippes H. (1972): Experimentelle Untersuchung des laminar-turbulenten Umschlags an einer parallel angeströmten konkaven Wand. *Heidel. Akad.*

Bissonnette L.R., Mellor G.L. (1974): Experiments on the behavior of an axisymmetric turbulent boundary layer with a sudden circumferential strain. *J. Fluid Mech.* **63**, 369.

Blackwelder R.F. (1989): Some ideas on the control of near-wall eddies. AIAA Paper No. 89-1009.

Blackwelder R.F., Eckelmann H. (1979): Streamwise vortices associated with the bursting phenomenon. *J. Fluid Mech.* **94**, 577.

Blackwelder R.F., Kaplan R.E. (1976): Wall structure of the turbulent boundary layer. *J. Fluid Mech.* **76**, 89.

Blackwelder R.F., Liu D., Jeon W.-P. (1998): Velocity perturbations produced by oscillating delta wing actuators in the wall region. *Experimental Thermal and Fluid Science*, to appear.

Bogar D.G., Tiederman W.G. (1986): Burst detection with single-point velocity measurements. *J. Fluid Mech.* **162**, 389.

Bradshaw P., Terrell M.C. (1969): The response of a turbulent boundary layer on an 'infinite' swept wing to the sudden removal of pressure gradient. NPL Aero Report No. 1305.

Chen C.-H. P., Blackwelder R.F. (1978): Large-scale motion in a turbulent boundary layer: a study using temperature contamination. *J. Fluid Mech.* **89**, 1.

Choi H., Moin P., Kim J. (1994): Active turbulence control for drag reduction in wall-bounded flows. *J. Fluid Mech.* **262**, 75.

Coller B.D., Holmes P. (1997): Suppression of bursting. *Automatica* **33**(1), 1.

Corino E.R., Brodkey R.S. (1969): A visual study of turbulent shear flow. *J. Fluid Mech.* **37**, 1.

Corrsin S. (1957): Some current problems in turbulent shear flows. *Symp. on Naval Hydrodyn*, Publ. No. 515, NAS-NRC, 373.

Emmerling R. (1973): Die Momentare Struktur des Wanddruckes einer Turbulenten Grenzschichtströmung. *Mitt. M.P.I. Strömungforschung*, Göttingen, No. 56.

Falco R.E. (1977): Coherent motions in the outer region of turbulent boundary layers. *Phys. Fluids* **20**, S124.

Falco R.E. (1979): Structural aspects of turbulence in boundary layer flows. *Sixth Biennial Symp. on Turbulence*, Rolla, 1-1.

Fan X., Hofmann L., Herbert T. (1993): Active flow control with neural networks. AIAA Paper No. 93-3273.

Gad-el-Hak M., Blackwelder R.F. (1987): A drag reduction method for turbulent boundary layers. AIAA Paper No. 87-0358.

Gad-el-Hak M., Blackwelder R.F. (1989): Selective suction for controlling bursting events in a boundary layer. *AIAA J.* **27**, 308.

Grass A.J. (1971): Structural features of turbulent flow over smooth and rough boundaries. *J. Fluid Mech.* **50**, 233.

Greenspan H.P., Benney, D.J. (1963): On shear-layer instability, breakdown and transition. *J. Fluid Mech.* **15**, 133.

Guezennec Y., Piomelli U., Kim J. (1989): On the shape and dynamics of wall structures in turbulent channel flow. *Phys. Fluids* **A1**, 764.

Hama F.H., Nutant J. (1963): Detailed flow field observations in the transition process in a thick boundary layer. *Proc. of the Heat Trans. and Fluid Mech. Inst.*, Stanford Univ. Press, Stanford, CA, 77.

Hites M., Nagib, H., Wark C. (1997): Velocity and wall shear- stress measurements in high Reynolds number turbulent boundary layers. AIAA Paper No. 97-1873.

Huerre P. (1983): Finite amplitude evolution of mixing layers in the presence of solid boundaries. *J. de Mecanique Theorique et Appliquee*, Numero Special, 121.

Ito A. (1980): The generation and breakdown of longitudinal vortices along a concave wall. *Trans. Japan Soc. Aero. and Space Sci.* **29**, 327.

Jacobson S.A., Reynolds W.C. (1995): An experimental investigation towards the active control of turbulent boundary layers. Dept. of Mech. Eng. Report No. TF-64, Stanford Univ.

Jung W.J., Mangiavacchi N., Akhavan R. (1992): Suppression of turbulence in wall-bounded flows by high-frequency spanwise oscillations. *Phys. Fluids A* 4, 1605.

Kim J. (1997): Taming Turbulence. AIAA Paper No. 97-1791.

Kim J., Moin, P. (1986): The structure of the vorticity field in turbulent channel flow—Part 1. *J. Fluid Mech.* **155**, 441.

Klebanoff P.S., Tidstrom K.D, Sargent L.D. (1962): The three dimensional nature of boundary layer instability. *J. Fluid Mech.* **12**, 1.

Kline S.J., Reynolds W.C., Schraub F.A., Runstadler P.W. (1967): The structure of turbulent boundary layers. *J. Fluid Mech.* **30**, 741.

Kovasznay L.S.G. (1970): The turbulent boundary layer. *Ann. Reviews of Fluid Mech.* **2**, 94.

Kovasznay L.S.G., Komoda H., Vasudeva B.R. (1962): Detailed flow field in transition. *Proc. of the Heat Transfer & Fluid Mech. Inst.*, Stanford Univ. Press, Stanford, CA, 1.

Laadhari F., Skandaji L, Morel R. (1994): Turbulence reduction in a boundary layer by a local spanwise oscillating surface. *Phys. Fluids* **6**, 3218.

Lee M.K., Eckelman L.D., Hanratty T.J. (1974): Identification of turbulent wall eddies. *J. Fluid Mech.* **66**, 17.

Lee C., Kim J., Babcock D., Goodman R. (1997): Application of neural networks to turbulence control for drag reduction. *Phys. Fluids* **9**, 1740.

Liepmann H.W. (1979): The Rise and Fall of Ideas in Turbulence. *American Scientist* **67**, 221.

Liepmann H.W., Brown G.L., Nosenchuck D.M. (1982): Control of laminar-instability waves using a new technique. *J. Fluid Mech.* **118**, 187.

Liepmann H.W., Nosenchuck D.M. (1982): Active control of laminar-turbulent transition. *J. Fluid Mech.* **118**, 201.

Lorkowski T., Rathnasingham R., Breuer K.S. (1997): Small- scale forcing of a turbulent boundary layer. AIAA Paper No. 97-1792.

Ludwig H., Tillman W. (1949): Untersuchungen über die Wandschubspannung in turbulenten Reibungsshicten. *Ind. Arch.* **17**(4), 288.

Lumley J.L. (1967): The structure of inhomogeneous turbulent flows. In *Atmospheric Turbulence and Radio Wave Propagation*, eds. A.M. Yaglom & V.I. Tatarski, Moscow.

Lumley J.L. (1996): Control of Turbulence. AIAA Paper No. 96-0001.

Michalke A. (1965): On spatially growing disturbances in an inviscid shear layer. *J. Fluid Mech.* **23**, 521.

Mito Y., Kasagi N. (1997): Turbulence modification with streamwise-uniform sinusoidal wall oscillation. *XI Symp. on Turbulent Shear Flows*, Grenoble.

Moin P., Shih T.-H., Driver D., Mansour N.N. (1990): Direct numerical simulation of a three-dimensional turbulent boundary layer. *Phys. Fluids A* **2**, 1846.

Myose R.Y., Blackwelder R.F. (1994): Selective suction for controlling the breakdown of streamwise vortices on concave walls. AIAA Paper No. 94-2216.

Nishioka M., Asai M., Iida S. (1979): An experimental investigation of the secondary instability. In *Laminar-Turbulent Transition*, eds. R. Eppler & H. Fasel, Springer Verlag, Berlin, 37.

Offen G.R., Kline S.J. (1974): Combined dye-streak and hydrogen bubble visual observations of a turbulent boundary layer. *J. Fluid Mech.* **62**, 233.

Oldaker D.K., Tiederman W.G. (1977): Spatial structure of the viscous sublayer in drag reducing channel flows. *Phys. Fluids* **20**, Supplement, S133.

Rathnasingham R., Breuer, K.S. (1997): System identification and control of a turbulent boundary layer. *Phys. Fluids* **9**, 1867.

Robinson S.K. (1990): The kinematics of turbulent boundary layer structure. Ph.D. Thesis, Stanford Univ.

Saric W.S., Carter J.D., Reynolds G.A. (1981): Computation and visualization of unstable wave streaklines in a boundary layer. *Bull. Am. Phys. Soc.* **26**, 1252.

Sendstad O., Moin, P. (1991): On the mechanics of 3-D turbulent boundary layers. In *VIII Symp. on Turbulent Shear Flows*, Sept 9–11, Munich.

Schubauer G.B., Skramstad, H.K. (1947): Laminar boundary layer oscillations and stability of laminar flow. *J. Aero. Sci.* **14**, 68.

Smith C.R. (1978): Visualization of turbulent boundary layer structure using a moving hydrogen bubble wire probe. In *Coherent Structure of Turbulent Boundary Layers*, Lehigh U., 48.

Smith C.R., Metzler, S.P. (1983): The characteristics of low-speed streaks in the near-wall region of a turbulent boundary layer. *J. Fluid Mech.* **129**, 27.

Sreenivasan K.R. (1989): The turbulent boundary layer. In *Frontiers in Exp. Fluid Mech.*, Lecture Notes in Engineering, vol. 46, ed. M. Gad-el-Hak, 159.

Swearingen J.D., Blackwelder R.F. (1987): The growth and breakdown of streamwise vortices in the presence of a wall. *J. Fluid Mech.* **182**, 255.

Swearingen J.D., Blackwelder R.F. (1988): The role of inflectional velocity profiles in wall bounded flows. In *Near Wall Turbulence*, ed. S.J. Kline, Hemisphere Pub. Corp.

Tani I. (1962): Production of longitudinal vortices in the boundary layer along a concave wall. *J. Geophysical Research* **67**, 3075.

Tani I., Aihara Y. (1969): Görtler vortices and boundary layer transition. *Z. Angew. Math. Phys.* **20**, 609.

Tani I., Sakagami J. (1962): Boundary layer instability at subsonic speeds. *Proc. of the International Council of the Aerospace Sciences*, ed. M. Roy, Spartan books, Washington, 391.

Temam R., Bewley T., Moin P. (1997): Control of turbulent flows. *Proc. 18th IFIP TC7 Conf. on System Modeling and Optimization*, Detroit.

Tiederman W.G., Luchik T.S., Bogard D.G. (1985): Wall-layer structure and drag reduction. *J. Fluid Mech.* **156**, 4.

Toms B.A. (1949): *Proc. of the International Congress on Rheology*, North-Holland Pub., Amsterdam,Sec. II, 135.

Trujillo S.M., Bogard D.G., Ball K.S. (1997): Turbulent boundary layer drag reduction using an oscillating wall. AIAA Paper No. 97-1870.

Tung S., Hong W., Huang J., Ho C.-M., Liu C., Tai Y.C. (1995): Control of a streamwise vortex by a mechanical actuator. In *Turbulent Shear Flows X*, Penn. State Univ., August 14–16.

Willmarth W.W., Lu S.S. (1972): Structure of the Reynolds stress near the wall. *J. Fluid Mech.* **55**, 65.

Wortmann F.X. (1969): Visualization of transition. *J. Fluid Mech.* **38**, 473.

Wortmann F.X. (1979): The incompressible fluid motion downstream of two dimensional Tollmien Schlichting waves. In *Laminar-Turbulent Transition*, eds. R. Eppler & H. Fasel, Springer, Berlin, 110.

4 Large-Scale-Structure Identification and Control in Turbulent Shear Flows

Joël Delville, Laurent Cordier and Jean-Paul Bonnet

Laboratoire d'Etudes Aérodynamiques, Université de Poitiers, 86036 Poitiers, France

Abstract. The control of turbulent shear flows can be achieved through the control of the large-scale structures. Indeed, even in fully turbulent shear flows, these large-scale structures are known to be of primary importance for most of the flow characteristics. Due to the turbulent character of flows under practical and industrial interests, the detection, analysis, prediction and control of the large-scale structures are quite complex. We present, in this chapter, several tools available for accessing these large-scale structures. Non conditional, stochastic methods, based on correlations, are preferentially detailed. In particular, the Proper Orthogonal Decomposition and the Linear Stochastic Estimation are described. As an illustration of the potentialities of these objective stochastic approaches, the particular case of the turbulent plane mixing layer is derived as a guide-line all along this chapter. In its last part this chapter will focus onto the way by which, using POD, low dimensional models of the structures can be derived, in the framework of a closed loop control of these structures. This approach, deeply related to the notion of deterministic chaos, is then emphasized. The important problem of the closure (mean flow/turbulent flow) appearing in this context is recalled. The last part of this chapter is devoted to a point that is specific and of importance for these stochastic approaches. The limits for the representation of the flow by these models when the flow configuration evolves have to be given. The methods able to take into account this evolution are of crucial importance and under rapid development.

1 Introduction

Industrial, applied and fundamental researchers alike are now convinced that large-scale, organized motions exist and play a crucial role in turbulent flows. These large-scale structures are known to have a recurrent character and most of the time they are quasi-periodic: at a given spatial location, they possess a preferential size and appear with a preferential frequency.[1] Indeed, these characteristics are smeared by the turbulent nature of the flow and, unless artificially excited, possess a random distribution in size, location, frequency etc. Large-scale structure can then only be defined in a statistical way or by using specific concepts that will be described later in this chapter.

[1] For example, in the case of a plane mixing layer, the preferred large-scale structure size is of the order of the vorticity thickness δ_ω with a typical frequency f_p corresponding to a Strouhal number $S_\omega = f_p\ \delta_\omega / U_m$ of the order of 0.3 (see Chap. 6 of this book).

M. Gad-el-Hak et al.: LNPm 53, pp. 199 - 273, 1998
© Springer-Verlag Berlin Heidelberg 1998

It has become increasingly evident that large-scale structures influence mixing, noise, vibrations, heat transfer, drag, lift etc. Therefore, understanding their morphology, their dynamics and how they interact with the surrounding fluid is often essential for the purpose of controlling turbulent flows.

As is the case for any type of flow control, large-scale structure control can be achieved by passive as well as by active means (for a review, see Chap. 1 of this book). However, regardless of which particular method is used to control the large-scale structures, it is first necessary to be able to *identify* them. In this first stage of flow control, experimentalists and numerical analysts are faced with two initial tasks which are to find out: 1) how to separate (extract) these structures from the background turbulence and 2) how their average characteristics (in terms of their more probable or dominant role) can be determined. These tasks are always complex and non-trivial because the large-scale structures are embedded in random fields and the technique used to determine when and where certain structures are passing or present is directly related to the definition of the coherent structures.

Section 2 will be devoted to this problem of large-scale structure identification. An overview of different methods will be discussed herein. A variety of detection or analysis methods (both multi- and single-point) are now available or are in various stages of development. The following is a list of the main methods that will be discussed: Topological Concept-based methods; Full Field Methods (e.g., pseudo flow visualization); Conditional Sampling (Vorticity-based and other methods); Wavelets; Pattern Recognition Analysis; Proper Orthogonal Decomposition; Stochastic Estimation. Detailed descriptions of these methods can be found in several reference papers (see for example (Adrian 1975), (Antonia 1981), (Glauser and George 1992), (Lesieur 1993), (Berkooz et al. 1993), (Schoppa and Hussain 1994)). The existence of numerous different methods can be surprising at first. This is related to the diversity of the nature of the data that are available from experiments and/or computations. The information available from experiments can be local (probes) or global (visualizations), time resolved (e.g. hot-wire anemometry) or randomly acquired, alternatively triggered by some event (e.g. laser Doppler velocimetry, visualization-based velocimetry). In general, the information available from experiments is poorly resolved in both time and space, and special efforts have to be made to address the global, large-scale character of the flow. This is particularly true when, as for most cases of practical interest, the flows are turbulent, three-dimensional and occur at high Reynolds numbers. On the other hand, and somewhat conversely, the information available from numerical simulations is quite complete, and is sufficiently resolved in both time and space, as in the case of Direct Numerical Simulation (DNS) or Large Eddy Simulation (LES) for example. However, in these cases, the amount of information may be considered too large to be handled easily and to be interpreted in terms of large-scale structure. Therefore, for numerical simulations, it is generally necessary to choose properly

what part of the data has to be processed for the purpose of large-scale structure qualification.
In addition, for *practical applications of flow control*, it is necessary to define the appropriate detectors and the appropriate data processing algorithms to be applied to the "detector" output (here the term "detector" stands for any physical diagnostic apparatus). Therefore, even when using a numerical approach, specific detection schemes for physical detector outputs must be chosen.

To appreciate the need for these techniques one must understand the character of high Reynolds number, often turbulent, motions. As modern, full Navier-Stokes computer simulations have made clear, knowing the data at many points in the flow does little in and of itself to make clear what is happening, due to the chaotic nature of the flow. The key to understanding usually lies in what is done to the data to bring the underlying structure to the foreground.

Most of the techniques that are described in the following sections have been utilized widely over the past decade. Several "revisits" of these techniques, mainly by several groups cross-checking the results obtained for the same data etc., have improved their reliability and have allowed for a better qualification of their limits of applicability.

Section 3 will be devoted to a presentation of the Proper Orthogonal Decomposition (POD) technique which represents by itself a specific approach and concept of large-scale structure identification. This approach, introduced by Lumley (1967), is now widely used for analyzing turbulent flows. Several characteristics of this decomposition are quite attractive in terms of large-scale structure identification: firstly, this approach is objective in the sense that no preconceived ideas about the structure are required. Secondly, the POD leads to a basis of eigenmodes which are representative of the flow. The governing equations of motion can then be projected onto these modes. By this approach, the behavior of a structure can be described in terms of the evolution of simple scalars (coefficients of projection). A simple set of Ordinary Differential Equations (ODE) are obtained.
This decomposition is optimal in the sense of kinetic energy representation: this means that no other decomposition can be better for describing turbulent energy. In addition, it has been proven that for most turbulent shear flows, a very small number of modes are necessary to correctly represent the dynamical behavior of the large-scale structure. This characteristic means that only a small number of ODE will be sufficient for most shear flows. Dynamical systems of low order can then be obtained. These aspects will be discussed in more detail in Sect. 4.

1.1 Tools and Methods

As stated before, several methods for structure identification are available and the choice of a particular one is guided both by the available information

or data and by the purpose itself of the identification: physical understanding, validation of prediction, flow control. In addition, this choice depends on the definition of the structure, but also on the experimental and numerical capabilities available. For example, from an experimental point of view, some approaches require multiple sensors in order to obtain simultaneous instantaneous information at several locations. Some approaches are well adapted to scalar results while others require vectorial information. Other approaches, however, only require knowledge at one or at most a few spatial locations. Moreover, it is necessary to choose the optimal experimental configuration in order to characterize the structures. The problem is equivalent to trying to find the simplest (minimum?) sensor arrangement that gains maximum significant information about the structures. It is also related to the complexity of the organization of the flow and, in most of cases, it requires simultaneous 3D measurements of the flow variables such as velocity.

The recent and rapid advances in, for example: data collection, flow simulation, instrumentation, digital data processing, and increases in computational, graphical and storage capabilities of computers, have resulted in an exponential increase in the application of various methods.

1.2 Active Control

The active control of large-scale structure can be defined as attempting to bring the structures from their present state to another desired state where some given feature of the flow will be enhanced, reduced or simply modified. In this chapter, active control is discussed mainly in terms of reactive flow control, i.e. a closed loop, feedback system (see Figs. 3 and 4 of Chap. 1).

As for any active flow control process, the control of large-scale structure should take into account the following key-points: detection, analysis, prediction, strategy and actuation. In the particular case of control through action on the large-scale structure, some specific remarks can be made:

Detection and Detectors: To be able to control the large-scale structure in turbulent flows, it is first necessary to detect the presence of the turbulent structure one wants to "play" with. This introduces the notion of the choice of the optimal *detector* which is well adapted to practical constraints for actual industrial applications: minimum flow perturbation, reliability, minimum cost etc. As an example, the rakes of hot wires used for several laboratory experiments can hardly be proposed for real airplanes, trains etc. Once the choice of the optimal detector is made (either for a laboratory or an industrial application), it is necessary to address the following points: How can these large-scale structures be extracted from the background turbulence? Is it possible to provide their "mean" characteristics, for a feedforward control for example? How can their contribution to the flow dynamics be determined?

This is certainly not a trivial task, due mainly to the jitter effect of the "random" turbulence (as opposed to "organized" motions) that introduces

an unavoidable phase turbulence. By itself, the separation of the turbulent activity into "turbulent" or "coherent structures", corresponding to different decompositions of the fluctuating fields, is not unique. Hence, the detection method itself cannot be unique. However, the different approaches should lead to equivalent results in terms of flow control.

Whatever the detection scheme is, for the purpose of active control, we need to access to *instantaneous, real time,* information about the large-scale structure. For evident, practical reasons, the number of detectors needs to be kept as small as possible. It is then necessary to know what kind of information is relevant and sufficient in order to access the flow characteristics. It is also necessary to know the limit of the description of the flow required for efficient control: spectral range, vectorial information (e.g. velocity components) or scalar data (e.g. only one component of velocity, temperature, density, concentration, pressure, ...), correlations, etc.

The optimal configuration of the detection and data processing procedures that can be used to obtain a relevant description of the structure at a given time should be determined.

Analysis: Once the existence of large-scale structure has been accepted, it is necessary to quantify the contribution to turbulence and/or to the surrounding flow.

Due to the non-stationary character of the large-scale structures, their control requires knowledge of not only the statistical properties, such as the Reynolds tensor, but also of the time-dependency. In terms of energy, the usual averaging method is useful because it permits a global analysis of flow regions of turbulent activity. However, this is not enough for controlling the turbulent process, providing that only the result and not the details of this process is known. In terms of time dependency, the usual spectral, harmonic (Fourier) analysis in time is useful and has in the past proven that it can be used for physical interpretation and theoretical analysis of turbulent flow. The description of the turbulent processes in terms of the energy cascade can still be used with some success, even for some open loop flow control. However, the harmonic decomposition is in general not detailed enough for active flow control. With the exception of some special use of spectral analysis, more sophisticated time dependency analysis is required.

Based on the above remarks, the usual Reynolds decomposition is insufficient, and thus alternate decompositions have been introduced, such as the double or triple decompositions. For these approaches, the flow is divided into coherent and incoherent motions. The coherent part corresponds to "conditional" contributions, which are the flow properties when a "predetermined" type of event occurs. Another solution is to make use directly of some kind of projection of the flow characteristics on either prescribed eigenfunctions (Fourier, Galerkin modes) or specific, flow dependent ones (POD). For these

approaches, no assumptions about the nature of the large-scale structure need to be made.

Regardless of the approach used, it is necessary to estimate the contribution of the large-scale structure to the global turbulent process that has to be controlled. For example, the contribution to turbulent kinetic energy production, to diffusion, to shear stress etc. has to be specified.

Prediction: In order to design a "smart", and probably more efficient control, it is necessary, based on the knowledge of the state of a given detected large-scale structure at a given time t, to predict the evolution of this large-scale structure for the time $t + dt$. Even "short" time prediction may be sufficient for control.[2] Ideally, the interaction of the large-scale structure with the whole flow has to be estimated, such as large scale/small scale interactions. This requires the ability to define a model for the temporal evolution. At the present time, DNS and LES predictions are obviously not suited for these purposes. Linearized approaches as Rapid Distortion Theory, or stability analysis can be used. In this context, any procedure allowing to transform a Partial Differential Equation (PDE) problem into a much simpler, Ordinary Differential Equation (ODE) problem is useful. This can be achieved by deriving quite simple differential equations that describe the temporal evolution of the projection coefficients. When these coefficients, which are characteristic of the structures, are available, the ODE can be used for short term predictions. It is then necessary, in the context of flow control, to be able to access a physical representation of these instantaneous coefficients. This approach will be described below.

Strategy: As stated before, it is necessary to introduce a specific strategy in order to define the flow perturbation required to bring the large-scale structure to the required state, while the imposed constraints are satisfied or at least approached.

For such a purpose, a deterministic approach to turbulence can be of great interest. The early works of Lorenz (1963) or Ruelle and Takens (1971), have shown that, for some simple cases, turbulent behavior can be described by low order dynamical systems, or, more precisely, that these systems can exhibit a chaotic behavior. Recent developments in chaos control (Shinbrot et al. 1993, Ott et al. 1990) have demonstrated the great sensitivity of this kind of system to initial conditions (butterfly effect).

One of the interests in this type of approach is that this sensitivity allows to conjecture that a very small amount of energy can be sufficient in order

[2] One particular point need to be recalled: in the approaches that will be derived later on, the notion of Dynamical System will be often used. However, in this last context, authors are generally interested into asymptotic behavior of the system: in closed-loop feedback control, the short time behavior of the system can be sufficient.

to stabilize (or de-stabilize) the system and leads it into an orbit where the desired characteristics are. Up until now, these approaches have been applied to systems with a very small number of degrees of freedom. In a non-chaotic dynamical system, it would be necessary to introduce a larger amount of energy in order to obtain the same result. It is clear that the presence of chaos is of interest in order to reduce the cost and to improve the efficiency of control (Shinbrot et al. 1992a, Shinbrot et al. 1992b).

Actuators: The last stage of the active control process is of course the need to define the suited "actuator": the mechanical (Ho et al. 1996) (or other: temperature, mass flow ...) device by which the flow will be driven toward the desired state. In any case, the gross characteristics of such actuators can generally be estimated from a global knowledge of the flows. As an example, the Strouhal number or the characteristic frequencies of the flows can be used to select the order of magnitude or the time response of the actuator. The size of the actuators, or their domain of influence, corresponds in general to the characteristic scales of the large-scale structure. Thus, to estimate an order of magnitude, it is sometimes only necessary to know a few details about the non-stationary character of the flow. For example, some flow visualizations or conventional spectral analysis can be used for dimensioning the devices.

Lastly, it has to be recalled that the aerodynamical properties of the actuators can be a priori not known, due to special shapes or, in some applications, unusual sizes (in general very small scales). This can be also true for hydrodynamical properties and for aeroacoustic characteristics. The Reynolds numbers can be out of the usual ranges, and in general, these devices operate in extremely turbulent environments. Some new research areas may stem from the need to obtain better knowledge of the "actuators flows". Some roads remains open for future research!

2 Large-Scale Structure Identification Scheme

2.1 Overview

The definition of large-scale structure is never straightforward. In ordinary turbulent flows, these structures are embedded inside the overall chaotic behavior of the turbulence field and are then difficult to detect and to extract. It is also difficult to determine their average characteristics (in the sense of probability or dominance). This is a non-trivial task because the coherent structures are generally hidden in a random field and also because the technique used to determine when and where certain structures are passing or present is *directly related to the definition* of the coherent structure itself.

Indeed, first of all it is necessary to try to define the large-scale structure. The term itself is still controversial. Sometimes called Organized Motion, Co-

herent Structure, Coherent Eddy, these events should agree with a minimum set of characteristics.

Several meetings held in the last few years were devoted to topics directly related to Coherent Structures. Detailed proceedings are available for these meetings (Moffat and Tsinober 1989), (Gyr 1990), (Lumley 1990), (Langley 1990), (Métais and Lesieur 1989), (Bonnet and Glauser 1993).

Among others, let us recall some available definitions:

From Lesieur : (Lesieur 1990), (Lesieur et al. 1993):
Suppose that, at a given time t_0 there exists a vorticity concentration within a domain $D_{t_0} \subset R^3$. Let D_t be the image of D_{t_0} at $t \geq t_0$. D_t is a *Coherent Structure (coherent vortex)* if : i) D_t retains a recognizable pattern for time delays greater (typically 5 times) than the turnover time $({\omega_0}^{-1})$. ii) D_t is unpredictable (i.e. extremely sensitive to small perturbations of initial conditions).

From Hussain : (Hussain 1981), (Hussain 1983):
"A *Coherent Structure* is defined as a flow module with instantaneous phase-correlated vorticity".

From Berkooz : (Berkooz et al. 1993):
Coherent Structures are defined as "organized spatial features which repeatedly appear (often in flows dominated by local shear) and undergo a characteristic temporal life cycle". A rational method for extracting such "features" was proposed by Lumley (1967) and will be described later in this chapter. This author (Lumley 1981) introduces the concept of "Building Blocks" (basis of non-specified functions) based on the notion of more or less "energetic modes" on which the velocity field is projected. Using the Shot-Noise theory (Rice 1954), typical representations of the Coherent Structures can be provided.

El Tahry in (Lumley 1990) reports a discussion where several other proposals were given:

- From Perry, a Coherent Structure is a pattern which occurs periodically but not necessarily ordered (scale and convection velocities being random), but its orientation is fixed.
- From Kline, Coherent Structures are recursive events contributing to the dynamics: Production of Reynolds stress.
- Wygnanski states that the Coherent Structure can be associated with the dominant modes of the instability. This proposal is in some sense contradicted by Jimenez.
- Stull defines Coherent Structures as entities which contribute to transport of momentum and passive scalars over given distances without considerable diffusion.

The concept of "Conditional Eddy" introduced by Adrian avoids in some sense the problems of the definition of Coherent Structure, these conditional eddies being defined by the event itself. This concept does not imply quasi-periodicity of the flow, nor any mechanism related to the generation of Reynolds stress (see for example (Adrian 1979), (Bonnet and Glauser 1993)). An extended review of this approach can be found in (CISM/ERCOFTAC Advanced Course 1996). Typical applications in the context of flow control will be given later in this chapter.

Other definitions can be used. Among them topological concepts have been introduced by Hunt et al. (1978), for example.

Each of the Structure Eduction methods then corresponds to one (or several) of these definitions.

In the case of numerical approaches such as DNS or LES, the information available is by definition fully detailed, so that any definition can be retained and any structure detection method is applicable. However, as previously stated, the huge amount of data issued from computations is a real handicap for the analysis of flows in terms of large-scale structure. An illustration of the multiple possibilities offered by numerical data can be found in (Moin and Moser 1989), (Adrian and Moin 1988), (Bonnet and Glauser 1993), or (TCFD 1993).

Contrarily, in the case of experimental approaches, it is first necessary to define the information which is available or accessible.

2.2 Accessing the Large-Scale Structure

Visualizations. Historically, one of the first and, in some sense, the most simple way to detect the large-scale structure was to visualize these events. Several visualization methods are available, the most popular being the use of dyes or smoke in incompressible flows, or Schlieren in compressible flows. It is simply necessary here to recall the well known spectacular visualizations obtained by Brown and Roshko (1974).

Although apparently basic, the visualization process is not obvious. When tracers are used, particular care should be taken in choosing the location of seeding so that the tracer follows the vorticity. In this case, it is necessary to assume that the molecular diffusion is negligible. Cimbala et al. (1988) have shown in a wake that misleading interpretations can be obtained when the seeding is introduced in different downstream positions.

Velocity Measurements. More quantitative analysis can be performed with conventional measurement techniques.

Hot Wire Anemometry is, up to now, the most appropriate method due to two main properties:

- it delivers velocity signals which are continuous in time with a good frequency range (the inertial range is easily well described and the dissipative scales can be reached if probes are well designed),
- due to its relatively low cost, it allows multi-point measurements. The number of hot-wires being used simultaneously is continuously increasing (Delville 1995): 48 hot-wires, (Citriniti 1996): 138 hot-wires. In one direction, spatial meshes close to the ones that can be obtained from numerical simulations can then be approached, while the temporal description (record lengths) remains several orders of magnitude higher than that numerical simulations can provide.

However, some limitations on the use of this technique remain:

- spatial integration,[3] due to the wire length: this effect can be reduced by using gold plated or Wollaston wires.
- The intrusive nature of this technique may restrict its application field. This is more crucial when multi-probe configurations are used.
- For practical, industrial applications, the fragility and sensitivity to external perturbations (dust, noise, etc) can prohibit the use of such apparatus.

The Particle Image Velocimetry (PIV) (2D or, better Holographic) associates visualization and multi-point velocity measurement, thus allowing to obtain both visual and quantitative velocity information. Potentially any detection method can be used in this case. At present, these approaches are limited to research laboratories, but are under rapid development and systematic use is probable in the very near future. For example, in an application to the backward-facing step, Huang (1994) was able to apply POD to PIV. However, up until now the temporal bandwidth of PIV has remained low (of the order of ten pictures per second) and applications to high Reynolds number and 3D flow are limited. Some attempts are presently made to combine hot wire rake measurements and PIV in order to obtain simultaneously good spatial and temporal descriptions (Glauser 1996).

Laser-based quantitative measurements, are generally not used in Coherent Structures eduction processes, due to limitations in the number of measurement locations, and to the discontinuous nature of the temporal information

[3] This spatial integration can be, in fact, a favorable point if spatial aliasing is considered: there is no other practical way to avoid spatial aliasing than playing with the spatial integration properties of the sensor. Comments about this can be found in (Citriniti and George 1997) or (CISM/ERCOFTAC Advanced Course 1996).

(linked to the random presence of the seeding particles involving a random occurrence of the signals). However, a few attempts have been made to use Laser Doppler Velocimetry (LDV) for Coherent Structures characterization purposes (Lehman and Mante 1993, (Koochesfahni et al. 1979). In these cases indeed, the non-intrusive character of the LDV can be a crucial advantage.

Use of scalar information. It is usual to analyze the large-scale structure from velocity measurements, with one or (best) several components. However, the use of velocity as an input for flow control may lead to a certain number of problems: for an industrial application, it may be difficult to access to instantaneous velocity components, mainly for complex flow geometries. On the other hand, this information may not be relevant, for example if the purpose of the process is to control temperature or pressure fluctuations: in these cases, it may be more useful to use temperature or pressure as input. Up to now, only very few applications can be found for approaches that use information other than that arising from the velocity. Temperature, considered as a passive contaminant, has been used successfuly for Coherent Structures detection by Antonia et al. (1986) among other authors. Pressure information is used extensively for most flow control in aeroacoustic problems. For wall flows this information is easy to obtain. However, in free shear flows, the local fluctuations of static pressure, which constitute one of the relevant quantities, are difficult to measure. Some attempts have been made in the case of high velocity flows (Long et al. 1993).

2.3 Excited vs Natural Approaches

For several flow configurations, such as free shear flows in particular, it is possible to use small amplitude excitations of the flow. If these excitations occur in the vicinity of the most amplified unstable modes present in the flow, they will, in some sense, "freeze" the flow patterns. The frequency domain of excitation can also correspond to harmonic or subharmonic frequencies. Hussain (1983) has shown that in the case of mixing layers, the resulting large-scale structures are of the same nature in natural and excited configurations. The interest of the excited configuration is that the large-scale structures are "cleaner" than in the natural case, and they can be detected by a simple triggering process, providing the reference signal is known.

Except for the excited case, usual Coherent Structures detection requires at least 2 point information, particularly when velocity is concerned. The early use of two point measurements was to compute the space-time correlation between two signals (see for example (Favre et al. 1976), (Townsend 1976)). Later, instantaneous analysis was made possible by using more complex data acquisition and processing.

2.4 Detection Methods

The aim of this section is to present an overview, and the state of the art of detection and analysis techniques. The next paragraphs are devoted to brief presentations of the most popular methods developed up to now for identifying large-scale structure in free turbulent flows. Most of these methods can be found in the proceedings of an IUTAM Symposium (Bonnet and Glauser 1993). We intentionnaly restrict this review to free shear flows. It is important to note however that most detection schemes presented here can be successfully applied to wall bounded shear flows as long as the unique problems associated with them are accounted for (e.g., probe interference, mesh requirements, etc.).

As shown in Table 1, from a general point of view, it is possible to classify the different approaches into two categories.

Table 1. Classification of detection methods.

CONDITIONAL	Non-CONDITIONAL
• Detection: ($\Leftrightarrow$ Structure definition) - Fluctuation Levels - 4 Quadrants - VITA - Gradients - TPAV - Tracers (temperature ...) - Visualizations - Topology	• Space-Time Correlation & Spectral Analysis • Orthogonal Decomposition
• Wavelets • Stochastic Estimation • Pattern Recognition	
STATISTICS:	
- Ensemble Average - Multiple Decomposition - Coherent Structures dynamics	- More Probable Characteristics - Modal Decomposition - Dynamical Systems
- Statistical Properties	

The first category, "conditional approaches", consists of the detection of the passage or presence of a given event when a prescribed condition is fulfilled. This detection allows one to collect events, to compute averages and then to compile the main characteristics of the Coherent Structures. This first approach requires variable degrees of subjectivity or preconceived notions of the flow characteristics.

The second kind of approach involves statistical information (such as space-time correlations, for example) to derive the characteristics of the Coherent Structures, which are responsible for these statistics. These approaches are entirely "objective" or, at least more "objective" than in the first case. They are, however, limited to stochastic information, although under certain conditions they can provide instantaneous characteristics and they can be associated with conditional approaches, thereby making the two approaches complementary.

From both approaches, in addition to the information on the morphology of the Coherent Structures, it is possible to determine their dynamics, their contribution to the turbulent transport processes, etc. .... These characteristics are essential for the purposes of analysis and control of the flows, for developing new computational methods and for validation of numerical simulations.

The Variable Integration Time Average (VITA) introduces a time scale in the selection process. VITA is now a popular method applied mainly to boundary layer flows, but easily appplicable to free flows. The principle was introduced by Blackwelder and Kaplan (1976). The raw velocity signal $u(\mathbf{x}, t)$ (with a variance σ_u) is integrated over a short time scaled on the characteristic time scale of the structure. A new signal is then generated

$$\hat{u}_T(\mathbf{x}, t) = \frac{1}{T} \int_{t-\frac{1}{2}T}^{t+\frac{1}{2}T} u(\mathbf{x}, t) dt \tag{1}$$

The variance of the new signal, $\sigma_{\hat{u}}$ is then thresholded and a detector function is built.

$$D(t) = \begin{cases} 1 & \text{if } \sigma_{\hat{u}}^2 > K\ \sigma_u^2 \\ 0 & \text{otherwise} \end{cases} \tag{2}$$

K is an arbitrary parameter defining the threshold.

The interpretation of the results is well established in bounded flows but less clear in free shear flows. As quoted by Ferré and Girault (1989a), this method is based on a local energy criterion. This criterion is not relevant for every Coherent Structure, particularly in free shear flows.

Wallace et al. (1977) have improved this approach by introducing *pattern recognition* criteria for the velocity signals. The signals are recognized after pre-defined typical behaviors such as strong acceleration followed by slow velocity decrease. Here also this approach is well suited to wall flows but not very convenient when the overall flow characteristics are unknown.

The Pattern Recognition Approach (PRA) has been introduced by Mumford (1982) and refined by several authors (Ferré and Girault 1989a), (Ferré and Girault 1989b) (see Ferré in (Bonnet and Glauser 1993)). This technique is an iterative process that allows one to determine the ensemble average of the Coherent Structure and to detect the patterns embedded in the time series. The process starts from an initial template of a conjectured trace of the Coherent Structure, and from a correlation analysis, converges towards a final template. This procedure has been shown to be practically independent of the initial template, but with low values of the correlation coefficient (Berkooz et al. 1993). The usual applications of the conditional sampling techniques (statistics, contributions to turbulent processes, etc.) are possible.

Conditional Sampling is the technique that traditionally has been related to the "conventional" definitions of Coherent Structures. These techniques educe the average (most dominant?) structure and can also instantaneously characterize the location of a given Coherent Structure. This method is also directly related to the theoretical and computational approaches based on the multiple decomposition of the turbulent fields (Hussain 1986). It consists of choosing, at some location(s) of the flow, any single or multiple reference signal (detector), and applying the appropriate criteria for determining the instant(s) in time which correspond(s) to the presence of a given event. Several approaches can be used, depending on the variable considered (velocity, vorticity, pressure, ...). The most popular methods are described in several reviews (see for example (Antonia 1981)). In the case of artificially excited flows this techniques becomes straightforward. More recent techniques are based on vorticity (Jeong et al., Hayakawa see (Bonnet and Glauser 1993)). These techniques are quite robust and slightly dependent on the threshold levels. A version of this approach, based on a weighted average gradient (WAG), has been applied by Bisset et al. (1990). These methods require a limited number of sensors. If rakes of sensors are available, a "Delocalized" Conditional Sampling can be used as in Bellin et al. see (Bonnet and Glauser 1993) in order to improve the efficiency of the detection and to obtain more detailed information on the Coherent Structures (statistics on scales, locations, etc.). Indeed, some specific techniques can be adapted to the given flow configuration. The aforementioned techniques require several adjustments for threshold levels and/or detector choices. The contributions from various terms of the multiple decomposition can then be computed. This information is of current interest for both understanding the dynamics of the structures and for numerical predictions.

The Wavelet Transform consists of building the equivalent of an analyzing "mathematical microscope": the signal is analyzed by associating locally a set of wavelets built from the different dilatations of the analyzing function

(Farge 1992). This approach allows for detection of the instantaneous discontinuities of the signals, which can be related directly to the footprint of the Coherent Structures (see Kevlahan et al. in (Bonnet and Glauser 1993)). In other recent applications, the wavelet transform has been used to define a time-frequency mask. This method has proven its efficiency in several flows, including turbulent free shear layers and a manipulated turbulent boundary layer. It allows to extract large-scale structure from the background turbulence (Bonnet et al. 1996) or (De Souza et al. 1997).

The Proper Orthogonal Decomposition (POD) as introduced by Lumley, consists of the identification of a coherent structure which has the largest mean squared projection on the flow field (Berkooz et al. 1993). This approach is optimal in the energy sense, has a rapid convergence, must be applied to inhomogenous directions and requires no a priori knowledge of the flow. Various applications of POD can be used; classical POD, snapshot POD, and POD based on scalar or vectorial fields. It has been shown that the contribution of the first POD modes to the instantaneous velocity field exhibits most of the large scale features observed in the original velocity fields. The POD can also be combined with conditional techniques. All of these aspects will be detailed in Sect. 3.

The Linear Stochastic Estimation (LSE) Technique as introduced by Adrian (1979) uses the conditional information specified about the flow at one or several locations, in conjunction with its statistical properties (correlations), to estimate information at other locations in the flow. This approach can be associated with complementary methods, such as POD, conditional sampling, quadrant analysis, etc. As examples, from an experimental point of view, LSE extends the possibility of Coherent Structures analysis with a given number of probes and permits the use of the dynamical reconstruction as developed by Gieseke and Guezennec in (Bonnet and Glauser 1993). This method will be described in more detail in last part of Sect. 3.

Filters: In several cases, the large-scale structures possess a marked signature in the frequency range. Generally this corresponds to cases where dominant structures exist and have spectral footprints appearing as sharp peaks of the energy spectral density at certain frequencies. In these cases, some filtering techniques can be used to separate the coherent contribution from the turbulent flow field. Such approaches have been developed by Brereton and Kodal (1994) or De Souza et al. (1997). The method consists in defining a frequency-based filter either by auto-recursive or by Fourier techniques. This kind of approach can be very efficient when the Coherent Structures footprint is very well localized in the frequency domain. Such is the case when vortex shedding occurs or when, for example, well defined unstable modes (such

as Kelvin-Helmoltz) are present. However, for more complex flow structures, these approaches will be in general inefficient.

Other Techniques. Other techniques have been either described or used to complement those noted above. We mention the Pseudo-Flow Visualization (PFV) Technique for rapid and simple visual analysis of raw data from rakes of sensors (see for example Bellin et al. in (Bonnet and Glauser 1993)). Recent results show that the so-called complementary technique, which combines LSE and POD, can be used to obtain time dependent information (i.e., the phase) from the POD while greatly reducing the amount of instantaneous data required (Bonnet and Glauser 1993), (Faghani 1996).

Remarks. These techniques are now reasonably mature enough to be widely used. Berkooz et al. (1993) have given a review of some of the abovementioned methods. Kevlahan et al. (see (Bonnet and Glauser 1993)) have compared the application of several methods to synthetic data. During a collaborative programme (Bonnet et al. 1993), some of these methods were applied to the same data base for a free, turbulent, incompressible shear flow. The main conclusions of this comparative study were: the methods applied are generally limited to 2D characteristics. It is clear that the 3D nature of Coherent Structures should be taken into consideration. Experiments to obtain 3D information are complex and great care must be taken to select the optimal experimental arrangements for hot-wire rakes for example. The comparison of results obtained from various techniques permits the determination of some common features and helps to avoid discrepancies appearing between the different approaches and related Coherent Structure definitions. The conclusion drawn from most of these comparisons of eduction methods was that the different methods lead to the same average characteristics.

However, major discrepancies are observed in the "efficiency" of the detection process. Some methods clearly "miss" more events than others. This is not a problem when only statistical properties are required. However, in terms of *flow control*, a poor efficiency can be dramatic: if the detection process ignores too many large-scale structures, the resulting action can be inefficient. Indeed, the individual efficiency of each conditional method can be improved by properly adjusting the unavoidable thresholds associated with any conditional method. This, however, is a sort of limitation of conditional sampling methods, providing that the abovementioned thresholds are flow dependant.

Finally, knowledge of the detailed characteristics and dynamics of Coherent Structures can suggest new approaches of flow control using either passive or active means.

3 The Particular Case of POD

In this section, a particular large-scale structure identification procedure, that is of interest for flow control, is analyzed and developed: the Proper Orthogonal Decomposition (POD). More exhaustive reviews on POD can be found in (Berkooz et al. 1993) and in a recent well documented book (Holmes et al. 1996). The aim of this section is first to recall the POD theory and some properties of this decomposition. Then a particular case, the plane mixing layer, will be used to illustrate what kind of information this decomposition can provide. At the end of this section special attention will be paid to the way by which, in the context of flow control, the instantaneous projection coefficients of the POD can be obtained.

3.1 The POD Approach in Brief

Lumley (1967) proposed a method, generalizing spectral analysis to non-homogeneous directions, applied to turbulent flow analysis. He showed that in this way the dominant large-scale structures can be defined in an *objective* and *unique* manner. The formalized approach is intensively described in the book "Stochastic Tools in Turbulence" (Lumley 1970). It suggests that the Coherent Structures within a random field can be identified with the realization of the flow that possesses the largest projection onto the flow field. This approach, the POD, is a classical tool in Probability theory (Loeve 1955). This method is also called, among other denominations, Karhunen-Loeve expansion in Pattern Recognition theory (Ash and Gardner 1975), (Fukunaga 1972) or Principal Component Analysis by statistical analysts. (Ahmed and Goldstein 1975).

Compared to many other classical methods used for large-scale structure identification (Conditional Methods, VITA, Pattern Recognition Analysis, ...), POD is very attractive because no a priori is needed for the eduction scheme. Only a set of flow samples is necessary. From these samples a two-point correlation tensor is constructed for one or several directions (spatial or/and temporal) and for one or several flow variables. Adding directions or variables leads to more complex decompositions but generally leads to more precise descriptions of the large-scale structure (Delville 1995).

Solving the POD problem can be reduced to determining the solutions of an integral eigenvalue problem (Fredholm equation) where the kernel is the correlation tensor. A basis of uncorrelated orthogonal functions (eigenfunctions or eigenvectors), which are characteristic of the most probable "flow realizations" is then obtained. This important property permits the decomposition of every flow realization onto the basis of eigenfunctions obtained. By definition, POD is optimal in terms of the description of the energy present within the flow.

This decomposition is an elegant procedure that allows two approaches, sometimes described as antagonist, to coexist: statistical and deterministic approaches of turbulence. Despite the fact that it is based on statistical methods, the POD allows some kind of deterministic formalism to be introduced for the large-scale structure.

3.2 Formal Definition of POD

POD consists of searching for a set of deterministic uncorrelated flow realizations that correspond to preferred modes $\boldsymbol{\Phi}(\boldsymbol{X})$ of the flow. Consider $\boldsymbol{u}(\boldsymbol{X})$ to be a set of realizations of the velocity field[4] ($\boldsymbol{X} = (x, y, z, t)$). To determine these modes it is simply required to search within the flow realizations $u_i(\boldsymbol{X})$ for the $\boldsymbol{\Phi}(\boldsymbol{X})$ "closest" in average to this set. At this level, the average is not defined, and will depend on the kind of POD used.

Mathematically this problem can be written:

$$\frac{\langle (\boldsymbol{u}, \boldsymbol{\Phi})^2 \rangle}{(\boldsymbol{\Phi}, \boldsymbol{\Phi})} \stackrel{!}{=} Max \tag{3}$$

where $(\boldsymbol{u}, \boldsymbol{v})$ corresponds to the scalar product $\boldsymbol{u}$ by $\boldsymbol{v}$ defined by:[5]

$$(\boldsymbol{u}, \boldsymbol{v}) = \int_{\mathcal{D}} \boldsymbol{u}(\boldsymbol{X}) \boldsymbol{v}^*(\boldsymbol{X}) d\boldsymbol{X} = \sum_{i=1}^{n_c} \int_{\mathcal{D}} u_i(\boldsymbol{X}) v_i^*(\boldsymbol{X}) d\boldsymbol{X} \tag{4}$$

n_c is the number of vectorial components that are taken into account for describing the random function $\boldsymbol{u}(\boldsymbol{X})$ used for the decomposition. The average operator $\langle \bullet \rangle$ can be a temporal, spatial, ensemble or phase average, depending on the approach used.
The POD approach can be compared to searching, in the space of velocity field realizations, for a direction that can describe the preferred organization of the flow in terms of energy. The remainder of this flow description is decomposed in the same way, and this process is repeated ad infinitum up to the determination of the last significant mode.

The problem of maximization (3), leads to a Fredholm integral eigenvalue problem (Lumley 1970):

$$\sum_{j=1}^{n_c} \int_{\mathcal{D}} R_{ij}(\boldsymbol{X}, \boldsymbol{X'}) \Phi_j(\boldsymbol{X'}) d\boldsymbol{X'} = \lambda \Phi_i(\boldsymbol{X}) \tag{5}$$

where R_{ij} is the two-point space-time correlation tensor, estimated over the studied spatial domain $\mathcal{D}$, and defined by:

[4] This choice is not the only one that can be considered. For example vorticity $\boldsymbol{\omega}(\boldsymbol{X}) = \boldsymbol{rot}\big[\boldsymbol{u}(\boldsymbol{X})\big]$ (see (Sanghi 1991)), the stream function Ψ, the pressure (Long et al. 1993), or any scalar or vectorial quantity of the flow can be used.

[5] Here, $(\bullet)^*$ corresponds to the complex conjugate.

$$R_{ij}(\boldsymbol{X}, \boldsymbol{X'}) = \langle u_i(\boldsymbol{X}) u_j^*(\boldsymbol{X'}) \rangle \tag{6}$$

3.3 The POD Theorem

The solution of the Fredholm integral equation (5) is discussed in the Hilbert-Schmidt theory (Riesz and Nagy 1955), (Temam 1988). For this theory to be applied, the integration domain has to be finite so that the integral (5) exists and the correlation tensor R_{ij} is symmetric and belongs to the L^2 space. In the particular case where homogeneous or stationary directions exist, the domain of integration becomes unbounded. In such a case, a different decomposition has to be applied: the harmonic decomposition is well suited to this task, and is generally preferred.

When these integration conditions are satisfied, the POD theorem can be derived (Loeve 1955). The main consequences of this theorem are given below:

1. The integral equation (5) has a discrete set of solutions satisfying:

$$\sum_{j=1}^{n_c} \int_{\mathcal{D}} R_{ij}(\boldsymbol{X}, \boldsymbol{X'}) \Phi_j^{(n)}(\boldsymbol{X'}) \, d\boldsymbol{X'} = \lambda^{(n)} \Phi_i^{(n)}(\boldsymbol{X}) \qquad n = 1,\ 2,\ 3, \cdots, +\infty \tag{7}$$

   where (n) is the order of the orthogonal decomposition and where $\lambda^{(n)}$ and $\Phi_i^{(n)}$ are respectively the eigenvalues and eigenvectors (or eigenfunctions) of POD.
2. The operator $\mathcal{R}$ is hermitian and non negative.[6] The eigenvalues are then real, positive and the corresponding series converges:

$$\lambda^{(1)} \geq \lambda^{(2)} \geq \lambda^{(3)} \geq \cdots \tag{8}$$

3. The eigenfunctions $\Phi_i^{(n)}$ can be chosen to be orthonormal: [7]

[6] $(\mathcal{R}\boldsymbol{u}, \boldsymbol{u}) \geq 0$ for each $\boldsymbol{u}$.

[7] This choice is arbitrary when these function are determined relative to a multiplicative constant. When a "snapshot" POD is involved (see for example (Rempfer and Fasel 1994a)), the eigenfunctions are chosen such that:

$$\sum_{i=1}^{n_c} \int_{\mathcal{D}} \Phi_i^{(p)}(\boldsymbol{X}) \Phi_i^{*(q)}(\boldsymbol{X}) \, d\boldsymbol{X} = \lambda^{(p)} \delta_{pq} \tag{9}$$

and the coefficients $a^{(n)}$ verify $\langle a^{(n)} . a^{(m)} \rangle = \delta_{mn}$. For numerical reasons, it is easier to use condition (10) for the "classical POD", and condition (9) for the "snapshot POD."

$$\sum_{i=1}^{n_c} \int_{\mathcal{D}} \bar{\Phi}_i^{(p)}(\boldsymbol{X}) \bar{\Phi}_i^{*(q)}(\boldsymbol{X}) \, d\boldsymbol{X} = \delta_{pq} = \begin{cases} 0 & \text{for } p \neq q \\ 1 & \text{for } p = q \end{cases} \tag{10}$$

4. Each realization of the random field $u_i(\boldsymbol{X})$ can be constructed from the deterministic eigenfunctions $\bar{\Phi}_i^{(n)}$:

$$u_i(\boldsymbol{X}) = \sum_{n=1}^{+\infty} a^{(n)} \bar{\Phi}_i^{(n)}(\boldsymbol{X}) \tag{11}$$

5. The random coefficients $a^{(n)}$, projections of $\boldsymbol{u}$ onto $\bar{\boldsymbol{\Phi}}$, are then calculated by using:

$$a^{(n)} = (\boldsymbol{u}, \bar{\boldsymbol{\Phi}}) = \int_{\mathcal{D}} u_i(\boldsymbol{X}) \bar{\Phi}_i^{*(n)}(\boldsymbol{X}) \, d\boldsymbol{X} \tag{12}$$

6. Mercer's theorem (Courant and Hilbert 1953) specifies that the correlations R_{ij} can be decomposed in the following way:

$$R_{ij}(\boldsymbol{X}, \boldsymbol{X}') = \sum_{n=1}^{+\infty} \lambda^{(n)} \bar{\Phi}_i^{(n)}(\boldsymbol{X}) \, \bar{\Phi}_j^{*(n)}(\boldsymbol{X}') \tag{13}$$

and that this series is uniformly convergent.

7. Points 6, 4 and 3 impose that the coefficients $a^{(n)}$ are mutually uncorrelated and satisfy:

$$\langle a^{(n)} . a^{*(m)} \rangle = \delta_{mn} \lambda^{(n)} \tag{14}$$

8. Points 6 and 3 allow one to write:

$$\int_{\mathcal{D}} \sum_{i=1}^{n_c} R_{ii}(\boldsymbol{X}, \boldsymbol{X}) \, d\boldsymbol{X} = \sum_{n=1}^{+\infty} \lambda^{(n)} \tag{15}$$

In particular, if $\boldsymbol{u}(\boldsymbol{X})$ is a velocity field, the sum of all the eigenvalues corresponds to the turbulent kinetic energy integrated over the domain $\mathcal{D}$. If $\boldsymbol{u}(\boldsymbol{X})$ is a vorticity field (Sanghi 1991), this relation leads to the system enstrophy. Relative to the notion of large-scale structure, the eigenvalues $\lambda^{(n)}$ of the problem (5) are then representative of the mean energy corresponding to the structure of order (n). These eigenvalues are then a measure of the relative importance of the different structures present within the flow.

9. The POD basis is optimal for describing energy. If $\bar{\Phi}_i^{(n)}(\boldsymbol{X})$ is the POD basis, and $\bar{\Psi}_i^{(n)}(\boldsymbol{X})$ any other orthonormal basis, one can write:

$$u_i(\boldsymbol{X}) = \sum_{n=1}^{+\infty} b^{(n)} \bar{\Psi}_i^{(n)}(\boldsymbol{X}) = \sum_{n=1}^{+\infty} a^{(n)} \bar{\Phi}_i^{(n)}(\boldsymbol{X}) \tag{16}$$

Berkooz (1991) show that for each N the following equality holds:

$$\sum_{n=1}^{N} \langle a^{(n)}.a^{*(m)} \rangle = \sum_{n=1}^{N} \lambda^{(n)} \geq \sum_{n=1}^{N} \langle b^{(n)}.b^{*(m)} \rangle \tag{17}$$

This last result is one of the reasons for using the POD to construct a low order dynamical system: the optimal convergence suggests that only a very small number of modes may be necessary to describe the large scale dynamics of the flow.

3.4 Different POD Approaches

Depending on the way the ensemble average $\langle \bullet \rangle$ is defined for calculating the kernel of the integral eigenvalue problem, different orthogonal decompositions can be obtained: classical, snapshot, extended, biorthogonal, ... For example, the ensemble average can consist of:

- a temporal average, under the ergodicity assumption in statistically stationary flows: *"classical" method.*
- a spatial average, estimated for N uniformly sampled discrete times $t_n = n\tau$ for $n = 1, \ldots N$, for which the instantaneous flow fields $u_i(\boldsymbol{x}, n\tau)$ are uncorrelated, where τ is a time scale, characteristic of the correlation time: *"snapshots" method* (Sirovich 1987a; 1987b; 1987c).
- a spatial average estimated for time realizations satisfying the symmetry group of the equation used to generate the signal: (Sirovich 1987a; 1987b; 1987c); (Breuer and Sirovich 1991) ; (Sirovich and Park 1990), (Park and Sirovich 1990) ; (Deane and Sirovich 1991) ; (Aubry et al. 1993).
- an ensemble average of time realizations with different initial conditions: *extended POD* (Glezer et al. 1989).
- a spatial average estimated for time realizations obtained with conditional measurements (in practice, phase average of background periodicity) (Sirovich 1989) ; (Sirovich et al. 1990b) ; (Rajaee et al. 1994).
- a spatial or time average estimated with space-time realizations of the flow $\boldsymbol{u}(\boldsymbol{x}, t)$ without assumptions as to the properties of the signal, such as ergodicity or statistical stationarity: *the Biorthogonal Decomposition* (Aubry et al. 1991).

In what follows, only two methods: the "classical" method and the "snapshots" method will be described.

"Classical" Method This approach is the one originated by Lumley (1967). In this case, the ensemble average $\langle \bullet \rangle$ is temporal and $\boldsymbol{X}$ is assimilated to the space variable $\boldsymbol{x} = (x, y, z)$.

The $\boldsymbol{\Phi}^{(n)}(\boldsymbol{x})$ are eigenfunctions of the Fredholm integral equation written:

$$\sum_{j=1}^{n_c} \int_{\mathcal{D}} R_{ij}(\boldsymbol{x}, \boldsymbol{x}') \, \Phi_j(\boldsymbol{x}') \, d\boldsymbol{x}' = \lambda \, \Phi_i(\boldsymbol{x}) \tag{18}$$

where the kernel is the **two-point spatial correlation tensor** R_{ij}, and is evaluated from a temporal average assimilated to an ensemble average, based on the assumptions of stationarity and ergodicity:

$$R_{ij}(\boldsymbol{x}, \boldsymbol{x}') = \frac{1}{T} \int_T u_i(\boldsymbol{x}, t) u_j(\boldsymbol{x}', t) \, dt = \sum_{n=1}^{N_{POD}} \lambda^{(n)} \Phi_i^{(n)}(\boldsymbol{x}) \Phi_j^{(n)*}(\boldsymbol{x}') \tag{19}$$

where T is a sufficiently long period of time for which the space-time signal $u_i(\boldsymbol{x}, t)$ is obtained and where N_{POD} is the number of POD modes.

The time dependent coefficients $a^{(n)}(t)$ can be estimated using the relation:

$$a^{(n)}(t) = \int_{\mathcal{D}} u_i(\boldsymbol{x}, t) \, \Phi_i^{(n)*}(\boldsymbol{x}) \, d\boldsymbol{x} \tag{20}$$

In this approach, the flow directions are decomposed in directions assumed homogeneous using a harmonic decomposition, and in inhomogeneous directions by applying the Proper Orthogonal Decomposition.

"Snapshots" Method. In this method introduced by Sirovich (1987a; 1987b; 1987c), the ensemble average operator $\langle \bullet \rangle$ is evaluated as a space average and the variable $\boldsymbol{X}$ is assimilated to time t.

It allows to overcome a critical size problem that can be encountered when applying the classical method: considering N_x, N_y and N_z the number of nodes of the experimental (or numerical) grid in directions X, Y, Z and n_c the number of velocity components used for the decomposition, the size of the integral problem (5) to solve, is $n_c \times N_x \times N_y \times N_z$. This size can quickly become too large to be solved. In the classical method, this point can be taken into account by decomposing flow directions in homogeneous and inhomogeneous directions. In the method of "snapshots", the size of the integral problem to be solved is only related to the number of temporal realizations N_t retained in the sample. This number is generally less than $n_c \times N_x \times N_y \times N_z$. Note that this method does not require any hypothesis concerning the homogeneity of the flow.

The eigenfunctions arising from this decomposition are now purely temporal. They are simply the $a^{(n)}(t)$ coefficients. The integral equation to solve is:

$$\int_T C(t, t') a^{(n)}(t') \, dt' = \lambda^{(n)} a^{(n)}(t) \tag{21}$$

where the kernel $C(t,t')$ of the eigenvalue problem is **the two-point temporal correlation tensor** defined as:

$$C(t,t') = \frac{1}{T}\int_{\mathcal{D}} u_i(\boldsymbol{x},t)u_i(\boldsymbol{x},t')\,d\boldsymbol{x} = \frac{1}{T}\sum_{n=1}^{N_{POD}} a^{(n)}(t)a^{(n)*}(t') \tag{22}$$

The spatial basis functions $\Phi_i^{(n)}(\boldsymbol{x})$ can be calculated from the velocities $u_i(\boldsymbol{x},t)$ and the coefficients $a^{(n)}(t)$, by integrating over a sufficiently long period of time T and normalizing by the eigenvalues $\lambda^{(n)}$:

$$\Phi_i^{(n)}(\boldsymbol{x}) = \frac{1}{T}(\lambda^{(n)})^{-1}\int_T u_i(\boldsymbol{x},t)a^{(n)*}(t)\,dt \tag{23}$$

Note that for the above two approaches of the orthogonal decomposition ("classical" and "snapshots"):

1. Each space-time realization $u_i(\boldsymbol{x},t)$ can be expanded into orthogonal basis functions $\Phi^{(n)}(\boldsymbol{x})$ with uncorrelated coefficients $a^{(n)}(t)$:

$$u_i(\boldsymbol{x},t) = \sum_{n=1}^{N_{POD}} a^{(n)}(t)\Phi^{(n)}(\boldsymbol{x}) \tag{24}$$

2. The spatial modes $\Phi_i^{(n)}(\boldsymbol{x})$ are specified to be orthonormal:

$$\int_{\mathcal{D}} \boldsymbol{\Phi}^{(n)}(\boldsymbol{x})\boldsymbol{\Phi}^{(m)}(\boldsymbol{x})\,d\boldsymbol{x} = \delta_{nm} \tag{25}$$

3. The temporal modes $a^{(n)}(t)$ are orthogonal:

$$\frac{1}{T}\int_T a^{(n)}(t)a^{(m)*}(t)\,dt = \lambda^{(n)}\delta_{nm} \tag{26}$$

In practice, the choice of the solution via the "classical" method (18) or via the "snapshots" method (21) is determined by the particular data set available for the evaluation of the kernels. Data sets from experiments typically consist of a long time history with moderate spatial resolution, whereas data sets from numerical simulation typically offer much higher spatial resolution but a moderate time history. Therefore, the data issued from an experimental approach will be generally[8] treated by using the "classical" method and data issued from numerical simulation by the "snapshots" method.

[8] An exception is the case of data sets obtained from Particle Image Velocimetry.

3.5 POD and Harmonic Analysis

To apply the orthogonal decomposition, the domain $\mathcal{D}$ defined in (5) should be bounded. It is thus necessary to pay special attention to flow directions assumed to be homogeneous, stationary or periodic.

For example, we can assume that the spatial direction OX_3 is homogeneous (a generalization including other directions is immediate). Splitting the space-time variable $\boldsymbol{X} = (x_1, x_2, x_3, t)$ into a homogeneous variable x_3 and inhomogeneous variables, we introduce a new variable $\boldsymbol{\chi} = (x_1, x_2, t)$ for which the Fredholm equation (5) is written as follows:

$$\sum_{j=1}^{n_c} \int_{\mathcal{D}} \Pi_{ij}(\boldsymbol{\chi}, \boldsymbol{\chi}'; k_3) \hat{\Phi}_j(\boldsymbol{\chi}', k_3) d\,\boldsymbol{\chi}' = \lambda(k_3) \hat{\Phi}_i(\boldsymbol{\chi}; k_3) \tag{27}$$

where:

1. $\hat{\Phi}_l$ is the Fourier series decomposition in the OX_3 direction of Φ_l.
2. Π_{ij} is the Fourier transform in the OX_3 direction of the correlation tensor R_{ij} :

$$\begin{aligned} \Pi_{ij}(\boldsymbol{\chi}, \boldsymbol{\chi}'; k_3) &= \int_{-\infty}^{+\infty} R_{ij}(\boldsymbol{\chi}, \boldsymbol{\chi}'; r_3) \exp(-2\pi j k_3 r_3) dr_3 \\ &= \int_{-\infty}^{+\infty} R_{ij}(\boldsymbol{\chi}, \boldsymbol{\chi}'; -r_3) \exp(2\pi j k_3 r_3) dr_3 \end{aligned} \tag{28}$$

In each homogeneous (or stationary) direction, the harmonic functions are solutions of the integral Fredholm equation. As a first approximation, the orthogonal decomposition can be viewed as the generalization of the harmonic decomposition to the inhomogeneous directions.

3.6 Evaluative Summary of the POD Approach

The POD approach by itself is neither a theory nor a closure method for turbulent flows. It is a technique for data analysis (as the classical Fourier analysis or wavelets are).

The main feature of the POD is that it is a decomposition:

- onto a "natural" basis of the flow: the eigenvectors of the two-point correlation tensor. It is then clear that this decomposition, because it isbased on "intrinsic" functions of the flow, will be more efficient than other decompositions based on functions that are given a priori: harmonic decomposition, Chebyshev polynomials, ...
- In this basis, the eigenfunctions can be considered as the preferred statistical directions of the flow.

- This basis is orthogonal, in the sense that the various modes are statistically uncorrelated.

Among the **advantages** related to this method are the following:

- This method is objective, methodic and rigorous.
- The POD is a linear process but it does not invoke the linearity of the process under study.
- The POD is efficient (best decomposition in terms of energy).
- The efficiency of POD increases with the level of inhomogeneity of the direction in which it is applied; it is then suited for the analysis of turbulent shear flows. In the particular case of an homogeneous direction, POD degenerates into a classical harmonic decomposition. This method is therefore complementary to harmonic methods.
- This decomposition is an interesting complement to dynamical systems theory in the sense that this theory requires systems of minimal order, while the POD captures a maximum of energy with a minimum number of modes.

Among the **disadvantages** related to this method the following points can be underlined:

- This technique requires the knowledge of a two-point correlation tensor over a great number of points. Its use can then be limited by the size of the data sets that can quickly become huge.
- One of the most important limitations of the POD is called the "phase indetermination". This indetermination is due to the use of two-point correlations and appears for directions where a harmonic decomposition has to be used. It can be easily proven that if $\Phi(\chi'; k_3)$ is a solution of (27) then every eigenfunction $\Phi(\chi'; k_3)\phi(k_3)$, where $\phi(k_3)$ is a random phase function, will also be a solution. However this indetermination occurs only for the directions where a harmonic decomposition has been used. For the classical POD in particular, it is impossible to obtain directly a description of the preferred modes in the physical space. However, complementary techniques can be used in order to palliate this problem (Herzog 1986) or (Moin and Moser 1989). Dynamical systems theory can also provide this information indirectly.
- Another limitation of the POD resides in the intrinsic nature of the eigenfunctions. These eigenfunctions are directly related to the flow configuration from which they have been derived. The extrapolation of these functions to flows of a different nature, or to the same flow but with other physical parameters (geometry) or control parameters (Reynolds number, ...), can be difficult to undertake (see Sect. 4.6).

3.7 Some Typical Applications of POD

We present here only a brief overview of some notable applications of POD which can be found in the literature. The reader can refer to Holmes et al. (1996) for a more complete review on the topic.

The POD method was first applied to experimental data in 1967 by Payne (1966), Payne and Lumley (1967) to study the data sets obtained by Grant (1958) in the wake of a cylinder. These data were limited to a small part of the two-point correlation tensor and the measurement mesh was quite coarse and incomplete. To palliate this poor resolution, the authors used an ensemble of complementary techniques: Gram-Charlier decomposition (Payne 1966), (Frenkiel and Klebanoff 1967); use of a mixing length hypothesis and the continuity equation to estimate the remaining part of the correlation tensor. Contrarily to what they expected, the first POD mode did not really dominate the subsequent modes.[9] However, the first mode of the POD confirmed the approach of Townsend (1976) according to which the flow organization is dominated by large scale counter-rotating eddies which are inclined with respect to the wake axis ("Double Roller Eddy Model").

POD in Wall-Bounded Flows: Herzog (1986) performed a complete three dimensional POD analysis of the wall layer of a turbulent pipe flow using the correlation tensor obtained experimentally with neither interpolation nor approximation. The measurements of the streamwise and spanwise components of the velocities were used to estimate the first three POD eigenfunctions. Herzog found that approximately 60% of the total kinetic energy is contained in the first eigenmode. By use of the "Shot Noise" technique to palliate the initial phase loss due to the use of the two-point correlation tensor, Herzog reconstructed the zero phase structure in physical space and found a pair of counter rotating vortices with physical characteristics that match the results of Bakewell and Lumley (1967).

Later, these eigenfunctions were used by Lumley's group to develop a low order dynamical model for the coherent structures (e.g. (Aubry et al. 1988)).

Using the channel-flow data base of Kim et al. (1987) obtained by direct numerical simulation, Moin and Moser (1989) consider in particular the problem of phase loss related to POD. They propose different techniques to determine the original phase of the dominant structure. In this manner, these authors obtain what they call "characteristic eddies". The dominant eddy is found to contribute to as much as 76% of the turbulent kinetic energy.

[9] This quite "disappointing" result can be explained by the low resolution of the data sets and by the great number of "complementary techniques" used in this study.

POD in Free Shear Flows: Except for the initial study by Payne and Lumley (1967) of the cylinder wake, one of the first free shear flows to be analyzed was the annular jet mixing layer by Glauser and George. After a first application of the POD to the streamwise velocity component by Glauser et al. (1985), this approach was generalized to all the velocity components by Glauser and George (1987a), Glauser and George (1987b), Glauser et al. (1987). For the first time the correlation tensor was estimated by means of rakes of hot wires. In these studies, the jet was assumed approximately homogeneous in the streamwise direction and periodic in the azimuthal direction. These assumptions facilitate the use of the harmonic decomposition in these directions. The main results obtained are: (i) the first POD mode contributes to 40% of the total turbulent kinetic energy, demonstrating the efficiency of the POD in capturing kinetic energy; (ii) by studying the shape of the eigenfunctions and eigenvalues, the important role of a secondary mode exhibiting hexagonal symmetry can be emphasized; (iii) the authors were then able to propose a "life cycle" for the jet's structures.

Rajaee and Karlsson (1990) use the snapshot POD based on conditional phase averaged measurements in a plane mixing layer. This approach was 2D in the sense that they only consider a slice of the flow. From this study a low order model has been proposed for the plane mixing layer (Rajaee et al. 1994).

Delville et al. (1990), Delville (1994), Delville (1995), Ukeiley (1995), Cordier (1996) apply the classical POD (3D approach) to a plane turbulent mixing layer. From these studies low order dynamical systems are developed. Selected results of this study will been presented later in this chapter.

Cao (1993) uses experimental data measured by Guezennec and Gieseke (1991) to apply POD in the far wake of a cylinder. Retrieving the typical wake organization, the author can derive a low-dimensional dynamical system based on the first mode of the POD.

POD in Transitional Flows: To study the transition to turbulence on a rotating flat disk, Aubry et al. (1994) applied biorthogonal decomposition techniques to experimental data from one-point measurements. The evolution of the system's global entropy with the Reynolds number is studied. As the Reynolds number increases, the entropy increases, revealing that the distribution of the energy tends to become more uniform between the different modes. The same typical results were obtained by Rempfer and Fasel (1991), Rempfer and Fasel (1994a) in the study of the transition over a flat plate.

3.8 Some Typical Results: Application to the Plane Mixing Layer.

We present here selected results which illustrate the application of the POD to a plane mixing layer experiment, where the applied decomposition is of increased complexity. The POD corresponds to the resolution of eigenvalue problems of the following type:

$$\sum_{j=1}^{n_c} \int_{\mathcal{D}} \Psi_{ij}(\boldsymbol{x}, \boldsymbol{x}'; \boldsymbol{k}) \Phi_j^{(n)}(\boldsymbol{x}'; \boldsymbol{k})\, d\boldsymbol{x}' = \lambda^{(n)}(\boldsymbol{k}) \Phi_i^{(n)}(\boldsymbol{x}; \boldsymbol{k}) \tag{29}$$

where n_c is the number of components used for this POD. In the above equation, $\Psi_{ij}(\boldsymbol{x}, \boldsymbol{x}'; \boldsymbol{k})$ is the cross-spectrum of $u_i u_j$ and corresponds to the Fourier transform of the space time correlation $R_{ij}(\boldsymbol{X}, \boldsymbol{X}')$ in the "homogeneous" directions. According to the value of n_c and the number of flow directions used in the POD resolution, different levels of decomposition can be defined, taken into account progressively the complexity of the flow organization.

Experiments which will be used as a guideline throughout this analysis were performed in the asymptotic region of a plane turbulent incompressible mixing layer (Fig. 1). These experiments were undertaken by using rakes of hot X-wires (up to 24 X-wires probes are simultaneously used) and simultaneous sampling. The advantages of using this measurement technique are twofold: space-time correlations can be calculated very easily (the number of measurement configurations is greatly reduced) - this provides a means to access the projection coefficients of POD (see (37)). A complete description of the experimental apparatus can be found in (Delville 1995).

Pure Spatial POD: $n_c = 1$, $\boldsymbol{x} \equiv y$, (here $\boldsymbol{k}$ is not taken into account).
For sake of simplicity, a one-dimensional decomposition is first considered, where only the u component and the inhomogeneous direction y are taken into account.

$$\int_L R(y, y') \phi_u^{(n)}(y')\, dy' = \lambda^{(n)} \phi_u^{(n)}(y) \tag{30}$$

where $\phi_u^{(n)}$ and $\lambda^{(n)}$ are the n^{th} eigenvector and eigenvalue and $R(y, y')$ is the two-point correlation.

For this decomposition, eigenvalues are real scalars. The first mode of the POD is found to account for about 37% of the turbulent energy and 63% is contained in the first three modes. The POD is typically seen as a generalization of harmonic analysis for the inhomogeneous directions, which is consistent with the fact that the POD eigenfunctions behave in the same

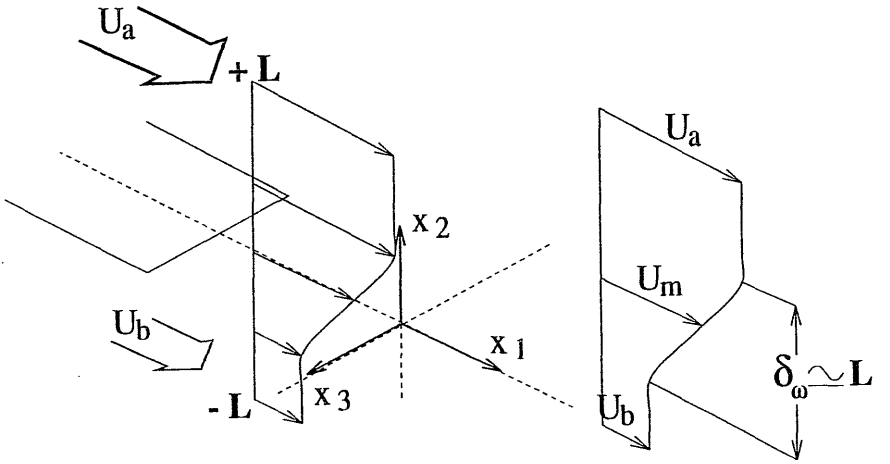

Fig. 1. Experimental configuration for the mixing layer experiment

manner as Fourier modes (Moin and Moser 1989), (Chambers et al. 1988), namely, the number of zero-crossings increases with the order of the eigenfunction. This feature is illustrated in Fig. 2 where the first 4 eigenfunctions obtained from a scalar POD based on the u component of the velocity are plotted.

We will now consider more complex decompositions, where the number of velocity components and/or the number of of spatial directions are increased.

POD in Space-Frequency Domain (POD_{uv}): $n_c = 2$, $\boldsymbol{x} \equiv y$, $\boldsymbol{k} \equiv f$.
In this POD, where the temporal dependence (via the frequency) and two components of velocity are considered, the eigenvalues are functions of frequency. By integrating these eigenvalues with respect to frequency, their relative contribution to the turbulent energy can be examined. The first mode is found to contain 44% of the energy while the first three modes contain about 71% of this energy. From Fig. 3, where the evolution with frequency of the first three eigenvalues obtained by this vectorial POD_{uv} are plotted, one can note the rapid convergence of the eigenvalues $\lambda^{(n)}(f)$, in accordance with the POD theorem. For each value of the frequency, the first mode dominates fully the higher modes.

The relative value of the eigenvalues expresses the level of organization of the flow for the mode and frequency considered. Hence, the amplitude of the eigenvalues increases with the importance of the associated organization. In the case of the POD_{uv}, the first mode is maximum for $f_{max}\delta_\omega/U_c = 0.3$, which is the typical Strouhal number found for the passage of structures

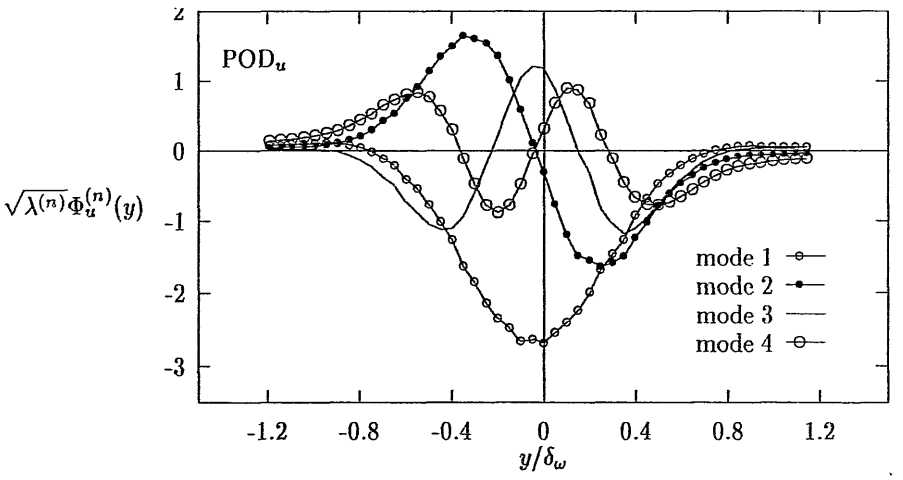

Fig. 2. Shape of the first four eigenvectors of the POD based on u in the plane mixing layer.

(from spectral analysis at the edge of the mixing layer). Hence, it seems that the first POD mode is able to capture a major feature of the flow: its spatio-temporal organization.

In this POD, eigenvectors are complex functions of y and f. Their moduli are plotted in Fig. 4. In this plot, the modulus is weighted by the square root of the corresponding eigenvalue, to take into account the statistic importance of the mode for the frequency domain considered. One can note the presence of two local maxima at $|y|/\delta_\omega \sim 0.5$ for $\Phi_u^{(1)}$, which can be interpreted as the footprint of the large-scale structure at the edge of the mixing layer.

POD$_{3D}$: $n_c = 3$, $\boldsymbol{x} \equiv y$, $\boldsymbol{k} \equiv (f, k_z)$.

In this more complex vectorial POD application, referred to in the following as POD$_{3D}$, the spanwise direction z and the temporal direction are assumed to be respectively homogeneous and stationary on average. Hence the eigenfunctions used in these directions are Fourier modes. The cross-stream direction y, which is strongly inhomogeneous, is examined with the POD. The integral Fredholm equation that must be solved for this application of the POD is then:

$$\sum_{j=1}^{n_c} \int_D \Pi_{ij}(y, y'; f, k_z)\Phi_j^{(n)}(y'; f, k_z)dy' = \lambda^{(n)}(f, k_z)\Phi_i^{(n)}(y; f, k_z) \tag{31}$$

$i = 1, \ldots, n_c$

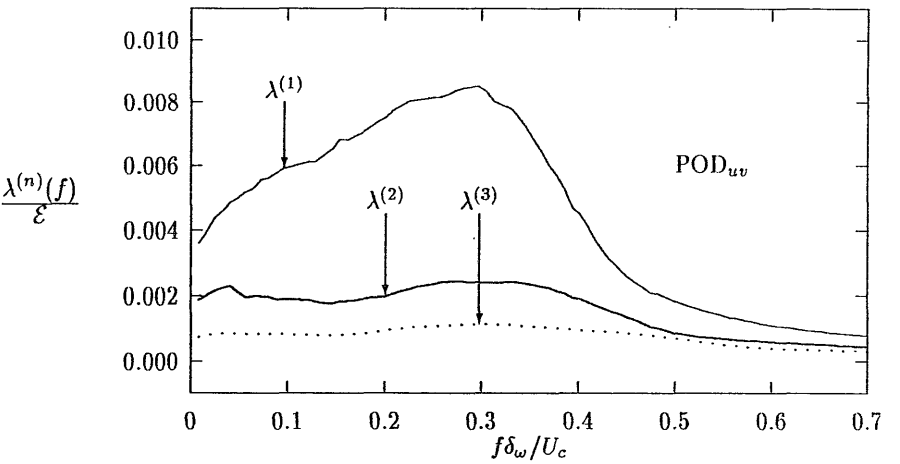

Fig. 3. First 3 eigenvalues. Vectorial POD based on uv. (here $\mathcal{E}$ is the turbulent energy contained in the whole domain.)

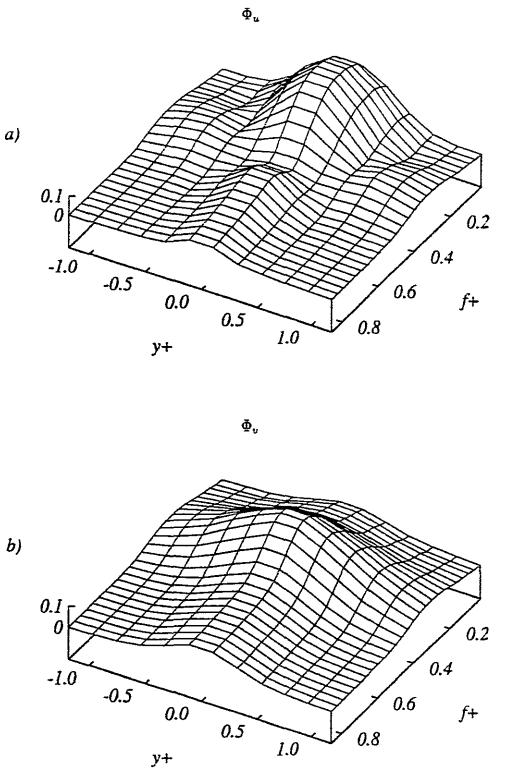

Fig. 4. Shape of the first eigenvector in the frequency domain. Vectorial POD based on uv. Plotted: $\sqrt{\lambda^{(1)}(f)} \cdot ||\Phi_i^{(1)}(y,f)||$. *a*) u component; *b*) v component. ($y+= y/\delta_\omega$ and $f+= f\delta_\omega/U_c$)

where $\Pi_{ij}(y, y'; f, k_z)$ is the *cross-spectral tensor* which is defined as the Fourier transform of R_{ij}.

• *Eigenvalues* In this POD eigenvalues are real functions that depend on frequency and spanwise wavenumbers. When integrated over wavenumbers and frequency the contribution of the first mode to energy is 49% and the contribution of the first three modes is 75%. When comparing the 3 PODs described here, it is remarkable that the amount of energy captured by the first modes increases with the number of degrees of freedom of the flow which are taken into account.

The shape of the eigenvalue spectra $\lambda^{(1)}(f, k_z)$ for the first mode is shown in Fig. 5(a). For this mode, two maxima are discernible: a very well defined maximum located at $f\ \delta_\omega/U_c \sim 0.3$ and another less pronounced one for $k_z\delta_\omega = 0.5$. These two maxima correspond to the dominant lengthscales present in the core of the mixing layer (Delville 1995) and are the footprint of the two main types of organization present within the mixing layer (quasi 2D large-scale structure and longitudinal vortices). Thus the POD is able to capture the main features of the flow. The rapid convergence of POD can be illustrated by analyzing Fig. 5(b). This figure (where the vertical scale is expanded by a factor of 5) presents the eigenvalue spectra of the second mode. The good representation of the first mode is also made evident when comparing the eigenvalue for this mode (Fig. 5(a)) to the summation of all the modes of the POD plotted in Fig. 5(c).

• *Turbulent Kinetic Energy Reconstruction:* $\boldsymbol{k} \equiv (f, k_z)$
For each value of y in the inhomogeneous direction, the local contribution of the different POD modes to the Reynolds stresses can be retrieved from the integral in the two homogeneous directions of the spectral tensor:

$$\overline{u_i' u_j'}(y) = \int_{-\infty}^{+\infty} \int_{-\infty}^{+\infty} \Psi_{ij}(y; f, k_z)\, df\, dk_z \tag{32}$$

In the same manner, we can determine the contribution of POD mode number (n) with the relation:

$$\overline{u_i' u_j'}^{(n)}(y) = \int_{-\infty}^{+\infty} \int_{-\infty}^{+\infty} \Psi_{ij}^{(n)}(y; f, k_z)\, df\, dk_z \tag{33}$$

where $\Psi_{ij}^{(n)}$ is rebuilt from the eigenvalues and eigenfunctions of the POD:

$$\Psi_{ij}^{(n)}(y; f, k_z) = \lambda^{(n)}(f, k_z)\Phi_i^{(n)}(y; f, k_z)\Phi_j^{*(n)}(y; f, k_z) \tag{34}$$

The Reynolds stresses reconstructed from the first POD modes (POD_{3D}) are compared, in Fig. 6, to those directly measured. For each y location in the inhomogeneous direction, the same trend is noted for the evolution of eigenvalues (see Fig. 5): the first mode is more energetic than the others, etc.

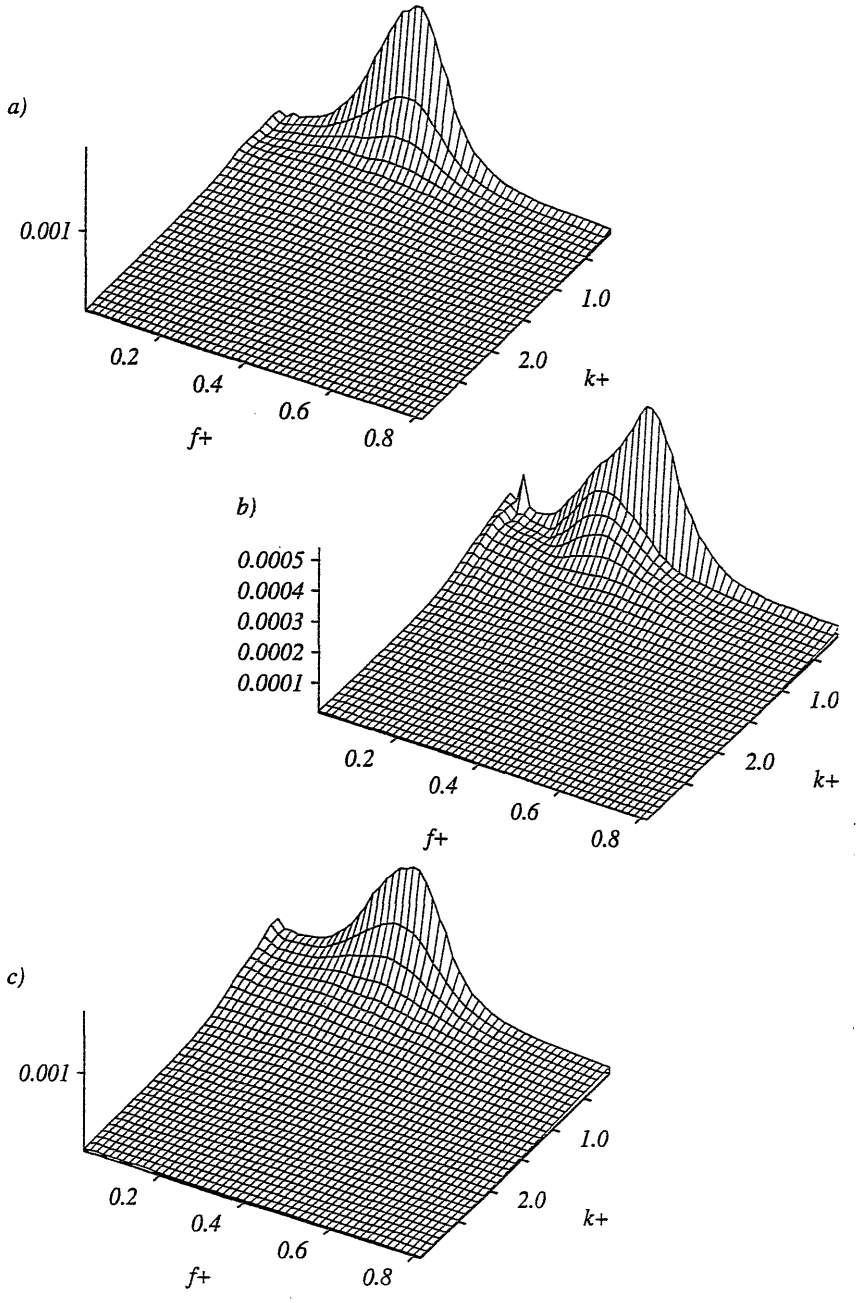

Fig. 5. Evolution of eigenvalues $\lambda^{(n)}(f, k_z)$. (POD_{3D}). *a*) mode 1; *b*) mode 2; *c*) cumulative contribution of all modes. $f+= \dfrac{f\delta_\omega}{U_c}$, $k+= k_z\delta_\omega$.

.... This result shows that the global rapid convergence of POD, which can be found from the eigenvalues, is also a local characteristic. Even if the POD is the best decomposition in terms of turbulent energy (i.e. for the trace of the Reynolds stress tensor) it is remarkable to see how well predicted the Reynolds stress component $\overline{u'v'}$ is. This behavior seems to be a universal characteristic of this decomposition and has already been mentioned by several authors (e.g. Moin and Moser (1989)).

Instantaneous Signal Reconstruction: In the framework of a feedback control of large-scale structures, it is necessary to obtain a real time description of the instantaneous flow field, at least in terms of large-scale structure. In the context of POD and dynamical systems, this questions the ability of POD to reconstruct instantaneous signals or velocity fields.

The phase indetermination of POD that was recalled on page 223 suggests that this may be impossible due to the use of two-point correlations. However if rakes of probes are used, this could become possible. The use of rakes of sensors allows one to access the instantaneous contribution of any given mode to the velocity field. For any type of POD used, the way to retrieve this contribution is to calculate first the projection coefficient on the POD basis (e.g. (12)) and then to construct the contribution of this mode to the velocity field (e.g. (11)). For example, in the case of POD_{uv} this can be done by computing as follows:

$$u_i^{(n)}(y,t) = \int \Phi_i^{(n)}(y, t-\tau) a^{(n)}(\tau)\, d\tau \tag{35}$$

or, in the Fourier space:

$$\widehat{u_i}^{(n)}(y,f) = \widehat{a}^{(n)}(f)\widehat{\Phi_i}^{(n)}(y,f) \tag{36}$$

where

$$\widehat{a}^{(n)}(f) = \sum_{i=1}^{n_c} \int_{\mathcal{D}} \widehat{u_i}(y,f)\widehat{\Phi_i}^{*(n)}(y,f)\, dy \tag{37}$$

Figure 7 shows an example of the contribution of the first POD modes to the velocity signal measured on the mixing layer axis when $n_c = 1$. Clearly the first mode is able to predict the behavior of the large scale evolution of the signal. When using three modes, the reconstruction is found to be very similar to the measured signal. An example of the reconstruction obtained when n_c=2 can be found in Fig. 10(a), where the same conclusion can be derived, when compared to the directly measured velocity plotted in Fig. 8(a).

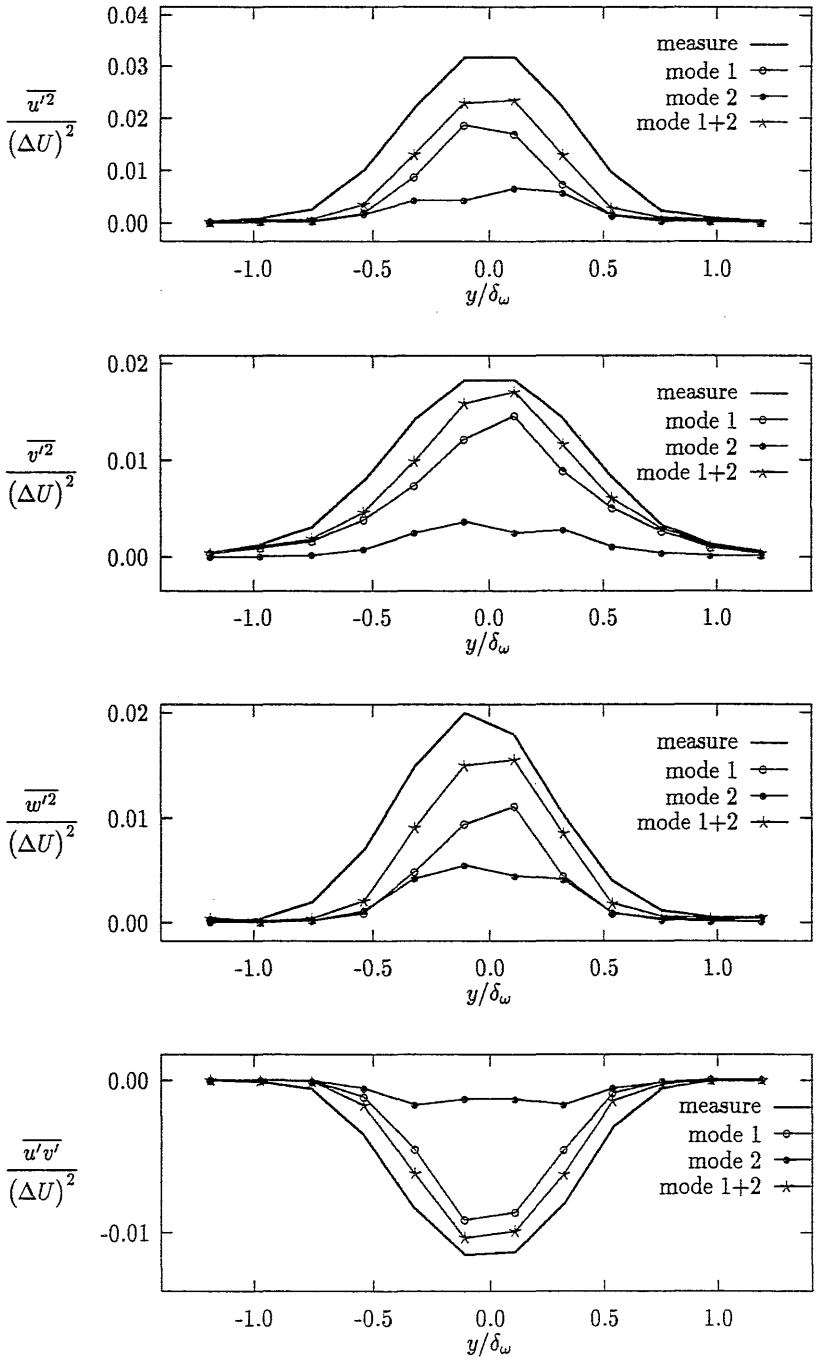

Fig. 6. Contribution of the first POD modes to the Reynolds stresses. (POD_{3D}). Plane mixing layer.

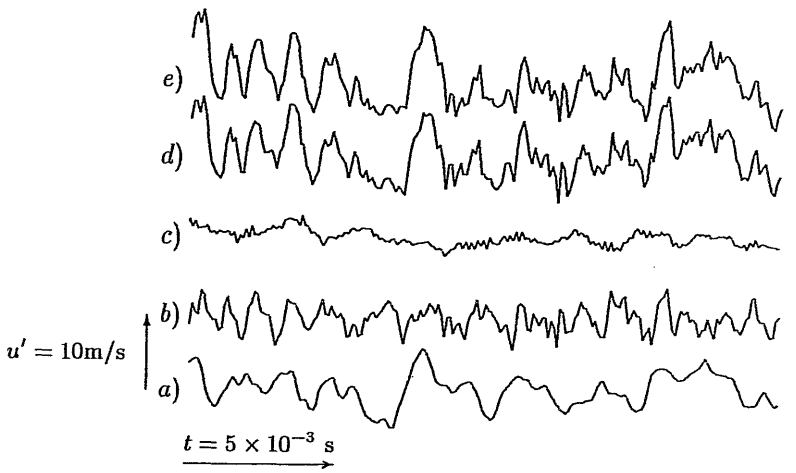

Fig. 7. Contribution of the first modes of the POD ($n_c = 1$) to the instantaneous velocity on the mixing layer axis: *a*) 1^{st} mode; *b*) 2^{nd} mode; *c*) 3^{rd} mode; *d*) summation over the first three modes; *e*) measured velocity.

Some Remarks Related to the Use of POD Based Dynamical System Approach. The above examples show several features that are favorable to the dynamical systems approach, based on the POD modes. Here, we limit our attention to the first mode. In terms of turbulence, this mode contains about 50% of the turbulent energy, and thus seems able to give a good approximation for the convective terms (function of k). It is also representative of the productive terms (function of $\overline{u'v'}$). In terms of flow organization, this mode contains most of the significant dominant scales of the flow. On the other hand, using the first modes of the POD, it is possible to reconstruct the instantaneous features of the large-scale structure.

However it should be noted that the best energy representation is obtained when the number of degrees of freedom is increased. More precisely, one can ask about conclusions that can be derived from a "degenerated" POD application. POD based on only one component of velocity is such a case.

3.9 LSE and Complementary Technique.

One important aspect in terms of flow control is to be able to access the coefficients $a(t)$ of the POD. We have seen that in order to be able to estimate the $a(t)$, it is necessary to know the velocity over the whole flow extent in such a way that (11) can be used. For practical considerations, this can be done only by performing flow simulations or very detailed laboratory experiments. For industrial applications, the number of sensors obviously has to be reduced. We present here a method by which this reduction can be achieved.

This method uses Linear Stochastic Estimation (LSE) as introduced by Adrian (1975). We will then focus on a complementary technique which employs the LSE method to estimate the $a(t)$ from a very reduced experimental configuration.

Linear Stochastic Estimation: Adrian (1975) studied conditional flow structures in isotropic turbulence by computing estimates of the velocity $u(y+r,t)$ given that the velocity at (y,t) assumes some specified value $u(y,t)$. It was found that this simple flow, when sampled in a statistical sense, demonstrates the existence of organized structures. Tung and Adrian (1980) studied the influence of the second, third and fourth order terms on the estimate. Their results indicated that the contribution from higher order terms to the overall estimate was insignificant, hence the use of the linear stochastic estimate can be justified in the present study.

A one-dimensional (in y) linear stochastic estimation yields an estimate

$$\tilde{u}_i(y',t) = A_{ij}(y')u_j(y,t) \tag{38}$$

with A_{ik} computed from

$$\overline{u_j(y)u_k(y)}A_{ik}(y') = \overline{u_j(y)u_i(y')} \tag{39}$$

where $\overline{u_j(y)u_k(y)}$ and $\overline{u_j(y)u_i(y')}$ are the Reynolds stress and two-point correlation tensors, respectively. It should be noted that for these systems of equations, only the two-point space (in y) correlation data is utilized. These systems **are not** a function of the condition being investigated. This estimation may be easily extended to several dimensions. For further discussion on the Stochastic Estimation theory see (Adrian and Moin 1988), (Cole et al. 1992) and (Guezennec 1989). For further details and discussion on the LSE theory, the reader can refer to Adrian (1996).

Stochastic estimation uses the conditional information specified about the flow at one or more locations in conjunction with its statistical properties (the two-point correlation tensor) to estimate the information at the remaining locations. Here the thrust will be to utilize the instantaneous velocity at select y locations in the flow to estimate the instantaneous velocity for all y locations. A simple test has been performed for the mixing layer data. Here the instantaneous velocity is available at all y locations (where there are probes). In many other experiments, this is not the case due to a lack of a sufficient number of channels of hot-wire anemometry data acquisition and A/D conversion. Hence, it is advantageous to use the rake data base since it allows us to check the validity of the approach by comparison between estimated

and measured time series. Note that a minimum of two probes and associated hardware are necessary to apply the following ideas to any experiment because of the need for the **two-point** statistics.

We estimate the velocity components across the mixing layer from the expansion of (38) using the actual velocity components at select positions in y. Here, it is not the intent to present a detailed discussion on what number of probes or their respective positions are the most appropriate to obtain the best estimate of the velocity field. These issues are discussed in (Delville et al. 1993) for the present mixing layer and in (Cole et al. 1992) for a jet mixing layer.

Figure 8(a) presents the vector plot of the **measured** velocity field. Figures 8(b) through (d) show various linear stochastic estimates of the vector field where the condition points are indicated by the arrows. Figure 8(b) presents a one-point estimate, whereas Figs. 8(c) and (d) present two-point estimates. For the two-point cases, the probes which supply the condition are equally spaced on either side of the centerline. Comparison of Figs. 8(b) through (d) with Fig. 8(a) indicates the quality of each respective estimate. It is clear that the estimate shown in Fig. 8(d) provides the best comparison. Note, in particular, that both the amplitude and phase of the velocity vector field are reasonably preserved with this estimate.

Three-Dimensional Estimation. This method can be easily extended to a three-dimensional estimation of the flow field. Such an estimation is given in Fig. 9. In this case, the information obtained from only five probes of the same rake have been used in order to estimate the full vorticity field surrounding the rake ($\Omega = (\omega_x^2 + \omega_y^2 + \omega_z^2)^{0.5}$) at a given time. To accomplish this, it was necessary to measure the full two-point correlation tensor for the spanwise and plate-normal directions. The third direction (streamwise) is dealt with by using Taylor's hypothesis. Note that signals containing information from only two components of velocity can be used to generate (through the intercomponent correlations) information about the third one through LSE.

Complementary Technique. The estimated time series shown in Fig. 8(d) will be used in conjunction with the POD to implement the complementary technique. This complementary technique consists of three main steps. First, the eigenvectors and eigenvalues are obtained from direct application of the POD to a two-point spectral tensor as discussed in Sect. 3. Second, the LSE is applied to the cross correlation tensor, and multi-point estimates of the random vector field are computed as presented above for the mixing layer. Third, the eigenvectors obtained from step one are projected onto the estimated velocity field obtained from step two to obtain *estimated* random coefficients. These estimated random coefficients are then used in conjunction with the

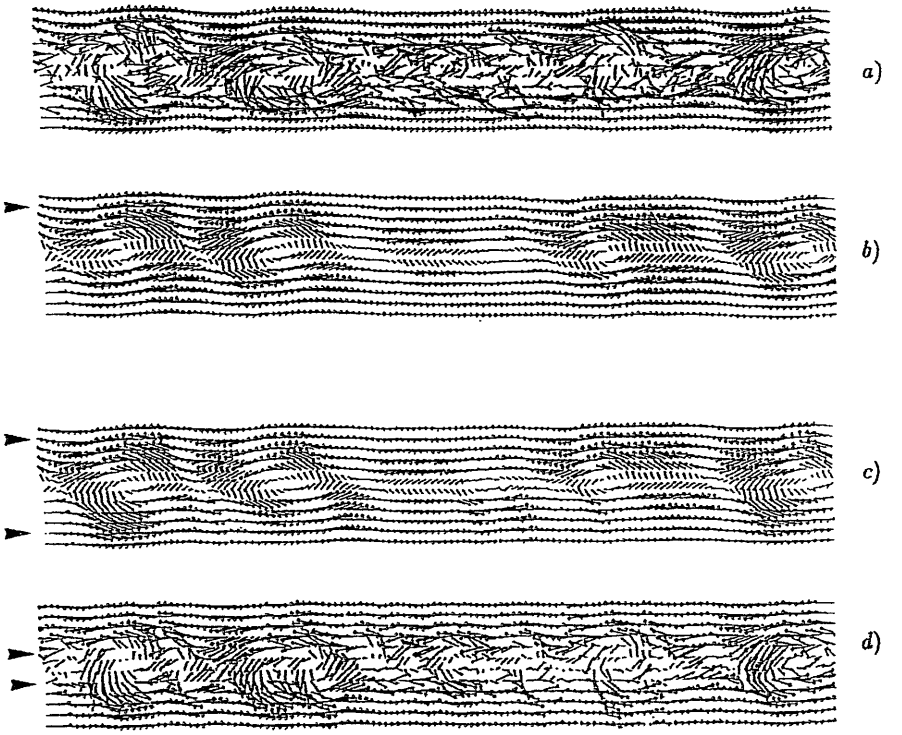

Fig. 8. Examples of Linear Stochastic Estimations for several conditions. (a) Original instantaneous velocity vector plot; (b) LSE with 1 condition; (c) and (d) with 2 conditions. The reference signals are indicated by the arrows on each example.

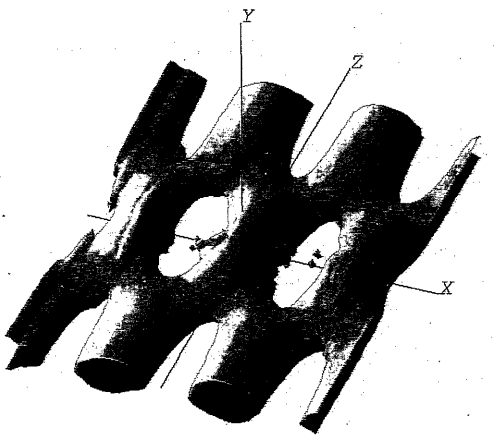

Fig. 9. Example of three-dimensional Linear Stochastic Estimation. Isosurface of the modulus of vorticity Ω. From Vincendeau (1995).

POD eigenvectors to reconstruct the estimated random velocity field.

Mathematically the stochastic estimates of the random coefficient are calculated from:

$$a_n^{est}(f) = \int \hat{u}_i^{est}(y,f)\psi_i^{(n)*}(y,f)dy \tag{40}$$

where in this case $\hat{u}_i^{est}(y,f)$ is the two-point linear stochastic estimate of the velocity field and $\psi_i^{(n)*}(y,f)$ is obtained from the original POD eigenvalue problem. The estimated streamwise velocity can be reproduced in Fourier space by

$$\hat{u}_i^{est}(y,f) = \sum_{n=1}^{\infty} a_n^{est}(f)\psi_i^{(n)}(y,f) \tag{41}$$

and then inversely transformed to obtain $\hat{u}_i^{est}(y,t)$. For further details on this technique refer to Bonnet et al. (1994), Glauser et al. (1993) and Ukeiley et al. (1993).

Figure 10(a) shows the contribution from the first POD mode using the **measured** instantaneous velocity field, Fig. 8(a), in the projection as presented in the previous section. The first POD mode retains most of the large scale features exhibited in the original field. The application of the complementary technique is shown in Fig. 10(b). Here the eigenvectors, obtained from direct application of the POD, are projected onto the estimated field using the estimated data presented in Fig. 8(d). Reasonable estimates of the large scale structure are obtained, even though only 17% of the **measured** instantaneous data has been used. In fact, one sees that Fig. 10(b) compares quite well to Fig. 10(a), which was computed using the full **measured** instantaneous velocity field.

In order to quantitatively assess the technique, the streamwise root mean squared (RMS) velocities are computed from the estimated and original velocity fields and comparisons are made, see Fig. 11. The percentage of the streamwise RMS velocity captured using the complementary technique is very close to that obtained from the direct application of the POD for the first mode. These results show that the complementary technique, which combines LSE and POD, allows one to obtain time dependent information from the POD while greatly reducing the amount of instantaneous data required. Hence, it may not be necessary to measure the instantaneous velocity field at all points in space *simultaneously* to obtain the phase of the structures, but only at a few select spatial positions.

A recent—and illustrative—use of this complementary method has been developed at the IMFT in Toulouse. From the work of Faghani (1996), the

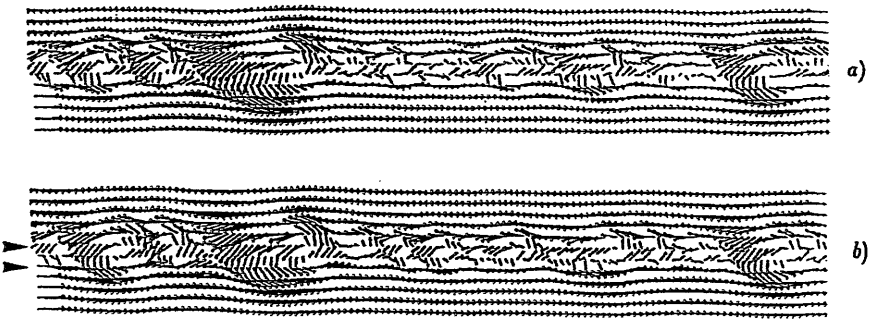

Fig. 10. Complementary technique. (a) first POD mode from full measurement field; (b) reconstructed using the stochastically estimated field. For original velocity field refer to Fig. 8(a).

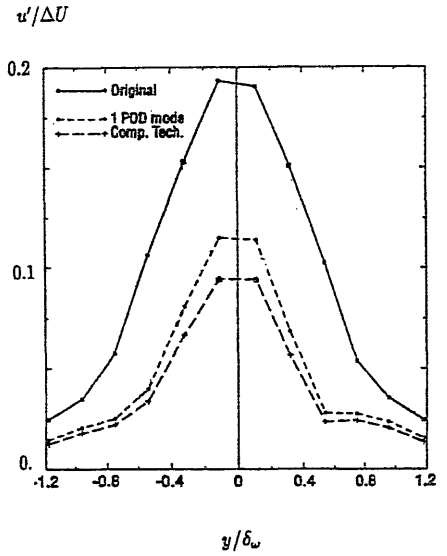

Fig. 11. Comparisons of RMS value of the u component

objective was to provide a POD analysis of a plane turbulent jet. Providing that only two probes were available, the author first used an artificially excited flow from which he was able to compute a phase locked average. Simple use of "instantaneous" reconstruction by POD is then possible. In addition, through LSE, the author was able to estimate the time histories from two available ("conditional" after Adrian) signals. The comparison between the direct POD and the complementary approach was quite successful, similar to the comparison between rakes of hot wires and complementary techniques which has been demonstrated. As a second step, Faghani used directly the complementary method in the case of a natural (unforced) plane turbulent jet. In this case no other validation is available but the comparison with

the excited case provides enough confidence in this approach. Based on our knowledge, this example represents the first use of the complementary method where no alternative to the instantaneous POD analysis exists.

4 Flow Control by POD based Dynamical Systems

4.1 Deterministic Approach of Turbulence

Low Order Dynamical System. Lorenz (1963) was the first who expressed the links between dynamical system and turbulence. His first objective was to elaborate a crude description of the earths atmosphere, that can be simulated on the small computers available at this time. As a first attempt, he proposed to model two-dimensional Rayleigh Bénard convection by a set of three ODE. These equations were obtained by a severe truncation of the Galerkin projection of the Boussinesq equations onto Fourier modes. For typical values of the control parameter, he demonstrated that this system can behave chaoticly.

Later, Ruelle and Takens (1971) conjecture for Navier-Stokes equations, defined on a bounded domain and under certain conditions, the existence of a mathematical object they called a strange attractor. They suspect that, for this system, a chaotic regime can be reached through a limited, finite, number of successive bifurcations. This hypothesis was contradictory with the scenario proposed by Landau (1944) or Hopf (1948). For these authors, turbulence corresponds to an infinite number of bifurcations, i.e. an infinite number of modes is necessary for a correct description. In constrast, the approach introduced by the work of Ruelle and Takens is then very attractive: *describe a problem of probably infinite dimension whose solutions are random, with a deterministic model of low dimension.* This reduction to a small number of interacting modes can find a physical justification in the sense that turbulence is a dissipative process.

Clearly, such an approach is of immediate interest for flow control. Indeed, if a limited set of ODE is sufficient to describe turbulent flows, the two objectives described above (see p. 204) can be fulfilled. It should be easier to test flow control strategies, and the short term prediction of the relevant dynamics of the flow can be computed in real time.

Limitations of Low Order Dynamical System Modelisation. The main question arising is to evaluate *up to which level a fully turbulent flow can be described by a low order system.* It should be recalled that, for the present approach of flow control, only the large-scale structure behavior is needed. In the case of confined flow - i.e. for systems strongly constrained by walls (Rayleigh Bénard convection, Taylor-Couette flow, ...) important progress has been obtained with this kind of model. For these flows, the initial instability and the transition to turbulence have been described by

several scenarios (see: Le chaos, théorie et expériences 1988, Swinney 1983). Nevertheless, for these kinds of confined flows only a limited amount of modes can interact ; mainly temporal chaos appears and the spatial organization remains relatively strong (see (Manneville 1991) for example).

However, when the degree of confinement decreases, the spatial disorder develops rapidly. An important number of temporal and spatial scales then interact. The standard approach of Dynamical Systems based only on a temporal evolution can then become useless for a correct description of turbulence. It follows that it may become intricate to relate Navier-Stokes equations to a low order system. But even when this is performed, the results, obtained from the low order system (e.g. existence of a strange attractor), may be difficultly extrapolated to the "real" configuration. As a consequence, a low order dynamical system modelisation of any given flow configuration cannot be guaranteed.

Low Order Models and Coherent Structures. Hussain (1986) argued about the role of large-scale structure or coherent structures in turbulence modeling: "*While turbulent flows (or for that matter, all flows) have infinite degrees of freedom, the motion of coherent structures, being large scale and organized, is likely to be low-dimensional.*" The existence of coherent structures within the fully turbulent flow is one of the elements that allows a model, based on a low order dynamical system, to lead to an efficient description. This is particularly true when large-scale structures are used to control is the flow.

It has been shown that the POD is a very powerful tool associated with the concept of large-scale structure. Then, it seems natural to make use of the corresponding eigenfunctions to build a dynamical system. In this case, the dynamical system will be based on the optimal—in an energetic sense—decomposition, with specific, flow dependent eigenfunctions. The following section will recall some fundamental points for the development of a dynamical system.

4.2 Development of POD Based Dynamical System

General Method. This part presents only the general method used to derive a low-order dynamical model of the flow under investigation, by use of a POD basis. The possibilities and limitations of this approach are investigated in detail by (Rempfer 1996).

If $\boldsymbol{u}(\boldsymbol{x},t)$ is a set of flow realizations,[10] Navier-Stokes equations for incompressible flows can be written symbolically as:

[10] Notations $\boldsymbol{u}$ and $\boldsymbol{x}$ are respectively the velocity vectors and the position within the flow.

$$\frac{\partial \boldsymbol{u}}{\partial t} = \boldsymbol{F}(\boldsymbol{u}) \text{ avec } \boldsymbol{u} = \boldsymbol{u}(\boldsymbol{x}, t) \;\; \boldsymbol{x} \in \mathcal{D} \text{ and } t \geq 0 \tag{42}$$

where $\boldsymbol{F}$ is a differential operator that contains only spatial derivatives and where $\mathcal{D}$ is the spatial domain under study. The problem is mathematically well defined with:

– boundary conditions[11]

$$\boldsymbol{B}\big(\boldsymbol{u}(\boldsymbol{x})\big) = \boldsymbol{h}(\boldsymbol{x}, t) \text{ with } t \geq 0, \boldsymbol{x} \in \partial\boldsymbol{\mathcal{D}} \tag{43}$$

– and initial conditions

$$\boldsymbol{u}(\boldsymbol{x}, 0) = \boldsymbol{u}_0(\boldsymbol{x}) \tag{44}$$

In order to transform the PDE (42) in a set of ODE, the development on the POD basis is introduced:

$$u_i(\boldsymbol{x}, t) = \sum_{m=1}^{N_{POD}} a^{(m)}(t) \bar{\Phi}_i^{(m)}(\boldsymbol{x}) \tag{45}$$

where N_{POD} is the number of modes used in the POD. The following equation is then obtained:

$$\sum_{m=1}^{N_{POD}} \frac{\mathrm{d}a^{(m)}(t)}{dt} \bar{\Phi}_i^{(m)}(\boldsymbol{x}) = \boldsymbol{F}\Big(\sum_{m=1}^{N_{POD}} a^{(m)}(t) \bar{\Phi}_i^{(m)}(\boldsymbol{x}) \Big) \tag{46}$$

The set of spatial eigenfunctions $\bar{\Phi}_i^{(m)}(\boldsymbol{x})$ being a basis, the RHS of (46) can be written as:

$$\boldsymbol{F}\Big(\sum_{m=1}^{N_{POD}} a^{(m)}(t) \bar{\Phi}_i^{(m)}(\boldsymbol{x}) \Big) = \sum_n \boldsymbol{\mathcal{F}}^{(n)}\big(a^{(1)}, \cdots, a^{(n)}(t)\big) \bar{\Phi}_i^{(n)}(\boldsymbol{x}) \tag{47}$$

Taking into account the orthogonality of the eigenfunctions $\bar{\Phi}_i^{(n)}(\boldsymbol{x})$ one obtains:

$$\boldsymbol{\mathcal{F}}^{(n)} = \left(\bar{\boldsymbol{\Phi}}^{(n)}, \boldsymbol{F}\Big(\sum_{m=1}^{N_{POD}} a^{(m)}(t) \bar{\Phi}_i^{(m)}(\boldsymbol{x}) \Big) \right) \tag{48}$$

Finally, the Galerkin projection of (42) onto the POD eigenfunctions, has to be evaluated:

$$\Big(\bar{\boldsymbol{\Phi}}^{(n)}, \frac{\partial \boldsymbol{u}}{\partial t}\Big) = \big(\bar{\boldsymbol{\Phi}}^{(n)}, \boldsymbol{F}(\boldsymbol{u})\big) \text{ for } n = 1, \ldots, N_{gal} \tag{49}$$

where N_{gal} is the number of Galerkin modes kept in the projection.

The set of PDE (42) can now be expressed as:

[11] The notation $\partial\boldsymbol{\mathcal{D}}$ represents the boundary of the domain $\mathcal{D}$.

$$\frac{da^{(n)}(t)}{dt} = \mathcal{F}^{(n)}\left(a^{(1)}(t), \cdots, a^{(n)}(t)\right) \text{ with } n = 1, \cdots, N_{gal} \tag{50}$$

The functions $\mathcal{F}^{(n)}$ defined by (48) are linear, if $\boldsymbol{F}$ is a linear operator. In the case of Navier-Stokes equations, because of the convective terms, $\mathcal{F}^{(n)}$ are quadratic functions of $a^{(n)}$.

In order to obtain a well posed mathematical problem, one needs to add a set of initial conditions to (50). These conditions can be directly inferred from the conditions (44) imposed by the original problem:

$$a^{(n)}(t=0) = a_0^{(n)} \text{ with } a_0^{(n)} = (\boldsymbol{u}_0(\boldsymbol{x}), \boldsymbol{\Phi}^{(n)}) \tag{51}$$

Boundary conditions. When comparing the initial problem described by (42) to (44) with the problem obtained after the Galerkin projection (50 and 51), it can be seen that these two problems are not equivalent. An equation is missing in the second formulation. This imposes to prescribe additional boundary conditions.

Before describing practical cases, a preliminary remark should be emphasized. An important property of the spatial eigenfunctions is that because they can be expressed in terms of flow realizations:

$$\Phi_i^{(n)}(\boldsymbol{x}) = \sum_{k=1}^{N_{POD}} q^{(n)}(t_k) u_i(\boldsymbol{x}, t_k) \qquad n = 1, \ldots, N_{POD} \tag{52}$$

these eigenfunctions possess the same properties as the flow field $u_i(\boldsymbol{x}, t)$ itself. Particularly, the continuity equation will be verified individually by each POD eigenfunction, therefore for incompressible flows, $\operatorname{div} \boldsymbol{\Phi}^{(n)} = 0$. In the same way, this consideration allows one to consider two cases where boundary conditions play a different role:

- if the boundary conditions (43) are homogeneous and linear then the POD eigenfunctions implicitely verify the same conditions and it is not necessary to add another equation.
- If this is not the case, special care is needed. This case can be found for example in:
  - the study of transition over a flat plate (Rempfer and Fasel 1994a), (Rempfer and Fasel 1994b), (Rempfer 1996),
  - the study of near wall region in a turbulent boundary layer (Aubry et al. 1988).

In the case where the boundary conditions are inhomogeneous, but known, they can be taken into account by adding complementary equations in a way similar to the method of Galerkin-Tau (Fletcher 1984).

Examples of Applications. In this section, we present a non exhaustive list of studies in which empirical eigenfunctions were used to construct low-dimensional models and some attempt was made to analyse their dynamical behavior. We especially provide a brief survey of applications related to flow control. We have selected two classes of typical flows: wall flows and open flows systems. A more complete and detailed review can be found in (Berkooz et al. 1993) and (Holmes et al. 1996).

Wall flows models: To this date, the best studied low-dimensional model is that developed for the wall region of a turbulent boundary layer. Mainly, two different groups work on this subject: Lumley's group (Berkooz, Holmes, Lumley: Cornell University; Aubry, Sanghi: B. Levich Institute; Stone: Arizona State University) and Sirovich's group (Sirovich, Zhou, Handler, Levich: Brown University). These approaches are based on the pioneering work of Aubry et al. (1988) who used the experimentally determined eigenfunctions of Herzog (1986) to develop a low-order dimensional system based on POD modelling of the near wall region of a turbulent boundary layer. This original model included five (complex) spanwise Fourier modes, a single ($k_x = 0$) streamwise mode, and a single family of eigenfunctions in the wall normal direction. Aubry et al. found that their model exhibit an heteroclinic cycle which persists over a range of control parameter and with different truncations. These authors argued that this dynamical characteristic can be associated to the bursting behavior of a turbulent boundary layer. Unfortunately, when no pressure field in the boundary layer is supplied, the time duration between bursts grows without bound. When they introduced a more realistic boundary by including a term representative of the pressure field, the interburst duration equilibriates rapidly. In conclusion, the most significant finding of this work is that the bursting phenomenon appears to be produced autonomously by the wall region, but also to be triggered by pressure signals from the boundary layer. In this description, the analysis required an inhomogeneous pressure term to be supplied from outside the theory.

In a parallel work, Zhou and Sirovich (1992) resume the study of the coherent structures dynamics in the wall region of a turbulent channel flow. Using the numerical database of Kim et al. (1987), they developed a method for the construction of wall eigenfunctions with full channel validity. The important consequence of this formulation is that a well posed mathematical problem is developed, in particular, no exterior pressure term is required. The resulting model equations exhibit the same qualitative behavior as the model of Aubry et al. (1988). However, in this model, the bursting and ejection events are no longer explained by the triggering mechanism of the pressure fluctuations but rather by the existence of propagating modes (or waves).

These different explanations for the same physical phenomenon have been discussed extensively by the two groups in (Berkooz et al. 1994) and (Sirovich and Zhou 1994).

Flow control applications for wall flows: Bloch and Marsden (1989) showed that for a certain class of nonlinear control system possessing homoclinic orbits, a control can be found such that the system exhibits arbitrarily long periods in a neighborhood of the homoclinic point. These authors tried to apply these ideas to the finite-dimensional model of the bursting phenomena developped by Aubry et al. (1988). Unfortunately, they obtained that in general one may not have sufficient control energy to overwhelm the heteroclinic structure and change the flow dynamics.

Later, in an attempt to model drag reduction on the near wall-region (by polymer addition, for example), Aubry et al. (1990) rescaled the eigenfunctions determined by Aubry et al. (1988). The main result of this study is that the qualitative behavior of the new dynamical system obtained after stretching the eigenfunctions was similar to that in the unmodified layer. The authors argued that their model equations retain much of their physically significant behavior under transformations resulting from stretching the flow. Afterwards, Berkooz (1992) proposed a control strategy based on boundary deformation for increasing the mean passage time between bursts in the heteroclinic attractor model proposed by Aubry et al. (1988).

The discovery of propagating modes in turbulent channel flow made previously by Zhou and Sirovich (1992), motivated the investigation by Handler et al. (1993) and Levich and Malomed (1993) of the effect of phase randomization of selected Fourier modes. These authors determined that such mechanism of phase randomization gives rise to a fully sustained drag reduction of about the same magnitude as found when small concentrations of long-chained polymers are introduced into the flow.

The study of Berkooz (1992) have been later extent by Coller et al. (1994a) and Coller et al. (1994b) in examining the effect on a naturally occuring streamwise vortex pair of a perturbing pair produced by an actuator. In particular, Coller et al. introduced a control strategy that reduces the bursting rate and hence the turbulent drag in the model equation. Recently, Carlson and Lumley (1996) investigate numerically in a minimal flow unit, the effect of an actuator, Gaussian in shape, on drag reduction. The test flow contained just one pair of coherent structures in the near wall region: a high and a low speed streak. They found that when the actuator is raised underneath a low-speed streak, an increase in drag is obtained and when the actuator is raised underneath a high-speed streak a reduction is obtained.

Work on open fluid flows: A dynamical model for the jet-annular mixing layer was constructed along the lines of the model of Aubry et al. (1988) for the wall layer by Glauser and coworkers ((Ukeiley et al. 1993) and (Zheng 1991)). In their dynamical systems simulations, cascade phenomena were observed where streamwise wavenumbers act as trigger modes to excite various helical modes, in particular azimuthal modes 4, 5 and 6. These results were then applied by Corke et al. (1994) to control the experimental setup of Corke and Kusek (1993). The higher helical modes were excited through

the experimental closed-loop feedback control scheme. Similar effects as in the dynamical systems simulations, such as mode competition and switching have been observed.

Another dynamical system of the mixing layer based on an experimental procedure can be found in (Rajaee et al. 1994). In this case, a snapshot POD is performed based on conditional measurements of an acoustically excited developing flow. Using the POD eigenfunctions, a low-order system of dynamical equations was constructed. The authors compared instantaneous modal coefficients with projections of experimental data for a sixteen mode problem. They obtained that the first two POD modes display remarkably good tracking of the experimental time evolution, while higher modes were less accurate, although their general level remains correct.

Some other results obtained by Cordier (1996) or Ukeiley in the case of a subsonic plane mixing layer, based on the eigenfunctions derived by Delville will be illustrated in section 4.5.

For practical flow predictions, the pressure should be included in the Navier-Stokes equations. This essential point induces some new difficulties that are adressed in the next section.

4.3 Navier-Stokes Equation: Pressure-Velocity Formulation

When the pressure term are taken into account, the Navier-Stokes equation can be written as:

$$\frac{\partial \boldsymbol{u}}{\partial t} + \overline{\overline{grad}}\, \boldsymbol{u}.\boldsymbol{u} = -\boldsymbol{grad}\, P + \frac{2}{Re}\boldsymbol{\Delta u} \tag{53}$$

As seen before, POD eigenfunctions automatically verify the continuity equation. Thus no further equation is needed to satisfy continuity.

Using the POD basis given in (45), the Galerkin projection (49) leads to the equation for the a's:

$$\begin{aligned} \frac{\mathrm{d}a^{(n)}}{dt} &= -(\boldsymbol{\Phi}^{(n)}, \boldsymbol{grad}\, P) + \frac{2}{Re}(\boldsymbol{\Phi}^{(n)}, \sum_m a^{(m)} \boldsymbol{\Delta}\boldsymbol{\Phi}^{(m)}) \\ &\quad -(\boldsymbol{\Phi}^{(n)}, \sum_{m,k} a^{(m)} a^{(k)} \overline{\overline{grad}}\, \boldsymbol{\Phi}^{(m)} \boldsymbol{\Phi}^{(k)}) \end{aligned} \tag{54}$$

for $1 \leq n, m, k \leq N_{gal}$.

In this equation, the pressure term, P, is unknown. Unfortunately, it cannot be expressed directly in terms of the projection coefficients $a^{(m)}(t)$, and of the eigenfunctions $\boldsymbol{\Phi}^{(m)}$ of POD.

In a similar way to the derivation of Poisson equation in conventional approaches, it is possible to take benefit of the fact that the divergence of the eigenfunctions $\boldsymbol{\Phi}^{(n)}$ is zero. Then, the divergence theorem allows the term of (54), in which the pressure P appears, to be rewritten as an integral over the domain boundary $\partial\mathcal{D}$:

$$(\boldsymbol{\Phi}^{(n)}, \boldsymbol{grad}\ P) = \int_{\partial\mathcal{D}} P\boldsymbol{\Phi}^{(n)}.\boldsymbol{n}\ dS \tag{55}$$

In this equation, $\boldsymbol{n}$ is the external normal to $\partial\mathcal{D}$. The pressure term in (54) can then be evaluated under the condition that pressure is known on the domain boundary.

There then exist a number of flow configurations where this term exactly vanishes. The form of (55) clearly shows that this will occur when the velocity component is normal to the domain (no slip conditions). This will be true also when the boundary conditions are periodic. In this last case the contributions of the periodic parts of the boundary $\partial\mathcal{D}$ cancel each other. Zhou and Sirovich (1992) use this property in their study of a channel flow by numerical simulation.

In the study of Aubry et al. (1988) the domain is limited to the near wall region of a turbulent boundary layer. The modelisation of the non zero pressure term then becomes necessary. For that purpose, Aubry et al. utilized numerical data coming from an LES of a channel flow by Moin (1984). Knowing pressure fluctuations at the upper boundary of the domain they could determine exactly the term (55).

In the study of the transition over a flat plate performed by Rempfer (1996), the upstream and downstream conditions of the domain $\mathcal{D}$ on which the POD is applied cannot be considered as periodic. This author, in order to avoid the difficulties in taking into account of the pressure term, uses another formulation based on vorticity. We describe, in the next section, this alternative approach.

4.4 Vorticity Transport Equation

The vorticity transport equation can be writen:

$$\frac{\partial\boldsymbol{\omega}}{\partial t} + \overline{\overline{grad}}\ \boldsymbol{\omega}.\boldsymbol{u} - \overline{\overline{grad}}\ \boldsymbol{u}.\boldsymbol{\omega} = \frac{2}{Re}\boldsymbol{\Delta\omega} \tag{56}$$

where the vorticity $\boldsymbol{\omega}$ is defined as the rotational of the velocity vector $\boldsymbol{u}$: $\boldsymbol{\omega} = \boldsymbol{rot}\ \boldsymbol{u}$.

In order to be able to perform a Galerkin projection of (56), flow realizations $\boldsymbol{u}(\boldsymbol{x}, t)$ and $\boldsymbol{\omega}(\boldsymbol{x}, t)$ both have to be expressed on a basis for which the temporal dependancy is carried by the same projection coefficients $a^{(n)}(t)$.

After applying POD to the set of flow realizations $\boldsymbol{u}$, and after (45), new sets of eigenfunctions $\boldsymbol{\Psi}^{(n)}$ can be defined as:

$$\boldsymbol{\Psi}^{(n)} = \boldsymbol{rot}\ \boldsymbol{\Phi}^{(n)} \tag{57}$$

This new ensemble of eigenfunctions are the eigenfunctions of the vorticity $\boldsymbol{\omega}$. This can be demonstrated by writing:

$$\sum_{n=1}^{N_{POD}} a^{(n)}(t)\boldsymbol{\Psi}^{(n)} = \sum_{n=1}^{N_{POD}} a^{(n)}(t).\boldsymbol{rot}\ \boldsymbol{\Phi}^{(n)} = \boldsymbol{rot}\ (\sum_{n=1}^{N_{POD}} a^{(n)}\boldsymbol{\Phi}^{(n)}) = \boldsymbol{\omega} \tag{58}$$

Hence, the set of eigenfunctions $\boldsymbol{\Phi}^{(n)}$ represent at the same time velocity and vorticity fields (via the definition 57 of $\boldsymbol{\Psi}^{(n)}$). The only practical limitation is that one has to check, for every new application, that the eigenfunctions $\boldsymbol{\Psi}^{(n)}$ are linearly independant.

4.5 The Plane Mixing Layer

We have defined all ingredients necessary to develop a POD based Dynamical System. In the next sections,[12] we will illustrate a specific application of this approach to the case of a subsonic plane mixing layer. This flow configuration has been described in Sect. 3.8. This example is generic for free shear flows.

Dynamical System Based on Experimental Data. From the experimental arrangement of the plane mixing layer, in an approach similar to the one of Aubry et al. (1988), a POD based dynamical system can be derived.

POD: Two assumptions are necessary in order to be able to apply this approach. The mixing layer is considered as being two-dimensional in the mean sense: the spanwise (z or x_3) direction is assumed homogenenous. The streamwise (x or x_1) direction is considered as being locally homogeneous. The POD is applied only in the direction of the mean velocity gradient y (or x_2). In the two other directions, a Fourier transform is applied.

The eigenvalue problem that has to be solved is then:

$$\sum_{j=1}^{3} \int_{\mathcal{D}} \Pi_{ij}(x_2, x_2'; k_{x_1}, k_{x_3})\Phi_j^{(n)}(x_2'; k_{x_1}, k_{x_3})dx_2' =$$
$$\lambda^{(n)}(k_{x_1}, k_{x_3})\Phi_i^{(n)}(x_2; k_{x_1}, k_{x_3}) \qquad n = 1, \ldots, +\infty \tag{59}$$

[12] In the sequel, the following notations will be used indifferently: coordinates x, y, z or x_1, x_2, x_3 ; velocity components u, v, w or u_1, u_2, u_3.

The cross-spectrum $\Pi_{ij}(x_2, x_2'; k_{x_1}, k_{x_3})$ is the Fourier transform in the two homogeneous directions x_1 and x_3 of the two-point space correlations $R_{ij}(x_2, x_2'; \delta_x, \delta_z) = \left\langle u_i'(x_2, x_1 = X_0, x_3 = 0) u_j'(x_2', X_0 + \ delta a_x, \delta_z) \right\rangle$. Here, the averaging process involved $\left\langle \bullet \right\rangle$ is a classical time average.

The set of eigenfunctions $\Phi_i^{(n)}(x_2; k_{x_1}, k_{x_3})$ is complete in the sense that the flow fields of the given ensemble can be expanded in terms of the eigenfunctions via:

$$\hat{u}_i(x_2; k_{x_1}, k_{x_3}, t) = \sum_{n=1}^{+\infty} a_{k_{x_1}, k_{x_3}}^{(n)}(t) \Phi_i^{(n)}(x_2; k_{x_1}, k_{x_3}) \tag{60}$$

where $\hat{u}_i(x_2; k_{x_1}, k_{x_3}, t)$ is the two dimensional Fourier transform of the fluctuation velocity $u_i'(x_1, x_2, x_3, t)$.

Governing Equations: Navier-Stokes equations in the form:

$$\frac{\partial u_i}{\partial t} + u_j \frac{\partial u_i}{\partial x_j} = -\frac{1}{\rho} \frac{\partial p}{\partial x_i} + \nu \nabla^2 u_i, \quad i = 1, 2, 3 \tag{61}$$

In a similar way as that followed by Aubry et al. (1988) and Zhou and Sirovich (1992), the homogeneity in directions x_1 and x_3 allows us to define, for each time t the ensemble average $\overline{(\bullet)}$ as a spatial integration:

$$\overline{(\bullet)} = \frac{1}{L_1 L_3} \int (\bullet) dx_1 dx_3 \tag{62}$$

where L_1 and L_3 correspond to the size of $\mathcal{D}$. Velocity and pressure fields can then be decomposed into mean and fluctuating fields:

$$\begin{aligned} u_i &= \overline{u_i} + u'_i \\ \text{and} \\ p &= \overline{p} + p' \end{aligned} \tag{63}$$

After a few manipulations, the equation for the fluctuating and mean part are respectively:

$$\begin{aligned} &\frac{\partial u'_i}{\partial t} + u'_j \frac{\partial u'_i}{\partial x_j} - \overline{u'_j \frac{\partial u'_i}{\partial x_j}} + u'_j \frac{\partial \overline{u_i}}{\partial x_j} + \overline{u_j} \frac{\partial u'_i}{\partial x_j} \\ &\quad + \frac{1}{\rho} \frac{\partial p'}{\partial x_i} - \nu \nabla^2 u'_i = 0 \end{aligned} \tag{64}$$

$$\frac{\partial \overline{u_i}}{\partial t} + \overline{u_j} \frac{\partial \overline{u_i}}{\partial x_j} + \overline{u'_j \frac{\partial u'_i}{\partial x_j}} = -\frac{1}{\rho} \frac{\partial \overline{p}}{\partial x_i} + \nu \nabla^2 \overline{u_i} \tag{65}$$

Adding classical mixing layer assumptions, like the thin-layer hypothesis ($\overline{u_2} = \overline{u_3} = 0$), homogeneity in the x_3 direction ($\frac{\partial \overline{(\bullet)}}{\partial x_3} = 0$), and using the

continuity equation for the mean velocity, we obtain $\overline{u_1} = \overline{u_1}(x_2, t)$. Finally, the Navier Stokes equations for the turbulent components reads:

$$\frac{\partial u'_i}{\partial t} + u'_j \frac{\partial u'_i}{\partial x_j} - \overline{u'_j \frac{\partial u'_i}{\partial x_j}} + u'_2 \frac{\partial \overline{u_1}}{\partial x_2} \delta_{i1} + \overline{u_1} \frac{\partial u'_i}{\partial x_1} + \frac{1}{\rho} \frac{\partial p'}{\partial x_i} - \nu \nabla^2 u'_i = 0 \tag{66}$$

Equations for the Dynamical System: As described in the previous section, the method consists of projecting the Fourier transform in x_1 and x_3 of (66) onto the empirical basis set (POD) using a Galerkin method. This projection yields a set of time dependent ODEs for the so-called random coefficients of the POD : $a_{k_{x_1}, k_{x_3}}(t)$. Three steps are then followed:

1. The Fourier transform of (66) using:

$$\hat{u}_i(k_x, k_z; y, t) = \int \int_{-\infty}^{+\infty} u'_i(x, y, z, t) \mathrm{e}^{-2\pi j (k_x x + k_z z)} \, dx \, dz \tag{67}$$

2. The introduction of POD decomposition (60).
3. The application of a Galerkin projection of the new equation obtained onto the eigenfunctions:

$$\left(\text{equation}, \Phi^{(n)}_{k_x, k_z}(y) \right) \text{ for } \quad n = 1, \cdots, N_{gal} \tag{68}$$

Note: that the dynamical system that is obtained is at least quadratic (due to the convective part of 64) and at worst cubic.

Closure: One of the remaining points to be solved is that the mean field $\overline{u}$ appears in (66). This field is not known at this level providing the ODEs are established for the a's, i.e. for the fluctuating part of the velocity field. The system is then open. For the system to be closed, an estimate of this field needs to be provided. This is in some sense, the equivalent to the closure problem of the Reynolds equation. However, in this case, the mean velocity field is the "new" additional unknown. The closure can be done explicitely, by using another transport equation for this quantity, or implicitely, by relating the mean part to the fluctuating one. In terms of flow control the second solution seems better in the sense that we want a system of low order with a minimum number of equations.

Depending on the assumptions made about the flow and of the flow configurations (wall bounded flows, free shear flows, etc. ...), several closure methods can be used:

- the simplest one is to use a prescribed mean field independent of time. The dynamical system obtained is then quadratic and no *feed-back* can be found between the fluctuating and mean fields. Note that, in this case, the mean field can be directly the measured one or derived from the contribution of the POD modes which are retained for the Galerkin projection (e.g. by using an eddy viscosity model).
- for a mixing layer, an eddy viscosity model (Boussinesq 1877) could be thought to be well suited. The integration of $\overline{u'v'} = -\nu_t \dfrac{\partial \overline{u}}{\partial y}$ gives:

$$\overline{u}(y) = -\frac{1}{\nu_t} \int_0^y \overline{u'v'}(y')\, dy' + \overline{u}(0) \tag{69}$$

  Unfortunately, it is clear that the two boundary conditions $\overline{u}(-L) = U_b$ and $\overline{u}(L) = U_a$ cannot be imposed at the same time.
- for the mixing layer configuration, Ukeiley (1995) uses a closure where a cutoff wavenumber is introduced. For wavenumbers less than this cutoff wavenumber, the velocity is considered as steady, while the feedback is driven by the highest wavenumbers.
- a specific closure has been used intensively in wall flow configurations (e.g. (Aubry et al. 1988) or (Zhou and Sirovich 1992)). However, with some success, a closure similar to this one has been used by Zheng (1991) for a jet flow configuration. This closure consists of using the average momentum equation, with the thin layer assumption, this equation can be written (Tennekes and Lumley 1972) as:

$$\frac{\partial \overline{u'v'}}{\partial y} = \nu \frac{\partial^2 \overline{u}}{\partial y^2} \tag{70}$$

  By integrating (70) twice, one obtains:

$$\overline{u}(y) = \frac{1}{\nu} \int_{-L}^{y} \overline{u'v'}(y) dy + C_1 y + C_2 \tag{71}$$

  Note: that this kind of closure can certainly be used for near wall regions where viscosity dominates but less efficiently for a free shear flow configuration.
- In a wake flow configuration, Cao (1993), uses for closure the additional equations:

$$\begin{aligned} U_e \frac{\partial \overline{u}}{\partial x} &= \frac{\partial \overline{u'v'}}{\partial y} \\ \frac{\partial \overline{u}}{\partial x} + \frac{\partial \overline{v}}{\partial y} &= 0 \end{aligned} \tag{72}$$

  This kind of assumption is justified by the far wake, low deficit characteristics.

It is clear that the problem of closure is crucial for the behavior of the dynamical system. A lot of work needs still to be done in this field.

Truncation: A truncation is then necessary to include only $Ngal$ (the first POD modes) and selected streamwise/spanwise modes. The order of the system that is obtained corresponds to the number of these POD and Fourier modes that are retained.

Introduction of a Numerical Dissipation. In a turbulent flow, energy is dissipated by viscous effects appearing at high wavenumbers. The truncation suppresses this high wavenumbers contribution, as well as the one of the highest POD modes. An artificial dissipation needs then to be imposed in order to preserve this contribution. The order of magnitude of this artificial viscosity can be found from a generalization of the Heisenberg spectral model (Aubry et al. 1988). As a result, an artificial viscosity $\alpha\nu$ is added to ν. In such approaches, α is the control parameter for the dynamical system.

General Form of the Dynamical System: Finally, the dynamical system of (66) can be written for the a's:

$$\begin{aligned}\frac{\mathrm{d}a_{k_x,k_z}}{dt}(t) &= \left[(1+\alpha)L^V_{k_x,k_z} + L^{BC}_{k_x,k_z}\right]\ a_{k_x,k_z}(t) \\ &+ \sum_{k'_x,k'_z} Q_{k'_x,k'_z,k_x,k_z}\ a_{k'_x,k'_z}(t)\ a_{k_x-k'_x,k_z-k'_z}(t) \\ &+ \sum_{k'_x,k'_z} C_{k'_x,k'_z,k_x,k_z}\ a_{k_x,k_z}(t)\ |a_{k'_x,k'_z}(t)|^2\end{aligned} \tag{73}$$

In this system, linear terms $L^V_{k_x,k_z}$ correspond to the viscous terms of the Navier-Stokes equation, the linear terms $L^{BC}_{k_x,k_z}$ depend on the boundary conditions used in the closure equation. Note that the cubic terms $C_{k'_x,k'_z,k_x,k_z}$ are zero when a time independant closure is used for the mean velocity.

Examples of Results. We present here a few selected results restricted to the plane mixing layer. The reader can refer to Holmes et al. (1996) for a more complete review of typical results.

Most Amplified Mode. We first consider a very strong truncation: only the first POD mode is considered. The only wavenumbers that are kept in the truncature are $(k_x, k_z = 0)$, so that the large scale (quasi two-dimensional) structures can be described. In a recent work, Cordier et al. (1997a) consider (66) where the viscous terms are imposed to be zero (i.e. $\alpha = -1$). Thus obtaining an inviscid configuration. A stability analysis of the dynamical system is then derived. It is possible to compare this analysis with the corresponding stability analysis of Michalke (1964).

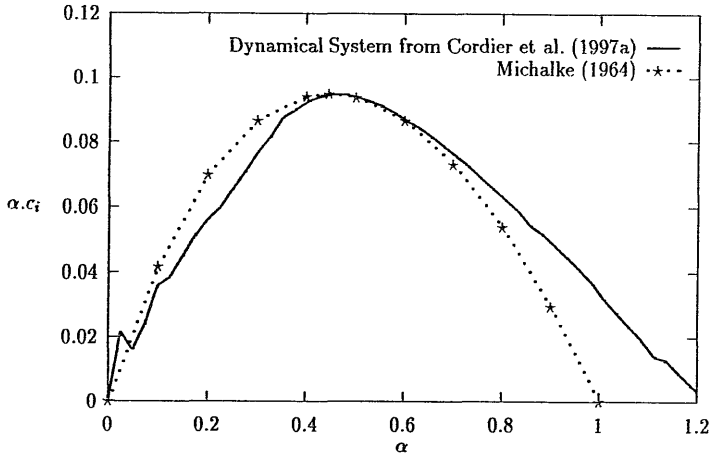

Fig. 12. Linear growth rate of the inviscid turbulent plane mixing layer

Figure 12 compares the linear growth rate obtained for an inviscid mixing layer by Michalke (1964) to the one obtained with the simplified dynamical system. An excellent agreement can be observed. Both the most linear unstable mode α^{max} and the value of its linear growth rate being comparable. It has here to be noted an important point: the dynamical system obtained from the POD is only based on the two point correlation tensor, (by opposition to Michalke's approach where the stability of the profile of the longitudinal velocity whas in concern). It is a striking result that both approaches lead to comparable results.

Three-Dimensional Model. A more complex, three-dimensional, dynamical system of the experimental mixing layer has been derived by Ukeiley (1995). By using 39 nodes (including both streamwise and spanwise wavenumbers), and a truncation based on the filter model described in the previous section, a complex behavior of the dynamical system has been observed. Large-scale quasi two-dimensional structures and streamwise vorticity tubes were found to coexist and interact (see Fig. 13).

Use of Large Eddy Simulation. From a three-dimensional Large Eddy Simulation of a plane mixing layer, Cordier et al. (1997b) applied a snapshot POD. From the eigenfunctions obtained, a dynamical system was derived. It has been found that with only a 10 equations model, the short time evolution of the flow can be predicted by this system, as illustrated in Fig. 14.

These examples are particularly encouraging for the use of POD based Dynamical System for flow control. The time is now close to being able to include these approaches either for building strategies of flow control or to be

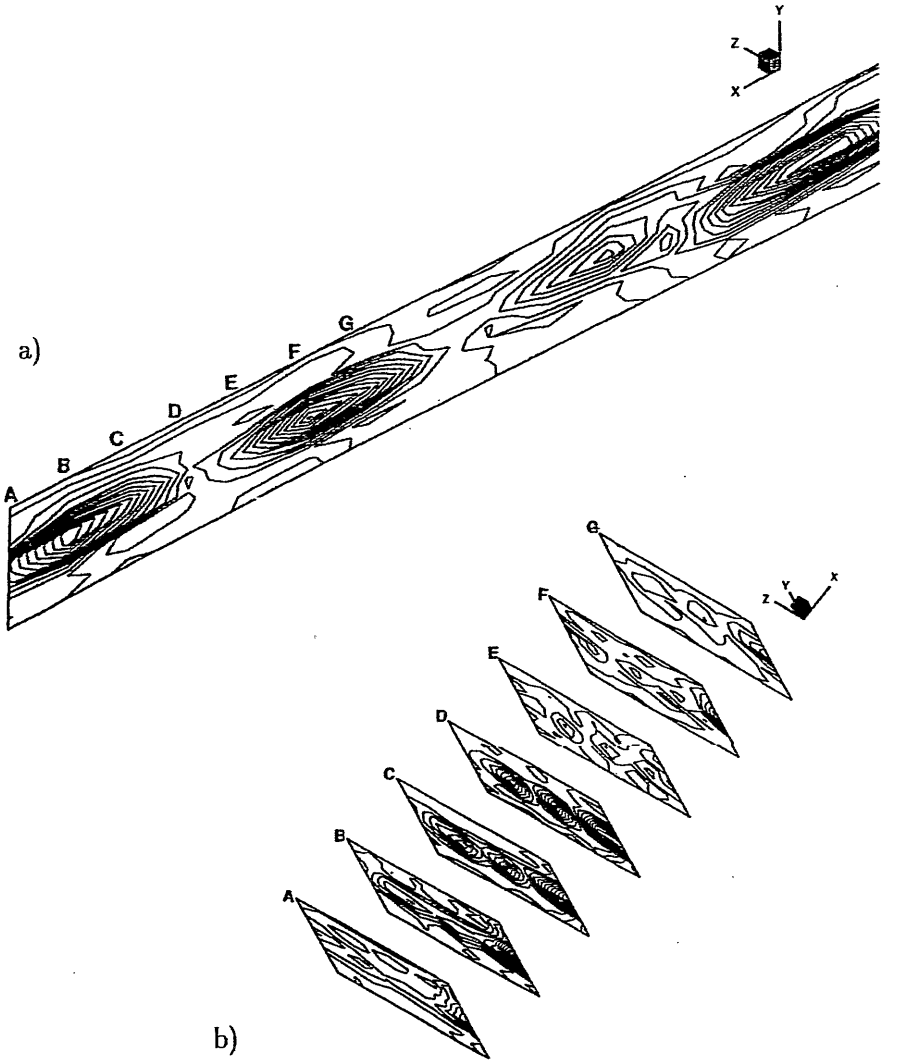

Fig. 13. Vorticity contours. (a) in the x_1-x_2 plane; (b) in x_2-x_3 planes. Dynamical System of the plane mixing layer (39 nodes—filter relashionship). α=0.39. From (Ukeiley 1995). Courtesy of L. Ukeiley.

directly used in the feedback process. A remaining question to be addressed before this ultimate goal is achieved is the universality and robustness of the POD eigenfunctions. This point is now addressed in the following section.

4.6 Representativity of the Dynamical System Model

Generally, studies related to low-dimensional dynamical systems based on POD, try, for a given flow configuration, to evaluate the ability of such sys-

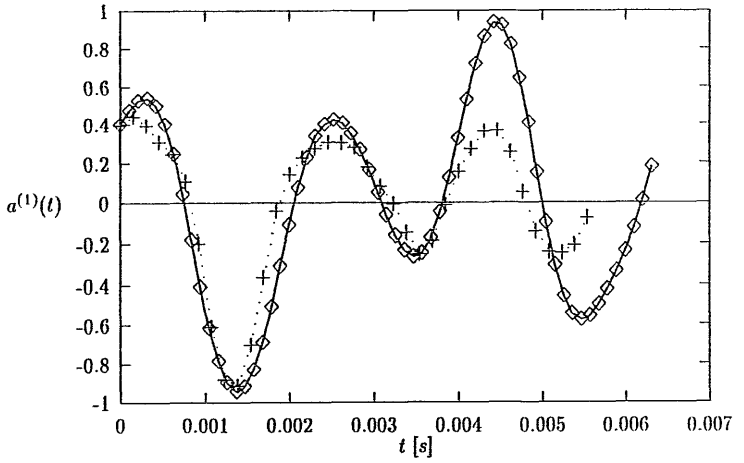

Fig. 14. Comparison of the temporal evolution of $a^{(1)}(t)$ from a direct application of POD and from a 10 equations Dynamical System. Large Eddy Simulation of the plane mixing layer.

tems to describe properly the dynamics of the flow. Once, the governing equations and the POD basis are known, the development of the system becomes straightforward. However, considering flow control, a fundamental question has to be asked: what is the robustness of the model when the flow realizations are more or less varied relatively to the ones from which the POD basis was derived? In other words what is the sensitivity of the model to variations of geometry, boundary conditions, control parameters, ...? This question is important when the flow control, will modify at least one of these points. This limitation is due to the "intrinsic to a flow" character of the POD. It has to be underlined that the optimal convergence property of POD, that makes this approach interesting, is also responsible of this limitation. This section will try to bring elements of answers to these questions.

General Considerations. The bifurcation parameter of a dynamical system appears generally in the time evolution equation, in an explicit manner as well as in an implicit manner (through the eigenfunctions of POD, for example). Hence, in terms of flow control, the effect of variations of the physical parameters on the eigenfunctions needs to be addressed. Early, in a series of papers (Sirovich 1987a), (Sirovich (1987b) 1987b), (Sirovich (1987c) 1987c), the problem of parametrization of POD in terms of the features of the flow (Reynolds number, Rayleigh number, ...) has been discussed. Following this discussion, let us denote generically by μ, the ensemble of flow parameters such as the Reynolds number. If the eigenfunctions $\Phi_0{}^{(n)}$ can be associated to the coherent structures of the flow for the specific value μ_0 of flow parameters, this is a priori no longer the case when $\mu \neq \mu_0$. In particular, the

relationship: $\langle a^{(n)} a^{(l)} \rangle = \delta_{ln}$, is verified only if $\mu = \mu_0$. However, the set $\Phi_0{}^{(n)}$ still forms a complete, orthonormal set satisfying the boundary conditions and flow properties (e.g. incompressibilty). The calculated set $\Phi_0{}^{(n)}$ might therefore be expected to be useful over a range of parameter space μ, at least for relatively small variations around μ_0.

Influence of Variation of the Control Parameter. The different methods, encountered in the literature, to take into account this variation depend strongly on the type of flow realizations used for solving the POD problem. Practically, two cases are found:

1. the realizations used to solve the POD problem are known only for *one* specific value μ_0 of the control parameter;
2. the realizations contain (implicitely or explicitely) different values of the control parameter.

POD Solved for One Specific Value $\mu = \mu_0$: In these approaches, a dynamical system is derived from the eigenfunctions determined at $\mu = \mu_0$. Then μ is made to vary in the system.[13] As claimed before, it can be expected that the eigenfunction set determined for μ_0 is useful to represent the dynamical evolution of the system for $\mu \neq \mu_0$. This has been effectively demonstrated in the case of the Ginzburg-Landau equation, in a study by Sirovich and Rodriguez (1987). These authors show that a relatively large region of the parameter space is very well described by a three mode approximation calculated from one particular set of parameters.

Chambers et al. (1988) studied a turbulence model based on a randomly forced one-dimensional Burger's equation with zero velocity boundary conditions. The solutions of this equation exhibit two very different statistical behaviour: a core region quasi homogeneous and wall regions (near the end of the study domain) where significant statistical spatial inhomogeneity exist. Correlation and covariance tensors are determined for three different Reynolds numbers. They show that outside the wall layers, the eigenfunctions are nearly identical for Reynolds numbers spanning a range of 16 : 1. However in thin viscous wall layers, the eigenfunctions depend strongly upon the Reynolds number. They note that this dependence can be reduced by rescaling the distance from the wall with the thickness of the viscous layer. Chambers et al. illustrate here a principle of large scale similarity for the Karhunen-Loeve eigenfunctions of a two-length scale process: "In the physical region outside of the wall layers and in the range of sequencies where the eigenfunction wavelength is large compared to the viscous length scale, both the structure of the eigenfunctions and the spectrum of the eigenvalues are independent of Reynolds number when scaled on outer variables".

[13] Note that μ appears explicitely in the dynamical system model via the governing equations that have been projected on POD basis.

Deane et al. (1991) applied the Snapshot POD method to data resulting from a detailed spectral simulation of two complex geometries: the flow in a periodically grooved channel and the wake of an isolated circular cylinder. Low-dimensional dynamical models for these systems are obtained by Galerkin projection of Navier-Stokes equations onto the empirically derived global eigenfunctions. The short and long term accuracy of the models is studied through numerical integrations, and bifurcation analysis is done using a continuation software called AUTO94 (Doedel 1981). Special attention is paid to estimate the ability of the low-order dynamical system to mimic the full simulations for Reynolds number beyond the values used for eigenfunctions extraction. When the results of the full simulation for the grooved channel flow are compared to those of a four equations model, Deane et al. found that the initial loss of flow stability ocurring through a supercritical Hopf bifurcation can be described with accuracy by the model. However, this four equation model is deficient when extrapolating the system behavior for Reynolds numbers away from the value used for the decomposition. Deane et al. identify a source for this deficiency: they noted that their model contains, as a constant part, the mean field corresponding to the Reynolds number at which the POD problem is solved. For other values of Reynolds number, the mean flow is very different from the one corresponding to the one for which POD was applied. If this change can be accurately spanned by the POD eigenfunctions at Re_0, one may still expect the model to work without further modifications. For the grooved channel flow problem, Deane et al. choose to account for variations in the mean flow with the Reynolds number by introducing an ad hoc **linear law of correction**:

$$\overline{\boldsymbol{u}}(Re) = \gamma(Re)\overline{\boldsymbol{u}}(Re_0) = \Big[\frac{c_1}{Re} + c_2\Big]\overline{\boldsymbol{u}}(Re_0) \tag{74}$$

where the parameters c_1 and c_2 are estimated such that the flow rates at different values of Reynolds number match those from the simulation. The new model system derived by this way, predicts very well the flow dynamics for Reynolds numbers away from the decomposition value. The Hopf bifurcation location is captured fairly accurately, being $R_0 = 292$ in the model as compared to approximately $R_0 = 300$ obtained by the full simulation. For the cylinder flow, the accuracy of the POD low-order model predictions rapidly deteriorates when the Reynolds number is made made to vary from the value at which the POD is performed. In the same study, Deane et al. try to estimate the ability of the eigenfunctions $\Phi_i^{(m)}(\boldsymbol{x}, Re_0)$ determined when $Re = Re_0$ to represent exactly the flow realizations at $Re = Re_p$. To quantify numerically this aspect, they defined a residual characteristic of the part of $\boldsymbol{u}(\boldsymbol{x}, t, Re_p)$ not spanned by the eigenfunctions $\Phi_i^{(m)}(\boldsymbol{x}, Re_0)$:

$$\text{Res}\,(\boldsymbol{u}, N_{max}) = \frac{\langle ||\boldsymbol{u}(\boldsymbol{x},t,Re_p) - \sum_{j=1}^{N_{max}} (\boldsymbol{u}(\boldsymbol{x},t,Re_p), \bar{\Phi}^{(j)}(\boldsymbol{x},Re_0))\bar{\Phi}^{(j)}(\boldsymbol{x},Re_0)|| \rangle}{\langle ||\boldsymbol{u}(\boldsymbol{x},t,Re_p)|| \rangle} \quad (75)$$

For the grooved channel flow ($Re_0 = 350$ and $Re_p = 1000$), there is about 8% ot energy not captured. This error is sufficiently low to permit the dynamical system built at $Re = 350$ to describe the long-term dynamics of the full simulations at $Re = 1000$. In the case of the cylinder flow, 65% of the dynamics at $Re = 150$ is not captured by the first six eigenfunctions determined at $Re = 100$. When 20 modes are included, the corresponding value of the residual is only 64%. This result means that, in this case, the flow changes with Reynolds number cannot be simply thought of as an "excitation of the next higher modes" in the $Re = 100$ hierarchy. Nevertheless, we can note that, even though the long-term dynamic predictions of such models may be sometimes inaccurate, their short-term prediction capabilities may still be useful, for example, in real-time flow control applications.

Deane and Mavriplis (1994) use the same analysis method as was developed by Deane et al. (1991), to describe the dynamics of the viscous flow past a thick airfoil NACA 4424 in the transitional regime. The spectral simulations have provided data for decomposition into empirical eigenfunctions at two different values of Reynolds number: $Re = 3000$ and $Re = 4000$. Comparing the two Reynolds number configurations, they show that the energy is spread over a greater number of modes as Reynolds number increases. Lastly, Deane and Mavriplis retain the twelve most energetic modes (which represent approximately 95% of the energy) to develop a low-order dynamical system for $Re = 3000$. This model is found, while not reproducing the detailed flow properties, to capture certain essential dynamical features, namely the shedding frequency and its low frequency modulation.

Liu et al. (1994) present experimental evidence, in a fully turbulent process, of the principle of large-scale similarity for the POD eigenfunctions, introduced previously by Chambers et al. (1988). In this study, Liu et al. show that in the outer region of wall-bounded turbulent flow, both the eigenfunctions and the eigenvalue spectra of the one dimensional Proper Orthogonal Decomposition have shapes that are independent of Reynolds number when scaled by the wall friction velocity and the outer length scale. By comparing the POD results of Lu and Smith (1991) for a boundary layer to their results for channel flow, they conjecture that the similarity principle can be extended from channel flow to a broader class of turbulent wall flows.

POD Solved for Samples Including Different Values of Control Parameters: The characteristics of the flow vary strongly in transitional flows, thus these flows are good test cases for studying the influence of the variation of the con-

trol parameters.[14] There are some systems where the evolution of the control parameters are intrinsically included. Such configurations can be found in the studies by Carrion (1993) and Aubry et al. (1994) of the turbulent transition over a rotating disk, where the bi-orthogonal decomposition was applied. In these configurations, for a fixed angular rotation, the transition to turbulence, can be studied by considering different radial locations.

Studies by Rempfer (1991), Rempfer (1993), Rempfer (1994), Rempfer and Fasel (1994b), Rempfer (1996) of the transitional flow over a flat plate are of the same nature. Evolving in the streamwise direction, the flow goes from a periodic, to a chaotic and then turbulent state. Rempfer (1993) uses data from a DNS from Rist and Fasel (1995), by using the "snapshots" methods, he determines eigenfunctions of the flow from which a low order dynamical system is derived (vorticity transport formulation). By examinating the Lyapunov exponents, he shows that the pre-turbulent stages are characterized by deterministic chaos. Rempfer (1994) uses three different spatial domains located along the streamwise direction (therefore at different transitional stages), for which the "snasphots" method is applied. Using this, he shows that convected structures can be defined by gathering successive pairs of eigenfunctions. The coefficients of the dynamical system, describing the non linear interactions between components of a same structure are found to be negligible. The dynamical system can then be expressed under the form of linear oscillators coupled by quadratic interactions. In a following paper, Rempfer and Fasel (1994b) uses these equations, to analyze the temporal evolution and the energetic balance of the coherent structures. More recently Rempfer (1996), in the context of the discussion between "classical" and "snapshots" schools ((Berkooz et al. 1994), (Sirovich and Zhou 1994)) about the best suited dynamical model for the near wall region, analyzes the possibilities and limitations of low order dynamical systems based on POD. In the same paper, to study the transition, Rempfer utilizes 60 spatial subdomains (thin slices normal to the streamwise direction) from the same simulation. For each of these sub-domains a dynamical system is derived, that is valid for a limited range of Reynolds number variation and possesses its own dynamics.

In these transitional configurations, the difficulties for taking into account the variations of the flow features are overcame. However the price payed for this is excessive: an important number of dynamical systems is needed. On the other hand, the continuity of the representativity of the system when parameters change is difficult to access, due to the use of a discrete set of dynamical models.

[14] Note that for these flows the low dimensional dynamical system approach can be an alternative method to classical ones (linear and weak non linear stability theories), that could allow access to the last stages of transition where strongly non linear phenomena dominate.

Another possibility for taking into account these variations consists of applying POD to samples of the flow including several values of the control parameters. The flow realizations need then to be selected in such a way that the various regimes encountered, for which one wants the model to be efficient, are considered. Unfortunately, this means that the eigenfunctions obtained through these decompositions are such that they cannot be identified to the coherent structures of the flow, whatever the value of the control parameters.

Christensen et al. (1993) apply this approach to the study of the flow in a cylindrical tank from which one end is rotating. The numerical study by Daube and Sørensen (1989) has shown that a Hopf bifurcation exists when the Reynolds number is in the range [2500; 2600]. Their objective is then to built a low dimensional dynamical systems that can exhibit this bifurcation.[15] In order to do this, Christensen et al. generate a set of "snapshots" at fixed Reynolds number, in the range $Re = 2200$ to $Re = 3000$. They introduce the notion of *displacement vector* (difference between the ensemble averages of the samples at fixed Reynolds number). These displacement vectors allow the resulting dynamical system to represent the flow dynamics for various Reynolds numbers. For example, by this method, the Hopf bifurcation can be predicted with an accuracy of 0.2%. This group utilizes this approach to describe the successive transitions occuring in this flow (Sørensen and Christensen 1995).

As seen in this review, the sensitivity of the model to variations of the control parameters, has been studied essentially more in terms of the influence of the variation of the flow parameters (e.g. Reynolds number) than in terms of the influence of the geometry or boundary conditions. However, Berkooz (1992) for example, has proposed a control strategy based on boundary deformation, in which a conformal change of coordinates allows to take into account these variations. In fact, the variations of eigenfunctions with the control parameter depend both on the nature of the flow and on the type of realizations retained when the POD is applied. Either, the eigenfunctions can be rescaled properly (e.g. Liu et al. (1994), Chambers et al. (1988), Lu and Smith (1991), Aubry et al. (1990)) or a specific method needs to be introduced. This last problem is crucial in transitional configurations, where the flow characteristics and dynamics can evolve strongly. In this configuration, the authors try to take into account the variation of the control parameter by to ways: either sets of ODE are derived over a range of discrete values of the control parameter (e.g. Rempfer 1996) or a unique set of ODE is derived that include implicitely the variation of the control parameter (e.g. linear evolution Deane et al. (1991), displacement vectors Christensen et al. (1993)). This last method, because it reduces greatly the number of equations to be used seems very promizing. The common penalty of these approaches of low

[15] A similar approach has been used with the same motivations by Cordier (1996) in the case of a flow between counter rotating disks.

order Dynamical Systems based on POD basis, is that eigenfunctions have to be determined for each flow configuration. This determination is generally costly and requires heavy computations or experiments. An important gain would be obtained if they could be determined a priori. Such a formalism, based on the stability analysis of the equation for energy, has been recently developped by Poje and Lumley (1995).

5 Concluding Remarks

As noticed all along this chapter, it is now well admitted that, by their presence, the large-scale structures have a considerable influence on the turbulent flow dynamics. Indeed, even in fully turbulent shear flows, the large-scale structures are known to be of primary importance for most of the flow characteristics. In the framework of control of turbulent flows, it is therefore necessary to recognize them, understand their influence and somewhat predict their short time evolution. The ultimate aim of any method involved in flow control has then to try to define methods allowing to interact with them in a apropriate, intelligent way. The purpose of this chapter was, in this context, to analyze a few points that are to be taken into account when wishing to monitor the Coherent Structures, developping in turbulent shear flows: mainly, the large-scale structures identification and the prediction of their short time evolution has been addressed.

Due to the turbulent character of flows under practical and industrial interests, the detection, analysis, prediction and control of the large-scale structures are quite complex. Even organized, these large-scale structures possess a large degree of randomness leading to specific detection methods, associated to specific detectors and associated data processing. The identification schemes are linked with the accepted definitions themselves. The usual tools for accessing the large-scale structures regroup the usual experimental methods: flow viz, one or several point measurements, instantaneous or random data collecting. A commmon feature of these approaches is that they are selective, in that they only retain very well defined events. A comparative analysis shows that the average characteristics, obtained by using various conditional methods, are close. Even more they can be compared to the ones that can be derived from stochastic approaches, as POD or LSE are. However, the efficiency of the detection is different, accordind the method used. This point should be taken into account for flow control strategies: how can a method, even precise in the average sense, but selecting only a few percent of occuring events, be efficient?.

Therefore, non conditional, stochastic approaches have to be considered. These methods can lead to an objective contribution description of the Coherent Structures to the instantaneous flow, that conditional methods cannot

in general. These approaches have been detailed in the present chapter. In particular, the Proper Orthogonal Decomposition and the Linear Stochastic Estimation have been presented. A bibliographical review, as well as a particular case "the plane mixing layer" shown that several important features of the flow can be gained: turbulent kinetic energy (as a direct consequense of the POD definition), shear stress $u'v'$ component (thus energy production). The main large-scale structures organization (trough dominant wavelengthes, or frequencies) is also very well described by POD approaches. These methods lead to the description of the behavior of projection coefficients, that we called the a's. An intricate problem is related to POD applications: the "phase indetermination", that avoid to gain the temporal bahavior of these coefficients. This indetermination can be solved only if the whole flow field is known, it could therefore seem that this kind of method is useless. However, the use of complementary methods based on LSE seems a powerful tool that can be efficient in the determination of the a's. Obtained results show that the complementary technique, which combines LSE and POD, allows one to obtain time dependent information from the POD while greatly reducing the amount of instantaneous data required. Hence, it may not be necessary to measure the instantaneous velocity field at all points in space *simultaneously* to obtain the phase of the structures, but only at a few selected spatial positions.

One point has to be recalled in the context of real time flow control: the estimation of the POD coefficients only requires (at each time) to evaluate a spatial integral value. This evalution, while involving only very simple linear operators can be very easily hardwared. This remains true also in the context of the complementary technique, based on LSE.

An interesting feature of the POD approach is that an optimal basis is determined, from which a low order dynamical system, modelling the large-scale structures of the flow, can be derived. With the Galerkin projection procedure, sets of ODE have been derived. However it has appeared that some assumptions need to be made and that a closure problem remains present. Two results, obtained in the mixing layer configuration, have shown that from the Dynamical Systems approach: the most amplified mode (due to instability) is well predicted by the first mode of POD – a low order system (10 equations) can be used to predict the short time evolution of the Coherent Structures. Clearly, even though the long-term dynamic predictions of such models may be sometimes inaccurate, their short-term prediction capabilities may still be useful, for example, in real-time flow control applications.

Indeed, if a limited set of ODE is sufficient to describe turbulent flows, two objectives can be fulfilled: it should be easier to test flow control strategies, and the short term prediction of the relevant dynamics of the flow can be computed in real time.

Generally, studies related to low-dimensional dynamical systems based on POD, aim at, for a given flow configuration, evaluating the ability of such systems to describe properly the dynamics of the flow. Once, the governing equations and the POD basis are known, the development of the system becomes straightforward. However, considering flow control, a fundamental question remains to be answered: what is the robustness of the model when the flow realizations are more or less varied relatively to the ones from which the POD basis was derived? In other words what is the sensitivity of the model to variations of geometry, boundary conditions, control parameters, ...? This question is quite important when the flow control will modify at least one of these points. This question is related to the "intrinsic to a flow" character of the POD. It has to be underlined that the optimal convergence property of POD, that makes this approach interesting, is also responsible of this limitation. Different methods, encountered in the literature, to take into account this variation are available. The developped methods depend strongly on the type of flow realizations used for solving the POD problem. The two practical cases that can be found (realizations used to solve the POD problem known only for *one* specific value of the control parameter - realizations containing different values of the control parameter) have been developped in this last section. An ensemble of various methods are now available that allow to take into account the variation of the control parameter. These methods are dependent of the flow configuration: for developped flows, a rescaling of the eigenfunctions can be sufficient. In more complex situations, as transitional flows, one needs to derive specific procedures. Whatever the approach used for taking into account the control parameters variation, this point needs to be considered when developping the dynamical system model.

Two additional remarks can be done. The first one concerns the rapid developpement of the low order dynamical system as a tool for prediction of complex flows: in a recent work Joia et al. (1997) have used the dynamical system of Aubry et al. to simulate a two-phase flow (bubbles in air). In their approach, the dynamical system provides the large scale motion of the flow, while a Lagrangian approach is used for the particles trajectories. The second remark concerns an other application of the Karuhnen Loeve theory in the framework of flow control, this decomposition can be used as a tool for the identifications of dynamical systems and can be used for defining predictive models directly from time series data (see Landa and Rosenblum (1991)).

To conclude this chapter, it is clear that further studies are necessary for the optimization of flow control through POD based Dynamical Systems. The use of numerical methods is possible. However, for real flows with configurations that mimic the industrial ones, detailed experimental studies remain unavoidable.

Acknowledgements

The authors gratefully aknowledge J.H. Garem, S. Bellin, E. Vincendeau, R. Manceau for their individual contributions to different parts of the results presented in this chapter. Several of the results presented here were obtained through collaborative studies with Prof. M.N. Glauser, Dr. L. Ukeiley who are also aknowledged for fruitful discussions and exchanges. The financial support of the French Ministery of Defense (DGA, formerly DRET) was appreciated.

References

Adrian R.J. (1975): On the role of Conditional Averages in Turbulence Theory. In *Proc. 4th Biennal Symp. on Turbulence in Liquids.*

Adrian R.J. (1979): Conditional Eddies in Isotropic Turbulence. *Phys. Fluids* **22** (11), 2065–2070.

Adrian R.J. (1996): Stochastic Estimation of the Structure of Turbulent Fields. In *Eddy Structure Identification*, ed. J. P. Bonnet, 145–195, Springer-Verlag, Berlin.

Adrian R.J., Moin P. (1988): Stochastic Estimation of Organized Turbulent Structure: Homogeneous Shear Flow. *J. Fluid Mech.* **190**, 531–559.

Ahmed N., Goldstein M.H. (1975): *Orthogonal Transforms for Digital Signal Processing.* Springer-Verlag, New York.

Antonia R.A. (1981): Conditional Sampling in Turbulence Measurement. *Annu. Rev. of Fluid Mech.* **13**, 131–156.

Antonia R.A., Chambers A.J., Britz D., Browne L.W.B. (1986): Organized Structures in a Turbulent Plane Jet: Topology and Contribution to Momentum and Heat Transport. *J. Fluid Mech.* **172**, 211–229.

Ash R.B., Gardner M.F. (1975): *Topics in Stochastic Processes.* Academic Press, New York.

Aubry N., Berkooz G., Coller B., Elezgaray J., Holmes P., Lumley J.L., Poje A. (1994): Low Dimensional Models, Wavelet Transforms and Control. In *Eddy Structure Identification Techniques in Free Turbulent Shear Flows*, ed. J. P. Bonnet, 271–331, Springer-Verlag, Berlin.

Aubry N., Chauve M.P., Guyonnet R. (1994): Transition to Turbulence on a Rotating Flat Disk. *Phys. Fluids* **6** (8), 2800–2814.

Aubry N., Guyonnet R., Lima R. (1991): Spatio-Temporal Analysis of Complex Signals: Theory and Applications. *J. Statis. Phys.* **64** (3/4), 683–739.

Aubry N., Holmes P., Lumley J.L., Stone E. (1988): The Dynamics of Coherent Structures in the Wall Region of a Turbulent Boundary Layer. *J. Fluid Mech.* **192**, 115–173.

Aubry N., Lian W., Titi E. (1993): Preserving Symmetries in the Proper Orthogonal Decomposition. *SIAM J. Sci. Comput.* **14** (2), 483–505.

Aubry N., Lumley J.L. & Holmes P. (1990): The Effect of Modeled Drag Reduction on the Wall Region. *Theoretical Computational Fluid Dynamics* **1**, 229–248.

Bakewell P., Lumley J.L. (1967): Viscous Sublayer and Adjacent Wall Region in Turbulent Pipe Flow. *Phys. Fluids* **10** (9), 1880–1889.

Bellin S. (1991): Etude Expérimentale des Structures Cohérentes d'une Couche de Mélange Plane Turbulente de Fluide Incompressible. Ph.D. Dissertation, Université de Poitiers, France.

Bellin S., Delville J., Vincendeau E., Garem J.-H., Bonnet J.P. (1992): Large-Scale Structure Characterization in a 2D Mixing Layer by Pseudo-Flow-Visualization and Delocalized Conditional Sampling. In *Eddy Structure Identification in Free Turbulent Shear Flows*, eds. J. P. Bonnet and M. N. Glause, Kluwer Academic Press, Dordrecht, The Netherlands.

Berkooz G. (1991): Turbulence, Coherent Structures, and Low Dimensional Models. Ph.D. Dissertation, Cornell University, Ithaca, New York.

Berkooz G. (1992): Feedback Control by Boundary Deformation of Models of the Turbulent Wall Layer. Report, Cornell University.

Berkooz G., Holmes P., Lumley J.L. (1993): The Proper Orthogonal Decomposition in the Analysis of Turbulent Flows. *Annu. Rev. Fluid Mech.* **25**, 539–575.

Berkooz G., Holmes P., Lumley J.L., Aubry N., Stone E. (1994): Observations Regarding "Coherence and Chaos in a Model of Turbulent Boundary Layer" by X. Zhou and L. Sirovich [*Phys. Fluids A* **4**, 2855 (1992)]. *Phys. Fluids* **6** (4), 1574–1578.

Bernal L.P. (1981): The Coherent Structure of Turbulent Mixing Layers. Ph.D. Dissertation, California Institute of Technology, Pasadena.

Bernal L.P., Roshko A. (1986): Streamwise Vortex Structure in Plane Mixing Layers. *J. Fluid Mech.* **170**, 499–525.

Bisset D.K., Antonia R.A., Brown L.W.B. (1990): Spatial Organization of Large Structures in the Turbulent Far Wake of a Cylinder. *J. Fluid Mech.* **218**, 439–461.

Blackwelder R.F., Kaplan R.E. (1976): On the Wall Structure of the Turbulent Boundary Layer. *J. Fluid Mech.* **76**, 89–112.

Bloch A. M., Marsden J. E. (1989): Controlling Homoclinic Orbits. *Theoret. Comput. Fluid Dynamics* **1**, 179–190.

Bonnet J.-P., Cole D.R., Delville J., Glauser M.N., Ukeiley L.S. (1994): Stochastic Estimation and Proper Orthogonal Decomposition: Complementary Techniques for Identifying Structure. *Exp. in Fluids* **17**, 307–314.

Bonnet J.P., Delville J., Glauser M.N. (1993): Workshop on Eddy Structure Identification in Free Turbulent Shear Flows, ERCOFTAC Bulletin **17**, 41–51.

Bonnet J.-P., Lewalle J., Glauser M.N. (1996): Coherent Structures: Past, Present and Future. In *Advances in Turbulence VI*, 83–90, Kluwer Academic Publishers, Dordrecht, The Netherlands.

Boussinesq J. (1877): Essai sur la Théorie des Eaux Courantes. *Mémoire Prśenté par Divers Savants à l'Académie des Sciences, Paris* **23** (1), 1–680.

Brereton G.J., Kodal A. (1994): An Adaptative Turbulence Filter for Decomposition of Organized Turbulent Flows. *Phys. Fluids* **6** (5), 1775–1786.

Breuer K. S., Sirovich L. (1991): The Use of Karhunen-Loève Procedure for the Calculation of Linear Eigenfunctions. *J. Comput. Phys.* **96**, 277–296.

Browand F.K., Ho C.M. (1983): The Mixing Layer: an Exemple of Quasi Two-Dimensional Turbulence. *J. de Mécanique Théorique et Appliquée*, Special Issue, 99–120.

Browand F.K., Troutt T.R. (1980): A Note on Spanwise Structure in the Two-Dimensional Mixing Layer. *J. Fluid Mech.* **97**, 771–781.

Browand F.K., Weidman P.D. (1976): Large Scales in the Developing Mixing Layer. *J. Fluid Mech.* **76**, 127–144.

Brown G.L., Roshko A (1974): On Density Effects and Large Scale Structure in Turbulent Mixing Layers. *J. Fluid Mech.* **64**, 775–816.

Cao N.Z. (1993): Analysis and Reduced Simulations of Laminar/Turbulent Wake Flows. Ph.D. Dissertation, City University of New York.

Carlson H.A., Lumley J.L. (1996): Active Control in the Turbulent Wall Layer of a Minimal Flow Unit. *J. Fluid Mech.* **329**, 341–371.

Carrion S. (1993): Reliability of Bi-Orthogonal Decomposition Applied to a Rotating Disk Boundary Layer. *Exp. in Fluids* **14**, 59–64.

Chambers D.H., Adrian R.J., Moin P., Stewart D.S., Sung H.J. (1988): Karhunen-Loève Expansions of Burger's Model of Turbulence. *Phys. Fluids.* **31** (9), 2573–2582.

Christensen E.A., Sørensen J.N., Brøns M., Christiansen P.L. (1993): Low-Dimensional Representations of Early Transition in Rotating Fluid Flow. *Theoret. Comput. Fluid. Dynamics* **5**, 259–267.

Cimbala J.M., Nagib H.M., Roshko A. (1988): Large Structure in the Far Wakes of Two-Dimensional Bluff Bodies. *J. Fluid Mech.* **190**, 265–298.

Citriniti J.H. (1996): Experimental Investigation into the Dynamics of the Axisymmetric Mixing Layer Utilizing the Proper Orthogonal Decomposition. Ph.D. Dissertation, State University of New York at Buffalo.

Citriniti J.H., George W.K. (1997): The Reduction of Spatial Aliasing by Long Hot-Wire Anemometer Probes. Accepted for publication in *Exp. in Fluids.*

Cole D.R., Glauser M.N., Guezennec Y.G. (1992): An Application of the Stochastic Estimation to the Jet Mixing Layer. *Phys. Fluids* **4** (1), 192–194.

Coller B.D., Holmes P., Lumley J.L. (1994a): Interaction of Adjacent Bursts in the Wall Region. *Phys. Fluids* **6** (2), part 2, 954–961.

Coller B.D., Holmes P., Lumley J.L. (1994b): Control of Bursting in Boundary Layer Models. *Appl. Mech. Rev.* **47** (6), part 2, S139–S143.

Cordier L. (1996): Etude de Systèmes Dynamiques basés sur la Décomposition Orthogonale aux Valeurs Propres (POD). Application à la couche de mélange turbulente et à l'écoulement entre deux disques contra-rotatifs. Ph.D. Dissertation, Université de Poitiers, France.

Cordier L., Manceau R., Delville J., Bonnet J.P. (1997): Sur la Relation Entre la Théorie de la Stabilité Linéaire et la Décomposition Orthogonale aux Valeurs Propres : le Cas de la Couche de Mélange Plane Turbulente. Accepted for publication in *Comptes Rendus de l'Académie des Sciences Paris.*

Cordier L., Delville J., Tenaud C. (1997): Low Dimensional Description of Large Scale Structures Dynamics in a Plane Turbulent Mixing Layer. *Turbulent Shear Flows 11th*, September 8–11, Grenoble, France.

Corke T.C., Glauser M.N., Berkooz G. (1994): Utilizing Low-Dimensional Dynamical Systems Models to Guide Control Experiments. *Appl. Mech. Rev.* **47** (6), part 2, S132–S138.

Corke T.C., Kusek S.M. (1993): Resonance in Axisymetric Jets with Controlled Helical Mode Input. *J. Fluid Mech.* **249**, 307–336.

Courant R., Hilbert D. (1953): *Methods of Mathematical Physics.* Interscience Publishers, New York.

Daube O., Sørensen J.N. (1989): Simulation Numérique de l'Écoulement Périodique Axisymétrique dans une Cavité Cylindrique. *C. R. Acad. Sci. Paris Série 2* **308**, 463–469.

Deane A.E., Kevrekidis I.G., Karniadakis G.E., Orszag S.A. (1991): Low Dimensional Models for Complex Geometry Flows: Application to Grooved Channels and Circular Cylinders. *Phys. Fluids* **3** (10), 2337–2354.

Deane A.E., Mavriplis C. (1994): Low-Dimensional Description of the Dynamics in Separated Flow Past Thick Airfoils. *AIAA J.* **32** (6), 1222–1227.

Deane A.E., Sirovich L. (1991): A Computational Study of Rayleigh-Bénard Convection. Part 1. Rayleigh-Number Scaling . *J. Fluid Mech.* **222**, 231–250.

Delville J. (1994): Characterization of the Organization in Shear Layers via the Proper Orthogonal Decomposition. *Applied Scientific Research* **53**, 263–281

Delville J. (1995): La Décomposition Orthogonale et l'Analyse de l'Organisation Tri-Dimensionnelle d'Écoulements Turbulents Cisaillés Libres. Ph.D. Dissertation, Université de Poitiers, France.

Delville J., Bellin S., Bonnet J.P. (1990): Use of the Proper Orthogonal Decomposition in a Plane Turbulent Miximg Layer. In *Turbulence and Coherent Structures*, eds. O. Métais, M. Lesieur, 75–90. Kluwer Academic Publishers, Dordrecht, The Netherlands.

Delville J., Bellin S., Garem J.H. , Bonnet J.P. (1988): Analysis of Structures in a Turbulent Plane Mixing Layer by Use of a Pseudo Flow Visualization Method Based Hot-Wire Anemometry. In *Advances in Turbulence II*, eds. H. H. Fernholtz, H.E. Fielder, p. 251. Springer-Verlag, Berlin.

Delville J., Ukeiley L. (1993): Vectorial Proper Orthogonal Decomposition, Including Spanwise Dependency, in a Plane Fully Turbulent Mixing Layer. In *Ninth Symp. on Turbulent Shear Flows*, Kyoto, Japan, August 16–18.

Delville J., Vincendeau E., Ukeiley L., Garem J.H., Bonnet J.P. (1993): Etude Expérimentale de la Structure d'une Couche de Mélange Plane Turbulente en Fluide Incompressible. Application de la Décomposition Orthogonale aux Valeurs Propres. Convention DRET 90-171, rapport final.

De Souza F., Delville J., Bonnet J.P. (1997): On the Large Scale Organization of a Turbulent Boundary Layer Disturbed by a Circular Cylinder. *Turbulent Shear Flows 11th*, September 8–11, Grenoble, France.

Doedel E.J. (1981): AUTO: A program for the Automatic Bifurcation Analysis of Autonomous System. *Congressus Numerantium* **30**, 265–284.

Faghani D. (1996): Etude des Structures Tourbillonnaires de la Zone Proche d'un Jet Plan: Approche Stationnaire Multidimensionnelle. Ph.D. Dissertation, INP Toulouse, France.

Farge M. (1992): Wavelet Transforms and their Applications to Turbulence. *Annu. Rev. Fluid Mech* **24**, 395–457.

Favre A., Kovasznay L.S.G., Dumas R., Gaviglio J., Coantic M. (1976): La Turbulence en Mécanique des Fluides. Gauthier Villars.

Ferré J.A., Girault F. (1989a): Pattern Recognition Analysis of the Velocity Field in Plane Turbulent Wakes. *J. Fluid Mech.* **198**, 27–64.

Ferré J.A., Girault F. (1989b): Some Tological Features of the Entrainment Process in a Heated Turbulent Wake. *J. Fluid Mech.*, **198**, 65–78.

Fletcher C.A.J. (1984): *Computational Galerkin Methods.* Springer-Verlag, Berlin.

Frenkiel F.N., Klebanoff P.S. (1967): Higher-Order Correlations in a Turbulent Field. *Phys. Fluids* **10** (3), 507–520.

Fukunaga K. (1972): *Introduction to Statistical Pattern Recognition.* Academic Press, New York.

Glauser M.N. (1996): Private Communication.

Glauser M.N., Cole D., Ukeiley L.S., Bonnet J.-P., Delville J. (1993): Stochastic Estimation and Proper Orthogonal Decomposition: Complementary Techniques for Identifying Structure. *Proc. Turbulent Shear Flow 9*, Kyoto, Japan, August 1993.

Glauser M.N., George W.K. (1987a): Orthogonal Decomposition of the Axisymetric Jet Mixing Layer Including Azimuthal Dependence. In *Advances in turbulence*, eds. G. Comte-Bellot , J. Mathieu, 357–366. Springer-Verlag, Berlin.

Glauser M.N., George W.K. (1987b): Orthogonal Decomposition of the Axisymetric Jet Mixing Layer Utilizing Cross-Wire Velocity Measurements. In *Sixth Symp. Turbulent Shear Flows.*

Glauser M.N., George W.K. (1992): Application of Multi-Point Measurements for Flow Characterization. *Experimental Thermal & Fluid Sciences* **5**, 617–632.

Glauser M.N., Leib S., George W.K. (1985): Coherent Structures in the Axisymetric Turbulent Jet Mixing Layer. In *Fifth Symp. Turb. Shear Flows.*

Glauser M.N., Leib S., George W.K. (1987): Coherent Structures in the Axisymetric Turbulent Jet Mixing layer. In *Fifth Turbulent Shear Flows*, eds. F. Durst, B. E. Launder, J. L. Lumley, F. W. Schmidt, J. H. Whitelaw. Springer-Verlag, Berlin.

Glezer A., Kadioglu A.J., Pearlstein A.J. (1989): Development of an Extended Proper Orthogonal Decomposition and its Application to a Time Periodically Forced Plane Mixing Layer. *Physics of Fluids* **1** (8), 1363–1373.

Grant H.L. (1958): The Large Eddies of Turbulent Motion. *J. Fluid Mech.* **4**, 149–190.

Guckenheimer J. (1976): A Strange Strange Attractor. In *The Hopf Bifurcation and its Applications*, eds. J. E. Marsden, M. McCracken, 368–381. Springer-Verlag, Berlin.

Guezennec Y.G. (1989): Stochastic Estimation of Coherent Structures in Turbulent Boundary Layers. *Phys. Fluids* **1** (6), 1054–1060.

Guezennec Y., Gieseke T.J. (1991): Multi-Point Stochastic Estimation of the Spatio-Temporal Evolution of the Far Wake of a Circular Cylinder. *Bul. Am. Phys. Soc.* **36** (10), 2863.

Handler R.A., Levich E., Sirovich L. (1993): Drag Reduction in Turbulent Channel Flow by Phase Randomization. *Phys. Fluids* **5** (3), 686–694.

Hayakawa M., Hussain A.K.M.F. (1989): Three-Dimensionality of Organized Structures in a a Plane Turbulent Wake. *J. Fluid Mech.* **206**, 375–404.

Herzog S. (1986): The Large Scale Structure in the Near-Wall of Turbulent Pipe Flow. Ph.D. Dissertation, Cornell University, Ithaca, New York.

Ho C.-M., Tung S., Tai Y.-C. (1996): Interactive Control of Wall Structures by MEMS-Based Transducers. In *Advances in Turbulence VI*, 413–416, Kluwer Academic Publishers, Dordrecht, The Netherlands.

Holmes P., Lumley J.L., Berkooz G. (1996): *Turbulence, Coherent Structures, Dynamical Systems, and Symmetry.* Cambridge University Press, Cambridge, United Kingdom.

Hopf E. (1948): A Mathematical Example Displaying the Features of Turbulence. *Comm. Pure Appl. Math.* **1**, 303–322.

Huang H. (1994): Limitations and Improvements to PIV and its Application to a Backward-Facing Step Flow. Ph.D. Dissertation, TU Berlin, Germany.

Hunt J.C.R., Abell C.J., Peterka J.A., Woo H. (1978): Kinematical Studies of the Flows Around Free or Surface-Mounted Obstacles; Applying Topology to Flow Visualization. *J. Fluid Mech.* **86**, 179–200.

Hussain A.K.M.F. (1981): Role of Coherent Structures in Turbulent Shear Flows. In *Surveys in Fluid Mechanics*, eds. Narasimha and Deshpande.

Hussain A.K.M.F. (1983): Coherent Structures—Reality and Myth. *Phys. Fluids* **26** (10), 2816–2850.

Hussain A.K.M.F. (1986): Coherent Structures and Turbulence. *J. Fluid Mech.* **173**, 303–356.

Joia A., Ushijima T., Perkins R.J. (1997): Numerical Study of Bubble Motion in a Turbulent Boundary Layer Using Proper Orthogonal Decomposition. ASME Fluids Engineering Division Summer Meeting.

Kim J., Moin P., Moser R.D. (1987): Turbulence Statistics in Fully Developed Channel Flow at Low Reynolds Number. *J. Fluid Mech.* **177**, 133–166.

Kolmogorov A.N. (1941): The Local Structure of Turbulence in Incompressible Viscous Fluid for Very Large Reynolds Numbers. *Dokl. Aked. Nauk. USSR* **30**, 299–303.

Koochesfahani M.N., Catherasoo C.J., Dimotakis P.E., Gharib M., Lang D.B. (1979): Two-Point LDV Measurements in a Plane Mixing Layer. *AIAA J.* **17** (12), 1347–1351.

Landa P.S., Rosenblum M.G. (1991): Time Series Analysis for System Identification and Diagnostics. *Physica D* **48** 232–254

Landau L.D. (1944): On the Problem of Turbulence. *Dokl. Aked. Nauk. USSR* **44**, 311.

Le Gal P., Peschard I., Chauve M. P., Takeda Y. (1996): Collective Behavior of Wakes Downstream a Row of Cylinders. *Phys. Fluids* **8** (8), 2097–2106.

Lehmann B., Mante J. (1993): Analysis of Turbulent Structure by Mean of a Two-Component Laser-Doppler Scanning Technique. In *Engineering Turbulence Modelling and Experiments 2*, eds. W. Rodi, F. Martelli, 415–424. Elsevier, New York.

Lesieur M. (1990): *Turbulence in Fluids*, second edition. Kluwer Academic publishers, Dordrecht, The Netherlands.

Lesieur M. (1993): Turbulence and coherent vortices. In *Computational Fluid Dynamics*, eds. M. Lesieur, P. Comte, J. Zinn-Justin. Elsevier, New York.

Levich E., Malomed B. (1993): Model of Boundary Layer Turbulence. Preprint.

Liu Z.C., Adrian R.J., Hanratty T.J. (1994): Reynolds Number Similarity of Orthogonal Decomposition of the Outer Layer of Turbulent Wall Flow. *Phys. Fluids* **6** (8), 2815–2819.

Loeve M. (1955): *Probability Theory.* Van Nostrand, New York.

Long D.F., Arndt R.E.A., Glauser M.N. (1993): The Orthogonal Decomposition of Pressure Fluctuations Surrounding A Turbulent Jet. Submitted to *J. Fluid Mech.*

Lorenz E.N. (1963): Deterministic Non-Periodic Flow. *J. Atmos. Sciences* **20**, 130–141.

Lu L.J., Smith C.R. (1991): Velocity Profile Reconstruction Using Orthogonal Decomposition. *Exp. in Fluids* **11**, 247–254.

Lumley J.L. (1967): The structure of Inhomogeneous Turbulent Flows. In *Atmospheric Turbulence and Radio Wave Propagation*, eds. A. M. Yaglom, V. I. Tatarski, 166–178. Nauka, Moscow.

Lumley J.L. (1970): *Stochastic Tools in Turbulence.* Academic Press, New York.

Lumley J.L. (1981): Coherent Structures in Turbulence. In *Transition and Turbulence*, ed. R. E. Meyer, 215–242. Academic Press, New York.

Manhart M., Wengle H. (1993): A Spatiotemporal Decomposition of a Fully Inhomogeneous Turbulent Flow Field. *Theoret. Comput. Fluid Dynamics* **5**, 223–242.

Manneville P. (1991): Structures Dissipatives, Chaos et turbulence. Collection Aléa Saclay.

Michalke A. (1964): On the Inviscid Instability of the Hyperbolic-Tangent Velocity Profile. *J. Fluid Mech.* **19**, 543–556.

Moin P. (1984): Probing Turbulence via Large Eddy Simulation. AIAA 22nd Aerospace Sciences Meeting.

Moin P., Moser R.D. (1989): Characteristic-Eddy Decomposition of Turbulence in a Channel. *J. Fluid Mech.* **200**, 471–509.

Mumford J.C. (1982): The Structure of the Large Eddies in Fully Developed Turbulent Shear Flows. Part 1. The plane jet. *J. Fluid Mech.* **118**, 241–268.

Obukhov A.M. (1941): Energy Distribution in the Spectrum of a Turbulent Flow. *Izvestya Aked. Nauk. SSSR, Ser. Geogr. Geophys.* **4-5**, 453–466.

Ott E.A., Grebogi C., Yorke J.A. (1990): Controlling Chaos. *Phys. Rev. Lett.* **64** (11), 1196–1199.

Park H., Sirovich L. (1990): Turbulent Thermal Convection in a Finite Domain: Part 2. Numerical results. *Phys. Fluids* **2** (9), 1659–1668.

Payne F.R. (1966): Large Eddy Structure of a Turbulent Wake. Ph.D. Dissertation, Pennsylvania State University, State College, Pennsylvania.

Payne F.R., Lumley J.L. (1967): Large Eddy Structure of the Turbulent Wake behind a Circular Cylinder. *Phys. Fluids* **10**, S194–S196.

Pécheux J., Vigor H. (1995): Instabilité de l'Écoulement dans une Cavité Cylindrique à Parois Contra-Rotatives. $2^{ème}$ *Congrès de Mécanique*, Casablanca, Morocco.

Poje A., Lumley J.L. (1995): A Model for Large Scale Structures in Turbulent Shear Flows. *J. Fluid Mech.* **285**, 349–369.

Rajaee M., Karlsson S.K.F. (1990): Shear Flow Coherent Structures via Karhunen-Loève Expansion. *Phys. Fluids* **2** (12), 2249–2251.

Rajaee M., Karlsson S.K.F., Sirovich L. (1994): Low-Dimensional Description of Free-Shear-Flow Coherent Structures and their Dynamical Behavior. *J. Fluid Mech.* **258**, 1–29.

Rempfer D. (1991): Koherente Struturen und Chaos beim Laminar-Turbulenten Grenzschichtumschlag. Ph.D. Dissertation, Stuttgart University, Germany.

Rempfer D. (1993): Low-Dimensional Models of a Flat-Plate Boundary Layer. In *Near-Wall Turbulent Flows*, eds. R. M. C. So, C. G. Speziale, B.E. Launder, 63–72. Elsevier Science Publishers, New York.

Rempfer D. (1994): On the Structure of Dynamical Systems Describing the Evolution of Coherent Structures in a Convective Boundary Layer. *Phys. Fluids* **6** (3), 1402–1404.

Rempfer D. (1996): Investigations of Boundary Layer Transition via Galerkin Projections on Empirical Eigenfunctions. *Phys. Fluids* **8** (1), 175–188.

Rempfer D., Fasel H.F. (1991): Evolution of Coherent Structures during Transition in a Flat-Plate Boundary Layer. *Proceedings of the Eight Symposium on Turbulent Shear Flows*. Munich, Germany.

Rempfer D., Fasel H.F. (1994a): Evolution of Three-Dimensional Coherent Structures in a Flat-Plate Boundary Layer. *J. Fluid Mech.* **260**, 351–375.

Rempfer D., Fasel H.F. (1994b): Dynamics of Three-Dimensional Coherent Structures in a Flat-Plate Boundary Layer. *J. Fluid Mech.* **275**, 257–283.

Rice S.O. (1954): Mathematical Analysis of Random Noise. *Bell System Technical Journal*, 282–332.

Riesz F., Nagy B.S. (1955): *Functionnal Analysis*. Ungar, New York.

Rist U., Fasel H.F. (1995): Direct Numerical Simulation of Controlled Transition in a Flat-Plate Boundary Layer. *J. Fluid Mech.* **298**, 211–248.

Ruelle D., Takens F. (1971): On the Nature of Turbulence. *Commun. Math. Phys.* **20**, 167.

Sanghi S. (1991): Mode Interaction Models in Near-Wall Turbulence. Ph.D. Dissertation, Cornell University, Ithaca, New York.

Schoppa W., Hussain F. (1994): New Aspects of Vortex Dynamics Relevant to Coherent Structures in Turbulent Flows. In *Eddy Structure Identification Techniques in Free Turbulent Shear Flows*, ed. J. P. Bonnet, 61–143. Springer-Verlag, Berlin.

Shinbrot T., Grebogi C., Ott E., Yorke J.A. (1992a): Using Chaos to Target Stationary States of Flow. it Phys. Rev. A **169**, 349–354.

Shinbrot T., Ditto W., Grebogi C., Ott E., Spano M., Yorke J.A. (1992b): Using the Sensitive Dependance of Chaos (the "Butterfly Effect") to Direct Trajectories in an Experimental Chaotic System. *Phys. Rev. Letters* **68** (19), 2863–2866.

Shinbrot T., Grebogi C., Ott E., Yorke J.A. (1993): Using Small Perturbations to Control Chaos. *Nature* **363**, 411–417.

Sirovich L. (1987a): Turbulence and the Dynamics of Coherent Structures. Part 1: Coherent Structures. *Quarterly of Applied Mathematics* **XLV** (3), 561–571.

Sirovich L. (1987b): Turbulence and the Dynamics of Coherent Structures. Part 2: Symmetries and Transformations. *Quarterly of Applied Mathematics* **XLV** (3), 573–582.

Sirovich L. (1987c): Turbulence and the Dynamics of Coherent Structures. Part 3: Dynamics and Scaling. *Quarterly of Applied Mathematics* **XLV** (3), 583–590.

Sirovich L. (1989): Chaotic Dynamics of Coherent Structures. *Physica D* **37**, 126–145.

Sirovich L., Ball K.S., Handler R.A. (1991): Propagating Structures in Wall-Bounded Turbulent Flows. *Theoret. Comput. Fluid. Dyn.* **2**, 307–317.

Sirovich L., Kirby M., Winter M. (1990): An Eigenfunction Approach to Large Scale Transitionnal Structures in Jet Flow. *Phys. Fluids* **2** (2), 127–136.

Sirovich L., Park H. (1990): Turbulent Thermal Convection in a Finite Domain. Part 1: Theory. *Phys. Fluids* **2** (9), 1649–1658.

Sirovich L., Rodriguez J. (1987): Coherent Structures and Chaos: a Model Problem. *Phys. Letters A* **120** (5), 211–214.

Sirovich L., Zhou X. (1994): Reply to "Observations Regarding Coherence and Chaos in a Model of Turbulent Boundary Layer" by X. Zhou and L. Sirovich [*Phys. Fluids A* 4, 2855 (1992)]. *Phys. Fluids* **6** (4), 1579–1582.

Sørensen J.N., Christensen E.A. (1995): Direct Numerical Simulation of Rotating Fluid Flow in a Closed Cylinder. *Phys. Fluids* **7** (4), 764–778.

Sparrow C. T. (1982): *The Lorenz Equations: Bifurcations, Chaos and Strange Attractors.* Springer-Verlag, Berlin.

Swinney H.L. (1983): Observations of Order and Chaos in Nonlinear Systems. *Physica D* **7**, 3–15.

Temam R. (1988): *Infinite-Dimensional Dynamical Systems in Mechanics and Physics.* Springer-Verlag, Berlin.

Tennekes H., Lumley J. L. (1972): *A First Course in Turbulence.* MIT Press, Cambridge, Massachusetts.

Townsend A.A. (1976): *The Structure of Turbulent Shear Flow*, second edition. Cambridge University Press, Cambridge, United Kingdom.

Tung T.C., Adrian R.J. (1980): Higher-Order Estimates of Conditional Eddies in Isotropic Turbulence. *Phys. Fluids* **23** (7), 1469–1470.

Ukeiley L.S. (1995): Dynamics of Large Scale Structures in a Plane Turbulent Mixing Layer. Ph.D. Dissertation, Clarkson University, Potsdam, New York.

Ukeiley L.S., Cole D.R. , Glauser M.N. (1993): An Examination of the Axisymmetric Jet mixing Layer Using Coherent Structure Detection Techniques. In *Eddy Structure Identification in Free Turbulent Shear Flows*, eds. J. P. Bonnet, M. N. Glauser. Kluwer Academic publishers, Dordrecht, The Netherlands.

Vincendeau E. (1995): Analyse Conditionnelle et Estimation Stochastique Appliquées à l'Étude des Structures Cohérentes dans la Couche de Mélange. Ph.D. Dissertation, Université de Poitiers, France.

Wallace J.M., Brodkey R.S., Eckelmann H. (1977): Pattern-Recognized Structures in Bounded Turbulent Shear Flows. *J. Fluid Mech.* **83**, 673–693.

Zheng X. (1991): A Low Dimensional Dynamical Systems Description of Coherent Structures in the Axisymmetric Jet Mixing Layer. Ph.D. Dissertation, Clarkson University, Potsdam, New York.

Zhou X., Sirovich L. (1992): Coherence and Chaos in a Model of Turbulent Boundary Layer. *Phys. Fluids* 4 (12), 2855–2874.

Books/Workshops

Le Chaos, Théorie et Expériences. Eyrolles Série Synthèse—Collection du Commissariat à l'Energie Atomique, 1988.

Turbulence and Coherent Structures, selected papers from "Turbulence 89: Organized Structures and Turbulence in Fluid Mechanics," Grenoble , eds. O. Metais, M. Lesieur. Kluwer Academic Publishers, Dordrecht, The Netherlands, September 1989.

Topological Fluid Dynamics, eds. H. K. Moffatt, A. Tsinober, 1989.

Wither Turbulence? Turbulence at the Crossroads, ed. J. L. Lumley. Springer-Verlag, Berlin, 1990.

Structure of Turbulence and Drag Reduction, ed. A. Gyr. Springer-Verlag, Berlin, 1990.

Boundary Layer Structure Workshop, Langley Research Center, Hampton, VA, August 1990.

Computational Fluid Dynamics, Les Houches, Session LIX, eds. M. Lesieur, P. Comte, J. Zinn-Justin. Elsevier Sciences Publishers, New York, 1993.

Eddy Structure Identification in Free Turbulent Shear Flows, eds. J. P. Bonnet, M. N. Glauser. Kluwer Academic Publishers, Dordrecht, The Netherlands, 1993.

Special Issue of Theoretical and Computational Fluid Dynamics **5**, 1993.

Eddy Structure Identification Techniques in Free Turbulent Shear Flows, CISM/ERCOFTAC Advanced Course, Udine, Italy, R. Adrian, J. P. Bonnet, J. Delville, F. Hussain, J. Lumley, O. Metais, C. Vassilicos. Springer-Verlag, Berlin, 23–27 June 1994.

5 Multiscale Active Flow Control

Pierre C. Perrier

Dassault Aviation, 92210 Saint-Cloud Cedex, France

Abstract. The physics of the multiscale patterns of flows is introduced in the first part: it is the foundation for analysis of the control of flow. Then a careful distinction is made between control as a passive mean for improving the properties of natural flows relevant to a given application, and control as a robust active tool to optimize a cost function. Improvements of the performances of engineering systems relying on flow of fluids may use passive means or active controller, sensors and actuators to withstand the external perturbations. Consideration of such types of active and passive control and of calming or increasing unsteadiness forms the subject matter of the following parts in flows of high Reynolds number relevant to major applications with turbulence or chaotic behavior. These progress towards increasing complexity of control: from the simpler control of amplitude of turbulence and chaos everywhere in the flow to achieve its homogenization to the more complex control aimed to reduce such amplitude. Methodology relying on a mix of experimental and numerical assessment of the problems and of possible solutions is needed for mastering the level of difficulties involved in complex flow control. The final part is devoted to the problems of applications, when a real-life controlled flow system is to be built, demonstrated and certified at the level of safety presently required for advanced aviation systems in operation.

1 Physics and its Modeling

1.1 Physics of Multiscale Flows

Sensitiveness. Underestimation of flow complexity is common in the field of fluid mechanics, both in applications and often in research. So much flow visualization at low Reynolds number and of computation with increased viscosity, by artificial dissipation of the numerical schemes, are now widespread, and have become the basis of physical knowledge of flows for many people. Both types of visualization succeed too much in extracting quasi-steady flow patterns, often the more attractive for researchers or engineers willing to consider simple explanations of mean properties of flows. Turning to a problem of active control implies that transient effects and their stability become of main importance in the study of control, and that the hypothesis of smooth mean flow properties is no longer relevant. Another error is to consider the behavior of the flow as a linear output of an excitation by actuators, and so assume that relevant unsteadiness is linear sum of forced outputs by the intended movements of actuators. Such framework of analysis of flows comes from the linear theory of the control of systems and is strictly valid only

M. Gad-el-Hak et al.: LNPm 53, pp. 275 - 334, 1998
© Springer-Verlag Berlin Heidelberg 1998

for linear systems. This is clearly what the flow of fluid is not, both when the Reynolds number is low because dissipation effects are predominant, and when the Reynolds number is large. Turbulent dissipation are then large particularly also in transitional regime because the transition process is highly nonlinear. Such remarks do not preclude the usefulness nor the efficiency of some basically linear controllers. However, in cases of failure of control at the design point, with large external perturbations, it reminds us that no useful analysis can be conducted from the linear viewpoint.

One basic characteristic of flows seen in practice at high Reynolds number is the capacity for a small perturbation to be convected and amplified on a space-time frame to many orders of magnitude larger than the initial perturbations entering the domain. Typically a small perturbation of $O(10^{-6})$ compared to mean external velocity and $O(10^{-3})$ compared to a characteristic length of the flow (width of a duct, wake, shear or boundary layer thickness) can fill all the domain with a perturbation $O(1)$. Such a process is therefore of major concern in the efficiency of any control aiming to reduce perturbations as far as very local control is not used (i.e. control reduced to the vicinity of the perturbation). The feeding of the unsteadiness of the flow by the actuators, designed for calming it, is a common output of linear control outside of its limited range of linear effect. Another parasitic effect is the transfer from one frequency (wavenumber) to another frequency (larger and smaller wave numbers) of the perturbation due to the nonlinear coupling of modes.

Major part of our knowledge in the field of control have been developed from the stability analysis of systems with reduced number of degrees of freedom or with clear separation of modes. It is usual in mechanical systems where a small number of eigen values keeps significant percentage of the energy stored from an impulsive solicitation. On the side of fluids such simplicity does not exist because the modes are not at fixed frequency regardless the fact that they may be seen (when a more amplified frequency lets a particular mode to appear) with more amplitude on some modes than on others. Mode frequency and possibly its shape will generally change downstream from the point of observation. So, the energy embedded in a given perturbation can be transfered to other frequencies, can be convected by mean flow or may have a significant relative traveling velocity, may eventually feed other modes. Such that the spreading of an initial perturbation is generally larger than anticipated from simple one-mode-convected linear analysis. One could consider as a challenge the control of flow patterns having such highly nonlinear behavior, but in fact it is the contrary. It means that the system constituted of the areas of interest is highly responsive to perturbations and so will be controlled with small inputs, if such inputs are adjusted to the possible self amplification where they are more sensitive. We need to turn to a sensitiveness analysis of the flowfield at least for the flow irregularities of interest for the goal of control (see Lions, 1996).

Compressibility. Another characteristic of many flowfields is compressibility. It implies that we have to add to the traveling waves of constant enthalpy perturbations, compressibility waves (isentropic at small amplitude and dissipative at high amplitude) coming from locally supersonic flows and acoustic sources. They are fed by interaction with turbulent flows or unsteady flows in shear layers in wakes or near the wall (induced by fluctuating separation, or vortex breakdown). It is generally at the sources of such unsteadiness where it is preferable to place an actuator because the control of the surface of shock waves in the field would need specific generators and cancelation seems difficult except with absorbing boundary materials out of the scope of this paper. Major problems are then related to the control of acoustic waves that focus in traveling shock waves or, in subsonic flows, that fill up all the domain at much higher velocity than traveling waves. They are however smaller amplitude than other perturbations. Acoustic waves have yet to be controlled for applications because a small percentage of energy fed into acoustic waves gives unacceptable level of perceived noise Moreover control has to avoid generating strident noise by the controller, because users do not accept such environmental attrition. Coupling of isentropic acoustic waves and entropy waves is also a main ingredient of the multiscale interacting process of traveling waves excitation. It is not a local process and is generally effective for large domain where interaction may have cumulative action in spite of large relative speed of convective modes and acoustic waves.

Vorticity. We can now turn to Fig. 1, which gives a reproduction of a drawing by Leonardo da Vinci, the famous engineer and painter of the Renaissance, that clearly indicates the effort in thinking needed to understand real vortical flows and to open the way for a control of their detrimental effects. Drawings are related to flow of water in the output of a watermill and represent the first realistic visualization of vortical flow. The great engineer's thought led to the deduction that losses of energy (height needed for waterfall) are present, generating vortical flows. However, without consideration of the boundary layer before, Leonardo da Vinci was led to try to control the vortex produced at the point of separation by an unsuccessful redesign of the downstream channel. Cancelling large turbulent vortex structures after generation is, of course, a difficult task.

Interacting Waves and Large Structures. Figure 2 will be the main basis for identification of the physical properties essential to the analysis of any control requirements, either to define realistic goals (acceptable cost function), or the physical phenomena that will be involved in the actuator action for control.

Figure 2 is an image, in a set of very high speed camera output, aimed to visualize the bidimensional unsteady flowfield around a lifting wing section (or compressor blade) having a large unsteady wake generated by separated

Fig. 1. Drawing by Leonardo da Vinci describing the complexity of vortical flows

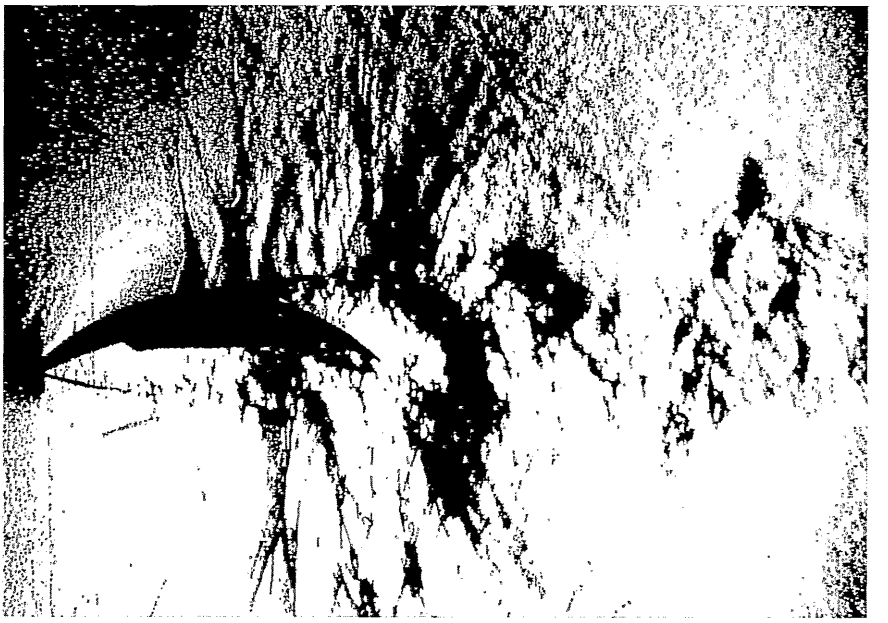

Fig. 2. Instantaneous Schlieren of transonic separated flow around cambered airfoil

shear layers on both sides of the section. Such a test case has been selected for its quasi bidimensional behavior. The carefully designed experimental apparatus by Professor Dymant of the Institut de Mécanique des Fluides de Lille, with parallel lighting, gives a pixel quality allowing identification of all phenomena. With a pixel size of 10^{-3} chord length, the duration of the lighting may be coherent with such an accuracy, so freezing all the waves and flow oscillation. The Reynolds number is roughly 3×10^6 and Mach number 0.8, giving a supersonic pocket on the upper surface with an oscillating separation. In Fig. 3 we have summarized the major flow patterns for better identification in the Schlieren picture of Fig. 2 and their scale related to chord c.

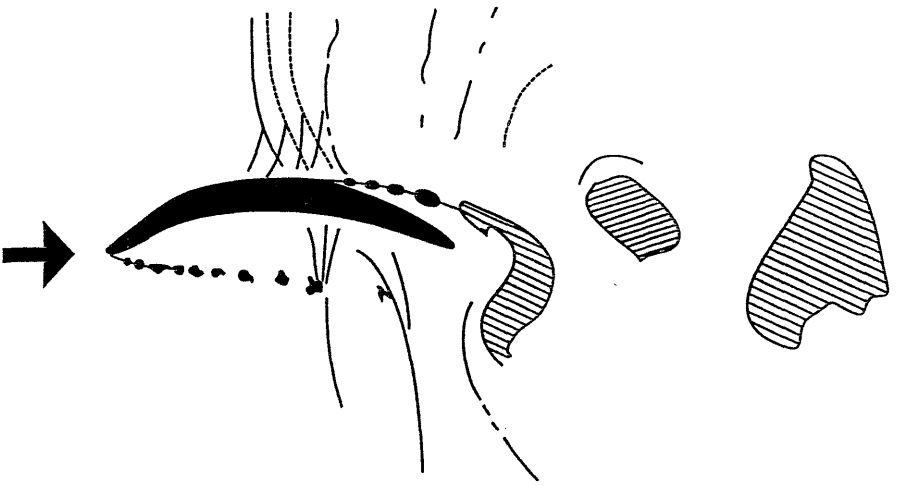

Fig. 3. Main characteristic pattern of instant flowfield of Fig. 2

For a good understanding of the multiscale problem, it is better to begin the survey of Fig. 2 by the shear layer generated on the lower part after leading edge. On the original picture it is possible to follow the growth of Kelvin Helmholtz instability from the level of 10^{-3} to 10^{-2} chord length before the bursting of regular vortex pairing. Such destruction is not exactly bidimensional leading to an indistinct generation of "puffs." It is to be noted that external flow in such mixing layer is supersonic when the internal returning flow is subsonic. The end of the regular separated area is closed by a shockwave that is generated by pulsating vortex layer structure in its rearward movement. Some residual perturbations coming from the preceding oscillation are visible as sound waves amplified by the reduction of height of the subsonic part near the leading edge. At the outer edge of supersonic pocket it is possible to see acoustic waves (or pressure waves as far as they have linear behavior at local speed of sound) traveling upstream and decreasing

in intensity with the diverging effect of reduction of the supersonic pocket upstream of the shock wave (the opposite effect of what we have identified before in the separated wedge beginning at leading edge). Such pressure waves are interacting in the separated wedge, with Kelvin-Helmholtz pairing clearly. However the external pressure waves can also interact with the incoming flow and so with the process of unsteady separation at the leading edge, but such process is in the 10_c^{-5} range. In summary we have identified that large instabilities are fed from 10_c^{-4} size processes. At least unstable processes and their saturated amplitudes are directly related to the nonlinear amplification process of large disturbances. We have to mode not only the local stability but the coupling with upstream traveling waves.

In practical configurations in low subsonic speeds the acoustic waves are very weak, but in transonic, and obviously in supersonic external flows, caution is to be kept for all perturbations generated in subsonic separated areas (and also in subsonic part of boundary layers). In low subsonic flow, a lot of flows (see Huerre and Monkewitz,1990) have absolute instability and will present such upstream interaction, but they are not so visible as acoustic waves due to their very small density fluctuation. If we turn now to fluctuation of separation on the upper part of the wing section, where the movement of the separation point is not 10_c^{-5} but 10_c^{-1}, it is possible to see also multiple shock waves with a large λ foot coming from the incoming laminar boundary layer flow, kept ahead due to accelerating flow. The pulsating flow, with large structures generated at separation, gives birth to a set of successive λ shocks that coalesce in a small number of shocks fed by downstream low frequency oscillations of separation bubble.

The building of Kármán-street-like structure, half a chord behind the wing section, is related to the interference between lower and upper separated shear layers mixing in that area in an extremely complex rolling process of the upper and lower shear layers. The upper layer has gained vortical structure of $5 \times 10_c^{-1}$ size at the trailing edge, while the bidimensionality has almost disappeared on the lower side. It is obvious that the mean flow behavior cannot be represented by an equilibrium turbulent k-ε model. It would be very uncertain to try to make the adjustment of a controller with such computational model when much more complex flowfield and exchange of energy, between large structure and microscale turbulence, has to take the predominant effect.

Bidimensionality and Tridimensionality. For control of fluid such real-life flow analysis teaches us to take into account the following phenomena:

- Natural mode amplification in the shear-layers of the flow.
- Upstream and downstream input and output of the perturbations coming from any local fluctuation.
- Sound or pressure waves travel with their focusing and dispersing effects.

– Low frequency coupling with the wind tunnel walls as a perturbation effect versus free flight.

We need a general multiscale approach in order to really control such phenomena in the flow at the suitable location, taking in account all their interactions and their increased complexity in 3-D flows. The phenomena of vortex-pairing and 2-D fluctuations of lines of separation has to be extended to real 3D phenomena that give birth to two new phenomena. First, the coupling of different non-planar entropy modes. Second, the helical destruction of local bidimensionality leading to an unstable balance between flow governed by helicity (more and more exact when separation lines are swept like in high-sweep delta wings) or by vorticity (more and more organized in Kármán street or toroïdal modes as low frequency coupling with 2D incoming flow prevails). Such 2D-3D partition is also valid for high angle of attack flow normal to upstream velocity, or for any locally bidimensional flow near leading or trailing edge. Return to isotropy is the major downstream process.

Multiscale Coupling. The problems related to multiscale flows are examined in Perrier (1996) with more details but we have to survey at least the process of amplification and phase locking of direct interest for active control.

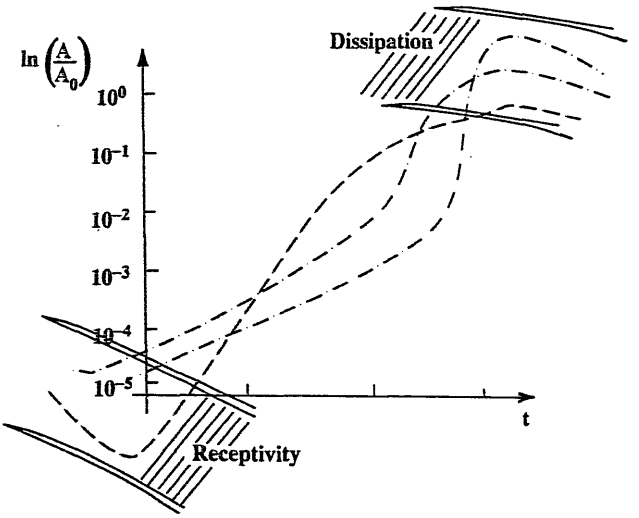

Fig. 4. Modes amplification and coupling

The process of amplification in time and of coupling in wavenumber is sketched in Fig. 4. It has to be remembered that, following a streamline in a Lagrangian coordinate, at least three modes are independently amplified among all the possible traveling waves in any direction in a small thickness

shear-layer. One is the normal mode without helicity and the two others are the conjugate modes with helicity. The angle with streamline of the more amplified transverse mode is near 45° at low speeds and low gradients but can be at higher angle (or lower) if the flow is accelerated or distorted by the local tensor of deformation. With these three oscillators, a level of 10^{-2} for fluctuating velocities compared to mean velocity may be sufficient for beginning a coupling between modes. Such nonlinear process can extract energy from the external flowfield with an excellent efficiency giving birth to the three lengths allowed for rolling a vortical flow to a chaotic flow feeding turbulence efficiently. So we have to separate

- $\tilde{n}$ in the 10^{-5} to 10^{-3} range, where linear independent amplification of modes takes place with selection of the most amplified modes (as can be seen experimentally where the Tollmien-Schlichting waves are generally only seen at level 10^{-2}.
- $\tilde{n}$ in the range of amplitudes of 10^{-3} to 10^{-1}, where coupling are taking place, as soon as the phasing of waves is correct.

The more efficient control will be at low level of amplitude, before the chaotic interference is present, and particular care has to be devoted to master it. The source of low amplitude waves is to be found in external entropy fluctuations and in pressure wave interference. External perturbations entering the viscous layer are generally damped except if at the critical wavenumber (frequency and orientation) because they do not enter with the receptive eigen distribution of perturbation. However the perturbations entering at the leading edge by convection, or acoustic waves, can made perturbations at the wall. Thereafter reduced fluctuation, although very small in amplitude, may be obviously sufficient for a coupling process involving non linearity near the zero velocity at the wall. Such a spot of fluctuation may then be amplified. It is the reason why the control at the wall may be very efficient with the help of a subsequent amplification, or be very detrimental by forcing all the modes to reach non linear amplitude that will later interfere for a chaotic amplification (Goldskin, 1996; Kerschen, 1996; Ruban & Duch, 1996; Terent'ev, 1996; Wu, 1996).

Sensitive Points. As a conclusion of this analysis of multiscale physics, it will be recommended at the beginning of any study of control of complex flow, that one should completely survey the unsteady phenomena present in the configuration of flowfield and near boundary conditions, to identify the more strongly amplified linear modes and their receptivity to external perturbation. Particular emphasis will be put on noise traveling waves and on focusing of such waves and of compressibility waves. Preliminary study will highlight the "sensitive points" in the flowfield for each of the waves, including the stationary waves that can push the non linear processes to be present very soon and very effective (Görtler vortices ...). Such preliminary study,

directed towards the problem of robustness of control, will also give the amplitude of maximal external perturbation that the controller can be expected to deal with. It is a point where we need improvement in measurements, and obviously need some new equipment able to identify in the noise the linear modes present at level $< 10^{-4}$, as well as new computations able to reach the direct evaluation of more amplified modes in the complete field.

1.2 Modeling of Unsteady Flows

Self Oscillation and Metastabilities. In the same line as Fig. 2, but with non cambered airfoil, one first test needed for qualification of Computational Fluid Dynamics in active flow control design, is to check capabilities of codes to rebuilt natural unsteadiness for transonic separated wing sections. Such test case is well documented for a lenticular arc airfoil in square test section. Rebuilding by 2D computation does not give the correct frequency for this periodic phenomena of iteratively separated flow on upper and lower surface induced by a movement of the shock waves. Correct answer is rebuilt with a 3D unsteady computation. Fig. 5 gives two Mach number contours in the cycle and shows the highly non linear behavior of the pressure for two chord positions. Such computation is a first step towards transonic buffet control on aircraft by appropriate deflection of the rear flap for damping the oscillations.

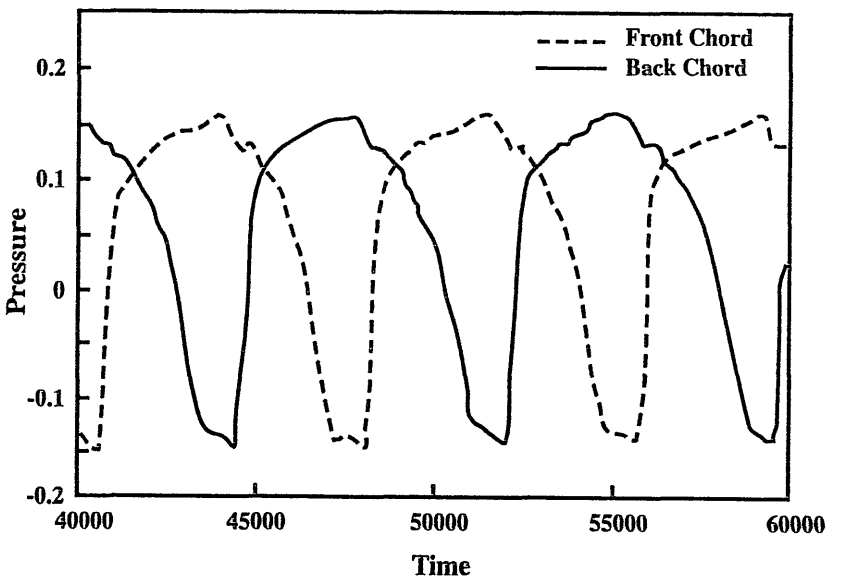

Fig. 5. Pressure in transonic separated oscillating flow

Another type of flowfield turbulence inducing buffet is generated when metastability is present in a part of the flight envelope of an aircraft or for

any complex flowfield. Such metastability can appear as a large hysteresis generator or as a small transient unsteady flow. In the first case the flowfield moves suddenly from a first pattern to another with increasing incidence and will have an inverse jump with decreasing incidence, but with an incidence delay. The control of such flow is difficult because it will be needed to smooth the jump and it requires, at least, that condition or angle of attack of the jump will have to be fixed by the control system. Another more efficient control will be to turn to a proportional oscillating transition. Such real flow exist in many natural multivalued flowfields: between the angle of attack of wing section α_1 where the state I is stable and so where a probability of 0 for state II is certain, and an angle of attack α_2 where probability of state II is 1, there is a transitory law of probability when checking a set of experiment with variation of angle of attack from α_I to $\alpha_I I$ and conversely. So a controller can work with a superimposed high frequency fluctuating forcing process from state I to state II, fixing a mean value at lower frequency and so giving a smooth transition without hysteresis. Such artificial mean behavior is of great interest for a flight control system of the aircraft. It is generally very insensitive to unpredictable hysteresis and jumps in aerodynamic characteristics that can be filtered out in this way by enforcement of their mean values.

The same strategy can be developed for the metastability of vortical flow around a pointed nose at high angle or attack of for vortex bursting as done by Lee (1996), Truong (1993). One may consider the large eddies in a highly turbulent flow with low frequency unsteadiness as requiring a similar enforcement. The asymmetry of the distribution of fluctuations of pressure compare to a normal law will sign the intermittency, requiring special consideration, see Gledzer et al. (1994). But such intermittency can appear in steady stable waves for large stationary structures in viscous layers That may bes seen in a laminar spinning body before unstable oscillations lead to turbulent flow by interaction of spiral vortices and Tollmien-Schlichting waves.

Elementary Phenomena. Such perturbations can be summarized in Table I, and are of increasing importance and complexity when compressibility or enthalpy production are present in the flowfield.

A major part of such nonlinear phenomena can appear in a boundary layer and is enhanced when perturbation velocity is large relative to mean velocity, as exemplified in near wall coherent structures; see e.g. Robinson (1989).

Equations for Modeling. So the modeling necessary to the computational analysis of any control of flow has to fulfill multiscale requirements that could be included in Direct Navier-Stokes solvers, but with a too-small Reynolds number. Large Eddy Simulation codes has a domain of computation generally too small for letting the slightly unstable modes to develop and to take in

account realistic receptivity coming from far upstream perturbations. The phenomena and equations are summarized in Table II.

Table I: Perturbations as emerging from linear quasi-steady viscous flows.

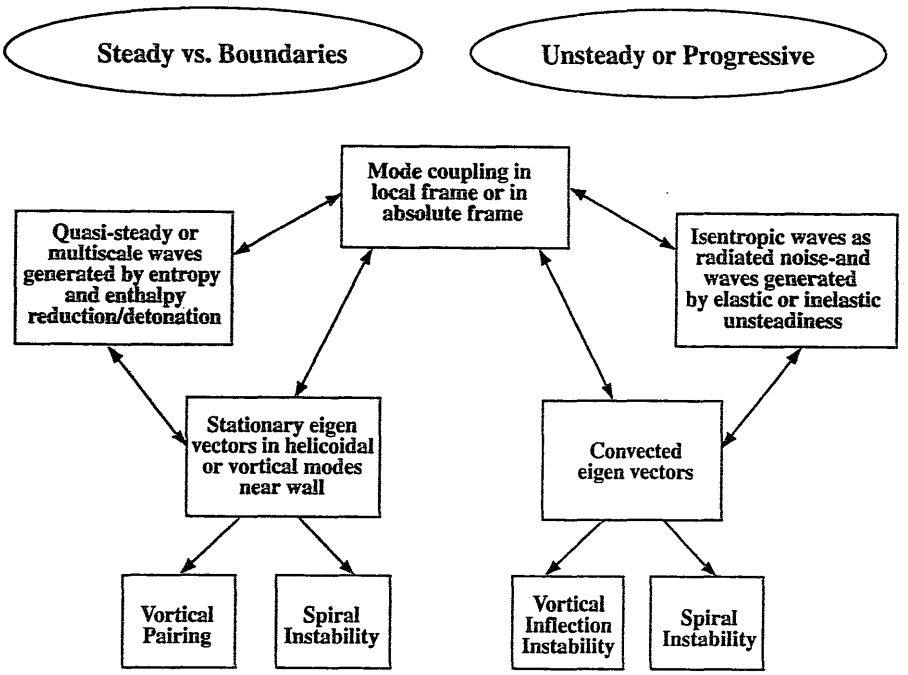
Steady vs. Boundaries
Unsteady or Progressive
Mode coupling in local frame or in absolute frame
Quasi-steady or multiscale waves generated by entropy and enthalpy reduction/detonation
Isentropic waves as radiated noise-and waves generated by elastic or inelastic unsteadiness
Stationary eigen vectors in helicoidal or vortical modes near wall
Convected eigen vectors
Vortical Pairing
Spiral Instability
Vortical Inflection Instability
Spiral Instability

Table II: Modeling constraints and equations

Global:

- Multiscale viscid modes—interaction and coupling in nonlinear range.
- Receptivity and emissivity between shear flows and viscid-inviscid perturbations.
- Energy transfer between viscid and inviscid flows—coupling with structure.
- Propagation of waves viscid and inviscid, diffraction and focusing.

Local:

- Interaction between waves number (Craya equation).
- Dispersion equation for different waves (Landau equation).
- Interaction between large structures of vorticity (Crocco equation).
- Local amplification factors in linear approximation (Orr-Sommerfeld ...).
- Multiscale homogenization due to small-scale turbulence (Pironneau-Papanicolaou).

Local Stability Analysis. Anyway the basis of any control analysis of the effect of an actuator on the flowfield has to be local stability analysis as initiated by Monkewitz (1989) and may be roughly characterized by hot wire or pressure sensor put in the flowfield. In Fig. 10, adapted from Monkewitz and Sohn (1988), the frequency distribution of peaks appearing in a hot jet is compared to the almost smooth frequency spectra of a typical cold jet. This is an example of the subsequent tracking of energy containing large structures that control has to manage. Table 3 of Huerre and Monkewitz (1990) gives the basic stability of the main different flow topology (jets, wakes, ...). Numerical tools able to give complete local stability prediction are lacking at present.

Propagation and Coupling. Linear amplification rebuilding is insufficient by itself if the propagation of waves is not also well reconstructed by Helmholtz-like equations in inhomogeneous media and the coupling of modes identified. The best mathematical ingredient for computation will be a deterministic equation for vortex interaction equation as the Crocco equation plus a stochastic triadic coupling for turbulent mean flow as the Craya equation, as implemented in Matthieu (1990) and Bertoglio (1987):

$$\frac{\partial \boldsymbol{\Phi}_{ij}}{\partial t} + \boldsymbol{\Psi}_{ij} = \boldsymbol{\Omega}_{ij} - 2\gamma k^2 \boldsymbol{\Phi}_{ij} \tag{1}$$

where $\boldsymbol{\Phi}_{ij}\ (\boldsymbol{k}, t)$ is the spectral tensor.

The closure of the equation is usually done by EDQNM over the triple correlations of the $\boldsymbol{k}$, $\boldsymbol{p}$, $\boldsymbol{q}$ triad. The integration over all possible triads gives a statistical closure of the equation, and so include the different waves emerging of the multiscale computation and then redistributes energy in the continuous spectra of established turbulent flow downstream, destroying the order preserved for large eigen vectors in Crocco equation

$$\frac{d}{dt} rot\boldsymbol{V} - rot\boldsymbol{V} \cdot \boldsymbol{V} = T\nabla S - \nabla h \tag{2}$$

For interaction of eigen vectors it is convenient to keep a deterministic formulation following the convection of vorticity field associated to eigen vectors through random stochastic medium. (see e.g. Carpenter, 1996). The controllability of propagating waves are addressed in Bardos et al. (1991; 1992).

Global Direct L.E.S. The next figure gives example of what is accessible by L.E.S. computation (Professor Lesieur, LEGI, Univ. Grenoble) as basic elementary flows: past a step in velocity formulation, for a turbulent Kelvin-Helmholtz convected instability as for vortical flow attached as a distinct vortex to a swept step and as periodic Görtler helical pattern to a ramp. Physical evidence of such structures are generally well substantiated as seen by physical visualization and may be found in Ducros et al. (1996), Mittal and Balachandar (1996), and Urbin and Métais (1997).

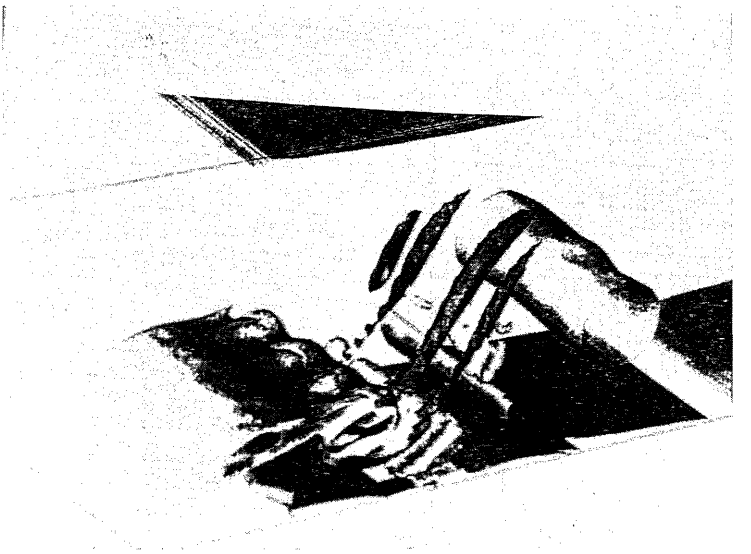

Fig. 6. L.E.S. fine vortical-helical pattern

The coupling between longitudinal and transverse vortical large structures is one of the main way to chaotic flows that is of major importance in flow control. This is particularly well identified in the visualization extracted from a LES computation of Métais (1992). However in real turbulent flows the complexity is generally higher as can be seen from the frequency spectra obtained by Bonnet et al. (1993) exemplifying complex anisotropic distribution of acoustic waves. So the reconstruction by computation has to be an ad-hoc work, relying on experimental measurements or equivalent well instrumented problems.

One cannot avoid the chain:

$$\text{Physics} \rightarrow \text{Numerical modeling} \rightarrow \text{Analysis} \rightarrow \text{Validated tool}$$

Validation may be done directly on the experiments if an approximation to the experimental data inputs may be extracted from direct measurements by a proper orthogonal decomposition (see the chapter by Delville et al. in this volume) or by any other discrete fitting. Such input approximation is necessary before LES computation may be compared for the flow pattern itself and its modeling which requires specific tests, experimental and numerical (D.N.S.), for a direct modeling from test cases relying on laboratory experiments.

Mesh Requirements. One important requirement in modeling is also to cover the topology of flows involved (at the size of the actuator flowfield

involved in the design process) in order to help the selection of optimal shapes including the control. If, for example, it may be useful to fix separation on a wing section for better control of the wake or inversely to let separation free with a domain of control at the size of possible actuators, the flow pattern has to be coherently rebuilt in either case. This requires a refinement where needed (blades, jets, suction holes, ...).

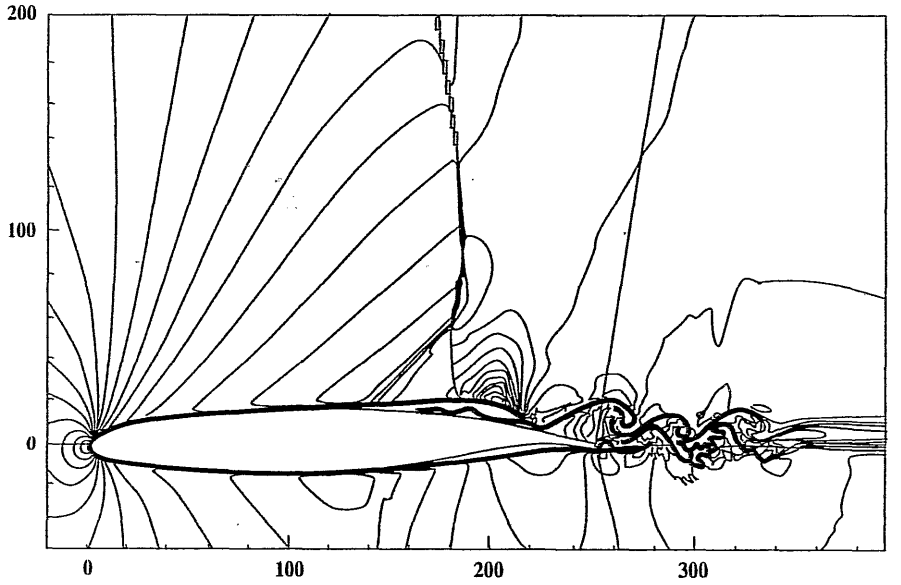

Fig. 7. Unsteady L.E.S. separated flow past an airfoil

Figure 7 gives a DASSAULT example of an industrial LES bidimensional computation of unsteady separated flow in transonic that is a basic tool for study of control of the transonic buffet induced at separation. The Reynolds number of the computation is 2.3×10^6 for 0.4×10^6 discretization points on an ONERA OALT 25 at $M = 0.8, \alpha = 2°$. The corresponding mesh is given in Fig. 8. The use of structured mesh leads to a large waste of degrees of freedom, so the future industrial codes will be probably in finite element unstructured mesh with a reduction of at least one order of magnitude in the number of points in three-dimensional flows. Such computation have been done in CTR and Dassault for a slice of bidimensional wing with a mesh able to cover $y^+ = 30$ in boundary layer. Some extra gain can be also obtain in time discretization if the order of the scheme allows it.

1.3 Theoretical Problems Related to Control

Three Ways for Handling the Control of Fluids. The complexity of the problem of control of flows of fluids is directly connected to the complexity

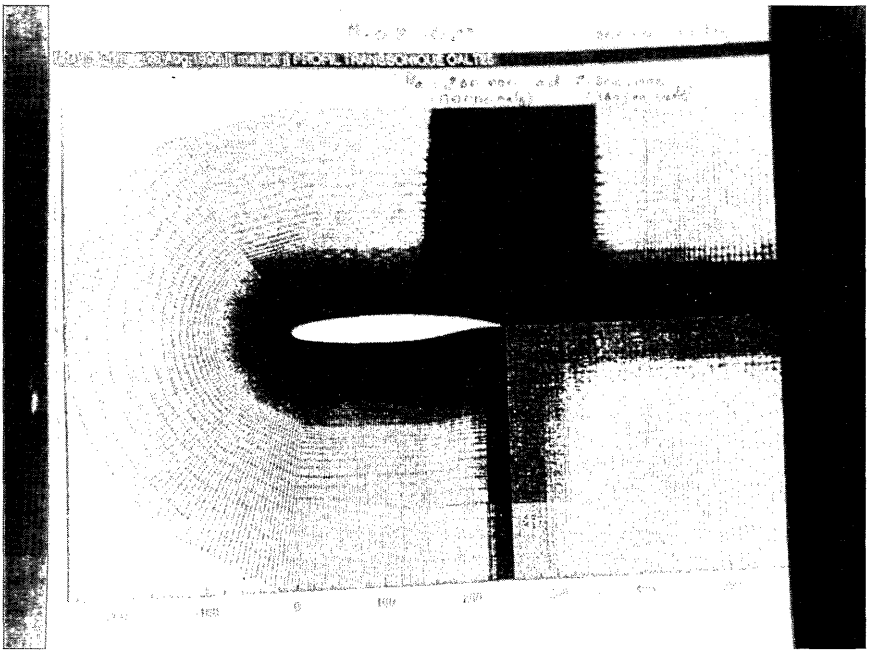

Fig. 8. Fine mesh needed for Fig. 7 computation

of the solutions of unsteady Navier-Stokes equation. So a rational approach cannot escape to a careful analysis of what can be afforded by mathematical theory of control and by past experience in the field of control of ordinary differential equations versus partial differential equations. It implies three ways for a rationality of the control of flows of fluids, two with reduced synthetic systems and one with numerical solution of flow equations with the boundary constraints and control law computation.

Dynamical Model. One way is to reduce the system to a "dynamical model," with a reduced number of degrees of freedom. The evolution of the system can then be considered as equivalent to a system of coupled ordinary differential equations. The coupled evolution of each of the parameters define the amplitude of each degree of freedom in which the system is reduced. If the actuators and sensors are also in reduced discrete number, such reduction may be equivalent to the standard black-box simulation of a dynamical system with a control loop, the vectors of parameters defining the state of the system. The input of actuators and the output of sensors are vectors of variables to be managed by the controller. The tools of classical control theory of simplified discrete system apply and are particularly efficient when the system is quasi-linear, linearity affording simple mathematical tools for evaluation of

stability and performances, non linearity appearing as a perturbation around local linearized behavior. Such linear approach (and the correlated spectral decomposition) is no longer valid when metastabilities or multivalued output come from unstable flows. A variant of the black-box approach may rely on an equivalent nonlinear dynamical system or any nonlinear synthetic model of the flow. A large literature on dynamical models helps to know the way to enforce convenient attractor trajectories, and direct control on such attractors. Unfortunately only limited number of flows, highly constrained by boundaries, seem tractable by such approach. However a proper orthogonal decomposition based on correlations between a set of snapshots of a flowfield may help to rebuild a linearly coupled dynamical behavior with an O.D.E. on first modes. Better understanding of the stability of equivalent P.O.D. for different control laws is to be recovered (see Tang et al., 1996).

Synthetic Model. A second way to rationality of control is to build an equivalent synthetic system that does not seek to eliminate the complexity of the control of a nonlinear black box. Direct consideration of the experimental problem is obtained by fitting a synthetic system without discretization of the continuous problem. The synthetic system is assumed to converge towards the real system behavior when experimental test is extrapolated to real-life conditions. Reduced set of experiments and reduced scale model are generally used in identification process, so extrapolation is needed in Reynolds number for a combination of parameters. Use of neural networks may be unique affordable process of identification of equivalent synthetic system. However, it is better to use neural network for identification of nonlinear part of model and to rebuild deterministic numerical model duplicating neural network model as frozen at the end of learning selected sequences. As Gunzburger states, it is possible to see such control as a "flow control without fluids."

Numerical P.D.E. Model. The control may be designed with a set of solutions of P.D.E. computed on a fine grid with a very large number of degrees of freedom. Convergence to continuous control, when the mesh is refined, is however to be proved. The mathematical optimal control may be computed at each time step. This gives the best setting for actuators to make the fastest transition to the targeted final state, and may take in account constraints and "least regret" as proposed by Diaz and Lions (1994) and Lions (1993) for a secondary cost function. The number and the location of the sensors may be also selected by their efficiency in the reduction of the transient behavior or of efficiency in the remaining error on control costs with perturbations.

Controllability and observability of the physical properties of the flow field are dual qualities of a given control or observation, one helping to define the minimum number and location of sensors, the other the minimum number, the location and the optimum shape of actuators. As short will be the wanted response time of control, as large will be the needed number of actuators

and sensors. This number is anyway in proportion with the complexity of the flow field involved in the transient trajectory. When crude mesh is used for evaluation of the control after observation of the flowfield from sensor data, crude control is generated (Bardos et al. 1991). Finer discretization means finer possible actuators and reduced energy required for control, but multiscale physics are then more involved in self-amplification of the action of the actuators. Specific multiscale unsteady modeling is therefore needed, and its pay-off will be net increase in the quality of the control.

The control may be evaluated step by step from an explicit computation of the solution of the basic equation in time and of the adjoint equation in reverse time from the targeted final state. Iterative control gives computation of optimal actions of actuators. The number of phenomena present in such computation constrained by boundary conditions will be at the level of complexity allowed by the discretization, and the quality of the control. True multiscale approach is generally required if the cost function is related to the properties of small scales such as mixing length, local pressure, skin friction or heat transfer. But multiscale approach is also required when small energy is available for control. Then the actuators have to rely on integrated effects coming from self amplification of perturbations and on nonlinear coupling of such effects. Considerations of large energy transfer recovered from external flow help to design the system with the level of instability convenient to such efficient control. In addition, the time constants of such amplification processes will govern the global time constant of the control in a hierarchical way; the transfer requiring a knowledge of the flow at the different involved scales, and the determination of convenient multiscale cost function.

Mathematical Point of View. If we consider a flowfield and a target for the system operating with such flowfield, a cost function J may be defined as distance of a better system state vector to present system defined by its state vector y. Then $J(y_j) < J(y_i)$ is the descent in cost with the constraint $A \cdot y = 0$, which is a symbolic expression of the differential operator A applied to the field vector y for fulfilling the Navier-Stokes equation as a constraint, the adjoint operator is A^* associated with an adjoint vector $\tilde{y}$ such that

$$< A\,y, \tilde{y} > = < y, A^*\,\tilde{y} > + b \tag{3}$$

The mathematical concepts of control of Navier-Stokes equations are now better formalized thanks to the work of Lions and his colleagues in the framework of Dolecki and Russel (1970). To obtain the control law for going from the state 0 to the state 1 will require the help of A and A^* . The differentiation of the cost function $J(y, \Phi)$, Φ being the control vector, gives the optimal control, if we solve the direct an the adjoint problem simultaneously. It is possible to reduce the optimal control to a suboptimal control working only on a time step from time t to time $t + \mathrm{dt}$ and using the formulation

of the discrete algorithm of integration in time as an approximation of the continuous equation without its complexity. However such approximation is not necessary thanks to automatic differentiation of the formulas for mathematical derivation of control vector or of sensitivity matrix in linearized perturbation equation. See Ito and Desai (1991), Gunsburger et al. (1991), Chacon (1995), and Lions (1971; 1986).

We may try a reduction of the discretized partial differential operator $\boldsymbol{A}$ to a much smaller reduced system ($\boldsymbol{a} \cdot \boldsymbol{y} = 0$) of ordinary differential equations by a proper orthogonal decomposition. Then each equation needs a control but the coupling between the different equations, coming from the original nonlinear Navier Stokes equation, implies that they have to be correlated. If so, outside of perturbations, the dynamical system will be put on stable orbits and theoretically needs only to be active when perturbations occur. However the approximations of real flow by a dynamical system is crude, continuous actions are needed and stability may be uncertain. The fact that such approach helps to separate the stable and unstable generalized modes of the flow field is a very useful piece of knowledge for optimizing the system of boundaries including actuators.

The same trend as the perturbations may be mastered by direct acting (being locally damped or self amplified by a convective or absolute local instability), the global control may lead to controllable or uncontrollable behavior. The general time lag or the parameter residual errors induced in a partially controllable system is generated by the controller itself from uncertain or incomplete observability. The computation of the better action (eventually to be balanced with simpler laws of control based on data of sensors as for a Kalman filtering in O.D.E.) requires the solution of the Riccati equation. Unfortunately this is a P.D.E. with 6 dimensions in space and 1 in time, difficult to compute except for a very small domain. One has to confine within limits of local specific control of prescribed modes. Targeted control, based on selection of coherent reduced state equation, requires also a selection of pertinent scales in flow computation (Lions, 1971; 1985; 1986; 1988; 1990; 1991; 1993).

Consideration of total energy may also help to identify control problems. First importance is knowing the energy that is under control compared to the residual uncontrolled energy able to destroy control by a back-scatter process. Then the control has reduced the energy only in one part of frequency or wavenumber range of the flow field. A feedforward effect may appear as excitation of convectively unstable large scale by perturbations from large or small scales when large scales are not properly controlled. A better way of scaling energy effects is to carry out an evaluation of energy in parts of the flow including vortical patterns from energy evaluated with vorticity and helicity integrals. For helicity the Arnold theorem (Arnold 1965, 1966, Wu 1991) confirm that stable configuration of vortical flow, in the Lyapunov sense, are maintained for extremes of energy in concentrated or diffuse vortical flows,

respectively with maximal and minimal energy. High dissipation may then be checked by enstrophy increase due to vortex stretching process in turbulent three-dimensional flow.

Present state of the art is far from giving precise mathematical conditions or constraints for controllability of Navier Stokes Equation. A review is given in Gunsburger (1995) but preliminary partial results are building (see Bardos, 1992); Furksikov, 1994; Coron, 1996). Recent results by Coron afford precise but limited answers to dual problem of observability-controllability.

Flows are characterized by a mix of local instability and of traveling wave dispersion. For wave control, as typified in Helmholtz equation, see results by Bardos and Lebeau (1992) and Bourquin (1993). The elementary results of mathematical rationalization of control are used in the following chapters.

Open loop control will apply constant amplitude control without use of sensor data related to instantaneous cost function, but feed-forward control will close the loop of control by adjustment to upstream identified set of parameters and evaluating some approximation of the cost from the sensors data.

Cost Functions and Characteristic Test Cases. General form of the cost function may be written as

$$\boldsymbol{J}(u,t) = \int_0^t [\boldsymbol{\Phi}(y(u)) + \boldsymbol{\Psi}(u)]\,\mathrm{dt} \tag{4}$$

The cost function for going from state 0 to state 1 is $\boldsymbol{J}(u,t_i)$ and has two parts, one related to the physical realization of the targeted control ($\boldsymbol{\Phi}$ being function of the distance between y and targeted $y\,t$), the other to some economical cost $\boldsymbol{\Psi}$ of the mastering of the flow field.

Two parts may be once more identified in $\boldsymbol{\Phi}$ as in $\boldsymbol{\Psi}$. The first one may be extracted from mean values of distance in y, for mean perturbations requiring mean deflections v_p of the actuators. The second is characteristic of extreme values of deflections for mastering extreme perturbations and distances between state 1 and 0. It is clear that the overall economic cost of acquisition of a control system is defined by the envelope of extreme needs in size, energy input and activity of the actuators. Conversely mean economic cost of operation is related to mean activity and on energy requirements for the operating life, as resulting from integral of activity throughout the service life.

This consideration of mean and extreme conditions of operation does not appear in the local problem of observability. Robustness of observation need a sufficient set of well located sensors always in operation. They have to be as numerous as needed for covering problems of uncertainties or duplication for failure in extreme conditions.

In addition to physical and economical costs, an additive term, acting as a penalty term, is often needed for inclusion of other intuitive cost functions.

these express distance to a desired behavior of the system seen as more globally productive, safe or comfortable and with respect to which least regrets are to be taken in consideration. Similarly, least regrets penalty may be constrained by margins for unanticipated phenomena, out of sensors location, by extreme uncertainties, or in physical cost (mean or extreme residual errors in operation) or in economical cost (mean or extreme reference cases for design).

For evaluation of the control laws minimizing the economical cost, the selection of test cases is a major concern in the design and qualification of active control of fluid flows. It requires the availability of multiscale codes for the generation of the large coherent boundary conditions in the reduced size domain of the flowfield around actuators and sensors system. For example it needs the use of a mesoscale generation of realistic atmosphere perturbations upstream of experimental or numerical tests. Specific activity of "assimilation" may be supported by advanced specific codes. If selection of a reduced (but pertinent) approximation of complex flowfields (P.O.D. of Lumley or L.E.S. filtered modes) is possible, a coherent targeted control may be tested on. It may help to analyze the control stiffness with various complex cost function.

2 Turbulence Enhancement Using Active and Passive Control

2.1 Enhancement of Perturbation Process

Energy Spreading. From an energetic point of view, whatever the specific cost function, the control has to be divided by the applications between control oriented towards the reduction of fluctuations and control oriented towards the increase of some property (like heat and mass transfer) related to increase of fluctuations at a certain scale.

If the Reynolds number is sufficiently large, as well as the complexity of the flow induced by boundary conditions, then reduction of perturbations will be much more difficult than enhancement of gradients. Thereafter such control aiming to increase fluctuations is to be considered first, and the relevant cost parameters are "minimum of energy" for control and "scale of homogeneity" resulting from actuators action. Better controls rely on self equilibrium of the turbulent scales and on self entrainment effects of the non turbulent parts of external or internal flows.

Denominations. Control of flows are often denominated "passive" when no addition of energy is supplied to the system and "active" when there is input of energy by actuators in the flow. However in the following analysis another denomination is retained. Passive integrated control is related to a free system without controller to control the position in time of the actuators, and active control is related to a system with a controller, the output of which

is the targeted position of the actuators. The controller is taking in account the knowledge of the state of the system by previous experiments or/and computations and by present outputs of the sensors.

A "passive" system of control may rely on fixed or free devices added to initial design or may rely on specific integrated design (e.g. rotating blade mixer enhancing a particular flow pattern). In that denomination frame, the vortex generators will be denominated as passive fixed flow control near separation of boundary layers and a local "Gaster bump" (bump at leading edge of a swept wing for accelerating flow contaminated by leading-edge turbulent boundary layer and so regaining laminar boundary layer downstream) a passive built-in flow control design. Similarly a slotted part of wing section with interrelation with another slot upstream of a shock-wave will be a "passive" device. A free-floating vane cutting large structures of turbulent flows in a tube will also be also a "passive" device. One of the main ingredients of the evaluation of the effectiveness of any active control will be its comparative value with the best of passive controls and the justification of its added complexity related to performances. The best passive control will then be named "passive reference" control.

2.2 Strategies of Control

By Force Action. It is possible to identify three paths to turbulence enhancement in a flow when more and more precise action on the flow is built and when strong action is replaced by small self-amplified local actions. The resulting turbulent fluctuation is u' and it is the sum of contribution of ordered modes u_i and of random fluctuations.

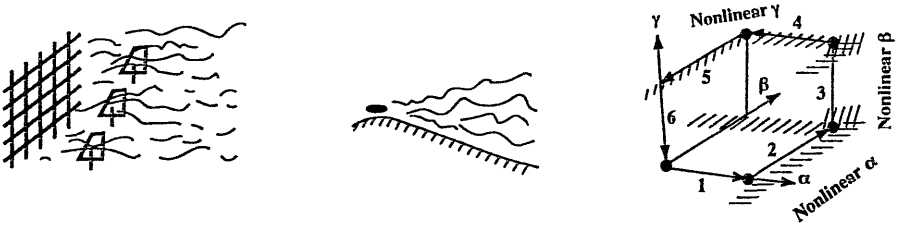

Fig. 9. The three paths to turbulence enhancement: forced turbulence seeding, self amplification, and bracket in a nonlinear strategy.

The first one consist in a strong production of more or less local source of intense turbulence that will be convected downstream, if the local instability allows more or less local behavior of the flow. Passive means are grids or

vortex generators. Active means are relying on added moving blades, injections, or moving walls. The proper design of the flow boundaries will help to have or retain intended diffusion downstream of turbulent energy injected in the local source spots. Clearly such path is irreversible and so specific to turbulence enhancement.

Mode Coupling Used for Action. The second one will rely on control of smaller scale structures of flow, and on identification of the areas of maximum receptivity of the flow to external actions or perturbations. The energy injected in the receptive part of the flow need to be in phase resonant with one amplified wave to be more effective, if active control is built. The use of acoustic or shock waves may be added to the means of turbulence enhancement, but the use of chaotic seeding of turbulent energy (Swanson & Ottino, 1991) is no more relevant. Selection of the more amplified waves leads to adjust size of passive means for excitation of unstable modes. Such modes are surviving to intermittency and low-scale turbulence in the case of turbulent incoming flow. Phase adjustment increases effectiveness of active means, asking for a precise acquisition by sensors of phase of incoming waves. The persistence of induced action in turbulent flow is a major practical and theoretical issue.

Receptivity Used for Action. The third path to turbulence enhancement is to turn control towards the coupling of modes. The process of transfer of energy from external flow field to fluctuating turbulent flows rely on nonlinear coupling of modes that extend in external flow. One mode at least has to be saturated or in highly nonlinear increase so that the coupling will be itself nonlinear, that is to say that it will extract energy from $\nabla \cdot \boldsymbol{u}$ (the gradient of external low-frequency fluctuating velocity) by the coupling term $\boldsymbol{u}'_1, \boldsymbol{u}'_2 \nabla u$, where the nonlinearity of u' will ensure the non-orthogonality of $\boldsymbol{u}'_1 \cdot \boldsymbol{u}'_2$. (Linear wave pattern of modal fluctuating velocities, $\boldsymbol{u}'_1$ and $\boldsymbol{u}'_2$ for the modes 1 and 2, causes $\boldsymbol{u}'_1 \cdot \boldsymbol{u}'_2 = 0$.)

It is clear that the larger the scalar product of fluctuating velocities, the larger will be the transfer and also the nearer the frequency of both mode, the better the phase adjustment and the better the locking in frequency. Then the locking in phase will give the continuity of production term relying on the nonlinear coupling behavior. Control has so to be adjusted to act on the phase and frequency of more energetic coupling. If a third mode may be put in the loop of nonlinear coupling, one builds a generative device for highly chaotic source of turbulence that is an extremely powerful mean for transfer of energy from external or boundary parts of shear flow to subscale turbulence. Such behavior of flows are eventually produced near the wall by the first three modes of instability of laminar boundary layer as very active spot of turbulence. Similar behavior may be built in turbulence shear layers with transverse vortices generated by passive or active means. A very active

set of command of actuators will rely on the bracket strategy of action (right side of Fig. 9).

In the first segment of the bracket a linear mode is pushed to saturation, before actuation of the second mode to its maximum value, the action on the first mode can be then released before release of the action on the second mode and new symmetric action. The saturation in nonlinear behavior of the first mode have not to be effective at the location of the actuator but at some station downstream, relying on the natural linear amplification as for other modes, but the localization of the interference have to be prescribed. The longitudinal modes that are pure helical modes, except in the case of curvature induced amplification (i.e. Görtler-type amplification), and are convected with a quasi-constant value of helicity. They may interact efficiently with rolling vortices normal to convection velocity: convected alternate in sign helicity helps to build nonlinear bracket coupling.

Reversibility of Action. Only small linear actions may be almost reversible and so lead to minimize entropy production. Wasting of energy appears when action is coupled with turbulent flow randomness. Use of near self-damping of neutrally stable modes are the more efficient process as being quasi-reversible actions; they are quite different of the finer actions for control and reduction of turbulence.

2.3 Cost Function and Heat and Mass Transfer Enhancement

Constrained Global Cost. The maximization of energy may not be a target, being not bounded. Added constraints need to be expressed as limiters, and cost function cannot rely only on maximization of turbulence because mechanical constraints may appear. If one considers for example a two dimensional mixing layer, mainly bidimensional turbulence will enhance a k^{-1} behavior (k is wavenumber, see Fig. 10). A continuous transfer to low frequency of the injected energy amplified by Kelvin-Helmholtz instability will enforce coupling with external flow of mean shear layer. Such transfer may put energy in low frequency mechanical parts of the system. A "least regret" cost function, (difference to a target in turbulence energy plus mechanical energy) taking in account given alternate fatigue-stresses constraints, will be the best expression of the global target of the control. A direct control of mean stresses may act in the controller for limitation of amplitude.

Local Homogeneity Indexed Cost. The homogeneity of resulting field of turbulent shear stresses may be chosen as the major target to be included in the cost function. For example, with sensors of turbulent shear, as efficient energy transfer are related to the square of the fluctuations of velocity, data of sensors may be taken in a cost function as least regret penalty contributors. Results are however very sensitive to sensor position and so preliminary

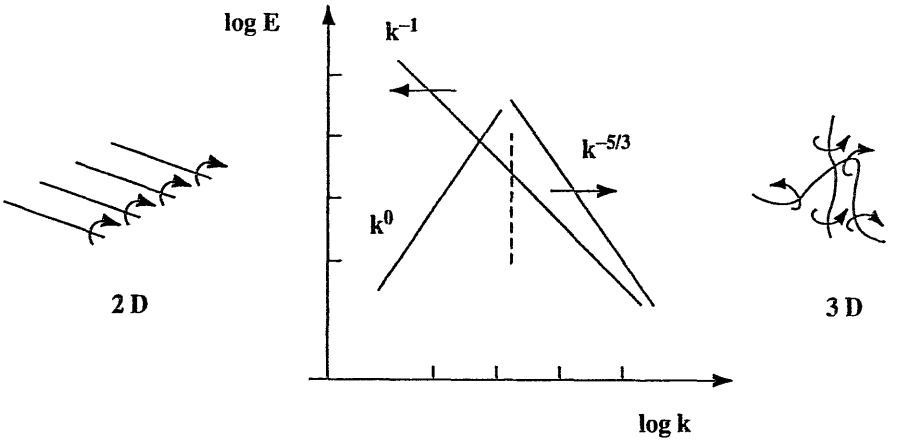

Fig. 10. 2D versus 3D energy transfer

analyses of sensitivity of flow to perturbations induced by actuators and of sensitivity of the sensors to distortion of the local versus global cost function are very useful. Algebraic methods for evaluation of stability of flow versus perturbations being local and generally unable to survey complex boundary conditions, the development of new numerical tools for such sensitivity is mandatory and complementary to introduction of reduced scale experiments. The knowledge of a model, identified with the support of experimental and numerical data, may also help to define controllers. The classical dynamics property of systems with reduced number of parameters may be recovered with convenient diagonalization of sensors and actuator linear correlation. However it is clear, from consideration of the bracket control strategy, that such modeling cannot really support advanced self-amplified to nonlinear saturation type of control. The rejection of some linear flow-structure coupling may also be conveniently studied in a linear approach with O.D.E. simplified models better than with complete P.D.E. coupled unsteady computation. So the addition of homogeneity and mechanical constraints may be done in the global cost formation without care of variety of sensors data involved if a partial energy decomposition is clearly defined.

Global Economy Indexed Cost. If we turn to economical constraints, it is clear that the energy required for a given efficiency is an index that has to be balanced with the complexity of the set of actuators and sensors and of the controller itself. Complexity and associated cost are key factors allowing to justify jump from passive means to complete active control system. It will

be addressed in Part 5.

Globally, we may keep a typical global cost function to minimize, either the performance index or the numerical cost index, or even better the ratio of cost C and performance or $C/e_f = c$:

$$c = c_e + c_p \tag{5}$$

$$c_p = \left(\frac{\alpha \cdot e_i + \beta \cdot e_s + \gamma \cdot e_h}{e_f} \right) \tag{6}$$

where c_p is the performance index cost, cost of energy input related to energy output, c_e is economical index cost (cost of sensors + actuators + controller) related to energy output, e_f is the turbulent energy injected in the flow domain to be controlled (integral), e_i is the input of energy in actuators, e_s is feedback input of mechanical energy above stress limit constraints, e_h is the defect of energy below mean e_f (integral of local defects in the flow domain of interest), and α, β, γ are parameters for weighting e_f, e_i, e_h.

2.4 Basic Flow Characteristics and their Use in Control

Stochastic Versus Deterministic. There are two basic flow characteristics which can be used for the turbulence enhancement control: or the quasi-random behavior of locally equivalent dynamical system or the organized one with multiscale structures. In the quasi equilibrium turbulence, it is possible to analyze in Fourier wavenumber the energy stored in turbulent flow within a well identified cascade. From the low-frequency part, continuous part with a high frequency dissipation, and power law spectra subpart. Then, with a forcing energy at a given wavenumber, a statistical triadic coupling extend the injected energy in lower and higher frequency, the global energy moving rapidly to equilibrium curve.

Stochastic Mixing. If the flow is excited with two frequencies, the triadic coupling, as modeled in EDQNM by Kraichnan, statistically redistribute energy. If wavenumbers $\boldsymbol{p}$ and $\boldsymbol{q}$ are fixed, giving birth to the complementary wavenumber vector r, a triple excitation is generated, and homogenization is better.

In the case of a specific excitation coupled to the response of the flow, the large eddy structure of the flow may be enhanced as a resonator amplifying input excitation. For example an excitation of the Káán street of a cylinder by transverse movement of the cylinder will give birth to a three dimensional quasi-isotropic wake. An impulsive start of transverse movement of the cylinder induce two oblique shedding wave packets, in pattern that are similarly excited by sinusoidal movement of the cylinder at resonant frequency in Gharib (1993) experiments. Generally, in established turbulence, the resonant behavior is without peak in the energy spectra because it is

smoothed by redistribution of Reynolds stress in wavenumber as exemplified in Binder and Tardu (1996). For an excitation at the end of the spectra in turbulence cascade, same behavior may appear with the forcing issued from the wake of a cylinder in the subscale of a shear layer. Efficient increase in mixing results from the return to isotropy of such forcing at frequency higher than the energy carrying scales. That process also reduces the transfer to low frequency, and so is an efficient mixing process in small scales, it allows devices to be efficient for improvement of the classical mixing in chemical industries with paddle wheel mixer. Another mixing enhancement may rely on the coupling between same structures, one being excited (see Lepera and Vandsburger, 1997) or excitation of the vortical separated flows (see Nelson et al., 1990; Nelson and Eaton, 1996).

Dynamical Mixing. Another multispectral enhancement of the turbulence may rely on equivalent dynamical system. The aim is the destruction of organized structure by excitation of the basic attractors of the flow. Two main transitions to patterns with chaos are possible, one relying on Hopf bifurcation following Ruelle-Takens scenario and cascade in power spectra as for Rayleigh Bénard convection, the other relying on the doubling of period scenario of Feigenbaum, see e.g. Argyris (1993). Both patterns may be induced by perturbations forcing specific equivalent global modes such as the first modes of a proper orthogonal decomposition of Lumley.

The building of low frequency by vortex pairing in a free layer is characteristic of the natural process that can be enhanced by proper excitation. Similarly chaotic advection helps to have efficient mixing at low Reynolds number (see Aref and Jones 1989).

Transitional Mixing. One can notice successively in a typical transitional situation:

1. Periodic emission of unstable waves.
2. Growth of low frequency perturbations (see Monkewitz, 1993).
3. Phase decorrelation of coherent structures induced by perturbations (see Ho, 1991).
4. First vortex merging (1st bifurcating process) and production of small-scale turbulence.
5. Spanwise fluctuation of resulting merged vortices.
6. Second bifurcating process with irregular secondary merging.
7. Irregular spanwise fluctuation in normal and transverse distorted flow.
8. Third bifurcating process and interaction of the three component distortions in nonlinear coupling. The nonlinearity occurs in lower speed areas (areas of greater relative distortion), near the wall for boundary layers.
9. Bursting phenomena coming from vortical high-shear engulfment of low-speed vortical flow and external potential flow. Transition and chaos are present with vortex stretching and intermittency building.

10. Return to isotropy and spectral equilibrium of turbulence generated by bursting. Nonlinear coupling of the three component fluctuations follows random spots of inviscid engulfed flow.
11. Established turbulence with usual behavior and eventually fractal intermittency.

This physical description of transition from correlated bidimensional rolling transverse vortices to three dimensional turbulent shear layers as expressed in Monkewitz (1993) and Ho (1982; 1991) and as schematically illustrated in Fig. 28 has been partially supported, in addition to flow visualization, by Large Eddy Simulation. LES does support phase 3 to 9 of the suggested sequence, if amplification is large, but transition to equilibrium turbulence need specific spectral modeling with spectral redistribution of eddy damped random process of transfer by Kraichnan (1976) and S.C.I.T. model of spectral closure. Matthieu and Jeandel (1994) Bertoglio and Jeandel (1987) and Bertoglio et al. (1994) were able to effect a return to classical turbulence modeling like that of Smagorinsky (1963) or k-ε models. For a multiscale physics homogenization closure is described in Pironneau's appendix to Mohammadi and Pironneau (1994).

Numerical Tools for Control. Assuming some validity and generality of the process of transient flow as described before, one may notice that phases 1-2-3 may not be modeled by realistic computations due to the length of growth of the irregular pattern of a flow. Linearized Navier Stokes solver would be good solver for rebuilding the receptivity problem of items 1-2. To control the linear perturbations induced by receptivity process need sufficiently small-scale discretization, otherwise the control will be turn to the damping of saturated nonlinear perturbation of items 3-5-7.

In fact the control at this 2-5-7 second level (first level is related to receptivity reduction by artificially increased damping of external perturbations) tries to control modal fluctuations of main rolling vortices as if it was in low Reynolds number range. Such behavior is physically possible, when fine structure of perturbations are almost homogeneous in small-scale turbulence. An equivalent low-Reynolds-number pattern is built by the turbulent Reynolds averaged stress tensor. Numerical tests in LES/DNS are therefore mandatory before testing robustness versus turbulent fluctuations of any control law.

Complex Physical Control Building. General control by minimization strategy relies on the building of "clean" basic modes of flow, to be maintained below the saturated nonlinear amplitude, but at a level allowing bifurcating laminar-like behavior. In dynamical system framework, one large amplitude orbit is maintained but its attractor basin is stabilized for avoiding transition to chaos. Such strategy is called O.G.Y control (Ott, Grebogi and York, 1990; Bergé and Pomeneau, 1988). Control is effective as far as one large orbit in

phase space remain the major large structure of the flow, i.e. with sufficient percentage of the fluctuating energy.

Conversely the present control, for increasing heat and mass transfer by properly increased turbulence in mid-scale, will use the enhanced large deterministic structure, pushed unto the saturated amplitude by the bracket strategy. The successive amplification of the three secondary modes superimposes chaos on main structures and helps to build an efficient bursting procedure (item 9). Turbulent spots feed a large range of wavenumbers in the mid-scale or fine scale, and so enhance turbulent energy on all the spectra (item 10–11).

It is clear that stabilization of the main structures to be excited downstream is firstly done by the proper geometrical design of the walls. It reduces the perturbations (item 1-2) and increases the phase correlation of main large eddies (items 3-4), around the critical points of bifurcation. For example, the optimum design of a laminar airfoil requires a careful control of the flow near the stagnation point, for an efficient damping of the external perturbations (low receptivity), particularly in spanwise direction. It also requires fixed chordwise laminar separation point, avoiding irregular downstream separation pattern. Forcing in order to increase downstream turbulence may eventually let the reattachment of the separated thin layer take place before trailing edge of the wing section. Such complex flow control will lead to a better stability of global flow thanks to the stabilization of the laminar part of the flow and the excitation of the turbulent part for better efficiency of turbulent mixing; mean flow pattern has to be regular. Active-passive coupling may be done by control of modes to be convected on a secondary or tertiary fixed device (example of such mechanism in receptivity may be seen numerically in Casalis, 1997).

2.5 Critical Point Design and Control

One major concern in aerodynamic design is the search for regular flow pattern whatever the angle of incidence or sideslip. Regular forces and moments on a vehicle will therefore be obtained. However the high angle of attack and sideslip involved in high performance design has put the challenge of regular behavior in domains where bifurcations are predominant. With large variations of wall separation patterns and of external flow patterns, with shock waves and vortex sheets or vortex lines, with bursting and reattachment induced processes, the challenge would be almost impossible to overcome. The control of large main structures in the flow would give robustness and monotonicity to the flow field at varying angles. That is, it is not necessary to search for stabilization of all large eddies but to stabilize low frequencies after first bifurcations.

Two types of large eddies are generated around the bodies in free flight or in ducts. One is induced along separation lines, the other in free shear layer or vortical layers. Stabilization of the separation lines may be better done with

upstream forced separation than downstream free control. Similarly, shear layer or vortical layers may be better fixed in their complex transition to chaos and turbulence by upstream forcing.

We will address the difficult problem of reduction of separation or of transition to chaos in the following part. Extension of high turbulence in a regular solution is easier to control. In each particular case we will always have to enhance a large structure and a mode coupling. For jets and wakes the strategy of control rely on the excitation of the basic toroïdal structure and of the normal modes (particularly streamwise vortices). For bodies it relies on helical swept separation (more stable than free bidimensional separation on curved surface). For ducts on longitudinal swirl and transverse large rolling structures. Each time it is the critical point concept that gives guidance to action.

Rennie and Jumper (1994) have shown the trailing edge control effectiveness and its unsteady behavior, and Lee and Ho (1993) experimented with the reduction in lift fluctuations by trailing edge suction. Wu and Wu (1991) identified the gain in swirl as obtained by suction in the central part of an S-shaped duct of square inlet and circular exit. This may also be achieved by passive control with vortex-generators (Reichert and Mendt, 1994).

Large amount of tests of excitation of modes of a round jet have shown that mixing may be multiply by a factor as large as 3, when secondary modes are excited. Recent results by Urbin and Metais (1997), in Grenoble University using LES computations, have supported numerically the high efficiency of modal unsteady excitation obtained experimentally by Bischop and Chan (1996). Active pulsed forcing of turbulent boundary layer at leading edge of a wing section has shown (Mochizuki, 1993) that reattachment takes place with very small injected mass airflow.

Passive control by small flaps at the nozzle exit (Binder and Didell, 1981; Zaman, 1994) or by cavities for supersonic jet forcing have been successful. Also successful, but more complex for the excitation devices, are pneumatic actuators that force different modes of the jet, so increasing its mixing for a given length.

Same type of pneumatic actuators have been used for jet and separation control. For jet excitation they may be applied on toroïdal modes or on three-dimensional modes (Jeung et al., 1994; Suprayon and Fiedler, 1994; Raman and Cornelius, 1994). Same strategy was applied for reduction of separation bubble on a flap or a sphere or cylinder (Eric and Fernholz, 1994; Bar-Sever, 1989; Huang et al.; 1987, MacManus et al., 1995).

For free shear layers, when building vortical shear layers like leading edge vortices, care must be taken of the stationary modes reinforced for specific sweep angles of the separation line. Fluctuations in the separation line is inducing the helicity fluctuations convected in the vortex core. For small sweep angles low helicity precludes shedding, while large sweep induced more stable flow pattern. Intermediate sweep generates alternate flow pattern becoming

more stable for specific sweep angles easier to control. Theoretical background in stability are presently lacking.

2.6 Noise Generation and Receptivity Control

One of the main element in reduction of the perturbations relevant to amplitude of control, is that the receptivity to entropy waves or perturbations is generally low, due to the damping process that take place in the initial part of each body, it is due to acceleration of flow from stagnation point (or line) to bifurcation or separation of large structures in shear layer. Comparatively the acoustic waves are of much lower amplitude in induced velocity, but they travel through viscous layers almost without damping and their fluctuating velocities may be source of downstream amplification if convenient frequency is selected (Ffowcs Williams, 1984; Lilley, 1972; Mitchell et al., 1995). From the time of Binder (1981) and Bechert (86) the components of the acoustic sources are better identified from the large structure (Tam, 1990) to small-scale shear-layer noise (Moose, 1977) to the screech (Lockwood, 1981) and the coupling effects (Viswanathan, 1994).

Present accuracy of DNS and LES does not allow to compute pressure fluctuations for noise generation modeling. However, recent modeling is better than in the past (Sohly, Lockwood and Walter, 1994; Sverdrop, 1996), and some realistic results may be obtained in a duct, where it can be seen that instant velocities in the centerline have preferred frequency that are associated with large structure of the flow. In aircraft engine exit noise generated by supersonic jet, screech tones are major source of noise. So control of noise have been tested and some success have been obtained particularly with local peaks for given frequencies.

Large range of loud speakers are available off the shelf from audio-visual applications for experiments in laboratories. Acoustic actuators may be therefore very useful for building fluctuations in the part of flows not receptive to incoming convected flow perturbations. But acoustic actuators are generally to be excluded from major practical engineering design, due to poor human ear tolerance to noise at the level of power required. They remain attractive, however, for use in laboratory experiments. By acoustic excitation it may be easily demonstrated if mode excitations by a controller in phase and frequencies are efficient as forcing process of the unstable modes of the flow (Huang et al., 1987).

2.7 Experimental Work in Progress

Major experimental results are supporting the increase of turbulence or chaos by local excitation. A large set of data may then be compared and help to understand better the underlined physical phenomena, although much remain to be checked.

For boundary layer's receptivity in turbulent flows see Binder and Tardu (1990); Joslin and Gunsburger (1995), and in separated-reattached flows see Hall (1984); Reisenthel (1985); Bar-Sever (1989); Michizuki (1993); Nelson (1990); McManus (1994); Fernholz (1994); Nelson (1996); Papadakis (1996).

For mixing layer's development, after the basic experiments of Fiedler (1981), Gaster (1985), Ho (1984), and Fiedler et al. (1988), more detailed analysis was performed by Buell and Huerre (1988) on stability leading to conditional sampling and compressibility analysis from Samimy (1990) to Bonnet (1993).

For jets same two steps lead from Zaman and Hussain (1980), Longmire (1984) Lee (1987), to Michalke (1991), after analysis by Monkewitz (1988), and to Martin (1991), Kusek (1990), Compton (1992), Jeung (1994), Vuillermaux (1994), Raman (1994), Vandsburger (1997), Bishop (1996), Sverdrop (1996), and L.E.S. by Urbin and Metais (1997).

For vortical flows from Provansal (1987) and Gad el Hak and Blackwelder (1987) vorticity and helicity, to Wu (1991), Roussopoulos (1993), Erikson (1994), Celik (1994), Park (1994), Blackwelder (1995) and Lee (1996), but the stability of vortical flows (see Yang, 1996) remains to be better known after first major work of Lopez and Perry (1992).

For cavity flow and its complex acoustic coupling eventually with elasticity of walls from Rossiter (1966), Rockwell (1980) to Ovelano (1995), McGrath (1996) and Terent'ev (1996).

For base flow used as a flame holder see McManus (1993), Candel (1992) and Gutmark (1994).

3 Turbulence Suppression by Passive and Active Control

3.1 Strategies of Control

Turbulence suppression is a very different target due to chaotic nature of turbulent flows. Strategies of control need therefore to involve much more advanced concepts of control than the concepts put forward in enhancement of chaos or in the transition to chaos.

Four different conceptual strategies seem relevant and may be used with increasing efficiency. These are discussed in turn in the following four subsubsections.

Addition of Local Stabilization. The simplest theoretical strategy of control is to spread a large set of actuators and many sensors of different scales in the field to be controlled and to let them operate as dampers of instabilities. In case of boundary layers, the actuators are to be spread better on the wall where turbulent spots are building main turbulent structures; due to the

saturated modes, that nonlinearly build turbulent spots, the control needs to reduce the vorticity ahead of the burgeoning of spots.

It is not obvious that such action is sufficient, and incoming flow may also need pacemaker. The present status of the research has to rely on numerical simulation by DNS with a modeling of the controller and of the actuators. Simulation is to be developed in the study before the experimental substantiation. Direct Navier Stokes Solvers are however working in a very low range of Reynolds number. They cannot be used for supporting evidence of true damping of high frequency or small-scale instability as well as for checking the increase or the decrease of perturbations. Some numerical tests done by Moin (1993), with perfect sensors and the help of an active controller developed by Temam (1993) using optimal control theory, show a significant reduction of the turbulent friction drag. Gains of 40 % in drag are obtained without the real suppression of turbulence. Partial suppression of turbulence, thanks to the avoidance of friction streaks, as the main source of the turbulent skin friction, is a realistic local control target. Large experimental gain might be anticipated by this strategy applied in multiple location, but no interference effect between local reduction processes have been evaluated and controlled yet. One may also try to move up the turbulent hairpins, reducing their coupling with high shear near the wall by a positive normal velocity bump, but the gains obtained by Lumley (1996) were lost in negative velocity phase of the wall displacement.

Reduction of Sources of Turbulence. An advanced strategy for the control of turbulence consists in pacing turbulence where it is produced, keeping perturbations low after, and simply adding downstream artificial damping. The first need is to identify and remove the sources of turbulence. Turning back to the description of the physics of generation of turbulence, in addition to the standard model of receptivity as presented before, one has to consider the catastrophic or by-pass production on local wall irregularities, on shock-wave interaction or on mixing with turbulent flow by concentrated eddies contamination. The strategy will be to use enhanced dissipation process by passive (grid, divergence of flow) or active (vibrating pads or blades ...) means. The target is to feed small dissipative scales of turbulence and to homogenize the turbulence for killing large-scale, deterministic intermittency where a part of flow is without dissipation.

It is a bracket control of the sources with the target of first increasing dissipation at high wavenumber and therefore using at small scale the actions previously described. However, this also requires a decrease of large scale structures. Small scale turbulent fluctuations build an equivalent eddy viscosity (equivalent low Reynolds number due to turbulent viscosity) and at the same time indeed dissipation increase, but possible unstable modes may be fed back and only large structures may grow until rebuilding large eddies. For example the dissipation of the wake of a cylinder by forced transfer of

the turbulent energy to small scale lets the Kármán-street large eddies form again themselves further downstream. So the control of new main modes is to be added to the source of turbulence control, and has to be kept active downstream. Such a strategy will follow a bracket strategy: damping (but not feeding) of structural modes to smaller amplitude, trying to reduce actively their amplitude when they are at their scale in the linear range and when passive means may not be efficient (local acceleration, curvature or continuous blowing/sucking). The bracket strategy is to be kept on longer streamline abscissa as being applied for a Lagrangian control of spots of turbulence. These spots are always able to birth and increase again downstream due to the receptivity to external perturbations (also to be kept by control at low amplitude). The forced dissipation of small scales tries to avoid such an amplification.

Local Emptying Hole in Spectra. A third strategy will be to build a hole in the deterministic part of the flow (intermittency) and/or in the stochastic energy versus wave number curve (Fig. 11). The first target in stochastic control is to cut the spill-over effect of the enhancement of dissipative length scales. If we consider a dynamical system, with a large number of degrees of freedom and weakly coupled interactions between modes, the control of large structures alone is not able to damp the system below a modest ratio of amplitude. This is so because the transfer of energy to high frequency modes has not damped itself and energy stored in such modes are not reduced in same amount and feedback large frequency eigen modes by a spill-over effect (Bourquin 1996). Such effect is to be expected with flows that have a large coupling between low- and high-frequency modes. This may be computed through triadic interaction with the Craya equations (1958) for randomly sparse eddies, giving the flux of energy to be absorbed for stabilization of the process by a hole in the spectra.

So strategic an issue will be cutting a sufficient gap of wavenumbers $K_1 - K_2$ by active control at their scale that once low frequencies are isolated, the control will turn to bidimensionalization of large-scale turbulence that may be well controlled because energy is transfered more efficiently in low frequency (Fig. 11) and the triadic effect feeding chaotic movement of eddies is reduced to dyadic which is easier to control. Bidimensionally controlled fluctuations are cutting the path to chaos such strategy may be summarized by the transfer to both extremities of spectra towards diffusion (high k) and linear control (low k). However, the turbulence gap needs a methodical control in the field which is not easy (passive honeycomb filter or active array of vanes) to implement and not yet carried out.

Periodic Paced Flow Enhancement. More advanced strategy has to rely on intermittency enhancement in addition to the previous control, using the sweeping-out concept coming from the mathematical theory of control (see

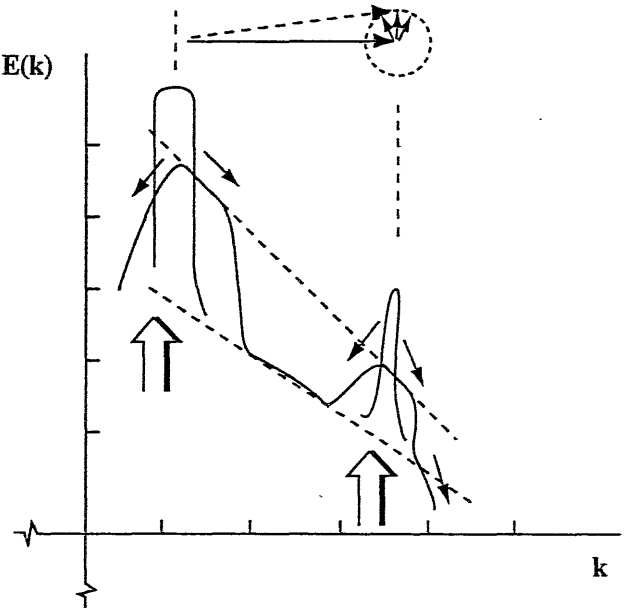

Fig. 11. Triadic interaction spreading turbulence towards all the spectra

Coron 1996). If the controllability in the domain of interest of a nonlinear partial differential equation is poor or not certain, within the limit of observability given by a large set of sensors for any initial condition, the only possible solution for control is to put the initial conditions (in every critical subdomain) in the right parameters' space of controllability. One simple set of initial conditions for a final laminarization of the flow field is evidently an undisturbed flow field. Such flowfield is only excited by external perturbations before they are amplified through receptivity effects, giving birth to local or total spreading of spots of turbulence. So the sweeping-out concept (or basin emptying) is a dynamical control where the source of turbulence or perturbations are swept out as soon as possible. The laminar intermittent domains that are generated are to be kept under control for filling downstream the whole domain. For example, in turbulent boundary layer this strategy will lead inviscid flow feeding of intermittent laminar subdomains coupled with a systematic suppression by suction of high shear layer near the wall. Avoiding a control of turbulent wall structures in order to avoid the perhaps intractable high-shear coupling needs putting out of control the flow near the local burst of an hairpin vortex in high stretching and its coupling transverse modes. Similarly, the high sheared parts of a wake or the center of a Kármán vortex street with small vortex filaments inducing transfer to chaotic flow difficult to control would have to be sucked out in such strategy. On a wing section, within that strategy, the shear layer generated at separation line will

be sucked out locally near the leading edge. Sweeping out concept will be applied where the flow is extremely unstable, and a blowing fixed jet will feed a concentrated vortex from a new shear layer allowing an inviscid stable domain underneath the vortex without Kelvin-Helmholtz instability, much easier to control (Fig. 12). Excitation of two convected modes may also localize interferences and local generation of induced stationary modes where needed.

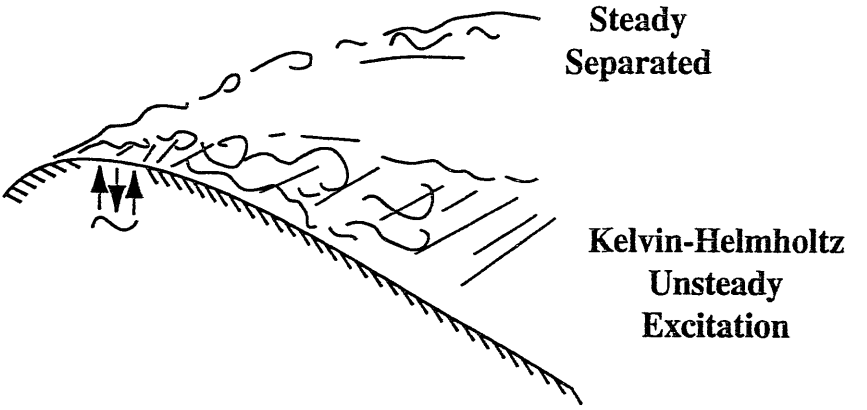

Fig. 12. Kelvin-Helmholtz forcing on shear layer induced by separation at leading edge.

3.2 Applicability of the Strategies

Basic Actions. Outside of the periodic curing of control domain by sweeping out turbulent spots the other strategies are addressing the control along three basic possible actions:

I. Dissipation of a local spot of turbulence.
II. Creation of a gap of low energy in the spectrum.
III. Direct control in space and time of catastrophic coupling.

Perhaps the level III is intractable if the flow outside the location of the catastrophic event is not convectively stable or absolutely stable and/or dissipative turbulent cascade is unable to damp low frequency large structures. Perhaps the level II is intractable because the needed gap width in frequency is too large and requires difficult phasing of controls. Perhaps the level I is intractable, outside of a better knowledge and observability of the flow field near the critical location at the wall.

The simple "passive" answers to the strategic issues may be exemplified on a flat plate in the following Fig. 13 with the successive devices: fine structure grid, honeycomb filter, bidimensional curvature and local suction. The

complex "active" answers would be similarly a moving grid screening the turbulent spots, a set of control vanes damping in a small bandwidth the fluctuations of the flow, a near the wall control by suction and blowing by a set of holes controlling the vortex generation at the internal boundary of the boundary layer.

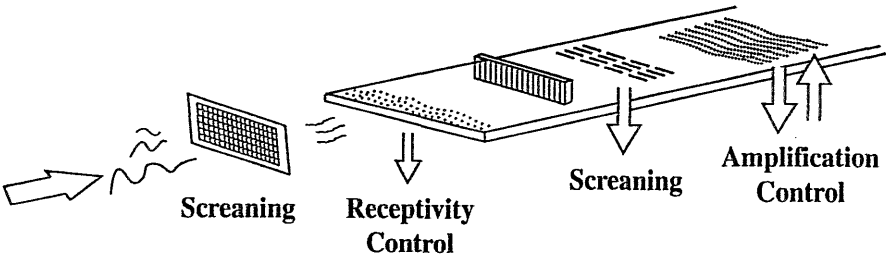

Fig. 13. Reducing turbulence in flow by high frequency dissipation + low frequency control.

Studies are to be developed on the following technological items for supporting such possible applications of the previous strategies.

Technology and Fluid Mechanics Studies. The major constraints on mechanical devices are clearly related to their cost (development and procurement cost for feasibility and affordability). Problems of scientific knowledge may delay or postpone their development: they are questioning the validity of the design tools for such studies, either experimental or numerical. The perturbations that a controller would have to withstand in real operation are to be simulated at the correct level of amplitude and spectral distribution. Good simulations are therefore not easy to validate. Experimental tests are done always with too low Reynolds number in wind tunnel. Numerical tests have always too high numerical dissipation built in solvers, has poor absorbing conditions on the boundaries or are not able to simulate generation of real quasi random perturbations.

The first studies to be advanced, in parallel to the validation of experimental and numerical tools, as seen necessary today, are related to specific works of technology needed for the control of fluids. Work for design of easier to control shapes and for easier to built controller and cheaper actuators and sensors and for their better locations. Always hidden behind such studies is general problems of controllability. Design for better or simpler controllable

systems address the problem of observability and also the selection of technology of sensors convenient for the cost function to be minimized. Sensors are to be specific to local or integral values of skin friction, heat or mass transfer, and pressure or other fluctuating physical parameters.

Specification of the cost function is a major concern for the applications. Whatever it appears as specific to each application, it generally involves a positive action to reduce fluctuations and a penalty for economy and safety.

Skin friction and heat transfer are convenient local measure of quality for wall boundary layers, diffusion for wakes and mixing layers. But global turbulence energy consideration is often the unique integral design parameter. The questions of stability or decoupling with other phenomena (vibrations, aeroelasticity ...), and of robustness of control versus "acceptable" fluctuations of the incoming flow are part more generally of evaluation of "acceptable" uncertainties in the environment of the system. That evaluation has to be the same for the system itself and for its modeling.

Behind all these scientific problems is the practical problem of certification or qualification of a passive or active system and of its "acceptability" and affordability with realistic improvement of performances.

3.3 Control of Flows with Internal Mode Coupling

Monodimensional Problem. Practical controls are very different if they include monodimensional, bidimensional or tridimensional coupling. The boundary conditions force each coupling as may be seen in the three following examples of graduated difficulty.

Considering, as a monodimensional problem, the interaction of mass flow entering a tube (with turbulent or irregular or chaotic fluctuations in time) and of the sound emission coming from exit of the tube in stationary or moving atmosphere. The problem is the exhaust tubes of cars or, more complex, problem of the chemical reaction chamber with elongated shape in the direction of the flow. It is clear that, outside the three-dimensional entrance and exit flowfield, there is a monodimensional coupling phenomenon between acoustic fluctuation of pressure, combustion or heat transfer and irregular inflow in the tube. For flows without combustion it is easy to compute an impedance for fluctuating velocities in the tube, to know the basic time constant of acoustic waves propagation (McManus et al., 1993) and to adjust the movement of a valve (obstruction of the flow or upstream incoming mass airflow control) for reducing acoustic emissions. By controlling pressure near the exit tube, it is easy to obtain reduction of more than 20 db; it has been achieving deriving control law from the monodimensional equation for flow. Similar results may be obtained with combustion in the tube, as far as a single monodimensional fluid mode is to be controlled while coupled together with linear acoustic modes. However, it is a stiff problem from the fact that the pressure-velocity relation at any position in the tube is modified by the command of the valve (subsonic flow). Noticeable are the periodic peaks of

massflow and its multiple resonant harmonics, requiring multi-frequency controller.

Bidimensional Problem. If we turn to a bidimensional cavity flow we have now to consider more complex problems of interaction of acoustic and viscous modes. On the monodimensional acoustics, the generation of the shear-layer tones interacting with cavity resonant modes is first added. Then the frequency for filling in or out the cavity and the frequencies of shear layer impinging on its downstream edge where there is low-speed compressible fluid are added to the sub-harmonic frequency coupling of the cavity and shear flow. Some coupling effects may also appear between the acoustics and the entropy modes as well as between the control and the uncontrolled filling of the cavity. Moreover, the intensity of radiated noise, generated at the impingment of shear layer on the downstream step of the cavity, is fed by shear layer large eddies structure. But again the radiated noise brings instability to the shear layer and the amplitude of its fluctuations. Such flow requires control that may counteract external bidimensional waves, because they are highly distorted by tridimensional effects as by compressibility effects.

Bidimensional control may be recovered with locally three dimensional flow, if turbulence enforce "subgrid" or subscale turbulent isotropic dissipation. The bidimensionality may be destroyed locally by roughness, as by a succession of small bumps. In a tridimensional bump problem, the helicity built in the vorticity layer contouring the bump is fed by helicity in the boundary layer shed off the bump but it is dissipated in 3D-turbulence and only influences stability and size of separated areas after the bump. The receptivity problem is of main importance, in the evaluation of the perturbations level and of the amplitude of the oscillations of boundary layer thickness and vortical flows superimposed. The control of the fluctuations of incoming flow is so related to the tridimensional receptivity (Fig. 14) if it allows stationary modes to appear when curvature is sufficient (Görtler instability). Bidimensional control is only possible if remaining helicity is not feeding such three-dimensional modes.

The effects of compressibility are important: as multiple 2D modes appear and so nonlinear processes shall appear sooner and have stronger influence on linear amplification (Fig. 15). Simple control with suction have a large effect on such unstable processes and on the transition location, it reduces secondary three-dimensional effects.

If we turn to the analysis of the bidimensional transition from 2D Tollmien-Schlichting waves to 2D turbulent flow, and to the control of the perturbation velocity by suction and/or blowing in a 2D slot, we can check that the perturbations in the field issued from the slot control are propagating upstream as well as downstream. Therefore the control has to counteract upstream perturbations which are generated by blowing or sucking through the slot (Fig. 16, from Gaster and Carpenter, 1994).

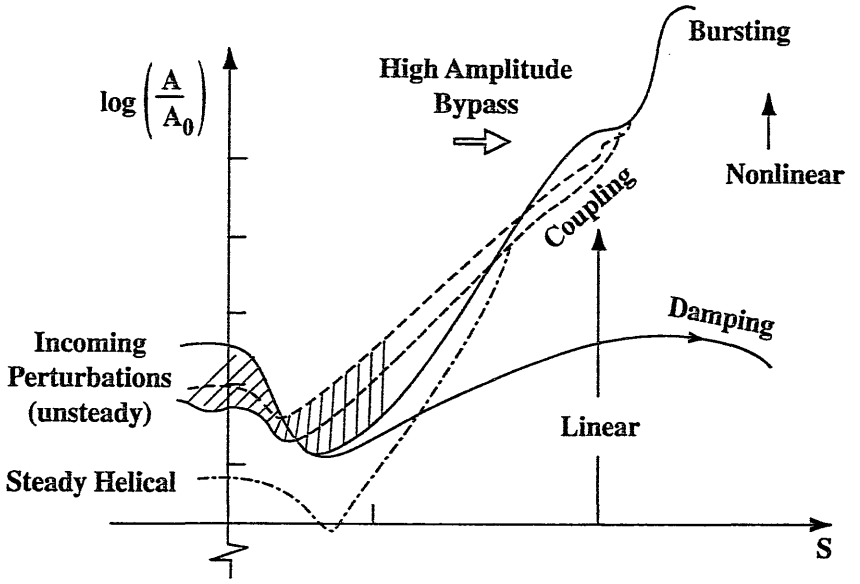

Fig. 14. Receptivity near leading edge

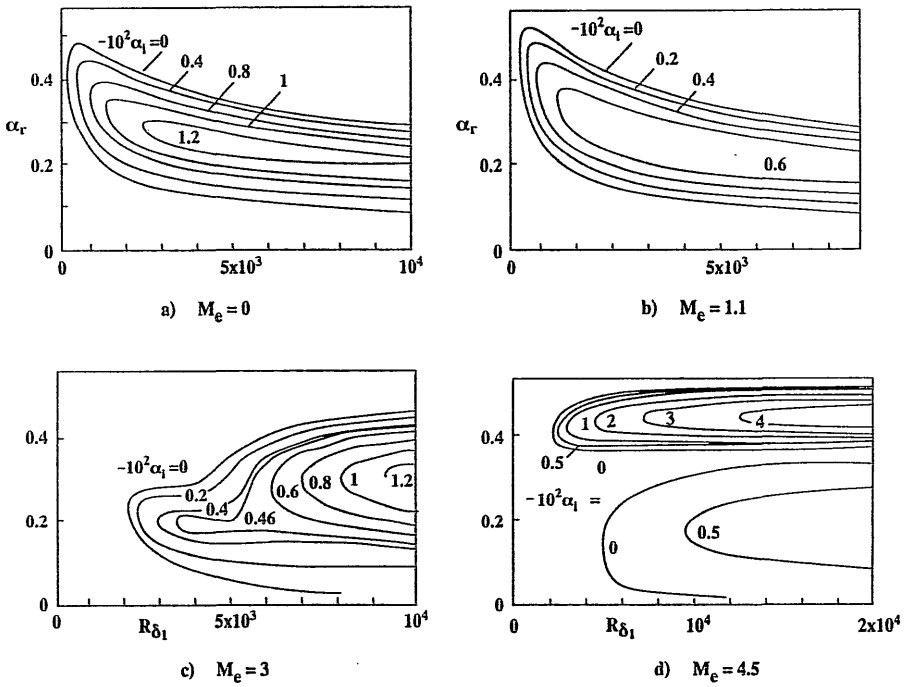

Fig. 15. Effect of compressibility on 2D adiabatic flat plate

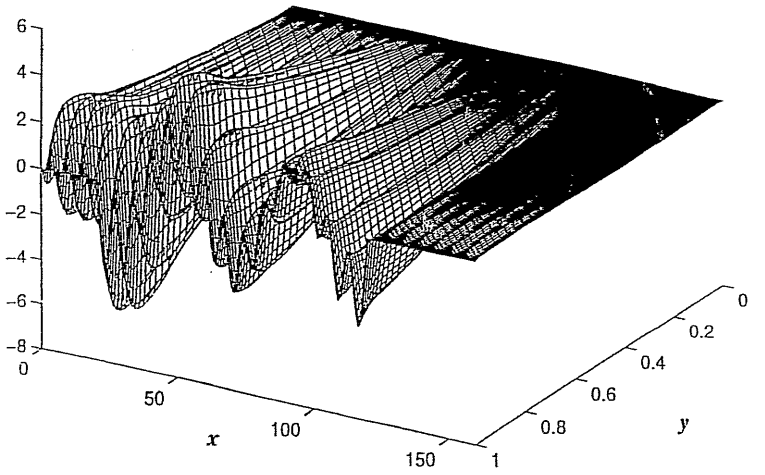

Fig. 16. Upstream perturbation generated by slot control of Tollmien-Schlichting waves.

Nonlinear control may be very powerful on such 2D self-perturbed flows either by the use of an intermittent control action, or by control of all periodic modes as perturbations of the basic mode used as a driven oscillator. O.G.Y. method relies on the alternate action of a stable mode and of an unstable one driven by the other in an alternate stable coupling. This is easily mastered in a bounded domain like with the basic mode in a channel flow (Ott et al., 1994; Keefe, 1993). Some comparative work with a D.N.S. solver has been done in Dassault Aviation on the control of the vorticity generation at the entrance of a two-dimensional channel flow, where the complexity of the flowfield is much larger that in a duct. It appears that the coupling between internal and external flows are of major importance so that it is at the lip that control by suction needs to be applied. Computation requires fine grid for the rebuilding of experimental turbulence level in the channel flow, but the turbulence control is not itself attained. Control succeeded by the suppression of irregular vortex emission feeding turbulence. Generation of turbulence is, therefore, better controlled at the source by direct suppression of the separation on the lip.

Tridimensional Problems. Tridimensional computation by L.E.S. code of Lesieur (1995) gives the explanation of turbulence feeding in the tridimensional structure of the real flow (Fig. 17). Main vortices generated on the lip added helical perturbations by structures parallel to the external velocity and coupling building the tridimensionalization of the separated flow.

Similarly if we turn back to the cavity flows, experimental evidence show sensitivity to tridimensionality in the turbulent rotational flow in the cavity whatever the fact that apparently (as obtained by Fourier analysis) the acous-

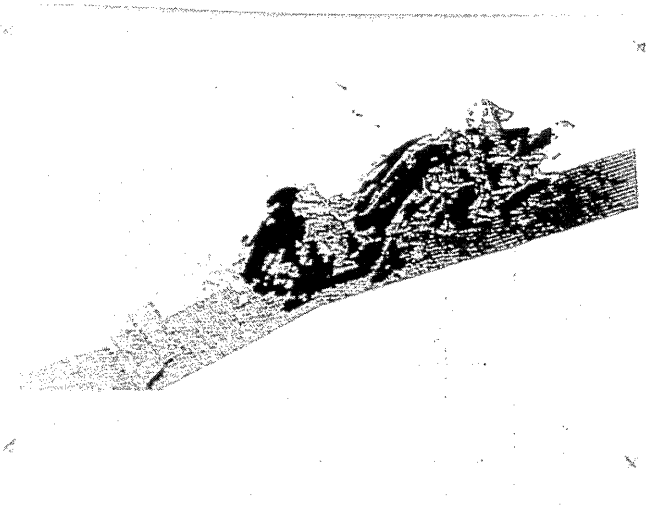

Fig. 17. LES of separated flow on a 2D ramp

tic basic modes are mainly two dimensional, or monodimensional. Such behavior comes from the dissipation of the non-resonant acoustic waves between the left and right modes. The vortical flow distortion by lateral walls help the turbulence not to remain bidimensional as is required by the tridimensionality of the vortex stretching process. On Figs. 18a and 18b experimental results obtained by Antonov et al. (1990) show a general turbulent trend to tridimensionality as exemplified by acoustic pressure spectra without large resonant peaks, for cavity as for upstream step or backward step. Therefore active control of the unstable Kelvin-Helmholtz modes of shear layer closing a rectangular cavity (Fig. 19) is able to reduce the monodimensional acoustic peaks and their detrimental effects on the shear layers but not the three-dimensional turbulence generated at lower scale in the reattachment region, at the beginning of recirculating flow on the downstream wall, where peaks of acoustic pressure appear (Grath and Show 1996, and Antonov 1990).

The analysis of aeroacoustic instabilities, generating the large perceived noise, shows that sound generation is correlated with the separation of the flow in large incidence. It is possible to identify the primary sources of noise at the trailing edge or at the separation line, with an exponent of the scaling effect versus the frequency of primary tones proportional to the 8^{th} power of the velocity. The generation of three-dimensional acoustic perturbations is complex, being on smaller scales than energy carrying large eddies. The direct control of noise generation would be very difficult as related to randomly sparse extreme distortions (peaks in Dalembertian local value). A better strategy would be to reduce large distortions that build the local peaks.

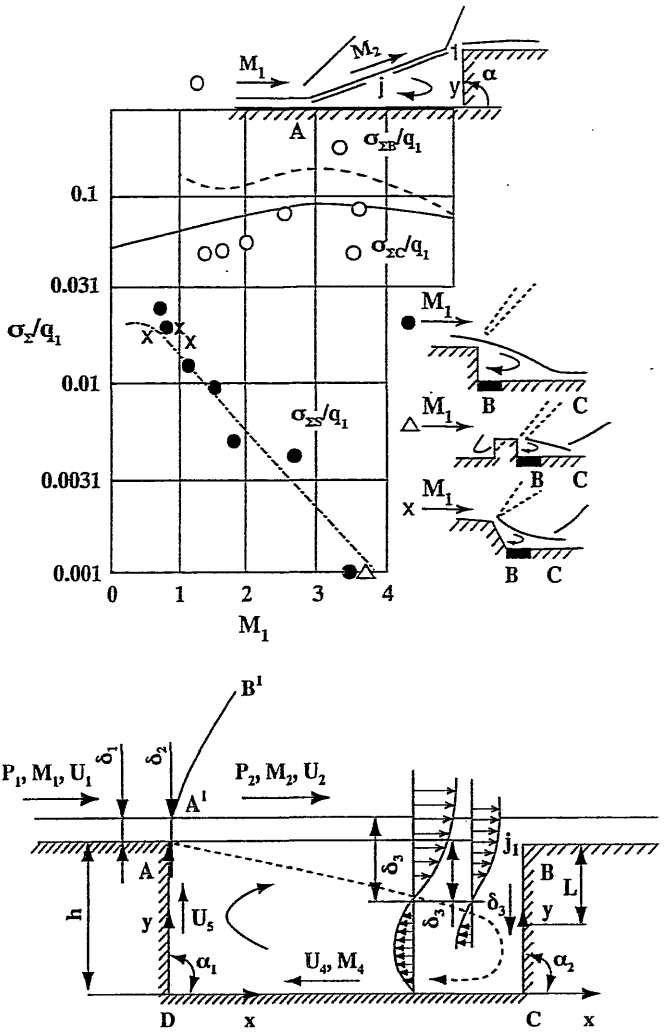

Fig. 18. Cavity pressure fluctuation analysis (comparison with step and ramp flow)

This is not quite different of the control of the flow instabilities that gives birth to the sources of noise, whatever the fact that damping large structures induced by flow instabilities is limited but efficient. See Sunyach and Ffowcs Williams (1986); Galland et al. (1991); Bera and Sunyach (1994).

It therefore appears that an action on the singular separation or reattachment processes, is the best strategy of control of main turbulent parts of a flow. The more efficient way of controlling separation is to fix singularities to maintain bidimensionality and to act on the unstable modes of the shear layers they generate. A large quantity of tests are supporting such evidence. However, the selection of the best velocity control and microblowing loca-

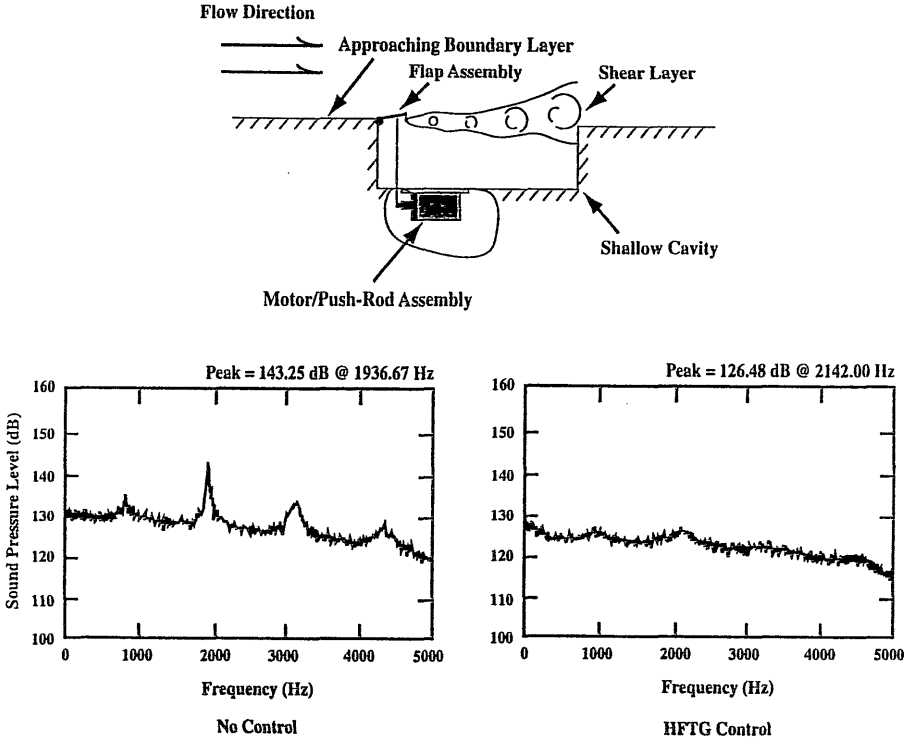

Fig. 19. Active control of rectangular cavity noise

tions is difficult, whatever the fact that it is in direct relation to the flux of velocity gradients feeding the large structure of eddies. All is beginning in the small thickness of boundary layers generating the separated shear layers. A classical example is given by the control of the unstable flowfield around a conical nose at high angle of attack. DNS or LES computation are now able to rebuild major characteristics of such flow (Lee et al., 1996).

3.4 Direct Control of Separation

If we turn to separation on a wing leading edge, where the boundary layer is very thin, we can only rely on Microsystems or MEMS for action of the size

of structures of incoming shear layers. Any large scale action with use of large blowing jets will be destroying mid-scale structures of the flux of incoming rotational flows. The amplification effect of the shear layers are alone, on a complete aircraft, so powerful as to build wing-rocks or large pitch-up or pitch-down movements. Use of large "by strength" blowing to control the vortex sheets, before or after its rolling up and its bursting, may lead to very large energy requirements for the control If the control is done late in the downstream development process of the large vortical flows induced on the wing it requires energy of the same importance as the vortical flow to be modified. The direct "in strength" control is to be avoided whatever the fact that it may then be done at the low frequency of the flight control systems. Large blowing effect may be used as a test of reference for more refined control effectiveness, defining more favorable flow patterns to be generated by more refined self amplified mini-actions.

Two self-amplified mini-actions strategies are conceptually promising:

- The former relies on reinforcement of the skin-function near separation, by excitation of the inner part of turbulent boundary layer, leading to the reduction of the shape factor of the boundary layer and delay in flow separation and control of separation point.
- The latter rely on the control of vorticity and helicity convected downstream by the shear layer generated at separation. This may be used for modulation of vortex-induced flowfield on the boundary or self-induced vortex breakdown location control (see Lopez, Perry, 1992). Both concepts are building enhancement or decrease of global turbulent energy but more complex target is anticipated (see Wu, 1991; Yang, 1996).

4 Problems in Practical Design of Flow Control Systems

4.1 Introduction to Engineering Problems

The scientific problems that engineers have to manage in the design and development of flow control systems are largely under-estimated. However acceptability of the concept is meeting some reluctance. Confidence is not always present when an active flow control system is anticipated for a given application, concurrently to simpler design. For many engineers the anticipated strategy for this new design is derived from the concept of "miniaturization" or "subscaling" of "by strength" control. Obviously that strategy is no longer efficient for facing new paradigms underlined in flow as in control.

However the problems to be solved are not without conceptually tested solutions and a great part of the addressed problems will be in line with a good methodology of development. Some of this problems will be better solved in the future if more basic research is done, taking in account their specificity.

The problems to be solved are to be put in a general framework answering to two different sets of questions. The first set is related to the usual demonstration of feasibility and ability to be affordable, the second is related to the capability of such new systems to be qualified for their robustness and flexibility for the product life cycle.

4.2 Problems of Methodology

Four Steps Methodology. The first necessity in development of active flow control is rational methodology. Four periods are to be discriminated in the studies plus production of an active flow control system:

- Conceptual studies: such studies has to cover the proof of concept work. Industry and research teams have to organize coordinated research works plus experiments to validate the concept and its technology. Less detailed or subscale designs within relevant flow parameters range have to anticipate that operation will be easy to do and support and that operation failures are conceptually not critical.
- Feasibility studies: for such studies, experimental tests are needed with reduced size and range of parameters but with a validation of extensions to real size and practical operational parameters. The economic cost of fabrication, operation and environmental acceptance should also be included. Of major concern are the uncertain evaluations relevant to risk-performance affordability for the venture and the prediction of programatic flexibility.
- Development studies: such studies need a set of comprehensive simulation tool by real life tests and/or virtual simulation of extreme conditions of use, with and without failures in simulation, including man interaction. These support the detailed design work and the necessary evaluation of critical design points.
- Fabrication and delivery.

In parallel to design and production studies there is a need to include the development of an "acceptance" program as far as confidence is to be built in such advanced product, because it is more or less soundly assumed by main possible users that "manipulation" of flow may be a dangerous process. Due to turbulence fluctuations and sensitiveness of metastable flows to external random perturbations, robustness afforded by a better mastering of passive natural multiscale bifurcating flows has to be well perceived. This has to be a step in technology beneficial to user, not only in performance but in safety.

Acceptance Program. It is that acceptance program, founded on a better evaluation of uncertainties and risks, that will specify a target robustness

associated with the new level of performance. It is to be built from the conceptual studies and need collaboration of research and industry, from the conceptual studies to the training of users and vendors. The use of advanced design tools, including computational virtual products and experimental benchmarking of representative tests, are mandatory in the acceptance program by certification authorities and users. Their evaluation, or at least the checking of program consistency with in-time delivery, are to take place before internal industrial go-ahead, because the virtual demonstration of a new level of mastering of flow, characteristic of "control," is a central issue. Clearly the absolute mastering of complexity of real turbulent flows may remain for a long time an incredible target. The practical experimental-numerical demonstration has to be done by reference to a passive, uncontrolled, no more totally mastered "reference system."

Conceptual Methodology. Conceptual studies are the major location of scientific cooperation between industry and research because the real problem of conceptual methodology needs to be sufficiently focused on affordable solutions. Otherwise, designs will be too costly either due to the cost of too numerous and complex actuators and sensors or due to the cost and time involved in research studies. Conceptual studies are basically multi-disciplinary studies. They ask for a multiscale approach not only in physics of flow and hardware but on the coordination of the different laboratories involved in the conceptual demonstrations. Probably a set of various scale demonstrations has to be done. It will include superscale tests with enlarged devices for better understanding of the microphysics and validation of modeling for feasibility, before real-life global multiscale validation.

4.3 Basic Problems for Design

Sensor Specification. Basic problems appear in the control system and in its parts, but first in sensor selection. Sensors may first be selected as offering the better compromise between their number and position and their accuracy. Unfortunately there is no real experimental sensor of the state of the dynamical system in fluids except with intrusive and very complex devices. What would be needed is:

1. Local maximum vortex stretching detector.
2. Local mode amplification detector.
3. Detector of balance of momentum and energy production, diffusion and dissipation in a bandwidth of wavenumbers.

First and last detectors allow to check turbulence behavior, the second gives the receptivity to perturbations and active mastering from local actuator. The "approximate" sensors detect gradients in pressure, velocity or density but generally in one dimension and not as a tensor, and heat fluxes or

shear stresses in the field or at the wall. Gradient sensors are generally assembly of elementary pressure and temperature sensors. Correlation between the "correct" sensor and a simplified sensor (e.g. pressure difference, heat flux, ...) may be obtain by computation, for a set of different resolution of Navier Stokes equation with varying boundary conditions. Cost trends (complexity, development, production, technology) will help to identify the cost/quality acceptable ratio for the sensor specification, particularly in reference to a low-cost, off-the-shelf, multi-purpose, industrial sensor.

Actuator Specification. Actuators are conceptually of three types. Deformation of the wall; mechanical protruding devices like flaps with variable angle of attack in the flowfield or near the wall; blowing and suction of air through holes of different shapes. The actuators are of large surface and deflection or of small surfaces. They then rely more or less on self amplification of perturbations near the wall. Problem of cost/efficiency is also the main driver in the specification design of actuators, particularly with a large number of devices working in a coordinated movement. The precise relative position and the large bandwidth of efficient activity are specifications parameters checked once the reliability is demonstrated. Reliability demonstration assumes the knowledge of design envelope particularly for the external perturbations and environmental aggressions (sand, dust, ...).

Controller Specification. Controllers are intrinsically either of simple design (linear matrix of local command or control with a given outphasing relative to local measurements) or much more complex with computation of amplitude and phase of a set of actuators in a coordinated way. The simple controller uses a knowledge-based building of controlled variables. Some good estimation of the state of the system may rely on neural network learning process and similarly on the side of controller output on a set of variables given by an empirical semi-linear approach. One or two significant parameters may help to adjust control laws to variables conditions, so building a feed-forward control, relying on those parameters measured in the incoming flow before actuators. On the side of the complexity it is possible now, with the speed and memory of new chips, to directly solve a P.D.E. with reduced number of discretization points and boundary conditions with "assimilation" fed by refreshed initial conditions taking in account the upstream measured parameters. Such computation of direct and adjoint problems will give a more elaborate estimation of the optimal setting of controlled variables, increasing quality and robustness. Moreover the cost function to minimize may be taking in account quality and robustness of the control. With reduced numbers of discretization points, a good modeling of multiscale effects is needed, with the time frame adjusted to phenomena to control. Between this maximum P.D.E. controller and the simple quasi-linear evaluation of output versus input as given by sensors, there is a lot of intermediate modeling of the system

as a P.D.E. with reduced number of dynamical variables. Cost of controller is in relation with its simplicity. If real mean flows are not complex, a minimum of complexity of controller is however required with regard to the complexity of flowfield in unsteady evolution. Targeted cost/quality of control may also need an advanced controller for reduction of size and number of actuators and sensors cost, or because the control is stiff.

In particular the time and cost for design of the controller and of the complete coherence of sensors, actuators and laws of control delivered by the controller may be the economic driver leading to selection of the complete system. This is to be done always in reference to a passive system.

4.4 Design for Qualification, Certification

Fail Safe Design. Major elements against decision to implement an active flow control system are related to anticipated problems of failures in service. A passive system addition is generally not supposed to lead to added failures and therefore not to increase significantly the cost of operation and of procurement. However, new devices are requiring sometimes specific care for keeping the system in good operative conditions. For example, external smart skins devices are easily destroyed by dust or internal open cavities devices have holes filled up during operations. Taking in account the specificity of an active system versus passive reference system, development of a new active control system need first to address a comprehensive demonstration of safe operation. It includes two items to be validated for aerospace vehicles:

- The robustness of the active system in the flight domain for aerodynamic control of the flow around the aircraft with perturbations.
- The ability, in case of failure to return to a safe operation in some "degraded" mode with the system being "inactivated" and actuators in their "failure position."

An active system might take in account reduced set of sensors/actuators or the reduced complexity of control laws with the controller partially inoperative.

The simplest system is in passive degraded mode where the actuators no more move. It is the safer mode, with loss of the performances afforded by active control, but it is practically extremely difficult to implement outside of very simple cases. Generally it is needed to stop controllers in a specific position at least, for example active small blades may become fixed vortex generators. More complex is the case where a specific action is needed, because the system operate safely in a larger domain of parameters with active control, and so need to return to a smaller domain of allowed parameters by an automatic sequence of controlled events with or without the pilot in the loop. For complex systems, the complete failure is avoided by detection and correction of failure on actuator, sensor, controller (on complete system,

there does exist specific actions aiming to operate without the non-operative equipments). The design effort is then to be directed towards the duplication or triplication of critical devices and their continuous test.

Qualification. The former analysis for the requirements of safety demonstrations of active flow control system favors the following rules of design and qualification:

- Sensors and actuators are to be large in number in order to reduce the impact of failure.
- Sensors, actuators and controller need to have their internal test of good operation and switching-out procedures.
- The extension of the domain of operation need specific procedures for safe return to passive system domains. Qualification has to cover the performances with and without failure as two states of the systems with control in active or in degraded mode.
- Heuristic or non deterministic systems are to be replaced by deterministic ones for clear demonstration of uncertain effects; e.g. neural network used in preliminary studies are to be replaced by deterministic codes giving same output for tested parameters.
- Numerical and experimental simulation of robustness of the system to external perturbations and internal failures or uncertainties is to be built at the preliminary design stage for correct appreciation of risks and errors in the major design drivers.

Reference to Nature. The reliability and performances of active flow control are not to be underestimated because a lot of natural functions are using it from the flight of insects to fishes' upgraded performances and efficient flow mixing for biochemistry. It is clear that, without the added level of performance and robustness of active flow control, many vital biological functions would be impossible.

Acceptance of active flow control may therefore have reference to natural robustness.

5 Parting Remark

One major output of the research for design and operation of future active and passive control systems is an increase of knowledge of how multiscale flows are working. Real unsteady flows are a mix of stochastic and deterministic and of local and global behavior. Better knowledge of such multiscale flows will help also to master better and to design the uncontrolled systems and identify the real uncertainties and the real boundaries of safe operations of present industrial products.

References

Abarbanel, S. S., Don, W. S., Gottlieb, D., Rudy, D. H., Townsend, J. C. (1991): Secondary Frequencies in the Wake of a Circular Cylinder with Vortex Shedding. *J. Fluid Mech.* **255**, 557–574.

Abid, M., Bracket, M.E. (1992): Mécanisme de Génération des Jets Latéraux dans les Jets Axisymetriques Forcés. *C. R. Acad. Sci. Paris.*

Antonov, Kouptov, Komanov (1990): Pulsatil davlenya. Moscow (in Russian).

Aref, H., Jones, S.W. (1989): Enhanced Separation of Diffusing Particles by Chaotic Advection. *Phys. Fluids A* **1**(3), 470–474.

Argyris, J., Faust, G., Haase, M. (1993): Routes to Chaos and Turbulence—A Computational Introduction. *Phil. Trans. R. Soc. London A.* **344**, 207–234.

Arnold, V.I. (1965): *Dokl. Akad. Nauk* **162**, 975–978. Moscow (in Russian).

Arnold, V.I. (1966): IZV. Vyssh. Uchcbn. *Zaved Mathematika* **54**(3). Moscow (in Russian).

Bailly, C., Lafon, P., Candel, S. (1994): Computation of Subsonic-Supersonic Jet Noise with a Modified k-ε Model. *Acta Acoustics* **2101**.

Balakumat, P., Hall, P. (1950): Optimum Section Distribution for Transition Control. *AIAA.*

Bardos, C., Bourquin, F., Lebeau, G. (1991): Calcul de Dérivées Normales et Méthodes de Galerkin Appliquée au Problème de Contrôlabilité Exact. *C. R. Acad. Sci. Paris* **313**, Série I, 757–760.

Bardos, C., Lebeau, G., Rauch, J. (1992): Sharp Sufficient Conditions for the Observation, Control and Stabilization of Waves from the Boundary. *S.I.A.M. J. Control & Optimization.* **30**(5), 1024–1065.

Bar-Sever, A. (1989): Separation Control on an Airfoil by Periodic Forcing. *AIAA J.* **27**(6), 820–821.

Batt, R.G. (1975): Some Measurements on the Effect of Tripping the Two-Dimensional Shear Layer. *AIAA J.* **13**(2), 245–247.

Bechert, W. D., Pfitzenmeier, E. (1976): On the Amplification of Broadband Jet Noise by a Pure Tone Excitation. AIAA Paper 76-489.

Bechert, W. D., Stahl, B. (1988): Excitation of Instability Waves in Free Shear Layers. Part 2. Experiments. *J. Fluid Mech.* **186**, 63.

Bera, J.C., Sunyach, M. (1994): Active Control of Bursting Phenomena in Transitional Boundary Layers. In *Proceedings of Euromech Colloquium 328.*

Bergé, P., Pomeau, Y. (1988): Le Chaos Theorie et Experiences. *Eyrolles Paris.*

Berkooz, G., Holmes, P., Lumley, J. L. (1993): The Proper Orthogonal Decomposition in the Analysis of Turbulent Flows. *J. of Fluid Mech.* **25**, 539–575.

Bertoglio, J.-P., Jeandel, D. (1987): A Simplified Spectral Closure for Inhomogeneous Turbulence: Application to the Boundary Layer. *Fifth Turb. Shear Flows* (Springer-Verlag, Berlin).

Bertoglio, J.-P., Shao, L., Parpais, S., Courty, J.C., Ravachol, M., Uny, G., De Vuyst, F. (1994): A Simplified Spectral Model for Inhomogeneous and Non Equilibrium Turbulence. *25th AIAA Fluid Dynamics Conference.* Colorado Springs, Colorado.

Bewley, T. R., Choi, H., Temam, R., Moin, P. (1993): Optimal Feedback Control of Turbulent Channel Flow. Technical Report, Annual Research Briefs 1993, Center for Turbulence Research, Stanford University, California.

Bilanin, A.J.,Covert, E.E. (1973): Estimation of Possible Excitation Frequencies for Shallow Rectangular Cavities. *AIAA Journal* **11**(3), 347–351.

Billoud, G., Huynh Huu, C., Galland, M.A., Candel, S. (1992): Adaptive Active Control of Combustion Instabilities. *Combustion, Sciences & Technology* **81**, 257–283.

Binder, G., Didell (1981): *AGARD Conference Proceedings on Aeroacoustics*, no. 308.

Binder, G., Tardu, S. (1990): Boundary Layer Response to Harmonic Forcing. INP Grenoble, France.

Bishop, K., Chen, E. (1996): Optical Tomography of the Effect of Excitation of a Heated Round Jet. AIAA Paper 96-2323.

Bonnet, Ouzaa, Sabrit, Gresillon (1993): Density Fluctuations and Acoustic Waves in Supersonic Mixing Layers. *9th Symposium on Turbulent Shear Flows.* Kyoto, Japan.

Bourquin, F. (1993): Approximation Theory for the Problem of Exact Controllability of the Wave Equation with Boundary Control. *Proc. Second SIAM Conference on Mathematical and Numerical Aspects of Wave Propagation.* Newark, Delaware.

Bristeau, M., Pironneau, O., Glowinski, R., Periaux, J., Perrier, P., Poirier, G. (1983): Application of Optimal Control and Finite Element Methods to the Calculation of Transonic Flows and Incompressible Viscous Flows. *Numerical Methods in Applied Fluid Mechanics*, ed. B. Hunt, pp. 203–312 (Academic Press, London).

Broze, G., Hussain, F. (1996): Transition to Chaos in a Forced Jet: Intermittency, Tangent Bifurcations and Hysteresis. *J. Fluid Mech.* **311**, 97–71.

Buell, J. C., Huerre, P. (1988): Inflow/Outflow Boundary Conditions and Global Dynamics of Spatial Mixing Layers. *Proceedings of the Summer Program*, Center for Turbulence Research, Stanford University, California.CTR.

Burdisso, T., O'Brien, F. (1994): Active Control of Spinning Acoustic Modes from a turbofan engine. AIAA Paper 94-0361.

Burns, J., Ou, Y. (1994): Active control of vortex shedding. AIAA Paper 94-0182.

Candel, S. M. (1992): Combustion Instabilities Coupled by Pressure Waves and their Active Control. *24th Symposium on Combustion.*

Carpenter, R. (1996): A Novel Velocity-Vorticity Formulation of the Navier-Stokes Equations for Application to Laminar Flow Control. *Eccomas 96.*

Casalis, G. (1997): Boundary Layer Receptivity and Unstable Waves Control. *C. R. Acad. Sci. Paris.*

Celik, Z., Roberts, L. (1994): Vortical Flow control on a Delta Wing by lateral Blowing. AIAA Paper 94-0509.

Chacon, T. (1995): Numerical Analysis of Optimal Control of Navier-Stokes Equations: Control of Large Scales. H.C.M. Report, Univ. Seville.

Chandrasekhar, S. (1996): NPS Monterey. AIAA Paper 96-1953.

Choi, H. (1995): Suboptimal Control of Turbulent Flow Using Control Theory. *International Symposium of Mathematical Modeling of Turbulent Flows.*

Choi, H., Temam, R., Moin, P., Kim, J. (1993): Feedback Control for Unsteady Flow and its Application to the Stochastic Burgers Equation. *J. Fluid Mech.* **253**, 509–543.

Chollet, J.-P., Lesieur, M. (1981): Unsteady Grid Modelling. *J. Atmos. Science* **38**, 2747–2757.

Compton, D. A., Johnston, J.P. (1992): Streamwise Vortex Production by Pitched and Skewed Jets in a Turbulent Boundary Layer. *AIAA J.* **30**(3), 640–647.

Coron, J.M. (1993): Controllability de l'Équation de Navier Stokes Incompressible Bidimensionnelle. *C. R. Ac. Sc. Paris* **317**, 271–276.

Coron, J.M. (1996): On the Controllability of 2D Incompressible Perfect Fluids. *J.M.P.A. 96.*

Craya, A., Curtet, R. (1955): Sur l'Évolution d'un Jet en Espace Confiné. *C. R. Acad. Sci. Paris*, 621–622.

Diaz, J., Lions, J.-L. (1994): No Regret and Low Regret Controls—An Introduction. *Environment, Economics and their Mathematical Models*, pp. 101–123 (Masson, Paris).

Dolecki, S., Russel, D. (1977): A General Theory of Observation and Control. *S.I.A.M. J. Control & Stabilization* **15**(2).

Ducros, F., Conte, P., Lesieur, M. (1996): Large-Eddy Simulation of Transition to Turbulence in Boundary Layer Developing Spatially over a Flat Plate. *J. Fluid Mech.* **326**, 1–36.

Ericsson, L., Mendenhall, M. (1994): On Forebody-Induced Wing Rock. AIAA Paper 94-0167.

Erk, P., Ferholtz, H. (1994): An Experimental Study of the Receptivity of a Separated Boundary Layer on a Low-Reynolds Number Airfoil at High Angle of Attack. *Proc. of Euromech Colloq.*, no. 328.

Estivalezes, J.L., Eradyn, E. (1992): Numerical Comparison of Outflow Boundary Conditions for the Simulation of Unsteady Compressible Mixing Layers.

Falkner, W., Schvek, S., Luttzen, H. (1994): Real Time Prediction and Control of 3D Unsteady Separated Flows Fields Using Neural Networks. AIAA Paper 94-0532.

Fernholz, H.-H. (1993): Management and Control of Turbulent Shear Flows. *ZAMM 73* 11, 287–300.

Ffowcs Williams, J.E., Kumpton, A. (199) The Noise from the Large-Scale Structure of a Jet. *J. Fluid Mech.* **84**, 673–694.

Fiedler, H.E. (1991): Ways and Possibilities of Controlling Turbulent Shear Flows—A Selection of Problems Pursued at HFI and DLR in Berlin. *29th Aerospace Sciences Meeting*, AIAA Paper 91-0330.

Fiedler, H.E., Dziomba, B., Mensing, P., Rösgen, T. (1981): Initiation, Evolution and Global Consequences of Coherent Structures in Turbulent Shear Flows. In *The Role of Coherent Structures in Modelling Turbulence and Mixing*, ed. J. Jimenez, *Lecture Notes in Physics* (Springer, Berlin).

Fiedler, H.E., Glezer, A., Wygnanski, I. (1988): Control of Plane Mixing Layer—Some Novel Experiments. In *Current Trends in Turbulent Research*, AIAA Series, vol. 112, pp. 30–64, eds. H. Branover, M. Mond & Y. Ungers.

Fiedler, H.E., Kim, J.-H., Köpp, N. (1991): The Spatially Accelerated Mixing Layer in a Tailored Pressure Gradient. *Eur. J. Mech., B/Fluids* **10**(4), 349–376.

Fursikov, A. (1982): Control Problems and Theorems Concerning the Unique Solvability of a Mixed Boundary Value Problem for the Three-Dimensional Navier-Stokes and Euler Equations. *Math. USSR Sbornik* **43**, 251–273.

Fursikov, A.W., Imanuvilov, O.Y. (1995): On Controllability of Certain Systems Simulating a Fluid Flow. *Flow Control*, ed. Gunsburger, IMA (Springer, Berlin).

Fursikov, A.W., Imanuvilov, O.Y. (1995): On Exact Boundary Zero Controllability of Two-Dimensional Navier-Stokes Equations. *Acta Appl. Math.* **37**, 67–76.

Gad-el-Hak, M., Blackwelder, R.F. (1987): Control of the Discrete Vortices from a Delta Wing. *AIAA J.* **25**, 1042–1049.

Galland, M.A., Billoud, G., Sebbani, M. (1991): Suppression des Oscillations Auto-Entretenues dans un Risonateur de Helmholtz par Contrôle Actif Auto-Adaptatif. *C. R. Acad. Sc. Paris* **312**, Sirie II(7), 695–700.

Gaster, M., Wygnanski, I. (1985): Large-Scale Structures in a Forced Turbulent Mixing Layer. *J. Fluid Mech.* **150**, 23–39.

Germano, M., Piomelli, U., Moin, P., Cabot, W. (1991): A Dynamic Subgrid-Scale Eddy-Viscosity Model. *Phys. Fluids A* **3**(7), 1760–1765.

Gharib, M. (1993): The Effect of Axial Oscillation on a Cylinder Wake. AIAA Paper 93-3240.

Gledzer, Villermaux, Kahlaleuras, Gajue (1994): Intermittency. LEGI/IMG Grenoble Univ. Press, France.

Glowinski, R., Lions, J.-L. (1994): Exact and Approximate Controllability for Distributed Parameter System. *Acta Numerical*, 269–378.

Glowinski, R., Lions, J.-L. (1995): Exact and Approximate Controllability for Distributed Parameter System. *Acta Numerical*, 159–333.

Goldskin (1996): AIAA Paper 96-2132.

Gunzburger, M., Hou, L., Svobodny, T. (1991): Analysis and Finite Element Approximation of Optimal Control Problems for Stationary Navier-Stokes Equations with Distributed and Neumann Controls. *Maths. Comput.* **57**, 123–151.

Gunzburger, M., Lee, H. (1994): Feedback Control of Fluid Flows. *Proc. 14th IMACS World Congress*, Atlanta.

Gunzburger, M., Lee, H. (1994): Analysis, Approximation and Computation of a Coupled Solid/Fluid Temperature Control Problem. *Comput. Methods Appl. Mech. Eng.* **118**, 133–152.

Gunzburger, M., Hou, L., Svobodny, T. (1991): Analysis and Finite Element Approximation of Optimal Control Problems for Stationary Navier-Stokes Equations with Dirichlet Condition. *Math Mod. Numer. Anal.* **25**, 711–748.

Gunzburger, M., Peterson, J. (1993): The Reduced Basis Method in Control Problems. *Computation and Control III*, eds. K. Bowers & J. Lund, pp. 211–218 (Birkhauser, Boston).

Gutmark, E.J., Shadow, K.C. (1994): Active Control of Bluff-Body Flame-Holder Combustor. AIAA Paper 94-0215.

Gutmark, E. J., Schadow, K.C., Yu, K.H. (1995): Mixing Enhancement in Supersonic Free Shear Flows. *Annu. Rev. Fluid Mech.* **27**, 375–417.

Ha Minh, H. (1994): Order and Disorder in Turbulent Flows—Their Impact on Turbulent Modelling. *Osborne Reynolds Centenary Symposium*, UMIST, England.

Hall, W. II (1984): Tests of Wall Blowing Concepts for Diffuser Boundary Layer Control. AIAA Paper 84-1276.

Hansen, M. (1994): Effect of Internal Acoustic Excitation on the Vortex Shedding of a Circular Cylinder. *Proceedings of Euromech Colloquium*, no. 328.

Hardouin, Micheau, Tartarin, Lemmonier (1993): An Anti-Pulsatory Device Used as an Active Noise Control System in a Duct. *Acta Acoustica* **I**, 289–198.

Heenan, A.F., Morrison, J.F. (1994): Control of Pressure Fluctuations Generated by Separated Flow. *Proceedings of Euromech Colloquium*, no. 328.

Henry, F.S., Pearcey, H.H. (1994): Numerical Model of Boundary-Layer Control Using Jet Generated Vortices. *AIAA J.* **32**(12), 2415–2424.

Hernandez, G., Schönfeld, T., Nicoud, F., Mangiavacchi, N. (1996): Numerical Active Control of Two-Dimensional Boundary Layer Separation. *First AIAA Theoretical Fluid Mechanics Meeting*, AIAA Paper No. 96-2142.

Ho, C.-M. (1982): Vortex Merging. *J. Fluid Mech.* **119**, 443–473.

Ho, C.-M. (1991): Phase Decorrelation of Coherent Structures in a Free Layer. *J. Fluid Mech.* **230**, 319–337.

Ho, C.-M., Huang, L.-S. (1982): Subharmonics and Vortex Merging in Mixing Layers. *J. Fluid Mech.* **119**, 443–473.

Ho, C.-M., Huerre, P. (1984): Perturbed Free Shear Layers. *Annu. Rev. Fluid Mech.* **16**, 365–464.

Hsiao, F.B., Shyu, J.Y. (1991): Influence of Internal Acoustic Excitation upon a Circular Cylinder. *J. Fluid & Structures* **5**, 427–442.

Huang, H., Kuo, C.C., Uhlig, O., Fiedler, H.E. (1994): Control of the Flow Behind a Backward Facing Step. *Proceedings of Euromech Colloquium*, no. 328.

Huang, L.S., et al. (1967): Separation Control over an Airfoil at High Angle of Attack by Sound Emanating from the Surface. AIAA Paper No. 67-1261.

Huang, X.Y. (1996): Feedback Control of Vortex Shedding from a Circular Cylinder. *Exp. Fluids* **20**, 218–224.

Huerre, P., Monkewitz, P.A. (1985): Absolute and Convective Instabilities in Free Shear Layers. *J. Fluid Mech.* **159**, 151–168.

Huerre, P., Monkewitz, P.A. (1990): Local and Global Instabilities. *J. Fluid Mech.* **220**, 473–537.

Hussain, A.K., Husain, H.S., Zaman, K.B., Tso, J., Hayakawa, M., Takaki, R., Hasan, M.A. (1986): Free Shear Flows—Organized Structures and Effects of Excitation. AIAA Paper No. 86-0235.

Hussain, F., Zaman, K.B.M.Q. (1981): The "Preferred Mode" of the Axisymmetric Jet. *J. Fluid Mech.* **110**, p. 3971.

Inoue, O. (1992): Double Frequency Forcing on Spatially Growing Mixing Layers. *J. Fluid Mech.* **234**, 553–581.

Ito, K., Desai, M. (1991): Optimal Control of the Navier-Stokes Equations. Center for Applied Mathematical Sciences Report No. 91-6, Univ. Southern California, Los Angeles.

Jendoubi, S., Strykowski, P.J. (1994): Absolute and Convective Instability of Axisymmetric Jets with External Flow. *Phys. Fluids* **6**(9), 3000–3009.

Jeung, W.R., Al-Sudone, A.S, Turner, J.T. (1994): Aerodynamic Excitation and Control of an Axisymmetric Turbulent Jet. *Proc. Euromech Colloquium*, no. 328.

Johnston, J.P., Nishi, M. (1990): Vortex Generator Jets—Means for Flow Separation Control. *AIAA J.* **28**(6), 989–994.

Joseph, D.D. (1980): *Stability of Fluid Motions. Springer Tracts in Natural Philosophy*, vols. 27-28 (Springer, Berlin).

Joslin, R.D. (1994): Control of Nonlinear Instabilities in Attachment Line Boundary Layer. AIAA Paper No. 94-0826.

Joslin, R.D., Nicolaides, R.A., Erlebacher, G., Hussaini, M.Y., Gunzburger, M.D. (1995): Active Control of Boundary Layer Instabilities—Use of Sensors and Spectral Controller. *AIAA J.* **33**(8), 1521–1523.

Katz, Y., Nishri, B., Wygnanski, I. (1989): The Delay of Turbulent Boundary Layer Separation by Oscillatory Active Control. *Phys. Fluids* **2**, 179–181.

Keefe, L.R. (1993): Drag Reduction in Channel Flow Using Nonlinear Control. AIAA Paper No. 93-3279.

Kerschen, A. (1996): AIAA Paper No. 96-2135.

Kim, J., Kline, S., Johnston, J. (1980): Investigation of Reattaching Turbulent Shear Layer—Flow over a Backward-Facing Step. *J. Fluids Eng.* **102**, 302–308.

Kiya, M., Shimizu, M., Mochizuki, O. (1993): Active Forcing of an Axisymmetric Leading Edge Turbulent Separation Bubble. AIAA Paper No. 93-3245.

Kiya, M., Shimizu, M., Mochizuki, O., Ido, Y., Tezuka, H. (1993): Active Forcing of an Axisymmetric Leading-Edge Turbulent Separation Bubble. AIAA Shear Flow Conference, Orlando, Florida, AIAA Paper No. 93-3245.

Kraichnan, R. (1980): Eddy Viscosity in Two and Three Dimensions. *J. Atmos. Sci.* **33**, 1521–153.

Kusek, Corke, Reisenthel (1990): Seeding of Helical Modes in the Initial Region of an Axisymmetric Jet. *Exp. Fluids* **10**, 116–124.

Lamp, A, Chokani, N. (1996): Active Control of Compressible Cavity Flows by Using a Smart Jet. AIAA Paper No. 96-0446.

Le Dimet, F.X., Talagrand, O. (1986): Assimilations Method. *Tellus* **38A**, 97–110.

Lee, M., Ho, C.-M. (1990): Lift Force of Delta Wings. *Appl. Mech. Rev.* **43**, 209–221.

Lee, M., Reynolds, W. C. (1987): Bifurcating and Blooming Jets. *Fifth Symposium on Turbulent Shear Flows*, pp. 1.7–1.12 (Springer, Berlin).

Lee, R., Hanff, E.S., Kind, R.J. (1996): Linear control of side forces and yawing moments wing the dynamic manipulation of forebody vortices. *ICAS. 96.2.10.1.*

Le Pera, S., Vandsburger, U. (1997): Coupled Multijet Excitation. AIAA Paper No. 97-0075.

Lesieur, M. (1996): *Turbulence in Fluids* (Kluwer, Dordrecht, Netherlands).

Leu, T.S., Ho, C.-M. (1993): AIAA Paper No. 93-3242.

Lilley, G. (1972): Generator and Radiation of Supersonic Jet Noise. Air Force Aerospace Lab. TR 72.

Lions, J.-L. (1971): *Optimal Control of Systems Governed by Partial Differential Equations* (Springer, Berlin).

Lions, J.-L. (1985): *Control of Distributed Singular Systems* (Bordas, Paris).

Lions, J.-L. (1986): Exact Controllability, Stabilization and Perturbations for Distributed Systems. The John Von Neumann Lecture, S.I.A.M. National Meeting, Boston.

Lions, J.-L. (1988): *Contrôlabilté Exacte des Systèmes Distribués* (Masson Paris).

Lions, J.-L. (1990): Are there Connections between Turbulence and Controllability. In *Lecture Notes in Control and Information Sciences*, vol. 144, eds. A. Bensoussan and J.-L. Lions (Springer, Berlin).

Lions, J.-L. (1991): Exact Controllability for Distributed Systems. In *Some Trends and Some Problems in Applied and Industrial Mathematics*, ed. R. Spigler, pp. 59–84 ((Kluwer, Dordrecht, Netherlands).

Lions, J.-L. (1993): Least Regrets Control. In *Boundary Value Problems for PDE and Applications.* Private communication.

Lions, J.-L. (1996): *Mathematical Topics in Fluid Mechanics. Vol. 1. Incompressible.* Oxford Series in Math. and its Appli., no. 3 (Clarendon, Oxford).

Lions, J.-L., Magenes, E. (1968): *Problèmes aux Limites Non Homogènes et Application* (Dunod, Paris).

Lockwood, M.K., Walker S.H. (1981) Modelling Structurally Damaging Twin Screech. *AGARD Conference Proceedings on Aeronautics*, no. 308.

Longmire, E.K., Duong, L.H. (1966): Bifurcating Jets Generated with Stepped and Sawtooth Nozzles. *Phys. Fluids* **8**(4), 978–992.

Lopez, J., Perry, A. (1992): Axisymmetric Vortex Breakdown. Part 3. Onset of Periodic Flow and Chaotic Advection. *J. Fluid Mech.* **234**, 449–471.

Lu, P.J, Yeh, D.Y. (1993): AIAA Paper No. 93-3285.

Lumley, J.L. (1996): Control of Turbulence. Dryden Lecture, *34th AIAA Aerospace Sciences Meeting*, Reno, Nevada.

Martin, J.E., Meiburg, E. (1991): Numerical Investigation of Three-Dimensionally Evolving Jets Subject to Axisymmetric and Azimuthal Perturbations. *J. Fluid Mech.* **230**, 271–318.

Martin, J.E., Meiburg, E. (1992): Numerical Investigation of Three-Dimensionally Evolving Jets under Helical Perturbations. *J. Fluid Mech.* **243**, 457–487.

Masuda, S., Obi, S., Aoki, K. (1994): Control of Turbulent Separating and Reattaching Flow by Periodic Perturbations. *ASME Fluids Engineering Summer Meeting.*

Mathieu, J., Jeandel, D. (1984): *La Simulation des Modèles de Turbulence et leur Application. Vol. 1. Turbulence et Approche Spectral* (Eyrolles, Paris).

McGrath, Shaw, L. (1996): Active Control of Shallow Cavity Acoustic Resonance. AIAA Paper No. 96-1949.

McManus, K.R., et al. (1995): Active Control of Aerodynamic Stall Using Pulsed Jet Actuators. AIAA Paper No. 95-2187.

McManus, K.R., Legner, H.H., Davis, S.J. (1994): Pulsed Vortex Generator Jets for Active Control of Flow Separation. AIAA Paper No. 94-2218.

McManus, K.R., Poinsot, T., Candel, S.M. (1993): A Review of Active Control of Combustion Instabilities. *Proc. Energy Combust. Sci.*, vol. 19, pp. 1–29.

Metais, O., Lesieur, M. (1992): Spectral Large-Eddy Simulation of Isotropic and Stably Stratified Turbulence. *J. Fluid. Mech.* **239**, 157–194.

Michalke, A.(1989): Survey on Jet Instability Theory. *Prog. in Aerospace Sci.* **21**, 159–199.

Mitchell, B., Lele, S., Moin, P. (1995): Direct Computation of Sound Generated by Vortex Pairing in an Axisymmetric Jet. AIAA Paper.

Mittal, R., Balachandar, S. (1996): AIAA Paper No. 96-0210.

Mohammadi, B., Pironneau, O. (1994): Analysis of the K-Epsilon Turbulence Model. *J. Wiley*, 149–182.

Moin, P., Kim, J. (1991): Numerical Investigation of Turbulent Channel Flow. *J. Fluid Mech.* **118**, 341–397.

Monkewitz, P.A. (1988): Global Linear Stability Analysis of Weakly Non-Parallel Shear Flow. *J. Fluid Mech.* **251**, 1–20.

Monkewitz, P.A. (1988): Oscillations in the Nearfield. *J. Fluid Mech.* **255**, 323–347.

Monkewitz, R.A. (1989): *Bulletin American Physical Society* **33**, p. 2273.

Monkewitz, P.A. (1989): Feedback Control of Global Oscillations in Fluid Systems. *2nd Shear Flow Conference*, AIAA Paper No. 89-0991.

Monkewitz, P.A., Fernholz, H.H., Weickgenannt, A. (1994): The Control of Vortex Shedding from Axisymmetric Bluff Bodies. *Proceedings of Euromech Colloquium*, no. 328.

Monkewitz, P.A., Huerre, P. (1982): Influence of the Velocity Ratio on the Spatial Instability of Mixing Layers. *Phys. Fluids* **25**(7), 1137–1143.

Monkewitz, P.A., Sohn, K.D. (1988): Absolute Instability in Hot Jets. *AIAA J.* **26**, 911–916.

Montividas, R.E., Acharya, M., Metwally, M.H. (1991): Reactive Control of an Unsteady Separating Flow. *AIAA J.* **30**(4), 1133–1134.

Moore, C.J. (1977): The Role of Shear-Layer Instability Waves in Jet Exhaust Noise.

Morgan, K., Peraire, J., Peiro, J. (1987): Unstructured Grid Methods for Compressible Flows. In *Unstructured Grid Methods for Advection Dominated Flows*, AGARD Conference Proceedings.

Morris, P.J. (1976): The Spatial Viscous Instability of Axisymmetric Jets. *J. Fluid Mech.* **77**, 511–529.

Myose, R.Y., Blackwelder, R.F. (1995): Control of Streamwise Vortices Using Selective Suction. *AIAA J.* **33**(6), 1076–1089.

Nagib, H., Reisenthel, P.H., Koga, D. (1985): On the Dynamical Scaling of Forced Unsteady Separated Flows. AIAA Paper No. 85-0553.

Nash, L.F. (1994): Laminar Boundary Layer Aeroacoustics Instabilities. AIAA Paper No. 94-0358.

Nelson, C.F., Eaton, J.K. (1996): Open Loop Control of the Unsteady Separated Flow Downstream of an Oscillatory Spoiler. AIAA Paper No. 96-0447.

Nelson, C.F., Koga, D.J., Eaton, J.K. (1990): Unsteady Separated Flow behind an Oscillating Two-Dimensional Spoiler. *AIAA J.* **28**, 845–852.

Nishioka, M., Asai, M., Yoshida, S. (1990): Control of Flow Separation by Acoustic Excitation. *AIAA J.* **28**(11), 1909–1915.

Nishri, B., Wygnanski, I. (1996): On Flow Separation and its Control. *ECCOMAS 1996.*

Olsson, M., Fuchs, L. (1996): Large Eddy Simulation of the Proximal Region of a Spatially developing circular jet. *Phys. Fluids* **8**(8), 2125–2137.

Orellano, A., Wengle, H. (1995): Numerical Simulation and Analysis of Manipulated Transitional Flow over a Fence. *IMACS-COST Conference on Three-Dimensional Complex Flows.*

Osswald, Y.G. (1993): Management of Dynamic Stall Phenomenon Through Active Control of Unsteady Separation. AIAA Paper No. 93-3284.

Ott, E., Grebogi, C., Yorke, J.A. (1990): Controlling Chaos. *Phys. Rev. Letter* **64**, 1196–1199.

Ott, E., Sauer, T., Yorke, J.A. (1994): *Coping with Chaos* (Wiley, New York).

Ou, Y., Sritharan, S. (1994): On the Robustness of the Navier-Stokes Global Attractor. *Proc. 14th IMACS World Congress.*

Papadakis, M., Lin, J. (1996): A Flow Physics Study of Vortex Generators on a Multi-element Airfoil. AIAA Paper No. 96.0548.

Park, D.S., Ladd, D.M., Hendricks, E.W. (1994): Feedback Control of von Kármán Vortex Shedding behind a Circular Cylinder at Low Reynolds Number. *Phys. Fluids* **6**, p. 2390.

Perrier, P. (1997): Some Problems and Paths to Next Century Unsteady Multiscale C.F.D. In *Computational Science for the 21st Century*, pp. 357–368 (Wiley, New York).

Petersen, R.A. (1978): Influence of Wave Dispersion on Vortex Pairing in a Jet. *J. Fluid Mech.* **89**, 469–495.

Pironneau, O. (1994): *Optimal Shape Design for Elliptic Systems.* (Springer, New York).

Poinsot, T.J., Lele, S.K. (1992): Boundary Conditions for Direct Simulations of Compressible Viscous Flows. *J. Computational Physics* **101**, 104–129.

Poinsot, T.J., Trouvé, A., Veynante, D., Candel, S., Esposito, E. (1987): Vortex Driven Acoustically Coupled Combustion Instabilities. *J. Fluid Mech.* **177**, 265–292.

Poje, A.C., Lumley, J.L. (1995): A Model for Large-Scale Structures in Turbulent Shear Flows. *J. Fluid Mech.* **285**, 349–369).

Provansal, M., Mathis, C., Boyer, L. (1987): Bénard-von Kármán Instability—Transient and Forced Regimes. *J. Fluid Mech.* **182**, 1–22.

Raman, G., Cornelius, D. (1994): Jet Mixing Control Excitation from Miniature Oscillating Jets. *AIAA J.* **33**, 365–368.

Reeder, M.F., Samimy ,M. (1996): The Evolution of a Jet with Vortex Generating Tabs—Real-Time Visualization and Quantitative Measurements. *J. Fluid Mech.* **311**, 73–118.

Reichert, A., Wendt, J. (1994): Improving S-Duct Performance by Secondary Flow Control. AIAA Paper No. 94-0365.

Reisenthel, P.H., Nagib, H.M., Koga, D.J. (1985): Control of Separated Flows Using Forced Unsteadiness. AIAA Paper No. 85-0556.

Rennie, R., Jumper, E. (1994): Experimental Measurements of Dynamic Control Surface Effectiveness. AIAA Paper No. 94-0504.

Robinson, S. (1989): Review of Vortex Structures and Associated Coherent Motions in Turbulent Boundary Layers. *2nd IUTAM Symposium*, Zürich, Switzerland.

Rockwell, D., Knisely, C. (1980): Observations of the Three Dimensional Nature of Unstable Flow Past a Cavity. *Phy. Fluids* **23**(3), 425–431.

Rockwell, D., Naudascher, E. (1982): Self-Sustained Oscillations of Impinging Free-Shear Layers. *Annu. Review Fluid. Mech.* **11**, 67–94.

Ross, F.W., (1996): Microblowing for Vortex Asymmetry Management on a Hemispherical Cylinder Forebody. AIAA Paper No. 96-1951.

Rossiter, J.E. (1966): Wind Tunnel Experiments in the Flow over Rectangular Cavities at Subsonic and Transonic Speeds. NACA R.M. No. 3438.

Roussopoulos, K. (1993): Feedback Control of Vortex Shedding at Low Reynolds Numbers. *J. Fluid Mech.* **248**, 267-296.

Ruban, Duch (1996): AIAA Paper No. 96-2123.

Samimy, M., Elliott, G. (1990): Effects of Compressibility on the Characteristics of the Free Shear Layer. *AIAA J.* **2813**, 439–445.

Schumm, M., Berger, E., Monkewitz, P.A. (1994): Self-Excited Oscillations in the Wake of Two-Dimensional Bluff Bodies and their Control. *J. Fluid Mech.* **271**, 17–54.

Sebbani, M., Sunyach, M. (1992): Contrôle Actif des Instabilitis Liies aux Ecoulements—Exemple du Pompage des Systhmes de Compression. *J. de Physique IV*, Colloque CI, 615–618.

Selby, G.V., Troeger, L.P. (1993): Passive and Active Control of Low-Speed Turbulent Separated Flow over Swept Backward-Facing Ramps. In *FED Symposium on Separated Flows*, vol. 149, pp. 27–41, ASME, New York.

Sigurdson, L.W. (1995): The Structure and Control of a Turbulent Reattaching Flow. *J. Fluid Mech.* **298**, 139–165.

Silveira-Neto, A., Grand, D., Métais, O., Lesieur, M. (1993): A Numerical Investigation of the Coherent Structures of Turbulence behind a Backward-Facing Step. *J. Fluid Mech.* **256**, 1–55.

Sinha, S.K., Pal, D. (1994): Controlling Unsteady Separation with Acoustic Active Surfaces. AIAA Paper No. 94-0183.

Smagorinsky, J. (1963): General Circulation Experiments with the Primer Time Equation. *Monthly Rev.* **91**, p. 99.

Smith, B.C. (1996): Pneumatic Control of Vortices on Different F-16 Forebodies Using Jets and Slots. AIAA Paper No. 96-0049.

Smits, P. (1993): After Failure in Supersonic. AIAA Paper No. 93-3248.

Soh, W.Y. (1994): Unsteady Jet Flow Computation Towards Noise Prediction. AIAA Paper No. 94-0138.

Sritharan, S.S. (1991): Dynamic Programming of the Navier-Stokes Equations. *Systems & Control Letters.* **16**(4), 299–307.

Sunyach, M., Ffowcs Williams, J.E. (1986): Contrôle Actif des Oscillations dans les Cavitis Excities par un Icoulement. *C. R. Acad. Sc. Paris* **303**, Sirie II, 1085–1088.

Suprayank, K., Fiedler, H.E. (1994): Structural Control and Management in a Waterjet by Axial Excitation and Vortex Generators. *Euromech Colloquium*, no. 328.

Sverdrop (1996): Unsteady Jet Flow Computation—Towards Noise Prediction. *AIAA Aerospace Sciences Meeting 96.*

Swanson, P., Ottino, J. (1990): A Comparative Computational and Experimental Study of Chaotic Mixing of Viscous Fluids. *J. Fluid Mech.* **213**, 227–249.

TA'Asan, S. (1994): Multigrid One Shot Methods for Optimal Control Problems—Infinite Dimensional Control. ICASE Report No. 52.

TA'Asan, S. (1995): Trends in Aerodynamics Design and Optimization—A Mathematical Viewpoint. *AIAA Conference Proceedings No. 95-1731-CP*, pp. 961–970.

Tam, C., Burton, D. (1990): Jet Noise Generated by Large-Scale Coherent Motion. *NASA R. Pub.* **1258**(1), 311–390.

Tang, K.Y., Graham, W.R., Peraire, J. (1996): Active Flow Control Using a Reduced Order Model and Optimum Control. *27th AIAA Fluid Dynamics Conference*, AIAA Paper No. 96-1946.

Terent'ev (1996): AIAA Paper No. 96–1980.

Truong, V.K. (1993): *19th Rotorcraft Eur. Forum*, Cernobbio.

Urbin, G., Metais, O. (1997): Large Eddy Simulations of Spatially-Evolving Round Jets—Vortex Control. *Phys. Fluids.*

Villermaux, E., Hopfinger, E. (1994): Self-Sustained Oscillations of a Confined Jet— A Case Study for the Nonlinear Delayed Saturation Model. *Physica D* **72**, 230–243.

Viswanathan, P.R. (1994): A Fluid Acoustic Coupled Simulation of Supersonic Jet Noise. AIAA Paper 94-0137.

Williams, D.R., Mans, H., Amato, C. W. (1992): The Response and Symmetry Properties of a Cylinder Wake Subject to Localized Surface Excitation. *J. Fluid Mech.* **234**, 71–96.

Witkowska, A., Juré, D. (1994): Numerical Estimation of Noise Generated by Homogeneous and Isotropic Turbulence. *C. R. Ac. Sc. Paris* **318**, 597–602.

Wood, A.C.R. (1995): Engine Integration. *AGARD Conference Proceedings*, no. 12.

Wood, N.J., Roberts, L. (1986): Experimental Results of the Control of Vortical Flow by Tangential Blowing. Technical Report, Stanford University, California.

Wood, N.J., Roberts, L. (1988): Control of Vortical Lift on Delta Wings by Tangential Leading-Edge Blowing. *J. Aircraft* **25**, 236–243.

Wu, X. (1996): AIAA Paper No. 96-2133.

Wu, X.H., Wu, J.Z. (1991): Guiding Principles for Vortex Flow Control. *29th Aerospace Sciences Meeting*, AIAA Paper No. 91-0617.

Wurtzler, K. (1994): Numerical Analysis of a Chined Forebody with Asymmetric Slot Blowing. AIAA Paper No. 94-0171.

Wygnanski, I. (1994): The Control of Separation by Oscillatory Blowing. *Proceedings of Euromech Colloquium*, no. 328.

Wygnanski, I. (1996): The Control of Fluid Separation. *ECCOMAS.*

Wygnanski, I., Seifert, A. (1994): The Control of Separation by Periodic Oscillations. AIAA Paper No. 94-2608.

Yang, H., Gursul, I. (1996): Vortex Breakdown over Unsteady Delta Wing and its Control. *AIAA J.* **35**(3), 571–574.

Yang, J., Ghia, K.N., Ghia, U., Osswald, G.A. (1993): Management of Dynamic Stall Phenomenon Through Active Control of Unsteady Separation. *AIAA Shear Flow Conference*, AIAA Paper No. 93-3284.

Zaman, K.B. (1994): Effect of Delta Tabs on Mixing and Axis Swelling. AIAA Paper No. 94-0186.

Zaman, K.B., Hussain, A.K. (1980): Vortex Pairing in a Circular Jet under Controlled Excitation. Part 1. General Jet Response. *J. Fluid Mech.* **101**, 449–491.

6 Control of Free Turbulent Shear Flows

Heinrich E. Fiedler

Technische Universität Berlin, Hermann-Föttinger-Institut für Strömungsmechanik, Müller-Breslau-Str. 8, D-10623 Berlin, Germany

Abstract. In this chapter major principles, methods and possibilities of control of free turbulent shear flows are explained. In the first part we present and summarise general characteristics of free shear flows and the whys and hows of their manipulation. The subsequent two parts are focussing on the three classical configurations—jets, wakes and mixing layers, where the major and largely established ways of controlling those flows for specific goals and purposes are discussed in some detail. In the fourth part combinations of classical free flows and of free and wall-bounded flows—complex scenarios of growing practical interest—are dealt with. Some of their characteristics are discussed and ways and possibilities for their control are shown.

1 Basics and Principles

1.1 Introduction

Observation of nature may provide valuable inspiration and insight into flow control mechanisms: Nature has—over many millenia of optimization—achieved and developed some amazingly elegant and efficient ways of flow control, the most widely known ones being the control of wing-flow of birds and the drag reduction mechanisms found with aquatic animals—particularly the dolphin and the shark. Some of the underlying principles are as yet still incompletely investigated and understood.

In recent time this topic has again been revived for two reasons: It is on the one hand a scientifically logical extension of the coherent structures research of the last two decades, and on the other hand the need for improved technical processes wherever a turbulent flow is involved, as well as the ubiquitous necessity for reduced energy consumption (e.g. drag reduction), which has economical as much as ecological implications. In the following we shall discuss major developments of recent in some depth. We shall—after a general introduction of the physical phenomena and principles involved—discuss specific flow scenarios in the light of their susceptibility to certain ways of control.

1.2 Description–Typology and Characterization of Free Shear Flows

We shall first establish some basic understandings and agreements. Thus the most basic question is:

M. Gad-el-Hak et al.: LNPm 53, pp. 335 - 429, 1998
© Springer-Verlag Berlin Heidelberg 1998

What are free turbulent shearflows?—to which a very general answer is readily given: Those are flows with a mean velocity gradient and free boundaries. A more detailed yet still general characterization has the following specifics:

- freely convoluting boundaries (→ intermittency)
- 'simple', freely evolving (coherent) structures
- mean velocity profiles with one or more inflection points (→ Kelvin-Helmholtz-unstable) and with asymptotic limits
- (mostly) constant momentum integrals
- Re-number independence
- decaying or with permanent 'drive' (as e.g. in a mixing layer)

To simplify and standardize the infinite number of possible flow configurations it has for long time been customary to distinguish between three classical abstractions, which are sketched in Fig. 1. They may be seen as basic building blocks or moduls of essentially all more complex configurations.

1.3 Control Versus Management

In this context the term flow control is used in a relatively well defined and limited way, distinguished from influencing a flow purely by design or by what we may call management, signifying a method of treating or trimming ('tailoring') a given flow to fit a desired specification, as e.g.

- in windtunnels to suppress background turbulence, or to create a prescribed structure, or
- to simulate an atmospheric boundary layer flow for model investigations in architectural aerodynamics.

Some possibilities and limitations of turbulence management are discussed by Nagib and Corke (1984a), Nagib and Marion (1984b), Counihan (1969).

Flow control proper on the other hand is a process or operation by which certain characteristics of a given flow are manipulated in such a way as to achieve improvements of a specific technical performance.

Thus, control acts typically indirectly via structures and their behaviour, which obviously necessitates an intimate knowledge of the latter. It is efficient and not immediate, since it is based on a flow development initiated by internal amplification of a small 'tailored' disturbance.

Management on the other hand describes a rather direct, immediate manipulation of the flow, for which in most cases no detailed knowledge is needed. An example for mangement is the reduction of turbulence level by screens or honeycombs. Figure 2 shows another, however related, application: the destruction of coherent structures in a jet by screens or honeycombs (see also Yajnik and Acharya 1977; Nieberle 1986).

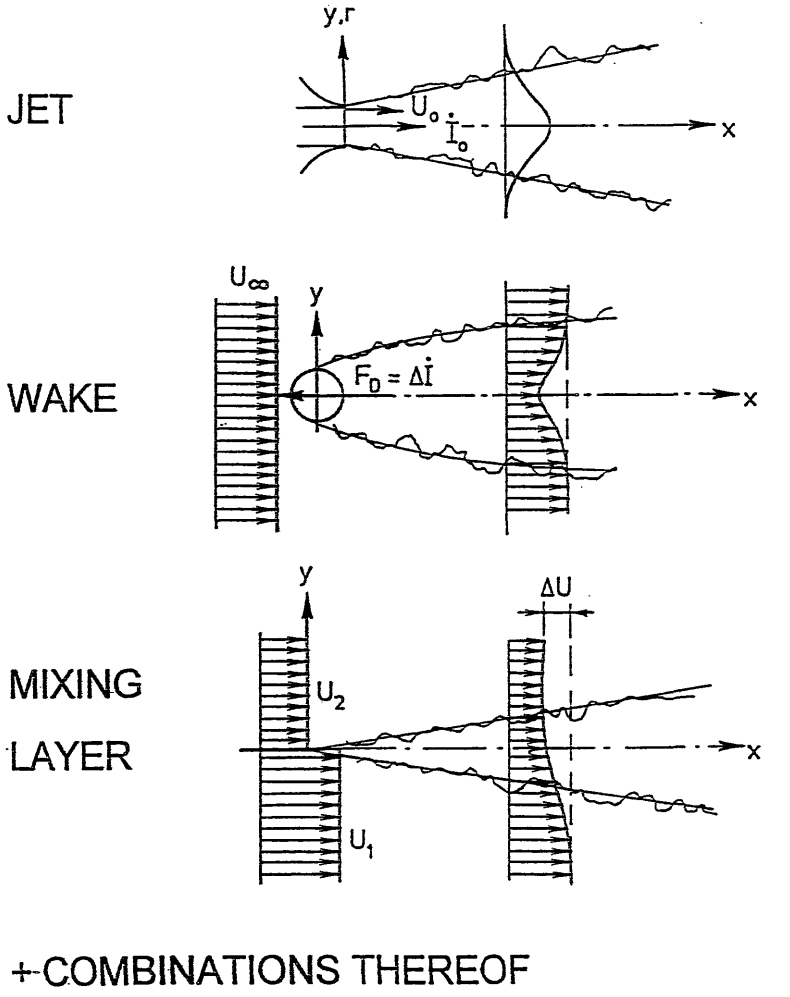

Fig. 1. Three basic modules of free shearflows.

1.4 Some History

Obviously, control is based on detailed knowledge of turbulent structures. Since when dates our knowledge of those? Here are some cornerstones in chronological succession:

- Boussinesq (1879)—introduction of the concept of turbulent viscosity
- Reynolds (1883)—the very beginning of the turbulence concept and it's mathemetical treatment; the phenomenon of transition
- Prandtl (1961)—phenomenological models, boundary layer theory etc.
- v. Karman—theoretical foundations
- Taylor (see Batchelor 1969)—statistical theory

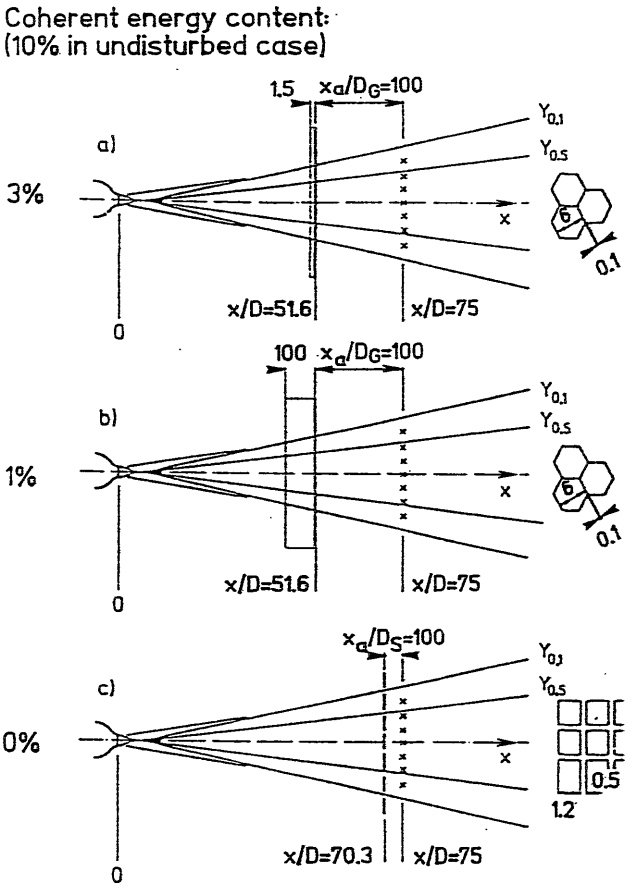

Fig. 2. Destruction of coherent structures in a jet: an example of flow management (Nieberle 1986).

In later years turbulence research became too widespread and diverse so that it is no longer possible to name individuals but rather concepts and methods which provided and signified progress. Thus, from 1960 on we observe a renaissance of phenomenology, which, among other things, led to the development of conditional sampling methods in experimentation and, in this context, to the discovery of coherent structures as a backbone of turbulence. Those coherent structures are, as we shall see, the major links to flow control.

Without, however, knowing about those specific elements, quite spectacular observations of dynamic flow control have been reported already more than one hundred years ago. The famous description by Tyndall (1867) relates to the observation by Leconte (1858) and extends it to a multitude of surprising possibilities of acoustically influencing and modifying gaseous

and liquid jets alike. It was only after many years that the topic was then taken up again by Brown (1935), who undertook a thorough study of jet flow and its sensitivity to sound, observing, describing and explaining many of the amazing consequences of sinusoidal excitation on jet flow, that were then again re-visited and deepened some thirty years later. And then there is the Coanda (1934) effect, which is based on the strong entrainment of turbulent flows, relating to the influence (deflection) of free turbulent flows by nearby walls. Early examples of control of true wall bounded flows are Dubuat's paradox (Dubuat 1779), where the drag of a plate was found to depend on the nature of the flow, i.e. whether the plate or the fluid was at rest. Here we have one of the first reported observations of flow control via laminar/turbulent transition, presumably by means of the turbulence level in the flow. The first use of a trip-wire to achieve premature transition was described by Prandtl (1914), who also introduced boundary layer suction as tool to control and prevent separation.

Only after ca. 1970 there seems to be renewed interest and activity for questions of flow control. This is clearly a consequence of the by then improved knowledge about the dominating structures in turbulent motion and their handling and on the other hand of the economic and ecologic needs which in this decade became an issue of worldwide recognition. Some of the recent developments are summerized in reviewers by Fiedler and Fernholz (1991a), Fernholz (1993) and Hussain et al. (1986).

Next we shall address the question of

1.5 What Do We Want to Achieve ?—*Aims of Control*

Flow control aims at improvements of flow processes in view of technology, ecology and economy. Since the use of control methods is mainly in industrial applications the demand for reliability provides a limiting condition of priority.

In free turbulent flows there are three principal areas for control application:

1. Mixing
2. Noise
3. Entrainment

1. *Mixing:* The question of mixing and its quantification is to this time still not settled. The process of turbulent mixing, preceding the final molecular mixing may be sub-divided into large-scale mixing = 'stirring', and small scale mixing. The major issue to enhance mixing is to achieve a maximum of contact surface between the species to be mixed for providing better conditions for the ensuing 'independent', i.e. uncontrollable, molecular mixing. Note that an increase of spread is not always indicative for an increase of mixing as is often assumed. In fact, in certain cases it may

indicate increase of stirring in a 'stabilizing mode', where the subsequent breakup into smaller structures is suppressed and small-scale mixing— the link between stirring and molecular mixing— largely reduced (see e.g. frequency excited structures in a mixing layers, Chap. 3).
We note here that mixing is primarily a small scale mechanism. In most cases, however, control of small scales in turbulence is not directly possible and can be achieved only by indirect routes via the large scales, which are more directly amenable to external manipulation.
Viewing the practical importance of mixing control some applications are immediately obvious, as e.g. in combustion (flame stabilization), improvement, localization or confinement of chemical reactions, in many applications of chemical engineering, and finally in heat- and mass transfer. While in those cases an increase is the typical result desired, reduced mixing may also be called for, as e.g. for increase of reach of fire jets.

2. *Noise production:* Source of aerodynamic noise is the non-linear dynamics of the amalgamation process of coherent structures (Laufer 1983; Michalke 1978). Its underlying mechanism is, therefore, connected to the large scales of the turbulent motion and thus directly amenable to control. Here the major interest is in the reduction of noise production, where typical applications are in airplane technology and in air-conditioning. The wish for increase of noise would be the exception, however conceiveable for whistles, sirens or in the design of actuators for—again—flow control. Note: Noise compensation by counter-noise is not flow control in the strict sense !

3. *Entrainment:* This is a phenomenon, the effect of which has probably first been recognized by Coanda (1934) (coanda effect). It is primarily the consequence of large scale mechanisms, its control is, therefore, possible by direct means.
Among the many conceiveable applications of this effect the two major ones are probably separation control and localized cooling, e.g. by jet vectoring (see in Chap. 2). Some examples sketched in Fig. 3a/b.

In addition to the practical purpose of flow control there is a scientific aspect: Controlled stabilization of coherent structures may enable or simplify their detailed investigation e.g. by phase averaging methods.

1.6 What Means Do We Command?—*Methods and Mechanisms*

According to control theory we distinguish between two control principles (see e.g. DiStefano et al. (1979))

- the simple, direct OPEN LOOP control, which necessitates external adjustments based on measurements or observations of some kind, and

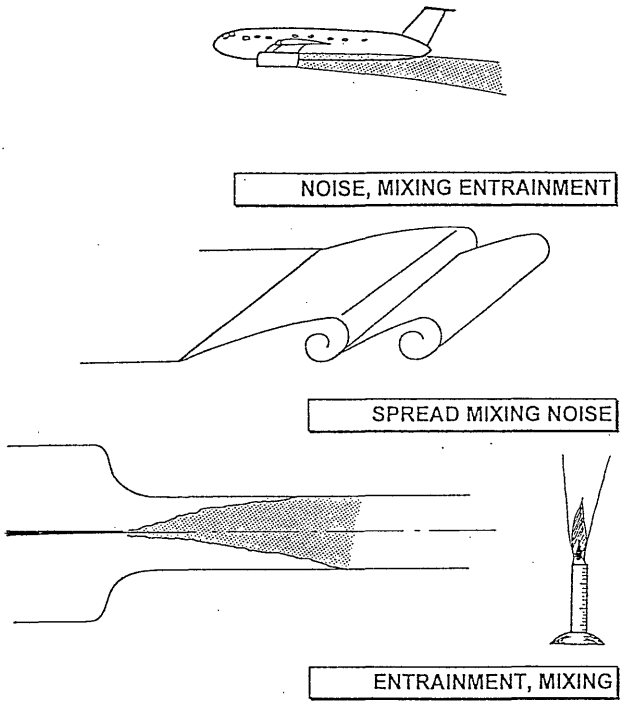

Fig. 3. a) Examples of control application.

– the more elaborate CLOSED LOOP, or 'feedback' control, where continuous adjustment is provided by a feedback of constantly monitored system output. The feedback is typically provided by an external, often adjustable or conditionable loop. The case of an internal, 'built-in' feedback is found in absolutely unstable systems (see below). Typical and often encontered terms and concepts in this context are adaptive feedback, 'intelligent' control, neural networks, fuzzy logic etc.

According to the terminology of control theory the system consists of the plant (the controlled system), a measuring or monitoring system and a controller. Figures 4a,b show block diagrams of the two control systems.

In a closed loop-, or feedback-, control system the difference between the actual value of the controlled output and the desired value of that output is used to change the value of the input to the system in such a manner as to maintain the output as close as possible to a desired value. A special situation of (b) is when this control loop is 'unstable', i.e. when any deviation is amplified (a situation which in common understanding is known as a feedback). A feedback situation, which may be external or internal, is characterized by threshold- and saturation- levels and is—in general—a non-linear phenomenon. In more specific terms we call a situation where feedback signal

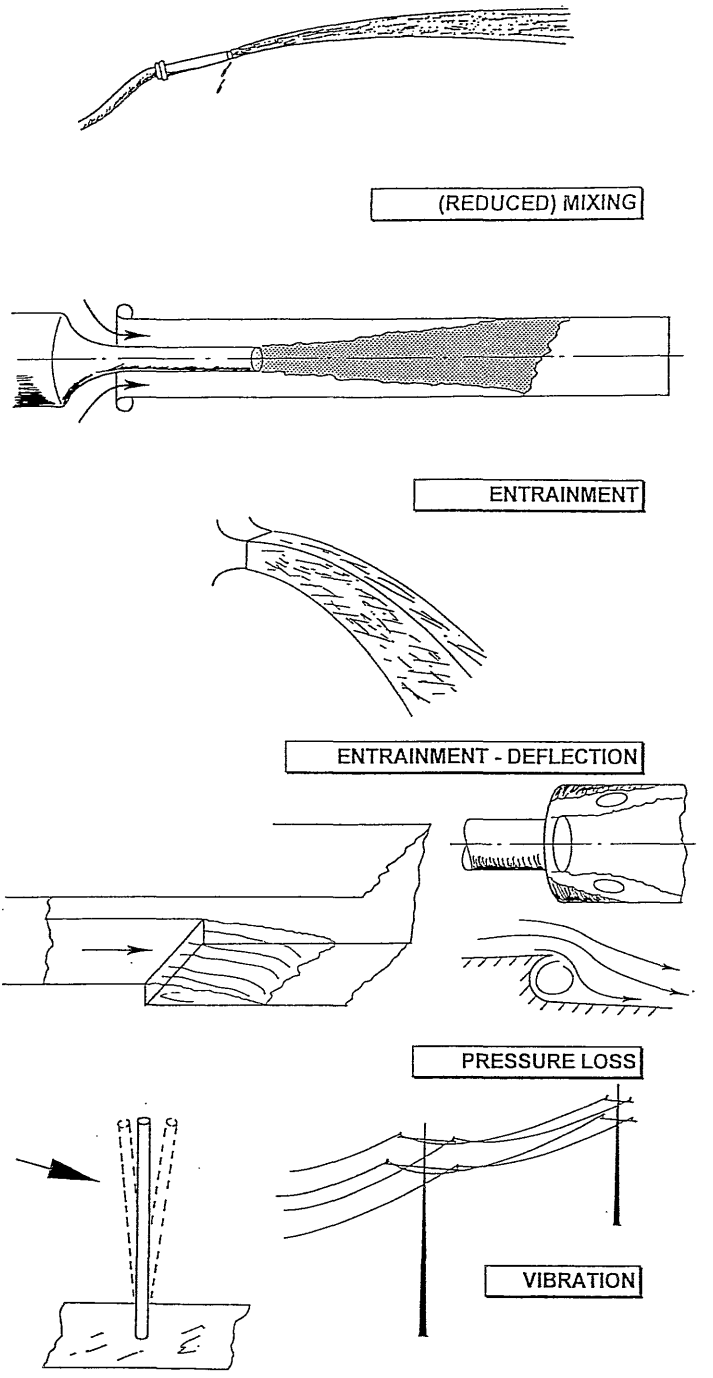

Fig. 3. b) Examples of control application.

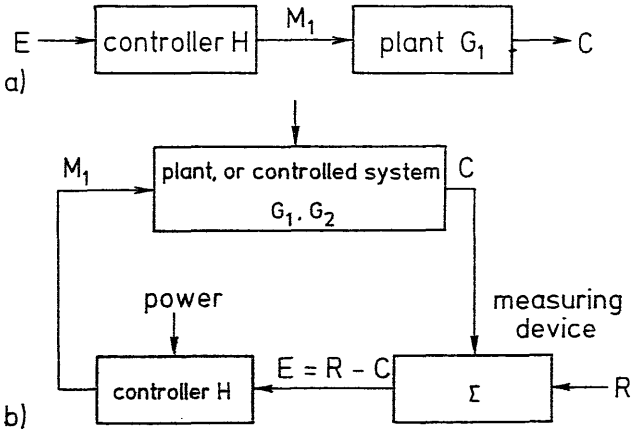

Fig. 4. Block diagrams of control circuits: a) open loop; b) closed loop.

and input signal are of opposite phase a negative (or degenerative) feedback. If both signals are of equal phase the feedback is positive (or regenerative).

As an example let us consider a plane mixing layer (the PLANT), which is easily controlled by periodic perturbations of appropriate frequency and amplitude. (see under 3.4).

Open loop control is then applied by forcing the flow (via loudspeaker or other appropriate means = the CONTROLLER) with an independently adjusted external periodic signal from, say, a frequency generator.

Closed loop control has various possibilities:

1. the frequency generator is controlled by some characteristic amplitude (e.g. the RMS-output) as obtained from the periodic fluctuations, measured at some station in the flow, or,
2. the (filtered) output signal is directly used to drive (via amplifier) the forcing unit (the CONTROLLER). Adjustment is possible through the amplifier, by a time shift of the feedback signal, or by spacial shift of the location where the control signal is obtained. This is the case of an external direct feedback loop.

Internal feedback can be provided by pressure waves or mechanical vibrations of the system. An obvious model relation is—as has been proposed by various authors (e.g. Ho and Nosseir 1981; Laufer and Monkewitz 1980) –

$$\frac{L}{U_P} + \frac{L}{a} = \frac{n}{f} \ ,$$

where L is a 'feedback-characteristic' length, U_P = phase velocity of the feedback wave in the flow (the 'structure'), f = feedback frequency, a = velocity of sound (by which the wave is transported upstream), and $n = 1$, 2, 3, ... representing the number of waves.

This can be expressed as a 'feedback Strouhal number':

$$S_F = \frac{n}{U_0/U_P + Ma} \ ,$$

with Ma = Mach number and U_0 = velocity of the basic flow.

The role of adaptive or 'intelligent' control by closed loop appears, however, to be small in free flow applications, in particular there is no laminar-turbulent transition control, since transition appears essentially already at the trailing edge, and also no separation control as in airplane applications—the two typical examples of adaptive feedback control. In free flows we find closed loop control almost exclusively in combustive applications.

A modern example of adaptive control in flow around an airfoil is shown in Fig. 5.

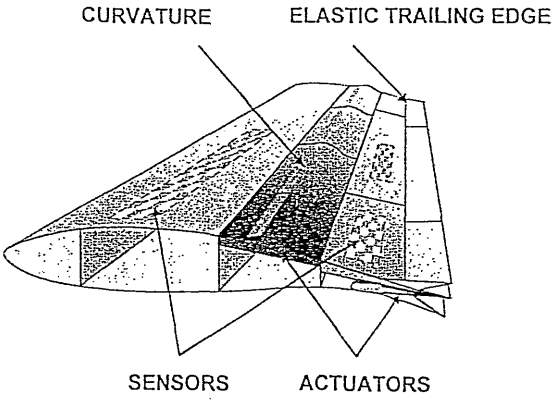

Fig. 5. Airfoil with adaptive control elements.

Stability—*The Key.* Discussion of stability of turbulent shear flows evokes their most obvious manifestation: Coherent Structures. What are coherent structures (CS)? We may describe them as characteristic transient, metamorphic structural entities or scenarios of quasi-regular repetition and existence or duration over a distinct period of time, comparable to a few of their turnover times (Fiedler 1988a).

Alternatively we see them as manifestations of concentrated and coherent vorticity of an instability mode of the (physically non-existent!) mean velocity profile. In view of this CS can be influenced or controlled as can laminar stability modes.

Note, however: Specific manifestations of a given coherent structure depend largely on the quality of interest. Examples are POD-reconstructions of velocity, energy, vorticity, temperature etc.. Figure 6 juxtaposes some of

those manifestations as measured in an accelerating mixing layer, where the vorticity distribution corresponds approximately to its visual manifestation, i.e. a smoke picture.

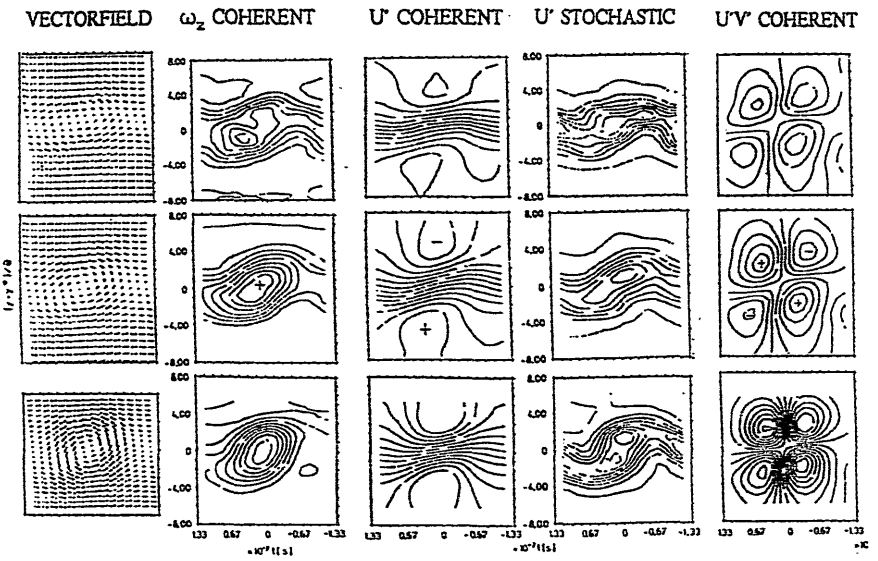

Fig. 6. Different manifestations of a coherent structure in an accelerated turbulent mixing layer (artificially stabilized) from Fiedler et al. (1991).

This definition leads to a number of questions, like:

1 How can a mean profile be unstable?
2 What fraction of turbulent energy is coherent?
3 What fraction of other turbulent qualities, e.g. shear stress, is coherent?

Here are some—in this context sufficient—answers:

(1) mean flow profile instability (leading to formation of coherent structures) may be understood when viewing it as a real flow profile with superimposed noise, of typical wave lengths an order of magnitude smaller than the instability wave, and therefore decoupled.

(2) coherent energy fraction: Coherent structures are most amenable to external flow control. Control efficiency or -potential may, therefore, be estimated by the relative energy content of the coherent structures as compared with the total turbulent energy. Because of the inherent uncertainty of the various eduction schemes for coherent structures, the following percentages provide only estimates:

Flow	$E_{coherent}/E_{total}$
plane mixing layer	20 %
accelerated mixing layer	25 %
near jet	>25 %
axisymmetric far jet	10 %
near wake	25 %
far wake	20 %
and for comparison:	
wall bounded flow	<10 %

On the basis of these data the idea of controlling turbulent flows by means of influencing their coherent structures seems promising. Are, however, these values as such meaningful? Indeed it is not primarily the energy of the coherent structure that determines its importance, but rather its distributive actions and in particular the ratio of the Reynolds-shear-stresses $(\overline{u'v'})_{coherent}/(\overline{u'v'})_{total}$, which may reach values of up to 95 % in the region of maximum structural organization of an excited mixing layer (region II, see Fig. 52). Still, those figures seem to be of importance only in an indirect way. We find that a jet flow in still ambient fluid with relatively weak coherent content is—owing to its configuration—easily controlled by periodic excitation in most spectacular ways (see Lee and Reynolds 1985). A wake on the other hand has a notably higher CS energy content, yet its controllability is—by comparison—limited. The major difference between those two flows is in its convective characteristics: In a jet the convection is of the same order as its diffusion and highly dependent on the state of excitation. In the wake on the other hand, being a flow deficit, the convection velocity of its structures in the far region are almost constant and large in comparison with it's diffusion, which reduces its controllability.

Let us—for better understanding—take a closer look at the different stability characteristics in free flows and in wall bounded flows: While wall-bounded flows are Orr-Sommerfeld unstable, where viscosity plays a crucial role, free flows are Rayleigh- (inflexion point) unstable. There the (largely negligible) effect of viscosity may only be of damping influence and the prime instability mechanism is by vortical induction. Flows dominated by this kind of instability tend to develop comparatively 'simple' instability modes which to a considerable extent persist in the random-turbubulent ambience, becoming prey of either mutual interaction or of secondary instabilities (pairing, tearing, wearing). Figure 7 gives a simplified picture of the evolving coherent structures in free- and in wall flows.

Flow stability, that is to say the stability of the coherent structures, obviously provides the key to control. It is responsible for such mechanisms as the laminar/turbulent transition, as well as for the origin (the creation) and to some extent the decay of structures by creation of smaller structures as a consequence of the instability of the former. We therefore distinguish

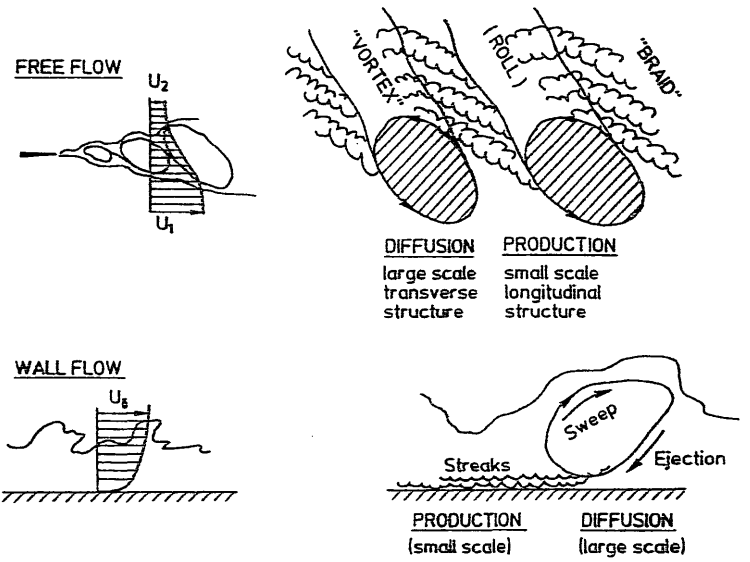

Fig. 7. Sketches of coherent structure scenarios in free- and wall-bounded (boundarylayer) flows.

between primary and secondary instability, which can manifest in various modes (denoted by numbers 0,1,2...n).

While the basic mechanism leading to a growth of perturbations may be one of many, a major and more general distinciton in stability behaviour, of particular importance for controllability, is provided by the temporal and spatial growth behaviour of the initial disturbances. We define (see Drazin and Reid 1981; Huerre and Monkewitz 1985): A flow is considered absolutely unstable if the group velocity of an unstable mode is equal to zero. In this case the amplitude of a given perturbation grows with time at a fixed x-position in the flow. This situation is tantamount to a closed loop system with internal feedback, i.e. an oscillator. It occurs typically in profiles with regions of reverse flow.

For convectively unstable flows all perturbation frequencies have positive group velocity. Thus, at a given $x > x_p$, where x_p defines the geometrical position at which the perturbation is introduced, the perturbation wave will reach a finite amplitude for a finite time only. The diagram in Fig. 8 gives a graphical explanation.

Huerre and Monkewitz (1990) have extended the scope of stability behaviour by introducing a distinction between local and global instability: Local instability denotes the situation of instability of a local velocity profile (being usually a function of x), while in global instability the entire flow field is concerned (see also Monkewitz 1989).

There are basic differences between those four conditions with respect

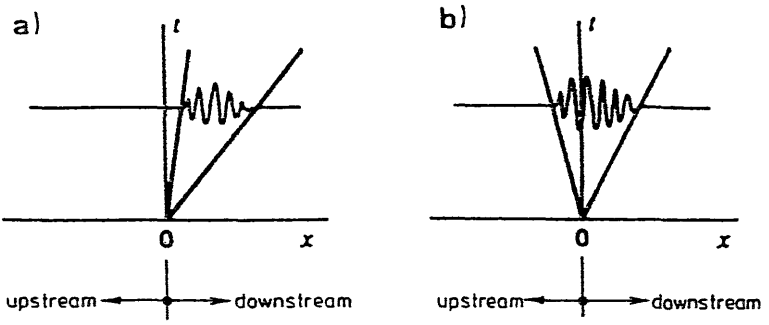

Fig. 8. Amplification of a perturbation at (a) convective- and (b) absolute instability.

to their control behaviour: Convectively unstable flows have characteristics of frequency selective, non-linear amplifiers. Accordingly they are sensitive to external forcing at a given frequency, while the amplifier characteristics themselves are modified by stationary boundary conditions.

Absolutely unstable flows, having an oscillator characteristic, are on the other hand comparatively resistant against external (periodic) forcing, being 'self-excited flows' according to Koch (1985). They can often be effectively influenced by minor changes introduced into the unstable flow regimes, as was demonstrated by Strykowski and Sreenivasan (1990) in the near wake behind a cylinder.

Locally unstable flows may—by modifications of their boundary conditions —become globally unstable (e.g. Fiedler et al. 1991b). Global instabilities are often indicative of a feedback situation. A control-relevant distinction in this context is whether the flow system behaves as an externally excitable amplifier or as an oscillator with characteristic global response (Monkewitz and Sohn 1986).

Finally there are 'mixed' situations, where a flow has locally limited regions of absolute instability. Those may lead to a self excited global response in a way similar to that of feedback mechanisms.

Temporal development of the perturbation frequency amplitude is found in absolutely and in globally unstable flows. There is a more than superficial similarity between the behaviour of absolutely unstable flow scenarios and flows with (natural) feedback, as observed by Hilberg and Fiedler (1989)—see in Chap. 4: Both situations show the characteristic transient behaviour. However, transient times in true feedback cases are typically shorter and the flow is more easily influenced by external forcing.

Receptivity—*The Door.* The location of maximum receptivity for control in a given free flow, in particular for periodic excitation, is essentially determined by two parameters:

1. The position where the mean velocity profile is most unstable: The mean velocity profile of a separating flow immediately at or downstream of the trailing edge (nozzle) is still very much a wall boundary layer profile. It needs a certain time to develop into the more unstable "free" profile (Michalke 1972, 1990) and
2. where a given (absolute) perturbation provides maximum relative perturbation. This is the case for minimum profile thickness.

It is for these two reasons that maximum receptivity of a separating flow is always near (order of the boundary layer thickness) to the point of separation, i.e. the trailing edge. Figure 9 shows this situation for a mixing layer. This therefore is the place where dynamic, but also static control measures will be most effectively introduced.

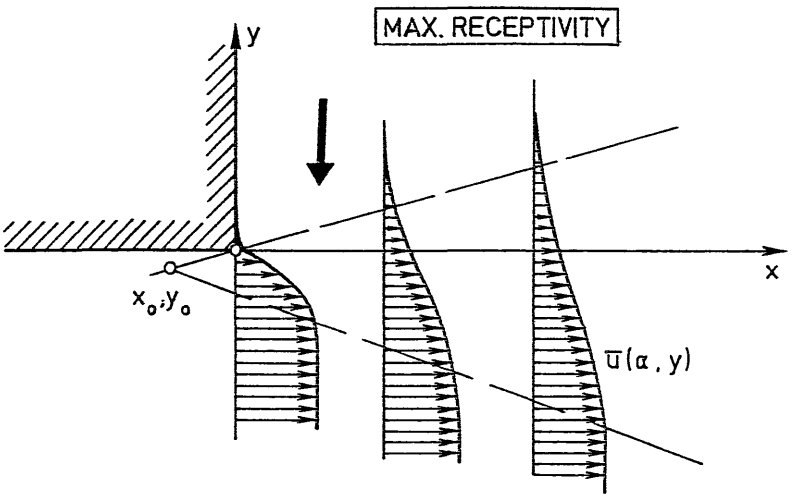

Fig. 9. Locus of maximum receptivity in a mixing layer.

Means of Control—*The Tool.* The major question to be asked at this point is: what and how do we control: Figure 10 outlines some essential paths.

From this picture it is insinuated, that control of substructures might provide a way of controlling the primary structures and thereby the overall flow behaviour. While this may be so in principle so, its practical realization appears to be much more difficult if not impossible. This is illustrated by

an example: The large structures in a plane mixing layer—displaying, when periodically excited, perfectly rolled up two-dimensional vortices—are composed of thin stretched shear layers. One might then think of exciting those wrapped layers with a frequency of, say, an order of magnitude above the basic excitation frequency, thereby enhancing the diffusion and the dissipation of the primary structures. Since, however, these smaller layers are curved and their convection velocity is a function of their position, it is not possible by simple means to impress onto them a constant frequency with constant wave length and phase position, necessary conditions for receptivity. In addition, these rolled up layers are stabilized by their curvature (higher velocity at larger radii of curvature). No specific receptivity of the plane mixing layer is indeed observed when forced at appropriately high frequencies.

Since control of turbulent flow is often synonymus with control of turbulent structures, the question as to its efficiency may best be answered by looking at the major structural constituents and their specific role in the flow—e.g. large scale for noise production and small scale for mixing. Thus the problem reduces to the question of possible minimum- and maximum states (saturation values of thoses structures, their specific stability (receptivity) and their interaction. What can be accomplished then depends on the role of the structure under control in the physical process. Thus mixing, being mainly controlled by small scale turbulence, may be increased by, say, 100 % or more by destruction or deformation of the large coherent structures. At the same time effects of comparable magnitude are observed in noise reduction, which is a direct consequence of the large scales and their amalgamations. Major limitations are by the fact that most control mechanisms affect the flow only in a limited spatial range, which is particularly true for evolving configurations as e.g. the turbulent jet, which develops from a wall boundary layer first into a mixing layer and only asymptotically to its final state.

Distinction is often made between:

- *Active control*, which describes all possibilities of externally activated dynamic control mechanisms.
- *Passive control*, on the other hand, encompasses both *dynamic control* by means which are internally activated (i.e. by the flow itself, as sketched in see Fig. 54), or *static control* by special design or other measures (e.g. fluid additives).

As a general rule we find that most control mechanisms act only on large scale structures (except for additives). Control of small scales (important for mixing) is therefore in most cases only indirectly possible by way of controlling the large scales.

Depending on what method of control is applied and what effects are expected we may select the 'place' of control in the flow at hand (not to be confused with the preceding receptivity discussion) according to Fig. 10.

How then can we introduce or impose the control onto the flow ? For this we have essentially two possibilities:

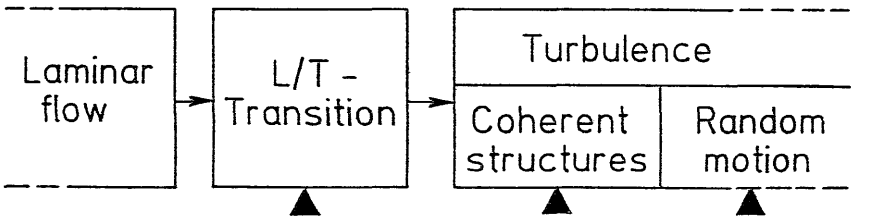

Fig. 10. Places of control 'along' the flow development.

1. by way of boundary conditions, and
2. by conditioning the flow itself, i.e. the medium

Control via boundary conditions is mostly done through the upstream boundary condition (i.e. at the trailing edge)—either dynamically by excitation of the instability mode to amplify the primary coherent structures, or by static means, which mostly do the opposite, namely introducing three-dimensional vorticity to break up the coherent primary structures (see Norum 1982; Soteriou and Ghoniem 1995b).

Major *parameters for dynamic control* are frequencies, amplitudes, modes, and signalforms.

Depending on the *actuator device* used (e.g. flaps (externally/internally activated), variable/flexible trailing edge, periodic local heating, periodic slit blowing, loudspeakers (direct/remote), the actual kind of perturbation is primarily by pressure-gradient- or vorticity fluctuation (Morkovin and Paranjape 1971; Rebel et al. 1992).

Static control is mostly done by winglets—leading to formation of longitudinal vortices and subsequent breakup of CS, by nozzle-/trailing edge shapes to introduce three-dimensionalities and again to break up CS. With the use of tripping devices upstream of the separation point early laminar-turbulent transition is achieved, and finally, there are possibilities for statically controlling the flow by prescribed flow condition through specifically tailored velocity profiles of the basic flow.

Control through side-boundary conditions is rather rare as it implies modification of the flow conduit as a whole. It is, however, encountered in special geometrical configurations as e.g. curvature or changes of the flow cross-section. The ensuing pressure gradients—longitudinal or transverse—may cause stabilization or destabilization of large structures. Those cases are by necessity cases of flow confinement, where the primary flow is no longer a free flow in the ideal sense. When the confinement is stronger, wall effects may come into play and three-dimensionalization may become an important feature.

Control of a flow via flow field and fluid, finally, can be done through the turulence level (intensity and scale) of the basic flow, which may lead to

premature transition of a laminar flow or to a breakup (randomization) of CS when the flow is already turbulent.

Slight distortion or inhomogeneities of the mean flow may have strong effects when influencing the stability characteristics (e.g. the 'control cylinder'—see Chap. 2)

While modification of the turbulence level provides only relatively small effects (which, incidentally, may to some extent be rather considered as flow management), control by tailoring the fluid characteristics may be more effective. A fluid is basically described by its density and its viscosity. Effects from changing those characteristics are well known; they are not control parameters in the proper sense, as they provide direct access to the flow development (see 1.2). Additives, on the other hand, are perfect examples of control agents. They act indirectly, where strong effects are achieved with extremely small amounts of additives. Those additives suppress the small scale structures in a turbulent flow, thereby reducing the dissipation rate of the larger structures, which are thus stabilized. Bulk effects are a reduced spread (which may be a desired feature for water jets) and a considerable reduction of friction in boundary layers. This is known as Toms' effect (Toms 1948). Figure 11 shows as an example the amazing reduction of friction factors for different concentrations of *Habon* (a polymere additive).

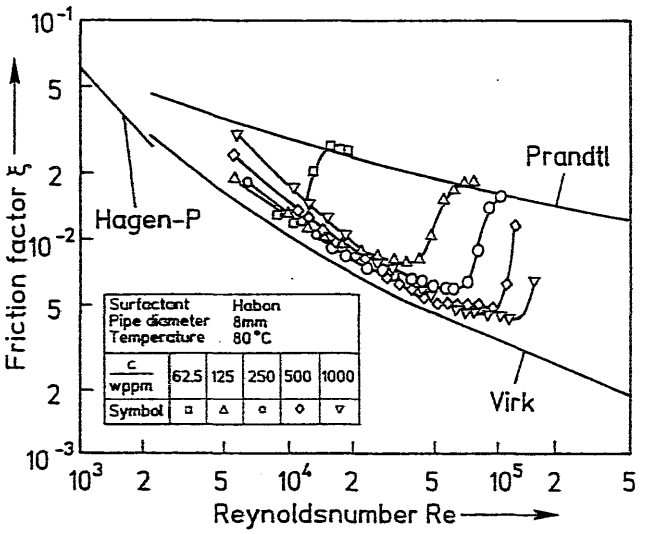

Fig. 11. Effect of concentration of Habon on friction factor in pipe flow.

Combinations. Only very few of the numerous conceiveable combinations of control methods have so far been studied. In most cases increased effects

have been observed albeit not to the amount that a simple (and mostly wrong) concept of superposition might suggest.

1.7 Effects of Compressibility

Compressibility in free shear flows affects the coherent structures in the sense that they are weakened and therefore the effect of control is reduced.

1.8 Goals and Gains—*The Question of Efficiency or is it Worth the Effort?*

There are two different aspects to this question:

1. A certain condition is to be met:
In this case the efficiency aspect is only relevant with regard to the goal to be achieved—not with regard to cost efficiency.
2. A condition is to be improved:
Here the cost aspect is—in most cases—of importance.

Reliability is a limiting condition, as is—in most cases—cost considerations. However: breaking even is not always the important question!

1.9 Summary and Charts

- the major aspects of control in free turbulent shearflows have been identified as *noise, mixing, entrainment*
- the control behaviour of a given flow is determined by its stability characteristics
- control is possible by dynamic or by static means. Dynamic control may be active or passive
- other than in wall flows applications of 'smart' technologies and of 'microactuators' is rather limited
- control of small scales—important for mixing—seems to be possible only via the control of large scales
- control efficiency depends on methods, demands and goals

Three basic control routes are outlined in the following charts (Figs. 12, 13, 14).

In the following Chaps. 2, 3, and 4 we are not primarily concerned with the question as to how or by what special means and/or control circuits a desired flow quality or specification may be achieved, but rather with the more elementary question as to how certain flows react to variations of their basic or boundary conditions. Detailed knowledge of this behaviour then provides the basis on which control circuits—open or closed loop, adaptive or by other, possibly more sophisticated means—may be devised.

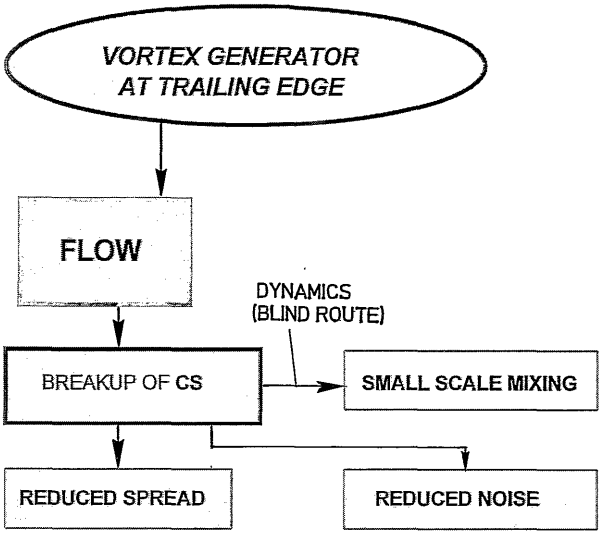

Fig. 12. Control chart for static upstream boundary conditions.

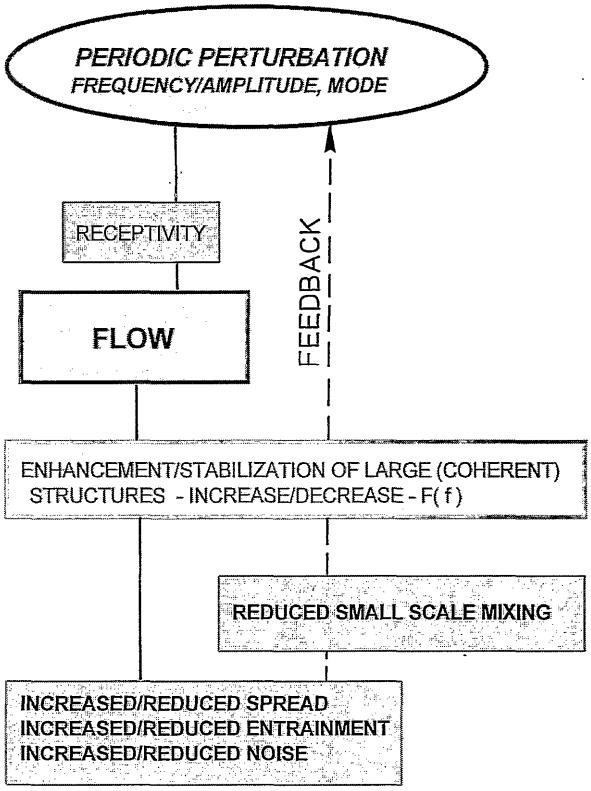

Fig. 13. Control chart for dynamic upstream boundary condition.

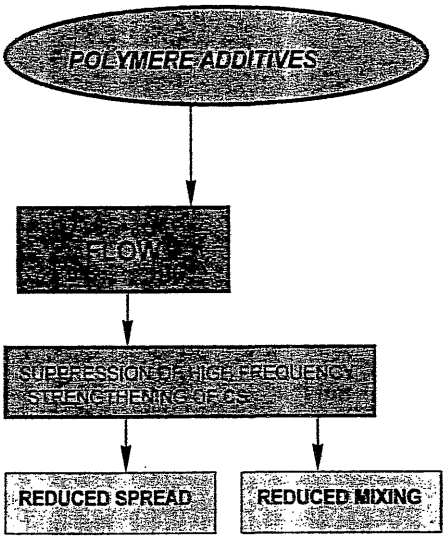

Fig. 14. Control chart for flow condition (polymere additives (Toms' effect).

2 Jets & Wakes

2.1 Introduction—*Definitions, Configurations, Concepts*

To understand the basics of jet and wake flow we shall first look at some visualizations. Figure 15a/b shows a few which have been taken from the 'album' by Van Dyke (1982).

From our general understanding— supported by those visualizations—we define a jet as a limited flow region of a given momentum flux of a given fluid and a given geometry emitting into an extended ambient fluid of another specific momentum flux, i.e. it constitutes a local momentum source. Its boundaries are unlimited and its velocity field is decaying. A wake follows the same definition where, however, the momentum flux introduced is negative, constituting a momentum sink. Figure 16 outlines this relationship between the two configurations in a generic series of a jet in a parallel ambient stream where the variation of the momentum flux ratio leads directly to the wake. Both flows are momentum conserving. A marked difference is in the ratio between convection and diffusion: The jet in still surrounding—the extreme and most often investigated jet configuration—is characterized by a constant ratio between convection and diffusion. All other cases—and in particular the wake flow— are increasingly dominated by convection, which in the case of a wake increases with increasing x asymptotically to the level of the undisturbed basic flow—while the diffusion goes asymptotically to zero. As a consequence jets and wakes in an ambient flow of constant velocity have a decreasing rate of spread with downstream distance while only the jet in

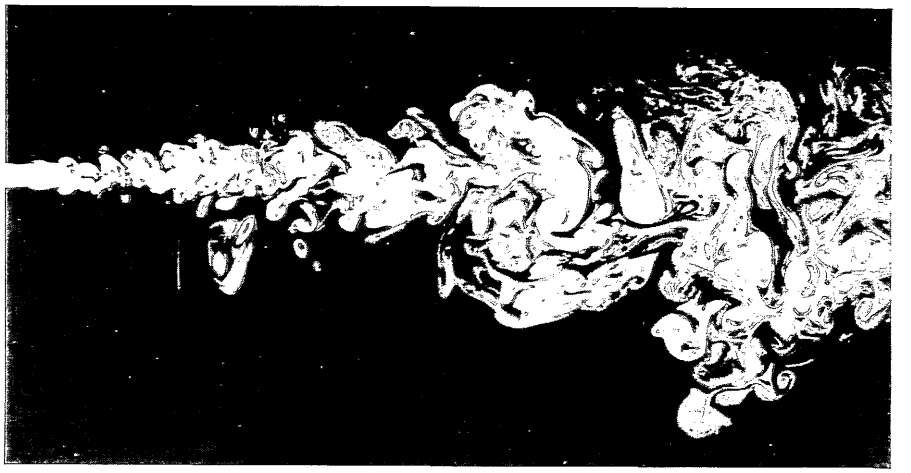

ROUND TURBULENT JET

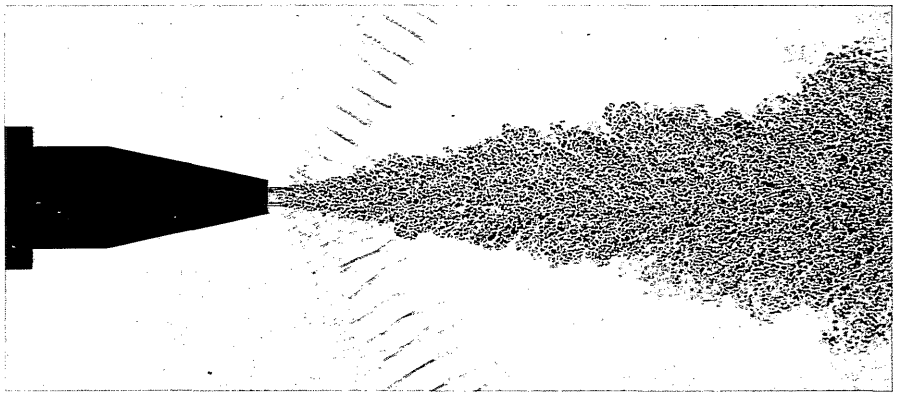

SUPERSONIC JET

Fig. 15. a) Jets—some visualizations.

still surrounding spreads linearly.

In order to reduce and standardize the infinite variety of jet and wake configurations we distinguish between a limited number of specific cases, viz.

- the submerged jet in still surrounding
- jets in moving streams
- jet-wake combinations
- wakes

Another distinction is by geometry, where we have

- plane geometries (*showing the largest effect of control*),
- axisymmetric, and

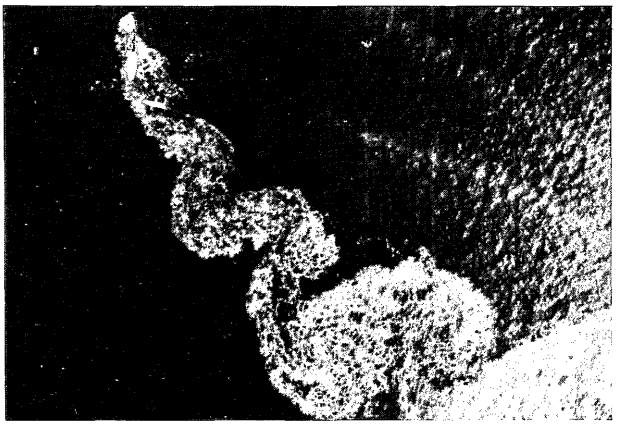

WAKE BEHIND A GROUNDED TANKSHIP

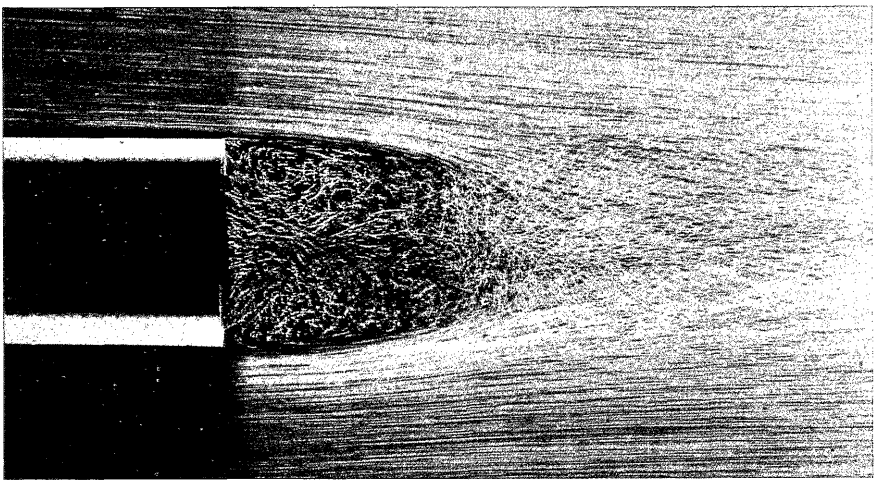

WAKE BEHIND AXISYMMETRIC BODY

Fig. 15. b) Wakes—some visualizations.

- three-dimensional geometries—which in themselves are again of unlimited variations and have therefore not been investigated extensively so far. Finally there are
- radial forms of which, to the knowledge of this author, only the jet has received some attention.

Next we shall consider the two configurations—jets and wakes—in more detail.

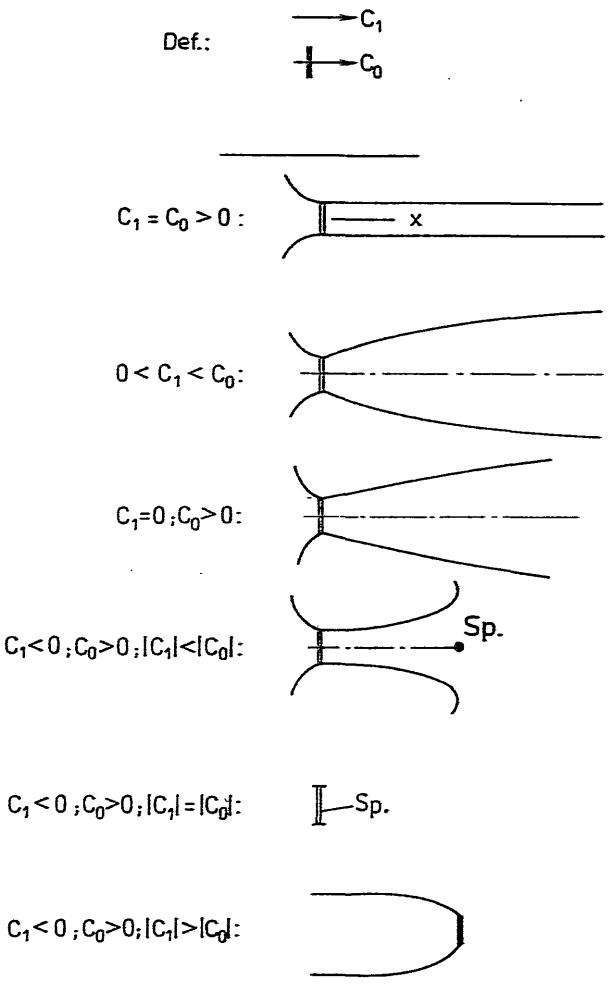

Fig. 16. Classification of jet- and wake flows (SP = Stagnation point).

2.2 Jets

Jet flow has often been studied as a ready object of control by external stimulation or manipulation (Rajaratnam 1976; Kibens 1989; Hussain and Husain 1988). Like the wake, it is a flow of evolving characteristics where the boundary layer of the nozzle wall develops first into a mixing layer and after the eventual merging of the mixing layer(s) the true jet flow develops into its final state (Fig. 17). It is only then that for certain configurations (ambient flow at rest or with 'tailored' pressure gradient) self similarity develops. This is the case after, say, 70 nozzle diameters in the axisymmetric case and around 120 for the plane jet in still surrounding. As a consequence we find the flow to be dominated by different structures or structural modes, depending on

the axial position we are looking at. Susceptibility for control depends also on the ratio of jet velocity to ambient velocity, and the self-similar jet in still surrounding provides the most convenient special case of highest instability and of highest interest for basic research. Traditional distinction in jet flow is made according to geometrical characteristics. Basic configurations are (in rising degree of complexity): plane-, radial-, axisymmetric-, co-axial-, three-dimensional- and confined jets, some of which are sketched in Fig. 18.

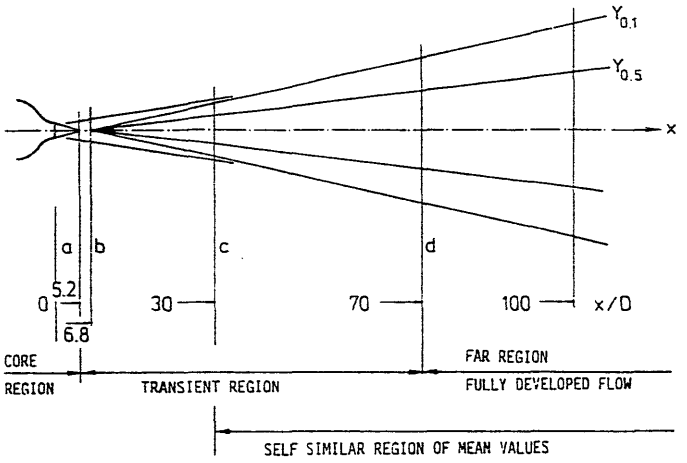

Fig. 17. Jet regions.

Jets can be easily controlled over a limited downstream range by various methods, e.g. by dynamic control, as by periodic forcing at one or more frequencies of the flow near the nozzle exit—with its characteristic manifestations of 'flapping', 'blooming' and 'pulsating'; and by static control, which is essentially imposed onto the flow by the nozzle geomety. Another possibility of exerting some influence on the flow behaviour is provided by the turbulence level of the primary stream. There are yet other possibilities of controlling the jet via its entrainment flow e.g. by a different density of the entrained medium. Jet development may be also influenced by a 'tailored' external flow (e.g. a jet in a diffusor flow). Finally there is the control mechanism of additives, particularly in the primary stream.

Many of these aspects have been investigated and a host of information may be found in the literature. Essential for understanding of the phenomena observed are the basic stability characteristics which lead to the dominant structures – vortex rings, line vortices, single- and multi-helices etc.—see e.g. Fiedler (1988a). A great number of investigations reported in the recent, say, two decades, have provided us with a relatively detailed picture of the coherent structures in the near-jet and in particular the characteristic phenomenon of the preferred mode (e.g. Crow and Champagne 1977; Arm-

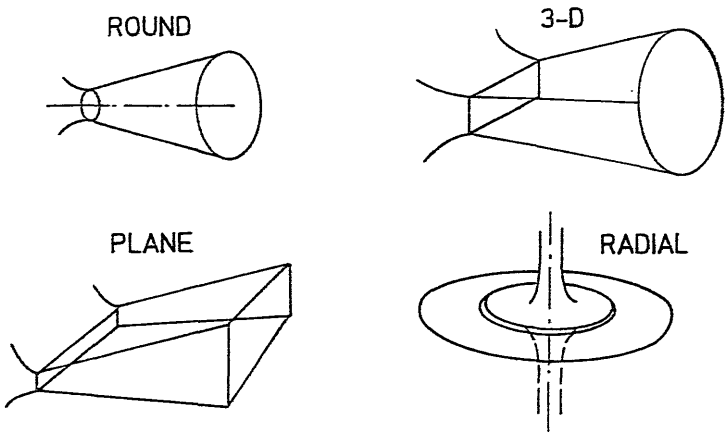

Fig. 18. Some basic jet geometries.

strong et al. 1977; Armstrong 1981; Peterson 1978; Eickhoff 1982; Peterson and Samet 1988; Gutmark and Ho 1983a; Gutmark and Ho 1983b). Owing to a higher degree of complexity and weaker structures, the picture is considerably less clear and detailed for the the far- field of turbulent jets, as we find from the few investigations known so far (e.g. Tso 1983; Tso et al. 1980; Tso and Hussain 1989; Kumori and Ueda 1985; Dimotakis et al. 1982; Nieberle 1986).

Most studies were concerned with axisymmetric jets. Less is known about the plane- and little about the coaxial jet (Bremhorst and Watson 1981; Szajner and Turner 1987). No structural investigation seems to have been devoted to the radial jet since Heskestad's (1966) work. There is, on the other hand, increasing interest in three dimensional configurations; some of their characteristic structures and global manifestations will be discussed below in some depth.

The primary stability behaviour of jets, as summarized by Michalke (1984), has been studied by a number of authors, e.g. Lessen and Paillet (1976), Morris (1976), Plaschko (1981), Bejan (1981), Michalke and Hermann (1982) and Morris (1983). A homogeneous jet is a purely convectively unstable flow. Exceptions, where absolute instability is observed, may turn up in the presence of density inhomogeneities, when the jet has lower density than the ambient fluid—see Monkewitz et al. (1990), Raghu et al. (1990).

The technical significance of turbulent jets is obvious: they are found in jet engines, in burners and mixers, in all kinds of exhaust applications,

for material cutting and erosion (manufacturing), in the wide field of air conditioning, and in fire extinction.

There are many applications of jet control, the most obvious ones are in combustion, fluidics, noise control, thrust control, mixing and entrainment enhancement (ejectors) and for continuous lasers. Some of those were discussed by Peters and Williams (1981), Crighton (1981), Bechert and Pfitzenmeier (1976), Kibens (1980), Laufer and Ta-Chun (1983), Michalke (1978), Roffman and Toda (1969), Norum (1982), Guicking (1988) and Gutmark et al. (1986). Some specific investigations and their major outcome are summarized below, where distinction is made according to the control method employed.

Goals. When thinking of the most important and basic applications of jet control fife specific goals come immediately to mind:

1. control of laminar-turbulent transition,
2. control of mixing and/or combustion,
3. control of noise production,
4. control of entrainment—which may be a question of mixing or—when not symmetric—of jet-deflection, is also known as 'vectoring'.
5. and control applications in fluidics.

L-T-Transition control is concerned with the state of the flow immediately at or near the nozzle exit. In most technical applications the boundary layer in the nozzle will be have become turbulent at the trailing edge so that this control aspect is rather limited. Premature transition of a laminar boundary layer is usually achieved by tripping devices (trip wire or the like in the nozzle near the exit plane). The importance of the condition of the separating bondary layer is in the subsequent evolution of the turbulent mixing layer and in particular its mixing potential.

Mixing is one of the most important aspects of jet flow control. It is central for combustion as well as in chemical engineering and wherever diffusive processes play a dominat role. Mixing is related to the size of the contact surface between the species to be mixed. Good mixing is achieved when this contact surface is maximized, which is the case at small turbulent scales. Control of mixing therefore has to aim at controlling the small scale structure of turbulence, which is typically possible only by indirect means via a forced breakup of the controllable large scales.

So far we have no generally accepted criterion for the quantification of turbulent mixing on the basis of flow- or turbulence characteristics and some criteria used are questionable. As an example, the often used spread rate of the mean flow is not always a useful criterion for turbulent mixing: In periodically excited flows strong spread is observed in regions of formation of large vortices, which are relatively stable and therefore rather suppress the small scale mixing process.

Noise production is understood to be the consequence of non-linear interactions of large-scale (coherent) structures. Those structures experience their strongest manifestations in the core region, where consequently also the strongest source of noise is found. Noise is thus a large scale effect and can be controlled (reduced) directly by tailored upstream boundary conditions designed for premature breakup of those structures.

Entrainment: Because of its entrainment a turbulent jet acts as a sink for the ambient fluid. Entrainment is a strong effect which is obvious from the numbers given in Fig. 19: The volume flux of a round jet doubles already at approximately every 8.5 nozzle diameters owing to the entrained fluid.

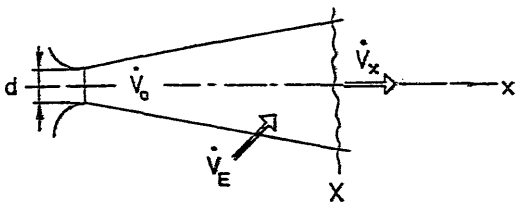

n	x/d (round)	x/d (plane)
2	8.6	19.8
3	12.8	44.5
4	17.0	79.0
5	21.3	124.0

$$\overline{\dot{V}}_E = \frac{d(\dot{V}_x/\dot{V}_0)}{d(x/d)} = 0.235 \quad \text{(round jet)}$$

$$= \frac{0.225}{\sqrt{x/d}} \quad \text{(plane jet)}$$

Fig. 19. Entrainment characteristics for round and plane jet. n = multiple of volume flux $\dot{V}_0$

A flow visualization showing the entrainment is shown in Fig. 20 (taken from Van Dyke 1982).

The mechanism of entrainment is based on the convolutions of the free boundaries of the turbulent flow, which are caused by the large scales of the turbulence. Entrainment is therefore directly amenable to control. How can those qualities be influenced in the best possible way? Since the question of control is always related to the characteristic flow structures and their stability, we shall now discuss some of these characteristics.

Stability and Structures. Figure 21 shows the neutral stability curves for jet and mixing layer (core region of the jet) flow as given by Joseph (1976). Obviously, the critical Reynolds numbers are at very low values, which shows that technologically interesting jets will be typically turbulent from the nozzle on.

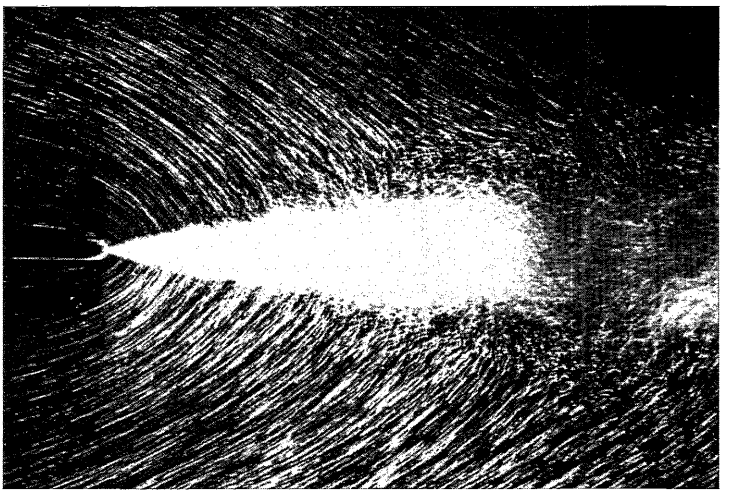

Fig. 20. Visualization of entrainment flow of a round jet.

The diagram in Fig. 22, which was given by Michalke (1972), demonstrates the influence of the Reynolds number on the stability of the 1th (helical) instability mode in the axisymmetric far jet. Again, for most cases of practical or technological interest only the dashed line giving the distribution for $Re = \infty$ is of relevance. There the Strouhal number for maximum instability based on the jet momentum thickness Θ is $S_\Theta = 0.11$. For a jet in still surrounding this leads to a Strouhal number based on the downstream coordinate of $S_x = 0.5$. The stability for different modes depending on the mean velocity profile shape as expressed by the ratio Θ/R (where Θ denotes again the momentum thickness of the velocity profile and R its half velocity radius) is given in Fig. 23. We find that the near jet is unstable for both, the 0th (symmetric) and the 1st mode, while the far jet is only unstable for the 1st mode.

According to the specific instability behaviour as discussed above we expect the characteristic structures of the jet to form as their manifestations, which can be excited, i.e. dynamically controlled according to their specific critical Strouhal numbers.

In the following ways and possibilities as well as some mechanisms and results of controlling a jet are discussed.

Static Control by Boundary Conditions. The region which can be controlled by static upstream boundary conditions is relatively limited, extending approximately over the core region, i.e. the first few diameters downstream of the nozzle.

Control is by different nozzle shapes, some of which are shown in Fig. 24. This kind of control always aims at disrupting or destroying or even sup-

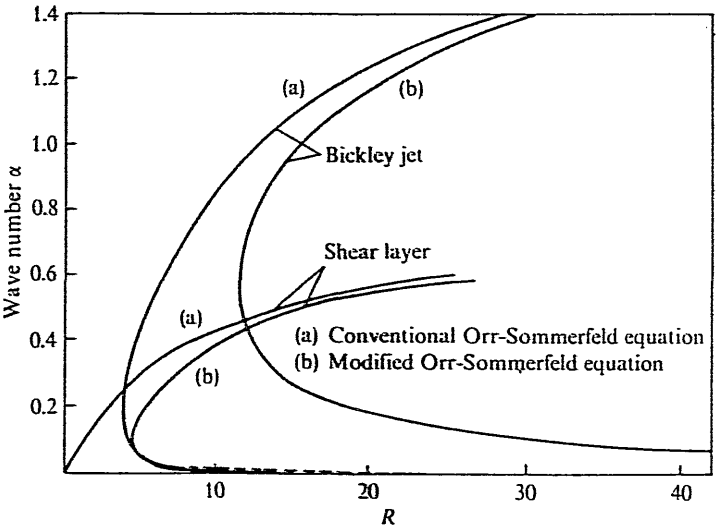

Fig. 21. Neutral stability curves for jet and mixing layer flows (Joseph 1976).

pressing the formation of the large coherent structures by introducing three-dimensionalities directly (by vortex generators) or indirectly by non-circular or non-symmetrical nozzle shapes: The primary structures which are forming past a non circular nozzle are unstable and are quickly distorted and disrupted due to self induction as is sketched in Fig. 24.

Control measures of this nature are often used to force premature transition, to increase global or local entrainment, enhance global or local mixing, and to reduce noise production. A very convincing example of how drastically the entrainment of a jet can be influenced by a relatively minor geometrical modification is shown in Fig. 25, which compares the entrainment characteristics of a jet from an elliptic nozzle to those of a round and a plane jet (see Husain and Hussain 1983; Gutmark and Ho 1983a).

Other static boundary conditions of some influence on the flow development are the velocity profile in the nozzle exit. This is, however, of relatively small effect, influencing to some extent the formation and strength of the primary structures in the near-nozzle regime (weaker structures for a pipe flow profile) and shifting the virtual origin. Stronger effects are observed with certain confinements. Thus, a plane jet spreading in y direction between two parallel walls of distance $\Delta Z \leq$ width of jet is known to develop a strong maeandering pattern (Giger 1987).

Another way to control turbulence in a liquid jet is by introducing additives (long chain polymeric molecules—e.g. 'Sapran', 'Polyox') into either the jet flow, the entrained fluid or in both. A major effect of this is the damping of small scales, which in turn provides a stabilization of large scales and con-

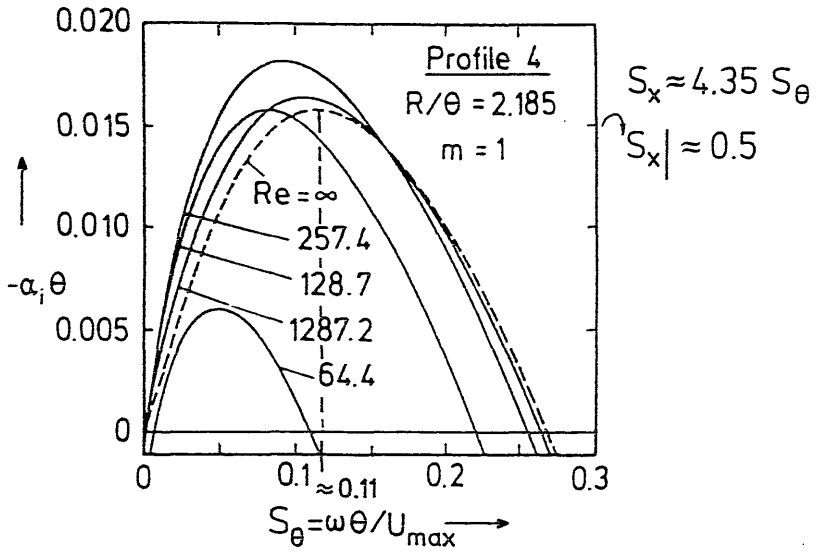

Fig. 22. Influence of Reynolds number for the stability of the axisymmetric far jet.

sequently reduces the spread. This effect is strongest when the additives are only in the jet fluid and smallest when it is only in the entrained fluid (Gyr 1997).

Density inhomogeneities, i.e. different densities (temperatures) of jet- and entrainment fluid when below a certain critical level is of little influence, since because of the strong entrainment the density differences are quickly decaying and equalized. The overall effect may be taken care of by a shifted virtual origin.

There is, however, a strong dynamic effect when $\rho_{\text{jet}}/\rho_{\text{ambient}} \leq 0.72$: Self sustained periodicity of stable frequency of Strouhal number $S = 0.44$–0.47 and high stability against external perturbation sets in as the flow is becoming absolute unstable. This effect is accompanied by formation of strong sidejets and a stepwise spread of the the visual jet diameter (scalar) however insignificant changes in velocity distribution and entrainment (Fig. 26).

Absolute instability in a jet achieved by upstream control was demonstrated by Strykowski and Niccum (1991), who applied suction in a circumferential slit around the jet nozzle, thereby creating a shear layer profile immediately downstream of the nozzle which fulfills the condition for absolute instability for a mixing layer (Fig. 27).

Dynamic Control via Boundary Conditions may be stochastic or periodic:

Stochastic control is scarcely used as direct tool to influence a given flow in a desired direction, since it is neither overly effective nor specific. It is

small $\Theta/R \rightarrow$ many modes, 0th & 1st mode dominating $\rightarrow$ **NEAR JET:**

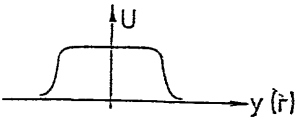

large $\Theta/R \rightarrow$ few modes, 1st mode dominating..., stable against 0th mode $\rightarrow$ **FAR JET:**

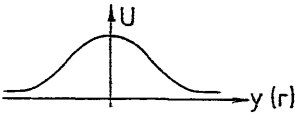

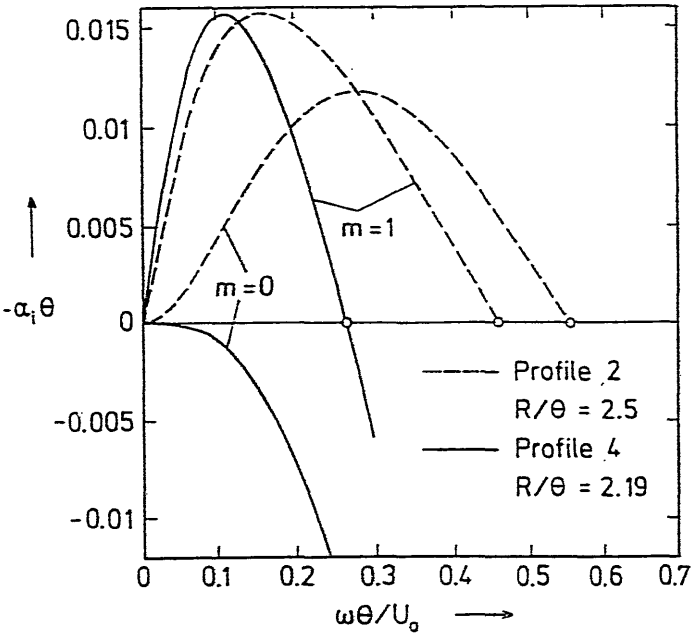

Fig. 23. Spatial growth rates of 0th and 1st mode for two velocity profiles (Michalke 1984).

more often an unwanted condition where one would only like to know its consequences. Its means are preferably a high turbulence level in either the entrained- or the primary jet fluid. The comparatively weak effect depends on the turbulence level as well as on its scale. It is most effective when the level is high and the scale is of the same order of magnitude as the structural scale of the turbulence to be controlled. Stochastic control of this kind may be purposefully used to increase entrainment or to accelerate laminar-turbulent transition. Its global effect in jet flow is a—mostly insignificant—increase of spread, which in essence amounts to an upstream shift of the virtual origin.

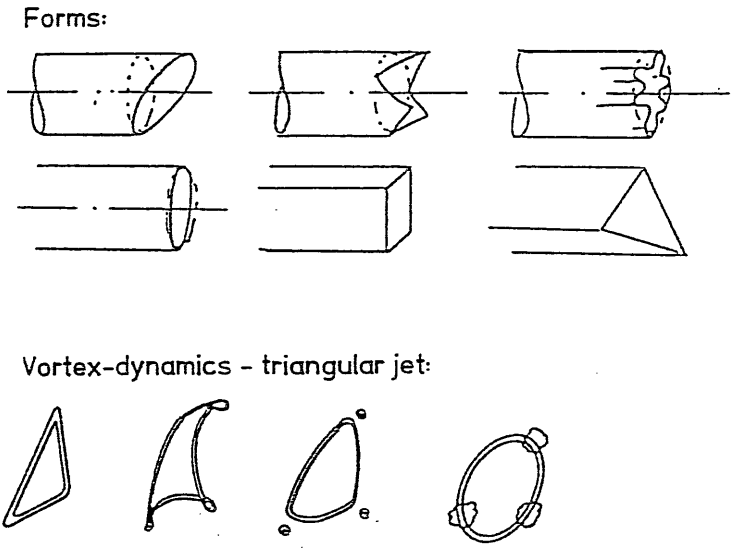

Fig. 24. Non-symmetric nozzle forms, and vortex dynamics of primary structure past triangular nozzle.

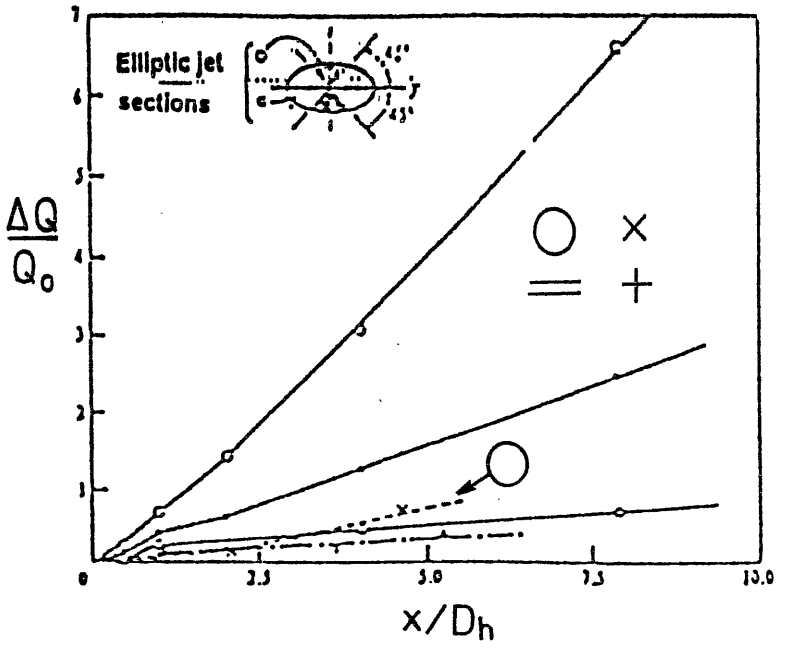

Fig. 25. Entrainment characteristics of elliptic jet (from Ho and Gutmark 1987).

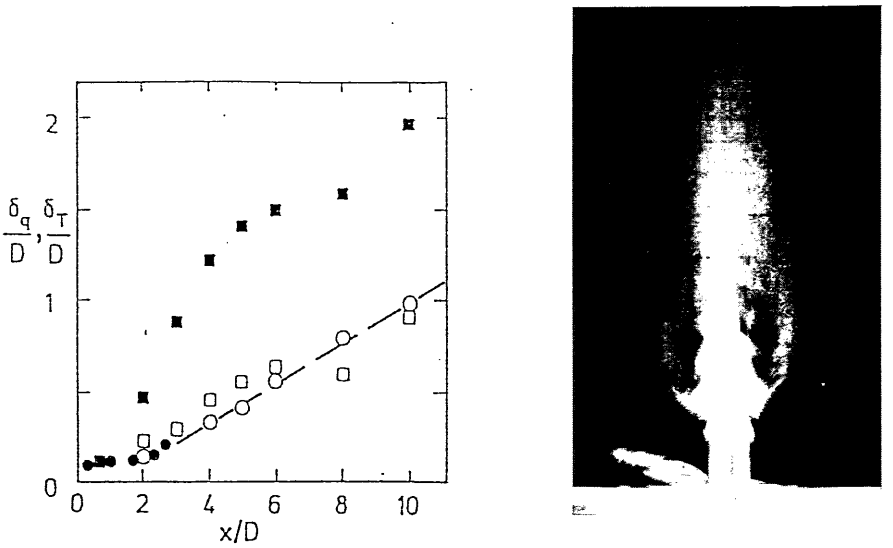

Fig. 26. Characteristics of the absolutely unstable jet (after Monkewitz et al. 1990.)

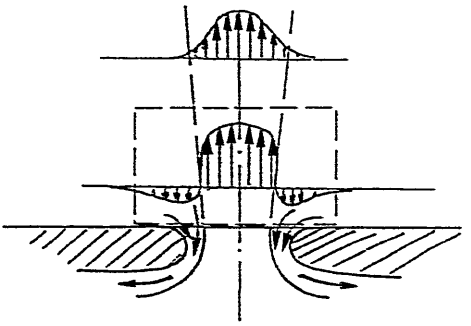

Fig. 27. Jet with circumferential suction at nozzle circumference (Strykowski and Niccum 1991).

The more effective and most often used way of dynamically controlling a turbulent jet is by

periodic excitation of the dominating instability modes. Excitation at a specific frequency $f_E$initiates the growth of the instability wave and causes the formation of concentrated vorticity—structures of a high degree of organization/ coherence—in a certain flow region. It is accompanied by a step-wise growth of the jet width, strong local entrainment and considerable increase of the Reynolds-stresses, in particular the shear stress. Some examples are shown in Figs. 28 and 29. Typical amplification factors are—depending on the excitation amplitude—of the order $\leq 10^2$. The region of strongest man-

ifestation of the periodicity is around the downstream position where the characteristic frequency $f_c(x)$ of the unexcited flow corresponds to the frequency f_E of excitation. Thus, the lower the excitation frequency is, the further downstream its controlling effect is found.

The following listing gives a general framework for the important frequencies or Strouhal numbers (d = nozzle diameter, U_o = exit velocity):

Control of the core region ($x/d \leq 6$):

- preferred mode: $0.2 \leq f_E d/U_0 \leq 0.6$
- shear layer mode: $0.8 \leq S_{x,max} = f_E x/U_0 \leq 1.5$
  (depending on forcing amplitude—see Fig. 28)

Control of the far region

- plane jet: $S_{x,max} = f_E x/U_{max}(x) \approx 1.0$
  (asymmetric mode) (Fig. 29)
- axisymmetric jet: $S_{x,max} = f_E x/U_{max}(x) \approx 0.5$
  (1st helical mode)

Attenuation of turbulence was observed at higher frequencies (Zaman and Hussain 1981).

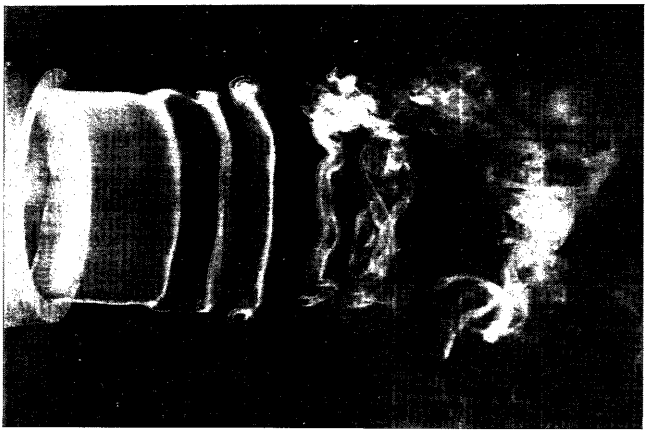

Fig. 28. Round jet with 0th mode excitation—shear layer mode (Michalke and Wehrmann 1964).

Amplitudes of forcing perturbation are typically low of the order $\leq 1\,\%$ of U_0, going up to $100\,\%$ ('pulsing jet' see Bremhors and Watson 1981). Wherever the flow is unstable to more than one mode, as in the core region, it may be controlled by combinations of different modes, whereby a variety

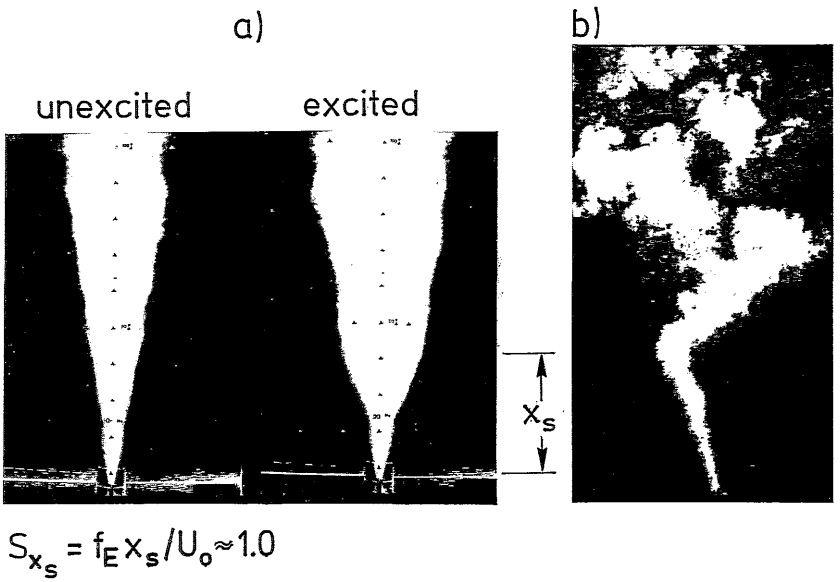

Fig. 29. Plane jets with 1st mode excitation. (a) Averaged spread (from Korschelt 1980 and (b) trajectory of deflected jet (from Hilberg 1996).

of effects are achieved. This was demonstrated by Paschereit et al. (1992), who applied mixed frequency- and mode forcing on a round air jet. Figure 30 shows schlieren pictures and a contour plot of cross-sections in the core region of the jet with different forcing conditions (see also Boree et al. 1996; Osthues 1986).

Combinations of specific forcing frequencies with their subharmonic may be particularly effective. Depending on the phase relationship between the two frequencies and provided that their phase velocity is equal over a sufficient distance, an energy transfer between the two waves may occur which amounts to an overall effect that exceed the sum of the individual effects if only single frequency forcing were applied (see Paschereit et al. 1995; Husain and Hussain 1995). This effect is often called 'subharmonic resonance'.

Many of other specific effects can be achieved by forcing with single frequencies or frequency combinations, as e.g. the so called 'blooming' or 'bi-/ tri-/ n-furcation' by double mode excitation as was reported by Lee and Reynolds (1985) (see Fig. 31) or the deflection of a jet ('vectoring') by forcing only part of the jet's circumference and thereby causing an asymmetrical distribution of the entrainment strength.

We summarize the effects achieved by periodic forcing as follows:

- **Periodic forcing leads to excitation of the inherent instabilities and to formation and stabilization of coherent structures.**

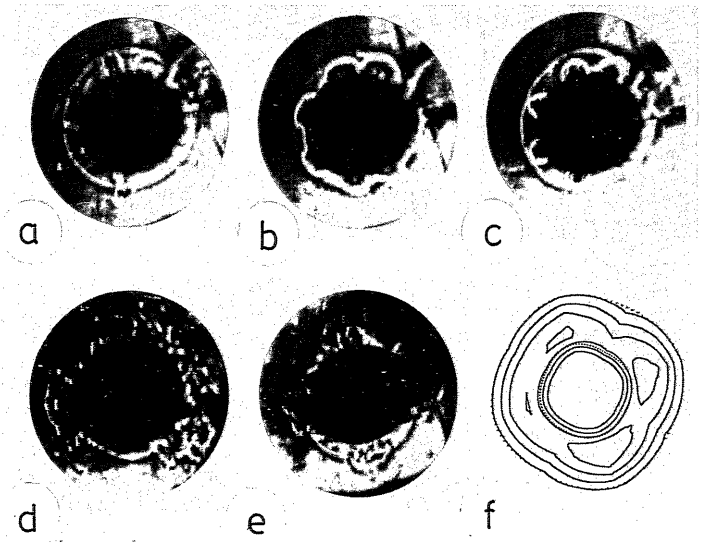

Fig. 30. Deformation of jet-cross-section by mixed frequency and mode forcing (small amplitude). a: no forcing, b: forcing at fundamental (m = 0), c: forcing at fundamental and subharmonic (m = 0), d: forcing at mode m = -1 and m = 2, e: forcing at mode m = 2 and m = -2, f: contours of u'^2 at forcing with modes m = -2/2—after Paschereit et al. (1992)

Major consequences are:

- **non-linear—locally increased—spread**
- **influence on mixing (typically reducing) and entrainment (increasing)**

Special effects achieved:

- **change of cross-section and amplification of small scales by mode combinations, blooming, folding (increased mixing)**
- **enhanced effect of forcing by subharmonic resonance**
- **deflection (vectoring) by non-symmetrical forcing**

At high Mach numbers reduced effects of control by periodic forcing are achieved.

Most applications of dynamic jet control is by open loop. Applications where closed loop control has been successful are particularly in combustion (see e.g. Gutmark et al. 1995; Parekh et al. 1996). Investigations of the possibility of flame stabilization by strong periodic forcing by Hilberg (1996) have shown that a jet-flame can be established at high velocity with a concentrated flame region by a folding mechanism as shown in Fig. 29b.

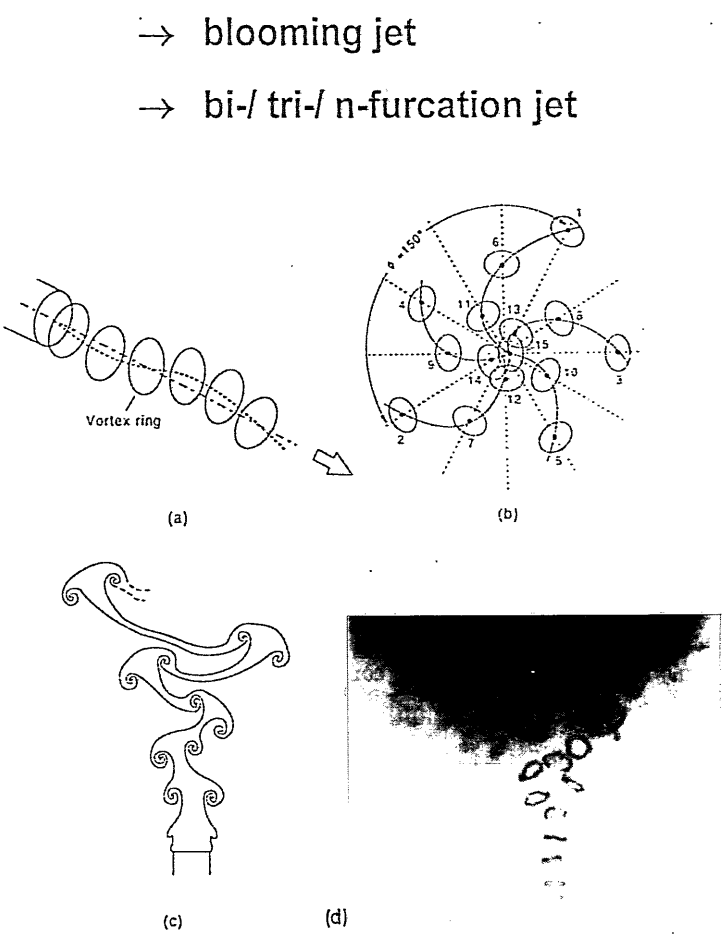

Fig. 31. Examples of specific forcing applications—double mode excitation (Lee and Reynolds 1985).

2.3 Wakes

Wakes in a constant velocity are only asymptotically self-preserving. They do not seem to reach a universal equilibrium state, developing instead in a way which depends on characteristics of the wake producing body: e.g. its shape and solidity, as was shown by Wygnanski et al. (1986). Wake flow is characterized by periodicity (Berger and Wille 1972), where typical (coherent) structures are similar to those in the jet, albeit stronger, and better organized with a multitude of modal developments in the axisymmetric case. In the two-dimensional case the two dominating modes—the sinusoidal and the varicose—are of comparable strength and probability, showing a tendency towards early development of three-dimensionalities.

Configurations. As in the jet we distinguish by basic geometry between plane-, axisymmetric- and three-dimensional wakes. Based on the different flow characteristics distinction is also made between the near wake, which is dominated by flow reversal and absolute instability behaviour (see Berger and Scholz 1990; Scholz 1985), and the far wake, which is convectively unstable (Fig. 32).

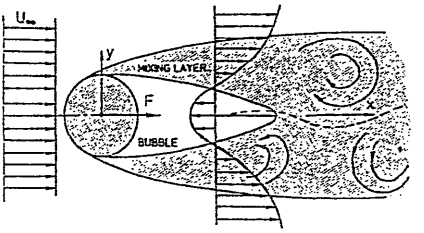

NEAR WAKE

$$c_D = \frac{F_D}{\left(\frac{\rho}{2} U_\infty\right) A}; \qquad S \approx 0.21 c_D^{3/4} \quad \text{(cylinder)}$$

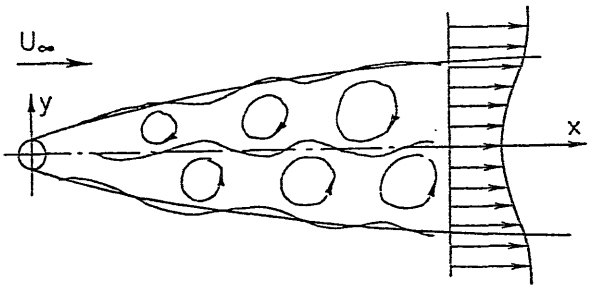

FAR WAKE

PLANE: symmetric / varicose mode

ROUND: multiple modes

Fig. 32. Wakes: configurations, definitions, regions.

Goals. There are three major goals for which control of wake flow is of interest. This is

- Reduction of drag (reducing with increasing Re)—an energy problem,
- suppression of vortex shedding—a mechanical and sometimes an acoustical problem, and
- increase or reduction of heat transfer—again an energy problem.

Other than for jets, wake flows are also of technological importance at low or medium Reynolds numbers. Let us therefore look at some characteristics of wake flow behaviour for different Reynolds number ranges:

Reynolds-Number Effects

$20 < Re < 100$:	increase of critical Re-number (46) up to 90 is possible
$100 < Re < 500$:	limited Suppression of vortex shedding is possible. Control is preferably by periodicity
$500 < Re < 200000$:	Synchronization of vortex shedding by periodic excitation is possible. There is a limited possibility of suppression of vortex shedding by periodic excitation with large amplitudes. Excitation of separated shear layers in the near wake with high frequenc forcing may be useful. **Stationary methods to influence the near-wake stability, (base bleeding, control wire) is superior to dynamic methods**

Stability Characteristics of the Near Wake. They depend on the geometry of the wake producing body. As an example let us consider only the near wake behind a circular disc, which—according to Berger et al. (1990) is dominated by three instability modes (Fig. 33):

- The High Frequency 'shear layer mode', characterized by $S_{SL} = f_{SL}D/U \approx 0.5$
- The Low Frequency 'pumping mode': $S_p \approx 0.05$
- The helical mode: $S_h \approx 0.135$

Static Control. There are three principal methods of statically- or passively controlling the near wake flow:

The first method is designed such as to suppress the initial vortex shedding by attenuation or suppression of the 'feedback information' between both sides of the cylinder. This is quite successfully achieved by a splitter plate (Roshko 1954) or by steady blowing ('base bleeding') or suction at the base of the body. Figure 34 shows the blowing and suction rates needed to suppress the vortex shedding behind a plate according to Schumm (1991).

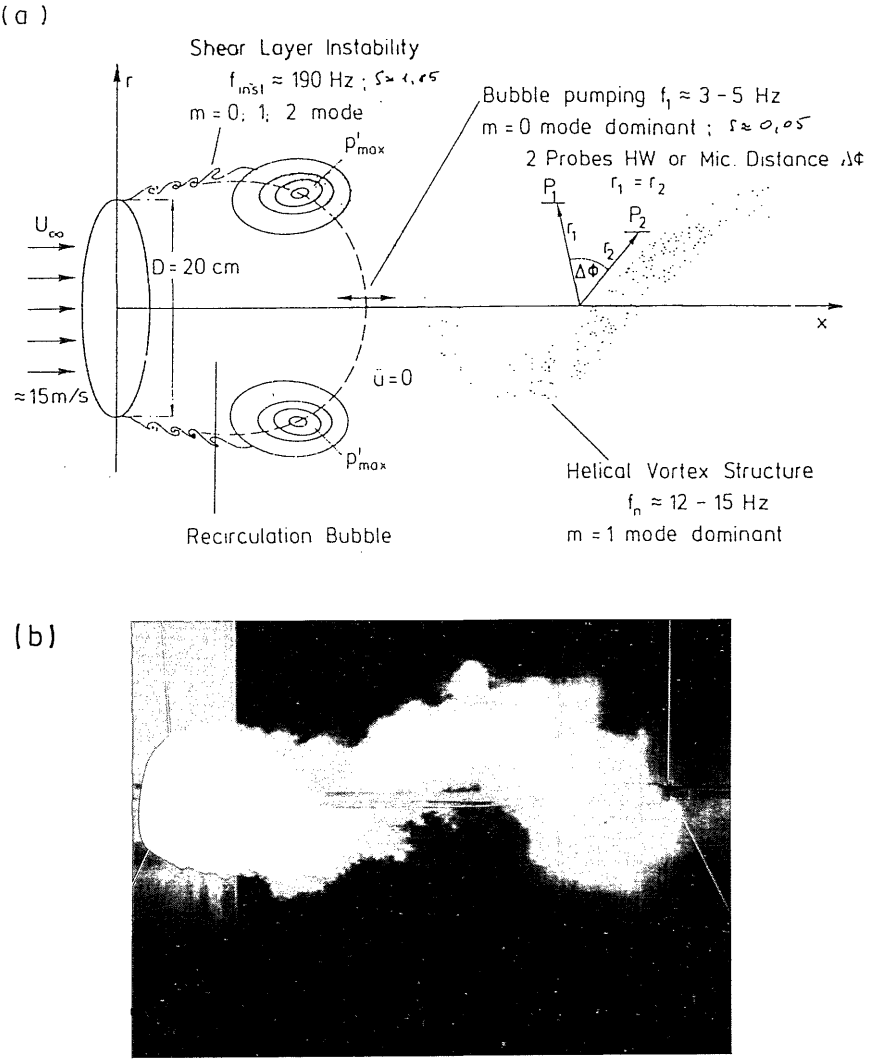

Fig. 33. Near wake of a circular disk—(a) Three regions/modes of instability; (b) Visualisation of wake with $m = 1$ excitation.

By the second kind the flow field is slightly modified such that the conditions for absolute instability are violated and the flow becomes only convectively unstable. This group encompasses control of the density field by heating of the body (in gas flows) or cooling it (in liquid) and the control wire as discussed by Strykowski and Sreenivasan (1990).

While the above methods are rather limited to low and medium Reynolds numbers, effective suppression of vortex sheedding at high—technologically relevant—Reynolds numbers (e.g. masts, chimneys, offshore structures) is

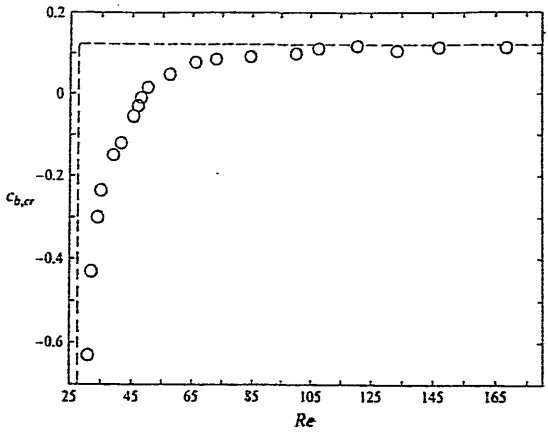

Fig. 34. Control of vortex shedding from cylinder by base bleeding or suction (after Schumm 1991). Critical flow rates, where $c_b = (U_b/U_\infty) \cdot (h/D)$. U_b = control velocity, U_∞ = free-stream velocity, h = slit hight, D = cylinder (wakes) diameter.

achieved by specific surface roughnesses, where the so called 'Scruton Spiral' (Scruton 1981) is particularly well known and found on many industrial chimneys and exhausts. This spiral introduces three-dimensional vorticity which causes a distortion of the shed vortices (ondulation along their axes) and subsequent disruption (see Fig. 35).

Dynamic Control. The near wake being an absolutely unstable flow cannot be controlled by external periodicity.

Stability Characteristics of the Far Wake. The far wake is convectively unstable. It can therefore, as was only recently shown by Wygnanski et al. (1986), be dynamically controlled to the same degree as the mixing layer, where again the characteristic three regions (I, II, III) as described by Fiedler et al. (1981) are found. An obvious practical aspect to this is the inherent possibility of changing the signature of wake- producing (aquatic) vehicles.

Static Control. In a practical sense this is only possible by additives.

Dynamic Control. Stochastic perturbations of the far wake by turbulence in the basic stream causes increase of the spread, as was shown by Symes and Fink (1978)— Fig. 36.

Control of the far wake by *periodic perturbations* is possible as in a jet. Since, however, the spread rate of the wake is considerably smaller than that of a jet, the frequency variation in downstream direction is also small and

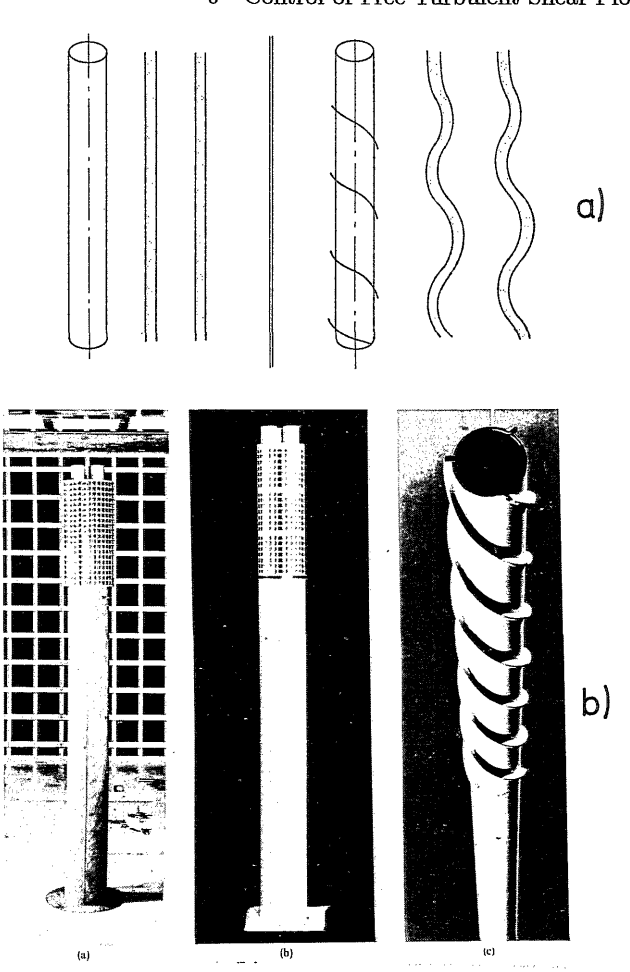

Fig. 35. Control by surface structures (Scruton 1981). (a) Structure deformation, (b) practical realizations.

the downstream extent of the range controlled, therefore considerably larger than in a jet. Possible means of controlling the far wake are by

- longitudinal fluctuations in the basic flow
- transverse fluctuation in the basic flow
- transverse vibration of the wake production body
- periodic rotation of the wake production body
- periodic blowing/suction through slots in the body's surface.

Special Methods and Effects. Experiments with closed loop control of a cylinder wake at $Re \approx 4\ 10^4$ by periodic blowing through slots in the cylinder surface reveal the following (Fig. 37):

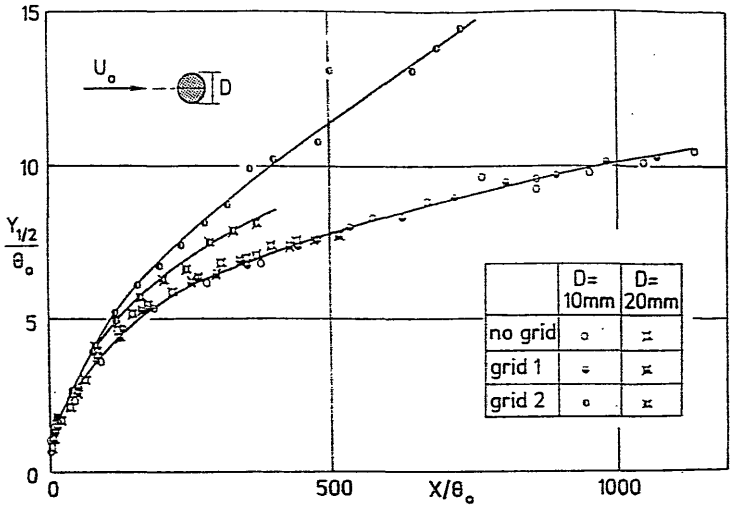

Specifics of external turbulence:

$\sqrt{\overline{u'^2}}\Big|_{external} / U_o = A(x/M)^{-B}$; $\Lambda/M = C(x/M)^D$

Grid	M(cm)	A	B	C	D
1	1.53	0.158	0.613	0.100	0.358
2	10.00	0.397	0.688	0.288	0.255

Fig. 36. Influence of turbulence level in the basic stream on mean spread of a cylinder wake. Θ_0 = Wake momentum thickness.

- *A general problem of feedback* is introduced by the time delay between the control signal and the signal to be controlled: this causes an amplitude modulation which prevents full suppression of the 'plant-signal'. Effective suppression is only possible when the delay time is zero, i.e. when the measuring device is not located at some position downstream of but at the 'plant', i.e. at the wake producing body itself. Moreover, there is the
- *problem of feedback in absolutely unstable systems:* Dynamic control appears to be possible only with the characteristic frequency or its subharmonic(s).

Still, a reduction of the coherent energy by approx. 40 % can be achieved, while the stochastic energy content remains essentially unaffected (Heine et al. 1997).

2.4 Juxtaposition and Summary

It is interesting and revealing to compare and juxtapose the different behaviour of jet and wake when exposed to periodic excitations of, say, the 0th, or the 1st mode as was discussed above. Obviously, the effect of forcing a structure must depend to a large extent on the ratio between vortex velocity and the velocity by which the structures are transported (other than by their own induction). Or to be more specific: the velocity field of the jet in

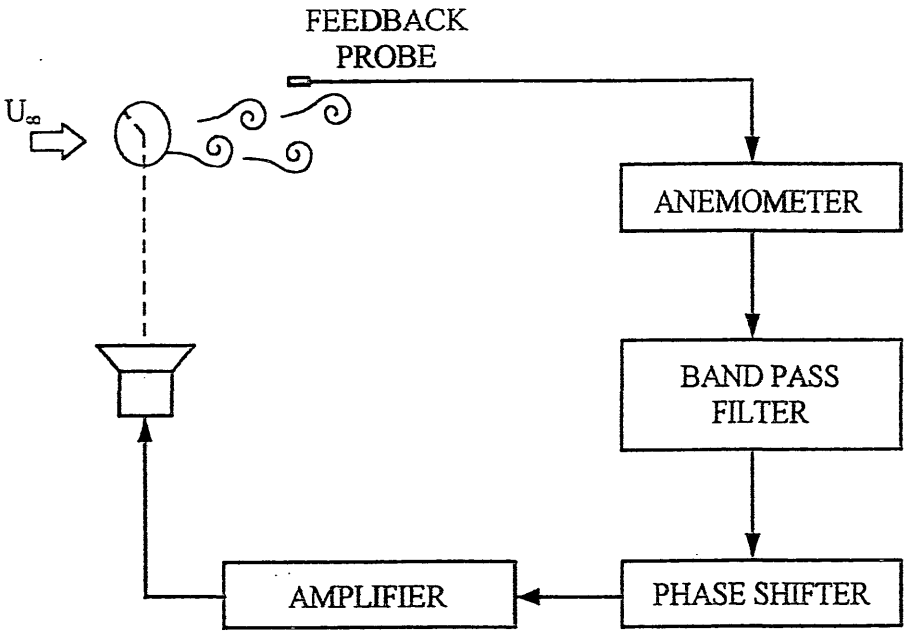

Fig. 37. Sketch of the feedback system

quiescent surroundings is a consequence of the induction of the dominating vortices. Perturbation of the latter is therefore directly reflected in the flowfield. Consequently, excitation of a jet structure is of comparatively strong effect.

In a wake, with its prevailing memory of initial conditions, the vortices themselves constitute only a perturbation of the basic convective flow. Their perturbation is therefore only of secondary effect—except for the near-wake region, where the flow is dominated by the large structures and their motion, and where the 'external' flowfield is then of reduced influence.

It is for this reason, that spectacular effects as observed in the excited jet in quiescent surrounding will not be found in wake flows, nor can they be expected for jets in a moving stream. The generic picture of jet- and wake flow as shown in Fig. 15 may serve to support this explanation.

A special jet-wake combination of some technological relevance is provided by the jet in a counter-stream (König and Fiedler 1991; Yoda and Fiedler 1996). Depending on the ratio of the jet velocity over the ambient

(counterstream-) velocity $R = U_J/U_0$ (where U_j = velocity of the jet and U_o = velocity of the counter-stream) we observe two different flow situations: A higly unstable flow for $R > 1.4$ where control by periodic forcing at reasonable amplitudes is of no visible effect, since the random motion of the flow in the stagnation region is of high amplitude, thereby causing phase scrambling of any periodic wave imposed onto the flow. For $R < 1.4$ the jet immediately wraps around the nozzle and creates a wake of some receptivity to periodic excitation at different modes.

3 Mixing Layers

Mixing layers have for long time been the favourite objects for turbulence researchers, surpassed in the number of papers devoted to them only by those on wall boundary layers. This is easily understood since the mixing layer represents the cleanest scenario for a free turbulent, non-decaying flow, being somewhat of a hybrid between jet and wake. For both flows the mixing layer provides the first configuration of transient and finite extent. General introductions and surveys on mixing layers were given by Birch and Eggers (1972), Ho (1982a), Fiedler et al (1981), Fiedler et al. (1988b), Browand and Ho (1983), Ho and Huerre (1984).

3.1 Introduction, Configurations, Definitions

Mixing layers are basic building blocks of a large variety of flows with often three-dimensional geometry, distortion or varying pressure. Classical objects of research are on the other hand the more basic, simple geometries—the plane mixing layer between parallel streams of 'infinite' extent and the axisymmetric layer—two flows of limited self similarity—see Fig. 38. In the general case the layer is formed between two streams of different velocity U_1 and $U_2 (< U_1)$ showing linear spread in the case of constant pressure. There is sufficient experimental support for the general validity of a transformation – widely known as the 'Abramovich-Sabin-rule' (Abramovich 1963; Sabin 1963) —by which the results for mixing layers between streams of different ratios U_2/U_1 can be reduced and generalized. Introducing a velocity parameter $\lambda = (U_1 - U_2)/(U_1 + U_2) = \Delta U/\Sigma U$ we find the local width b in the general case to be described by

$$b = \lambda b_0 \ ,$$

where b_0 = width of the single stream mixing layer ($U_2 = 0$) at the same x-position. A relation between local width as defined by the momentum thickness Θ and downstream position x is given as $\Theta/\lambda x \approx 0.032$.

Figure 39 shows a general velocity profile of a plane mixing layer flow and gives some definitions and relations.

In recent years the interest on flow geometries with parallel primary streams was extended, following a growing interest in more complex configurations and their control. Thus, constraining and distorting geometries were looked into and finally the study of general three-dimensional mixing layers between two non-parallel streams in parallel planes was taken up.

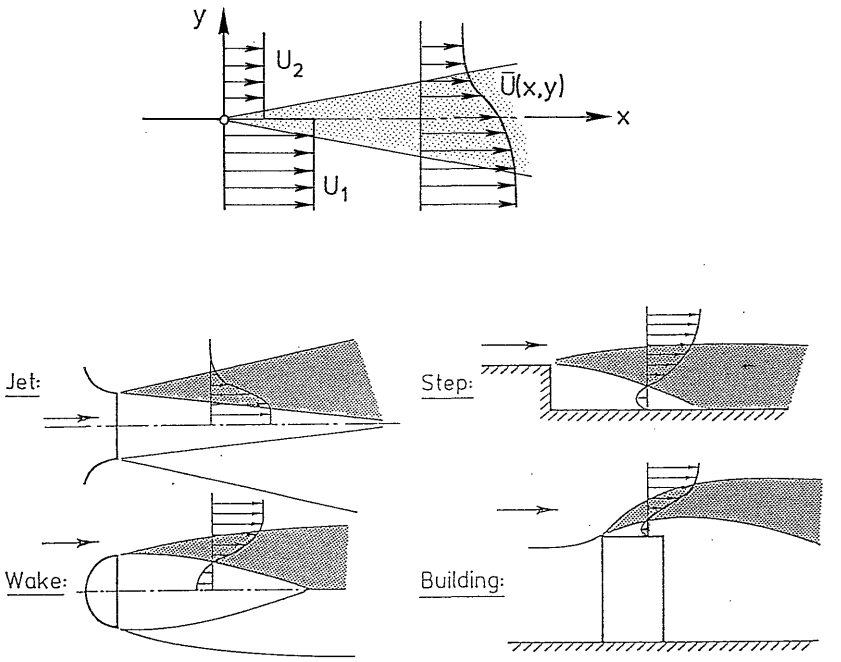

Fig. 38. Mixing layers as building blocks of other, more complex flows, and the basic, plane configuration.

3.2 Purpose of Control—Goals

There are numerous examples as to the aim and purpose of mixing layer control. Most obvious ones are

- enhancement or reduction of turbulent mixing—either in an overall sense or locally, i.e. 'tailored to measure'—important for chemical and combustive processes
- modification or adjustment of local spread, which is closely related to
- modelling and manipulation of (coherent) structures. This provides a basic mechanism for
- control of entrainment, as well as for

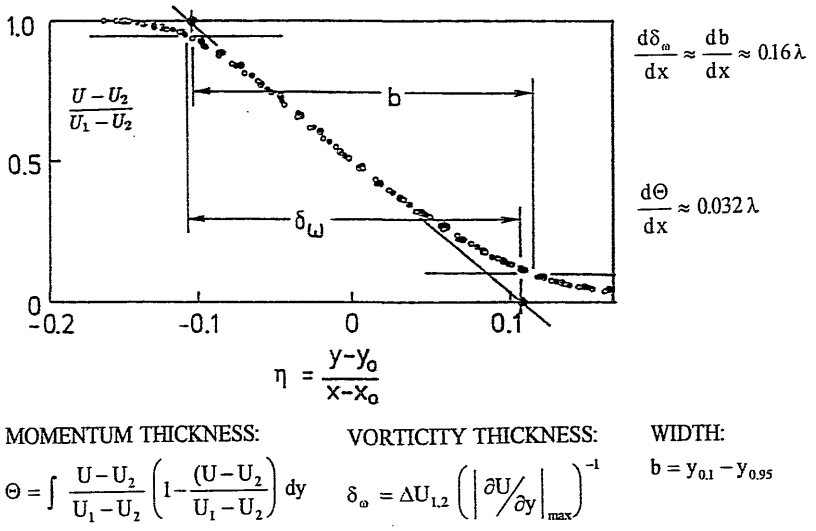

Fig. 39. Definitions, mean velocity characteristics and spread parameters of the plane mixing layer.

– control of noise production

Since, as we have already have seen, control is essentially based on manipulation of coherent structures making use of the stability characteristics of the flow to be controlled, we shall first discuss the

3.3 Stability and Structures

A mixing layer provides a perfect example for a Rayleigh-unstable flow. Figure 40 shows amplification curves for various velocity ratios—expressed by the flow parameter λ, as obtained by Monkewitz and Huerre (1982) for spatial amplification of a laminar flow. Its applicability to a turbulent flow was shown by Gaster and Kit and Wygnanski (1985). Obviously the one-stream layer ($\lambda = 1$) is the most unstable configuration. The value for maximum amplification is gradually reduced for lower values of λ, approaching the temporal amplification curve for $\lambda \to 0$.

The evolving coherent structures, appear in a comparatively simple scenario, as can be seen in shadowgraphic flow visualizations (Fig. 41). Many streakline visualizations have shown the typical spanwise structures of large scale and the superimposed longitudinal vortices, where the latter are often triggered and their spacing determined by minute upstream irregularities in the primary flow. Only the complete three-dimensional structure provides for turbulent (small scale-) mixing, the enhancement of which, therefore, requires the control of three-dimensionalities.

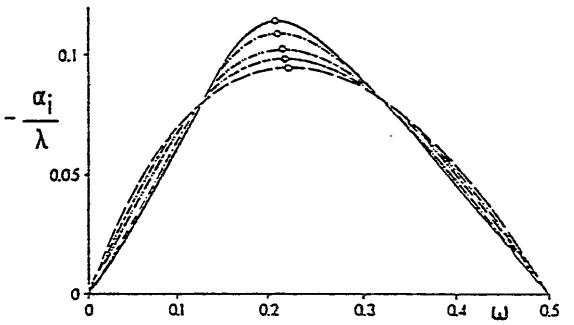

Fig. 40. Amplification curves for different flow parameters (after Monkewitz and Huerre 1982). Spatial amplification rate $-\alpha_1$ vs. frequency, ω for plane shear layer (tanh-profile); — $\lambda = 1$, – · – $\lambda = 0.9$, – ·· – $\lambda = 0.7$, – ··· – $\lambda = 0.5$, – – $\lambda << 1$ (temporal).

The coherent structures scenario is then as follows: primary structure is the line vortex with axis parallel to the trailing edge, which forms as a consequence of Rayleigh-instability of the basic flow. Those primary structures are called 'rollers'. Soon after their formation, secondary instability sets in, which leads to their spanwise undulation, followed by the formation of secondary structures, so called 'streaks'. Those are longitudinal counterrotationg vortex pairs with average spacing of the order of the downstream distance (wave length) of the rollers. A conceptual sketch of the complete structural scenario is shown in Fig. 42.

Although beyond an overall Reynolds number of order $Re_x \geq 10^5$ the global rate of spread of the flows seems to have achieved its asymptotic, Re-independent value (Birch and Eggers 1972) there is a 'diffusion critical Reynolds number' (defined by Konrad 1977),

$$Re_{\delta,\mathrm{crit}} = \frac{\Delta U_{1,2}^2}{\nu \left[\frac{\partial U}{\partial y}\right]_{\max}} \approx 2 \times 10^4 \ ,$$

below which turbulent mixing is at a very low level. This critical Reynolds number was first determined from the 'unmixedness' distribution and is related to the development of three-dimensional small scale motion, as shown in Fig. 43 (after Dimotakis 1991).

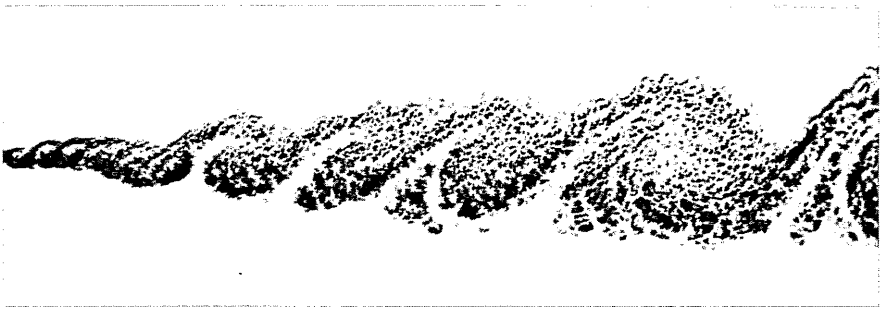

Fig. 41. Shadowgraph of mixing layer showing roller-structures (after Brown and Roshko 1974).

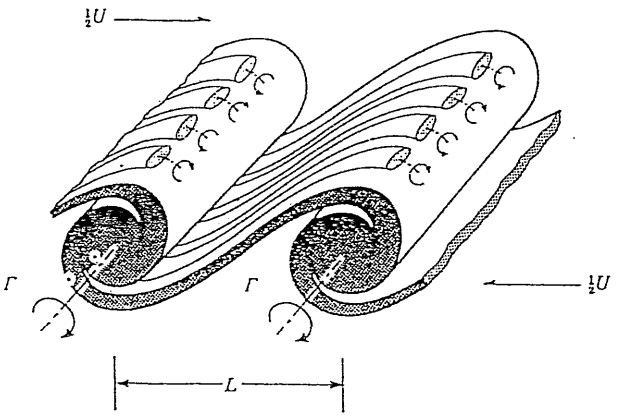

Fig. 42. Coherent structure scenario of the plane mixing layer (after Bernal 1981; Bernal and Roshko 1986.)

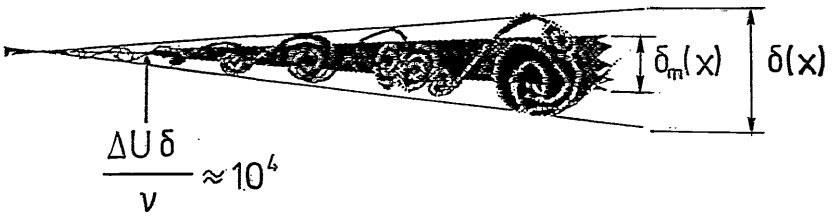

Fig. 43. The 'reduced' region of small scale mixing in a mixing layer (hatched area).

3.4 Control via Boundary Conditions

In the following we shall again discuss the different possibilities of control, distinguishing primarily between static (passive) and dynamic (mostly active) methods.

Static Upstream. The condition of the separating splitter-plate boundary layer is the most basic parameter of influence for the evolving mixing layer, a condition which had been overlooked in many early investigations and gave rise to controversies. Only as late as in the 70's Batt (1975) and Foss (1977) investigated the different developments of turbulent mixing layers starting from laminar and from turbulent (tripped) wall boundary layers. Later investigations concerning the effect of splitter plate geometry and of the boundary layer(s) were done by Hussain and Zedan (1978a), Hussain and Zedan (1978b), Husain and Hussain (1979), Dziomba (1981), Gurecki (1981), Dziomba and Fiedler (1985), Bell and Mehta (1992).

According to most investigations the length $x_{\text{asymptotic}}$ of the development region from the boundary layer to the final asymptotic mixing layer state is given by

$$400 < \lambda x_{\text{asymptotic}}/\Sigma\Theta < 600 \ ,$$

where $\Sigma\Theta = \Theta_1 + \Theta_2 + h$ = sum of the momentum thicknesses of the two boundary layers at the trailing edge plus the thickness h of the trailing edge itself. In the case of a one-stream layer $\Sigma\Theta = \Theta_1$. This is less than the conservative value of 1000, which was proposed by Bradshaw (1966) and considered a standard since then. In the transitional region of the mixing layer developing from a turbulent boundary layer the spread rate and the turbulence level is generally below that of the fully developed mixing layer. In the separating laminar boundary layer flow there is first an overshoot of spread rate and turbulence intensity (owing to the highly agitated flow during the L/T transitional process), before the flow reaches asymptotic values. For equal momentum thicknesses at TE the tripped flow— while providing a better defined upstream condition—needs slightly longer to reach the asymptotic condition. Trip wires to achieve turbulent conditions at separation may be of different shape, e.g. straight or bent wires or coarse sand paper. A criterion for dimensioning the trip wire number is

$$Re = \frac{dU}{\nu} \geq 900 \ ,$$

where d = diameter of trip wire and U = free stream velocity.

Other, more elaborate means of passive control are provided by shaping the trailing edge geometry, thereby directly triggering and controlling the formation and the characteristics (spacing, strength) of the streaks. Typical TE-geometries used for this purpose are those which are

- variable in x-y-direction = sawtooth geometries

- variable in x-z-direction = corrugated trailing edge (e.g. Lasheras and Choi 1988; Lasheras and Cho 1986)—Fig. 44
- vortex generators on the surface of the splitter plate near the trailing edge. A long established application of this is the so called Seifert-winglet, which is used for closed loop—open test section wind tunnels to break up the coherence of the large scales in the enclosing mixing layers and thereby preventing the unwanted and higly disturbing pumping characteristics often found in such tunnels.

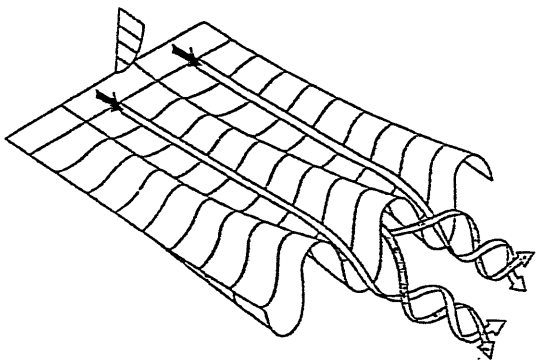

Fig. 44. Formation of longitudinal vorticity past corrugated trailing edge.

Static control by upstream boundary condition is by definition limited to a certain downstream length, after which the flow asymptotically retains its neutral state. This length is, however, by no means small and therefore negligible, depending inversely on the velocity parameter λ. The following Fig. 45, 46, 47 demonstate the far reaching influence of trip wires of various diameters and boundary layers of different thicknesses and characteristics on the development of a mixing layer with $\lambda = 0.33$ and $\lambda = 0.42$ (Dziomba and Fiedler 1985).

Static Overall. This offers but few possibilities for control; an obvious one is by *pressure gradients:*

1. $\boxed{\frac{\partial p}{\partial z}} \rightarrow$ a transverse pressure gradient is achieved by a curvature of the flow in the x-z-plane. This will cause a mean swirl vector pointing in downstream direction. Thus, apart from a three dimensional turbulent structure, the flow becomes three-dimensional in the mean.
2. $\boxed{\frac{\partial p}{\partial y}} \rightarrow$ the mean flow remains two-dimensional; the influence is only on the structure. We distinguish between a stablilizing curvature (towards

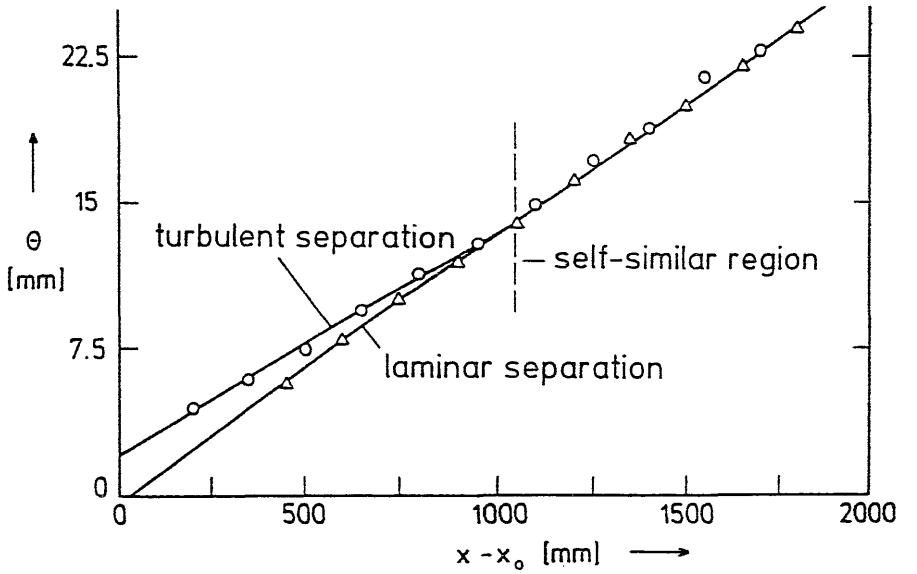

Fig. 45. Spread of tripped and untripped mixing layer for turbulent and laminar separation at TE (Θ = momentum thickness, x_o = virtual origin).

the low velocity side) with the effect of reducing the spread, and destabilizing curvature with the opposite effect (Plesniak et al. 1994).

3. $\boxed{\frac{\partial p}{\partial x}}$ → there again the mean flow retains its two-dimensionality. For positive gradients the mean flow is decelerated and vice versa. In a decelerated flow the vortex dynamics and thus the mixing capacity is enhanced (König and Fiedler 1995); acceleration stabilizes the large scale structures, thereby deactivating vortex dynamics and reducing the small scale mixing. Strongest stabilization is achieved when the characteristic frequency becomes constant throughout the flow (Fiedler et al 1991b).

Figure 48 sketches the geometries for the three pressure gradients. The influence of various longitudinal pressure gradients is most obvious from three flow simulations shown in Fig. 49.

Distortion and Confinement ($p \neq p(x, y, z)$ = const.). Another way of passively controlling the development of a mixing layer is by flow distortion or confinement. Here are two examples:

1. *Distortion:* The mixing layer develops in a test section of gradually changing cross section with downstream distance. In this situation the flow is influenced or controlled by axial strain on the coherent structures. Compression destabilizes the structures, thereby increasing the mean spread

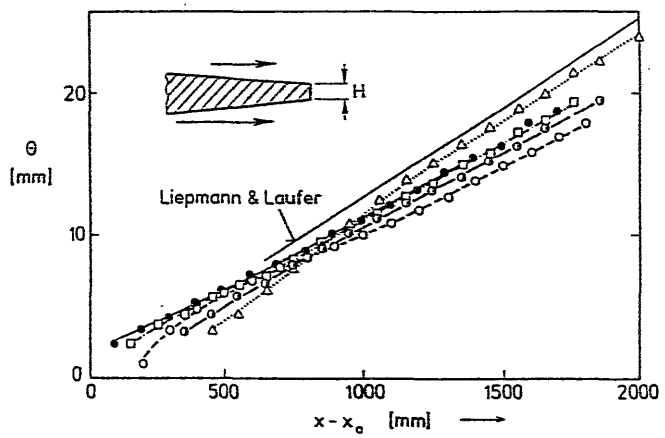

Fig. 46. Mean spread of mixing layer for different upstream conditions.

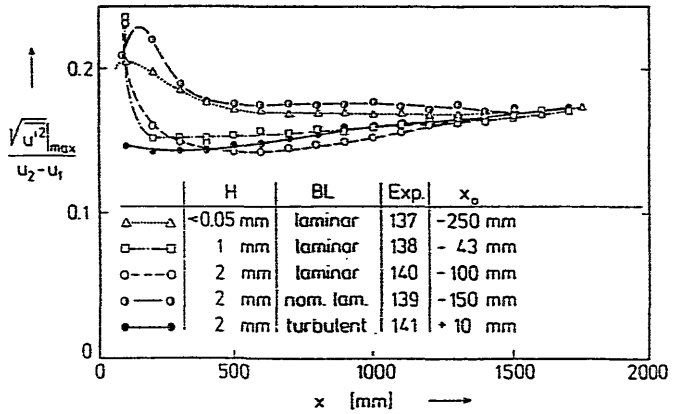
0.2
0.1
0
0
500
1000
1500
2000
x [mm]
H | BL | Exp. | x₀
<0.05 mm | laminar | 137 | -250 mm
1 mm | laminar | 138 | - 43 mm
2 mm | laminar | 140 | -100 mm
2 mm | nom. lam. | 139 | -150 mm
2 mm | turbulent | 141 | + 10 mm

Fig. 47. Development of maximum intensity of longitudinal turbulence intensity for different upstream boundary conditions.

and reducing the Reynolds stresses, in accord with the reduced maximum gradient of the mean velocity distribution. Stretching of the dominating vortices has the opposite effect. Figure 50 shows the configuration and some typical effects as were e.g. studied by Paschereit et al. (1989) and Keffer et al. (1978).

2. *Confinement:* Growth and structure of a free mixing layer are found to be considerably influenced by the lateral extent of the flow at reduced relative side wall distance. First investigations of this condition in a one stream layer ($\lambda = 1$) were reported by Hilberg and Fiedler (1989), (see also Dimotakis and Brown 1976): With increasing aspect ratio $A = L/h$ (where h is the sidewall distance and L the length of the test section—see Fig. 51) a periodicity develops in the spectrum, accompanied by con-

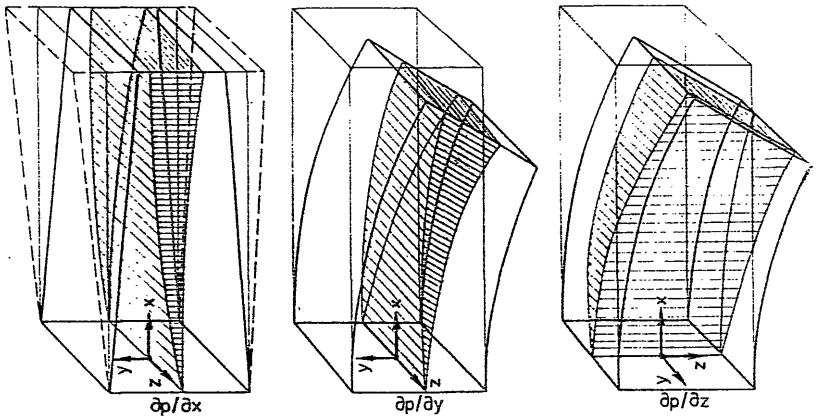

Fig. 48. Pressure gradients—three different configurations.

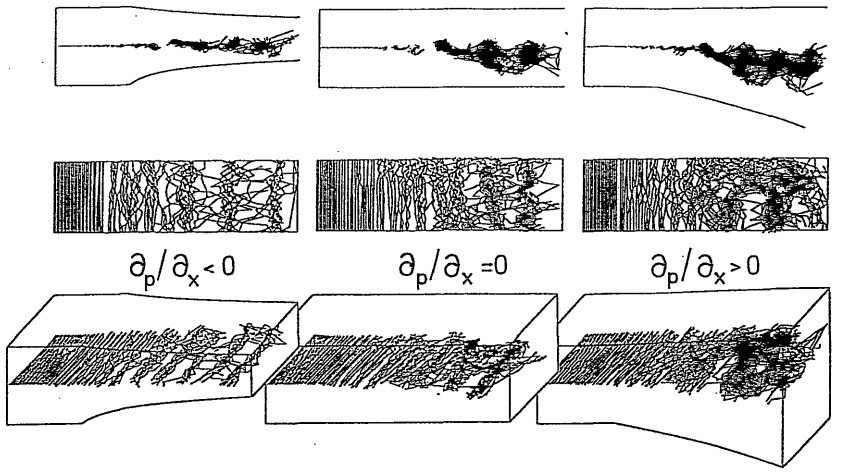

Fig. 49. Simulations of three longitudinal pressure gradients by DVS (Spieweg 1994).

siderable increase of spread. The amplitude of this periodicity reaches saturation for $\Lambda > 40$, corresponding to $h/\Theta_L \approx 1$ (Θ_L = momentum thickness of the mixing layer at test section exit).

This effect, which appears to be quite spectacular in flow visualization and less so in the measurements, is demonstrated in Fig. 51. Here we have a case of feedback of pressure waves from the two trailing edges of the test section side walls to the trailing edge of the mixing layer (as was already conjectured by Dimotakis and Brown (1976). Those pressure waves are uncorrelated at large values of h, and then unable to maintain a feedback cycle. The feedback frequency scales with a Strouhal number of $S = fL/U_1 = 1.0$.

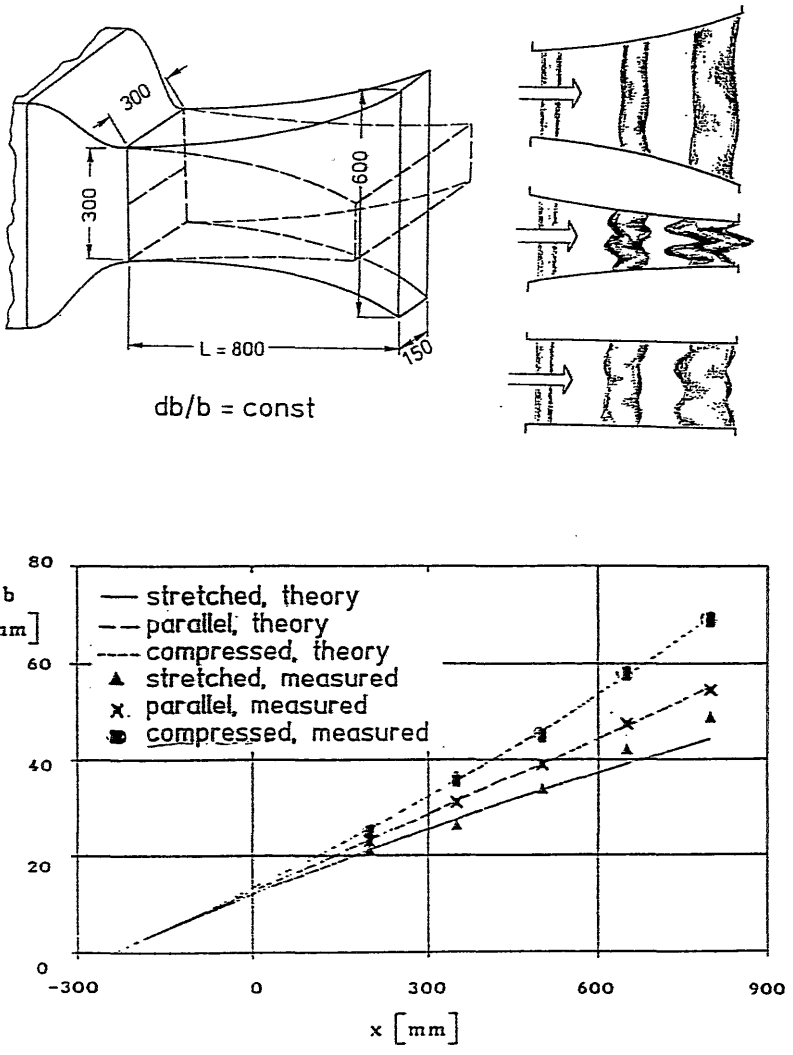

Fig. 50. Distorted mixing layer—configuration and some results.

Suppression or attenuation of the feedback loop is possible by modification of the sources of the feedback signal, i.e. the sidewall trailing edges by short flexible (energy absorbing) or by indented (scrambling) trailing edge extensions. Reduction of the feedback effect is also provided by increased turbulence level of the basic flow and by reducing the relative distance of the bottom wall of the test section from the mixing layer.

Dynamic. Periodic forcing was probably the first conscious application of mixing layer control. Some early investigations of the axisymmetric case date

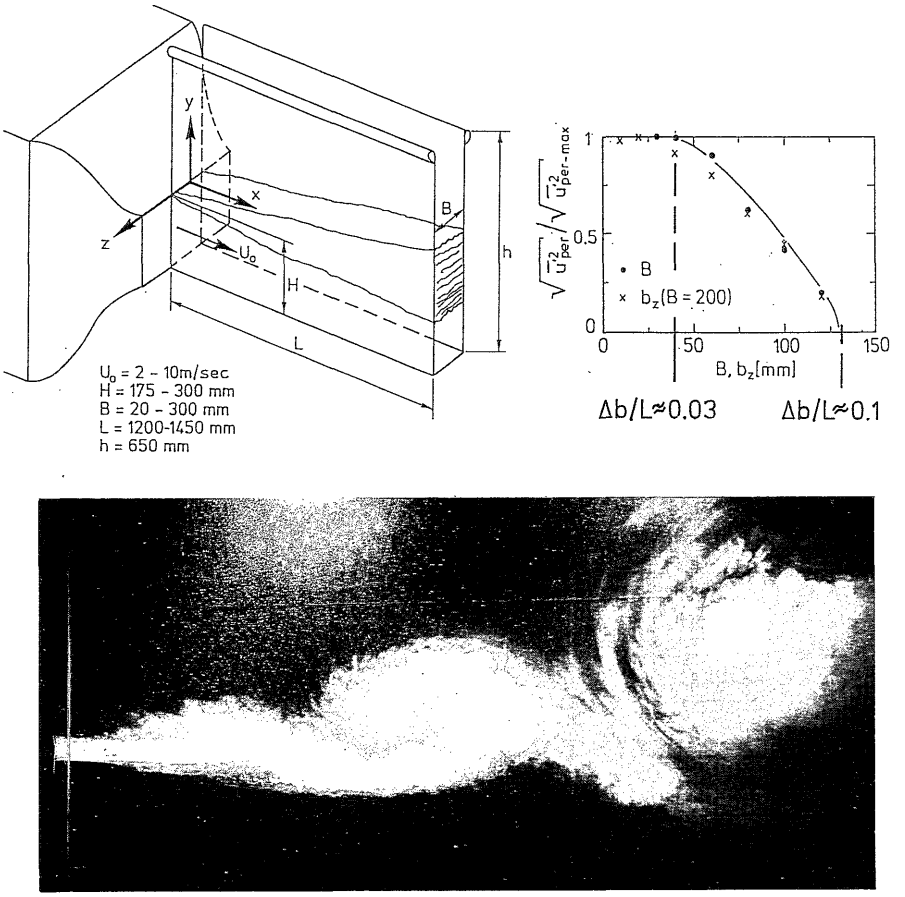

Fig. 51. Confined mixing layer by reduced aspect ratio.

back to the '50s, yet only in the '70s did this technique attract serious interest and detailed investigation in plane flow were then undertaken (Bechert and Michel 1975; Oster et al. 1978; Fiedler et al. 1978a). Many aspects were clarified by a host of investigations to follow, the major results of which are summarized by Ho and Huerre (1984). Here we mention only a the work by Bechert (1985), Bechert and Stahl (1988), Dziomba and Fiedler (1985), Fiedler and Mensing (1985), Fiedler and Thies (1978b), Oster and Wygnanski (1982), Weisbrot and Wygnanski (1988), Wygnanski and Petersen (1985),Michalke (1965), Ho and Huang (1982b).

By periodically exciting the flow with f_e at the trailing edge an (in z coherent) instability wave is triggered and subsequently amplified—according to the amplification curve shown in Fig. 40—to reach its most amplified state near the position of the characteristic frequency f_c of the mixing layer flow,

where in the plane case and $p = \text{const.}$ $f_c \propto 1/x$. Thus, with periodic forcing we control the formation and stability of the Rollers. The most obvious effect of single-frequency forcing is a local widening of the flow of up to 100%, accompanied by an increase of the Reynolds stresses and the coherence (stabilization) of the dominating structures.

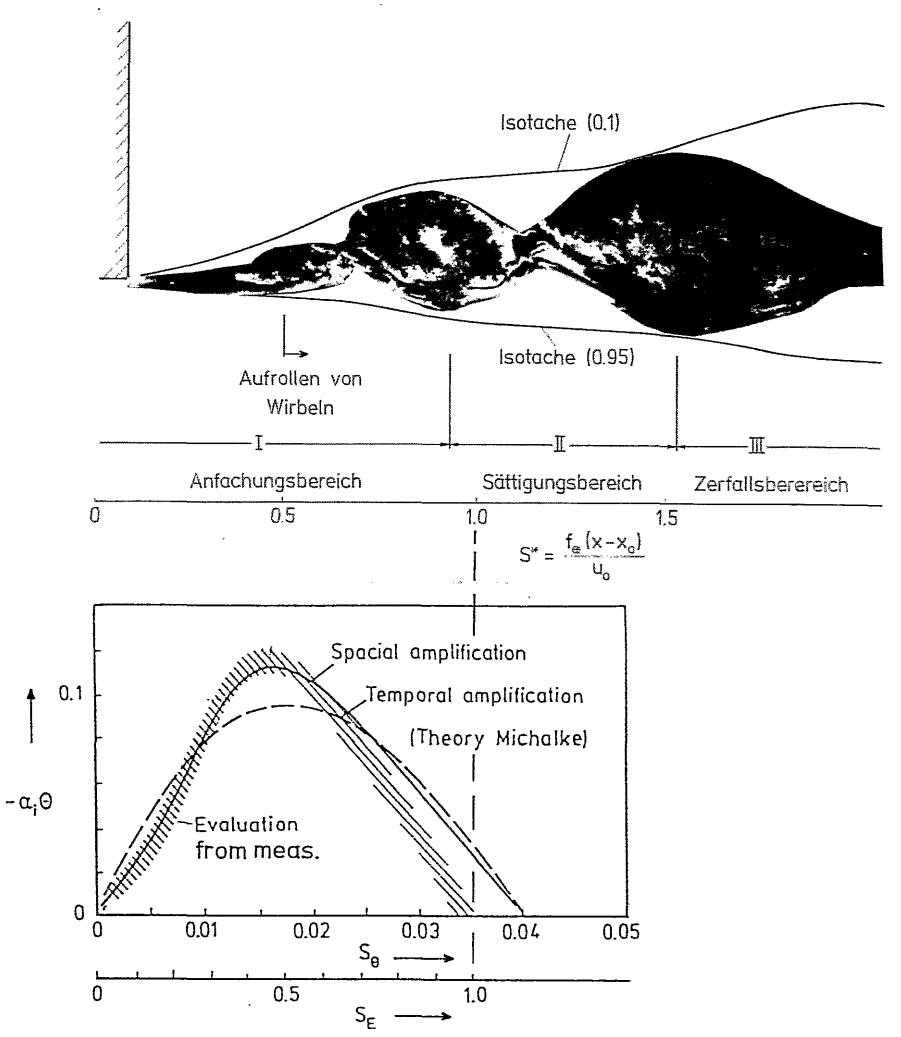

Fig. 52. Stability, amplification of periodicity and flow deformation (taken from Fiedler et al. 1981.)

Figure 52 illustrates this situation by juxtaposing a smoke picture of an excited flow bordered by two isotachs and below the corresponding amplification curve (same scale), where in addition to the theoretically obtained curves (Michalke 1972) the hatched distribution gives the range of amplification curves evaluated from actual measurements of coherent velocity components of the excited turbulent flow above.

For very high excitation amplitudes we even may find small regions of negative spread rate and negative production. The development of the amplified signal along x is —when properly normalized—self similar in a wide range of forcing amplitudes (Fig. 53). The entrainment flux undergoes a maximum, followed by a minimum, after which the flow asymptotically returns to its neutral state. The essence of this is sketched in Fig. 54 (see Ho and Huang 1982b; Roberts 1985).

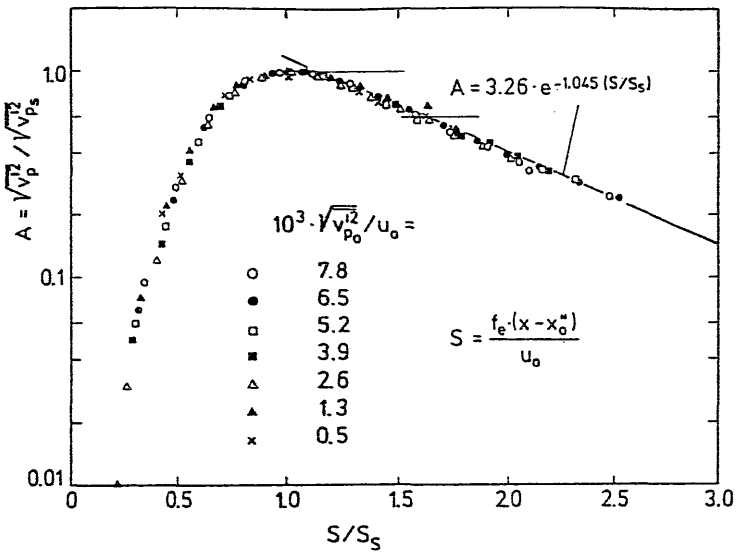

Fig. 53. Generalized development of amplified flow component for different initial (forcing) amplitudes. S_s = Stouhal No. at saturation—after Fiedler and Mensing (1985).

Recent investigations concentrate on more elaborate excitation schemes, as e.g. by multiple frequency forcing (Ho and Huang 1982b), wave packets, amplitude modulated excitation, three-dimensional forcing etc. (Fiedler et al. 1988b; Nygaard and Glezer 1991; Inoue 1992) by which specific influences—particularly on small scale mixing—can be exerted.

There are many uses of controlling the rollers, as e.g. in mixing, entrainment and noise production (coherent pressure fluctuations) as well as in stabilization of structures at very small amplitudes for the purpose of their detailed investigation, as is shown in Fig. 55.

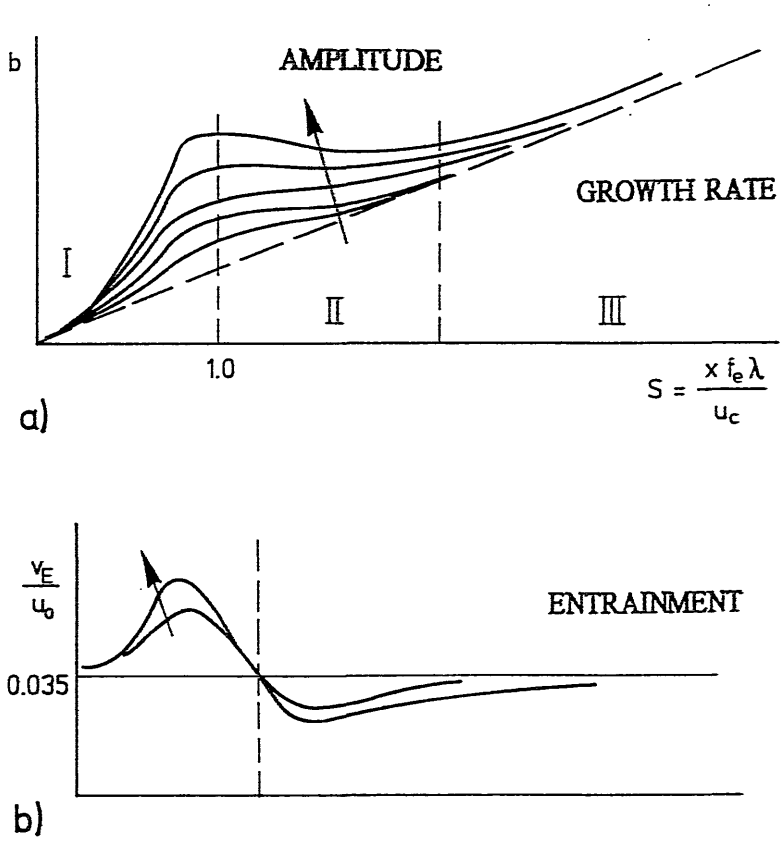

Fig. 54. Characteristics of excited plane mixing layer: a) non-linear spread vs. downstream coordinate and b) entrainment rate, for increasing excitation amplitude.

Periodic forcing can also be applied for the control of longitudinal structures (Streaks) by introducing spatial periodicity, i.e. three-dimensionality, by transverse periodic forcing amplitude.

Some specific aspects:

- *Introduction of the periodic signal* into the mixing layer flow at the trailing edge (the place of maximum receptivity) can be done by remote sources (loudspeaker)—see Bechert and Stahl (1988), Bechert and Michel (1975) and Rebel et al. (1992) – as well as more directly, flexible and adaptive by local actuators at the trailing edge, e.g. by jets, moving pins, heat pulses, flaps or other means. Amplitudes of the forcing signal are—unfortunately—often given only in geometric or electric dimensions, which are meaningless if not supplemented with details of the actuator characteristic. In terms of lateral fluctuation intensity or vorticity fluctuations the typical amplitudes applied are of the order $\leq 1\,\%$ of the mean velocity difference $\Delta U_{1,2}$

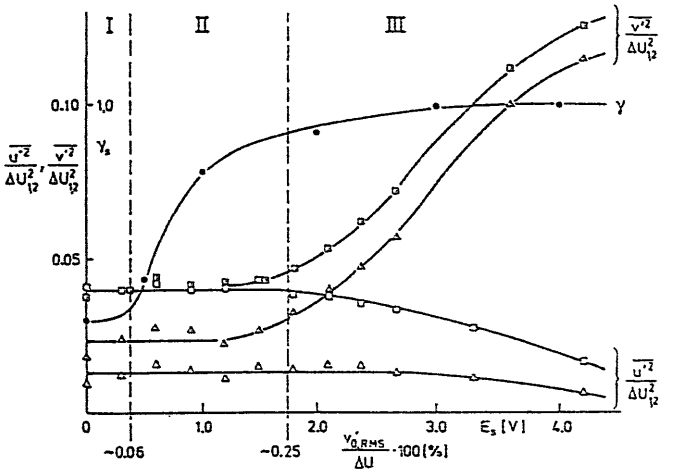

Fig. 55. Influence of excitation amplitude on flow (from Fiedler et al. 1991b). Region I: stabilization of periodicity. Region II: 'filling up' of structural intermittency. Region III: influence on structure itself.

- *Combinations* of control methods, e.g. combination of control of rollers and streaks is useful to introduce three-dimensionality at low frequencies and thereby enhance turbulent stirring and subsequent mixing, since the essence of mixing is the increase of reaction surface. Once again: Increased spread is not tantamount to mixing improvement, as is often assumed.
- *Modes:* Turbulent shearflows are often unstable to various modes, all of which may be excited to control the flow in various ways. Axisymmetric mixing layers have an infinite number of instability modes of which, however, only the first few are significant and provide a basis for control. Plane mixing layers can be correspondingly controlled by periodic waves, which—by introducing a phase shift along the trailing edge permit an infinite variety of control modes (see below). Combinations of modes may be used to achieve specific circumferential mean-flow and intensity distributions and thereby to control the small scale turbulence in a secondary way (see Paschereit et al. (1992) and Fig. 30).
- *Combinations of frequencies—resonance:* A mixing layer can be simultaneously forced with two frequencies. Special effects occur when those two frequencies are one octave apart. Energy exchange takes place between the corresponding wavetrains over a certain distance provided their phase velocities are equal. This may entail to particularly strong forcing effects. In this situation we speak of 'subharmonic resonance'. Since the phase velocities depend on the frequency, becoming constant and equal only for higher frequencies (Cohen and Wygnanski 1987a, 1987b), the effect is not found at low forcing frequencies (Paschereit et al. 1955). Figure 56 has some results (see also Husain and Hussain 1995).

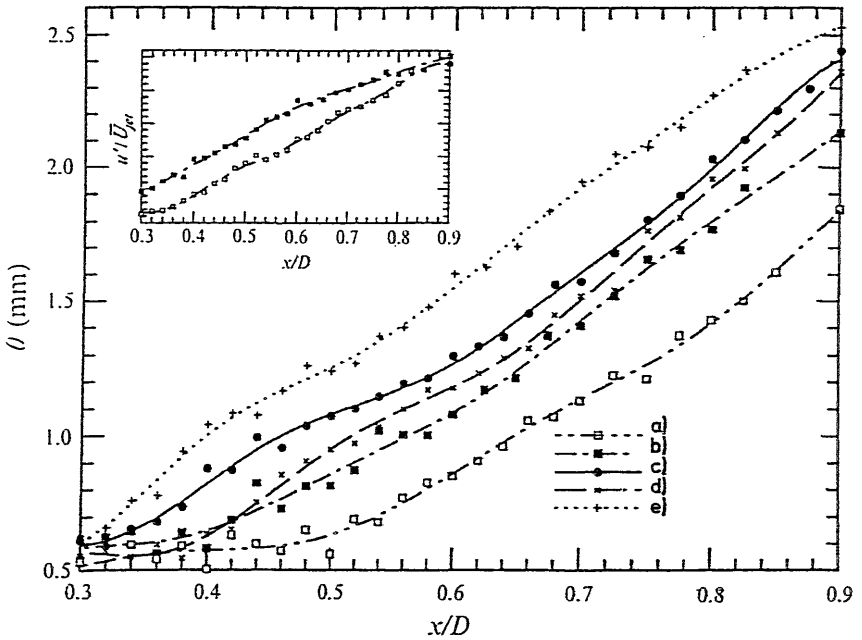

Fig. 56. Evolution of momentum thickness and maximum turbulence intensity along x/D for various cases of double-frequency forcing with subharmonic and various conditions of the separated boundary layer of the nozzle. $U_{rmjet} = 8$ m/s, $D = 50.8$ mm, $Re_D = 2800$. (a) natural, untripped BL; (b) natural, tripped BL; (c) untripped BL, forcing at $f_{\text{subharmonic}} = 184$ and $f_{\text{fundamental}} = 368$ Hz, amplitude ratio $A_{\text{sub}}/A_{\text{fun}} = \gamma = 0.1$; (d) untripped BL, 1184 and 368 Hz, $\gamma = 1.6$, $\Delta\phi = 0°$; (e) tripped BL, 184 and 368 Hz, $\Delta\phi = 90°$. $\Delta\phi$ = phase shift between fundamental and subharmonic wave. Max. forcing levels normalized with jet velocity werde 3.2 % in cases (c) and (d), and 6.5 % in case (e).

- *Actuators:* Typical actuators for periodic forcing at the trailing edge are sketched in Fig. 57 together with three examples of actuators which are driven by the flow itself ('passive' dynamic control).
- *Feedback:* This is seldom used in controlling free turbulent shearflows. 'Natural' Feedback may inadvertently be present in a flow as e.g. in the case shown in Fig. 51, where complete elimination is achieved by simple damping. This case is described by the block-diagram shown in Fig. 58. Amplification of periodicities is always possible, attenuation or even cancellation not, as long as there is a delay time between the initiation of the perturation and the sensor is not zero. Global feedback may, however, be useful in the sense that a certain characteristic is monitored (e.g. the entrainment flow or—in case of combustion—the flame temperature) which then serves for adjusting amplitude or frequency of the forcing signal (see also Monkewitz 1989; Dimotakis and Koochesfahani 1987).

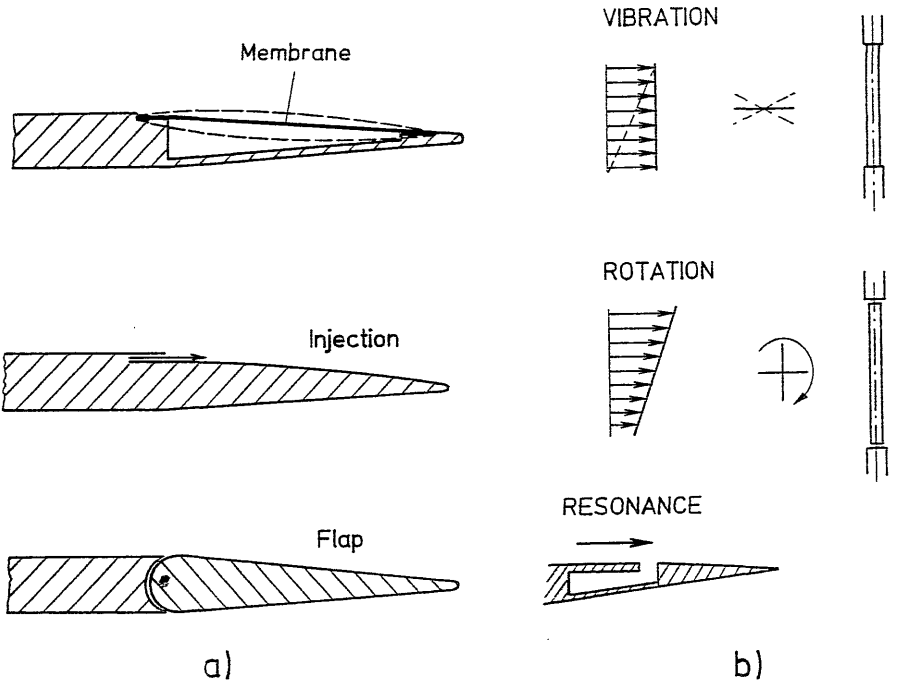

Fig. 57. Actuators for dynamic forcing of the flow. (a) active (b) passive.

3.5 Control via Flow Field / Field Effects

Static. *Density effects:* Influences of density differences of the two streams on the strength of coherent structures have been investigated and are documented in the literature (e.g. Rebollo 1972; Abramovich 1993; Fiedler et al. 1993; Soteriou and Ghoniem 1995a; Soteriou et al. 1991; Lummer 1989; Fulachier et al. 1989, Nottmeyer 1990). It was found that the influence of density ratio on the formation of coherent structures and mean spread is well described by stability theory: Coherent structures are stabilized (and thereby the spread reduced) in a situation where the higher density is on the high velocity side and vice versa ('co-gradient'- and 'counter-gradient'-configuration). Figure 61 shows stability diagrams for different cases of $\lambda_u = \Delta U_{1,2} / \sum U_{1,2}$ and $\lambda_\rho = \Delta \rho_{1,2} / \sum \rho_{1,2}$. The quantity most sensitive to the density ratio is the ρ'-u'-correlation, while the ρ'-v'-correlation remains largely indifferent to inhomogeneities. The overall spread is a function of the density ratio, being larger in the counter-gradient case, with stronger effects on the

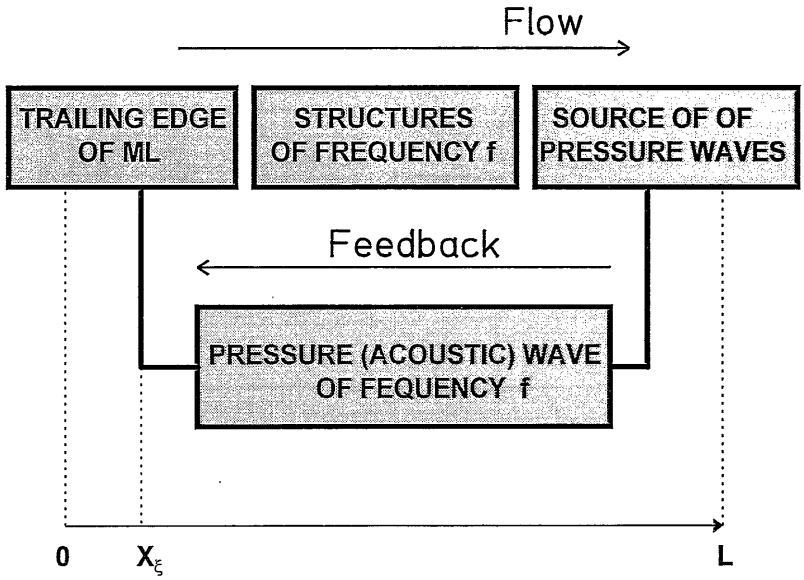

Fig. 58. Block diagram of the natural feedback.

low density side of the flow. On the basis of his measurements Nottmeyer (1990) suggests an extended 'Abramovich-Sabin-rule' for the spread of the density field as $b/b_{oo} = \lambda(1-0.627\tanh(2\lambda\rho))$, where b_{oo} spread for a velocity parameter $\lambda = \lambda_u = 1$ and a density parameter $\lambda_\rho = (\rho_1 - \rho_2)/(\rho_1 + \rho_2) = 0$.

Polymere additives: This important aspect ('Toms' (1948) effect') was – among othersg—studied by Kwade (1982) and by Riediger (1989), who found small amounts of long chained high-polymeres (e.g. Separan) to provide a significant reduction of small scale turbulence (corresponding in its effect to a laminarization, i.e. suppression of dissipation), which in turn strengthens and stabilizes the coherent transverse vortices—the rollers. The total spread was found to be smaller in the presence of additives—owing to different behaviour of the two flows in the initial region-yet the spread rate was higher by more than 40 %—see Fig. 60.

Dynamic. Periodic control by the overall flow field—as introduced by, say, a periodically fluctuating external stream—is, because of the receptivity at the trailing edge, tantamount to forcing at the upstream boundary. This is also the case for a periodicity embedded in random turbulence of the basic stream(s), as e.g. from a blower or some other vibrating component in the flow conduit. Only small effect on the flow development is from

Random turbulence: Dubuat's paradox, according to which the drag of a body at rest in a moving fluid exceeds that of a moving body in a fluid at rest, at closer inspection turned out to be an early example of flow control by disturbed flow conditions (high turbulence level). Dziomba (1981),

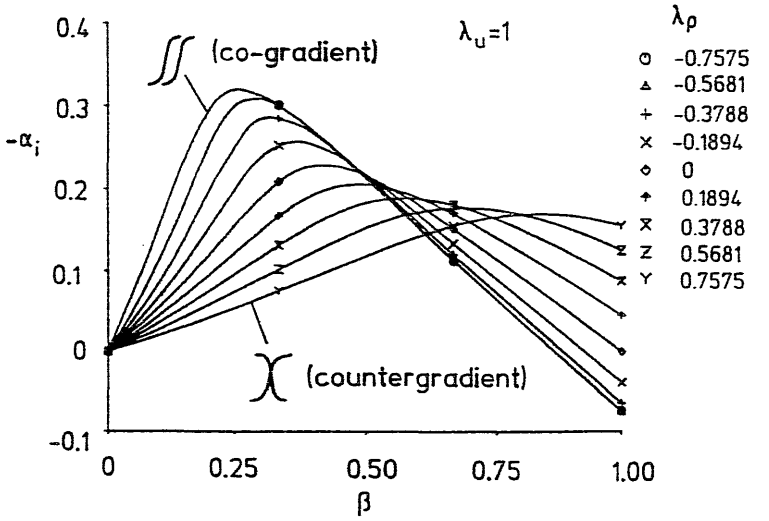

Fig. 59. Influence of λu and $\lambda \rho$ on the stability of a mixing layer (after Lummer 1989, see also Koochesfahani and Frieler 1987).

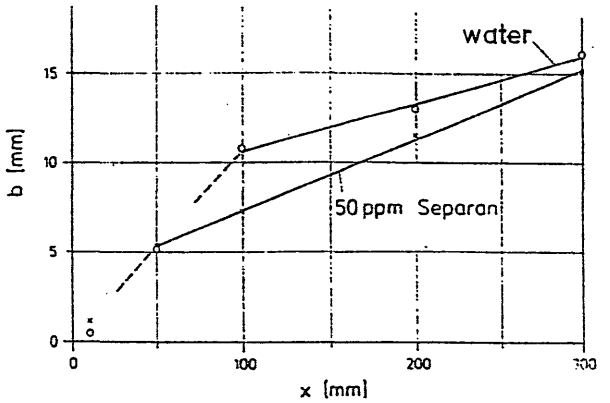

Fig. 60. Spread of an additive-controlled mixing layer.

Tavoularis and Corrsin (1987), Chandrsuda et al. (1978) and Tanner (1989) have invested some effort into the study of the consequences of turbulence in the primary streams on the subsequent flow development. Dziomba found the flow to reach an early self similar state for initial (but decaying) turbulence levels of approx. 2 %, exceeding the rate of spread for low turbulence levels at otherwise same conditions by approx. 10 %. This is accompanied by a reduced turbulence level in the flow by again 10 %. Tavoularis and Corrsin (1987) and Chandrsuda et al. (1978) were rather concerned with questions of structure. Particularly in the work of Tavoularis and Corrsin (1987) it was shown that

the turbulence level does not seem to interfere with the (spontaneous) creation and development of coherent structures, which appears contradictory to the findings reported by Chandrsuda et al. (1978), and Tanner (1989) gives spread rates for different external turbulence levels, which he finds strictly on theoretical grounds. His results (which need experimental corroboration) show, that in any case—according to expectation—increased external turbulence levels give rise to increased spread. The overall effect depends on the velocity parameter λ. It is almost negligible for $\lambda \to 1$, becoming, however, significant for small values of λ and may cause 100 % spread increase for, say, $\lambda = 0.14$ and a turbulence level of (only) 3 %. Tanner's theoretical results may be approximated by $b/b_0 \approx 60(Tu_1 + Tu_2)/\lambda + 1$, where b = flow width in the presence of external turbulence, b_0 = flow width for negligible external turbulence, and $Tu_{1,2}$ = turbulence intensities of streams 1 and 2, respectively. There is then apparently no way to give an upper critical level for the external turbulence below which there will be no influence, since this is a function of λ: for small values of λ, i.e. small velocity differences $\Delta U_{1,2}$, the equilibrium turbulence level produced in the mixing layer itself will be equally low and may approach the external turbulence level, which, by usual standards would be considered 'innocent' (see also Bell and Mehta 1992).

3.6 Three-Dimensional Configurations and Special Effects

Most basic investigations of flow control as discussed in the foregoing consider only two-dimensional and axisymmetric cases. Flows of technical importance are, however, mostly three-dimensional and extrapolation of results obtained in idealized geometries are problematic. Moreover, we know that mixing is enhanced by additional shear in y-z-plane, and that three-dimensionality destabilizes and destroys two-dimensional structures responsible for noise production and mixing suppression.

Some examples of technological and other situations where threedimensional mixing layers play an important role are listed below (see Fiedler et al. (1997); Fiedler 1995):

- Flow over swept wings, sails, tilted roofs, corners; over and past tapered cylinders or bodies of non-axisymmetric shape (wind engineering).
- Confined flows
- Aerodynamic flow, flow over ship hulls, automobiles.
- Flow past finite wings (ventilators, turbine blades).
- Shearflow between inhomogeneous or non-parallel streams.
- Swirling flows—airplane jet; mixer flow in jet engine, etc.
- Jets from non-circular or 2-D nozzles.
- Jets in crossflow.
- Basic elemens of turbulent and transitional flow.
- Meteorology.

Three dimensionalities in mixing layers is always found in random turbulence, unless suppressed by, say, MHD forces or buoyancy. It is also characteristic for large scale structural elements, unless control by periodic forcing is applied (stabilization of the rollers), and it may be a characteristic of the mean flow (primary three-dimensionality). Here is a more

Detailed Classification.

1. Primary three-dimensionality by geometry or boundary condition:
   - corrugated or slanted TE
   - streamwise variable test-sections
   - excitation with spanwise variable amplitude, phase, or frequency
   - flows not at right angles to splitter plate
2. Primary three-dimensionality by basic flow inhomogeneity or three-dimensionality:
   - non-parallel streams
   - non-homogeneous streams—including separating boundary layers
3. Secondary three-dimensionality by structural development:
   - deformation of rolls $\rightarrow$ formation of 'streaks'
   - excitation with odd mode or combinations

A particularly interesting case of structural three-dimensionalities is shown in Fig. 61, depicting the laminar-turbulent transition in an axisymmetric mixing layer (initial region of a jet) as reconstructed from a series of LIF visualizations.

A definition of three-dimensional configurations is shown in Fig. 62.

Following we shall discuss a few cases of primary and secondary three-dimensionality, and possibilities for their control in some detail:

Four Special Cases.

1. Mixing layer between oblique grazing streams—symmetric plane configuration *(primary three-dimensionality*—see Gründel and 1992; Fiedler et al. 1995; Gründel et al. 1995; Luo and Fiedler 1997)
   The mean velocity field is described by $\underline{C} = \{U;\ V(x,y);\ W(x,y)$, where $\Psi_1 = \Psi_2 = 15°/30°$ and $C_1 = C_2 = 8$ m/s. Figure 63 shows flow geometry and visualizations.
   This is now a temporally (convectively) growing parallel vortex layer (in z-direction) with the following characteristics:
   - Primary structures develop as spatially steady helices with axes parallel to the x-axis.
   - Helical pairing of those structures is observed.

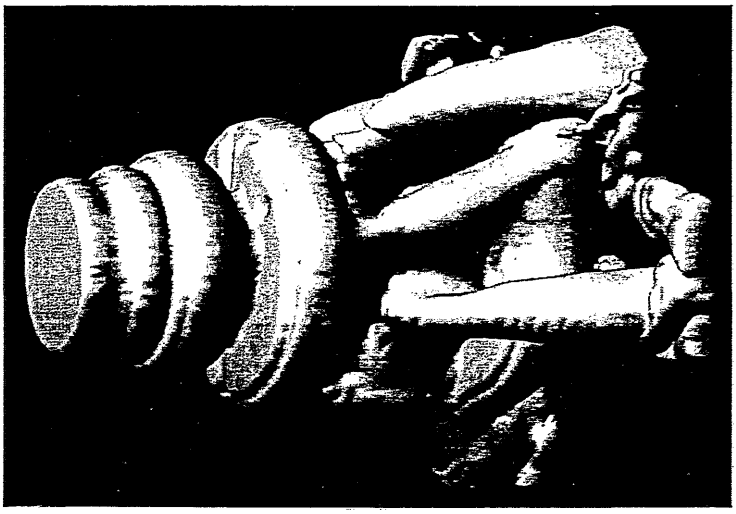

Fig. 61. Reconstruction of a transitional near jet—development of structural three-dimensionalities.

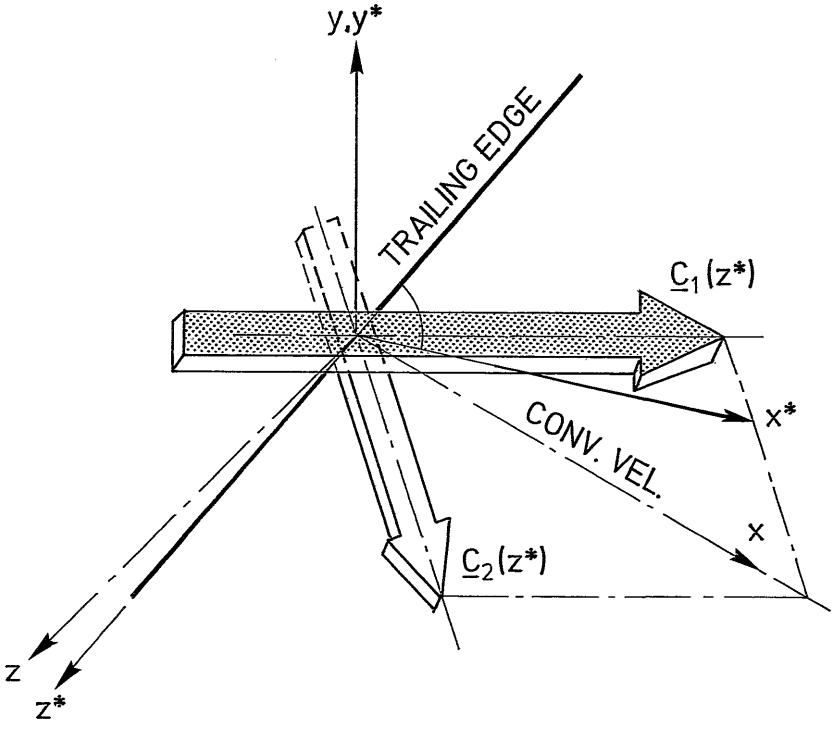

Fig. 62. Definitions and coordinate systems of three-dimensional mixing layers.

- three-dimensional mixing layers between oblique streams are qualitatively similar to two-dimensional mixing layers regarding their bulk quantities, e.g. spread, their structural development and their control behaviour.
- Well organized coherent structures form only when the wave vector of most the amplified instability wave is normal to the mean vorticity vector. This is only the case in symmetrical configurations.
- The flow may be characterized by a generalized (vectorized) flow parameter

$$\lambda_v = \frac{|\underline{U}_1 - \underline{U}_2|}{|\underline{U}_1 + \underline{U}_2|} \ .$$

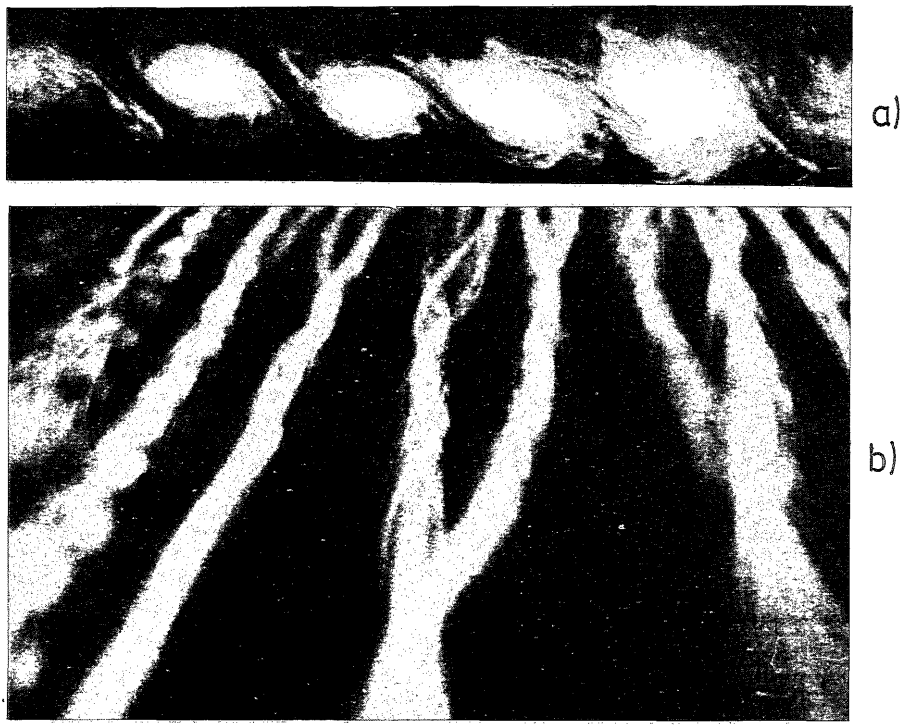

Fig. 63. Symmetric mixing layer between grazing oblique streams—visualizations. (a) cross-section (y-z-plane); (b) top view.

2. Oblique parallel mixing layer with $\lambda = 1/3$ *(asymmetric case—primary three-dimensionality*—see Gründel et al. 1995; Kibens et al. 1988; Blümel 1993; Luo and Fiedler 1997; Spieweg 1994):
The mean velocity field is described by $\underline{C} = \{U(x,y);\ V(x,y);\ W(x,y)\}$.
Figure 64a shows the basic configuration and definitions.

A flow of this kind has special characteristics, as e.g.

- Structures in the plane mixing layer between parallel oblique streams are weak and—on the average—at right angles to the mean flow, i.e. parallel to the mean vorticity vector $\overline{\Omega}$.
- spanwise pairing is observed. The flow develops stronger three-dimensionalities (vortex dynamics, mixing) than the classical o two-dimensional mixing layer.
- Oblique waves parallel to the trailing edge may develop when periodic forcing is applied. This was not found in naturally evolving flows.
- In numerical simulation of a forced flow we find a checkerboard pattern of structures in the top-view. This demonstrates the fact that the mean vorticity vector and the instability wave are not parallel. Side view reveals that the structures (i.e. the concentrated vorticity lines) are actually not interlaced but staggered. This interaction (misalignment) of instability wave and vortex lines is responsible for the weak structural organization (Fig. 64b).

3. Secondary three-dimensionalities in a nominally two-dimensional mixing layer, with mean velocity field $\underline{C} = \{U(x,y);\ V(x,y);\ 0\}$:
This kind of three-dimensionalities are often found, developing from imperfections in the test section and the primary flows. In the first place they tend to influence the separating boundary layer and in particular their laminar-turbulent transition. In the mixing layer flow downstream of the splitter plate those inhomogeneities are amplified to affect the turbulence structures over a long region.
This effect may be eliminated by a trip wire upstream of the trailing edge, which homogenizes the boundary layer (see Fig. 65).
4. Primary three-dimensionalities by three-dimensional periodic forcing:
This offers many possibilities for enhancement of turbulent mixing. Here are a few cases:
   - Three-dimensional forcing seems to have been first applied by Nygaard and Glezer (1991) who used elaborate heating schemes on the splitter plate in a two stream water tunnel, whereby almost any conceivable two- and three-dimensional static and dynamic forcing condition could be adjusted. This permits the introduction of longitudinal vorticity in a predetermined way, thereby providing possibilities for selective control of small scale mixing enhancement.
   - Oblique excitation with flap at TE (phase shift in z-direction) was studied in a special situation by Gründel et al. (1995).
   - Flap-excitation with spanwise variable amplitude. This case was investigated by Paschereit and Fiedler.

   Figure 66 shows four cases of discrete vortex simulations (Spieweg 1994) of three-dimensionally excited plane mixing layers: Juxtaposed are (1) the natural flow, (2) the flow with oblique excitation (phase variation in z), (3) a flow situation where plane excitation is applied over half of the

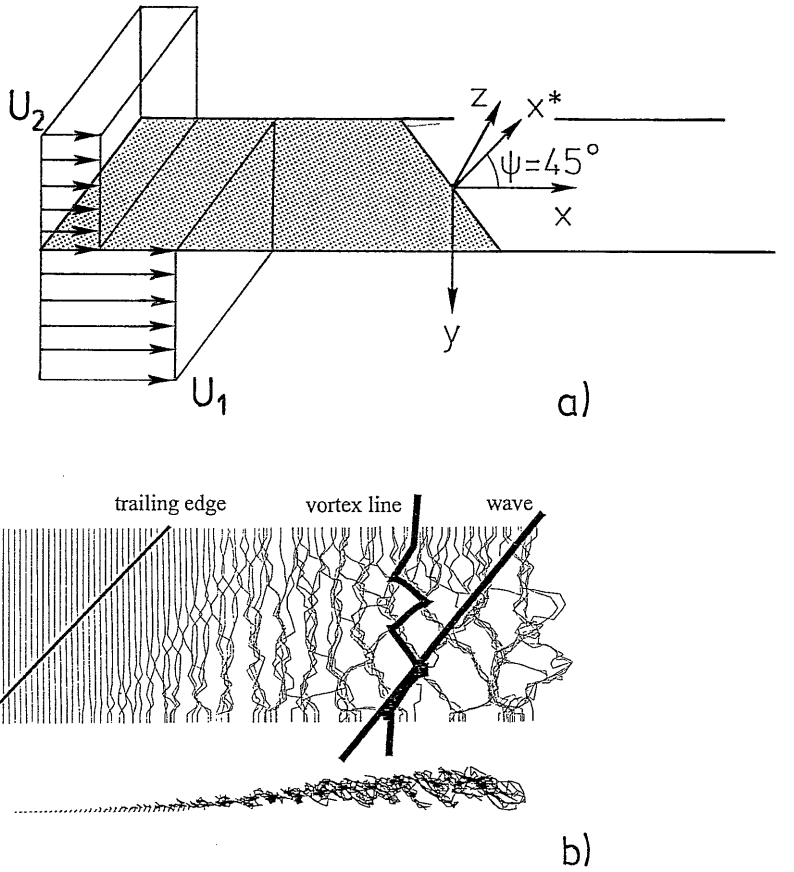

Fig. 64. (a) Configuration and definitions of the oblique parallel mixing layer; (b) Formation of diamond-shaped vortex pattern: top- and side-view of a discrete vortex simulation.

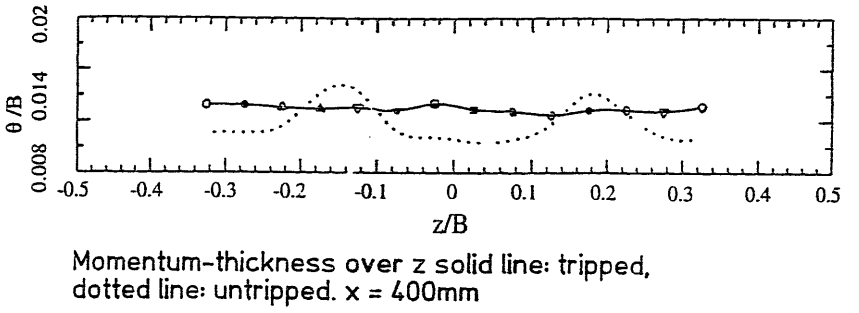

Fig. 65. Homogenization of separating boundary layer by a trip wire on the splitter plate.

depth (step change of amplitude along z), and (4) the same situation as in (3) yet with oblique forcing at constant amplitude over one half of the flow depth. There is enhanced vortex dynamics and production of small scale in the wedge developing between the neighboring conditions, in the angle of which corresponds approximately to the spread angle of the natural flow. Continuous succession of alternating forcing amplitude then may be expected to provide a versatile way to control the mixing layer for better mixing.

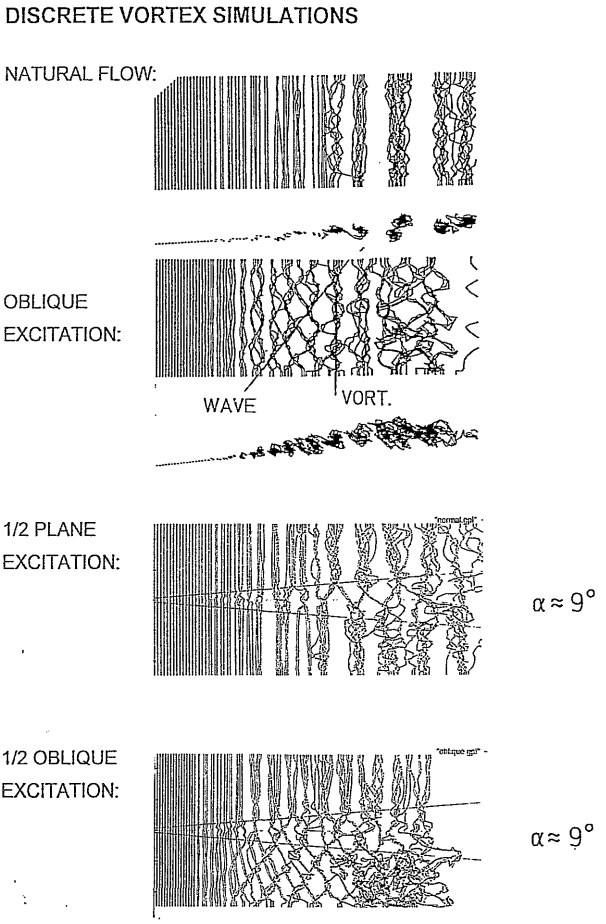

Fig. 66. Discrete vortex simulations of mixing layer with various three-dimensional forcing conditions.

Structures in Three-Dimensional Mixing Layers—Summarizing Observations. As in all shear flows coherent structures in mixing layers are

related to and a consequence of their instability behaviour. Accordingly we observe in the experiment primary structures which are also found in stability calculations (Luo and Fiedler 1997), ranging from rolls with axes parallel to the trailing edge in a plane configuration (Fig. 42) to trailing vortices with axes normal to the trailing edge in the case of a mixing layer between grazing streams in symmetrical configuration (Fig. 63). In fact, the primary structures are always oriented such that their axis is parallel to the direction of the mean vorticity vector. Well defined structures seem to be formed, however, only in symmetric configurations, as outlined in Fig. 67, i.e. when the **instability wave vector** and the **mean vorticity vector** are at right angles. All other configurations appear to be wakly organized. Accordingly we should expect symmetric flows to be better suitable and susceptive for dynamic control than asymmetric ones.

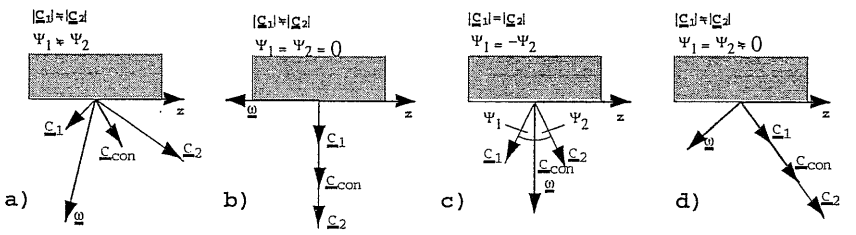

Fig. 67. Symmetric and asymmetric three-dimensional ML-configurations: (a) und (d): asymetric cases; (b) and (c): symetric cases.

Control. There are two possibilities:

1. **Direct excitation of the flow instability.**
   In general the flow is excited by introduction of periodic vorticity fluctuations Ω' at the trailing edge (e.g. by flap or loudspeaker), where

$$\Omega' = \Omega'_{\mathrm{O}}(z)\sin(\omega t + kz) \ .$$

   The temporal term ωt stands for the periodic wave travelling in downstream direction. This alone is applied to trigger the rollers in the plane mixing layer (symmetrical case).
   The spatial variation of vorticity—expressed by kz, with k = wavenumber in z-direction—is applied in the symmetrical mixing layer between oblique grazing streams, where the structures are steady and may be excited and stabilized by vortex generators on the splitter plate.
   In all other—non-symmetrical—cases control is possible only by a combination of temporal and spatial forcing, which in any case, however, is useful and efficient for mixing enhancement.

2. **Indirect control**

   This can be done by manipulating the mean flow field by as e.g. by suction or blowing through the trailing edge. In this way it is possible to suppress the instabilities and the subsequent formation of structures by the wake past the splitter plate, thereby stabilizing the mixing layer structures.

Other Effects. There are many other parameters affecting the stability of a mixing layer flow and the formation of ist structures. Let us have a quick look at two of them:

- **Compressibility:** this has for all shearflows an attenuating effect on the instability (see Fig. 68): Consequently the formation of coherent structures is weakend and so is its controllability (see also Lu and Lele 1994; Gutmark et al. 1995;; Reynolds 1883.

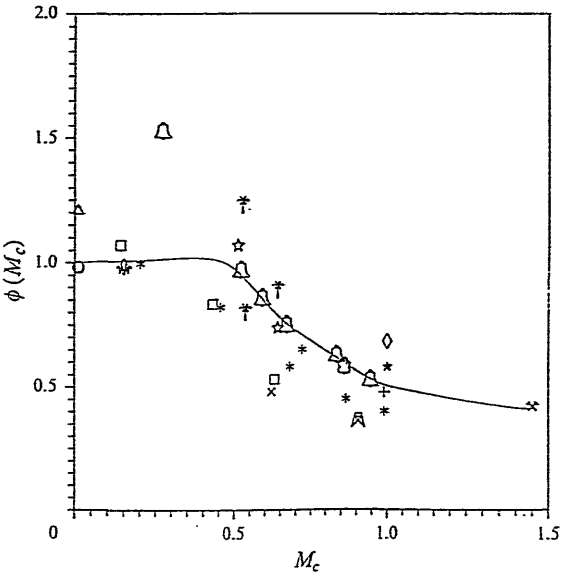

Fig. 68. Attenuation of mixing layer spread with increasing convection Mach number (after Barre et al. 1994).

- **Buoyancy:** This has—in a way similar to curvature—two sides to the coin: depending on whether the Richardson number is positive or negative we experience reduced or increased spread of the flow (e.g. Schowalter et al. 1993).

4 Mixed Cases

4.1 Introduction

Quasi idealized situations of clean flows as were discussed in the foregoing chapters are comparatively scarce in practical applications. More often than not we find combinations of flows as in a separating boundary layer which has characteristics of both ingredients—the wall bounded flow and the free shear flow. Following we shall discuss a few cases of recent interest.

4.2 Separating/Separated Flows (Mixing Layer with Wall Effects)

Separation of a boundary layer flow may be caused by many things, as e.g. sharp edges, shocks or gradual pressure gradients. At closer inspection we find, however, that the cause for separation is always the same: the existence of a longitudinal positive pressure gradient, which reduces the kinetic energy of the streamlines in the immediate vicinity of the surface, thereby rendering them unable to overcome further increase of pressure. There is a clear distinction between what we may call *weak separation* and *strong separation*, where the former encompasses all cases of undefined, i.e variable, separation locations, while the latter describes flow situations with fixed separation. In this sense all flows discussed in Chaps. 2 and 3 are of course separated flows – strong as in the cases of jets or mixing layers or wakes of sharp edged bodies, or weak as in wake flows past bodies with smooth surfaces. Other than in those cases we shall deal in this chapter only with separated flows where effects of the wall are still present to such an extent that it strongly influences the flow considered (Gad-el-Hak and Bushnell 1991).

Weak (Undefined) Separation. A typical example of a weakly separating flow and at the same time a flow of high practical importance is the boundary layer at incipient separation as e.g. on an aerodynamic wing surface. Given the possibility to control this flow, thereby preventing or delaying separation, we have an instrument to control its aerodynamic performance—in particular the lift and drag characteristics. Again, such a separating boundary layer may be influenced by passive or by active means. The point or line of separation depends essentially on the surface contour, the pressure gradient and the boundary layer profile.

Separation on an airfoil may be caused by genuine separation of the boundary layer itself or by bursting of the leading edge separation bubble. In both cases the wall boundary layer leaves the wall and develops into a free shear layer which is still influenced on one side by the wall. Since the free shear layer is by far more susceptible to control than the boundary layer, it is the former which can be influenced most easily. Attempts to control this kind of flow effectively and reliably date back to early times in aerodynamic

history. True success is, however, only of recent. Apart from passive methods as e.g. optimal shaping of the wing section or introducing longitudinal vorticity to increase the vertical exchange of energy and momentum by vortex generators, substantial increase of lift coefficients seems to be possible only through active control methods. Those are either by boundary layer suction, influencing the L/T-transition via feedback, or based on periodic forcing of the separated boundary layer, which, when properly agitated, increases its entrainment on the lower side and may therefore reattach (Coanda effect).

Various technologically feasible means for introducing the periodic vorticity into the boundary layer near its incipient separation have been suggested and investigated, e.g.

1. vibrating flaps as e.g. by piezoelectric actuator (Nishri and Wygnanski 1996),
2. acoustic excitation, (Stone and McKinzie 1984; Ahuja and Burrin 1984), or
3. periodic tangential blowing.

It appears that tangential blowing—under certain circumstances with steady blowing added—has been most thoroughly investigated (e.g. Nishri and Wygnanski 1996; Seifert et al. 1993a, 1993b) and provides one of the best ways of separation control of high efficiency. At elevated Mach numbers ($Ma > 0.3$) steady blowing is of reduced effect. An even more efficient way of introducing periodicity is by piezoelectric actuators. There, however, it is important to choose the proper location of the flap, since its efficiency is only guaranteed when it is upstream and near to the point of separation. The effect of periodic tangential blowing is on the other hand less sensitive to its location, which is typically near the leading edge of the profile (Fig. 69).

In fact, an excited separated boundary layer (becoming a mixing layer when separated) will approximately follow the curved surface contour, thereby causing a pressure distribution on the surface which in turn provides considerable lift increase although true reattachement may never be achieved. If separation is achieved, it is importand to observe the fact, that the lift characteristic (C_L)*vs.* angle of attack (α) is typically hysteretic: Once the flow stalls at a given α, the angle of attack has to be taken back to much smaller values to achieve reattachement—see Fig. 70.

Strong (Defined) Separation. Cases of strong, i.e. defined separation of a flow which is influenced by a nearby wall are abundant in technological applications. While separating flows over smooth ramps or through diffusors (two- and three-dimensional) may still be categorized under 'weakly' separating flows, whenever those ducts have sharp edges—as will be mostly the case for manufacturing reasons—the separation is fixed to those edges.

A classical model case for this kind of flow is the backward facing step. Its two-dimensional configuration has been abundantly investigated for various

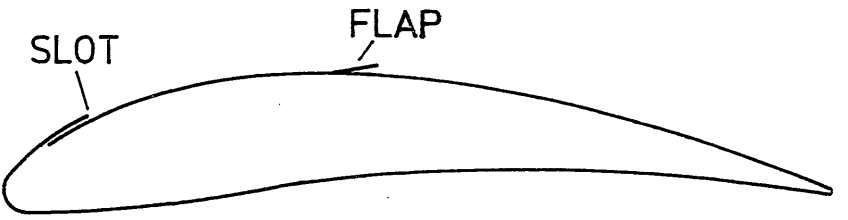

Fig. 69. Typical locations of actuators on wing surface.

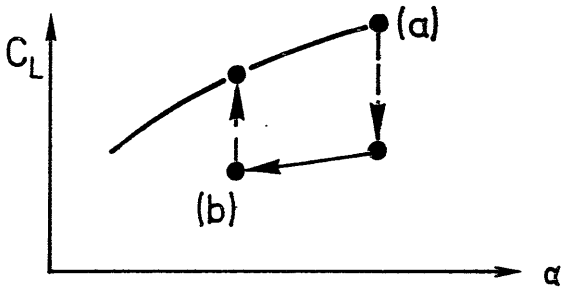

Fig. 70. Lift hysteresis for airfoil with periodic tangential blowing – (a) separation, (b) reattachment.

boundary conditions and parameters. To control this flow with the major purpose of reducing its pressure loss (e.g. for a sudden axpansion in a pipe) or its drag as in the case of a truck or a train, we have the following possibilities at our command (for configurations see Fig. 71):

1. Passive control by
   - giving it an appropriate form—e.g. as a 'cusp-diffusor' (Ringleb 1951),
   - perturbed upstream boundary conditions (shaping the trailing edge such as to introduce longitudinal vorticity).
2. Active control by
   - suction and/or blowing, or by
   - periodic excitation of the separated flow.

The diagrams of Fig. 72a–72d summarize results recently obtained for two step configurations where the normalized reattachment length x_R/s serves a criterion. Step (1) was investigated in a water tunnel at a Reynolds number of $Re = U_0 s/\nu \approx 4000$ and a step aspect ratio of $b/s = 2.5$. Investigations

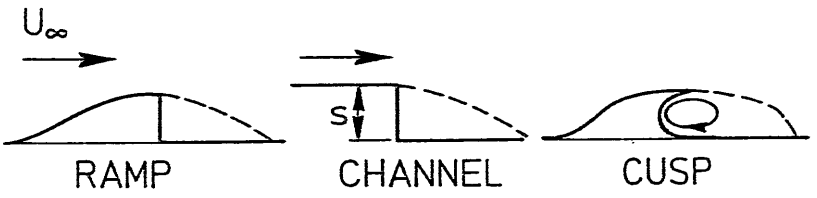

Fig. 71. Configurations of backward facing step.

with step (2) were done in a wind tunnel at $Re = 4800$, 15000, 27000, and aspect ratio $b/s = 15$ (s is the step height and b is the width).

Figures 72a–72d show the major results, where the suction rate is defined as $\dot{V}^* = \frac{\dot{V}_{\text{suction}}}{sbU_0}$.

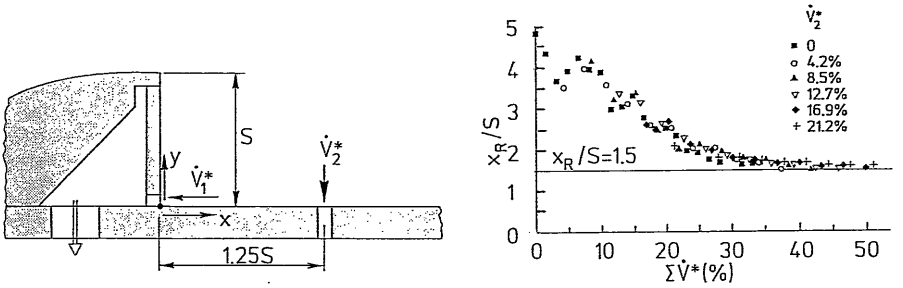

Fig. 72. a) Normal step with two suction ports.

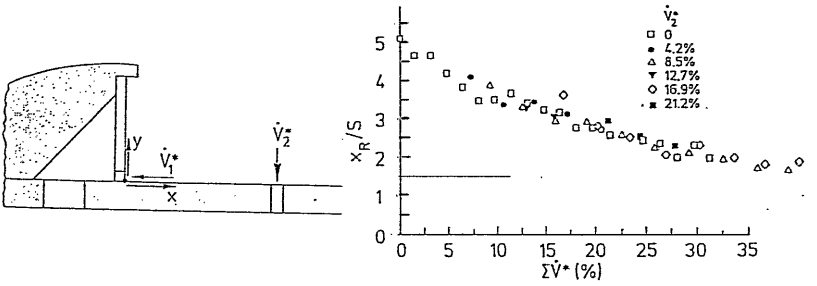

Fig. 72. b) Step with extended trailing edge (approximation of cusp)—two suction ports.

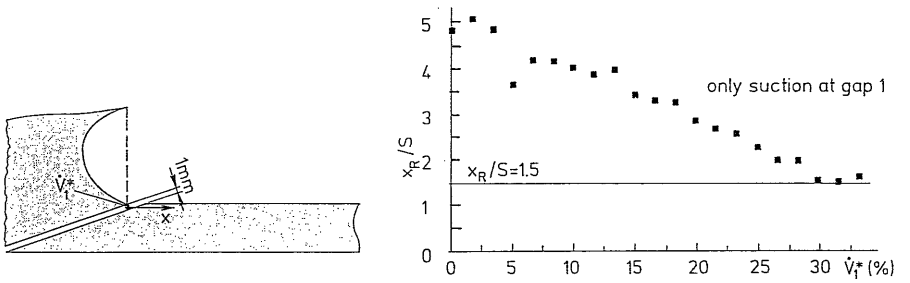

Fig. 72. c) Cusp with one suction port.

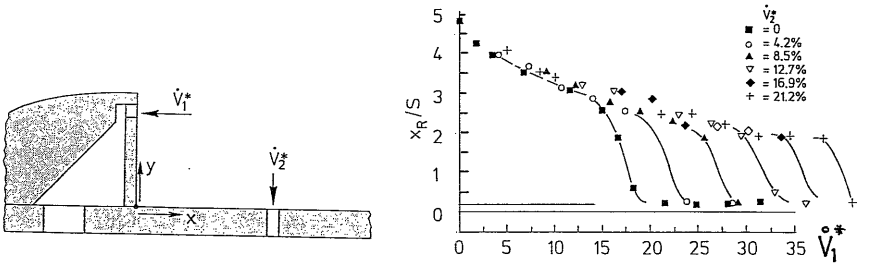

Fig. 72. d) Normal step. Suction through port below TE and port at bottom.

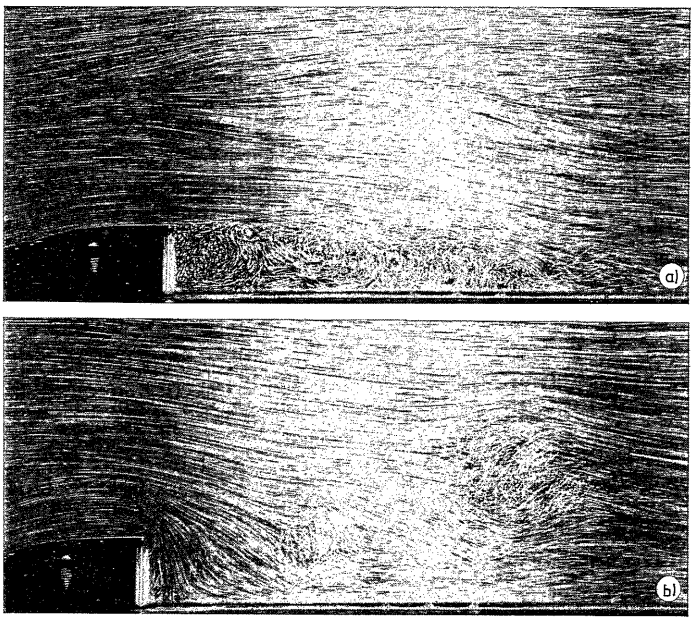

Fig. 73. Visualisations: (a) 'natural' flow; (b) full flow deflection as achieved in the configuration as in Fig. 72d.

Some results obtained with step (2) are shown in Fig. 74 (a,b).

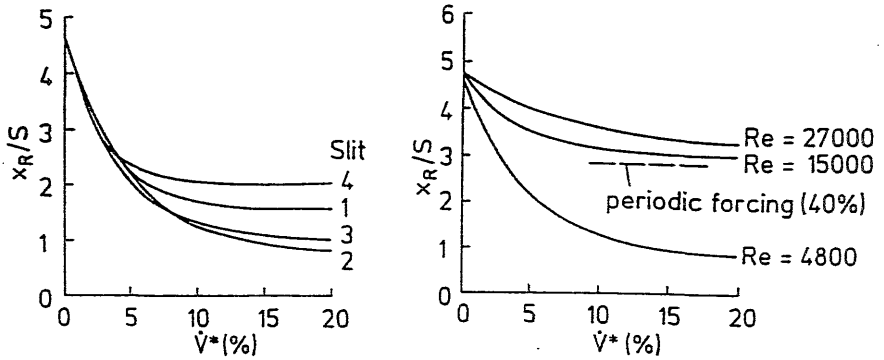

Fig. 74. Effects of control by suction—step (2): (a) Influence of suction rate and location of suction port; (b) influence of Reynolds number.

Based on those results the effect of control by suction on the step flow performance may be thus summarized:

- Suction has strong effect on the reattachement length, particularly for suction rates $5\,\% \leq \dot{V}^* \leq 10\,\%$; for $\dot{V}^* > 10\,\%$ the effect is comparatively small.
- In the uncontrolled flow $x_R/S \approx 5$. Minimum reattachement length which is achieved by suction at locations other than at or near the TE is $x_R/S = 1 - 1.5$ for $\dot{V}^* > 30\,\%$, where the location of the suction port is irrelevant as long as it is not too far downstream.
- With $\dot{V}^* < 5\,\%$ the flow downstream of the step is unstable, becoming more stable for $\dot{V}^* > 10\,\%$.
- Strong suction stabilizes the corner vortex behind the step without extension. Better stabilization, also for lower suction rates, is achieved with extension of TE.
- The effect of a cusp form as well as of a TE-extension on x_R is insignificant.
- **Suction with $\dot{V}^* \geq 20\,\%$ near the TE without extension causes complete deflection of the flow (no separation). In this case a region of high turbulence level is found further downstream (see Fig. 73).**
- With suction through the backward facing wall with $\dot{V}^* > 10\,\%$ a particular vortex shedding downstream of the step is observed. It is characterized by a Strouhal number $St = fs/U \approx 0.03$.
- **With increasing Reynoldsnumber the effect of suction is reduced.**
- With respect to efficiency the investigated direct control through steady suction is by far inferior to the indirect control by periodic forcing at the TE (discussed below), since the latter utilizes the amplification characteristic of the mixing layer flow with a typical gain of order 100.

– Extreme situations, as e.g. full flow deflection, seem, however, possible only via steady suction, while the dynamic method appears to be limited to $x_R/s_{min} \approx 2$.

In some technical applications where the step is in a flow region of elevated pressure, it might be possible to provide effects as found for suction simply by local bleeding. Combining suction with blowing at the same flow rate into the separated region may cause the step flow to become absolutely unstable.

The possibility of controlling the step flow by periodic perturbations introduced at the trailing edge was studied by Sung and Chun (1996). His setup is shown in Fig. 75, with the major effects achieved with high forcing at amplitudes of 35 % and 50 % of U_0 given in Fig. 76. Lower levels of forcing are needed for laminar separation (Huppertz and Janke 1997). Applications for this method are found in combustion control as described by McManus et al. (1993).

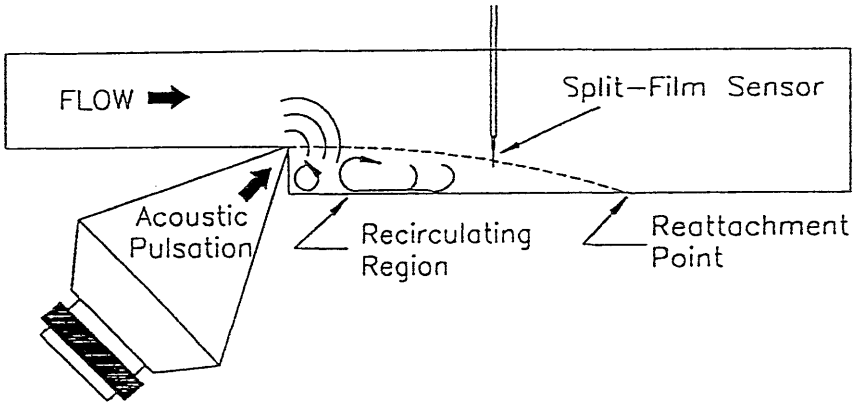

Fig. 75. a) Sung and Chun's (1996) setup for periodically excited step flow.

4.3 Confined Flow

Interactions may often cause self sustained oscillations as a consequence of internal feedback in the flow. Various cases of flow interaction and self sustained oscillation have been described by Rockwell and Naudascher (1979), Weir and Bradshaw (1974) and Ziada and Rockwell (1981). The influence of the system response on the coherent structures in a confined shear layer was studied by Veynante et al. (1986).

Growth and structure of a free mixing layer are found to be considerably influenced by the lateral extent of the flow at reduced relative side wall distance and may under certain conditions cause undesired perturbations in

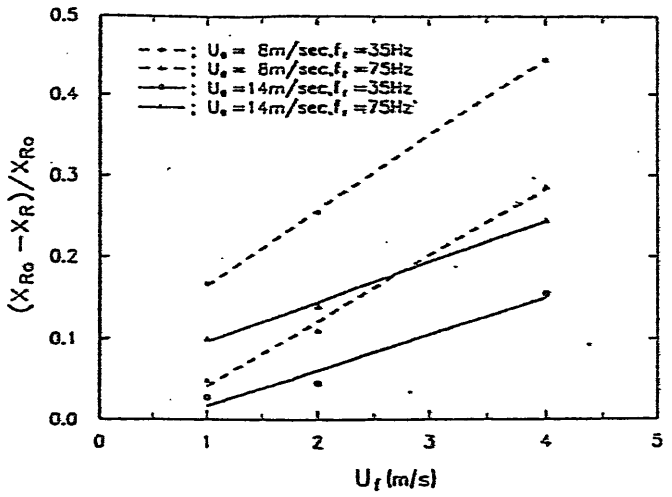

Fig. 75. b) Reduction of relative reattachment length $\frac{X_{R_0} - X_R}{X_{R_0}}$ achieved by periodic excitation (Sung and Chun 1996), versus pulsating velocity.

the flow to be studied. Investigations of this condition in a one-stream layer ($\lambda = 1$) were reported by Hilberg and Fiedler (1989): With increasing aspect ratio $A = L/h$ (see discussion in Chap. 3) a periodicity develops in the fluctuation spectrum, accompanied by considerable increase of spread. Phenomenologically similar observations of strong periodicity, which are, however, caused by different physical mechanisms, were reported by Giger (1987) for two-dimensional jets in shallow water (e.g. river estuaries). Active feedback interaction experiments in a shear layer have been reported by Dimotakis and Koochesfahani (1987).

4.4 Combined Flows

Classical combinations of shear flows are obtained by combinations of the basic model flows, e.g. wall jets and wall wakes. There is a considerable body of knowledge about controlling those flows, in particularly the wall jet (e.g. Zhou et al. 1996). We shall discuss here only a few special cases.

Confined/Combined Flow. *Mixing layer in a pipe:* This is a configuration of some potential for mixing and heat transfer. In all realistic cases of mixing layer flow there is always a wall influence present, albeit often negligible, and it may not be unwelcome under all circumstances. Thus, the confined mixing layer in a pipe is not a simply a superposition of a mixing layer and pipe flow, and visualization discloses a variety of phenomena which so far are not explained. This is particularly true for the case of periodic flow

excitatiation at low Reynolds numbers where one observes singular critical mixing phenomena, which are not known from the 'ordinary' mixing layer and are also not found in a simple pipe flow (Wang and Fiedler).

Flow-Body/Surface-Interaction—Impinging Flows. A summary of basic configurations and possibilities for natural feedback in flows with flow-body interaction was presented by Rockwell and Naudascher (1979). The configurations shown in Fig. 76 which are taken from this paper may be useful for designing control actuators; they may in other situations obviously be detrimental for flow and structures.

An example of flow control by utilizing an interaction effect of this kind is shown in Fig. 77. The pressure loss of a sudden expansion in a pipe can be reduced by approximataly 25 % with an orifice insert which by interaction causes a periodicity in the flow comparable to a periodically excited step flow as discussed above. This is an example of an efficient possibility of a simple and robust passive control, which, wherever its noisyness is of no importance, can be used in a large number of technological applications at high Reynolds numbers. Figure 77 shows relative reduction or increase of pressure loss parameter as a function of the orifice ratio d^*/d and the relative diaphragm position x/d for a given expansion ratio of $D/d = 2.24$.

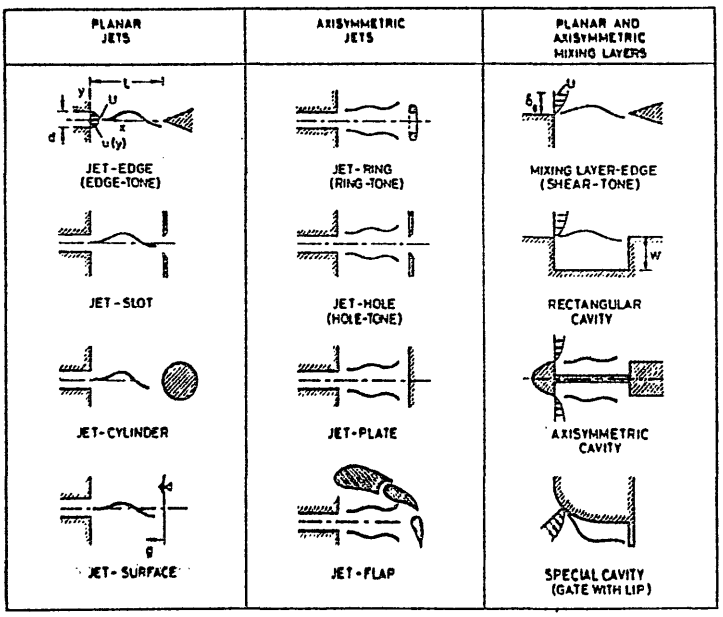

Fig. 76. Basic configurations of flow body interaction creating periodic fluctuations after Rockwell and Naudascher (1979).

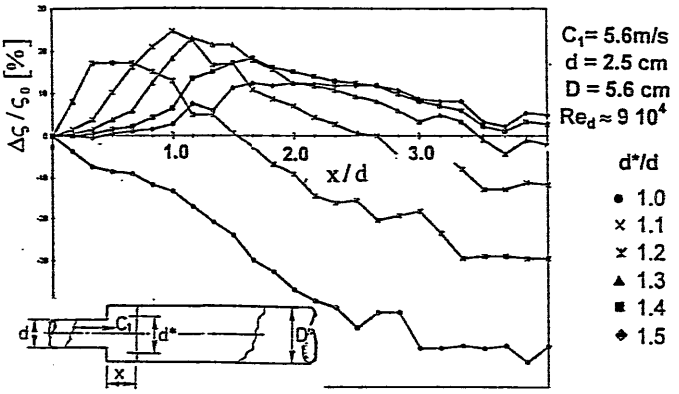

Fig. 77. Control of a sudden-expansion flow in a pipe by diaphragm insert.

4.5 Summarizing Remarks

Mixed configurations provide a multitude of control possibilities which are typically Reynolds number dependent. Some important onservations are:

1. Separation and lift in weakly separating flows can be controlled by passive means, e.g. stationary surface structures, and actively through suction, periodic excitation, or by L-T-transition control via adaptive feedback.
2. Strong separation flow can be controlled by suction (large effect, low efficiency) or by periodic excitation (small effect, high efficiency). Passive control by special contours is of small effect.
3. Feedback control of confined flow has good applications in combustion. Confined flows show large control effects—often by natural feedback (absolute instability).
4. Low Reynolds number confined flow is highly selective to frequency forcing with strong mixing potential.
5. Flow body interaction may cause strong, self-sustained periodicity.

5 General Summary

In trying to reduce the control problem to its essentials all of the above can be re-traced to two key phenomena:

1. turbulent mixing (re-distribution/diffusion) and—even more fundamentally:
2. turbulence creation/destruction, with its three aspects:
   - laminar/turbulent transition,
   - production,
   - dissipation.

What can be accomplished by control depends entirely on

1. the stability characteristics of the flow,
2. the efficiency of the control method applied, and
3. the interaction of the scales and energy mechanisms.

Thus, increasing the spread of a given free flow by 100 % is a comparatively easy task if one uses the proper 'tool': periodic excitation—thereby controlling the (creation and stabilization of) coherent structures. This may often provide the best results. And indeed also the mixing process, which is primarily related to the smaller eddies, "trapped" as it were in the large coherent ones, are controlled, however indirectly, by controlling the large ones. Other indirect ways of control, e.g. via entrainment (turbulence level of the primary streams) is, by comparison, only of small effect. The situation may be inverted for flows of strongly reduced instability, e.g. for mixing layers with low values of λ. Another parameter of influence is the ratio of convection to diffusion in a flow as discussed in the comparison of jet- and wake flow.

Reductions of certain characteristics, e.g. spread, on the other hand appears to be more limited. This is equally true for free flows and even more so for wall bounded flows, where the achievable reduction in frictional drag seems to be limited to approximately 10 %. What is of importance in any case is how, i.e. to what extent, the quality to be controlled depends on the quality which is (most easily and effectively) controllable.

There are two general spects to control: (1) Control proper: Initiation of control manifestations—instability modes ('tickling of flow' with high amplification gain) and (2) the reponse of the flow to modifications of basic—or boundary conditions. Ways and stratagems to influence a given flow and to achieve useful results in comparison with the efforts needed necessitate a clear knowledge about turbulent structural interplay, stability behaviour and amplification rates. Apart from the direct control of flow instability and thus of the primary structures by one or more frequencies, we have a number of passive mechanisms to influence turbulent structures, as e.g. by

- influencing the stability characteristics of the basic flow (walls, field effects), by modifying the mean velocity field, by
- influencing the stability of the basic coherent structure (wall geometry, field effects, upstream boundary conditions), thereby—in certain cases—, by
- influencing the feedback characteristics of the flow.

Finally: In mixed cases best conditions will be achieved when combining flow control with a control-adapted design.

Acknowledgement. I am grateful to Deutsche Forschungsgemeinschaft (DFG) for their support of some of the work presented, to the authors and publishers of some of the figures used in this text for their permission to do so, and finally to Frau S. Nordt and Frau E. Kulzer for their invaluable and ever patient help in preparing the manuscript.

References

Abramovich G. N. (1963): The theory of turbulent jets. MIT Press, Cambridge Mass.

Ahuja K. K., Burrin R. H. (1984): Control of flow separation by sound. *AIAA Paper 84-2298.*

Armstrong R. R. Jr. (1981): Influence of mach number on coherent structure relevant to jet noise. *AIAA Paper 81-4133.*

Armstrong R. R., Michalke A., Fuchs H. V. (1977): Coherent structures in jet turbulence and noise. *AIAA Journal* **15** (7), 1011–1017.

Barre S., Quine C., Dussauge J. P. (1994): Compressibility effects on the structure of supersonic mixing layers: experimental results. *J. Fluid Mech.* **259**, 47–78.

Batchelor G. (ed.) (1969): The scientific papers of G. I. Taylor. Vol. II, (Cambridge University Press).

Batt R. G. (1975): Some Measurements on the effect of tripping the two-dimensional shear layer. *AIAA Journal* **13** (2), 245–247.

Bechert D. W. (1985): Excitation of instability waves. *Z. Flugwiss. Weltraumforschung* **9**, 56–361.

Bechert D. W., Michel U. (1975): The control of a thin free shear layer with and without a semi-infinite plate by a pulsating flow field. *Acoustica* **33**, 287–307.

Bechert W. D., Pfitzenmeier E. (1976): On the amplification of broadband jet noise by a pure tone excitation. *AIAA Paper 76-489.*

Bechert W. D., Stahl B. (1988): Excitation of instability waves in free shear layers. Part 2, Experiments. *J. Fluid Mech.* **186**, 63pp.

Bejan A. (1981): On the buckling property of inviscid jets and the origin of turbulence. *Letters in Heat and Mass Transfer* **8**, 187–194.

Bell J. H., Mehta R. D. (1992): Measurements of streamwise vortical structures in a plane mixing layer. *J. Fluid Mech.* **239**, 213–248.

Berger E., Scholz D., Schumm M. (1990): Coherent vortex structures in the wake of a sphere and a circular disk at rest and under forced vibrations. *J. Fluids and Structures* 4, 231–257.

Berger E., Wille R. (1972): Periodic flow phenomena. *Annual Review of Fluid Mechanics* 4, 313–340.

Bernal L. P. (1981): The coherent structure of turbulent mixing layers. I: Similarity of primary vortex structure. II: Secondary streamwise vortex structure. PhD thesis CALTECH.

Bernal L. P., Roshko A. (1986): Streamwise vortex structure in plane mixing layers. *J. Fluid Mech.* **170**, 499–525.

Birch S., Eggers M. (1972): A critical review of the experimental data for developed free turbulent shear layers. Free Turbulent Shear Flows. *NASA SP-321*, 11–40.

Blümel B. (1993): Computergestützte Strömungssichtbarmachung. Diplomarbeit, Technische Universität Berlin.

Boree J., Atassi N., Charnay G. (1996): Phase averaged velocity field in an axisymmetric jet subject to a sudden velocity decrease. *Experiments in Fluids* **21**, 447–456.

Boussinesq J. (1879): Theorie de l'ecoulement tourbillant. Me. pre. par. div. Sav. XXIII, Paris.

Bradshaw P. (1966): The effect of initial conditions on the development of a free shear layer. *J. Fluid Mech.* **26** (2), 225–236.

Bremhorst K. Watson R. D. (1981): Velocity field and entrainment of a pulsed core jet. *J. Fluid Eng. Trans. ASME* **104** (4), 605–608.

Browand F. K., Ho C.-M. (1983): The mixing layer: an example of quasi two-dimensional turbulence. *J. de Mechanique Theorique et Appliquee* **99**.

Brown G. B. (1935): On vortex motion in gaseous jets and the origin of their sensitivity to sound. *Phys. Soc. XLVII* 4, 703-732.

Brown G. L., Roshko A. (1974): On density effects and large structure in turbulent mixing layers. *J. Fluid Mech.* **64** (4), 775–816.

Chandrsuda C., Mehta R. D., Weir A. D., Bradshaw P. (1978): Effect of free-stream turbulence on large structure in turbulent mixing layer. *J. Fluid Mech.* **85**, 693–704.

Coanda H. (1934): Procede et dispositif pour faire devier une veine fluide penetrautre fluids. French Patent 788, 140.

Cohen J., Wygnanski I. (1987a): The evolution of instabilities in the axisymmetric jet. Part 1. The linear growth of disturbances near the nozzle. *J. Fluid Mech.* **176**, 191–219.

Cohen J., Wygnanski I. (1987b): The evolution of instabilities in the axisymmetric jet. Part 2: The flow resulting from the interaction between two waves. *J. Fluid Mech.* **176**, 221–235.

Counihan J (1969): An improved method of simulating an atmospheric boundary layer in a windtunnel. *Atm. Env.*, p. 197–214.

Crighton D.G. (1981): Jet noise and the effects of jet forcing. In *The Role of Coherent Structures in Modelling Turbulence and Mixing*, (ed. J. Jimenez), *Lecture Notes in Physics* **136**. (Springer).

Crow S. C., Champagne F. H. (1977): Orderly structure in jet turbulence. *J. Fluid Mech.* **48**, 567.

Dimotakis P. E. (1991): Turbulent free shear layer mixing and combustion. In *High Speed Flight Propulsion Systems*, eds. B. Murthy, E. T. Curran. *Progress in Astronautics and Aeronautics* **137**.

Dimotakis P. E., Brown G. L. (1976): The mixing layer at high Reynolds number: large structure dynamics and entrainment. *J. Fluid Mech.* **78** (3), 535–560.

Dimotakis P. E., Koochesfahani M. M. (1987): Activ feedback interaction with a shear layer. *Ann. Prog. Rept. AFOSR-84-01ss20.*

Dimotakis P. E., Miake-Lye R. C., Papantoniou D. A. (1982): Structure and dynamics of round turbulent jets. *GALCIT Report FM82-01*, CALTECH.

DiStefano J. J., Stubberud A. R. Williams (1979): "Schaums Outline"—Theory and Problems of Feedback and Control Systems with Applications to the Engineering, Physical and Life Sciences. McGraw Hill.

Drazin P. G., Reid W. H. (1981): Hydrodynamic stability. Cambridge Monographs on Mechanics and Applied Mathematics. Cambridge University Press.

Dubuat (1779): *Principes d'hydraulique.* Paris.

Dziomba B. (1981): Experimentelle Untersuchung zum Einfluss von Anfangs- und Randbedingungen auf die Ausbreitung einer freien zweidimensionalen Scherschicht. Dissertation, Technische Universität Berlin.

Dziomba B., Fiedler H. E. (1985): Effect of initial conditions on two-dimensional free shear layers. *J. Fluid Mech.* **152**, 419–442.

Eickhoff H. (1982): Instability and coherent structures in jet flames. In *Recent Contributions to Fluid Mechanics*, ed. W. Haase (Springer).

Fernholz H.-H. (1993): Management and control of turbulent shear flows. *ZAMM* **73** (11), 287–300.

Fiedler H. E. (1988a): Coherent structures in turbulent flows. *Prog. Aerospace Sci.* **25**, 231–269.

Fiedler H. E., Dziomba B. Mensing P., Rösgen T. (1981): Initiation, evolution and global consequences of coherent structures in turbulent shear flows. In *The role of coherent structures in modelling turbulence and mixing*, ed. J. Jimenez. *Lecture Notes in Physics* (Springer).

Fiedler H. E., Fernholz H.-H. (1991a): On management and control of turbulent shear flows. *Prog. Aerospace Sci.* **27**, 305–387.

Fiedler H. E., Glezer A., Wygnanski I. (1988b): Control of plane mixing layer: Some novel experiments. In: *AIAA Series, Current trends in turbulent research* **112**, 30–64, eds. H. Branover, M. Mond, Y. Ungers.

Fiedler H. E., Gründel H., Spieweg R. (1995): Some observations in three-dimensional mixing layers. Proceedings, Indian Institute of Science, Bangalore, India.

Fiedler H. E., Kim J.-H., Köpp N. (1991b): The spatially accelerated mixing layer in a tailored pressure gradient. *Eur. J. Mech. B/Fluids* **10** (4), 349–376.

Fiedler H. E., Korschelt D., Mensing P. (1978a): On transport mechanism and structureof scalar field in a heated plane shear layer. In *Structure and Mechanisms of Turbulence II*, ed. H. E. Fiedler. *Lecture Notes in Physics* **76**, 58–72 (Springer).

Fiedler H. E., Lummer M., Nottmeyer K. (1993): The plane mixing layer between parallel streams of different velocities and different densities. *Advances in Turbulence*, eds. H. Branover, Y. Unger. *AIAA Series on Progress in Aeronautics and Astronautics.*

Fiedler H. E., Mensing P. (1985): The plane turbulent shear layer with periodic excitation. *J. Fluid Mech.* **150**, 281–309.

Fiedler H. E., Nayeri C. N., Spieweg R., Paschereit C. 0. (1997): Three-dimensional mixing layer. *Experimental Thermal and Fluid Science*, in press.

Fiedler H, Thies H. J. (1978b): Some observations in a large two-dimensional shear layer. In *Structure and Mechanisms of Turbulence I*, ed. H. E. Fiedler. *Lecture Notes in Physics* **75**, 108–771 (Springer).

Foss J. F. (1977): The effects of the laminar/turbulent boundary layer state on the development of a plane mixing layer. In *Turbulent Shear Flows*, proceedings, pp. 11.33–11.42. Pen. State Univ.

Fulachier L., Borghi R., Anselmet F., Parantheon P. (1989): Influence of density variations on the structure of low-speed turbulent flows: A report on EUROMECH 237. *J. Fluid Mech.* **203**, 577–593.

Gad-el-Hak M., Bushnell D. (1991): Separation control: Review. *J. Fluids Eng.* **113**, 5–30.

Gaster M., Kit E., Wygnanski I. (1985): Large scale structures in a forced mixing layer. *J. Fluid Mech.* **150**, 23–39.

Giger M. (1987): Der ebene Freistrahl im flachen Wasser. Dr. thesis, ETH Zürich.

Gründel H., Fiedler H. E. (1992): The mixing layer between non-parallel streams. *European Turbulence Conference (ETC) 4*, Delft, 167–171.

Gründel H., Spieweg R., Fiedler H. E. (1995): The mixing layer behind a slanted trailing edge. *Advances in Turbulence V*, ed. R. Benzi (Kluwer), 171–178.

Guicking, D. (1988): Active noise and vibration vontrol. Reference bibliography, 3rd edition, Göttingen.

Gurecki D. J. (1981): Effect of modification of the trailing edge of a separating wall on the downstream mixing of parallel flowing streams. MS-thesis, Air Force Institute of Technology, Ohio.

Gutmark E., Ho C.-M. (1983a): On a forced elliptic jet. *Proc. 4th Turbulence Shear Flow Conf.*, Karlsruhe, Germany.

Gutmark E., Ho C.-M. (1983b): Preferred modes and the spreading rates of jets. *Phys. Fluids* **26** (10), 2932.

Gutmark E., Schadow K. C., Wilson K. J., Parr D.M. (1986): Small scale mixing enhancement in acoustically excited jets. *10th Aeroacoustics Conf.*, Seattle, Wa. *AIAA Paper 86-1885.*

Gutmark E. J., Schadow K. C., Yu K. H. (1995): Mixing enhancement in supersonic free shear flows. *Annu. Rev. Fluid Mech.* **27**, 375–417.

Gyr A. (1997): Effects of polymer additives on the large scale structure of a two-dimensional submerged jet. To appear in *Experiments in Fluids.*

Heine C., Spieß M. C., Möser M., Fiedler H. E. (1997): The influence of feedback control on the vortex dynamics in a turbulent cylinder wake. *Euromech Coll. 361*, Technische Universität Berlin.

Heskestad G. (1966): Hot-wire measurements in a radial turbulent jet. Trans. of the ASME. *J. Appl. Mech.* pp. 417–424.

Hilberg D. (1993): Die seitlich eng begrenzte Scherschicht. Dissertation, Technische Universität Berlin.

Hilberg D. (1996): Repeatedly deflected jets and flames. Unpublished. Hermann-Föttinger-Institut, TU-Berlin.

Hilberg D., Fiedler H. E. (1989): The spanwise confined mixing layer. *Advances in Turbulence* **2**, eds. H.-H. Fernholz and H. E. Fiedler (Springer).

Ho C. M. (1982a): Local and global dynamics of free shear layers. In *Numerical and Physical Aspects of Aerodynamic Flow*, Chap. 30, ed. T. Cebeci (Springer).

Ho C. M., Gutmark E. (1987): Vortex induction and mass entraiment in a small aspect ratio elliptic jet. *J. Fluid Mech.* **179**, 383–405.

Ho C. M., Huang L. S. (1982b): Subharmonics and vortex merging in mixing layers. *J. Fluid Mech.* **119**, 443–473.

Ho C.-M., Huerre P. (1984): Perturbed free shear layers. *Ann. Rev. Fluid Mech.* **16**, 365–424.

Ho C. M., Nosseir N. (1981): Dynamics of an impinging jet. Part 1. The feedback phenomenon. *J. Fluid Mech.* **105**, 119–142.

Huerre P., Monkewitz P. A. (1985): Absolute and convective instabilities in free shear layers. *J. Fluid Mech.* **159**, 151–168.

Huerre P., Monkewitz P. A. (1990): Local and global instablilites in spatially developing flows. *Ann. Rev. Fluid Mech.* **22**, 473–537.

Huppertz A., Janke G. (1997): Some user results on the control of the flow over a backward forcing step. *Euromech Colloquium 361*, Technische Universität Berlin.

Husain Z. D., Hussain A. K. M. F. (1979): Axisymmetric mixing layer: Influence of the initial and boundary conditions. *AIAA Journal* **17** (1), 48–55.

Husain Z. D., Hussain A. K. M. F. (1983): Controlled excitation of elliptic jets. *Phys. Fluids* **26** (10), 2763-2766.

Husain Z. D., Hussain A. K. M. F. (1995): Experiments on subharmonics in a shear layer. *J. Fluid Mech.* **304** 343–372.

Hussain A. K. M. F., Husain H. S. (1988): Passive and active control of jet turbulence. In: *Turbulence management and relaminarization*, eds. H. W. Liepmann and R. Narasimha (Springer).

Hussain A. K. M. F., Husain H. S., Zaman K. B. M. Q., Tso J., Hayakawa M., Takaki R., Hasan M. (1986): Free shear flows: organized structures and effects of excitation. *AIAA Paper 86-0235.*

Hussain A. K. M. F., Zedan M. F. (1978a): Effects of initial condition on the axisymmetric free shear layer: Effects of the initial momentum thickness. *Phys. Fluids* **21**, 1100–1111.

Hussain A. K. M. F., Zedan M. F. (1978b): Effects of initial condition on the axisymmetric free shear layer: Effects of initial fluctuation level. *Phys. Fluids* **21**, 1475–1481.

Inoue O. (1992): Double frequency forcing on spatially growing mixing layers. *J. Fluid Mech.* **234**, 553–581.

Joseph D. D. (1976): Stability of Fluid Motions I and II. *Springer Tracts in Natural Philosophy*, vols. 27 and 28. (Springer).

Keffer F. F., Kawall J. G., Hunt J. C. R., Maxey M. R. (1978): The uniform distortion of thermal and velocity mixing layers. *J. Fluid Mech.* **86** (3), 465–490.

Kibens V. (1980): Discrete noise spectrum by an acoustically excited jet. *AIAA Journal* **18**, 434–441.

Kibens V. (1989): Jet flows and turbulence control. *AIAA Paper 89-105.*

Kibens V., Wlezien R. W., Kegelman J. T. (1988): Trailing-edge sweep and three dimensional vortex interactions in jets and mixing layers. *AGARD CP 438.*

Koch W. (1985): Local instability characteristics and frequency determination of self-excited wake flows. *J. Sound Vibr.* **99**, 53–83.

König O., Fiedler H. E. (1991): The structure of round turbulent jets in counterflow: a flow visualization study. In *Advances in Turbulence* **3**, 61–66, eds. A. V. Johansson and P. H. Alfredsson (Springer).

König O., Fiedler H. E. (1995): Some experimental results on a decelerated mixing layer. *Advances in Turbulence* **V**, 276–280, ed. R. Benzi (Kluwer).

Konrad J. H. (1977): An experimental investigation of mixing in two-dimensional turbulent shear flows with application to diffusion-limited chemical reactions. Ph.D. thesis. CALTECH.

Koochesfahani M. M., Frieler C. E. (1987): Inviscid instability characteristics of free shear layers with non-uniform density. *AIAA 25th Aerospace Sciences Meeting*, Reno, Nevada. *AIAA Paper 87-0047.*

Korschelt D. (1980): Experimentelle Untersuchung zum Wärme- und Stofftransport im turbulenten ebenen Freistrahl mit periodischer Anregung am Düsenaustritt. Dissertation, Technische Universität Berlin.

Kumori S., Ueda H. (1985): The large-scale coherent structure in the intermittent region of the self-preserving round free jet. *J. Fluid Mech.* **152**, 337–359.

Kwade M. (1982): Beeinflussung der Turbulenzstruktur in der ebenen Mischungsschicht zweier Ströme durch Polymerzusätze. *Rheologica Acta* **21**, 120–149.

Lasheras J. C., Cho J. S., Maxworthy T. (1986): On the origin of streamwise vortical structures in a plane, free shear layer. *J. Fluid Mech.* **172**, 231–258.

Lasheras J. C, Choi H. (1988): Three-dimensional instability of a plane shear layer: an experimental study of the formation and evolution of streamwise vortices. *J. Fluid Mech.* **189**, 53–86.

Laufer J., Monkewitz P.A. (1980): On turbulent jet flow in a new perspective. *AIAA Paper 80-0962.*

Laufer J., Ta-Chun Y. (1983): Noise generation by a low mach number jet. *J. Fluid Mech.* **134**, 1–31.

Leconte J. (1858): On the influence of musical sounds on the flame of a jet of coal-gas. *Philos. Magazine J. Sci.* **XV**, 235–239, London, Edinburgh and Dublin.

Lee, M. Reynolds W. C. (1985): Bifurcating and blooming jets. *Fifth Symposium on Turbulent Shear Flows*, pp. 1.7–1.12 (Springer).

Lessen M. Paillet F. (1976): Marginal instability of turbulent shearing layers and the break point of a jet. *Phys. Fluids* **19**, 943.

Lu G., Lele S. K. (1994): On the density ratio effect on the growth rate of a compressible mixing layer. *Phys. Fluids* **6** (2), 1073–1075.

Lummer M. (1989): Numerische Untersuchung der inkompressiblen ebenen Scherschicht zwischen Gasen unterschiedlicher Dichte. Dissertation, Technische Universität Berlin.

Luo J. S., Fiedler H. E. (1997): On the evolution of large scale structures in three-dimensional mixing layers. Submitted to J. Fluid Mech.

McManus K. R., Poinsot T., Candel S. M. (1993): A Review of Active Control of Combustion Instabilities. *Prog. Energy Combust. Sci.* **19**, 1–29.

Michalke A. (1965): On spatially growing disturbances in an inviscid shear layer. *J. Fluid Mech.* **23**, 521–544.

Michalke A. (1972): The instability of free shear layers. *Prog. Aerospace Sci.* **12**, 213–239.

Michalke A. (1978): On source coherence affecting jet noise. In *Structure and Mechanisms of Turbulence II*, ed. H. Fiedler, *Lecture Notes in Physics* **76** 171–180 (Springer).

Michalke A. (1984): Survey on Jet Instability Theory. *Prog. Aerospace Sci.* **21**, 159–199.

Michalke A. (1990): On the inviscid instability of wall-bounded velocity profiles close to separation. *Z. Flugwiss. Weltraumforsch.* **14**, 24–31.

Michalke A., Hermann G. (1982): On the inviscid instability of a circular jet with external flow. *J. Fluid Mech.* **114**, 343–359.

Michalke A., Wehrmann O. (1964): Akustische Beeinflussung von Freistrahlgrenzschichten. *Proc. Intern. Council Aeronaut Sci., Third Congress*, Stockholm, Washington, London, pp. 773–785.

Monkewitz P. A. (1989): Feedback Control of Global Oscillations in Fluid Systems. *AIAA 2nd Shear Flow Conference*, March 13-16, Tempe, Az., *AIAA Paper 89-0991.*

Monkewitz P. A., Bechert D. W., Barsikow B., Lehmann B. (1990): Self-excited oscillations and mixing in a heated round jet. *J. Fluid Mech.* **213**, 611–639.

Monkewitz P. A., Huerre P. (1982): Influence of the velocity ratio on the spatial instability of mixing layers. *Phys. Fluids* **25** (7), 1137–1143.

Monkewitz P. A., Sohn K. D. (1986): Absolute instability in hot jets and their control. *AIAA Paper 86-1882.*

Morkovin M. V., Paranjape S. V. (1971): On acoustic excitation of shear layers. *Z. Flugwiss.* **19**, 328–335.

Morris P. J. (1976): The spatial viscous instability of axisymmetric jets. *J. Fluid Mech.* **77**, 511–529.

Morris P. J. (1983): Viscous instability of compressible axisymmetric jets. *AIAA Journal* **21**, 481–482.

Nagib H. M., Corke T. C. (1984a): Wind microclimate around buildings: Characteristics and control. *J. Wind Eng. Indust. Aero.* **16**, 1–5.

Nagib H. M., Marion A. (1984b): On the design of contractions and settling chambers for optimal turbulence manipulation in wind tunnels. *AIAA Paper 85-0536.*

Nieberle R. (1986): Entwicklung einer Methode der Mustererkennung zur Analyse kohärenter Strukturen und ihre Anwendung im turbulenten Freistrahl. Fortschrittsberichte VDI, Reihe 7: Strömungsmechanik, Nr. 106 (VDI Verlag).

Nishri B., Wygnanski I. (1996): On Flow separation and its control. ECOMASS.

Norum, T. D. (1982): Screech suppression in supersonic jets. *AIAA Paper 82-0050.*

Nottmeyer K. (1990): Experimentelle Untersuchung der Ausbildung und Turbulenzstruktur von turbulenten Scherschichten zwischen Gasströmen unterschiedlicher Geschwindigkeit und Dichte. Dissertation, Technische Universität Berlin.

Nygaard K. J., Glezer A. (1991): Evolution of streamwise vortices and generation of small-scale motion in a plane mixing layer. *J. Fluid Mech.* **231**, 257–301.

Oster D., Wygnanski I. (1982): The forced mixing layer between parallel streams. *J. Fluid Mech.* **123**, 91–130.

Oster D., Wygnanski I., Dziomba B., Fiedler H. E. (1978): On the effect of initial conditions on the two-dimensional turbulent mixing layer. In *Structure and Mechanisms of Turbulence I*, ed. H. Fiedler. *Lecture Notes in Physics* **75**, 48–64 (Springer).

Osthues J. (1986): Experimentelle und theoretische Untersuchungen an einem periodisch schwingenden turbulenten Freistrahl. VDI-Verlag, Reihe 7 (Strömungstechnik), Vol. 105 .

Parekh D. E., Kibens V., Glezer A., Wiltse J. M., Smith D. M. (1996): Innovative Jet Flow Control: Mixing enhancement experiments. *AIAA Paper 96-0308.*

Paschereit C. O., Fiedler H. E.: The formation and suppression of a three-dimensional structure in a plane shear layer initiated by secondary vortices in the wind tunnel nozzle. Submitted for publication.

Paschereit C. O., Oster D., Long T. A., Fiedler H. E., Wygnanski I. (1992): Flow Visualization of Interactions among large coherent structures in a axisymmetric jet. *Experiments in Fluids* **12**, 189–199.

Paschereit C. O., Schüttpelz M., Fiedler H. E. (1989): The mixing layer between non-parallel walls. *Advances in Turbulence* **2**, eds. H.-H. Fernholz and H. E. Fiedler (Springer).

Paschereit C. O., Wygnanski I., Fiedler H. E. (1995): Experimental investigation of subharmonic resonance in an axisymmetric jet. *J. Fluid Mech.* **283** 365–407.

Peters N., Williams F.A. (1981): Coherent Structures in Turbulent Combustion. In *The Role of Coheren Structures in Modelling Turbulence and Mixing*, ed. J. Jimenez (Springer).

Peterson R. A. (1978): Influence of Wave Dispersion on Vortex Pairings in a Jet. *J. Fluid Mech.* **89** (3), 469–495.

Peterson R. A., Samet M. M. (1988): On the prefered mode of jet instability. *J. Fluid Mech.* **194**, 153–173.

Plaschko P. (1981): Stochastic model theory for coherent turbulent structures in circular jets. *Phys. Fluids* **24** (2), 187–193.

Plesniak M. W., Mehta R. D., Johnston J. P. (1994): Curved two-stream turbulent mixing layers: three-dimensional structure and streamwise evolution. *J. Fluid Mech.* **270**, 1–50.

Prandtl L. (1914): Der Luftwiderstand von Kugeln. Nachr. Ges. Wiss. Göttingen, Math. Phys. Klasse, 177–190.

Prandtl L. (1961): Gesammelte Abhandlungen in 3 Teilen, eds. W. Tollmien, H. Schlichting, H. Görtler and F. W. Riegels (Springer).

Raghu S., Lehmann B., Monkewitz P. A. (1990): On the mechanism of side-jet generation in periodically excited axisymmetric jets. *Third European Turbulence Conference*, Stockholm.

Rajaratnam N. (1976): Turbulent Jets. Elsevier, Amsterdamm.

Rebel J., Grützmacher V., Neuwald P., Ronneberger D. (1992): Towards the control of free shear layers: Accoustic pressure gradient versus vorticity wave. *Proc. 14th Aeroacoust. Conf.* 949–957, *AIAA Paper 92-02-162.*

Rebollo M. R. (1972): Analytical and experimental investigation of a turbulent mixing layer of different gases in a pressure gradient. PhD Thesis, CALTECH.

Reynolds 0. (1883): An experimental investigation of the circumstances which determine whether the motion of water shall be direct or sinuous, and of the law of resistance in parallel channels. *Phys. Trans. R. Soc.*, **174**, 935–982, Lond.

Riediger S. (1989): The influence of drag reduction additives on the coherent structures in a free shear layer. *Advances in Turbulence* **2**. Proceedings, eds. H.-H. Fernholz, H. E. Fiedler (Springer).

Ringleb F. O. (1951): Theory and application of the flow over a cusp. United States Navy, ONR, Contract N6onr-27016, Princeton University, Aeronautical Engineering Laboratory, Report no. 192.

Roberts F. A. (1985): Effects of periodic disturbance on structure and mixing in turbulent shear layers and wakes. Ph.D. thesis, CALTECH.

Rockwell D., Naudascher E. (1979): Self-sustained oscillations of impinging free shear layers. *Ann. Rev. Fluid Mech.* **11**, 67–94.

Roffman G. L., Toda K. (1969): A discussion of the effects of sound on jets and flueric devices. *J. Eng. Industry*, pp. 1161–1167.

Roshko A. (1954): On drag and shedding frequency of two-dimensional bluff bodies. *NACA TN-3169.*

Sabin C. (1963): An analytical and experimental study of the plane, imcompressible, turbulent free shear layer with arbitrary velocity ratio and pressure gradient. *Tech. Rep. MD.* **9**, Stanford Univ., Stanford, California.

Scholz D. (1985): Kohärente Wirbelstrukturen im Nachlauf einer ruhenden und einer schwingungserregten Kreisscheibe. Dissertation TU-Berlin.

Schowalter D. G., Van Atta C. W., Lasheras J. C (1993): A Study of streamwise vortex structures in a stratified shear layer. *J. Fluid Mech.* **11**, 1–100.

Schumm M. (1991): Experimente zum Problem der absoluten und konvektiven Instabilität im Nachlauf zweidimensionaler Körper. Dissertation, Technische Universität Berlin.

Scruton C. (1981): An Introduction to wind effects on structures. *Engineering design guides* **40**. Oxford University Press.

Seifert A., Bachar T., Koss D., Shepshelovich M., Wygnanski I. (1993a): Oscillatory blowing: a tool to delay boundary-layer separation. *AIAA Journal* **31** (11), 2052–2060.

Seifert A., Daeaby A., Nishri B., Wygnanski I. (1993b): The effects of forced oscillations on the performance of airfoils. *AIAA Shear Flow Conference*, Orlando, Fla. *AIAA Paper 93-3264.*

Soteriou M. C., Ghoniem A. F. (1995a): Effects of the free-stream density ratio on free and forced spatially developing shear layers. *Phys. Fluids* **7** (8), 2036–2051.

Soteriou M. C., Ghoniem A. F. (1995b): The effect of the inlet boundary conditions on the mixing and burning in the exothermic shear flow. *33rd Aerospace Sciences Meeting and Exhibit*, Reno, Nv. *AIAA Paper 95-0807.*

Soteriou M. C., Knio O. M., Ghoniem A. F. (1991): Manipulation of the growth rate of a variable density, spatially developing mixing layer via external modulation. *29th Aerospace Sciences Meeting*, Reno, Nevada. *AIAA Paper 91-0081.*

Spieweg R. (1994): Strukturen in turbulenten Scherschichten mit schräger Abströmkante. Diplomarbeit, Technische Universität Berlin.

Stone J. P., McKinzie D. J. (1984): Acoustic excitation—a promising new means of controlling shear layers. *NASA Technical Memorandum 83772.*

Strykowski P. J., Niccum D. L. (1991): The stability of countercurrent mixing layers in circular jets. *J. Fluid Mech.* **227**, 309–343.

Strykowski P. J., Sreenivasan K. R. (1990): On the formation and suppression of vortex shedding at low Rexynolds numbers. *J. Fluid Mech.* **218**, 71–107.

Sung H. J., Chun K. B. (1996): Control of Turbulent Recirculation Flows Behind a Backward-Facing Step by Acoustic Pulsations. *2nd International Symposium on Engineering Turbulence Modelling and Measurements*, Florence, Italy.

Symes C. R., Fink L. E. (1978): Effects of external turbulence upon the flow past cylinders. In *Structure and Mechanisms of Turbulence I*, ed. H. Fiedler, *Lecture Notes in Physics* **75**. (Springer).

Szajner A., Turner J. T. (1987): Coherent structures in a free circular jet surrounded by a pulsed annular jet. *Proc. 6th Symp on Turbulent Shear Flows*, Toulouse, France.

Tanner M. (1989): Calculation of the rate of spread of two-dimensional turbulent mixing layers. *Z. Flugwiss.* **13** (6), 393–398.

Tavoularis S., Corrsin S. (1987): The structure of a turbulent shear layer embedded in turbulence. *Phys. Fluids* **30** (10), 3025–3033.

Toms B. A. (1948): *Proc. 11st. Int. Cong. Rheol.* **2**, 135–141, North Holland, Amsterdam.

Tso J. (1983): Coherent structures in a fully developed turbulent axisymmetric jet. PhD thesis, Johns Hopkins University Baltimore.

Tso J., Hussain F. (1989): Organized motions in a fully developed turbulent axisymmetric jet. *J. Fluid Mech.* **203**, 425.

Tso J., Kovasznay L. S. G., Hussain A. K. M. F. (1980): Search for Large-Scale Coherent Structures in the Nearly Self-Preserving Region of an Axi-symmetric Turbulent Jet. *AIAA Paper 80-1355.*

Tyndall J. (1867): On the action of sonorous vibrations on gaseous and liquid jets. *Philos. Magazine J. of Sci.* **33**, 375–391, Lond, Edinburg, Dublin.

Van Dyke M. (1982): An Album of Fluid Motion. The Parabolic Press. Stanford California.

Veynante D., Candel S. M., Martin J. P. (1986): Influence of the system response on the coherent structures in a confined shear layer. *Phys. Fluids* **29** (12), 3912–3914.

Von Karman T.: Collected works.

Wang G., Fiedler H. E.: Turbulent mixing in a confined mixing layer. Submitted for publication.

Weir A. D., Bradshaw P. (1974): The interaction of two parallel shear layers. Dept. of Aeronaut., Imperial College, London, *AR 74-09.*

Weisbrot I., Wygnanski I. (1988): On coherent structures in a highly excited mixing layer. *J. Fluid Mech.* **195**, 137–159.

Wygnanski I., Champagne F., Marasli B. (1986): On the large scale structure in two-dimensional small deficit, turbulent wakes. *J. Fluid Mech.* **168**, 31–71.

Wygnanski I., Petersen R. A. (1985): Coherent motion in excited free shear flows. *AIAA Shear Flow Control Conference*, Boulder.

Yajnik K.S., Acharya M. (1977): Non-equilibrium Effects in a Turbulent Boundary Layer due to the Destruction of Large Eddies. In *Structure and Mechanisms of Turbulence I*, ed. H.Fiedler, *Lecture Notes in Physics* **75**, p. 249–260 (Springer).

Yoda M., Fiedler H. E. (1996): The round jet in a uniform counterflow: flow visualization and mean concentration measurements. *Experiments in Fluids* **21**, 427–436.

Zaman K. B. M. Q., Hussain A. K. M. F. (1981): Turbulence suppression in free shear flows by controlled excitation. *J. Fluid Mech.* **103**, 133–159.

Zhou M. D., Heine C., Wygnanski I. (1996): The effects of excitation on the coherent and random motion in a plane wall jet. *J. Fluid Mech.* **310**, 1–37.

Ziada S., Rockwell D. (1981): Generation of higher harmonics in a self-oscillating mixing layer-wedge system. Report, Lehigh University.

7 Near-Wall Turbulence Control

Andrew Pollard

Department of Mechanical Engineering, Queen's University at Kingston, Ontario, K7L-3N6 CANADA

Abstract. The control of near-wall turbulence is the topic of this contribution to the shortcourse volume on Flow Control. Turbulent boundary layer structure and near-wall turbulence structure in particular is considered and how passive and active modifications to the structure can produce a diminution in drag. This contribution examines various methods for passive and active control of these structures, which include riblets, humplets, spanwise wall oscillations, selective interference and selective introduction of turbulence at scales different to those already existing within a boundary layer.

1 Introduction

The effects of wall roughness on the transfer of momentum, heat and mass has been central to many investigations; however, most of these, at least to the early 1950's, were concerned with maximizing heat/mass transfer and accepting the drag penalties that arise therefrom, Jayatilleke (1969). The collection and assessment of data, which included both two and three dimensional roughness elements, gives some evidence that skin friction reduction is achieved, although this is dismissed as possible poor experimental control. Heat and mass transfer studies normally have been conducted with the view to significantly enhancing their rates over smooth surfaces. In the last decade or so, insight into the structure of turbulence in boundary layers and the structure near-walls in particular has increased to the point that certain inherent features have been identified and cause-effect relationships suggested. This opens the possibility of control of these structures to effect changes in skin friction and heat and mass transfer.

In this contribution, various techniques are examined that have the ability to interfere with near-wall structure. The first part considers a passive method called riblets, the basic ideas behind near-wall structure and the effects that riblets have on t hem are discussed. Other sections follow that consider alternative and complementary techniques for achieving greater interaction with these structures through both passive and active control methods.

2 Riblets

It is well recorded that streamwise aligned micro-groove striations or riblets, see figure 1, affect the magnitude of skin friction drag, Coustols and Savill

M. Gad-el-Hak et al.: LNPm 53, pp. 431 - 466, 1998
© Springer-Verlag Berlin Heidelberg 1998

(1992). The investigations include many experiments, aimed at either measuring the skin friction Wilkinson *et al.* (1989) or understanding the details of the turbulence structure and the comparative effects of introducing riblets (see, for example, Baron *et al.* 1993) or isolating, by conditional sampling, a small portion of the structure (for example, a quasi-streamwise vortex, QSWV, Robinson 1991) and again comparing results obtained from flat wall against walls populated by riblets, Tang and Clark (1991), Tardu *et al.* (1993) and references cited therein. Computationally, various laminar (Fioc 1991, Choi *et al.* 1991) and single point closure (Khan 1986, Djenidi and Antonia 1993) approaches have been applied, direct numerical simulations performed by Chu *et al.* (1992), Choi *et al.* 1993), and Chu and Karniadakis (1993) and also the application of near-wall viscous models (NWVM) by Chapman and Kuhn (1986), Tullis (1992) to riblets of various geometries, Tullis and Pollard (1993a), (1993b) (1994). However, after approximately 25 years of research effort, the full explanation of why riblets work, or why they only produce about 8-10% drag reduction still baffles those interested either in this technique of drag reduction or (and) in the control of turbulence. Clearly, the answer remains shrouded by either our still incomplete knowledge of what constitutes the turbulence structure near a wall or by not fully understanding what it is that needs to be controlled (for example, what precisely produces the instantaneous skin friction?). Interesting perspectives on some of these issues are revealed in the recent articles by Smith *et al.* (1991), Falco (1991), Robinson (1991) and Morrison *et al.* (1992).

About 70% of the energy that sustains turbulence is generated in the lower 10% of the boundary layer. The spectrum of scales of turbulence are significant in the wall region. As $y^+ \longrightarrow 0$, however, the viscous effects become large, and indeed, with riblets affixed to the wall, the viscous effects can be considered of paramount importance in the absence of structure Bechert and Bartenwerfer (1989), Luchini *et al.* (1991). It is known that turbulent structures exist and intrude randomly into riblet grooves, see, for example, Tang and Clark (1993), Tullis and Pollard (1993a), Chu and Karniadakis (1993), thereby having a deleterious effect on the amount of drag reduction that can be achieved, Pollard etal (1993). Not considered here, therefore, are investigations that resort to either laminar flow or those that use time averaged Reynolds stress modelling.

Large Eddy Simulation, LES, to the author's knowledge has not been applied to flows on walls populated by riblets. The technique has been applied to transitional, low and high Reynolds number flows, but many authors have conveniently overlooked the near-wall region by introducing a simplified log-law or wall function model to link the wall to the interior, Klein and Freidrich (1989), Rizk and Menon (1988). At low Reynolds numbers, the need for wall functions is deemed unnecessary Germano *et al.* (1991), Yang and Ferziger (1993) and Zang *et al.* (1993); however, there are still some considerable differences between the LES calculations and results from either direct

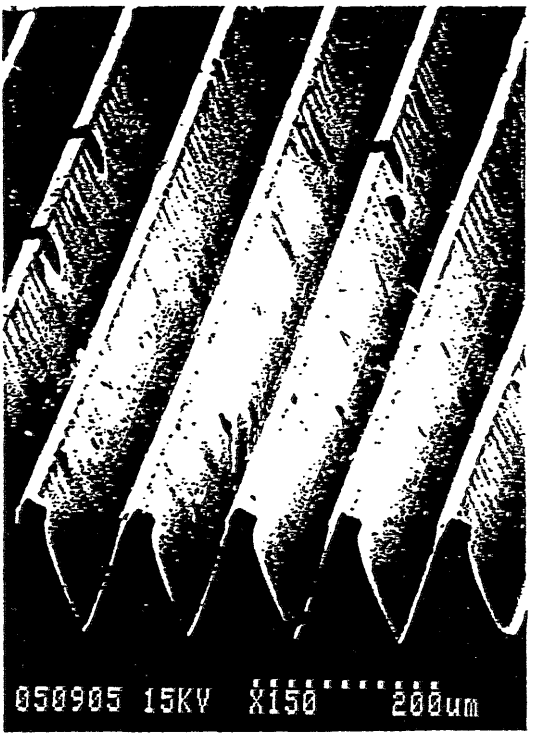

Fig. 1. Profile of v-groove riblet, distance between crest and depth of riblet is 120 and 130 microns, respectively. Note the curved face, near the peak of the riblet, is due to cutting, and the niches in the riblets. The riblets do not have sharp peaks, but display a flat land. Photograph courtesy of M. Weiss, Nova Husky Research, Calgary

numerical simulations (mean velocities, Reynolds normal stresses) Yang and Ferziger (1993) or experimental data (Reynolds normal and shear stresses), Zang *et al.* (1993). At very high Reynolds numbers, the recent work by Manhardt and Wengle (1993) is encouraging. However, the maturity of LES will be realised only when sub–grid scale models more fully reflect and accommodate and link the resolvable scales. An attempt in this direction has been suggested by Sullivan and Pollard (1994), which incorporates Gram-Charlier reconstruction, linear stochastic estimation and wavelet filters thereby permitting the sub grid scales to be reconstructed through de-convolving of the filtered velocity field and the filter function.

Two alternative approaches for modelling a turbulent boundary layer, on either smooth or riblet walls, are either direct numerical simulations (DNS) or a simplified model of the wall region ($y^+ \leq 40$). While, clearly, DNS must have greater realism than something that purports to account for the near-wall region in simplified ways, the over–abundance of data generated by a DNS calculation can easily mask or hinder the thought processes. Thus,

complementarily, there is value in making rationale arguments about what may be considered important *a priori*, and testing these, which is a basis for using a simplified model. The computational costs are considerably less than that required for DNS.

Here an assessment is made of results obtained from these two approaches to computing the flow over riblets. The assessment includes the results and the methods used to obtain them and comparison to the accumulated information on non-manipulated turbulent boundary layers. In any turbulent flow situation, the skin friction ideally to be obtained would be the laminar skin friction value at the same Reynolds number. This is, of course, behind the concept of compliant surfaces and laminar flow control; however, without direct recourse to these methods, it is appropriate to investigate if this can be otherwise achieved.

2.1 Methods for Simulating Flow Over Riblets

The data base on turbulent flow over riblets is limited to three types of studies: direct numerical simulations from (a) spectral-element, Chu *et al.* 1992), Chu and Karniadakis (1993) or finite volume methods, Choi *et al.* (1993), which physically identify many riblets and solve the three-dimensional time-dependent forms of the Navier-Stokes equations; (b) a spectral–element method, which imposes a spatially localised body force that opposes the flow velocity to create a riblet-like surface, Goldstein *et al.* (1995); (c) a model of the viscous wall region, applicable to turbulent boundary layers, but which is applied to riblet surfaces, using a control volume finite element method Tullis and Pollard (1993a,b)(1994) and Pollard *et al.* (1996). From these studies, various insights into the effect of riblets on near-wall coherent structures have been gained.

The basic parameters used in the simulations of flow over riblets are summarised in Table 1, to which reference will be made in the following sections.

2.2 Spectral-Element-Fourier Methods

One way of solving the Navier Stokes equations:

$$\frac{\partial \rho u_i}{\partial t} + \frac{\partial \rho u_i u_j}{\partial x_j} = -\frac{\partial p}{\partial x_i} + \frac{\partial}{\partial x_j} \mu \frac{\partial u_i}{\partial x_j} \tag{1}$$

is to assume the velocity field can be created using:

$$\mathbf{u}(\mathbf{x}, t) = \Sigma_{n=-N/2}^{N/2-1} \Sigma_{m=-M/2}^{M/2-1} \Sigma_{p=0}^{P} \; \mathbf{a}_{nmp} T_p(y) e^{i(2\pi n x/L_x + 2\pi m z/L_z)} \tag{2}$$

where

$$T_p(y) = cos(p \; cos^{-1} y) \quad , \tag{3}$$

Parameter	Princeton Chu & Karniadakis 1993	Stanford Choi etal. 1993	Brown Goldstein etal. 1995	Queen's Tullis & Pollard 1993a,b, 1994 Pollard etal. 1996
$\overline{U}H_{MR}/\nu$	3500			—
$U_\ell(H/2)/\nu$		4200		—
$\overline{U}H/\nu$	3684	5600(?)	3607 (*)	—
Re_{u_τ}	131	180	125	Various
L_x^+ (stream)	677	570	1250	1215
L_y^+ (norm)	271	?	250	≤ 50
L_z^+ (span)	271	160	375	100
Δx^+	42	35	26	—
Δy^+	0.43	0.1	0.15	0.7
Δz^+	0.42	0.64‖1.28	1.5	0.6
$T_l^+ = t(H/2)/U_\ell$	?	500	23[1]	?
$T_t^+ = t\nu/u_\tau^2$	300	4000	100	243
h^+	17.1	20,34.6‖10,17.3	5.3‖9.4	Various
s^+	17.1	40,40‖20,20	18‖11.7	Various
Shape	V-groove	V-groove	V-groove	V, U, L, etc.
No. of Riblets	10	4‖8	21	3→8
Computer	Cray iPSC/860	Cray	Cray	SGI IRIS

Table 1. Comparison of major parameters used in simulating riblet flows. H, H_{MR} refers to channel height and channel wall to mid-height location of riblet, respectively. U_ℓ refers to mean laminar velocity. L is domain size in given direction. Δx is smallest grid spacing in x direction. T is time period over which statistics are collected. h & s are riblet height and spacing. Further details for Queen's entries are given in Table 3. (*) see, Sirovich *et al.* (1991). (?) Estimated. ‖ implies X ‖ Y - X drag neutral or drag increasing, Y drag decreasing.

and $T_p(y)$ is a Chebyshev polynomial (see, for example, Canuto *et al.* 1987) applicable to the non-homogeneous direction (wall-to-wall) and the exponential term represents a Fourier series applicable to the two homogeneous (periodic) directions.

In all the DNS methods, (first three columns of table1), the flow is sustained by specifying either a pressure drop or a mass flow rate in the streamwise direction. In the latter case, the pressure is a consequence of this decision. Frictional changes are then reflected in either an increase in mass flow rate or diminution in the pressure gradient.

Karniadakis and his group (Princeton entry) consider a channel with one wall populated by v-groove riblets. The Navier Stokes equations are solved using spectral-elements in the cross-stream direction and spectral Fourier

expansions in the homogeneous streamwise direction. Third-order accurate advancement in time is used. "Turbulence" is claimed to be sustained with as little as 4 Fourier-modes in the streamwise direction, but the full spectrum of scales certainly can not be resolved with this number of modes. In the references cited here-in, 16 modes are used. While the computational parameters employed in those calculations reported seem to be consistent with those of others, the time over which statistics have been gathered appears short, since the *average* eddy turn over time is about equal to the computational time used. It would appear that Chu and Karniadakis paid particular attention to the resolution requirements around the riblet peaks, although the grid spacing seems a little large in the streamwise direction. As noted in table 1, the domain considered here (and by the Stanford group) is limited in streamwise extent. QSWV have a spectrum of diameters ($5 \leq d^+ \leq 115$, mean value ≈ 30, Robinson 1991) and their approximate length of about 100 - 200 y^+, Robinson (1991), or even larger Lyons *et al.* (1989), but retain their identity as they are convected downstream over several channel widths. It is difficult to say what effect the domain length has on the calculations. Recent investigations of a temporally evolving wake indicate that the evolution of the large scale structures is not at the same rate as those at smaller scales as predicted by similarity arguments, and thus their evolution is probably influenced by the calculation domain size being too small, McIlwain *et al.* (1996).

The calculations of Goldstein *et al.* (1995) (Brown, table1) use the method of Kim *et al.* (1987) applied to a channel flow. The riblet surface, on one wall, is modelled, not as a solid, but as a virtual surface. This is achieved by imposing point forces such that, at this virtual location, all fluid is brought to rest. It is interesting to note that a domain is used that is substantially larger than other simulations, and the time over which statistics have been obtained is equivalent to about 23 large eddy turn over times (based on H/u').

2.3 Finite Volume Methods

The finite volume method, as employed by Choi *et al.* (1992) (1993) (Stanford, table 1) solves Equation (1), over physically defined riblets on one wall of a plane channel. A non-orthogonal mesh is employed with concentrations of the grid around the riblets peaks. Second order central differencing is used for all spatial derivatives. Advancement in time is accomplished using a fully implicit method. Thus, the Courant-Friedrichs-Lewy (CFL) number ($[\Sigma(\mid u_i \mid)/\Delta x_i]\Delta t$) that normally limits the time step for explicit methods, can be violated. However, the time step Δt^+, or more precisely the CFL number, is shown to have considerable effect on the results. When compared to results from using spectral methods, the centreline (at $y^+ = 80$) rms velocities are over-predicted (streamwise, u), and underpredicted (wall normal v) and (spanwise w) by about 30%, 12.5% and 22% respectively as $0.5 \leq \mathrm{CFL} \leq 3$ or $0.2 \leq \Delta t^+ \leq 1.2$, Choi *et al.* (1992). Interestingly, when $CFL \geq 4$, a laminar flow solution is obtained. The time step ($\delta t^+ \approx 0.4$, $CFL = 1$) is chosen

from agreement with spectral results for plane channel flow and deemed appropriate for the flow over riblets. The sensitivity of the results as a function of the CFL number is a little disturbing because, as is known, the shear stress around the riblet peaks is much larger than that found for plane walls; thus, from the definition of the CFL number, the ratio of velocity to grid spacing will be significantly elevated around the riblet peaks (relative to that for a flat wall), requiring a much smaller time step to properly resolve the time evolution of the flow. There probably exists in the flow locally laminar regions that will, when integrated over time, have the effect of damping the turbulence.

2.4 Viscous Wall Region Modelling

Sufficient evidence exists, from both experimental Choi (1989), Hooshmand (1985), Clark (1989) and computational Choi *et al.* (1993) investigations that the effect of riblets is limited to the region $y^+ \simeq 40$. This enables the use of a near wall, viscous, (driven eddy) model, NWVM, which involves modelling the region between the wall and the outer edge of the viscous wall region (the inner edge of the log-law region) at $y^+ \simeq 40$. The notion of restricting attention only to a thin region close to the wall has been examined extensively by Hanratty and co-workers, Hanratty *et al.* (1977), Hatziavramidis and Hanratty (1979), Finnicum and Hanratty (1988a), Lyons *et al.* (1988) (see also references cited therein), Walker and co-workers, Peridier *et al.* (1991a,b) Ersoy and Walker (1987), and Smith *et al.* (1991) (see also references cited therein), Perry and co-workers, Perry and Chong (1982), Perry and Li (1990), Perry *et al.* (1993), (1994) (see also references cited therein), Chapman and Kuhn (1986), Aubry *et al.* (1988), Berkooz *et al.* (1993) (see also references cited therein) and most recently by Kravchenko *et al.* (1993) and Orlandi and Jimenez (1994). The models of Hanratty *et al.* and Chapman and Kuhn have been used by Tullis and Pollard, (1991), (1993a,b), (1994) and Tullis (1992) and are described below, for the convenience of the reader.

The computational domain consists of a cross-sectional y–z plane with $0 \leq y \leq y_o$ and $0 \leq z \leq z_o$ where $y_o^+ \simeq 40$ and the spanwise size of the domain (z_o) depends on the particular variation of the model but is usually in the range of 100–200 wall units.

The main modelling assumption of the method is the specification of the velocities along a fictitious boundary located at y_o. These specifications can vary slightly; however, the fluctuating velocity components specified at the upper boundary are periodic in time and spanwise location, and are representative of QSWV. Consequently, the an exact representation of the flow is not intended, but provides a model of the eddy structure in the viscous wall region.

The conditions for the fluctuating velocities are periodic in both the spanwise direction (z) and in time. The fluctuating velocity components usually have two scales: one that dominates wall normal momentum transport and

is roughly the size of the streak spacing and a larger scale accounting for the influence of all large "outer flow eddies". The full form of the specified boundary conditions, as given by Nikolaides (1984) is:

$$U_e = \bar{U}_e + \hat{u}_1 \cos\left(\frac{2\pi}{T_1}t + \phi_{u1}\right)\cos\frac{2\pi}{\lambda_1}z + \hat{u}_2 \cos\left(\frac{2\pi}{T_2}t + \phi_{u2}\right)\cos\frac{2\pi}{\lambda_2}z \quad (4)$$

$$v_e = \hat{v}_1 \cos\left(\frac{2\pi}{T_1}t + \phi_{v1}\right)\cos\frac{2\pi}{\lambda_1}z + \hat{v}_2 \cos\left(\frac{2\pi}{T_2}t + \phi_{v2}\right)\cos\frac{2\pi}{\lambda_2}z \quad (5)$$

$$w_e = \hat{w}_1 \cos\left(\frac{2\pi}{T_1}t + \phi_{w1}\right)\sin\frac{2\pi}{\lambda_1}z + \hat{w}_2 \cos\left(\frac{2\pi}{T_2}t + \phi_{w2}\right)\sin\frac{2\pi}{\lambda_2}z \quad (6)$$

where U_e, v_e and w_e are the specified upper edge velocities. λ_1 and λ_2 are the spanwise periods and T_1 and T_2 are the time periods for each of the two eddy scales. Each of the time periodicities (fluctuations) has a phase angle ϕ relative to some reference cycle. The amplitudes ($\hat{u}_1$, $\hat{u}_2$, $\hat{v}_1$, $\hat{v}_2$, $\hat{w}_1$ and $\hat{w}_2$) for each velocity component are for each of the two scales. The model of Chapman and Kuhn does not use all terms in Equation 5, as noted below. The terms in the above equations are ascribed values obtained from experimental data. The three model sets are summarised in table 2.4. The rationale for these choices, based on data available to the originators, are outlined below and this section may be omitted by the reader without loss of continuity.

NWVM Parameter Selection The relative amplitudes of the velocity components in the two scales are expressed as the energy fraction contained in the smaller scale eddies (e.g. $E_{u1} = \hat{u}_1/(\hat{u}_1^2 + \hat{u}_2^2)$).

The periods λ_1 and λ_2 are chosen to represent the spanwise sizes of two eddy scales. In all the models, the smaller scale (λ_1) is chosen to agree with the spacing of low speed streaks in the viscous sublayer. Sensitivity of the results to the choice of period has been documented, see for example, Lyons *et al.* (1988). These regions of low downstream momentum fluid are elongated in the streamwise direction and have spanwise spacing of approximately 100 wall units (Smith and Metzler 1983). The streaks are generally considered to be the result of the lift up of low momentum fluid near the wall by a streamwise vortex or vortex pair.

The larger spanwise scale (λ_2) accounts for the influence of larger scale streamwise vortices, particularly on the spanwise velocity fluctuations (w). Nikolaides used a representative value of $\lambda_2 = 400$, based on a rough evaluation of the $R_{ww}(y_o, \Delta z)$ correlations measured by Grant (1958) and Tritton (1967). Chapman and Kuhn did not select a specific value for the size of the λ_2 scale. Instead, only the smaller scale eddies were considered to have a spanwise periodicity. The value of the spanwise periodicity of the larger scale is then effectively infinite ($\lambda_2 = \infty$).

The time periods T_1 and T_2 are usually set to roughly the same values as λ_1 and λ_2. The value of T_1 was chosen to agree with experimentally measured

Parameter	Model		
	Chapman & Kuhn	Nikolaides-1	Nikolaides-2
λ_1	100	100	100
$\lambda_2(u,v,w)$	∞, –, ∞	400, –, –	400, 400, 400
T_1	143	100	100
$T_2(u,v,w)$	143, –, 286	400, –, –	400, 400, 400
E_{u1}	0.34	0.2025	0.15
E_{v1}	1	1	0.75
E_{w1}	0.74	1	0.4
ϕ_{u1}	0 (reference)	252^o	216^o
ϕ_{u2}	0	150^o	194.4^o
ϕ_{v1}	0	72^o	36^o
ϕ_{v2}	–	–	90^o
ϕ_{w1}	90^o	0 (reference)	0 (reference)
ϕ_{w2}	120^o	–	270^o

Table 2. Comparison of model parameters for near-wall viscous model

flat wall bursting (streamwise velocity fluctuation) frequencies in all of the models.

Chapman and Kuhn use values for the different velocity components $T_{w2} = 2T_{u2}$ which is based on a hypothetical statistically staggered large scale eddy flow. The value of T_{u2} is specified from the mean streamwise autocorrelation data:

$$T^+ = \frac{5\delta}{U_\infty} \tag{7}$$

where δ is the boundary layer thickness and U_∞ is the free stream velocity. This means that they consider the larger time scale to be dependent on the Reynolds number. By considering a Reynolds number of $Re_\delta \simeq 14000$, Chapman and Kuhn specified $T_{u2} = T_1 = 143$ and avoided the question of whether the larger eddies scale with inner or outer variables. Nikolaides used the same experimental relationship (Equation 7) but specified a Reynolds number of $Re_\delta \simeq 80000$ to obtain the single value of $T_2 = 400$ for all of the velocity components.

The amplitudes of fluctuations at the different scales ($\hat{u_1}$, $\hat{u_2}$, $\hat{v_1}$, $\hat{v_2}$, $\hat{w_1}$ and $\hat{w_2}$), are related to the energy fractions of the velocity components in each of the scales. These are selected mainly based on agreement between the specified upper boundary conditions and experimental data for the flow over flat walls at a height of $y^+ = 40$. For example, the values of $E_{u1} = \hat{u}_1/(\hat{u}_1^2+\hat{u}_2^2)$) were chosen so that the value of the Reynolds stress correlation coefficient at the upper boundary matched the experimental value of 0.45. The selection of the energy fractions for the v and w velocities is based on the assumption that the most (or nearly all) of the vertical momentum transport

is associated with the smaller scale eddies while the larger scale eddies account for at least a large fraction of the spanwise momentum transport.

The phase angles (ϕ's) between the various periodic terms are selected based on the experimental measurements of the average size of the near-wall eddies and the use of computer optimisation. Since the phase angles are only relative values, a reference ϕ value must be specified. Chapman and Kuhn selected both ϕ_{u1} and ϕ_{v1} as the reference values. A value of $\phi_{w1} = 90^o$ was chosen to match experimental values for the slope of $d\overline{v^2}/dy$ at the upper edge of the domain. Computer optimization was used to select the values for ϕ_{u2} and ϕ_{w2} to provide as good agreement as possible for the mean streamwise velocity profile, the Reynolds shear stress distribution and the streamwise skewness levels.

The parameters that describe the near-wall viscous model (NWVM) are tabulated in table 2.4. In the work reported here, the model of Chapman and Kuhn (essentially their model 1) was used exclusively.

Control Volume Finite Element Method The NWVM requires coupling the Navier Stokes equations and the upper surface boundary conditions. The walls over which the flow can be calculated could be of any shape. The control volume finite element method (CVFEM) was used for this purpose, where all terms are made non-dimensional using wall coordinates. The advantage of the method is the use of triangular shaped control volumes that precisely outlines the cross sectional shape of any riblet (within the limit of small straight lengths) and that local grid refinement can be used, especially around the riblet peaks. The equations are discretised using standard finite-volume methods Tullis (1992), Masson *et al.* (1994). The method integrates the restricted form of equations 1 (periodic in time and spanwise spatial direction) using non-dimensional time steps $\Delta t = 2$, chosen after extensive testing alternative values, Tullis (1992). The parabolic nature of the method causes the initial conditions (Laplacian equation for downstream momentum in the cross flow plane) to have significant effect on the results, so the equations are solved over 5 large eddy turn over times , discarding the results from at least the first three of these times before gathering the statistics. The convective terms in the equations are discretised using a flow oriented, equal order method that incorporates elemental (grid) Peclet numbers, thereby minimising false diffusion effects, Tullis (1992).

The CVFEM, which incorporates the NWVM models, assumes periodicity in the spanwise and streamwise (in time) direction. It therefore can not create any three dimensionality resulting from mean shear gradients and so turbulence can not be self-sustaining: it is driven by the out-edge boundary conditions.

2.5 Results from Near-Wall Viscous Model and Direct Numerical Simulations

The structure, the dynamics and the etiology of near-wall turbulence is perhaps best summarised, to ~1990, by Robinson (1991), Smith *et al.* (191), Falco (1991) and Morrison *et al.* (1992). The features so educed are used here to provide insight to the interaction between riblets and these features. A point of caution, however, is warranted. Some turbulence structure has been educed, in part, from data and simulations that use either data that are unreliable, or techniques that are inappropriately applied. A case in point is the use of Variable Interval Time Averaging (VITA). VITA pre–defines a time–scale and threshold for the passage of a "structure" and examines the localized RMS velocity for peaks with respect to the long–time RMS of the signal. Since these peaks will represent either accelerations or decelerations either spatially or temporally in the signal, VITA will detect shearing events, not the peak of the acceleration or deceleration. As shearing events do not necessarily have a unique phase relationship with structure passage, this makes identification problematic, see, for example, Morrison *et al.* (1989) and Sullivan *et al.* (1995), where the latter paper introduces an extension to VITA that utilizes a wavelet basis thereby provides a more objective structure identification method (see Bonnet's contribution to this volume).

The mean axial velocity at the riblet peaks is larger than that on a flat wall, while it is decreased in the valleys, and with concomitant changes in the wall shear stress. This feature is common for all riblet configurations that reduce skin friction, and is a consequence of the laminar-like flow inside the valleys, Bechert and Bartenwerfer (1989), Luchini *et al.* (1991). Thus, plotting the drag reduction gained as a function of the riblet spacing s^+, as $s^+ \to 0$, the drag must equal the smooth wall behaviour at a rate that is dependent on the limiting laminar flow within that riblet geometry, see, for example, figure 6 of Bruse *et al.* (1993). Indeed, the ultimate goal of any riblet shape must be to optimise the way in which the structural component of the flow is permitted to merge with the laminar asymptote. Thus, the ability of riblets to keep the wall isolated from the turbulence is a key component to their successful operation, Tullis and Pollard (1991), (1993a,b), (1994), Pollard *et al.* (1994), Bruse *et al.* (1993). Of course, turbulence will invade the valleys, exchanging high for low momentum fluid and destroy the relatively docile behaviour of the valley flow. A measure of this activity, is revealed by the higher order statistics of the turbulence field.

The statistics of the velocity fluctuations are considerably modified by the presence of riblets. In the case of triangular riblets, which have received the most attention, the general findings from all simulations and experiments, confirm, for the most part that, when drag reduction is achieved, the intensities of all velocity components are lower than those at the same non-dimensional distance from a flat wall. As well, the Reynolds shear stress, at least $\overline{uv}$, also displays a diminution in the valleys (in fact, it is almost zero)

while achieving large excursions from the flat wall values over the peaks. Indeed, the cross-stream gradient within the valleys is so small that the structural events ("sweep" and "ejection") have been effectively displaced (away from the wall) by the riblets. In a drag neutral case, the maximum stress occurs about 14 wall units from the riblet peak (similar to flat wall), suggesting that, unlike the drag reducing situation, which appear to displace the wall surface for momentum transfer, the drag neutral riblets protrude into the turbulent flow with an attendant considerable momentum transfer towards and away from the riblet peaks. There are no data available on either the $\overline{uw}$ or the $\overline{vw}$ stresses.

Skewness, the third moment of velocity or the first measure of asymmetry in a probability density distribution, can be related to structural events. A positive value implies many more small positive than the equivalent negative events, outside the standard deviation. The skewness in the streamwise velocity becomes significantly greater than the flat wall values (see, also, Tardu *et al.* 1993) as the riblet sizes (s^+) change from the drag reducing to drag increasing size, except in the riblet valleys; and the skewness of the wall normal or transverse velocity is more greatly affected and outside the valleys becomes large and positive, especially below $y^+ \leq 20$. In the valleys, the skewness becomes large and negative. The skewness in the lateral velocity is largely unaffected, although, in the DNS results, a small negative value could be a direct result of the periodic boundary conditions. These trends are displayed in figure 2 taken from Choi *et al.* (1992) and Chu (1992. Experimental evidence, using a both orthogonal X and V array hot wires give somewhat contradictory evidence of the skewness distribution of the lateral and wall normal velocity, Park (1992). A comparison between the DNS data Chu and Karniadakis (1993), Choi *et al.* (1993) indicates a possible Reynolds number dependence (intensities are too low, due, possibly to the CFL number problem identified earlier) as even the flat wall data for all velocity components are not in agreement either against themselves or against those data of Park (1992), Johansson and Alfredsson (1982).

Flatness, the fourth moment of velocity is a measure of the peakedness of a distribution relative to a normal one (flatness factor = 3) and, hence, indicates the relative importance of the small events in the tails of the distribution (large deviation from the mean or intermittency). The flatness in the streamwise velocity is significantly greater than the flat wall values as the riblet sizes (s^+) change from the drag reducing to drag increasing size, except in the riblet valleys. This is at odds with the experimental data of Tardu *et al.* (1993), which show that there is a decrease in the bursting frequency over riblets (recall that Walsh 1990 summarises that bursting is little altered by the presence of riblets). The flatness of the wall normal velocity (DNS) is significantly lower than that for a flat wall, at least below $y^+ \leq 15$ and there is an increasing diminution with increasing riblet size, see figure 2. It is interesting to note that Hooshmand (1985), as quoted by Walsh (1990), found

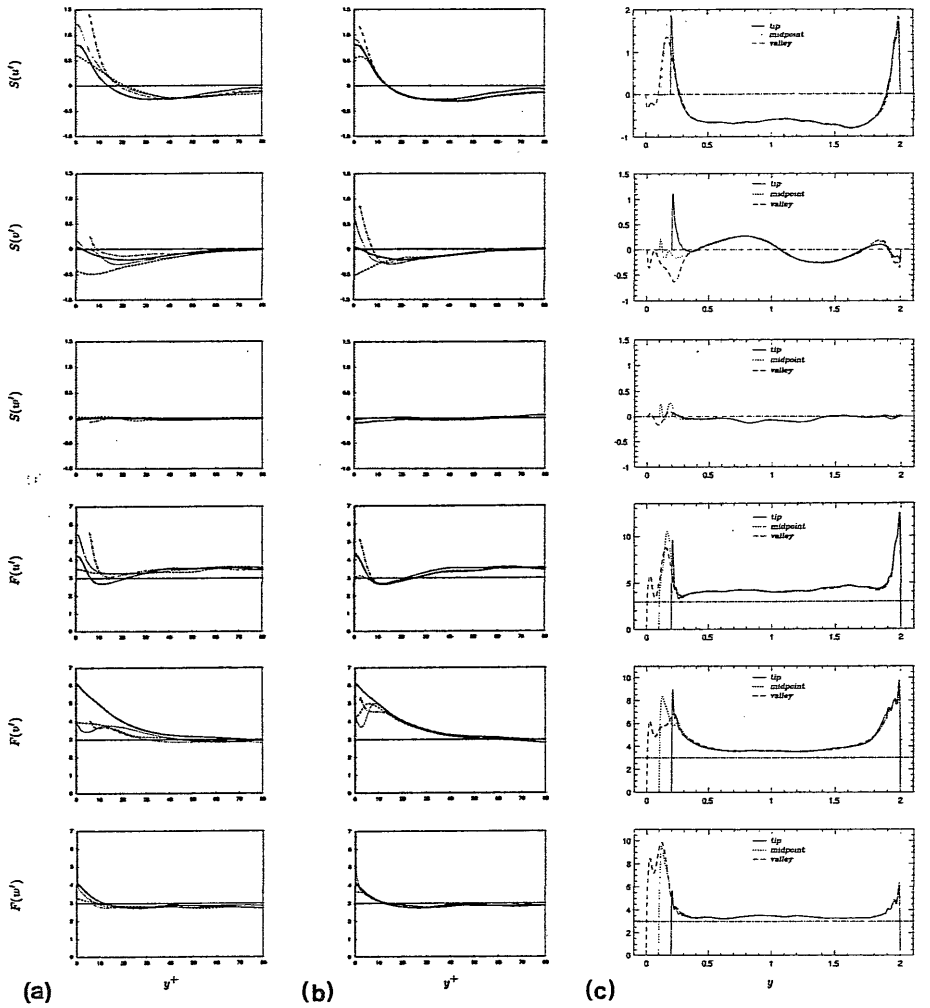

Fig. 2. Skewness, S, and flatness, F, factors in streamwise (u), wall normal (v) and span (w) directions for DNS results over riblets. Left column $s^+ = 40$, $h^+ = 34.6$, and centre column $s^+ = 20$, $h^+ = 17.3$, both from Choi etal. (1992) and right column $s^+ = 17.1$, $h^+ = 17.1$, Chu (1992). For Choi etal. ——— flat wall; —— . —— above tip; - - - - above valley; . . . . . above mid-height of riblet

(experimentally) that the transverse velocity flatness increases over riblets (greater intermittency); this damping is confirmed by Chu and Karniadakis (1993) and, as noted below, is indirectly confirmed by Goldstein *et al.* (1995) but in disagreement with Choi *et al.* (1993). The NWVM can add nothing to this argument.

The above behaviour of skewness and flatness implies that wallward directed fluid (a splat), occurring occasionally, but with large amplitude, reaches

into the riblet cavity. On a flat wall, this splat would spread out radially; the upstream direction perhaps being similar to the negative streamwise valley flow noted by Chu and Karniadakis (1993) giving rise to a high shear stress and high pressure spikes (recall the rather large streamwise spacing used by these authors, which may cast some doubt on this result). On a wall populated by riblets, the pressure pulse would be imprisoned within a valley or at most three valleys (an example is shown in figure 3, Tullis and Pollard (1993a), (1994). There is too little experimental evidence Choi (1987) to either confirm or refute this. The splat clearly gives rise to secondary flows within the valleys, washing out the low momentum fluid (observed in the NWVM and DNS results), see figure 4, and is quite probably the reason why riblets alter from reducing to increasing skin friction as s^+ increases.

DNS have only been applied to simple geometries, the computational cost probably acting as a deterrent to investigation of more interesting possible arrangements. The NWVM, on the other hand, has been applied to a variety of riblet shapes, as seen in table 3. From these studies, the effects of splatting (a non-continuous event) on the expulsion of low momentum fluid from the valleys has been found to be reduced if compound riblets are used. That is, replacing a full-height riblet by one that is, for example, half its height reduces the wetted area. Furthermore, in line with the idea that laminar conditions are ideal, the compound riblets act to further intervene with the sporadic motions of the structures so that any secondary flow engendered by the splats interacting with the riblets is quickly damped by the laminar-like fluid contained and constrained by the sub–riblet, as can be inferred from the results of the NWVM applied to thin element riblet/sub-riblet geometries, figure 5. Some data (obtained in very carefully controlled experimental conditions) exist on skin friction for this general concept, Bruse *et al.* (1993), which indicate that the additive effects of the riblet and sub–riblet are slightly advantageous (maximum skin friction reduction 10.2%). It is significant to note that for (see table 3) $h_2/s_1 \approx .25$, and $s_1/h_1 = 0.25$ the extent over which skin friction reductions are greater than 8% is about twice to three times that obtained for v-groove riblets. At the time of writing, the NWVM has not been applied to *optimized* riblet/mini–riblet geometries.

There appears to be some consistency in the effect of riblets on two point velocity correlations. Baron and Quadrio (1993), used v-groove riblets, ($s^+ = h^+ = 12$) and hot wires (of active length $\ell^+ = 8.6$) so some caution is necessary interpreting results that have some spatial averaging. Suzuki and Kasagi (1993a) used particle tracking velocimetry, PTV, over flat valley v-groove riblets, which creates a time averaged map of local velocities by adding together at given (periodic) spatial locations instantaneous realizations from particles. Pulles (1988) and Gallagher and Thomas (1984) used hot wire anemometry. From Suzuki and Kasagi (1993) and Goldstein (1995) close to the riblet surface ($y^+ \approx 14$) the spanwise variation of the longitudinal two-point correlation R_{uu} cross the zero axis at about $z^+ \approx 30$ and reach

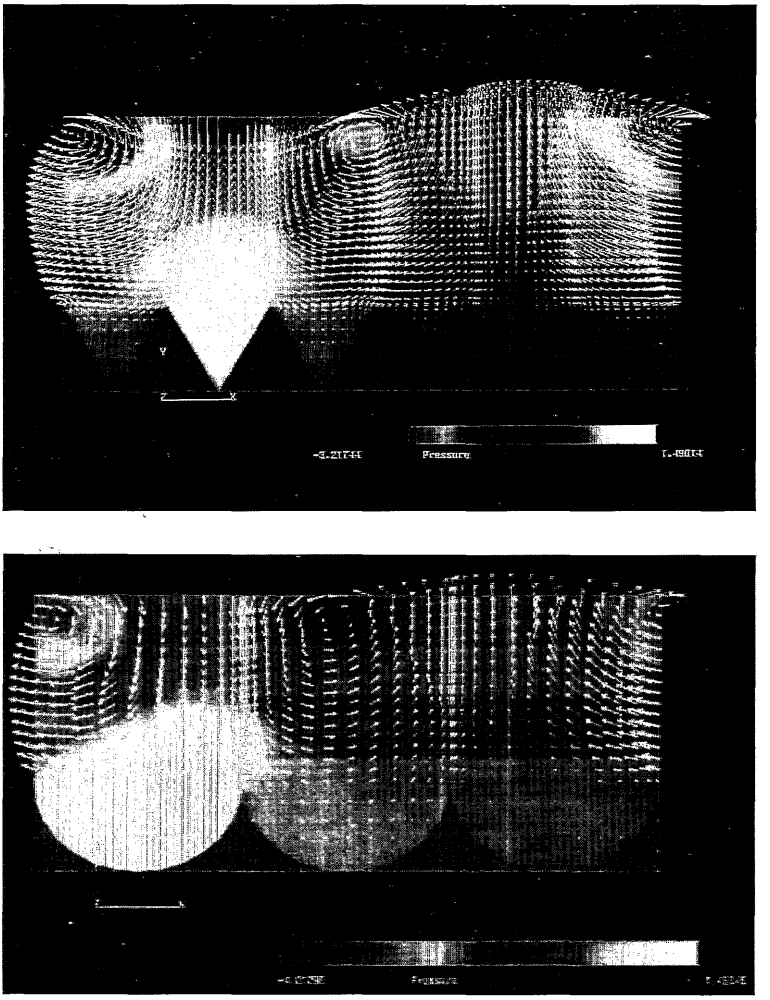

Fig. 3. Cross-sectional view, into the flow, over v-groove and large U-groove riblets. Arrows indicate cross-stream velocities and light areas inside riblets represent high pressure regions

a minimum (≈ -0.2) at $z^+ \approx 50$. There seems to be some effect of riblet size on the results (particularly for the larger riblets of Suzuki and Kasagi (1993a), which may not be entirely reliable, Pollard *et al.* 1996). Thus, it seems that riblets have some effect on the correlations, but there is insufficient evidence to clearly demonstrate that their effect is to the alter the QSWV spacing. (It is noteworthy that polymer addition greatly enhances the spanwise correlation, as will be referred to below). Similarly, the literature is dotted with claims that riblets somehow stabilise the meandering of the structures, a good summary of which is given by Walsh, (1990). The

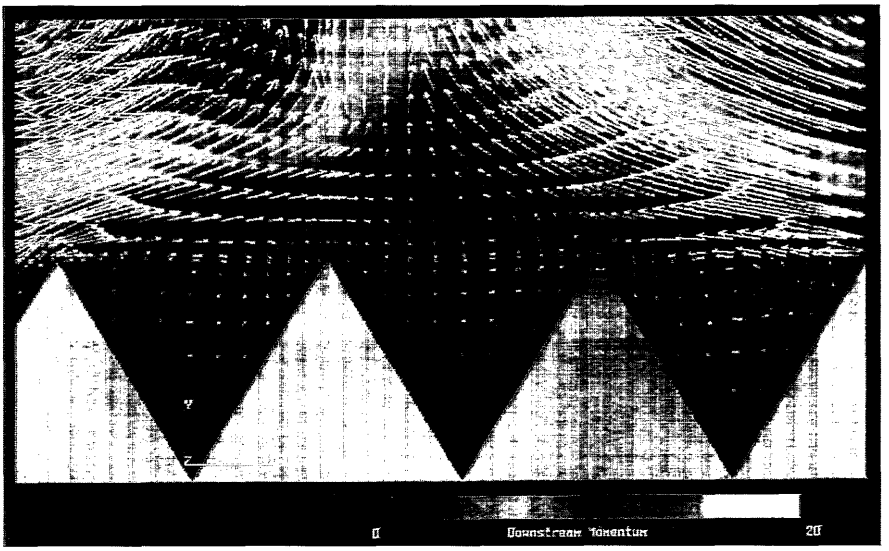

Fig. 4. Cross-sectional view, into the flow, over v-groove riblet. Arrows indicate cross-stream velocities. Note the secondary flows, particularly in the right-hand side groove as splat causes cross-stream velocity to move horizontally, thereby washing out laminar-like fluid inside groove.

in–depth examination of a DNS flat wall boundary layer, Robinson (1991), unfortunately, has not been duplicated for a wall populated by riblets. Certainly, flow visualisation (integration by eye) is subjective and inconclusive. The NWVM results reveal streaky structure, Tullis (1992); however, it can not be claimed that the structures are in anyway damped by the presence of the riblets since the boundary conditions are imposed. It is interesting to note that Goldstein *et al.* (1995) demonstrate that the effects of riblets on the flow can be recreated by damping the lateral or spanwise velocity, at some

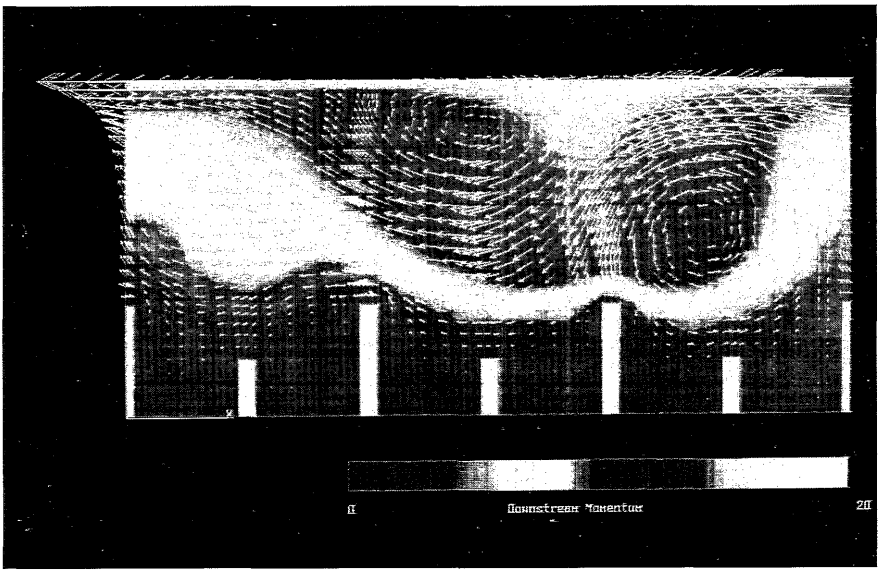

Fig. 5. Cross-flow view of thin element riblets

location above the riblets (this will be more fully explored below) that "displace the streaks upward", which is synonymous with concept of a protrusion height Bechert and Bartenwerfer (1989) and in accord with the idea that the QSWV need to be displaced and kept apart, Pollard (1994). The spanwise correlation coefficients are certainly very similar, at least close to the riblet "surface".

3 Alternative and Complementary Techniques

Up to this point, two-dimensional riblets have been the focus of attention and evidence has been presented as to their effects on near-wall structures and the concomitant effects on skin friction. It can be surmised that, while 10% reduction in skin friction may be realisable, perhaps there maybe alternative ways to achieve even greater reductions. In this section, some possible alternative or complementary techniques to riblets, gleaned from recent work, are suggested. While links are made where possible to earlier sections of this paper, the research reported is still in its infancy: speculation and uncertainty are expected, but foreshadows future directions.

The four sub-sections that follow are arranged in a manner that emphasises their similarity through physical actions.

Riblet Shape	h_1^+	h_2^+	s_1^+	s_2^+	t^+	h_p^+
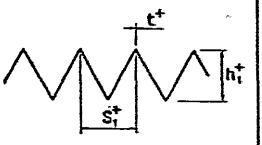	16.7		33.3			4.7
	16.7		16.7			3.6
	15		20			3.28
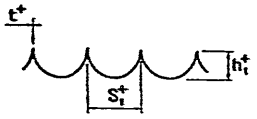	16.7		33.3			6.4
	15		20			3.84
	8.3		16.7			3.2
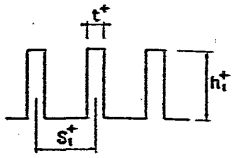	16.7		33.3		2.4	6.0
	15.0		20.0		0	4.41
	10.0		12.5		1.0	2.3
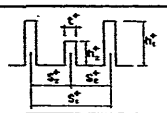	16.7	8.3	33.3	16.7	2.4	2.5(?)
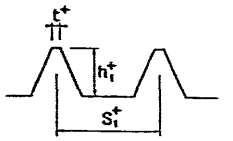	20.9		33.3		1.0	5.83
	15.0		20.0		0	3.99
	9.0		14.3		0	2.79

Table 3. Cross-sectional shapes of riblets studied by Queen's group. Non-dimensional sizes (h^+, t^+) and spacing (s^+) and their protrusion heights (h_p). t^+ refers to riblet thickness.

3.1 Three Dimensional Riblets or Humplets

The evolution in time of structures in a turbulent boundary layer Robinson (1991) (and accompanying video) indicates that the QSWV and other structures are not aligned exclusively in the streamwise direction, although there is a preference for this alignment, especially for $y^+ \leq 15$. Even so, the instantaneous wall shear stress is spanwise non-homogeneous (at least as revealed by the contour levels *chosen* by Robinson) accompanied by areas that display some skewing of the shear stress contours with respect to the streamwise direction. This could be due to non-symmetric wallward sweeps or splats. The propensity for structures to be three-dimensional, whose birth, evolution and

death are stochastic in space and time suggests the notion of using three dimensional riblets, or say "humplets". That is: are two dimensional riblets, of the type almost exclusively examined to date, the reason why only about 10% reduction in skin friction has been realised?

In any practical application, a boundary layer grows and it would be expected that the physical size of the riblets should reflect the physical dimensions of the layer in which they are immersed (tailor the riblet to the application). Also, as noted by, for example, Bechert (1987) shark scales have humplets (that, of course, may have evolved to satisfy both structural and frictional requirements; also, it is known that on any given shark, the riblets size, shape and orientation vary from head to tail of the body), so spatial variation in their placement should lead to at least as good a reduction to that found for streamwise aligned riblets. Tests indicate that uniformly shaped and homogeneously placed humplets do not yield significant differences in drag reduction over that obtained using streamwise aligned riblets (perhaps 1%, Enyutin and Lashkov 1987), but as the wall shear was not measured directly, there could yet be some advantage in further investigations.

As in the NWVM that has led to further insights into complicated geometries of riblets, a three dimensional version would undoubtedly likewise be useful. In this regard, Liu and Liu (1993) have used a non-orthogonal, finite-volume method with multi-grid acceleration for DNS investigation of the transition over three dimensional protuberances or humplets, as shown in figure 6. This method could be applied to optimising a three dimensional humplet shape, size, orientation (it may be that a slight skewing in the hump relative to the mean flow direction is advisable) and distribution pattern.

The best indication for active control and the most recent evidence of applying simulation methods to humplets has been the work of Carlson (1995) and Carlson and Lumley (1996). They used direct numerical simulation to predict the time dependent effects of raising a humplet from a wall into a turbulent boundary layer (channel flow), the intrusion being limited to $y^+ \leq 12$. Three calculations were performed: a rising symmetrical Gaussian shaped humplet underneath a low speed streak and under a high speed streak and a Gaussian shaped humplet with aspect ratio about 2:1 with the longer dimension aligned with the spanwise flow direction rising underneath the high speed streak. This idea of using a broader shaped humplet is in keeping with suggestions by Pollard (1994) that minimum drag should be attainable if the QSWV are kept apart, away from the wall and are well separated to minimise their interaction. The humplets rise from the wall as the calculation proceeds, thereby allowing their influence on the dynamics of the near-wall flow to be quantified. In the case where the humplet rises under a low speed streak, there is a small drag penalty, see figure 7. When raised under a high speed streak, there is about an equal but opposite amount of drag benefit. In the case of a non-symmetric actuator, the drag benefit increases over the whole cycle of the actuator movement, so that an estimated 7% reduction in skin

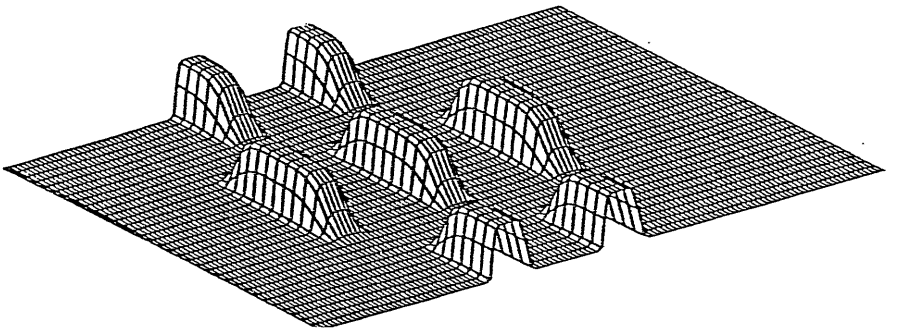

Fig. 6. A roughness element, that can be viewed as a humplet, courtesy of C. Liu, Louisiana Tech. University

friction is claimed. It is unknown whether this method can be practically implemented, but there is continued effort in this regard, especially using micro-electromechanical systems, see other contributions in this volume.

3.2 Wall Oscillation

Active control of turbulence can take various forms including: sensing an event and reacting to it Choi *et al.* (1993), washing the area using sound thereby trying to suppress and/or augment many (or just one) scales of turbulence at once, Welsh *et al.* (1990) introducing turbulence with a spectrum of scales and energies that interfere with that which already exists, using, for example, LEBU's. Here, some possible techniques are examined that may lead to control of turbulence. Compliant surfaces , wall suction and blowing are not directly considered, although they can be usefully employed in addition to those methods outlined below (see, for example, Bushnell and Mcginley (1989) and Wilkinson (1990).

Turbulent flow, oscillated in the streamwise direction, has received considerable attention in the literature, *e.g.* Ronneberger and Ahrens (1977), Cousteix *et al.* (1981), Mao and Hanratty (1986), Gajdeczko and Ramaprian (1987), Brereton and Reynolds (1991), Tardu and Binder (1993). The mean values are largely unaffected by the oscillation. Thus, the logarithmic region normally remains distinct. Brereton and Reynolds (1991), examined the turbulence and energy redistribution on a streamwise oscillating flow over a flat plate (oscillation frequencies less than 1/2 the supposed bursting frequency

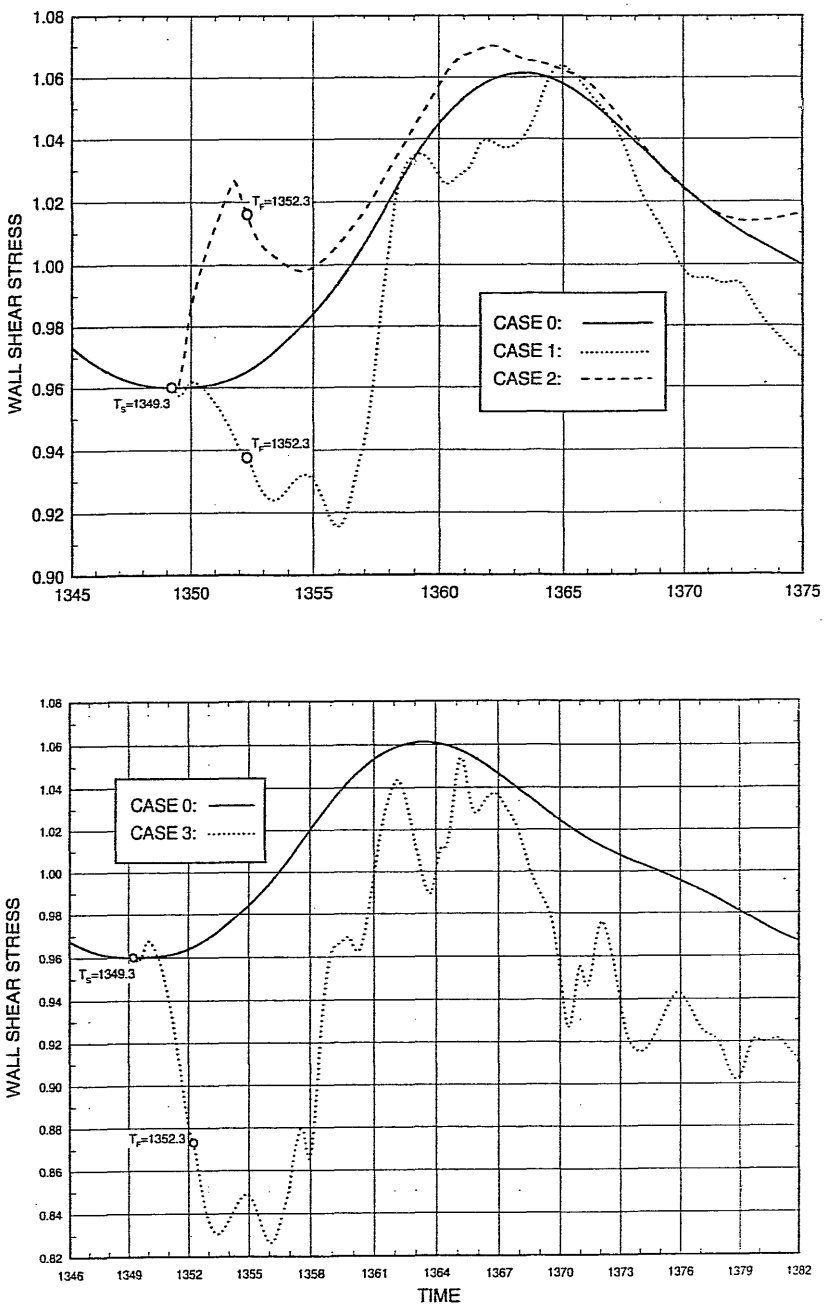

Fig. 7. Evolution of wall shear stress over rising Gaussian-shaped humplets. Solid line is for flat wall; case 1 for humplet rising underneath a high speed streak, case 2 for under a low speed streak; case 3 for broad Gaussian humplet rising under high speed streak. The humplet begins to rise at T_S and reach their full height ($y^+ = 12$) at T_F. Note the extended period, in the latter case, where skin friction reduction is achieved. Taken from Carlson (1995)

on stationary walls) showing that the turbulence production is increasingly dampened with increasing frequency in the near-wall; however, the wall normal extent of the effects of the oscillation decreases with increasing frequency. Tardu and Binder (1993) find that with increasing frequency there is a departure from the modification to the ratio of amplitudes of fluctuating wall shear and that computed assuming the Blasius solution is valid during each instant during the oscillation. This, in general, coincides with Mao and Hanratty (1986), but not with Finnicum and Hanratty (1988b). It is suggested by Tardu and Binder that geometrical factors may account for the difference implying that larger eddies play a role in the relaxation mechanism near the wall. Clarification of this is required. However, streamwise oscillations, imposed by vibrating the wall itself appears to have been seldom examined, Kobashi and Hayakawa (1981).

Jung *et al.* (1992) oscillated, in the lateral direction, the lower wall of channel, using DNS. They found that for oscillation periods $25 \leq T^+_{osc} = tu^2_\tau/\nu \leq 500$ produced drag reductions of up to 40%, the maximum at $T^+_{osc} = 100$. The normal and Reynolds shear stresses were both significantly damped (streamwise, u, 14% reduction; wall normal, v, 30% reduction; lateral, w, 35% reduction; uv 40% reduction) and that the maxima in each stress moved away from the wall toward, but never reaching, the centreline. The mean velocity profile, under maximum skin friction reduction conditions, shows a small logarithmic region, with a concomitant increase in the thickness of the buffer layer and an almost non-existent linear shear region ($u^+ = y^+$). It is argued that a reduction in the number and intensity of turbulent bursts is responsible for the observed behaviour. This was deduced, it seems, from noting a significant increase in the spatial homogeneity of constant vorticity magnitude ($\mid \omega \mid = 1.1u^2_\tau/\nu$) with the introduction of wall oscillation. This implies that the wall oscillation reduces the flow to more or less two dimensions, since spanwise variation is significantly reduced. Interestingly, in the conference presentation of the same work Akhavan *et al.* (1992), when the contour value of constant vorticity is increased ($\mid \omega \mid = 1.2u^2_\tau/\nu$) the rather flat, carpet -like surface seen above is replaced by streaks the distance between them is wider than in the natural wall case, but also, the streaks tend to merge together. These results seem contradictory and experimental evidence needs to be gathered to clarify this issue. Breuer *et al.* (1989) use membranes stretched transversely to the main flow, each separated by small spanwise solid surface gaps. They demonstrate the evolution and control of a large amplitude and highly three-dimensional disturbance in a laminar boundary layer (a turbulent spot). Activating the membranes decreases the amplification rate of spanwise vorticity and thus delays the formation of the spot. In view of Jung *et al.* , perhaps it is appropriate to repeat the experiment with the active components rotated and aligned with the flow.

3.3 Selective Interference

Goldstein *et al.* (1995) find that damping of lateral velocities close to the wall is all that is needed to explain the effects of riblets in turbulent flow. Goldstein *et al.* and Choi *et al.* (1992) apply damping to the velocity field in different ways. That is, by artificially introducing velocities in– or out–of phase with that which already exists will either amplify or nullify them, (*e.g.* $w(x,0,z) = \alpha\, w(x,h,z), -1 \leq \alpha \leq 1$, h is the non-dimensional height above the wall where the velocity vector is detected, and with either the same or the opposite value applied at the wall and the optimum is found to be at about $h = 10$). Spectacularly, both wall normal and lateral velocity out of phase control (velocity cancellation) gave about either 25% or 30% reduction, respectively, in the pressure gradient. Similar control applied to the streamwise velocity gave about 10%, which is similar to that obtained with riblets. The streamwise and spanwise distribution of the longitudinal correlation coefficient is noticeably altered when spanwise control is employed (spanwise distribution of R_{uu} crosses the zero axis at about $z^+ \approx 100$ and reaches a minimum (of ≈ -0.1) at $z^+ \approx 150$ and at $y^+ \approx 0.2$ and the general shape does not seem to be altered as $0.2 \leq h \leq 15$). When wall normal control (v) is used, the same correlations do not change appreciably from that obtained without control, while the longitudinal distribution of R_{uu} is severely shortened in streamwise extent (for $h \approx 0.2$, $R_{uu} \approx 0$ at $\Delta x^+ \approx 200$ whereas without control, the coefficient approaches zero as $\Delta x^+ \geq 800$). This implies that control (of the type employed) de-correlates the "normal" wall turbulence, at least in the longitudinal direction very close to the wall. When spanwise control is used, the streamwise extent of R_{uu} is larger than without control, especially when the control is sensed at $y^+ \approx 5$. R_{vv} and R_{ww} are little affected in all cases, implying that effects of applying control, in the simulations, may be a direct result of satisfying continuity. Interestingly, the spanwise two-point spatial correlation coefficient with polymer addition to the sub-layer, Fortuna and Hanratty (1972), shows an increasing spatial separation between the structures. Indeed, as the drag reduction saturates to its maximum, the correlation length remains positive.

An interesting aspect of the above is revealed in a series of papers by Sirovich *et al.* (1990) (1991) and Handler *et al.* (1993). The latter paper provides, I believe, critical information for the future. In a DNS, the velocity field is generated using equation (2). It can be reconstructed using the Karhunen-Loève procedure, or Proper Orthogonal Decomposition, Lumley (1967), (1970), which generates empirical eigenfunctions from the velocity correlations. From these, various eigenmodes can be identified that make up the velocities in the three coordinate directions. It turns out that a significant amount of the energy in the flow is contained in the non-propagating streamwise roll modes (streaky structure), and minimum energy (~20%) is contained in the propagating transverse wave modes. An interesting finding is the limited quadrant analysis, (see Willmarth 1975) that demonstrates,

Sirovich *et al.* (1990) the spectrum of occurrences of the Q2 events can only be re-created if the fast modes (propagating modes) and the slow modes (roll modes that are non-propagating) interact: remove one and there is very little Q2 activity, which clearly indicates that the ejection mechanism and the concomitant production of both Reynolds and wall shear stress should be reduced, Willmarth (1975).

Handler *et al.* (1993) choose to interfere with various Fourier modes (not eigenmodes of POD), introducing this randomisation at different specified frequencies. They claim upwards of 58% drag reduction, which is similar to polymer addition, Lumley (1969), Virk (1975), by just random forcing of a relatively small subset of the available Fourier modes in the DNS simulation and thereby, it is speculated, destroying the "coherence" of the turbulence producing structures. Since these turbulence producing structures are propagating modes, associated with waves at angles to the roll modes, it is inferred by the present author that removing the interaction reduces the flow to spanwise periodic two dimensional flow. Unpublished work by Handler (private communication 1993) claims that a non-random or constant phase shift gives drag reduction; moreover, drag increase is achieved if the phase relationships are maintained between the wave modes. Experiments are currently underway to see if phase randomization can be achieved (Levich, private communication).

An little emphasized feature of the results, Handler *et al.* (1993), is the dramatic change in the magnitudes and wall-normal distributions of the three RMS velocity fluctuations. At around maximum drag reduction (the shortest time between randomizing the modes) the maximum in both the spanwise and wall normal components double in magnitude and the maximum moves from $y^+ \approx 25$ to $y^+ \approx 125$, which is at the centre of the channel. As well, the longitudinal velocity component approximately doubles in magnitude; however, its maximum remains at $y^+ \leq 25$. Physically, this implies that the production of turbulence is shifted away from the wall and the flow is approaching a laminar-like condition (see below). Indeed, the spanwise wave-number spectrum of the streamwise velocity component, which highlights the spanwise streaky structure, shows, for the smallest period between mode randomization ($y^+ = 14.8$), a destruction of smaller scales and a concomitant increase in the smaller wave numbers. For larger periods between randomization, for which skin friction reduction first increases (to its maximum of 58%) before diminishing with increasing time between randomization, the spectrum does not change in the smaller scales implying that it is the large scales, or at least their location with respect to the surface, that control skin friction. That riblets have been found to perform the same function (as demonstrated by the protrusion height) seems to confirm the notion that they do so, but inefficiently.

The out of phase lateral and wall normal velocity control strategy of Choi *et al.* (1992), the phase randomization of Handler *et al.* (1993) and polymer

additions to liquids ($u^+ = 11.7\ ln\ y^+ - 17.$, Virk's asymptote, Virk 1975) leads to the alteration of the log-law region of the mean velocity profile. At $y^+ = 100$, $u^+ \approx 17$ (Newtonian flow) and $u^+ \approx 37$ for polymers; however, the out of phase control lifts $u^+ \approx 20$ (recall only about 25–30% reduction in skin friction) while the phase randomization gives $u^+ \approx 22.4$ when maximum friction reduction (58%) is achieved. The out of phase control ($\alpha = -1$) retains some semblance of a log-law region, while the phase randomization almost eliminates it. This is illustrated in figure 8.

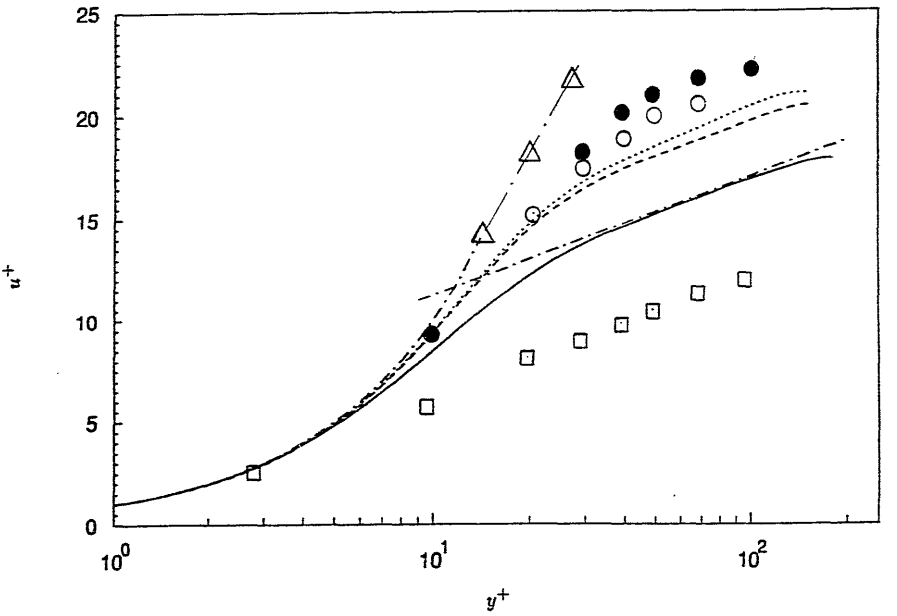

Fig. 8. $U^+ vs. Y^+$ for flat wall turbulence (——), with spanwise (. . . . .) and wall normal (- - - -) control, Choi etal. (1992); with phase randomization, run LK(2) (•), Handler etal. (1993); Virk's (1975) asymptote (Δ) for polymer addition; spanwise control $\alpha = 1$,(2) and $\alpha = -2$,(O), Jimenez (1994)

Illustrated, as well are the results from Jimenez (1994) (note the claim is made in this paper that riblets increase the spanwise width between the streaks; significant contradictory evidence in the literature exists on this).

The parameters used by Jimenez ($w(x,0,z) = \alpha w(x,h,z)$, *etc.*) were the same as Choi *et al.* , but $-2 \leq \alpha \leq 1$, which, for $\alpha = -2$ implies a local reorganization of the spanwise velocity (substantial acceleration of flow on the wall in the direction opposite to that at the detection point at $h = 10$) produces a greater diminution in the size of the log-law region. In addition, this control strategy moves the structures away from the wall, confirming the speculations on the action of riblets. It is difficult to imagine the effect of this type of boundary condition since it is sporadic; however, simply, as illustrated in figure 9 the fountain-like eruption of fluid from the impingement of two high speed streams could move a pair of QSWV further out into the core of the flow since the eruption is between the pair, the sense of rotation of which is opposite and toward the wall. Opposite to this is the elimination of the high shear region between a pair of QSWV and the wall and the inflectional velocity profile so engendered ($\alpha = 1$, or pure slip control) would seem to play an important role in generating shear stress, since the velocity profile is dramatically altered to consist entirely of a logarithmic region. That is, again simply, figure 9, the imposition of wall velocities in–phase with that sensed at the detection point would tend to draw towards the wall a pair of QSWV, thereby increasing the wall shear stress. The similarity here with studies of vortex cores impinging a wall (see, for example, Chu and Falco 1988) is appealing. It is not clear whether the imposition of the no–slip out–of–phase condition ($\alpha \pm 1$) on the spanwise velocity would produce effects similar to that observed by Jung *et al.* (1992).

It is interesting to speculate that the erosion of the log-law region noted above, may be linked to the inner-outer region scaling controversy. Falco (1991) suggests that the backs of the large scale motions in a boundary layer, upon which there are located what has been often referred to as his "typical" eddies are important in the dynamics of the boundary layer. As the Reynolds number increases, both the longitudinal rms velocity fluctuation and the Reynolds shear stress, when normalised with wall shear velocity, fail to scale with y^+ for $y^+ \geq 15$. However, when normalised using length and velocity scales deduced from an average "typical" eddy, then for wall equivalent scaling $15 \leq y^+ \leq 200$, and the maximum extent increasing with increasing Reynolds number, scaling is achieved. The minimum extent ($y^+ \approx 15$) maybe reducible (but not to zero), so that, it is argued, the "typical" eddies influence the wall region as well. This implies (but does not necessarily confirm) that the logarithmic region dynamics are altered when control or phase randomisation are employed by interfering with the transport of events to or from this region. Interestingly, Orlandi and Jimenez (1994), using a variant of the NWVM approach, argue that the wall shear in turbulent flows is larger than that in laminar because (over very short times $t^+ \ll 1$) any spanwise velocity imposed on an initial uniform shear serves to increase the average wall shear stress. As well, the transport of high speed fluid towards the wall is thus more important than ejection of low speed fluid away from it; this is confirmed experimentally, Wark and Nagib (1991).

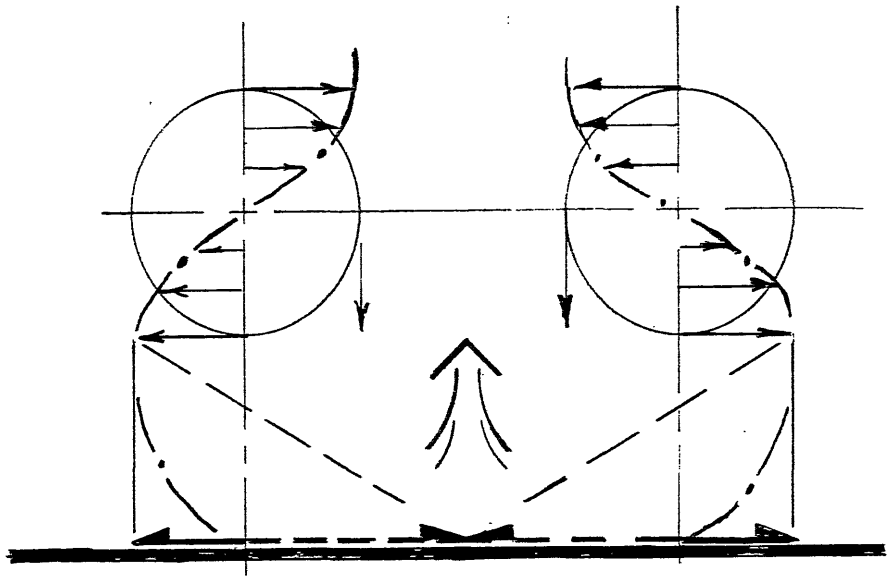

Fig. 9. Cartoon of a pair of QSWV near the wall. If detection of spanwise motion on lower boundary of QSWV is used, the zero-slip velocity profile (— . —) would alter to (——) if slip condition imposed on wall and if wall motion is applied in direction opposite to QSWV direction, then profile alters to (- - - -), giving rise to fountain-like eruption of near-wall flow which would lift away from the wall and separate the QSWV

3.4 Selective Introduction Techniques

The skin friction benefits obtained from lateral oscillation of a channel wall Jung *et al.* 1992) or phase randomization Handler *et al.* (1993) introduces interesting possibilities for alternative methods for interacting with near-wall turbulence. The introduction of small scales into the boundary layer through the wake of a body (for example, an airfoil or large eddy breakup device (LEBU), Coustols and Savill 1992) gives rise to a diminution in the wall skin friction downstream of the device. It is known, too, that a ribbon, vibrating in the wall normal direction produces spanwise variations in the RMS amplitude of the streamwise velocity, see, for example Kachanov (1994), and the

amplitude of these fluctuations can be adjusted using sound, Gedney (1983). Of course, instantaneously, there exists spanwise variations in all velocity components in a natural boundary layer, as shown by, for example, Kline *et al.* (1967).

In essence, the phase randomization and spanwise wall oscillation reorganises and diminishes the bursting events, in a manner not yet understood, while the wake of a body can introduce a spectrum of scales that provides spanwise variations in the velocity. Is it possible to introduce into the near-wall region a spectrum of scales, with streamwise oriented vorticity, with the "right" length scales, that will interact in the manner appropriate to decreasing the spatial coherence of the near-wall structures?

Osaka and Fukushima (1994) use plates of various sizes and lateral periodicity and alter their location to be either inside or outside the entrainment boundary of a turbulent boundary layer. The results from this study are encouraging, showing that widely spaced airfoils can generate significant spanwise variations in wall shear stress and that the effect of these airfoils extend 150 boundary layer thicknesses downstream. Caution, however is warranted in interpreting the skin friction results as they are obtained using Preston tubes.

A variety of scales can be introduced into the boundary layer by using a ribbon oscillating in the spanwise direction. Using Jung *et al.* (1992) as a guide, the optimum wall oscillation is $T^+_{osc} = tu^2_\tau/\nu = 100$, so that, assuming the wall shear velocity is the correct scaling parameter, Pollard *et al.* (1993b) obtained data that gave some hint that the wall skin friction could be forced to be below that obtained using a stationary ribbon, but perhaps the real benefit will be derived from enhancing mixing applications.

4 Concluding Remarks

We have reviewed controlling near-wall turbulence, using both passive and active methods. It has been surmised that the reason that riblets give only about 10% reduction in skin friction over that obtained from smooth walled flow is due to their inefficient interaction with QSWV. The QSWV are a predominant feature of near-wall turbulence; and it seems that the key to increased reduction in skin friction is to disallow them from approaching the wall. This review has surmised as well, from available evidence, that the re-organization of the near-wall structures should lead to or mimic as closely as possible a quasi-periodic spanwise organization of them. To accomplish the task of minimising the interacting between longitudinal rolls and other "waves" in the boundary layer, humplets may be an interesting passive method, since they can be of various sizes and orientations in the plane of the flow.

The manipulation and control of turbulence is in its infancy; however, the insights gained from simulations are becoming greater, especially as the

ability to handle and interrogate the huge amount of "data" generated by them. Even so, there continues to exist computational limitations that may have produced results that are not devoid of errors: as with other experiments, policing and reporting of computational errors and limitations of results need to be encouraged.

This material formed part of the author's contribution to the shortcourse Flow Control: Fundamentals and Practices held at the CNRS Laboratory, Cargése, Corsica, June 24-28, 1996 and at the University of Notre Dame, September 9-13, 1996. This contribution has used material excerpted from the same authors' contributions to Emerging Techniques in Drag Reduction, Choi, Prasad and Truong (eds.) 1996 and Progress in Aerospace Sciences, submitted for publication, 1997.

Acknowledgments

Funding for the work was provided in part by: a NATO Collaborative Research Grant, Natural Science and Engineering Research Council of Canada.

References

Akhavan, R., Jung, W.J. and Mangiavacchi, N. (1992): Turbulence control in wall bounded flows by spanwise oscillations. Advances in Turbulence IV, Nieuwstadt (ed) Kluwer Academic Publ., See also Applied Scientific Research, 51:299-303.

Aubry, N., Holmes, P., Lumley, J.L. and Stone, E. (1988): The dynamics of coherent structures in the wall region of a turbulent boundary layer, *J. Fluid Mechanics*, **192**:115-173.

Berkooz, G., Holmes, P. and Lumley, J.L. (1993): On the relation between low-dimensional models and the dynamics of coherent structures in the turbulent wall layer, *Theoretical Comp. Fluid Dynamics*, 4:255-269.

Cousteix, J., Houdeville, R. and Javelle, J. (1981): Response of a turbulent boundary layer to a pulsation of the external flow with and without adverse pressure gradient. *Proceedings, IUTAM Symposium on Unsteady Turbulent Shear Flows*, pp 120–144.

Baron, A. and Quadrio, M. (1993): Some preliminary results on the influence of riblets on the structure of a turbulent boundary layer. *International J. Heat and Fluid Flow*, **14**(3), 223–230.

Baron, A., Quadrio, M. and Vigevano, L. (1993): On the boundary layer - riblet interaction mechanisms and the prediction of turbulent drag reduction. *Intl. J. Heat and Fluid Flow*, **14**(4), 324–332.

Bechert, D.W. (1987): Experiments on three dimensional riblets. In *Turbulent Drag Reduction by Passive Means*, Royal Aeronautical Society, London.

Bechert, D.W. and Bartenwerfer, M. (1989): The viscous flow on surfaces with longitudinal ribs. *J. Fluid Mechanics*, **206**:105–129.

Benhalilou, M. Anselmet, F., Liandrat, J. and Fulachier, L. (1991): Experimental and numerical investigation of a turbulent boundary layer over riblets. In *Proc., 8th Symposium on Turbulent Shear Flows, Munich.*

Brereton, G.J. and Reynolds, W.C. (1991): Dynamic response of boundary layer turbulence to oscillatory flow. *Physics Fluids A*, **3**:178-187.

Breuer, K.S., Haritonidis, J.H. and Landahl, M.T. (1989): The control of transient disturbances in a flat plate boundary layer through active wall motion. *Physics Fluids A*, **1**:574-582.

Bruse, M., Bechert, D.W., vander Hoeven, J.G., Hage, W. and Hoppe, G. (1993): Experiments with conventional and with novel adjustable drag-reducing surfaces. In B.E.Launder R.M.C.So, C.G.Speziale, Editors, *Near-wall turbulent flows*, pages 719 – 738. Elsevier Publishers, B.V.

Bushnell,D. and McGinley, C. (1989): Turbulence control in wall flows. *Annual Review of Fluid Mechanics*, **21**:1–20.

Carlson, H.A. (1995): Direct numerical simulation of laminar and turbulent flow in a channel with complex, time-dependent wall geometries, Ph.D. thesis, Cornell University, May.

Carlson, H.A. and Lumley, J.L. (1996): Flow over and obstacle emerging from the wall of a channel, *AIAA J.*, **34**(5):924-931.

Canuto, C., Hussaini, M.Y. Quarteroni, A. and Zang, T.A. (1987): *Spectral Methods in Fluid Dynamics.* Springer Verlag, Berlin.

Chapman, D.R. and Kuhn, G.D. (1986): The limiting behavior of turbulence near a wall. *J. Fluid Mechanics*, **170**:265–292.

Choi, K-S. (1987): The wall pressure fluctuations of modified turbulent boundary layer with riblets, in *Turbulence Management and Relaminarization*, Springer Verlag, Liepmann and Narasimha (eds.).

Choi, K-S. (1989): Near-wall structure of a turbulent boundary layer with riblets. *J. Fluid Mechanics*, **208**:417–458.

Choi, K-S. (1993): Breakdown of the Reynolds analogy over drag - reducing riblet surface. *Applied Scientific Research*, **50**:563–567.

Choi, H., Moin, P. and Kim, J. (1991): On the effects of riblets in fully developed laminar channel flows. *Physics Fluids A*, **3**:1892–1896.

Choi, H., Moin, P. and Kim, J. (1992): Turbulent drag reduction: Studies of feedback control and flow over riblets. Technical Report Report TF-55, Dept. Mechanical Engineering, Stanford University, California.

Choi, H., Moin, P. and Kim, J. (1993): Direct numerical simulation of turbulent flow over riblets. *J. Fluid Mechanics*, **255**:503–540.

Choi, H., Theman, R., Moin, P. and Kim, J. (1993): Feedback control for unsteady flow and its application to the stochastic burgers equation. *J. Fluid Mechanics*, **253**:509–544.

Chu, D.C., Henderson, R. and Karniadakis, G.E. (1992): Parallel spectral element fourier simulation of turbulent flow over riblet mounted surfaces.

Theoretical and Comp. Fluid Dynamics, **3**:219–229.

Chu, D.C. and Karniadakis, G.E. (1993): A direct numerical simulation of laminar and turbulent flow over riblet mounted surfaces. *J. Fluid Mechanics*, **250**:1–42.

Clark, D.G. (1989): Boundary layer flow visualization patterns on a riblet surface. Technical Report QMC-EP-1081, Queen Mary and Westfield College, University of London.

Coustols, E. and Savill, A.M. (1992): Turbulent skin-friction drag reduction by active and passive means. In Coustiex, J. Editor, *Special course on skin friction drag reduction, Report 786.* AGARD.

Chu, D.C. (1992): A direct numerical simulation of laminar and turbulent flow over streamwise aligned riblets. Master's thesis, Department of Mechanical and Aerospace Engineering, Princeton University.

Chu, C.C. and Falco, R.E. (1988): Vortex ring/viscous wall layer interaction model of the turbulence production process near-walls, *Experiments in Fluids*, **6**:305-315.

Djenidi, L. and Antonia, R.A. (1993): Riblet flow prediction with a low-Reynolds-number k-ϵ model. In K. Krishna Prasad, Editor, *Further developments in turbulence management*, see also: *Applied Scientific Research*, **50**:267-282.

Enyutin, G.V., Lashkov, Y.A., Samoilova, N.V., Fedeev, I.V. and Shumilkina, E.A. (1987): Experimental investigation of the effect of longitudinal riblets on the friction drag of a flat plate. *Fluid Dynamics*, **23**(2):284–289.

Ersoy, S. and Walker, J.D.A. (1985): Viscous flow induced by counter-rotating vorticies. *Physics Fluids*, **28**(9):2687–2698.

Falco, R.E. (1991): A coherent structure model of the turbulent boundary layer and its ability to predict Reynolds number dependence. *Philosophical Transactions Royal Society London A*, **336**:103–129.

Finnicum, D.S. and Hanratty, T.J. (1988): Effect of favorable pressure gradients on turbulent boundary layers. *American Institute Chemical Engineering Journal*, **34**(4):529–540.

Finnicum, D.S. and Hanratty, T.J. Influence of imposed flow oscillations on turbulence. Physico-chemical Hydrodynamics, 10:585-596.

Foic, F. (1991): *Etude Numerique de L'ecoulement sur une paroi striee (A numerical study of the flow over streamwise grooves).* PhD thesis, L'Ecole Natioanl Superieure de L'Aeronautique et de L'Espace, Marseille.

Fortuna, G. and Hanratty, T.J. (1972): The influence of drag-reducing polymers on turbulence in the viscous sublayer. *J. Fluid Mechanics*, **53**(3):575-586.

Gallagher, J.A. and Tomas, A.S.W. (1984): Turbulent boundary layer characteristics over streamwise grooves, AIAA paper 84-2185.

Gajdeczko, B. and Ramaprian, B.R. (1987): Experiments on periodic turbulent boundary layers in adverse pressure gradients. In *Proc., 6th Symposium on Turbulent Shear Flows, Toulouse*, pages 4.3.1–4.3.6.

Gedney, C.J. (1993): The cancellation of sound-excited Tollmein-Schlichting waves with plate vibration, *Physics Fluids*, **26**:1158-1160.

Germano, M., Piomelli, U., Moin, P. and Cabot, W.H. (1991): A dynamic sub-grid scale eddy viscosity model. *Physics of Fluids A*, **3**:1760–1765.

Goldstein, D., Handler, R. and Sirovich, L. (1995): Direct numerical simulation of turbulent flow over a modelled riblet covered surface. *J. Fluid Mechanics*, **302**:333-376.

Grant, H.L. (1958): The large eddies of turbulent motion. *J. Fluid Mechanics*, 4:149–190.

Handler, R.A., Levich, E. and Sirovich, L. (1993): Drag reduction in turbulent channel flow by phase randomization. *Physics of Fluids A*, **5**:686–694.

Hanratty, T.J., Chorn, L.G. and Hatziavramidis, D.T. (1977): Turbulent fluctuations in the viscous wall region for Newtonian and drag reducing fluids. *Physics Fluids*, **20**(10):S112–S119.

Hatziavramidis, D.T. and Hanratty, T.J. (1979): The representation of the viscous wall region by a regular eddy pattern. *J. Fluid Mechanics*, **95**:655–679.

Hooshmand, A. (1985): *An experimental investigation of the influence of a drag reducing, longitudinally aligned, triangular riblet surface on the velocity and streamwise vorticity fields of a zero-pressure gradient turbulent boundary layer.* Ph.D. thesis, University of Maryland.

Jimenez, J. (1994): On the structure and control of near-wall turbulence. *Physics Fluids*, **6**:994-953.

Johansson, A.V. and Alfredsson, P.H. (1982): On the structure of turbulent channel flow. *J. Fluid Mechanics*, **112**:295–314.

Jung, W.J., Mangiavacchi, N. and Akhavan, R. (1992): Suppression of turbulence in wall bounded flows by high-frequency spanwise oscillations. *Physics of Fluids A*, **8**:1605–1607.

Kachanov, Y.S. (1994): Physical mechanisms of laminar boundary layer transition, *Annual Review of Fluid Mechanics*, **26**:411-482.

Khan, M.M.S. (1986): A numerical investigation of the drag reduction by riblet surfaces. AIAA paper 86-1127.

Kim, J., Moin, P. and Moser, R. (1987): Turbulence statistics in fully developed channel flow at low Reynolds number. *J. Fluid Mechanics*, **177**:133–166.

Klein, H. and Freidrich, R. (1989): Manipulating large-scale turbulence in a channel and a boundary layer. In *Seventh Symposium Turbulent Shear Flows, Stanford.*

Kline, S.J., Reynolds, W.C., Schraub, F.A. and Runstadler, P.W. (1967): The structure of turbulent boundary layers, *J. Fluid Mechanics*, **30**:283-325.

Kobashi, Y. and Hayakawa, M. (1981): Structure of a turbulent boundary layer on an oscillating flat plate. Proceedings, IUTAM Symposium on Unsteady Turbulent Shear Flows, pages 67-76.

Kravchenko, A.C., Choi, H. and Moin, P. (1993): On the relation of near-

wall streamwise vortices to wall skin friction in turbulent boundary layers, *Physics Fluids*, **5**:3307-3309.

Kravchenko, A.C., Moin, P. and Moser, R. (1996): Zonal embedded grids for numerical simulations of wall bounded turbulent flows. *J. Computational Physics*, **127**:412-423.

Liu C. and Liu, Z. (1993): Multigrid methods and high order finite difference for flow in transition. In *11th AIAA Computational Fluid Dynamics Conference, Orlando*, number 93-3354.

Sirovich, L., Ball, K.S. and Handler, R.A. (1991): Propogating structures in wall bounded turbulent flows. *Theoretical and Computational Fluid Dynamics*, **2**:307–317.

Sirovich, L., Ball, K.S. and Keefe, L.R. (1990): Plane waves and structures in turbulent channel flow. *Physics of Fluids A*, **2**:2217–2226.

Luchini, P. Manzo, F. and Pozzi, A. (1991): Resistance of a grooved parallel flow and cross-flow. *J. Fluid Mechanics*, **228**:87 – 109.

Lumley, J.L. (1967): The structure of inhomogeneous turbulent flows, *Atmoshperic Turbulence and Radio Wave Propogation*, Yaglom and Tatarsky, Editors, Nauka Publ., Moscow.

Lumley, J.L. (1969): Drag reduction by additives. *Annual Review of Fluid Mechanics*, **1**:367–384.

Lumley, J. (1970): *Stochastic Tools in Turbulence*. Academic Press, New York.

Lyons, S.L., Nikolaides, C. and Hanratty, T.J. (1988): The size of turbulent eddies close to a wall. *American Institute Chemical Engineering Journal*, **34**(6):938–945.

Lyons, S.L., Hanratty, T.J. and McLaughlin, J.B. (1989): Turbulence producing eddies in the viscous wall region, *AIChE J.*, **35**(12):1962-1974.

Manhardt, M. and Wengle, H. (1993): A spatio-temporal decomposition of a fully inhomogeneous turbulent flow filed. *Theoretical and Computational Fluid Dynamics*, **5**:223–242.

Mao, Z.-X. and Hanratty, T.J. (1986): Studies of the wall shear stress in a turbulent pulsating pipe flow. *J. Fluid Mechanics*, **170**:545-564.

Masson, C., Saabas, H..J. and Baliga, B.R. (1994): Co-located equal-order control volume finite element method for two dimensional axisymmetric incompressible fluid flow. *Int'l. J. Numerical Methods in Fluids*, **18**:1–26.

McIlwain, S., Ewing, D. and Pollard, A. (1996): Evolution of large and small scale coherent structures in non-homogeneous shear flows, Bulletin of APS, Div. Fluid Dynamics, paper HI-6, November, Syracuse, New York.

Morrison, J.F., Subramanian, C.S. and Bradshaw, P. (1992): Bursts and the law of the wall in turbulent boundary layers. *J. Fluid Mechanics*, **241**:75–108.

Morrison, J.F., Tsai, H.M. and Bradshaw, P. (1989): Conditional sampling schemes for turbulent flow based on the VITA algorithm, *Experiments in Fluids*, **7**:173-189.

Nikolaides, C. (1984): *A Study of the Coherent Structures in the Viscous Wall Region of a Turbulent Flow.* Ph.D. thesis, Dept. of Chem. Eng., University of Illinois, Urbana.

Orlandi, P. and Jimenez, J. (1994): On the generation of turbulent wall friction, *Physics Fluids*, **6**:634-641.

Osaka, H. and Fukushima, C. (1994): Variation of skin friction for a turbulent boundary layer interacting with the controlled longitudinal vortex arrays. In Truong, T.V., Choi, K-S., Prasad, K. Krishna, Editor, *Emerging Techniques in Drag Reduction*, IMechE. (see also, JSME, Series B, Vol. 39, No. 1 1996).

Park, S.-R. (1992): *An experimental study of passive drag reduction in a turbulent boundary layer by a riblet surface.* PhD thesis, University of Maryland.

Peridier, V.J., Smith, F.T. and Walker, J.D.A. (1991): Vortex induced boundary layer separation. part 1. the unsteady limit problem, Re $\longrightarrow \infty$. *J. Fluid Mechanics*, **232**:99–131.

Peridier, V.J., Smith, F.T. and Walker, J.D.A. (1991): Vortex induced boundary layer separation. part 2. unsteady interacting boundary layer theory. *J. Fluid Mechanics*, **232**:133–165.

Perry, A.E. and Chong, M.S. (1982): On the mechanism of wall turbulence. *J. Fluid Mechanics*, **119**:173–217.

Perry, A.E. and Li, J.D. (1990): Experimental support for the attached-eddy hypothesis in zero pressure gradient turbulent boundary layers. *J. Fluid Mechanics*, **218**:405–438.

Perry, A.E., Maru, I.šić, and Li, J.D. (1993): Some recent ideas and developments in the modelling of wall turbulence. In Launder, B.E., So, R.M.C. and Speziale, C.G., Editors, *Near-wall turbulent flows*, pages 1–25. Elsevier Publishers, B.V.

Perry, A.E., Maru, I.šić, and Li, J.D. (1994): Wall turbulenceclosure based on classical similarity laws and the attached eddy hypothesis, *Physics Fluids*, **6**:1024-1035.

Pollard, A. (1994): Riblets, skin friction and near wall turbulence, Invited lecture, 11th Canadian Symposium Fluid Dynamics, Edmonton, Alta.

Pollard, A., Tullis, S. and Wang, X. (1993a): Flow over pyramid, rectangular and compound rectangular shaped riblets, including higher order statistics. Presentation, *8th. European Drag Reduction Meeting, Lausanne, Switzerland.*

Pollard, A., Delville, J. and Bonnet, J.P. (1993b): Skin friction reduction using a laterally oscillating ribbon. Presentation, *8th European Drag Reduction Meeting, Lausanne, Switzerland.*

Pollard, A., Tullis, S. and Wang, X. (1994): Skin friction drag reduction: A computational study of riblets. Proceedings, CFD Society of Canada, CFD'94, Toronto, Ontario, Gottlieb and Ethier (eds).

Pollard, A., Savill, A.M., Tullis, S. and Wang, X. (1996): Effects of thin

element, compound thin element and trapezoidal valley riblets on near-wall turbulent flow. *AIAA J.*, **34**(11):2261-2268.

Pulles, C. J. A. (19988): Drag reduction of turbulent boundary layers by means of grooved surfaces, Ph.D. Thesis, Technische Universiteit Eindhoven.

Rizk, M.H. and Menon, S. (1988): Large eddy simulations of axisymmetric excitation effects on a row of impinging jets. *Physics Fluids*, **31**(7):1892–1903.

Robinson, S.K. (1991): The kinematics of turbulent boundary layer structure. Technical Report TM-103859, NASA.

Ronneberger, D. and Ahrens, C.D. (1977): Wall shear stress caused by small amplitude perturbations of turbulent boundary layer flow: an Experimental investigation. *J. Fluid Mechanics*, **83**:433-464.

Smith, C.R. and Metzler, S.P. (1983): The characteristics of low-speed streaks in the near-wall region of a turbulent boundary layer. *J. Fluid Mechanics*, **129**:27-54.

Smith, C.R., Walker, J.D.A., Haidari, A.H. and Sobrun, U. (1991): On the dynamics of near-wall turbulence. *Philosophical Transactions Royal Society London A*, **336**:131–175.

Sullivan, P., Day, M. and Pollard, A. (1995): Enhanced vita techniques for turbulent structure identification. *Experiments in Fluids*, **18**(1/2):10-16.

Sullivan, P.E. and Pollard, A. (1994): Large eddy simulation sub-grid-scale reconstruction using Gram Charlier with stochastic estimation and wavelet filters, Proceedings, 2nd. Annual Conference, CFD Society of Canada, Toronto, Ethier and Gottlieb (eds).

Suzuki, Y. and Kasagi, N. (1993): Drag reduction mechanism on micro-grooved riblet surface. In *Near-wall Turbulent Flows*, So, Speziale, and Launder, (Eds), pages 709–718. Elselvier Science Pub.

Tang, Y.P. and Clark, D.G. (1991): On turbulence generating events over drag reducing riblets. Technical Report QMW-EP-1087, Queen Mary and Westfield College.

Tang, Y.P. and Clark, D.G. (1993): On near-wall turbulence-generating events in a turbulent boundary layer on a riblet surface. *Applied Scientific Research*, **50**:215–232.

Tardu, S., Truong, T.V. and Tanguay, B. (1993): Bursting and structure of the turbulence in an internal flow manipulated by riblets. *Applied Scientific Research*, **50**:189–213.

Tardu, S. and Binder, G. (1993): Wall shear stress modulation in unsteady turbulent channel flow with high imposed frequencies. *Physics of Fluids A* **5**:2028-2037.

Tritton, D.J. (1967): Some new correlation measurements in turbulent boundary layers. *J. Fluid Mechanics*, **28**:439–462.

Tullis, S. (1992): Modelling the time dependent flow over riblets in the viscous wall region. Master's thesis, Dept. of Mechanical Engineering, Queen's University at Kingston.

Tullis, S. and Pollard, A. (1991): Modelling the flow over riblets including

their effects on near-wall turbulent eddies. Presentation, 6th. European Drag Reduction Working Meeting, Eindhoven, Netherlands.

Tullis, S. and Pollard, A. (1993): Modelling the time dependent flow over riblets in the viscous wall region. *Applied Scientific Research*, **50**:299–314.

Tullis, S. and Pollard, A. (1993): A numerical ivestigation of the turbulent flow over v and u groove riblets using a viscous wall region model. In *Near-wall Turbulent Flows*, So, Speziale, and Launder, (Eds), pages 761–770. Elselvier Science Pub.

Tullis, S. and Pollard, A. (1994): The time dependent flow over v and u groove riblets of different sizes. *Physics of Fluids A*, **6**(2):1000–1001.

Virk, P.S. (1975): Drag reduction fundamentals. *AIChE J.*, **21**:625–656.

P.Vukoslavčević, Wallace, J.M. and Balint, J-L. (1987): On the mechanism of viscous drag reduction using streamwise aligned riblets: a review with new results. In *Turbulent Drag Reduction by Passive Means*, pages 290–309. Royal Aeronautical Society.

P.Vukoslavčević, Wallace, J.M. and Balint, J-L. (1992): Viscous drag reduction using streamwise-aligned riblets. *AIAA J.*, **30**(4):1119–1122.

Walsh, M.J. (1990): Riblets. In Bushnell, D.M. and Hefner, J. Editors, *Viscous Drag Reduction in Boundary Layers, Progress in Astronautics and Aeronautics*123.

Wark, C. and Nagib, H. (1991): Experimental investigation of coherent structures in turbulent boundary layers, *J. Fluid Mechanics*, **230**:183-208.

Welsh, M.C., Hourigan, K., Welch, L.W., Downie, R.J., Thompson, M.C. and Stokes, A.N. (1990): Acoustics and experimental methods: the influence of sound on flow and heat transfer, *Exp. Thermal and Fluid Science*, **3**:138-152.

Wilkinson, S.P. (1990): Interactive wall turbulence control. In Bushnell, D.M. and Hefner, J., Editors, *Viscous Drag Reduction in Boundary Layers, Progress in Astronautics and Aeronautics*123.

Wilkinson, S.P., Anders, J.B., Lazos, B.S. and Bushnell, D.M. (1989): Turbulent drag reduction research at NASA Langley - progress and plans. *International J. Heat and Fluid Flow*, **9**:266 – 277.

Willmarth, W.W. (1975): Pressure fluctuations beneath boundary layers. *Annual Review Fluid Mechanics*, **7**:13-38.

Yang, K.S. and Ferziger, J.H. (1993): Large eddy simulation of turbulent obstacle flow using a dynamic sub-grid scale model. *AIAA J.*, **31**:1406–1413.

Zang, Y., Street, R.L. and Koseff, J.R. (1993): A dynamic mixed subgrid scale model and its application to turbulent recirculating flows. *Physics Fluids A*, **5**:3186–3196.

8 Combustion Enhancement by Active Control

E. Haile, O. Delabroy, D. Durox, F. Lacas, and S. Candel

Laboratoire E.M2.C., École Centrale Paris, 92295 Châtenay-Malabry Cedex, France

Abstract. Active control has many potential applications in the domain of combustion. Active instability control has been successfully demonstrated in a variety of laboratory combustors and its practical use is currently being explored. Active control methods also appear to be suited to the optimization of combustion system operation. The external controller may be used for example to extend the stability margin of the system, reduce the pollutant emission levels, augment the combustion and thermal efficiency, or modify the temperature distribution in the exhaust gases. This article describes applications of active control towards improving combustion, with specific attention paid to pollutant emissions reduction. Some background material on active combustion control is given, along with a discussion of strategies for NO_x reduction, and a review of experiments on flame interactions with external perturbations. The possibilities for active management of the reactive region are described. Applications of active control are illustrated by typical results obtained in recent experiments.

1 Introduction

Active combustion control is a subject of current fundamental and technological interest. The general objective of active control is to improve combustor operation. One wishes, for example, to augment the stability of the flame, enhance the rate of conversion of the reactants, improve the temperature distribution at the combustor exhaust, or diminish the levels of pollutant emission. Control is also seen as a means for monitoring the proper operation of a system.

Initial demonstrations of the basic concepts were achieved mainly on small-scale laboratory combustors. Reduction of combustion instabilities was investigated in a variety of geometrical configurations including Rijke tubes, laminar flame burners, and turbulent combustors. Some more recent studies were carried out on higher power devices. While active control was achieved with some success, it has also led to new detailed investigations of unsteady combustion processes. Active control has allowed analysis of the mechanisms leading to limit cycle oscillations of a combustor and has been used to study flame extinction mechanisms related to pressure waves.

It was concluded from these initial experiments that active control had potential applications in combustion enhancement. Instability control is one major area of concern. It is, for the moment, the most advanced, but has

M. Gad-el-Hak et al.: LNPm 53, pp. 467 - 499, 1998
© Springer-Verlag Berlin Heidelberg 1998

not yet given rise to large-scale application. Active control is specifically considered for ramjets, lean premixed combustors, afterburners, and segmented solid propellant rocket motors. Many aspects of active combustion instability control are reviewed by McManus et al. (1993), therefore this topic is not covered extensively in what follows. We here focus on other applications of active control and deal specifically with the active reduction of pollutant emissions.

A first case of interest is the lean premixed combustors being developed to reduce gas turbine exhaust emissions. These modern devices have excellent emission characteristics and bring a significant reduction of nitric oxide levels. Unfortunately, the lean premixed mode of operation is also quite sensitive to pressure waves and features instabilities and associated side effects like flashback or flame blowout. Active control may then be used to avoid unstable operation, or at least augment the stability margin of the combustor. This is an indirect application of active combustion instability control to combustion enhancement: control prevents instability thus allowing smooth operation of a low emissions combustor.

The second case of interest concerns standard combustors operating in the non-premixed mode. The reactants are introduced separately, often leading to poor mixing and long flames with large regions at elevated temperatures. Emission levels may be quite high in such circumstances. Active control can here be used to enhance mixing, thereby modifying the reactant conversion rate, combustion efficiency, flame temperature and pollutant formation and destruction. Active control may also be used to reorganize the flame structure by redistributing fuel and oxidizer to "stage" the regions of conversion.

Such direct applications of active control could be used to retrofit existing configurations in order to comply with more stringent regulations.

In what follows, we treat the direct application of active control to combustion enhancement. The next section contains some background material and a review of active control systems (open-loop, closed-loop, and adaptive closed-loop control). Section 3 deals with the methods of optimizing combustion processes, while section 4 describes the possible interactions of external excitation with flames. The flame response to perturbations and the resulting modification of the flow pattern are essential aspects of combustion control. The flame dynamics may be obtained from experiments reviewed in this section. Section 5 presents in detail the principles of active NO_x emissions reduction (mixing enhancement, flame structure modification) in light of the results discussed in section 4.

2 System review

The first mention of the effects of sound on combustion is due to Leconte (1858), who studied the response of flames to the music produced by a cello. The inverse mechanism, the production of sound by oscillating flames, or

"singing flames", was also studied at this time by Tœpler (1866), who used the Schlieren visualization technique to follow the phase-decomposed movements of the flame. As early as the 19th century, the sensitivity of flames to sound was exploited in acoustic measurements. Lord Rayleigh (1896), and especially Tyndall (1867), studied the response of flames to acoustic excitation, and determined that flames are most sensitive at their base, the point of stabilization. The necessary condition is that the flames be on the point of "flaring", that is, at the laminar/turbulent transition point. Their observations, incidentally, led Reynolds (1894) to formulate his criterion for turbulent transition.

2.1 Background material on coupling mechanisms

Flames are therefore sensitive to small perturbations. This observation of the last century returned to the forefront of engineering science with the development of rocket motors (see for example Crocco & Cheng (1956)) and the combustion instabilities encountered in these high-performance devices. Given the large volumetric heat release rates of rocket engines, resonant coupling between combustion and acoustics can attain very high energetic levels. These combustion instabilities caused the failure of many of the first launch vehicles. Ariane 1 on its second flight was destroyed when combustion oscillations coupled with the eigenmodes of the reservoirs, leading to large-amplitude pogo oscillations.

The measurements made on real motors and laboratory models gave rise to a classification, proposed by Barrère & Williams (1968) and Putnam (1971), depending on the system components implied in the instability:

- system instabilities, characterized by oscillations involving all of the system components, from the reservoirs to the exhaust;
- chamber instabilities, that only concern the combustion chamber, the characteristic dimensions being smaller, the instability frequencies are higher and transverse oscillation modes generally present;
- intrinsic instabilities, involving chemical kinetics and transport mechanisms, and having very high characteristic frequencies.

The coupling between heat release and acoustic modes can be formally understood by considering Euler's equations with source terms: (Harrje & Reardon (1972), Culick (1988), Clavin et al. (1994))

$$\frac{d\rho}{dt} + \rho \nabla \cdot \boldsymbol{u} = \dot{m} \tag{1}$$

$$\rho \frac{d\boldsymbol{u}}{dt} + \nabla p = \boldsymbol{F} \tag{2}$$

$$\rho c_v \frac{dT}{dt} + p \nabla \cdot \boldsymbol{u} = \dot{q} \tag{3}$$

where ρ, $\boldsymbol{u}$, T and p respectively designate fluid density, velocity, temperature and pressure. The unsteady energy source term $\dot{q}$ appears in the energy balance. In these expressions, d/dt is the material derivative defined as $d/dt \equiv \partial/\partial t + \boldsymbol{u} \cdot \nabla$. A mass source related, for example, to the evaporation of a condensed phase appears in the mass balance, and a force $\boldsymbol{F}$ acts as a momentum source. These last two terms will be neglected in what follows.

Using the equation of state for ideal gases: $p = \rho r T$, the equations for mass and energy conservation may be combined, yielding an equation for pressure:

$$\frac{dp}{dt} + \gamma p \nabla \cdot \boldsymbol{u} = \dot{m} r T + (\gamma - 1)\dot{q}, \tag{4}$$

where γ is the ratio of specific heats, $\gamma = c_p/c_v$. For a homogenous medium at rest, or with a vanishingly small Mach number, the material derivative may be replaced by the partial derivative with respect to time: $d/dt \approx \partial/\partial t$. This simplification yields the following system of equations.

$$\rho \frac{\partial \boldsymbol{u}}{\partial t} + \nabla p = 0 \tag{5}$$

$$\frac{\partial p}{\partial t} + \rho c^2 \nabla \cdot \boldsymbol{u} = (\gamma - 1)\dot{q} \tag{6}$$

where $c = \sqrt{\gamma r T}$ is the isentropic speed of sound. By taking the divergence of equation (5), deriving equation (6) with respect to time, and by subtracting the resulting expressions on obtains the inhomogeneous wave equation:

$$\frac{\partial^2 p}{\partial t^2} - c^2 \nabla^2 p = (\gamma - 1)\frac{\partial \dot{q}}{\partial t}. \tag{7}$$

This expression indicates that unsteady heat release acts as a source term for the pressure field. The resulting waves can, in return, modify the unsteady heat release, and, according to Rayleigh, if heat is released in phase with the pressure oscillation, the system receives energy, and can become unstable if the gain exceeds losses. However, if heat is added out of phase with respect to the pressure, energy is subtracted from the system, and the fluctuations are damped. The system is subsequently stable. The exact mechanism through which pressure waves are coupled to unsteady heat release must be determined and modeled to predict the occurrence of instability. Several possible coupling mechanisms exist, and are presented in a number of reviews (Barrère & Williams (1968), Culick (1988), Candel (1992)). Two are especially important in understanding what follows:

1. The acoustic velocity modifies the flame surface, folding and stretching it. This mechanism may excite parametric instabilities (Markstein (1965), Baillot et al. (1992), Boyer & Quinard (1990), Searby & Rochwerger (1991), Cambray & Joulin (1994))

2. Acoustic waves may excite hydrodynamic instabilities or induce the shedding of large-scale vortices. These, in turn, change mixture rates and can lead to unsteady combustion (Smith & Zukoski (1985), Poinsot et al. (1987), Yu et al. (1987)).

Both of these mechanisms depart from the framework of the simplified equation (7) given above.

In many practical situations (see for example Candel (1992)), the flame response is controlled by hydrodynamic instabilities. These instabilities are extremely sensitive to acoustic perturbations. Under external excitation, they are organized into coherent structures that are synchronized with the excitation. These structures control the development of non-reacting mixing layers. Crow & Champagne (1971) demonstrated the importance of these structures in the development of a turbulent jet by exciting the instability modes with a loudspeaker situated upstream of the jet nozzle. Brown & Roshko (1974) found that the same structures dominate the two dimensional shear layer. Oster & Wygnanski (1992) and Ho & Huang (1982) studied their evolution and nonlinear interaction.

In reacting flows, coherent structures induce unsteady heat release. This unsteadiness can then excite the acoustics of the installation and, if Rayleigh's criterion is satisfied, generate combustion instabilities (Schadow & Gutmark (1992)). Trouvé et al. (1988) have shown that driving by hydrodynamic instability was determined by the total time lag related to the phase speed of the instability wave on the jet of reactants entering their dump combustor and the speed of sound at which information is fed-back to the inlet conditions. This lag defines the phase of the heat release with respect to the acoustic eigenmodes of the installation. Yu et al. (1987) and Yu et al. (1991) have shown the relationship existing between coherent structures and combustion instability in their geometry.

In many other cases, coupling relies on the formation of a vortex at the entrance to the combustion chamber. This kind of instability is commonly referred to as a vortex instability (Poinsot et al. (1987), Smith & Zukoski (1985)). The vortex grows as it advects downstream, entraining reactants. This fluid structure can then interact with another vortex or with the chamber walls further downstream. This interaction results in a strong turbulent mixing of the reactants with burnt gases, leading to impulsive heat release. The pressure wave created travels upstream, triggering the shedding of another vortex (Menon & Jou (1990)). If no obstacle exists in the chamber, the vortex will continue to entrain reactants and products into its core. Vortex core ignition can then be observed (Thévenin & Candel (1995)). The rapid combustion in the core creates a pressure wave which propagates upstream and closes the resonance loop.

The dynamic counter-reaction can be tentatively modeled by a resonant feedback loop (fig. 1). The system (in dashed lines) is perturbed at its entry by pressure or heat release fluctuations. These fluctuations are converted

into heat release or pressure fluctuations, respectively. These latter, at the system exit, perturb the inputs through a counter-reaction. The simplest model consists of representing each of the blocks A and B in Fig. 1 with a linear filter, having a determined gain and delay, applied to the system inputs and outputs.

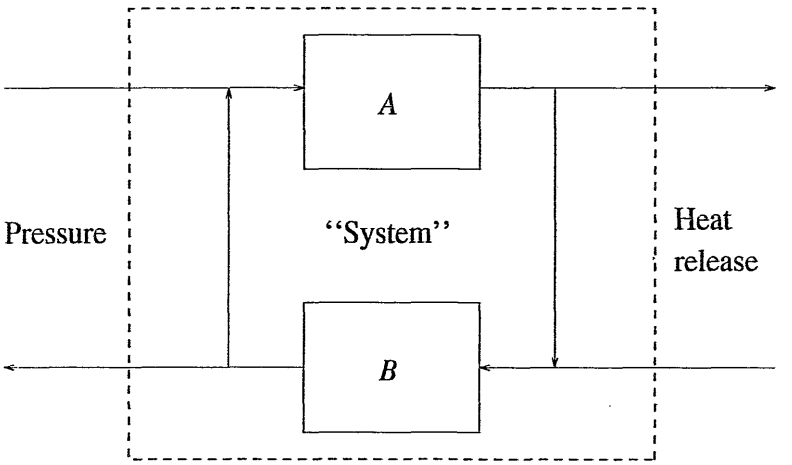

Fig. 1. Schematic representation of the coupling existing in combustion chambers. The linear filters A and B determine the degree of coupling between pressure oscillations and variations in heat release rate.

2.2 Pulse combustion

The coupling mechanisms cited above are equally present in pulse combustors. To benefit from the effects of combustion oscillations (increased heat transfer to the chamber walls, reduced pollutant emissions, smaller reaction zone, see Zinn (1992), Keller et al. (1994), Keller & Hongo (1988)), some combustion systems are designed to be unstable. Pulse combustion models are similar to those developed in the field of combustion instabilities (see Keller et al. (1988), Keller et al. (1987), Tang et al. (1995)). In most practical chambers, the driving mechanisms involve hydrodynamic instabilities or vortex shedding that control the mixing of reactants in the chamber and impose the ignition delay. The combustor is unstable if these mixing and reaction times retard the heat release with respect to the chamber eigenmodes, so that Rayleigh's criterion is satisfied.

2.3 Active combustion control

Active control techniques provide unique insights into the mechanisms of combustion instabilities. These methods can be used to stabilize an unstable

combustor, allowing steady operation over a wide range of regimes. It is also possible to establish an unstable mode of operation, a practice known as controlled pulsed combustion. This principle can be exploited to obtain the benefits of unstable combustion under controlled conditions in a stable burner configuration, or to identify the coupling mechanisms responsible for unstable operation. These possibilities are explored later in greater detail.

The first theoretical studies of active combustion instability control were carried out in the 1950s (Tsien (1952), Marble (1953), Marble & Cox (1955)), but its practical application had to wait for the technological advances of the 1980s.

In its simplest form, active combustion instability control can be summarized as in Fig. 2. A sensor is placed somewhere in the system to measure a signal representative of the instability (pressure oscillations, chemiluminescent intensity variations). The sensor signal serves as input to the control algorithm. The amplified and retarded signal is then re-injected upstream of the combustor by means of an actuator (for example, an acoustic driver unit), which creates fluctuations in pressure or heat release out of phase with respect to the instability. This technique is inspired by the principles of anti-noise as developed, for example, by Ffowcs Williams (1984). However, active instability control acts at the source of the phenomenon that is to be controlled. As such, less energy is required. Initial demonstrations were carried out by Heckl (1985) on Rijke tube geometries and by Bloxsidge et al. (1987) on ducted turbulent flames. This kind of control has been successfully demonstrated by Lang et al. (1987) and Gulati & Mani (1992) (among others) in the case of laminar premixed flames. Poinsot et al. (1989) and Billoud et al. (1992) applied this technique to turbulent non-premixed flames. More recently, Hermann et al. (1996) and Hantschk et al. (1996) have extended these results to the case of turbulent spray flames. Similar results are reported by Stirneman et al. (1995) with industrial burners.

If the gain and delay necessary to control the instability are not known *a priori*, adaptive control strategies may provide a solution (fig. 3). In this case, another sensor detects the global response of the system to the control effort. This signal is then used to update the parameters of the controller in order to minimize some error function (see Widrow (1970)). Active adaptive instability control has been successfully tested by Billoud et al. (1992) on a laboratory mock-up. This algorithm has certain limitations, however. Notably, in the experience of the authors, if the auxiliary path of the filtered-U algorithm is unknown, it must be identified before control can be attempted. Adaptive filters must also be constrained in order to remain stable whatever the system response. The adaptation cycle must also be longer than the closed-loop control cycle to ensure stability.

Note that if the suppression of instability is not the only objective, more complicated adaptive control algorithms exist which optimize error functions of several system parameters, taking into account noise levels and volumet-

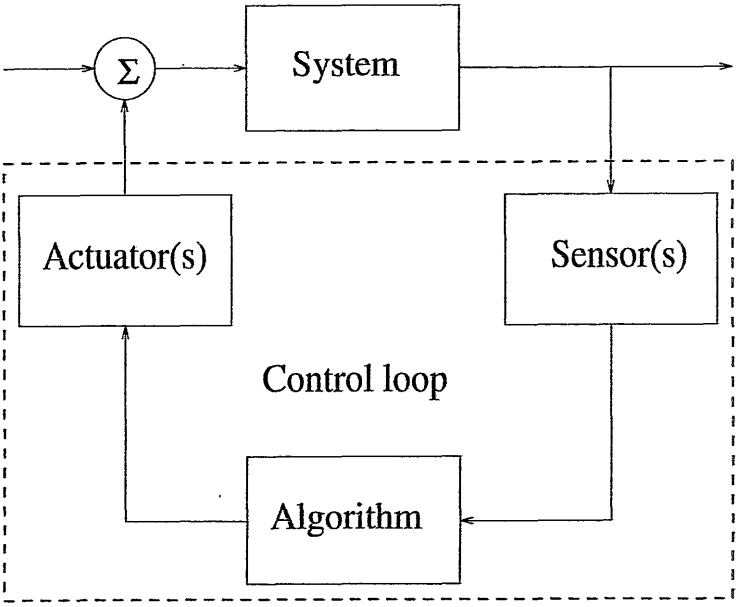

Fig. 2. Principle of closed-loop active control. A signal detected in the system is filtered and reintroduced upstream by the controller.

ric heat release rates, for example (Padmanabhan et al. (1995)). Allen et al. (1993) have shown the feasibility of low-frequency adaptive control of a turbulent spray flame using artificial neural networks. This result opens the way to new complex control strategies and to the control of more complex systems.

2.4 System identification

Figure 3 contains a filter representing an "auxiliary path" in the adaptive control loop. This component, essential to the filtered-U algorithm, is a model of the system to be controlled, incorporating the response of the system to the actuator's signal, and the sensor's detection of this response. The determination of this transfer function, known as system identification, may be carried out by exciting the combustor at very small amplitudes and recording its response. Given the excitation signal and the sensor signal, the corresponding transfer function can be inverted to filter the algorithm inputs. This tedious step is necessary for the convergence of the controller. The quality of the control obtained depends critically on the precision of the system representation by the auxiliary path transfer function. The principle of system identification is shown schematically in Fig. 4.

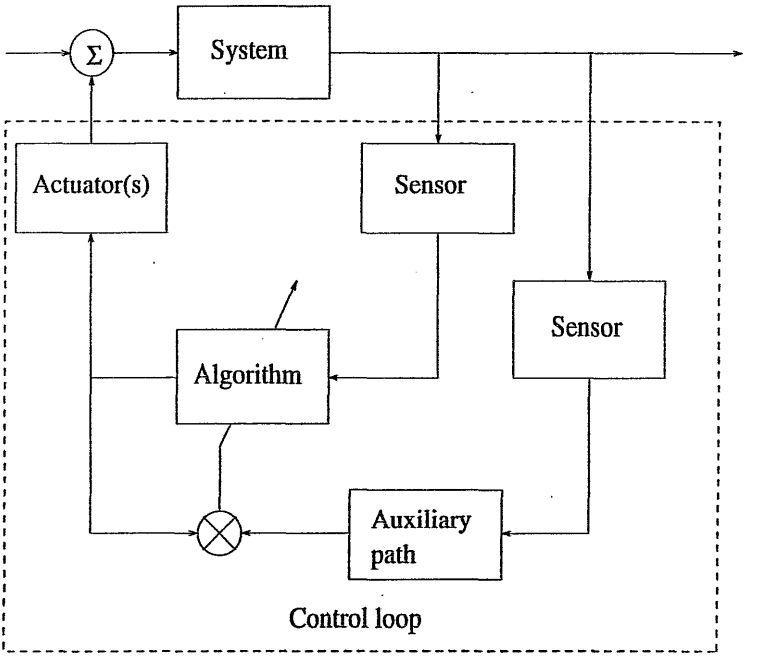

Fig. 3. Principle of active adaptive control. A second sensor detects the global response of the system to the control signal, and is used to update the coefficients of the control algorithm.

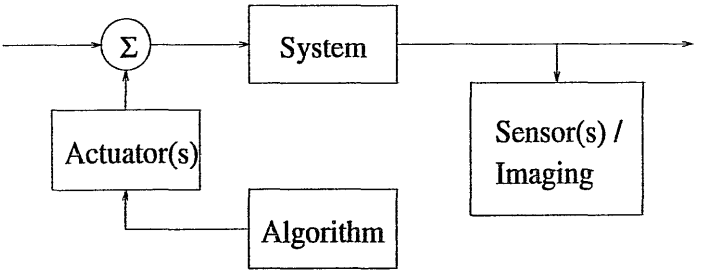

Fig. 4. The principle of system identification and open-loop control.

2.5 Active fluid mechanics and active combustion control

Active combustion control can be used to other ends than the suppression of instabilities. Gad-el-Hak (1994) gives a review of the new possibilities offered by active fluid mechanics, or flow control. This new field employs the techniques of active control to modify the development of a given flow. The properties of a fluid medium can be changed, increasing entrainment, drag or turbulence levels, for example. The work of Longmire & Eaton (1994) has shown that it is possible to actively control the dispersion of particles in a jet

by controlling the development of coherent structures in the unstable shear layer through acoustic excitation. Wiltse & Glezer (1996) have demonstrated the possibility of acting on the entrainment of jets in a quiescent medium. The entrainment of compressible jets through excitation of the origin of the shear layer has also been explored by Parekh et al. (1996).

The properties of combustors depend on the properties of the flow in which the flame develops. By exerting control over the flow, one can control the structure of the flame. By changing the local flame structure, as will be shown, the global characteristics of the combustor may be changed, such as the stability, pollutant emissions or volumetric heat release rate.

Gutmark et al. (1989) and, more recently, Chao & Jeng (1992) have used active control techniques to stabilize a lifted flame. A controlled acoustic excitation is applied to the lifted jet flame, creating coherent structures in the jet shear layer. These structures periodically reattach the flame to the burner exit, stabilizing it beyond the lean extinction limit. Recently, Yu et al. (1996) have obtained similar results using unsteady injection of liquid fuel droplets coupled with acoustic excitation. The periodic interaction between the vortices organized by the acoustic driving and the injected fuel drops is sufficient to stabilize the spray flame near the point of fuel injection.

Willis et al. (1994) and Pont et al. (1996) have increased the toxic waste disposal efficiency of their incinerator by acoustically driving the chamber. Coherent vortices are generated which interact with the flame. The toxic wastes are entrained by the vortices, increasing their residence time in the chamber, and thereby increasing the quantity of waste destroyed. Gutmark et al. (1994) have reported a reduction in the quantity of soot produced by a non-premixed propane-air flame when the fuel and air flows are acoustically excited in phase. For certain excitation frequencies and certain relative phases between the air and propane modulations, the mixing rate of the reactants is radically changed. The yellow sooting flame becomes blue, and the quantity of soot produced is decreased. The amount of nitrogen oxides produced by a domestic fuel-oil furnace has been reduced by applying a controlled acoustic excitation to the air flow rate (Delabroy et al. (1996b)). The application of this technique to a small (1 MW) industrial furnace has yielded similar results (Delabroy et al. (1996a)). Reduction in NO_x emissions are also reported by Charon et al. (1993) in a gaseous non-premixed burner.

McManus & Bowman (1990) (see also McManus et al. (1990)) have tested different types of actuators to excite the shear layer behind a dump plane in a combustion chamber. Like Yu et al. (1991), in this case, they noted the efficiency of this action in reorganizing the flow downstream of the dump, and the structure of the flame that develops in the shear flow. Using these techniques, they were able to increase the volumetric heat release rate in the chamber. The dynamic response of premixed flames subjected to acoustic fluctuations has been studied by Durox et al. (1996). They have shown that it is possible to change the average flow structure, thereby changing the average

structure of the flame. This complete reorganization of their Bunsen burner flow compacts the flame, which changes from its typical conical shape to a flattened hemisphere.

Many of the changes in combustor performance reported in the literature are due to structural modifications of the flow field. Global changes can be explained by local effects. A more compact flame reduces the residence time of nitrogen molecules in the high temperature reaction zone, thereby reducing the formation of NO through the thermal Zel'dovich mechanism. Lovett & Turns (1990) and Lovett & Turns (1993) have studied the structure of turbulent non-premixed gaseous flames subjected to external acoustic forcing. They report an increase in the entrainment of the jet which diluted the combustion products in their configuration. For the case of a confined flame, like that studied by Delabroy et al. (1996a), the same mechanisms increase mixing of the reactants. In a similar study, Gutmark et al. (1989a) showed by laser induced fluorescence of OH radicals that local extinction may take place downstream of vortical structures, in the braid region where strain rates are high. High strain rates inhibit the production of nitric oxide. This particular aspect (pollutant reduction by active control) is a challenging and technologically interesting field. Consequently, an entire section of this paper will deal with the mechanisms involved in NO_x control (section 5).

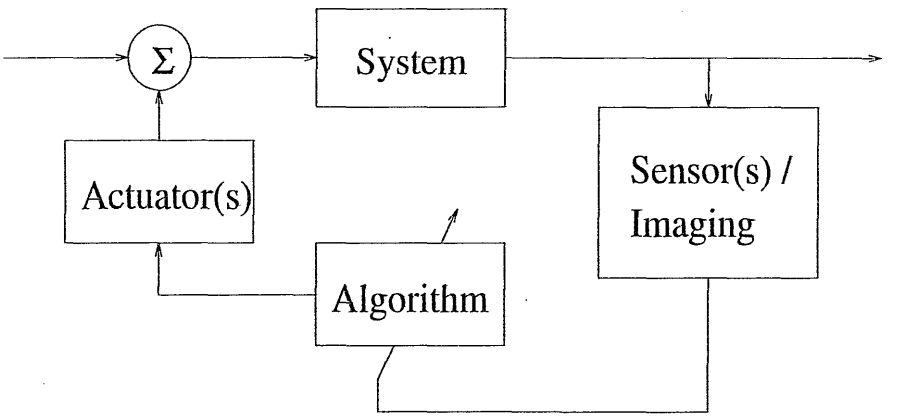

Fig. 5. Principle of closed-loop control with adaptive adjustment of external modulation. In this scheme, the algorithm serves to optimize the combustor operation.

Enhancement of combustion by active control can be successfully achieved in a variety of configurations. It is however possible and instructive to classify the different strategies and to give a few indications on how these strategies were effectively tested.

3 Control methods for combustion optimization

Whatever the objective of the control strategy may be (NO_x or soot reduction, efficiency, toxic waste elimination, flame stabilization, etc.), one is faced with two major issues. The first is the choice between open (Fig. 4) and closed-loop (Figs. 2, 3 and 5) control strategies. The second issue is technical and concerns actuators and sensors. Both are, in fact, linked as will be apparent from the following discussion.

3.1 Actuators

In all control strategies, the actuator is a central component of the system and deserves special attention. The choice of actuator is determined by the phenomenon to be controlled, as it must be able to act on the control parameters. As seen before, the control strategy may be a simple change in the combustor operating point. In this case, control will be effected by adapting the air flow rate (the primary or the nozzle atomizing air) or the fuel flow rate (see Table 1), and the actuators will be driven servo-valves.

If strong modification of the flame structure is sought, a sufficient amount of energy must be added to the flow. Flames are quite susceptible to acoustic perturbations, as will be shown later, so that one may use acoustic drivers to modulate the flow. Higher levels of modulation may be obtained with electro-pneumatic actuators or rotating valves. Acoustic drivers have been used most extensively (see Table 1 and especially Table 2), due to their extended frequency range and relative ease of use.

In some cases, one may wish to operate with more than one actuator. For instance, it is possible to act on the air flow with an acoustic driver (to form large-scale structures), using an actuator on the fuel line to synchronize fuel injection with the coherent structures (Yu et al. (1996)). Under these circumstances, it is possible not only to control the characteristics of one signal (its amplitude or frequency) but also to act on the phase between two signals and their relative amplitude. This type of control offers a range of new possibilities and should find more and more applications. However, more and more complex algorithms will be needed to manage the increasing number of actuators. Where before, with one actuator, there were two independent parameters in the cost function, with n actuators, the number of independent variables becomes at least $3n - 1$ assuming only frequency, amplitude and phase variations.

The effectiveness of the control strategy will also depend on the efficiency with which the actuator translates the control signal. Using acoustic drivers to generate vortices may not be the most efficient choice, whereas periodic jets may be more effective. It is therefore necessary to determine the sensitive parameters that control combustion enhancement. Such experimental work is reviewed in section 4.

3.2 Closed-loop control

Table 1. Closed-Loop Combustion Enhancement

Closed-Loop				
Authors	**Control objective**	**Sensor or Imaged radical**	**Actuator**	**Modified Flow**
Brouwer et al. (1990)	Optimize CO_2, CO, & soot	Gaz probe, radiative flux	Servo-valves	Atomizing & primary air
Gutmark et al. (1990)	ANN	CH*, C_2*, & OH*	Acoustic driver	Air flow
Gutmark et al. (1991)	Stabilize flame	CH* & C_2*	Acoustic driver	Premixed
Allen et al. (1993)	ANN	OH*	Valves	Atomizing & primary air
StJohn & Samuelsen (1994)	Optimize NO & efficiency	Gas analysis	Magnetic valves	Excess air & swirl
Padmanabhan et al. (1995)	Optimize heat release & noise	Piezoelectric transducer, photodiode	Loudspeaker & vortex jets	Premixed
Burkhardt et al. (1995), Burkhardt (1996)	ANN	Chemiluminescence	Valves	Air & fuel
Hermann et al. (1996)	Control instability	OH*	Piezo-actuator	Liquid fuel
Hantschk et al. (1996)	Control instability	OH*	Servo-valve	Liquid fuel

A set of articles using closed-loop control is given in Table 1. Combustion control is obtained by modulating the flow rates of air (Brouwer et al. (1990), Allen et al. (1993)), fuel (Hermann et al. (1996), Hantschk et al. (1996)), or both in non-premixed configurations. It is also useful to distinguish between rapid acoustic modulations and slower optimization of the burner operating point. The strategy used to slowly modify the operating point corresponds to that presented in Fig. 5. In such applications, the control strategy is not a direct feedback closed loop like that used in active combustion instability control (Figs. 2 and 3), in the sense that the sensor signal is not delayed, amplified, and re-injected into the system by the actuator. Instead, this information is used to optimize the combustor operating point or the parameters of an open-loop strategy like that depicted in Fig. 4.

In most of these applications, the output of the controller is essentially a mean reactant flow rate value. The combustor is brought to a new operating point, and the controller checks if a change has to be made to minimize a certain cost function. This is a slow but suitable way of finding the optimal operating conditions without directly modifying the flame structure. This approach is then well adapted to closed-loop operation, since in-depth understanding of the mechanisms involved is not necessary. The control strategy is often reduced to minimizing a cost function or maximizing a performance index evaluated from variables like CO_2, CO or NO mole fractions, thermal efficiency, volumetric heat release rate or sound pressure levels (Brouwer et al. (1990), StJohn & Samuelsen (1994), Padmanabhan et al. (1995)). Various experiments have proven the feasibility of this concept. New generations of controllers, like neural networks, are well suited to these operations and are beginning to emerge (Gutmark et al. (1990), Allen et al. (1993), Burkhardt et al. (1995), Burkhardt (1996)).

As an example of adaptive combustion enhancement, Padmanabhan et al. (1995) have used a closed-loop algorithm, with a more complex actuator-sensor system. A loudspeaker and jet vortex generators are used as actuators to change the flame structure (McManus et al. (1990), McManus & Bowman (1990)). A piezoelectric pressure transducer coupled with a photodiode measure the volumetric heat release rate and sound pressure level. The algorithm optimizes these two global response parameters, minimizing a predefined cost function, by changing the actuators' control parameters. The controller acts on the flame without *a priori* knowledge of the detailed flame structure or response, by minimizing an error function. However, this result was obtained after extensive open-loop experimentation to develop actuators and identify the combustor response showed that it was indeed possible to optimize the combustor performance in this manner.

The work of Allen et al. (1993) has shown that it is possible to train an artificial neural net (ANN) to recognize an optimal spray flame configuration from a video image of chemiluminescent emission. The ANN is then capable of changing the air and fuel flow rates in order to bring the flame to a given predefined optimal state. The training of such algorithms is equivalent to system identification and open-loop experimentation. This kind of control is also subject to the same limitations as other adaptive algorithms, in so far as the learned system response must not change over time, due to an accidental modification of the system, for example, the blockage of fuel injectors.

3.3 Open-loop control

A list of open-loop experiments is given in Table 2. There is no feedback in these experiments, but they form an essential first step towards active closed-loop control, as indicated above. Open-loop experiments allow the study of interactions between fluid motion, flame structure, and pollutant formation, for example. The information obtained from these experiments serves as a

model of the "auxiliary path" shown in Fig. 3, and guides the choice of actuator, as discussed above.

Imaging systems are often used in lieu of sensors (Table 2). Images can provide useful information about flame stabilization (Gutmark et al. (1989b), Gutmark et al. (1990), Chao & Jeng (1992)), reactant mixing and flame structure (Gutmark et al. (1989b), Vermeulen et al. (1982), Durox et al. (1996)), and pollutant formation (Gutmark et al. (1994), Delabroy et al. (1996b), Haile et al. (1996), Delabroy et al. (1997)). Some aspects concerning the flame response to external perturbations and pollutant control will be developed in the next section.

Active open-loop control can also be used as a finished product. For example, system driving or forcing has been used in incineration for years to eliminate particle deposition on the infrastructure of large industrial installations. It is also claimed (but yet to be independently proven) that infrasonic excitation of these incinerators increases burning rates and reduces pollutant emissions, mainly by improving mixing in fluidized beds. This type of control can be rendered adaptive by adding a sensor that measures the global response of the system to the external forcing. The information could then be used to modify the forcing frequency or amplitude until a minimum was found, as Padmanabhan et al. (1995).

Table 2. Open-Loop Combustion Enhancement

Open-Loop				
Authors	**Control objective**	**Sensor or Imaged radical**	**Actuator**	**Modified parameter**
Vermeulen et al. (1982)	Mixing	Temperature	Acoustic driver	Dilution air
Gutmark et al. (1989b)	Stabilization	OH*	Acoustic driver	Air & fuel
McManus et al. (1990)	Shear layer vortices	CH* & NO_x	Acoustic driver	Premixed
Gutmark et al. (1990)	Stabilization	Schlieren & PLIF OH	Acoustic driver	Premixed
Lovett & Turns (1990, 1993)	Pollutants	Gaz analysis, imaging, & velocimetry	Acoustic driver	Fuel
Schadow et al. (1992)	Control instability	CH* & pressure	Acoustic drivers	Fuel
Chao & Jeng (1992)	Stabilization	PLIF OH	Acoustic driver	Premixed
Gutmark et al. (1994)	Soot	IR, tomography, PLIF OH	Pneumatic driver	Air & fuel
Yu et al. (1996)	Stabilization	Tomography	Pneumatic driver & valves	Air & fuel (liquid)
Willis et al. (1994), Pont et al. (1996)	Incineration rate	Gas analysis, OH*, PLIF NO, PIV	Acoustic driver	Premixed
Durox et al. (1996)	Compact flame	CH*, Schlieren	Acoustic driver	Premixed
Delabroy et al. (1996a, b)	NO_x	CH* & gas analysis	Rotary valve	Air
Davis & Lin (1995)	Structure	Laser deviation	Acoustic driver	Air
Haile et al. (1996)	Structure	CH*	Acoustic driver	Air

4 Flame response to external perturbations

The response of a flame to external excitation is of central importance in active control. Identification of interaction mechanisms, resulting flame patterns and characteristic features of the excited flow constitutes the main building block in designing an active control system. Clearly the flame response will be highly dependent on the specific geometry, injection scheme, type of fuel, flow regime, etc. In general, the external excitation modifies entrainment, mixing and flow pattern. It also organizes the flame by setting a phase reference. Even small perturbations have a pronounced effect on the flame pattern, as will be shown below. Flames are generally quite sensitive to external perturbations because they often develop in a flow which is hydrodynamically unstable. The possible resonance of the confinement chamber may also enhance the response to a weak input. The large number of possible flame interactions are illustrated below by some typical examples. We successively consider laminar premixed flames interacting with upstream flow oscillations, premixed turbulent ducted flames forced by longitudinal acoustic modes, and turbulent spray flames subjected to air flow modulations. We also consider a case where both the liquid fuel and the air stream are simultaneously modulated. These three examples illustrate the possibilities of control.

4.1 Interactions between laminar flames and upstream flow modulations

It is quite informative to consider the simple situation of a laminar premixed flame anchored on the lip of a cylindrical pipe. Velocity oscillations are imposed on the upstream flow by a loudspeaker placed at the base of the duct, 0.2 m from the pipe exit. The loudspeaker is excited harmonically at various frequencies. Details on this experiment may be found in Baillot et al. (1992). In the low frequency range (typically around 100 Hz), the flame exhibits a strong response to very weak oscillations. Figure 6 shows the flame front visualized by a four-color Schlieren method. The front is wrinkled by the upstream modulations and features characteristic undulations which evolve into cusps.

The appearance of cusps is favored in longer flames, obtained with a high mean fresh gas velocity or low laminar flame speed. The cusp formation limit can be calculated, provided a reactive Strouhal number be defined, taking into account the flow velocity and the presence of a combustion wave (Baillot et al. (1996)). The relevant velocity then accounts for both the laminar flame speed and the flow velocity. With this definition, the intensity of flow fluctuations as a function of the reactive Strouhal number determines the limit of cusp appearance. As most flow oscillations remain weak, typically 20%, the flame front oscillates at the same frequency as that imposed on the upstream flow. The deformation of the front is due to traveling hydrodynamic waves created at the base of the flame and convected along the front at a

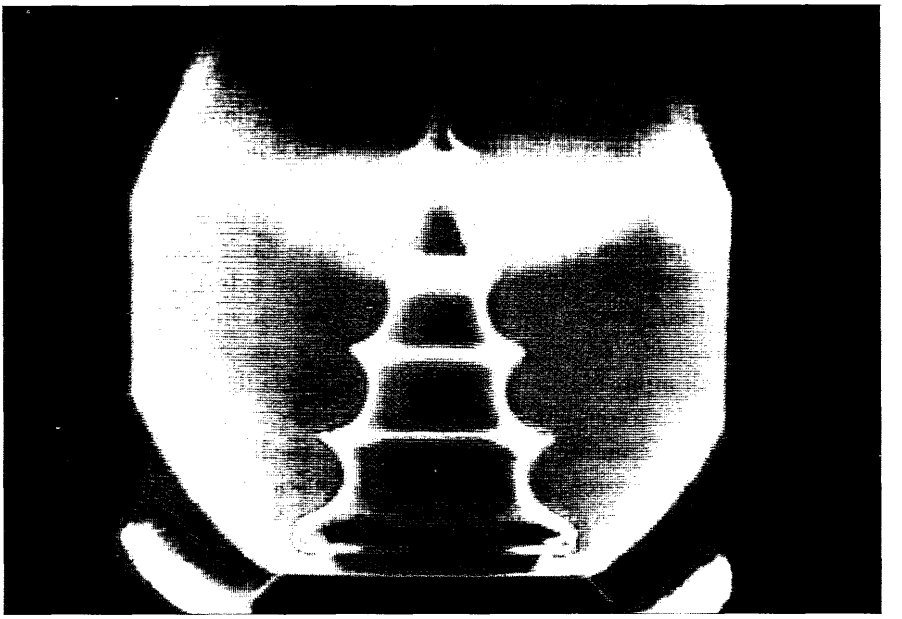

Fig. 6. Image of a Bunsen flame acoustically forced at 200 Hz (17.2% fluctuation intensity) acquired using a four-color Schlieren technique. The burner exit diameter is 30 mm.

phase speed which is a fraction of the flow velocity (De Sœte (1964)). More precisely, Boyer & Quinard (1990) have observed that the phase velocity of undulations is roughly equal to the local unburned gas velocity parallel to the flame front. Baillot et al. (1992) have improved upon this result through kinematic calculations. Their results underline the importance of two characteristic propagation velocities: the mean flow velocity projected along the flame front $V \cos \alpha$, and the phase speed of the flame front perturbations $V/\cos \alpha$. V is the mean flow velocity and α the half-angle of the steady flame cone. This second characteristic velocity is prevalent.

As the perturbation amplitude increases, the flame adapts its response by increasing the curvature of wrinkles and reducing its height (Durox et al. (1995)). However, the flame response to acoustic excitation becomes nonlinear when the excitation becomes too strong (Lang (1991)). Le Helley (1994) has shown that the heat release is a nonlinear function of the perturbation amplitude and that saturation occurs in the flame response. Davis & Jumppanen (1993) have also observed this saturation in diffusion flames. According to Le Helley (1994), heat release fluctuations are strongly correlated with

fluctuations in the flame surface area. The agreement in phase and amplitude are excellent, even for large acoustic velocity amplitudes. This result is true only when integrated over the entire reaction zone, since heat release can vary locally as a result of differential diffusion effects. Integrated over the entire flame surface, these local effects are compensated.

Premixed flames also behave as filters. While very sensitive to low frequency oscillations, flames are insensitive to low-amplitude high-frequency fluctuations. Work by Durox et al. (1995) has shown that beyond 250 Hz, methane-air flames stabilized on a burner 22 mm in diameter with a fluctuation intensity in the fresh mixture of 12% are not perturbed. This cut-off behavior of Bunsen flames can be compared with the results of flame-vortex interactions simulated by Poinsot et al. (1990) and experimentally investigated by Roberts et al. (1993). The sensitivity of flames to acoustic forcing is also influenced by the equivalence ratio of the mixture. Tests carried out at different equivalence ratios show that lean methane-air flames are more easily wrinkled than rich flames. This capacity to wrinkle is due to stretch effects (Law (1988)). A first analysis can be made based on the Lewis number. If less than unity (which is the case for lean methane-air flames), the competition between diffusive terms favors the appearance of instabilities and wrinkles, whereas they are inhibited by Lewis numbers greater than unity. This result agrees with the data obtained with premixed turbulent flames by Lee et al. (1993) and Lee et al. (1995). These authors have shown that turbulent flames wrinkle more easily if the Lewis number is less than unity. They consequently have a larger flame surface density.

These experiments may be used to determine the transfer function of the flame (the ratio of the fluctuating heat release to the velocity fluctuation imposed on the upstream side of the flame) in situations where the flame can no longer be considered infinitely small with respect to the wavelength of the disturbances created by the oscillating acoustic pressure.

At higher frequencies (typically around 1 kHz) and for large amplitudes of oscillation, the flame responds in a very different way. In some cases, the flame front takes a flat hemispherical shape as shown in Figure 7. In this example, it has been demonstrated that the acoustic field imposes the flame position (Durox et al. (1996)). The flame front lies on an equipotential of the pressure field and, in order to maintain equality between the laminar flame velocity and the flow component perpendicular to the front, strongly deflects the flow at the burner outlet. The flow pattern is, in this case, completely modified by the presence of the high-frequency large-amplitude oscillations of the incoming flow.

4.2 Forcing of a turbulent ducted flame by longitudinal acoustic modes

In this second example, a premixed turbulent flame is anchored on a V-shaped flame holder placed in a rectangular combustor. The channel is fed

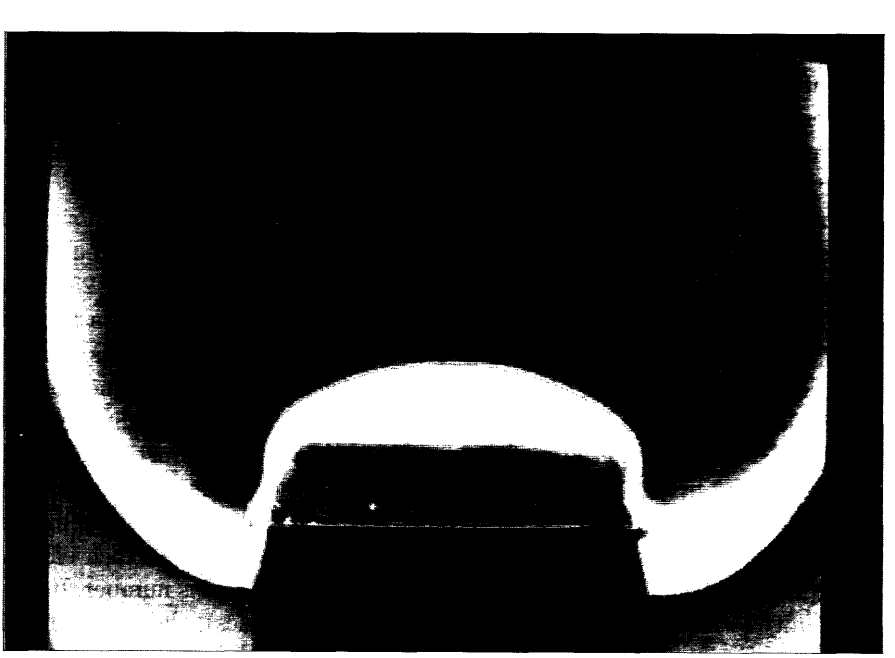

Fig. 7. Image of the same Bunsen flame forced at 1000 Hz. A parametric instability is excited, radically changing the flame structure and average flow field. The burner exit diameter is 22 mm.

with a mixture of air and propane. Experiments were carried out for a set of equivalence ratios ($0.6 < \phi < 0.9$) and mass flow rates (see Yu et al. (1991) for further details). The flame is excited by two driver units located on the upstream channel, producing longitudinal acoustic modes. Weak pressure oscillations produce a striking wrinkling of the turbulent flame front (as illustrated in Figure 8). The flame responds over a broad range of frequencies with a maximum for a Strouhal number based on the stabilizer size and flow velocity at the stabilizer lip $St = fh/U$ of order one. It is quite remarkable to note that the flame response is essentially flat over a broad spectral range (300 to 1800 Hz). Here again, the strong response observed may be related to the hydrodynamic instabilities of the flow.

4.3 Modulation of a turbulent spray flame

While gaseous flame forcing has been studied rather extensively, much less has been done on spray flames. This topic is of special interest because many combustors are fed with liquid fuel. A spray is usually formed by a mechanical or air-assisted atomizer. Experiments described in this section are carried out on a spray flame formed by a pressure atomizer and stabilized behind a small plate. The fuel is injected through a central hole in the flame holder plate. The air passes around the flame holder and mixes with the small droplets in

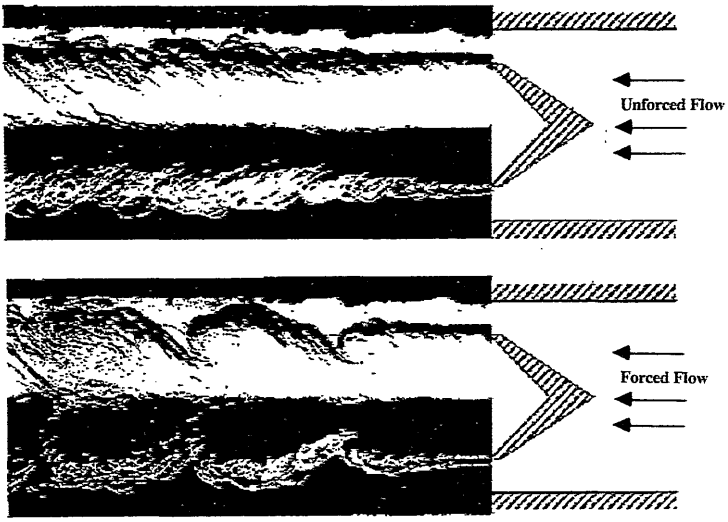

Fig. 8. Schlieren photograph of a turbulent premixed flame subjected to acoustic perturbations (from Yu et al. (1991)). The modulation reorganizes the flame holder wake into coherent structures. The global heat release rate is increased by the forcing.

the wake. Heat released by combustion vaporizes the remaining fuel droplets and the gaseous fuel released by this process mixes and burns with the downstream air. The natural flame obtained in this configuration is displayed in Figure 9 together with the fuel injector geometry. The burner and the active control system are shown in Figure 10.

A loudspeaker may be used to modulate the air stream. Another actuator, located on the fuel line and comprised of a fast electrovalve, is used to modulate the fuel stream. The forced flame is visualized by acquiring phase-locked images with a CCD camera equipped with an interferential filter centered on the CH* emission peak wavelength (430 nm). The modulation of the air stream reorganizes the flame structure as shown in Figure 11.

On the basis of simple physical considerations, the response of this type of flame to external excitation has been analyzed (Haile et al. (1996)). It is found that the flame responds best to structures whose characteristic length scale is the same as that of the reaction field, that is, having $St = fD/U \approx 1$. If the coherent vortices produced by the acoustic forcing are of the same size as the flame holder diameter D, they can effectively reorganize the entire reaction zone. They mix the fuel that is located close to the burner axis with the fresh air and combustion products. What is more, the droplet mechanical relaxation time should be less than the turn-over time of these coherent structures, so that they can be effectively entrained and mixed with the fresh air and products. This favors lower forcing frequencies, and may explain in part

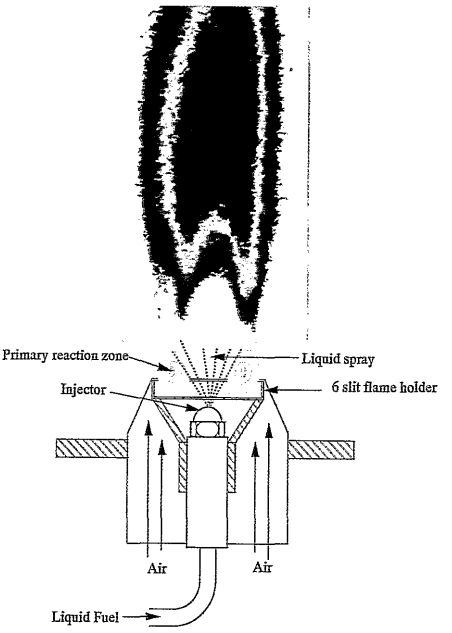

Fig. 9. Direct view of the unforced turbulent spray flame CH* radical emission. The color scale is linearly proportional to the emission intensity from red (least intense) to blue (most intense). The burner geometry is shown to scale.

the cut-off phenomenon observed in the acoustic response and NO emission reductions (Delabroy et al. (1996a)).

Using the liquid-fuel actuator, it is possible to stage actively the fuel distribution in the combustion chamber, and to synchronize fuel injection with the roll-up of the coherent vortices organized by the acoustic forcing. Figure 10 shows how this is accomplished experimentally. The loudspeaker is driven as before, and the acoustic excitation organizes the reaction zone into periodic coherent vortices. A microphone mounted on a wave guide at the burner exit plane on the chamber wall measures the acoustic pressure oscillations inside the combustor. Its signal is pass-band filtered around the forcing frequency. The liquid-fuel actuator is then used to synchronize the injection of the spray into the chamber with this signal. Both actuators operate at the same frequency, but their relative phase (measured between the valve's opening and the positive zero-crossing of the acoustic pressure signal) can be varied.

Figure 12 (taken from Haile et al. (1997)) shows the results obtained by forcing the flame acoustically and staging the liquid fuel injection at 124 Hz. The relative phase between the liquid-fuel actuator's opening and the microphone signal changes by 45° between each image. The relative phase is nil in image 12(a). The images were acquired in phase with the liquid

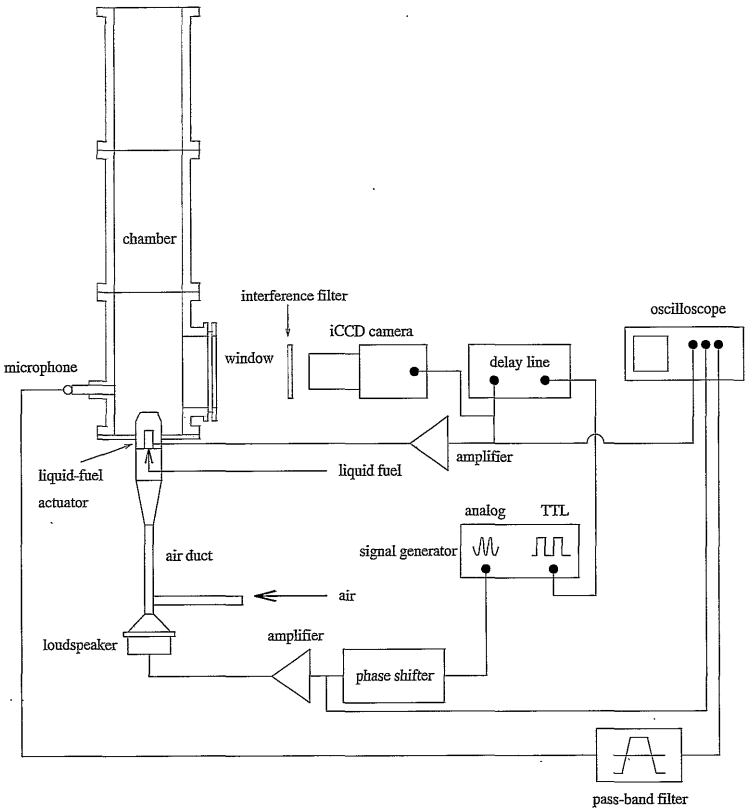

Fig. 10. Experimental set-up for active spray flame control.

fuel actuator, so that the phase of the coherent structures advances by 45°, while the packet of liquid fuel remains stationary. This latter is located at the center of each image, as shown by the region of intense CH* activity. As the coherent structure advances into the chamber, it interacts with the packet of droplets. Yu et al. (1996) have shown that periodic vortex-droplet interactions can be used to stabilize a spray flame in a dump combustor. In the present experiments, reductions in the sound pressure level of approximately 20 dB at the forcing frequency can be obtained with respect to the case of steady fuel injection when the droplet packet and vortex are out of phase (image 12(d)). When the two are in phase, the pressure fluctuations are maximized, and the apparent reaction zone length is minimized (image 12(h)). The effect on pollutant emissions is yet to be investigated for this particular case of dual excitation. However, the results previously obtained pointing to the improved mixing of reactants and reduced apparent reaction zone length are promising. How these changes bring about reduced NO_x emissions is the subject of the next section.

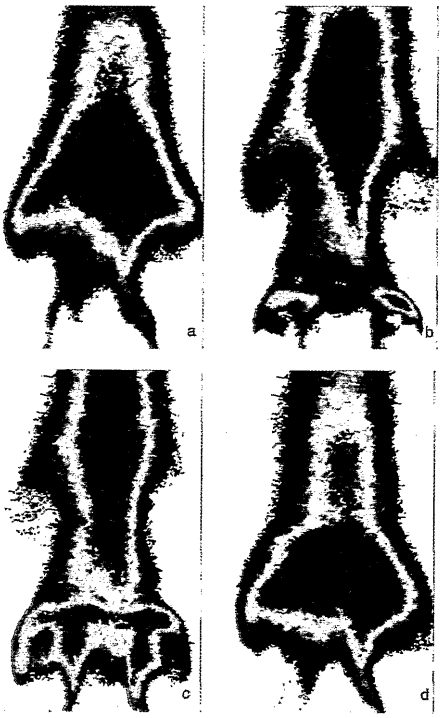

Fig. 11. CH* emission image of the flame under acoustic modulation. The image is acquired by phase-locking the camera with the excitation signal. The flame is excited at 82 Hz 5 Pa zero-peak. Each image corresponds to a different phase of the acoustic cycle, separated by 90° from its neighbors. The color scale is the same as in figure 9.

5 Application to pollutant emission

The interactions between a flame and large-scale coherent structures, as described in the previous section, have a major impact on pollutant emission. Long-term research effort is needed to design and commercialize new low-NO_x burners, while there is an urgent need for solutions to industrial applications faced with more demanding regulations on pollutant emissions. Active control can be used to retrofit a variety of existing burner configurations to comply with new legislation. It appears then as a viable alternative to acquiring completely new burners. This approach has been developed for a 20 kW liquid-fueled burner (Delabroy et al. (1996b)) and for a larger 900 kW system (Delabroy et al. (1996a), Delabroy et al. (1997)).

The goal of this section is to describe how active combustion control can lead to the observed NO_x emission reductions, using the results presented in the previous section concerning active control of a turbulent spray flame (Fig. 11). Open-loop experiments indicate reductions of 20% in NO_x emis-

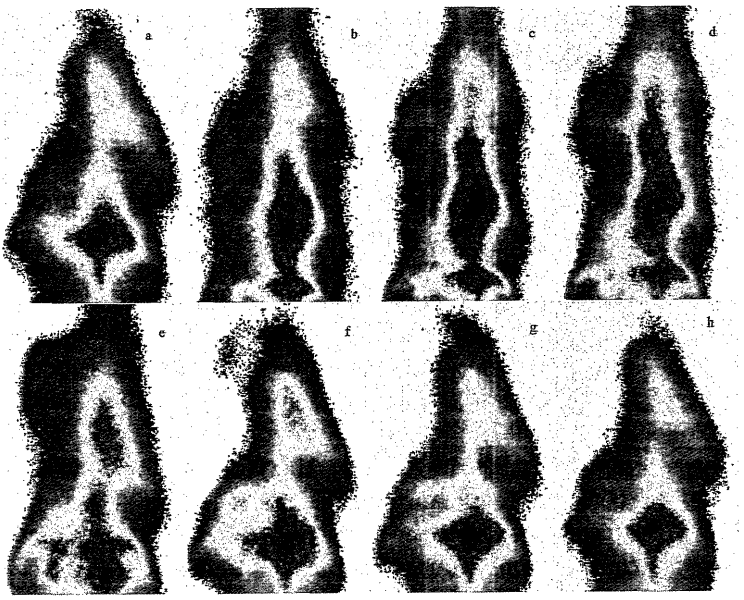

Fig. 12. Phase-locked images of the CH* radical emission of the flame. The color scale is the same as in figure 9. Both the air and the fuel are modulated at 124 Hz. The relative phase of the air modulation with respect to the valve's opening changes by 45° per image. The image is acquired for a fixed phase of the fuel valve cycle. ($\Delta\phi = 0°$, (a) ; $\Delta\phi = 45°$, (b) ; $\Delta\phi = 90°$, (c) ; $\Delta\phi = 135°$, (d) ; $\Delta\phi = 180°$, (e) ; $\Delta\phi = 225°$, (f) ; $\Delta\phi = 270°$, (g) ; $\Delta\phi = 315°$, (h))

sions are achievable (Delabroy et al. (1996b)). The different mechanisms presented in this section can be extrapolated to other systems featuring similar interactions between the flame and large-scale structures.

5.1 NO_x reduction: global effects

In order to understand the observed reduction in NO_x emission during active control experiments, one has to consider both the global and local effects of acoustic forcing on the flame. Globally, acoustic excitation systematically reduces the visible flame length (L_f) (Delabroy et al. (1996b)). This phenomenon has been observed in other configurations (Lovett & Turns (1990, 1993)). The residence time of burnt gases in high temperature zones is therefore reduced. This contributes to reducing thermal NO formation (Hayhurst & Vince (1983)). Note that empirical correlation of NO_x production (Peters & Donnerhack (1981), Stansel et al. (1995)) scale as L_f or ${L_f}^3$. Therefore, reducing L_f will diminish NO_x generation. The previous discussion concerns thermal NO. Because the residence times are relatively short in many situations, the thermal mechanism is not the only source of NO. To understand

the reduction mechanisms for prompt or fuel NO, it is important to examine the modifications in the local flame structure.

5.2 NO_x reduction: local effects

The non-premixed flame which develops in the combustion chamber downstream of the flame-holder is wrapped-up in the braids of the coherent vortex educed by the acoustic excitation (Fig. 11(b & c)). Here, the flame is subjected to high strain rates (Thévenin & Candel (1995)). Thermal NO_x formation rate decreases with increasing strain rate (Drake & Blint (1989), Vranos & Hall (1993)), and is therefore reduced in the vortex braids. Procter (1994) already suggested that the strain rates existing in pulse combustors were responsible for low NO_x levels.

Further downstream (Fig. 11(d & a)), the vortex grows, entraining fuel and air into its core, where a lean premixed flame ignites. The temperature field is more homogeneous and lower temperatures are attained than in diffusion flames. Such conditions reduce thermal NO production (Pompei & Heywood (1972), Lyons (1980)). Prompt NO formation is also reduced mainly because of the superequilibrium concentrations of O and OH prevalent in these flames (see Keller et al. (1994)). The chemistry of NO_x formation is presented in detail in the review by Miller & Bowman (1989).

Actively pulsed combustion also promotes reburning through the induced modifications of the flow field. Consider the primary flame zone, stabilized behind the flame-holder (Fig. 13). The structure of this rich primary flame is not modified by the air flow modulation. Due to the rich environment, a large quantity of CH_i radicals is produced. In the actively controlled flow, these radicals are entrained away from the burner axis by the coherent structures (Fig. 13) and may now react with the NO formed in the premixed vortex core through reactions like:

$$\begin{aligned} &CH + NO \rightarrow HCN + O, \\ &CH + NO \rightarrow N + HCO, \\ &CH + NO \rightarrow CNO + H. \end{aligned}$$

This mechanism is quite similar to reburning, or fuel staging, (Kolb et al. (1988)). In the modulated flame the staging is dynamic and internal. Other methods inducing internal staging exist (Beer (1994)), but the solution proposed here does not require major structural modifications to the burner and can be easily applied to many systems. This reduction mechanism affects all types of NO, and explains why actively pulsed combustion influences prompt as well as fuel NO. To illustrate this point, the nitrogen content of heavy fuel oil was simulated by doping domestic heating oil with pyridine and burned in a 900 kW burner (Delabroy et al. (1996a), Delabroy et al. (1997)). A reduction of 30% was achieved, demonstrating that active control can reduce the production of fuel NO.

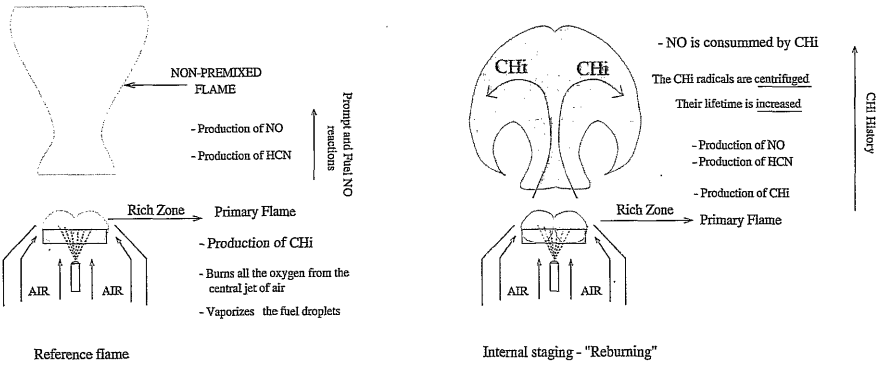

Fig. 13. Flame structure without (left) and with (right) control.

6 Conclusions

Active control methods have considerable potential in combustion. Experiments carried out on small and medium scale systems indicate that active control may be used to reorganize the flame region, improve mixing, modify the flame volume, or obtain a dynamic staging of the reaction zone. Open-loop control has already been employed to reduce nitric oxide emission levels. Further progress in this area will require a deeper understanding of flame interactions with external perturbations. In particular, it is necessary to develop basic studies on combustion/acoustic coupling and examine how modulations of air and fuel can be synchronized to attain optimal operation. Active control is also potentially useful in reducing instabilities that may appear in advanced systems like the lean premixed combustors which are now being developed for gas turbines and aircraft engines. While these systems produce low NO_x levels, they are often unstable. Pressure oscillations which appear under unstable conditions may then lead to flashback or flame blowout. Active control might be useful in preventing this unacceptable dynamical response and, in this sense, it might also help enhance the operation of the combustion system. Practical application of active control concepts is not straightforward. It will require further studies of basic mechanisms, examination of scaling problems, as well as more technological investigations focusing on sensors, actuators, and control algorithms. Reliability concerns in hostile environments will have to be treated carefully.

Acknowledgments

The authors gratefully acknowledge the financial support provided by the European Community, ADEME, MENESR, DRET and Bertin & Cie., and the technical support of the team of engineers and technicians at E.M2.C.

References

Allen, M. G., Butler, C. T., Johnson, S. A., Lo, E. Y., & Russo, F. (1993): An imaging neural network combustion control system for utility boiler applications. *Comb. Flame, 94*, 205–214.

Baillot, F., Bourehla, A. & Durox, D. (1996): The characteristics method and cusped flame fronts. *Combust. Sci. and Tech., 112*, 327–350.

Baillot, F., Durox, D., & Prud'homme, R. (1992): Experimental and theoretical study of a premixed vibrating flame. *Comb. Flame, 88*, 149–168.

Barrère, M. & Williams, F. A. (1968): Comparison of combustion instabilities found in various types of combustion chambers. *Eleventh Symposium (International) on Combustion.* The Combustion Institute, Pittsburgh.

Beer, J. M. (1994): Minimizing NO_x emissions from stationary combustion: reaction engineering methodology. *Chem. Eng. Sci., 49*, 4067–4083.

Billoud, G., Galland, M. A., Huu, C. H., & Candel, S. (1992): Adaptive active control of combustion instabilities. *Combust. Sci. and Tech., 81*, 257–283.

Bloxsidge, G., Dowling, A., Hooper, N., & Langhorne, P. (1987): Active control of reheat buzz. In *25th Aerospace Sciences Meeting.* AIAA.

Boyer, L. & Quinard, J. (1990): On the dynamics of anchored flames. *Comb. Flame, 82*, 51–65.

Brouwer, J., Ault, B., Bobrow, J. E., & Samuelsen, G. S. (1990): Active control for gas turbine combustors. In *Twenty-Third Symposium (International) on Combustion*, (pp. 1087–1092). The Combustion Institute, Pittsburgh.

Brown, G. L. & Roshko, A. (1974): On density effects and large structures in turbulent mixing layers. *J. Fluid Mech., 64*, 775–816.

Burkhardt, H. (1996): Image analysis and control of combustion processes. In *Active Combustion Control for Propulsion Systems*, AGARD Workshop. Athens, Greece.

Burkhardt, H., Oest, L., & Tao, W. (1995): Vision-guided flame control. In *SENSOR 95*, Nürnberg, Germany.

Cambray, P. & Joulin, G. (1994): Length-scales of wrinkling of weakly-forced, unstable premixed flames. *Combust. Sci. and Tech., 97*, 405–428.

Candel, S. (1992): Combustion instabilities coupled by pressure waves and their active control. In *Twenty-Fourth Symposium (International) on Combustion*, (pp. 1277–1296). The Combustion Institute, Pittsburgh.

Chao, Y.-C. & Jeng, M.-S. (1992): Behavior of the lifted jet flame under acoustic excitation. In *Twenty-Fourth Symposium (International) on Combustion*, (pp. 333–340). The Combustion Institute, Pittsburgh.

Charon, O., Jouvaud, D., & Genies, B. (1993): Pulsated O_2/fuel flame as a new technique for low NO_x emission. *Combust. Sci. and Tech., 93*, 211–222.

Clavin, P., Kim, J. S., & Williams, F. A. (1994): Turbulence-induced noise effects on high-frequency combustion instabilities. *Combust. Sci. and Tech., 96*, 61–84.

Crocco, L. & Cheng, S. L. (1956): Theory of combustion instability in liquid propellant rocket motors. In *AGARDOGRAPH 8.* NATO, Buttersworth Science Publication.

Crow, S. C. & Champagne, F. H. (1971): Orderly structure in jet turbulence. *J. Fluid Mech., 48*, 547–591.

Culick, F. E. C. (1988): Combustion instabilities in liquid-fueled propulsion systems. An overview. In *AGARD Conference.* NATO.

Davis, M. R. & Lin, L. H. (1995): Structures induced by periodic acoustic excitation of a diffusion flame. *Comb. Flame, 100*, 101–110.

Davis, M. R. & Jumppanen, P. C. (1993): Optical detection of the response of a diffusion flame to excitation. *Comb. Flame, 93*, 349–374.

De Sœte, G. (1964): Etude des flammes vibrantes: Application à la combustion turbulente. *Revue de l'Institut Français du Pétrole & Annale des combustibles liquides. 19*(6), June.

Delabroy, O., Haile, E., Candel, S., Pollard, A., Sobiesiak, A, & Becker, H. A. (1997): Passive and active control of NO_x in industrial burners. To appear in *Exp. Thermal & Fluid Sci.*, special volume reporting on *Workshop on Flow Control*, Cargèse, Corsica.

Delabroy, O., Haile, E., Veynante, D., Lacas, F., & Candel, S. (1996): Réduction de la production des oxydes d'azote (NO_x) dans une flamme de diffusion à fioul par excitation acoustique. *Rev. Gén. Therm. Fr., 35*, 475–489.

Delabroy, O., Lacas, F., Poinsot, T., Candel, S., Hoffmann, T., Hermann, J., Gleis, S., & Vortmeyer, D. (1995): A study of NO_x reduction by acoustic excitation in a liquid fueled burner. *Comb. Sci. and Tech., 119*, 397–417.

Drake, M. C. & Blint, R. J. (1989): Thermal NO_x in stretched laminar opposed flow diffusion flames with $CO/H_2/N_2$ fuel. *Comb. Flame, 76*, 151–167.

Durox, D., Baillot, F., Searby, G., & Boyer, L. (1996): On the shape of flames under strong acceleration: a mean flow controlled by the unsteady flow. Submitted to *J. Fluid Mech.*

Durox, D., Schulz, B. & Rudent, P. (1995): Sensitivity of premixed flames submitted to sinusoidal excitation. In *Joint Meeting of the French and German Sections of the Combustion Institute.* Mulhouse, France.

Ffowcs Williams, J. E. (1984): Anti-sound. *Proc. Roy. Soc. London, Series A, 395*, 63–88.

Gad-el-Hak, M. (1994): Interactive control of turbulent boundary layers: a futuristic overview. *AIAA J., 32*(9), 1753–1765.

Gulati, A. & Mani, R. (1992): Active control of unsteady combustion-induced oscillations. *J. Prop. and Power, 8*(5), 1109–1115.

Gutmark, E., Parr, T. P., Hanson-Parr, D. M., & Schadow, K. C. (1989): Azimuthal structure of an annular diffusion flame. *Comb. Flame, 75*, 229–240.

Gutmark, E., Parr, T. P., Hanson-Parr, D. M., & Schadow, K. C. (1989): On the role of large and small-scale structures in combustion control. *Comb. Sci. and Tech., 66*, 107–126.

Gutmark, E., Parr, T. P., Hanson-Parr, D. M., & Schadow, K. C. (1990): Use of chemiluminescence and neural networks in active combustion control. In *Twenty-Third Symposium (International) on Combustion*, (pp. 1101–1106). The Combustion Institute, Pittsburgh.

Gutmark, E., Parr, T. P., Hanson-Parr, D. M., & Schadow, K. C. (1991): Closed-loop amplitude modulation control of reacting premixed turbulent jet. *AIAA J.*, *29*(12), 2155–2162.

Gutmark, E. J., Parr, T. P., Hanson-Parr, D. M., & Schadow, K. C. (1994): Control of sooty high energy fuel combustion. In *1994 Spring Meeting of the Western States Section.* The Combustion Institute.

Gutmark, E., Parr, T. P., Parr, D. M., & Schadow, K. C. (1989): Stabilization of combustion by controlling the turbulent shear flow structure. In 7^{th} *Symp. on Turbulent Shear Flows.* Stanford Univ., CA.

Haile, E., Delabroy, O., Lacas, F., & Candel, S. (1996): Structure of an acoustically forced turbulent spray flame. In *Twenty-Sixth Symposium (International) on Combustion.* The Combustion Institute, Pittsburgh.

Haile, E., Lacas, F., & Candel, S. (1997): Active combustion control through pulsed liquid fuel injection. Submitted to *C. R. Acad. Sci. Paris.*

Hantschk, C., Hermann, J., & Vortmeyer, D. (1996): Active instability control with direct drive servo-valves in liquid-fueled combustion systems. In *Twenty-Sixth Symposium (International) on Combustion.* The Combustion Institute, Pittsburgh.

Harrje, D. T. & Reardon, F. H. (1972): Liquid propellant rocket instability. Technical Report SP-194, NASA.

Hayhurst, A. & Vince, I. M. (1983): The origin and nature of prompt nitric oxide in flames. *Comb. Flame*, *50*, 41–57.

Heckl, M. A. (1985): Active control of the noise from a Rijke tube. In Comte-Bellot, G. & Ffowcs-Williams, J. E. (Eds.), *Aero- and Hydro-acoustics*, (pp. 211–216). IUTAM, Springer.

Hermann, J., Gleis, S., & Vortmeyer, D. (1996): Active instability control (AIC) of spray combustors by modulation of the liquid fuel flow rate. *Comb. Sci. and Tech.*, *118*, 1–25.

Ho, C. M. & Huang, L. S. (1982): Subharmonics and vortex merging in mixing layers. *J. Fluid Mech.*, *119*, 443–473.

Keller, J. O., Bramlette, T. T., Barr, P. K., & Alvarez, J. R. (1994): NO_x and CO emissions from a pulse combustor operating in a lean premixed mode. *Comb. Flame*, *99*, 460–466.

Keller, J. O., Bramlette, T. T., Westbrook, C. K., & Dec, J. E. (1988): Pulse combustion: the quantification of characteristic times. Sandia Report SAND87-8832, Sandia National Laboratories.

Keller, J. O., Dec, J. E., Westbrook, C. K., & Bramlette, T. T. (1987): Pulse combustion: the importance of characteristic times. Technical Report SAND87-8783, Sandia National Laboratories.

Keller, J. O. & Hongo, I. (1988): Pulse combustion: the mechanisms of NO_x production. Technical Report SAND88-8602, Sandia National Laboratories.

Kolb, T., Jansohn, P., & Leuckel, W. (1988): Reduction of NO_x emission in turbulent combustion by fuel-staging: effects of mixing and stoichiometry in the reduction zone. In *Twenty-Second Symposium (International) on Combustion*, (pp. 1193–1203). The Combustion Institute, Pittsburgh.

Lang, W. (1991): Harmonic frequency generation by oscillating flames. *Comb. Flame, 83*, 253–262.

Lang, W., Poinsot, T., & Candel, S. (1987): Active control of combustion instability. *Comb. Flame, 70*, 281–289.

Law, C. K. (1988): Dynamics of stretched flames. In *Twenty-Second Symposium (International) on Combustion*, (pp. 1381–1402). The Combustion Institute, Pittsburgh.

Le Helley (1995): Etude théorique et expérimentale des instabilités de combustion et de leur contrôle dans un brûleur laminaire prémélangé. Ph.D. Thesis. Ecole Centrale Paris.

Leconte, J. (1858): On the influence of musical sounds on the flame of a jet of coal-gas. *Phil. Mag., 15*, 235.

Lee, J. G., Lee, T. W., Nye, D. A. & Santavicca, D. A. (1995): Lewis number effects on premixed flames interacting with turbulent Karman vortex streets. *Comb. Flame, 100*, 161–168.

Lee, T. W., North, G. L. & Santavicca, D. A. (1993): Surface properties of turbulent premixed propane/air flames at various Lewis numbers. *Comb. Flame, 93*, 445–456.

Longmire, E. K. & Eaton, J. K. (1994): Active open-loop control of particle dispersion in round jets. *AIAA J., 32*, 555–563.

Lord Rayleigh, J. W. S. (1896): *Theory of Sound.* MacMillan, London, reproduced by Dover (1945).

Lovett, J. A. & Turns, S. R. (1990): Experiments on axisymmetrically pulsed turbulent jet flames. *AIAA J., 28*(1), 38–46.

Lovett, J. A. & Turns, S. R. (1993): The structure of pulsed turbulent nonpremixed jet flames. *Combust. Sci. and Tech., 94*, 193–217.

Lyons, V. J. (1980): Fuel/air nonuniformity - effect on axisymmetrically pulsed turbulent jet flames. *AIAA J., 20*, 660.

Marble, F. E. (1953): Servo-stabilization of low-frequency oscillations in liquid propellant rocket motors. *ZAMP, 6*(1), 1–35.

Marble, F. E. & Cox, D. W. (1955): Servo-stabilization of low-frequency oscillations in a liquid bipropellant rocket motor. *Am. Rocket Soc. J.*, 63–81.

Markstein, G. H. (1965): Nonsteady flame propagation. In *AGARDOGRAPH 75.* NATO.

McManus, K. R. & Bowman, C. T. (1990): Effects of controlling vortex dynamics on the performance of a dump combustor. In *Twenty-Third Symposium (International) on Combustion.* The Combustion Institute, Pittsburgh.

McManus, K. R., Poinsot, T. & Candel, S. (1993): A review of active control of combustion instabilities. *Prog. in Energy and Comb. Sci., 19*, 1–29.

McManus, K. R., Vandsberger, U., & Bowman, C. (1990): Combustor performance enhancement through direct shear layer excitation. *Comb. Flame, 82*, 75–92.

Menon, S. & Jou, W.-H. (1990): Large-eddy simulations of combustion instability in an axisymmetric ramjet combustor. In 28^{th} *Aerospace Sciences Meeting.* AIAA Paper 90-0267.

Miller, J. A. & Bowman, C. T. (1989): Mechanism and modeling of nitrogen chemistry in combustion. *Prog. Energy Combust. Sci., 15*, 287–338.

Oster, D. & Wygnanski, I. (1982): The forced mixing layer between parallel streams. *J. Fluid Mech., 123*, 91–130.

Padmanabhan, K. T., Bowman, C. T., & Powell, J. D. (1995): An adaptive optimal combustion control strategy. *Comb. Flame, 100*, 101–110.

Parekh, D. E., Kibens, V., Glezer, A., Wiltse, J. M., & Smith, D. M. (1996): Innovative jet flow control: mixing enhancement experiments. In 34^{th} *Aerospace Sciences Meeting, Reno.* AIAA. Paper 96-0308.

Peters, N. & Donnerhack, S. (1981): Structure and similarity of nitric oxide production in turbulent diffusion flames. In *Eighteenth Symposium (International) on Combustion*, (pp. 33–41). The Combustion Institute, Pittsburgh.

Poinsot, T., Bourienne, F., Candel, S., Esposito, E., & Lang, W. (1989): Suppression of combustion instabilities by active control. *J. Propulsion, 5*(1), 14–20.

Poinsot, T., Trouvé, A., Veynante, D., Candel, S., & Esposito, E. (1987): Vortex driven acoustically coupled combustion instabilities. *J. Fluid Mech., 177*, 265–292.

Poinsot, T., Veynante, D., & Candel, S. (1990): Diagrams of premixed turbulent combustion based on direct simulation. In *Twenty-Third Symposium (International) on Combustion*, (pp. 613–619). The Combustion Institute, Pittsburgh.

Pompei, F. & Heywood, J. B. (1972): The role of mixing in burner-generated carbon monoxide and nitric oxide. *Comb. Flame, 19*, 407.

Pont, G., Willis, J. W., Karagozian, A. R., & Smith, O. I. (1996): Effects of external acoustic excitation on enhanced transport in a resonant incinerator. In *Twenty-Sixth Symposium (International) on Combustion.* The Combustion Institute, Pittsburgh.

Procter, D. (1994): In *Workshop on Pulsating Combustion and Its Application.* Technical report.

Putnam, A. A. (1971): *Combustion driven oscillations in industry.* American Elsevier, New York.

Reynolds, O. (1894): *Phil. Trans. Roy. Soc. A, 186*, 123.

Roberts, W. L., Driscoll, J. F., Drake, M. C. & Goss, L. P. (1993): Images of the quenching of a flame by a vortex - to quantify regimes of turbulent combustion. *Comb. Flame, 94*, 58–69.

Schadow, K. C. & Gutmark, E. (1992): Combustion instability related to vortex shedding in dump combustors and their passive control. *Prog. Energy Combust. Sci., 18*, 117–132.

Schadow, K. C., Gutmark, E., & Wilson, K. J. (1992): Active combustion control in a coaxial dump combustor. *Comb. Sci. and Tech., 81*, 285–300.

Searby, G. & Rochwerger, D. (1991): A parametric acoustic instability in premixed flames. *J. Fluid Mech., 231*, 529–543.

Smith, D. A. & Zukoski, E. E. (1985): Combustion instability sustained by unsteady vortex combustion. In 21^{st} *Joint Propulsion Conference.* AIAA/SAE/ASME/ASEE.

Stansel, D., Laurendeau, N., & Senser, D. (1995): CO and NO_x emission from a controlled-air burner: experimental measurements and exhaust correlations. *Comb. Sci. and Tech., 104*, 207–234.

Stirneman, A., Graf, H. R., & Ziada, S. (1995): Sound reduction potential with different controllers on industrial noise sources. In *Applications of active control to the reduction of noise and vibrations.* CETIM, Senlis, France.

StJohn, D. & Samuelsen, G. S. (1994): Active, optimal control of a model industrial, natural gas-fired burner. In *Twenty-Fifth Symposium (International) on Combustion*, (pp. 307–316). The Combustion Institute, Pittsburgh.

Tang, Y. M., Waldherr, G., Jagoda, J. I., & Zinn, B. T. (1995): Heat release timing in a nonpremixed Helmholtz pulse combustor. *Comb. Flame, 100*, 251–261.

Thévenin, D. & Candel, S. (1995): Ignition dynamics of a diffusion flame rolled up in a vortex. *Phys. Fluids A., 7*(2), 434–445.

Tœpler, A. (1866): Vibroskopische Beobachtungen über die Schwingungensphasen singender Flammen (der chemischen Harmonica) mit Benutzung des Schlierenapparates. *Pogg. Ann. Phys. Chem., 128*, 126–139.

Trouvé, A., Candel, S., & Daily, J. W. (1988): Linear stability of the inlet jet in a ramjet dump combustor. In *26^{th} Aerospace Science Meeting, Reno.* AIAA.

Tsien, H. S. (1952): Servo-stabilization of combustion in rocket motors. *Am. Rocket Soc. J., 22*, 256–263.

Tyndall, J. (1867): *Sound.* Longmans, London.

Vermeulen, P. J., Odgers, J., & Ramesh, V. (1982): Acoustic control of dilution-air mixing in a gas-turbine combustor. *Trans. ASME, 104*, 844–852.

Vranos, A. & Hall, R. J. (1993): Influence of radiative loss on nitric oxide formation in counterflow diffusion flames at high pressure. *Comb. Flame, 93*, 230–238.

Widrow, B. (1970): *Adaptive filters.* Holt, Rinehart and Winston, New York.

Willis, J. W., Cadou, C., Mitchell, M., & Karagozian, A. R. (1994): Destruction of liquid and gaseous waste surrogates in an acoustically excited dump combustor. *Comb. Flame, 99*, 280–287.

Wiltse, J. M. & Glezer, A. (1996): Direct high-frequency excitation of turbulence in free shear flows. In *34^{th} Aerospace Sciences Meeting, Reno.* AIAA. Paper 96-0309.

Yu, K. H., Parr, T. P., Wilson, K. J., Schadow, K. C., & Gutmark, E. J. (1996): Active control of liquid-fueled combustion using periodic vortex-droplet interaction. In *Twenty-Sixth Symposium (International) on Combustion.* The Combustion Institute, Pittsburgh.

Yu, K. H., Trouvé, A., & Candel, S. (1991): Combustion enhancement of a premixed flame by acoustic forcing with emphasis on the role of large-scale vortical structures. In *29^{th} Aerospace Sciences Meeting.* AIAA Paper 91-0367.

Yu, K. H., Trouvé, A., & Daily, J. W. (1987): Low frequency pressure oscillations in a model ramjet combustor. In *24^{th} Combustion Meeting.* JANNAF.

Zinn, B. T. (1992): Pulse combustion: recent applications and research issues. In *Twenty-Fourth Symposium (International) on Combustion*, (pp. 1297–1305). The Combustion Institute, Pittsburgh.

9 Chaos, Coherence and Control

Troy Shinbrot

Northwestern University, Evanston, Illinois 60208, U.S.A.

Abstract. In 1976, Werner Heisenberg lay dying. On his deathbed, he is reported to have said (Gleick, 1988) that he had two questions for God: why relativity, and why turbulence. "I really think," said Heisenberg, "He may have an answer to the first question." In this paper we focus on a tiny piece of the second question, "why turbulence?" Specifically, we try to understand just enough of that question to be able to decide whether or how turbulence could possibly be controlled. This is an ambitious agenda, and to study it we break the problem into manageable topics. So here we discuss two things. First, we review progress over the past decade on the control of low-dimensional, temporally chaotic dynamics. Second, we explore recent work which demonstrates how the dynamics of spatially chaotic, but temporally regular, systems can be manipulated. We conclude by very briefly discussing the prognosis of this research for the control of truly turbulent problems, which are unpredictable both in space and in time.

1 Historical Setting

Our story begins nearly a century before Heisenberg's death, in 1890. Prior to 1890, it was universally accepted that physical bodies were well described by the "clockwork universe." That is, given a set of bodies and a mathematical description of how they interact, it was believed that we could, given sufficient resources, calculate the positions of these bodies for all future times. Bodies should interact predictably and their trajectories should be prescribed forever.

This view was to be contradicted in 1890 by Henri Poincaré. On January 21, 1889, in celebration of the 60^{th} birthday of King Oscar II of Sweden, a prize was awarded to Poincaré for his work on the reduced celestial 3 body problem: the problem of an infinitesimal body in the gravitational fields of two larger bodies. In a 200 page manuscript published in the prestigious *Acta Mathematica*, Poincaré demonstrated that formal series solutions to this problem converge, and consequently there was thought to be hope that celestial problems such as the orbit of the moon around the earth could be stable.

Our story would end there, except for one thing: Poincaré's proof was wrong. In a later, 270-page paper, Poincaré provided the correct proof (Poincaré, 1957), which demonstrated that celestial orbits can in fact be unstable. All copies of his earlier work were systematically sought out and destroyed (Peterson, 1993). Poincaré's proof in itself was controversial (Poincaré, 1896), though the controversy was moderated somewhat by his demonstration

M. Gad-el-Hak et al.: LNPm 53, pp. 501 - 527, 1998
© Springer-Verlag Berlin Heidelberg 1998

(Sternberg, 1969) that the series would nevertheless asymptotically describe the motion of the three bodies (Poincaré, 1893; Schlissel, 1977). Nevertheless his proof presented a profoundly disconcerting idea, for as Poincaré pointed out,[1] "perhaps one day a mathematician will show by rigorous reasoning that the solar system is unstable." Thus one day, the moon could crash into the earth—or the earth could escape from the solar system altogether. More disconcerting still, given no amount of resources can we compute whether or not these catastrophes will occur. The fateful day presaged by Poincaré did not for practical purposes come until quite recently—a century after Poincaré's seminal proof—when careful computations showed conclusively that chaos—long term unpredictability—is readily to be found in the solar system (Laskar, 1989; Sussman and Wisdom, 1992).

The words of Poincaré, recognized at the time as the "greatest living mathematician" (Segré, 1980), a man who became the youngest ever president of the French Academy of Sciences, fell largely on deaf ears. To this day, Physics is largely taught as if Poincaré never lived—as if we live in a clockwork universe where everything can be predicted, everything understood. Yet we know this to be false. We know that even exceedingly simple systems can defy all attempts at prediction. We know further that the source of this unpredictability is the exponential growth of uncertainties in what we now call 'chaotic' systems (Li and Yorke, 1975).

One need look no further for a practical example of chaos than Goldstein (1950), the standard Classical Mechanics text. On page 12 of Goldstein's classic, one finds the double pendulum (sketched in inset to Figure 1)—one of the simplest of physical devices—described as an example of coupled oscillation. And indeed, for small oscillations one can use this device, as remarked by Professor Goldstein, to demonstrate the existence of normal modes. In addition to normal modes, however, if one studies the double pendulum for larger oscillations—where linearization is no longer appropriate—one can prove quite readily the existence of chaos, and the presence of trajectories which diverge exponentially in time (Shinbrot et al., 1992) (Figure 1). Thus in the very same system which exhibits linear, stable and completely predictable motion, one can find alongside nonlinear, chaotic and unpredictable behavior. The co-existence of these two antithetical behaviors is a theme that we will return to.

2 Control of Temporal Chaos

Apparently very simple systems can be extremely sensitive to tiny perturbations. There are many examples; the double pendulum is just one. The question that several teams of researchers have raised over the past decade is, "can this sensitivity be used to control chaotic systems?"

[1] "... un jour peut-être un mathématicien fera voir, par un raisonnement rigoureux, que la systeme planétaire est instable" (Garnier and Leray, 1953).

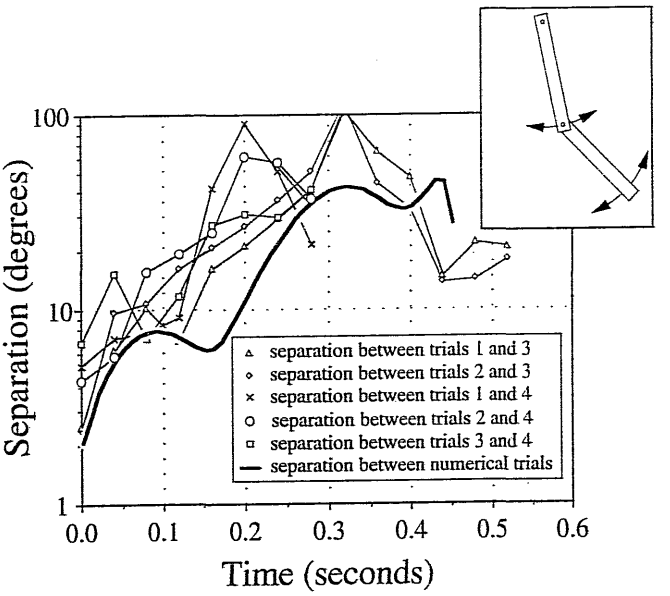

Fig. 1. Inset: Sketch of double pendulum. Main plot: Experimental separations between states of double pendulum released from, as nearly as possible, identical initial conditions during multiple trials; bold curve is numerical result.

The first practical contribution to the control of a chaotic system came from NASA (Wisdom, 1987). A little over a decade ago, NASA had an interesting problem. The comet Giaccobini-Zinner was due to travel through our solar system, and NASA scientists wanted to send a spacecraft through its tail. At the time, this had never been done before. But NASA couldn't budget a spacecraft to do this; it would have cost billions of dollars. What NASA did have was a craft that had previously been used to study the solar wind. This craft, the International-Sun-Earth-Explorer-3 (ISEE-3), was parked in a "halo orbit"—a controlled, elliptic trajectory—encircling a so-called Lagrange point, where the gravitational attractions of the earth and sun cancel out.

Because of the essential nonlinearity in celestial mechanics remarked upon by Poincaré a century earlier, NASA was able to send the craft—renamed the International-Cometary-Explorer-3 (ICE-3)—in a complex, unstable trajectory *halfway across the solar system* to meet the comet, using only small amounts of residual hydrazine fuel left over from its solar wind mission. It is important to stress that this was made possible only by the nonlinearity of the 3 body problem; NASA's maneuver would not have been possible in a linear system. In a linear system, a large effect requires a proportionately large control. Only in a nonlinear system can one achieve disproportionately large effects using small controls.

NASA's method was customized to their task and is exceedingly interesting (Efron et al., 1985; Dunham and Davis, 1985; Farquhar et al., 1985; Muhonen and Folta, 1985; Muhonen et al., 1985). What they did in the ISEE-3/ICE-3 mission (and what they do today in planning new missions) was to compile a library of maneuvers that would take them from one kind of trajectory to another. For example, they would calculate a single slingshot trajectory around the moon or a multiple slingshot with an orbit around the earth intervening, and so forth. Then they looked for ways to piece maneuvers from this library end-to-end in such a way that they could get from their starting point to their target. Fuel was reserved to redirect the spacecraft from one maneuver to another and for periodic mid-course corrections

This brings us to the first of the major topics of this paper: the control of temporal chaos. The study of modern, computational chaos began with Ed Lorenz in the 1960s. Lorenz is a meteorologist who studied simplified weather models. In his seminal paper (Lorenz, 1963), "Deterministic Nonperiodic Flow," Lorenz sought to study convection in a computational fluid model. This model involved a modal truncation, whereby a PDE is reduced to a set of ODE's by examining the dynamics of the lowest order coefficients of a Fourier expansion.

The earliest reference we find to the control of chaos, in fact, deals with the grandfather of all convective flows: the weather. In about 1950, Johann von Neumann gave a talk at Princeton on the subject of weather control. In his talk von Neumann foretold of a day when (Dyson, 1988) "as soon as we have some large computers working, the problems of meteorology will be solved. All processes that are stable we shall predict, and all processes that are unstable we shall control..." Thus Von Neumann imagined that, "a committee of computer experts and meteorologists would tell airplanes where to introduce small disturbances in order to make sure that no rain would fall on the Fourth of July picnic."

2.1 Using Chaotic Sensitivity

Clearly the spirit, if not the precise implementation, of the control of chaos has a long history. In the remainder of this section we will describe a few generic methods for the control of temporally chaotic systems.

As we have shown, chaotic systems are extremely sensitive to tiny perturbations. So if at time $t = 0$ we can adjust some parameter in a chaotic system, we expect generically that the future trajectories of the system will diverge exponentially in time as indicated on the sketch shown in Figure 2.

Here we see that if a particular chaotic trajectory follows the solid curve at the nominal parameter value, $p = p_o$, then by perturbing the system a little—i.e. by changing the parameter to $p = p_o + \delta p$ —we expect the trajectory to veer away exponentially, as shown in the dashed curve. This means that by choosing a suitable perturbation between 0 and δp, we can reach any point

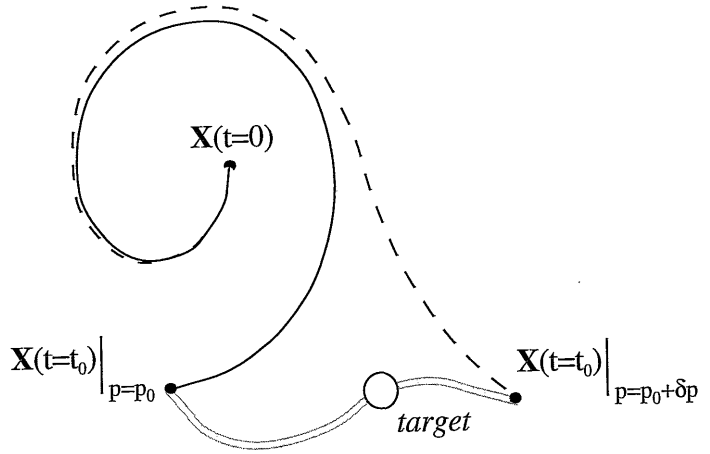

Fig. 2. Exponential growth of disturbance in a chaotic system. Solid line indicates trajectory at nominal parameter value, p_o; dashed line at perturbed value, $p_o + \delta p$. Thus any target on grey curve—which typically grows exponentially in length with time—can be struck using a perturbation between zero and δp.

on some grey curve shown in the figure. Thus if we want to reach a particular target, our job will be to sweep the grey curve forward in time until it strikes the target, and then identify the parameter which leads to the target region.

2.2 Implementations

Let's see how the idea works. In Figure 3 we show everyone's favorite attractor, originally produced by Ed Lorenz in 1963. If you want to study simple caricatures of turbulent flow, this is a good place to start, for as we mentioned, the attractor defines the state of convection rolls in the chaotic regime. Indeed, the Lorenz equations can be used to describe the motion of a narrow upright torus filled with fluid and heated from below (Yorke et al., 1987) (sketch to right of Figure 3).

We imagine that we want to direct the trajectory from any arbitrary starting point on the attractor to, say, a neighborhood of the unstable stationary point of the flow, the origin (encircled region in Figure 3). This is an interesting region because it contains exceedingly low measure: only 1 in 1010 orbits around either lobe of the attractor falls within the target region shown. To put this in perspective, the probability that a flipped coin will end up resting on its edge is a factor of a million *greater* than this (Murray and Teare, 1993).

As in any real physical problem, we imagine that we have control over some parameter, p —some knob or flow control, say. For our problem, we imagine that the parameter represents an asymmetric heating rate in the

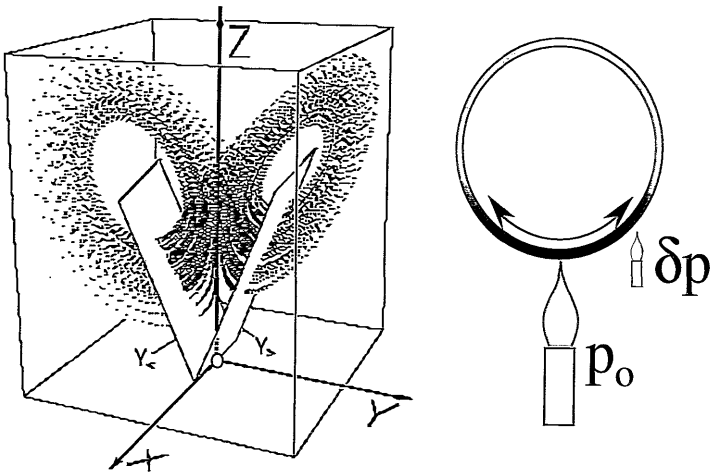

Fig. 3. Lorenz attractor (left) and heated fluid loop (right), which Lorenz equations can be used to model.

Lorenz system (small candle labelled δp in the fluid loop sketched in Figure 3). To direct a trajectory to this target, in a computer model of the Lorenz system, we perturb the flow by adjusting this parameter by some amount $p(t) = \pm\delta p$. Analytically, the Lorenz system with this parametric adjustment is written:

$$\begin{aligned} \dot{X} &= \sigma\,(Y - X) \\ \dot{Y} &= -X\,Z + r\,X - Y + p(t) \\ \dot{Z} &= X\,Y - b\,Z \end{aligned} \tag{1}$$

where we use Lorenz' values for the parameters: $\sigma = 10$, $r = 28$, and $b = 8/3$.

We trace these two trajectories forward in time until they eventually fall on opposite sides of the target. We can identify these events by placing planes through the origin, labelled $Y_<$ and $Y_>$ in the figure, and noting when a trajectory passes through one or the other plane. Once the trajectory associated with $p = p_o - \delta p$ strikes one plane and the trajectory associated with $p = p_o + \delta p$ strikes the other, if our system is sufficiently low-dimensional and well behaved, then we expect that some perturbation in the range between $p_o - \delta p$ and $p_o + \delta p$ will strike the target. All that remains is to refine the estimate of the correct perturbation, which can easily be done, for example by successively halving the parameter range and choosing the halves which contain the target.

Readers may recognize this as a simple shooting method. What is new here is that this simple method has been applied to a chaotic system, and far

from linearizing the problem—as is frequently done for control calculations—we include the full nonlinearities of the system. In so doing we can turn the exponential sensitivity of the system to our advantage.

Through this procedure, we can choose the perturbation to any accuracy we desire which should get us from any point on the attractor to a neighborhood of the origin—or any other target on the attractor—in a short time. How short? We mentioned that only 1 in 10^{10} orbits around the lobes of the attractor will fall in a small neighborhood of the origin. By contrast, this technique typically brings us to the origin in 5 to 10 orbits, again using only small perturbations. This represents a factor of a *billion* improvement in the time required to reach the target. This improvement is accomplished in this example using controls which amount to less than a tenth of a percent of the nominal heating rate, p_o.

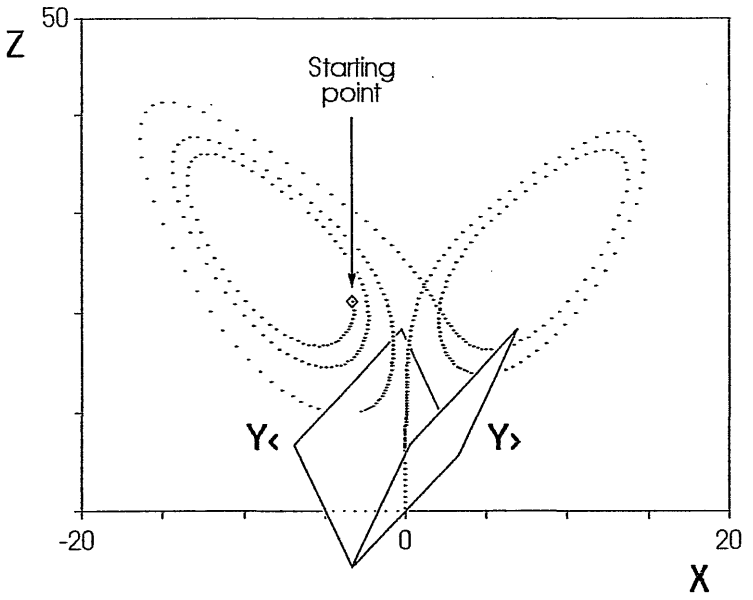

Fig. 4. Targeting of origin in Lorenz system

In Figure 4 we show a typical trajectory brought to the origin in a numerical experiment including additive noise. The same trajectory without control leads nowhere near the origin in any sensible amount of time (cf. Figure 3). Again, our recipe is to calculate a perturbation in a 'model' Lorenz system, and then to apply the perturbation in a separate 'real' system including additive noise.[2] To deal with noise, we re-apply the targeting algorithm periodically to obtain mid-course corrections. This is the same thing that

[2] For experiments done on this system, see Singer et al. (1991).

NASA did in their ISEE-3/ICE-3 mission and that every other robust controller does, and it can easily be shown that through these corrections we can reduce the exponential growth of errors to a growth that is no worse than linear.

Notice that we are playing both sides of the street here: because this system is chaotic, we can make use of exponential sensitivity to rapidly steer trajectories to highly improbable states. But because we correct the trajectory regularly, we can prevent the exponential build-up of errors in the trajectory.

There is, of course, nothing magic about the origin as a target; any other accessible state would work as well. For example, in Figure 5 we show a chaotic trajectory which is brought to a figure-eight unstable orbit. Unlike targeting of the origin, in this case we only need one plane, and we identify trajectories which strike one or the other side of the target point on this single plane.

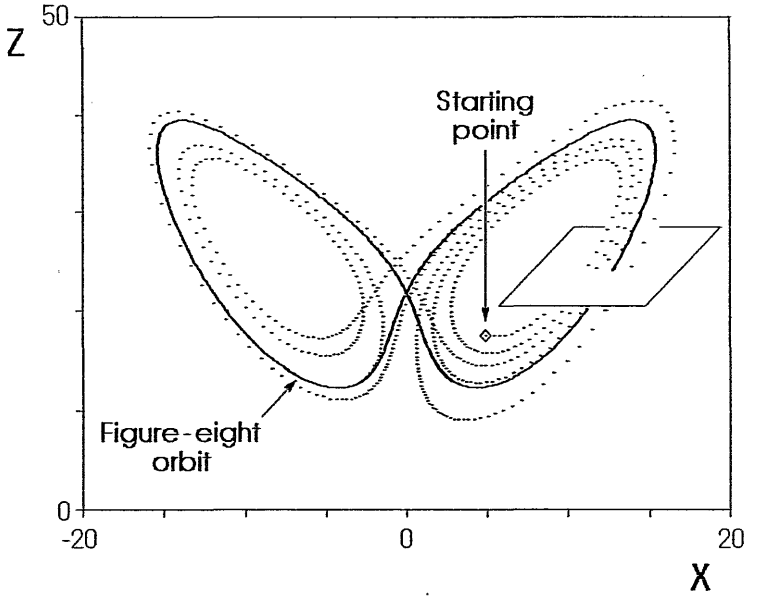

Fig. 5. Targeting of figure-eight orbit in Lorenz system

Once near this orbit we can apply the same targeting algorithm to bring the state back to the same orbit in the shortest possible time. Thus the targeting technique can be applied to stabilization of unstable periodic orbits (UPOs) as well, with the added advantage that targeting, requiring a global model, includes all nonlinear effects and requires no linearization (cf. Ott et al., 1990; now a classic for stabilization in chaotic systems). A further feature of targeting is that it can be used to send signals (Hayes et al.,

1993; 1994a; 1994b). In one implementation which has been developed, one UPO of a nonlinear transmitter is associated with a zero, and a second UPO is assigned to a one. By targeting one UPO and then the other, one can switch the system state in such a way as to send digital information. Indeed, since there are typically an infinite number of periodic orbits embedded in a chaotic attractor (Grebogi et al., 1988), one is not restricted to base-2; one can efficiently send information in any base that might be desired (Barretto et al., 1995).

2.3 Higher Dimensionality

We have so far shown that straightforward techniques can be used to steer trajectories to a desired state in simple, temporally chaotic systems like a heated fluid loop. For problems of this kind, it should not be surprising that control is possible. Indeed recent research has proven that there is an intimate relation between ergodicity—a hallmark of dissipative chaos—and controllability (Colonius and Kliemann, 1993). For the Lorenz case, this relation is facilitated by the low dimensionality of the problem: the correlation dimension (Schuster, 1989) of the Lorenz attractor for the parameters used in Figure 3 is 2.06. The technique we have described works by detecting intersections between the flow and surfaces of section (e.g. the plane shown in Figure 5), on which the dimension is 1.06. So we have a nearly one-dimensional problem which we are controlling using one parameter (Shinbrot et al., 1992). It comes as no surprise that control is readily achievable.

What about higher-dimensional problems? Here we can play the following game, which we illustrate using the Hénon system:

$$\begin{aligned} X_{n+1} &= p + 0.3\, Y_n - X_n^2 \\ Y_{n+1} &= X_n \end{aligned} \tag{2}$$

where we use a nominal value for the parameter p of $p_o = 1.4$. Equations (2) define the discrete time evolution of points (X_n, Y_n) at times n. The chaotic attractor (Ruelle,1980) resulting from these equations is shown in Figure 6(a). We imagine that the current system state is defined by $A = (X_o, Y_o)$, and we want to reach a new system state, $B = (X_t, Y_t)$. If we continuously vary a control parameter, we can sweep out a short[3] line segment, identified by $F^1(A)$ in Figure 6(b). By iterating this segment using the map (2), we obtain F^2, F^3, etc., and in a chaotic system, we expect the lengths of these curves to grow roughly exponentially in time. We repeat these iterations until the length of the curve is on the order of the size of the attractor.

[3] For the plots shown in Figure 6, we use a total parameter variation $p = 0.001 p_o$, where again $p_o = 1.4$. In this example, the starting point is: (0.94228972, 0.8512537).

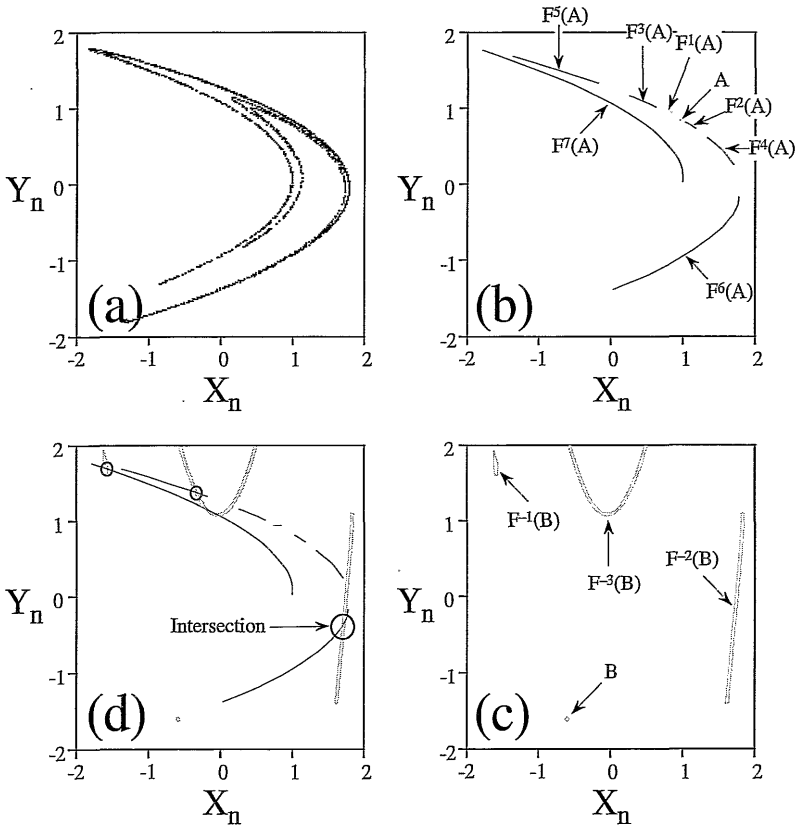

Fig. 6. Targeting in Hénon system

Next, we surround the target point with a small[4] circle (for higher-dimensional problems a hyper-surface), and iterate this circle *backward* in time, using the inverse map, F^{-1}. For the Hénon map (2), this inverse is unique; for other problems multiple branches may result, but the same idea still holds for any given branch (Kostelich et al., 1993). We repeat this process until, once again, the size of the circle is on the order of the attractor size. We then search for intersections between the forward iterates emanating from A and the backward iterates from the circle surrounding B. These intersections represent trajectories that start at A and end near B. Intersections typically exist due to the hyperbolic structure of stable (Figure 6(c)) and unstable (Figure 6(a)) manifolds characteristically found in chaotic systems. Moreover, because of the exponential growth which is characteristic of chaotic systems in both forward and backward evolutions, the time required to reach a target using this technique is exceedingly short, and goes only as the logarithm of the target size (Shinbrot et al., 1990).

[4] In the example shown, we use the target point, (0.5999968, −1.58540), and surround this point by a circle of radius 0.01 (in units defined by Equations (2)).

Chaos control methods have been applied to numerous practical problems. In multi-mode lasers, the stable power output has been boosted by over an order of magnitude (Gills et al., 1992; Ditto and Pecora, 1993). In phase locked loops, the range of entrainment has been broadened, again by a large factor (Bradley, 1993). In communication and switching devices, chaotic instability is used to reduce switching times and provide encryption strategies (Pecora and Carroll, 1990; Cuomo and Oppenheim, 1993; Barretto et al., 1995). In chemical and catalytic reactions, product concentrations and reaction rates are controlled (Parmananda et al., 1993; Petrov et al., 1993). And so forth. All of these examples are chaotic in time, but not (significantly) in space. This brings us to the second part of this paper: the control of systems which are chaotic in space, but not in time.

3 Control of Spatial Chaos

In this section we focus on a mechanism which can sometimes counteract the mixing influence of chaotic fluid flows. We begin by asking the relatively straightforward question of whether chaotic fluid flow can be controlled in any way. If we want to control chaotic fluid flow in a certain region, our first thought might be to make use of a chaos control technique, such as the ones we have described. Existing control techniques can do things like target or stabilize an unstable fixed point in a chaotic system. So we might ask what happens if we try to stabilize an unstable point in a chaotically advecting fluid.

The difficulty in a fluid is that in any practical application, it doesn't do any good to stabilize a single point. A single point has measure zero; what is needed is to control a cluster—a blob—of points. A spot of dye in a bucket of paint ... reactants in a mixing tank ... a hairpin vortex on an airfoil .... In all of these examples, it is the behavior of a group of points that is of interest, not a single point alone.

The problem fundamentally is that fluid flows are in general[5] volume conserving. If we apply a typical control procedure to a conservative problem, we find the following. In Figure 7 we show the standard map, defined as:

$$\begin{aligned} Y_{n+1} &= Y_n - k \sin(X_n) \\ X_{n+1} &= X_n + Y_{n+1} \end{aligned} \tag{3}$$

The standard map is a convenient paradigm which shares many of the features of fluid flow (Aref, 1984; Shinbrot, 1996). The map defines the evolution of points (X_n, Y_n) at discrete times n in the periodic domain $[-\pi, \pi]$. Because the map is discrete in time and involves only simple algebraic calculations, it is computationally much simpler to analyze than fluid flow dynamics.

[5] With notable exceptions such as Sommerer (1993) and Husain et al. (1995).

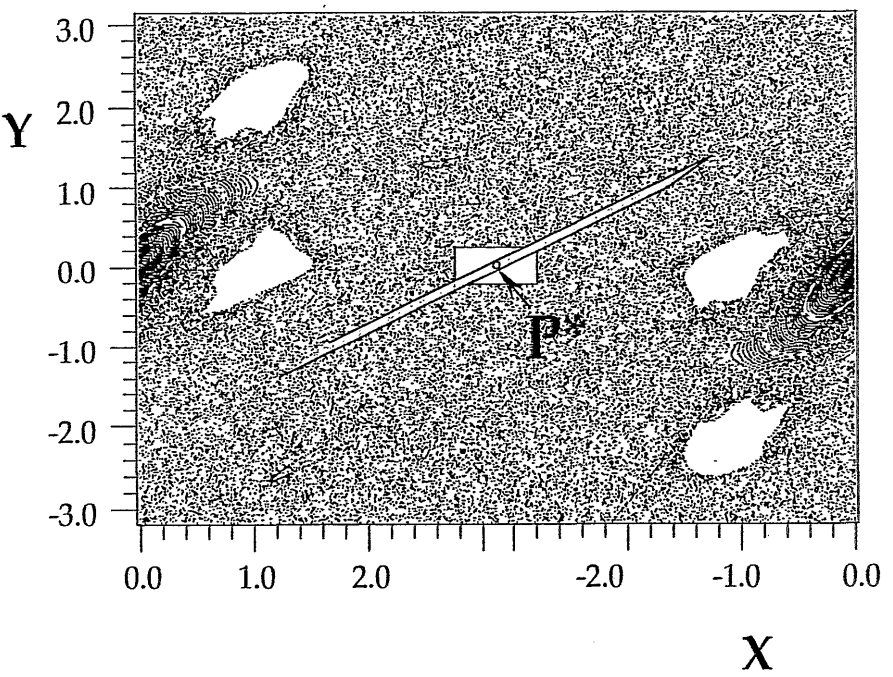

Fig. 7. Hyperbolic stretching in standard map

At the center of Figure 7 is a hyperbolic point, denoted P^*. If we evolve a set of points (white rectangle in Figure 7) surrounding a hyperbolic point, after one iteration of the map (grey quadrillateral in Figure 7), the set will be drawn away along the unstable manifold of the point. If we apply control, any one point in the initial set can be brought to the hyperbolic point, but all of the other initial points will still be drawn away along the unstable manifold. Precisely the same thing happens in chaotic fluid flows.

The problem in detail is that common control techniques leave the (hyperbolic) structure of the fixed point intact. In a non-conservative system, there is no problem: the goal of control is to make the desired fixed point attractive to all points in a certain neighborhood.[6] In a volume-conserving problem like the standard map or a typical fluid flow, however, no point can ever be attracting.

To control a cluster of initial points, we need to change the topology around the fixed point so as to keep the cluster together within the sur-

[6] See, for example, Ogata (1990).

rounding chaotic sea. How might this be done? It so happens that nature has provided us with copious examples, not just in spatially chaotic flows, but in actual turbulent flows as well.

A prototypical coherent cluster—or structure—in a turbulent flow is the Great Red Spot of Jupiter, originally discovered in 1664 by Robert Hooke (Hooke, 1665-6). This is a highly turbulent flow: the Reynolds number near the red spot is on the order of 10^5. Yet the spot has survived for more than three hundred years. Thus we ask: "how has this spot persisted within Jupiter's turbulent atmosphere? Given its presence, why hasn't the surrounding turbulence destroyed it?"

This question is not new; nor is it restricted to turbulence problems; the Great Red Spot is only one example of a coherent structure; these structures are observed in an astonishing variety of very different physical systems ranging from turbulent fluid flow to the human heart.

For more than 30 years, physiologists have studied so-called 'circus' waves in the heart, in which a localized region of the heart will talk only to itself rather than interacting with the rest of the heart muscle (Wit and Cranfield, 1978).

In Hurricane Andrew several years ago, it was determined that most of the damage was caused not by the hurricane's sustained winds; rather the damage was principally caused by coherent vortices in which the winds were driven to nearly twice the sustained wind speed (Hecht, 1993).

Coherent structures appear in virtually every scientific discipline: in catalytic chemistry; in epidemiology; in meteorology; in the study of Josephson junction arrays; in neural processing .... What do these very different problems have in common? No one would be surprised to see regular structures in regular flows, but why do they always seem to crop up in *ir*regular flows?

So this is a set of fundamental questions that we might ask. Beyond these, there are practical questions that we must answer if we hope ever to control spatially chaotic systems.

In particular, given that coherent structures often do pop up in complicated flows, we want to study what holds them together. Given that we might want to control chaotic fluid flow, can coherent structures be made to appear or vanish under our control? What underlying mechanisms keep one region of fluid in a chaotic flow intact, while fluid all around is quickly dispersed? And supposing that a structure already exists, what do its internal dynamics depend on? Can we vary the mixing within a structure, for example? Can we put a spot of reactant dye in a bucket tank of polymer and mix the polymer all around the reactant, keeping the reactant intact? And can we then mix the reactant with the polymer inside a little region, and then if we choose perhaps parcel out aliquots of diluted reactant?

3.1 Horseshoes in Mixing Flows

These are also questions that we would like to answer. To make a start, consider the following Gedanken experiment. Chaotic mixing is known to be produced by repeated stretching and folding. Stephen Smale (Smale, 1967) originated this idea when he introduced the horseshoe map in 1967, and Osborne Reynolds (Reynolds, 1894) commented on a similar idea in 1894. The benefit of repeated stretching and folding for the purpose of mixing can be explained as follows.

Suppose we observe that a rectangle of fluid is stretched by a fixed amount every unit time. For example, stretching due to shear is depicted in the top sketches of Figure 8. Thus after one unit time (say a second), a region of length L_o is typically stretched to a new length $L_1 \cong < \Lambda > L_o$, where the average stretching is $< \Lambda > \cong 2$. After another second $< \Lambda > \cong 3$, and in general after n seconds, the average stretching is $< \Lambda > \cong n+1$, or:

$$L_n \cong L_o\ (n+1) \tag{4}$$

The effect of linear stretching on a rectangle half filled with grey material and half with white is shown in the bottom sketches in Figure 8: after 5 seconds, the mean stretching is by a factor $< \Lambda > \cong 6$.

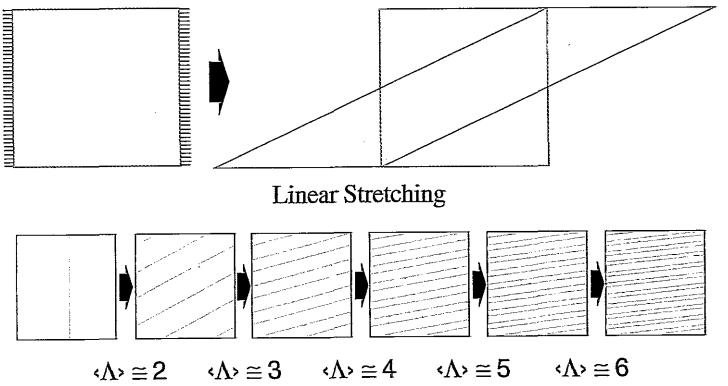

Fig. 8. Top: Linear stretching in box periodic at left and right. Each time unit, bottom moves fixed distance to left, top moves fixed distance to right. This is the situation encountered in simple shear flows. Bottom: Results of repeated applications of shear on box initially half grey, half white. In this progression we use periodicity at side walls to copy stretched material back into original box. The mean stretching after the final time step is $< \Lambda > \cong 6$.

We compare this with the situation in which a region of fluid is repeatedly stretched and folded. As shown in the top of Figure 9, after each time step (again say a second), a rectangle is stretched by a factor of two and is folded to lie in the same region as initially. This stretching and folding operation is

termed a 'horseshoe,' and if the region near the fold is neglected, this is termed a 'Smale horseshoe.' Material contained within the rectangle is stretched by a factor of two every second, so that after n seconds the stretching is given by $< \Lambda >= 2^n$. Thus a small initial region of length L_o will grow after n stretching and folding operations to a length:

$$L = L_o \ 2^n \tag{5}$$

This exponential growth is the hallmark of chaos. Now after 5 seconds the total stretching is by a factor of $< \Lambda > = 32$, as compared with the factor of 6 in the linear stretching case. As shown in the bottom of Figure 9, a half-grey initial state is visibly better mixed as compared with the linear stretching case shown in Figure 8.

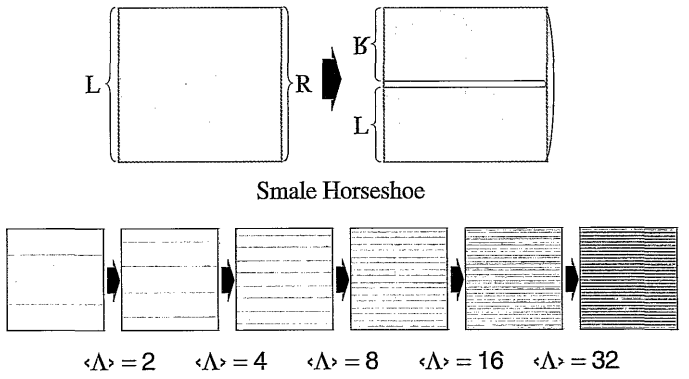

Fig. 9. Top: Horseshoe stretching and folding. Each time unit the rectangle is doubled in length and then folded over into shape shown. This is the situation encountered in simple chaotic flows. Bottom: Results of repeated applications of horseshoe on box initially half grey, half white. The mean stretching after the final time step is $< \Lambda >= 32$.

For the purposes of control, the thing to notice here is that the horseshoe consists of two actions: stretching *and* folding. In conjunction, these two operations lead to exponentially fast mixing, but by separating the two operations from one another, we can achieve a new type of control. That is, rather than putting the fold any old place, we can choose to put a fold where we want a coherent structure. This idea is shown in its simplest manifestation in Figure 10. Now we include a second fold, on the left of the rectangular region, resulting in two topologically identical horseshoe maps, one shown in light grey and the second in dark grey. Each time we stretch the fluid, we may double its length, but each time we fold it, we halve the length. So it should come as no great surprise that systems which compose stretching with folding exhibit chaotic regions side by side with coherent ones, which come or go depending on the happenstance of fold location

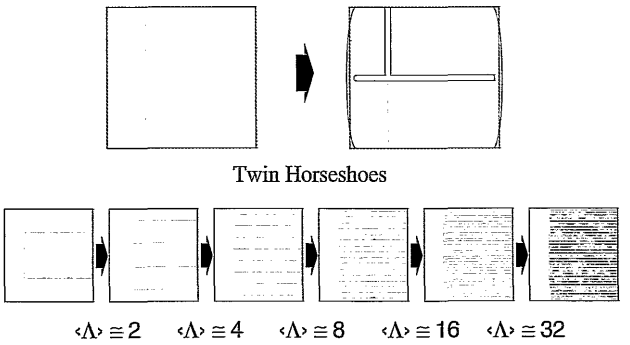

Fig. 10. Top: Twin horseshoes, resulting in two separated mixing regions. Bottom: Stretching is still exponential in time within either region, but there is no interpenetration between regions.

As indicated in the sketches at the bottom of Figure 10, the horseshoe structure results in exponential stretching still, but the dynamics in the two different grey regions are separated. In this figure, we consider the case where both regions exhibit identical horseshoes; alternatively we could permit different dynamics in one region—for example in the light grey region we could prohibit stretching altogether, or we could fold from top to bottom rather than bottom to top. The point here is that by including an additional fold we isolate the dynamics in one region from those in another, and this has important implications for the control of spatially extended and volume-conserving problems.

The horseshoe maps shown in Figures 9 and 10 are not completely general, since the initial rectangles shown have edges (L and R in Figure 9) which are folded together. In a container of fluid, say a stirred coffee cup, material can still be stretched and folded, but there are no edges to pull apart and rejoin. The same idea holds in more general flows where a continuous fluid is stretched and folded, as shown in Figure 11. Here the rectangles shown are periodic at the left and right edges—this is the situation one would see in an annular container. On the top of Figure 11 we show a horseshoe which would result from stretching the entire contents of the annulus to three times its original circumference, then folding the contents and reinserting it back into the container. Material is everywhere stretched in this operation, and mixing is global. If we insert folds into the central region we obtain the situation shown on the bottom of Figure 11. Now the light grey, 's' shaped region remains intact after repeated stretchings and foldings and does not mix with the outer dark grey region.

Independent of the geometry of the problem (i.e. Figure 10 vs. Figure 11), the point to stress is that the horseshoe map—the presence of stretching and folding—is a *universal* mechanism common to a broad class of problems. Fluid problems involving chaos or turbulence are convenient for study because this

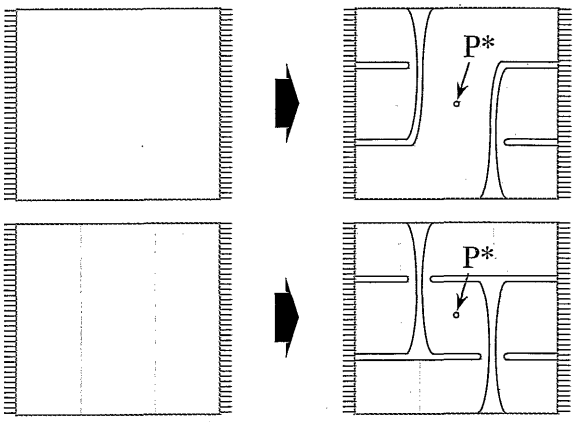

Fig. 11. Top: Horseshoe in box periodic at left and right. Point in center, P^*, is hyperbolic. Bottom: Additional 's' shaped horseshoe included in central region results in two separated mixing regions indicated by light and dark grey. P^* is again hyperbolic, and mixing within each region is chaotic.

stretching and folding occurs in physical space where we can readily visualize it; in other problems it occurs in phase space. Nevertheless, any system that stretches and folds can in principle be manipulated in this way to create coherent structures in the presence of repeated stretching. The location of the fold is the key.

Moreover, instead of repeatedly folding the region from bottom to top again and again, we can fold from bottom to top the first time, and then from top to bottom the next. By repeating this protocol, we can change the dynamics within the structure from something that repeats once per cycle to something that repeats once in two cycles ... or three cycles ... or eight .... In addition, effective stretching only occurs on the legs of the horseshoe. In the fold itself, the fluid can circulate, but need not stretch chaotically. By varying the proportion of fluid in the fold compared with the legs, the fraction of material that is chaotic or regular can be changed correspondingly. Thus by studying the horseshoes—which are known to underlie complicated flows (Ottino, 1994)—we can develop strategies to control the topology, mixing and extent of coherent structures.

3.2 Implementations

Let's see how this works in a few problems. We'll start with the easiest case, a 1D map, then we'll look at a 2D Hamiltonian map, and finally we'll apply these ideas to chaotic fluid advection.

One of the very simplest 1D maps is the tent map, shown in Figure 12(a). This map is defined by the following equation:

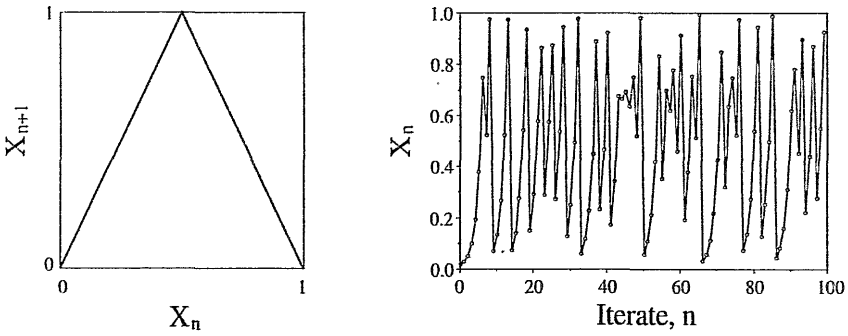

Fig. 12. Left: Tent map. Right: Evolution of initial point near origin under repeated application of tent map.

$$X_{n+1} = \begin{cases} 2\,X_n & \text{if } 0 \le X_n < \frac{1}{2} \\ 2\,(1 - X_n) & \text{if } \frac{1}{2} \le X_n < 1 \end{cases} \tag{6}$$

Thus Equation (6) defines the evolution of a scalar quantity, X, at discrete times n. The map and its evolution are shown in Figure 12. On the left we plot the functional form determined by Equation (6), and on the right we show the evolution of a point starting near the origin: $X_o = 0.01$. This map stretches a typical neighborhood by a factor of 2 in length—thus a point very near to X_o would diverge over time from the state X_n according to Equation (5). Now suppose we want to add a 'fold' to break this map into two disjoint domains. We can do this by shifting the map by a phase, α:

$$X_{n+1} = \begin{cases} 2\,(\alpha - X_n) & \text{if } 0 \le X_n < \alpha \\ 2\,(X_n - \alpha) & \text{if } \alpha \le X_n < (\frac{1}{2} + \alpha) \\ 2\,(1 + \alpha - X_n) & \text{if } (\frac{1}{2} + \alpha) \le X_n < 1 \end{cases} \tag{7}$$

This map and its evolution are shown in Figure 13. The new fold is visible as a 'v' shape in the lower corner of the plot on the left, and the effect of the fold is visible from the evolution shown on the right. Now the same initial point shown on the right of Figure 12 remains always within the light grey region shown; likewise trajectories initially within the dark grey region remain in that region for all time (solid line shown in evolution plot on right of Figure 13). Yet within each domain, typical neighborhoods are again stretched by a factor of two according to Equation (5). In fact, in this example, we see from the plot to the left of Figure 13, that there are simply two copies of the tent map, one of which is inverted, so the dynamics within each domain are naturally the same as in the original map. This doesn't have to be the case; for example, we can arrange the map to be whatever we like within either colored box provided that the map never extends beyond the box. To take an example, we could produce an attractive fixed point (dotted lines in

upper right of map shown in Figure 13; corresponding trajectory also shown as dotted line in evolution plot to right) in one of the maps, or if the map in one of the grey boxes leaves the box (dashed line in lower left of map), then the maps in the two regions can interact to whatever degree we choose. Although neither of these modifications are area preserving in the 1D case, these behaviors can be seen in higher-dimensional, area-preserving problems.

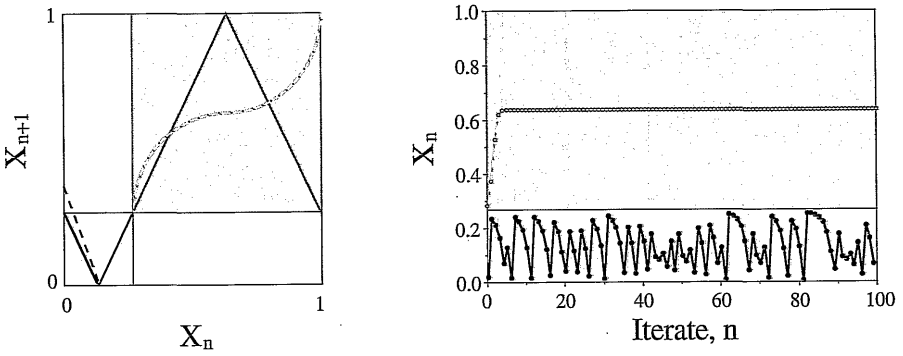

Fig. 13. Left: Shifted tent map. Right: Evolution of same point near origin as shown in Figure 12. Now dynamics within light and dark grey regions are separated. Dotted lines indicate possible modification in dynamics within dark grey region; dashed line indicates mechanism to permit controlled intermixing between two regions.

3.3 Coherent Structure Creation in Standard Map

Let's turn next to a 2D example: the standard map. We saw what happens near a hyperbolic point in the standard map earlier (Figure 7). The standard map has a sinusoidal nonlinearity (Equation (3)), and as we mentioned, this produces a hyperbolic fixed point, P^*, at $X = \pi$, $Y = 0$ for the amplitude chosen ($k = 2.5$). Can folds really be used to create a coherent region around P^*? Let's insert a couple of folds near P^* by modifying the standard map's sinusoidal nonlinearity. In a model problem such as the standard map, we can do this analytically: in the inset of Figure 14, we show the nonlinearity of Equation (3) with a cubic polynomial inserted at $X = \pi$, where the unmolested standard map exhibited a hyperbolic point (cf. Figure 7).

The effect of this modification is evident in the main plot of Figure 14. Now the same rectangle which formerly (Figure 7) was stretched hyperbolically away from P^* is stretched and folded in the vicinity of P^*. It is notable that formally the local stretching around P^* has been doubled: if we examine an interval around the fixed point, we find after one iterate of the map that the interval is stretched by about a factor of 2.5 for the standard map, and by about 5, twice as much, for this modified standard map. But there are

two folds to counteract this stretching. Each fold halves the effective stretching, which is thus reduced from a factor of 5 to a factor of 5/4—or a little over 1—which is to say, to only slightly worse than no stretching at all. And indeed, this modified standard map exhibits an isolated structure exactly in the vicinity of the folds. This is shown in Figure 15, where we expand the central region of Figure 14. Here we see clearly that there is an overlapping region between the initial rectangle (white) and the folded region (grey) that results from the application of the modified map. If we examine trajectories in this region (inset to Figure 15), we find that they remain trapped within a region of overlap between the original rectangle and the fold (outlined in main plot of Figure 15). If you looked closely, you'd find that there are stochastic regions as well as stable islands within this structure, which is what you'd expect. By changing the details of the folds, you can modify these features as well—I'll show you a little of this later on.The appearance of the map far from the new structure is unchanged.

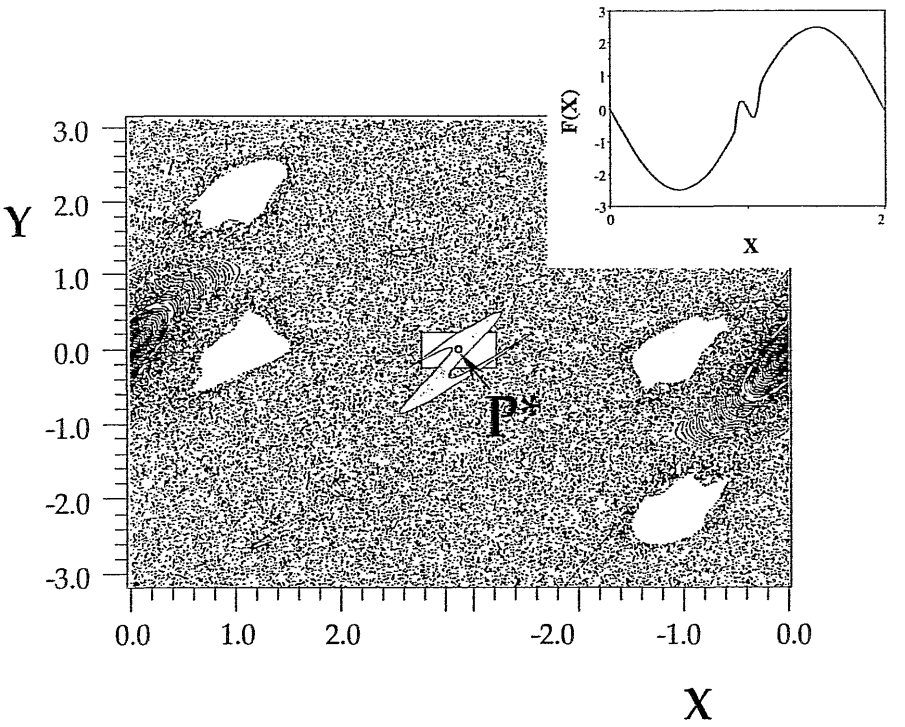

Fig. 14. Standard map with fold inserted in center. Inset: Fold incorporated into sinusoidal nonlinearity.

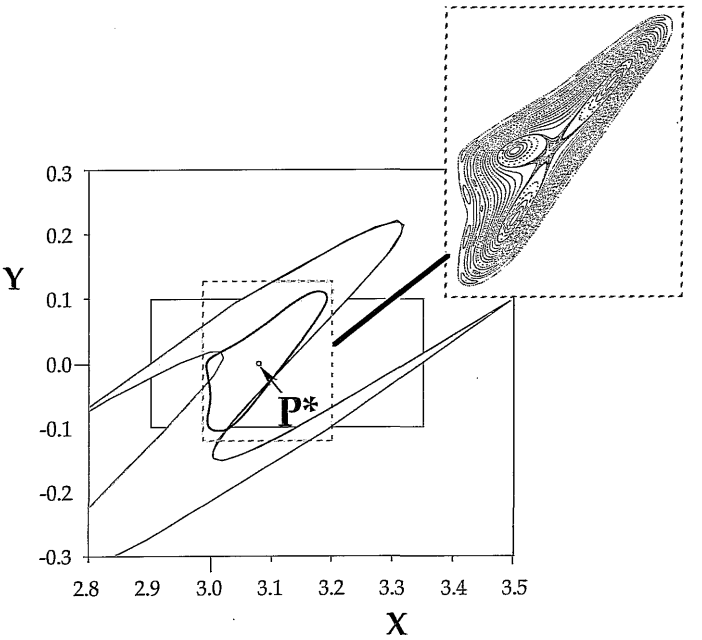

Fig. 15. Expanded view of folded region in modified standard map. Inset: Coherent structure which results from overlap between fold and original rectangle.

3.4 Coherent Structure Creation in Chaotic Fluid Flow

As we have indicated, it is possible to insert folds analytically into a model problem such as the standard map, but what about real problems? In Figure 16 we show an example: flow of a viscous liquid held between two eccentric cylinders, each of which is free to rotate. In the figure, we show computational images[7] looking into the cavity between the cylinders from above. By alternately rotating the inner and then the outer cylinders, it is well known (Swanson and Ottino, 1992) that we can produce chaotic mixing throughout the fluid. We have discussed so far the relevance of horseshoe folds to coherent structures (Bresler et al., 1997; Ottino et al., 1994), and in many chaotic mixing problems these folds are readily identified. In Figure 16(a), we show how a rectangle of dye drawn into the fluid becomes deformed after one cycle of slowly rotating the inner and outer cylinders.[8] The deformed rectangle takes the shape of a stylized 'z,' with folds lying far from the initial rectangle. This is the situation shown in the top sketches of Figure 11, and as we would expect, there is good chaotic mixing in the region surrounding

[7] The experimental counterparts to these images appear in Bresler et al. (1997).

[8] Here one cycle is defined by rotating the inner cylinder by $-1080°$, then the outer by $-240°$, and finally the inner again by $-1080°$. We choose the convention that positive angles represent clockwise rotation.

the rectangle. This is demonstrated in Figure 16(b), where we show how a small blob of dye would be advected after 14 cycles.

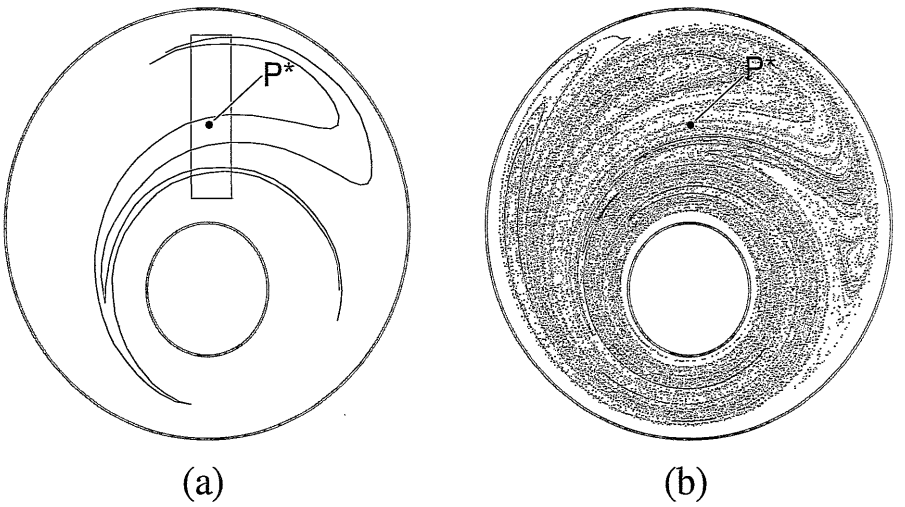

Fig. 16. (a) 'z' shaped Smale horseshoe between two eccentric cylinders rotated according to prescribed protocol. Initial rectangle of marker particles shown. (b) Resulting global chaotic advection of small blob of markers after 14 rotation cycles.

By contrast, if we perform the same experiment but this time add a counter-clockwise rotation of the outer cylinder,[9] we can bring the folds of the 'z' shown in Figure 16(a) close to the initial rectangle. This is shown in Figure 17(a), and in Figure 17(b) we display the resulting advection results, clearly showing a coherent structure precisely in the region where the folds intersect the initial rectangle.

To summarize, our recipe is to create—or conversely to destroy—coherent structures by moving horseshoe folds. Three properties are required to make a coherent structure in this way:

1. The structure must possess a periodic point, so that points in a given region return to that region,
2. The structure must contain a fold, so that the points are not drawn out of the region, and
3. The fold must be sufficiently compact and close to the periodic point that the underlying stretching is effectively defeated.

Thus we can use the idea of moving horseshoe folds as a tool to create coherent structures in spatially chaotic fluid flows. By reversing the process and moving folds away, we can destroy existing structures as well. Three facts

[9] Now we rotate the outer cylinder by $-32°$, the inner by $-1080°$, the outer by $-170°$, and finally the inner again by $-1080°$.

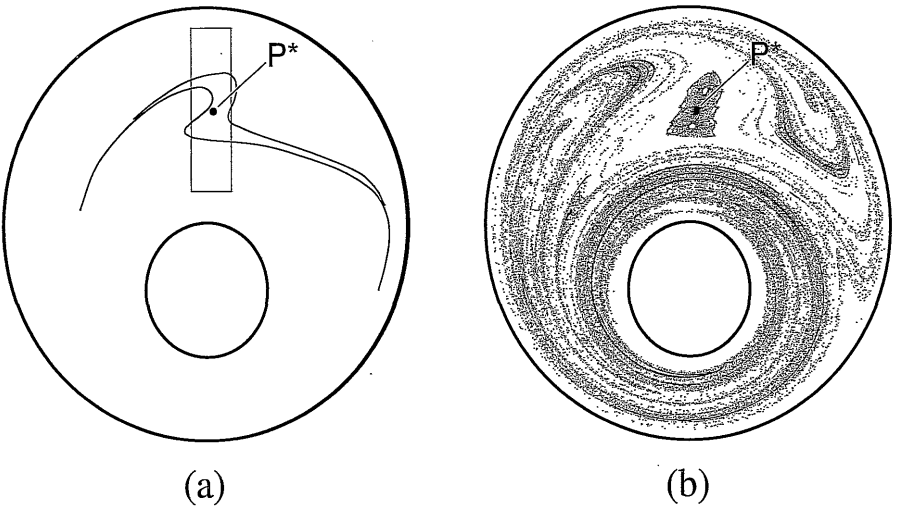

Fig. 17. (a) 'z' shaped horseshoe between eccentric cylinders rotated according to new protocol. There is now overlap between original rectangle of marker particles and folds of horseshoe. (b) Resulting advection of small blobs of markers after 14 rotation cycles: blob placed outside of coherent structure is stretched chaotically; blob placed within structure remains trapped despite stretching and folding.

deserve emphasis.

First, the analysis that we have presented has been based entirely on global arguments. No amount of local analysis—for example around P^* in Figure 16 or 17—will tell us anything whatsoever about the global behavior in the surrounding structure. The behavior of folds, for example, does not depend on the local behavior in the interior of the horseshoe—we saw this in the tent map example, where we could make the interior dynamics within a coherent region anything we wanted—for example an attractive fixed point—without affecting the barrier to mixing between regions. We saw this again in the standard map, where the stretching rate was 5 within a coherent region, and we see this once more in our chaotic fluid flow example by examining the structure shown in Figure 17(b). This structure contains two elliptic islands surrounding a hyperbolic point. The hyperbolic point is actually the remnant of P^*, which was hyperbolic before the creation of the coherent structure as well as after. That is, we can keep this point hyperbolic and create, destroy or modify the surrounding structure in the ways that we have described without changing the underlying local character of the central point. Local expansions can tell us many useful things, but only about local behavior. Only by global analysis—in this case of the surrounding folds—can we hope to understand global features of fluid behavior. It is these global features that dictate important structural features which can dominate complex flow dynamics.

Second, in a real experiment with only an approximate model, the struc-

ture may not appear or vanish precisely at the parameter values that we predict, but if a suitable fold can be moved by adjusting a parameter, then we expect that at some parameter value, a coherent structure can indeed be created or destroyed (Bresler et al., 1997). It is important here to be clear. That is, using the caricature of the horseshoe map, we cannot possibly hope to create as complete or detailed picture of a given problem as is possible using more sophisticated methods. For example, if we try to calculate the precise amount by which we should change a parameter in order to create or destroy a given structure in a particular problem, the parameter value isn't going to be exact, but if we construct our map properly, the topological structure of the problem should be qualitatively correct. More importantly, by using the simple caricature provided by horseshoe maps, we can quickly and accurately identify what kinds of structures are achievable, and how—and to what extent—they can be controlled. And most fundamentally, we can understand what underlying mechanisms keep them intact in the first place.

Third, it is surprising that the mere existence of a suitable fold is sufficient to imply the possibility of coherence. This is not obvious. We wouldn't think that the mere fact that a system is chaotic—i.e. that it has horseshoe folds—could tell us very much at all. But in reality, this fact alone tells us both how coherent structures can be created and where. More than this, we have learned that coherence should not be viewed as an aberration in chaotic flows. Coherence is not simply an alternative to chaos; rather, coherence can be *caused* by chaos.

4 Prognostication

Since Heisenberg's time, we have learned a great deal about applications of simple dynamical tools. While we cannot today say that we have uncovered the secrets of turbulence, we can fairly say that we have made a start at a better understanding of structural features of complex systems which can be exploited for the purposes of control. It is crucial here to stress that it was only knowledge of the *structures* of the systems which we have described that made control possible.

- It was knowledge of the structure of chaotic stretching that permitted us to achieve a billion-fold improvement in the time to reach a target using simple shooting techniques.
- It was knowledge of the hyperbolic structure of dissipative chaotic systems that allowed us to achieve targeting in higher-dimensional chaotic systems.
- And it was knowledge of the topology of horseshoes in conservative dynamical systems which allowed us to predictably manipulate coherent structures in a spatially chaotic sea.

The essential challenge for the field in the decades to come is to determine whether or how spatially and temporally chaotic problems can be controlled or manipulated as well. Here again, progress in the control of turbulent systems can only occur through an understanding of the structure of these problems.

Progress to date in this field already shows the importance of structure: a number of authors have been able to find systems whose apparent dimension is high or infinite, but whose actual dynamics live in a controllable, low-dimensional subspace. Anyone who is familiar with Proper Orthogonal Decomposition knows what I am talking about. The real challenge for the future is not, however, to ask when or how an existing low-dimensional problem can be controlled; the real challenge is to ask why the dynamics are low dimensional in the first place. Without low-dimensional dynamics, unless we plan to invest astronomical resources fiddling with the dynamics on every possible length and time scale, the control of turbulent dynamics ought to be out of the question. Ought, except for one bit of magic that we have no rational reason for expecting. And that is the presence, the persistence and the prevalence of low-dimensional coherent structures in biology; in physics; in chemistry—in virtually every single discipline that we know of.

The understanding of the origin and structure of low-dimensional dynamics within infinite-dimensional, turbulent systems is a big problem. It is not going to be solved overnight. We have no reason to expect low-dimensional dynamics in high-dimensional problems. The phenomenon is based on no physical principles that we know of; we have no right to it. But the fact that these structures do exist and that they are prevalent leads to hope. Without this kind of behavior, we surely have no hope for control.

References

Aref H. (1984): Stirring by Chaotic Advection. *J. Fluid Mech.* **143**, 1–21.

Barreto E., Kostelich E.J., Grebogi C., Ott E., Yorke, J.A. (1995): Efficient Switching Between Controlled Unstable Periodic Orbits in Higher Dimensional Chaotic Systems. *Phys. Rev. E* **51**, 4169–4172.

Bradley E. (1993): Using Chaos to Broaden the Capture Range of a Phase-Locked Loop. *IEEE Trans. on Circ. & Sys.* **40**, 808–818.

Bresler L., Shinbrot T., Metcalfe G., Ottino J.M. (1997): Isolated Mixing Regions: Origin, Robustness and Control. *Chem Eng Sci.*, in press.

Colonius F., Kliemann W. (1993): Some Aspects of Control Systems as Dynamical Systems. *J. Dyn. & Diff. Equation* **5**, 469–494.

Cuomo K.M., Oppenheim A.V.(1993): Synchronized Chaotic Circuits and Systems, with Applications to Communications. *Phys. Rev. Lett.* **71**, 65–69.

Ditto W.L., Pecora L.M. (1993): Mastering Chaos. *Sci. Am.*, August, 78–84.

Dunham D.W., Davis S.A.(1985): Optimization of a Multiple Lunar-Swing by Trajectory Sequence. *J. Astronautical Sci.* **33**, 275–288.

Dyson F.J. (1988):*Infinite in All Dimensions.* (Harper & Row, NY).

Efron L., Yeomans D.K., Schanzle A.F. (1985): ISEE-3/ICE Navigation Analysis. *J. Astronautical Sci.* **33**, 301–323.

Farquhar R., Muhonen D., Church L.C. (1985): Trajectories and Orbital Maneuvers for the ISEE-3/ICE Comet Mission. *J. Astronautical Sci.* **33**, 235–254.

Garnier R., Leray J., eds. (1953): Oeuvres de Henri Poincaré, **8**. (Gauthier-Villars, Paris).

Gills Z., Iwata C., Roy R., Schwartz I.B., Triandaf I. (1992): Tracking Unstable Steady States: Extending the Stability Regime of a Multimode Laser System. *Phys. Rev. Lett.* **69**, 3169–3172.

Gleick J. (1988): *Chaos: Making a New Science.* (Viking, NY).

Goldstein H. (1950): *Classical Mechanics.* (Addison Wesley, Cambridge, MA).

Grebogi C., Ott E., Yorke J.A. (1988): Unstable Periodic Orbits and the Dimensions of Multifractal Chaotic Attractors. *Phys. Rev. A* **37**, 1711–1724.

Hayes S., Grebogi C. (1993): Coding Information in the Natural Complexity of Chaos. SPIE **20**, *Chaos in Communications.* 1–9.

Hayes S., Grebogi C., Ott E. (1994a): Communicating with Chaos. *Phys. Rev. Lett.* **70**, 3031–3040.

Hayes S., Grebogi C., Ott E., Mark A. (1994b): Experimental Control of Chaos for Communication. *Phys. Rev. Lett.* **73**, 1781–1784.

Hecht J. (1993): Andrew's High-Speed Winds Whipped Up Trouble. *New Scientist*, 13 February, 10.

Hooke R. (1665–6): A Spot in one of the Belts of Jupiter, *Phil. Trans. Roy. Soc. A* **2**.

Husain H.S., Hussain F., Goldshtik M. (1995): Anomalous Separation of Homogeneous Particle-Fluid Mixtures: Further Observations. *Phys. Rev. E* **52**, 4909–4923.

Kostelich E., Grebogi C., Ott E., Yorke J.A. (1993): Higher-Dimensional Targeting. *Phys. Rev. E* **47**, 305–310.

Laskar J.A. (1989): A Numerical Experiment on the Chaotic Behavior of the Solar System. *Nature* **338**, 237–238.

Li T.-Y., Yorke J.A. (1975): Period Three Implies Chaos. *Amer. Math. Monthly* **82**, 985–992.

Lorenz E.N. (1963): Deterministic Nonperiodic Flow. *J. Atmos. Sci.* **20**, 130–141.

Muhonen D., Davis S., Dunham D. (1985): An Alternative Gravity-Assist Sequences for the ISEE-3 Escape Trajectory. *J. Astronautical Sci.* **33**, 255–273.

Muhonen D., Folta D. (1985): Accelerometer-Enhanced Trajectory Control for the ISEE-3 Halo Orbit. *J. Astronautical Sci.* **33**, 289–300.

Murray D.B., Teare S.W. (1993): Probability of a Tossed Coin Landing on Edge. *Phys. Rev. E* **48**, 2547–2551.

Ogata K. (1990): *Modern Control Engineering*, second edition. (Prentice Hall, Englewood Cliffs, NJ).

Ott E., Grebogi C., Yorke J.A. (1990): Controlling Chaos. *Phys. Rev. Lett.* **64**, 1196–1199.

Ottino J.M., Jana S.C., Chakravarthy V.S. (1994): From Reynolds' Stretching and Folding to Mixing Studies Using Horseshoe Maps. *Phys. Fluids* **6**, 685–699.

Parmananda P., Sherard P., Rollins R.W., Dewald H.D. (1993): Control of Chaos in an Electrochemical Cell. *Phys. Rev. E* **47**, R3003–R3006.

Pecora L.M., Carroll T.L. (1990): Synchronization in Chaotic Systems. *Phys. Rev. Lett.* **64**, 821-824.

Peterson I. (1993): *Newton's Clock: Chaos in the Solar System.* (Freeman, NY).

Petrov V., Gáspár V., Masere J., Showalter K., (1993): Controlling Chaos in the Belousov-Zhabotinsky Reaction. *Nature* **361**, 240–243.

Poincaré H. (1896): *Comptes Rendus des Seances de L'Academie des Sciences* **179**, 497ff. & 557ff.

Poincaré H. (1957): *La Mécanique Céleste, Tome 1.* (Dover Publications, NY).

Poincaré H.(1893): *Solutions Asymptotiques, Méthodes Nouvelles de la Mécanique Céleste, Tome II.* (Gauthier-Villars et Fils, Paris).

Reynolds O. (1894): Study of Fluid Motion by Means of Coloured Bands. *Nature* **50**, 161–169

Ruelle D. (1980): Strange Attractors. *Mathematical Intelligencer* **2**, 126–137.

Schlissel A. (1977): Poincaré's Contribution to the Theory of Asymptotic Solutions. *Archive for History of the Exact Sciences* **16**, 325ff.

Schuster H.G. (1989): *Deterministic Chaos.* (VCH, Weinheim).

Segré E. (1980): *From X-Rays to Quarks.* (WH Freeman & Co, NY).

Shinbrot T., Bresler L., Ottino J.M. (1996): Control of Transport in a Chaotic Lattice. *Physica D* **93**, 191–209.

Shinbrot T., Grebogi C., Wisdom J., Yorke J.A. (1992): A Chaos in a Double Pendulum. *Am. J. Phys.* **60**, 491–499.

Shinbrot T., Ott E., Grebogi C., Yorke J.A. (1990): Using Chaos to Direct Trajectories to Targets. *Phys. Rev. Lett.* **65**, 3215–3218.

Shinbrot T., Ott E., Grebogi C., Yorke J.A. (1992b): Using Chaos to Direct Orbits to Targets in Systems Describable by a One-dimensional Map. *Phys. Rev. A* **45**, 4165–4168.

Singer J., Wang Y.-Z., Bau H.H. (1991): Controlling a Chaotic System. *Phys. Rev. Lett.* **66**, 1123–1125.

Smale S. (1967): Differentiable Dynamical Systems. *Bull. Amer. Math. Soc.* **73**, 747–768.

Sommerer J.C., Ott E. (1993): Particles Floating on a Moving Fluid: A Dynamically Comprehensible Physical Fractal. *Science* **259**, 335–339.

Sternberg S. (1969): *Celestial Mechanics, Part II.* (WA Benjamin, NY).

Sussman G.J., Wisdom J. (1992): Chaotic Evolution of the Solar System. *Science* **257**, 56–62.

Swanson P.D., Ottino J.M. (1992): A comparative Computational and Experimental Study of Chaotic Mixing of Viscous Fluids. *J. Fluid Mech.* **237**, 227–249.

Wisdom J. (1987): Urey Prize Lecture: Chaotic Dynamics in the Solar System. *Icarus* **72**, 241–275.

Wit A.L., Cranefield P.F. (1978): Reentrant Excitation as a Cause of Cardiac Arrhythmias. *Am J. Physiol.* **235**, H1–H17.

Yorke J.A., Yorke E.D., Mallet-Paret J. (1987): Lorenz-Like Chaos in a Partial Differential Equation for a Heated Fluid Loop. *Physica D* **24**, 279–91.